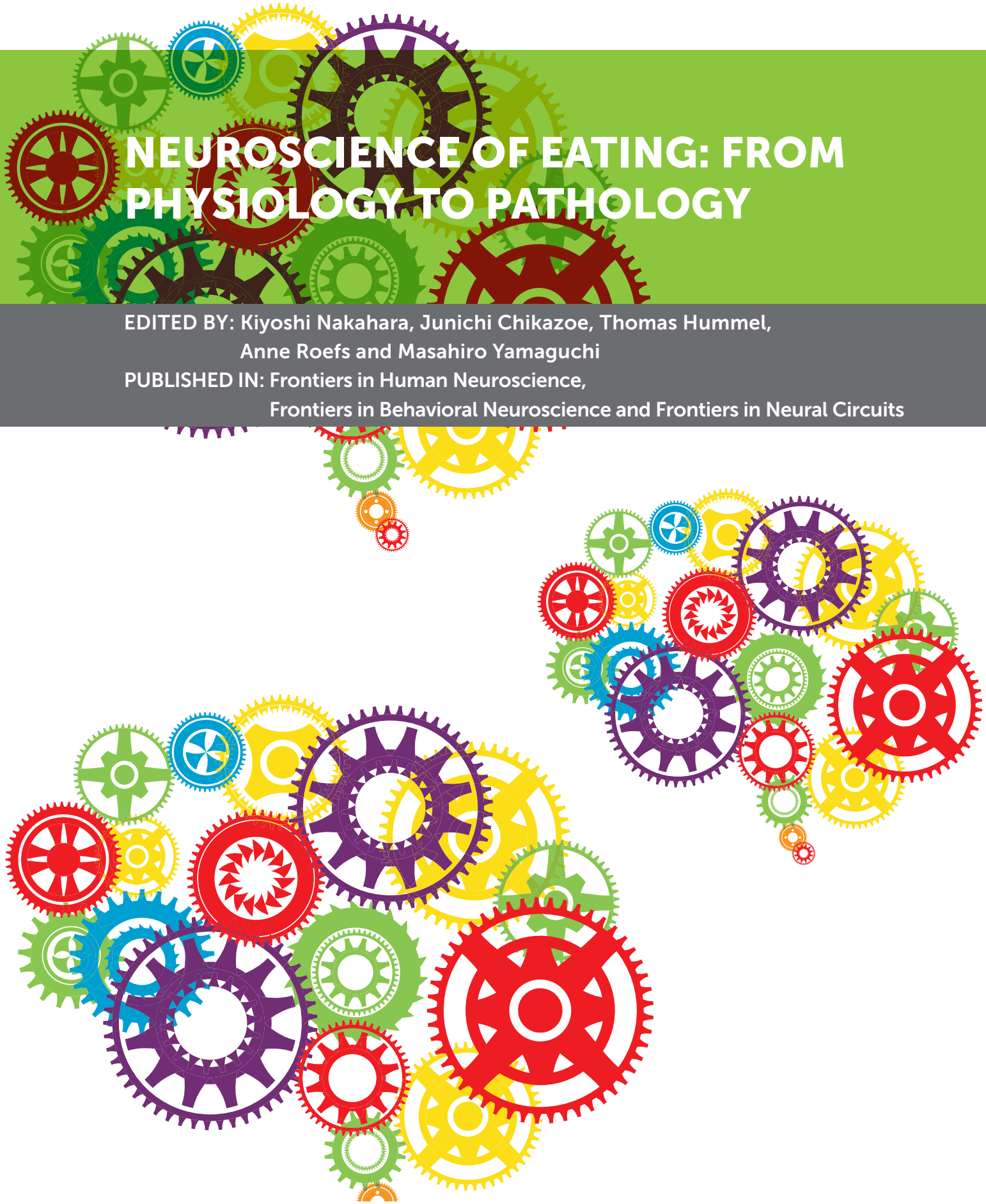

NEUROSCIENCE OF EATING: FROM PHYSIOLOGY TO PATHOLOGY

EDITED BY: Kiyoshi Nakahara, Junichi Chikazoe, Thomas Hummel, Anne Roefs and Masahiro Yamaguchi

PUBLISHED IN: Frontiers in Human Neuroscience, Frontiers in Behavioral Neuroscience and Frontiers in Neural Circuits

frontiers Research Topics

frontiers

ISSN 1664-8714
ISBN 978-2-88974-636-1
DOI 10.3389/978-2-88974-636-1

About Frontiers

Frontiers is more than just an open-access publisher of scholarly articles: it is a pioneering approach to the world of academia, radically improving the way scholarly research is managed. The grand vision of Frontiers is a world where all people have an equal opportunity to seek, share and generate knowledge. Frontiers provides immediate and permanent online open access to all its publications, but this alone is not enough to realize our grand goals.

Frontiers Journal Series

The Frontiers Journal Series is a multi-tier and interdisciplinary set of open-access, online journals, promising a paradigm shift from the current review, selection and dissemination processes in academic publishing. All Frontiers journals are driven by researchers for researchers; therefore, they constitute a service to the scholarly community. At the same time, the Frontiers Journal Series operates on a revolutionary invention, the tiered publishing system, initially addressing specific communities of scholars, and gradually climbing up to broader public understanding, thus serving the interests of the lay society, too.

Dedication to Quality

Each Frontiers article is a landmark of the highest quality, thanks to genuinely collaborative interactions between authors and review editors, who include some of the world's best academicians. Research must be certified by peers before entering a stream of knowledge that may eventually reach the public - and shape society; therefore, Frontiers only applies the most rigorous and unbiased reviews.
Frontiers revolutionizes research publishing by freely delivering the most outstanding research, evaluated with no bias from both the academic and social point of view. By applying the most advanced information technologies, Frontiers is catapulting scholarly publishing into a new generation.

What are Frontiers Research Topics?

Frontiers Research Topics are very popular trademarks of the Frontiers Journals Series: they are collections of at least ten articles, all centered on a particular subject. With their unique mix of varied contributions from Original Research to Review Articles, Frontiers Research Topics unify the most influential researchers, the latest key findings and historical advances in a hot research area! Find out more on how to host your own Frontiers Research Topic or contribute to one as an author by contacting the Frontiers Editorial Office: frontiersin.org/about/contact

NEUROSCIENCE OF EATING: FROM PHYSIOLOGY TO PATHOLOGY

Topic Editors:
Kiyoshi Nakahara, Kochi University of Technology, Japan
Junichi Chikazoe, National Institute for Physiological Sciences (NIPS), Japan
Thomas Hummel, Technical University Dresden, Germany
Anne Roefs, Maastricht University, Netherlands
Masahiro Yamaguchi, Kōchi University, Japan

Citation: Nakahara, K., Chikazoe, J., Hummel, T., Roefs, A., Yamaguchi, M., eds. (2022). Neuroscience of Eating: From Physiology to Pathology. Lausanne: Frontiers Media SA. doi: 10.3389/978-2-88974-636-1

Table of Contents

frontiers in Behavioral Neuroscience

BRIEF RESEARCH REPORT
published: 21 April 2020
doi: 10.3389/fnbeh.2020.00046

Neural Correlates of Food Cue Exposure Intervention for Obesity: A Case-Series Approach

Sieske Franssen, Anita Jansen, Ghislaine Schyns, Karolien van den Akker and Anne Roefs*

Department of Clinical Psychological Science, Faculty of Psychology and Neuroscience, Maastricht University, Maastricht, Netherlands

Background: People with overweight have stronger reactivity (e.g., subjective craving) to food cues than lean people, and this reactivity is positively associated with food intake. Cue reactivity is a learned response that can be reduced with food cue exposure therapy.

Objectives: It was hypothesized that participants after food cue exposure therapy would show reduced neural activity in brain regions related to food cue reactivity and increased neural activity in brain regions related to inhibitory-control as compared to participants receiving a control lifestyle intervention.

Method: Neural activity of 10 women with overweight (BMI $\geq$ 27 kg/m^2) in response to individually tailored visually presented palatable high-caloric food stimuli was examined before vs. after a cue exposure intervention (n = 5) or a control lifestyle (n = 5) intervention. Data were analyzed case-by-case.

Results: Neural responses to food stimuli were reduced in food-cue-reactivity-related brain regions after the lifestyle intervention in most participants, and generally not after the cue exposure therapy. Moreover, cue exposure did not lead to increased activity in inhibitory-control-related brain regions. However, decreased neural activity after cue exposure was found in most participants in the lateral occipital complex (LOC), which suggests a decreased visual salience of high-caloric food stimuli.

Conclusion: Receiving a cue exposure therapy did not lead to expected neural responses. As cue exposure relies on inhibitory learning mechanisms, differences in contexts (e.g., environments and food types) between the intervention setting and the scanning sessions may explain the general lack of effect of cue-exposure on neural activity.

Keywords: obesity, exposure therapy, functional MRI, case-series, cue reactivity

OPEN ACCESS

Edited by:
Liana Fattore,
Italian National Research Council, Italy

Reviewed by:
Claire Jennifer Foldi,
Monash University, Australia
Jamie Peters,
University of Colorado, United States

****Correspondence:***
Sieske Franssen
sieske.franssen@maastrichtuniversity.nl

Specialty section:
This article was submitted to Motivation and Reward, a section of the journal Frontiers in Behavioral Neuroscience

Received: *18 December 2019*
Accepted: *16 March 2020*
Published: *21 April 2020*

Citation:
Franssen S, Jansen A, Schyns G, van den Akker K and Roefs A (2020) Neural Correlates of Food Cue Exposure Intervention for Obesity: A Case-Series Approach. Front. Behav. Neurosci. 14:46. doi: 10.3389/fnbeh.2020.00046

INTRODUCTION

The prevalence of obesity has reached pandemic proportions (World Health Organization, 2018). Overweight people frequently engage in weight loss attempts, but success in the long-term is rare (Bish et al., 2005; Wing and Phelan, 2005). The main cause for obesity is a long-term energy imbalance, in which the number of consumed calories exceeds the number of expended calories

for an extended time (Mitchell et al., 2011; Hall et al., 2012). Therefore, developing effective interventions to change behavior and reduce body weight is important. One possible intervention is food cue exposure therapy (CE) (Jansen et al., 2016; van den Akker et al., 2016).

CE aims to reduce food cue reactivity, which is defined as appetitive responding – like increased salivation and self-reported craving – in response to food-associated cues. Food cue reactivity serves as a physiological and psychological preparation for eating (Jansen et al., 2016). Food cues can be internal, such as hunger, satiety, emotions and thoughts, but also external, such as the smell, sight and taste of food, or environmental contexts (Boswell and Kober, 2016; Jansen et al., 2016). As compared to lean people, overweight people have a stronger food cue reactivity (Ferriday and Brunstrom, 2011), which is related to increased food intake (Boswell and Kober, 2016). Food cues become associated with food intake through classical conditioning (Jansen et al., 2016). As soon as food cues are reliable predictors of intake, they will elicit reactivity (Jansen et al., 2011, 2016), which in turn can lead to food intake. In CE, overweight people are repeatedly exposed to food cues while (over)eating is prevented (Bouton, 2004, 2011; Jansen et al., 2011, 2016; van den Akker et al., 2014). Exposure to food cues first *in*creases food cue reactivity, but after prolonged and repeated non-reinforced exposure sessions, this reactivity *de*creases (Jansen et al., 2011, 2016). The CE rationale is that a new association between a food cue and intake is formed: the food cue does *not* predict intake. Importantly, this does not mean that the old association is *un*learned (Bouton, 2004; Jansen et al., 2016). As a result of this inhibitory learning, reactivity to food cues diminishes (extinction). To optimize this inhibitory learning, maximizing "expectancy-violation" is a key element of successful therapy (Craske et al., 2014). Expectancy violation is the reduction in a person's belief in his/her food-related expectancies (e.g., "If I feel exhausted and chocolate is available, then I will lose control and eat all chocolate"). CE has been shown to be an effective method to reduce food desires and overeating (Boutelle and Bouton, 2015; Jansen et al., 2016; Schyns et al., 2016), and it leads to short-term weight loss (Jansen et al., 2011, 2016; Schyns et al., 2016).

To gain insight in the mechanism of change, examining neural correlates of food cue reactivity may be valuable. A recent review described the following food-cue-reactivity-related brain regions: ventral striatum with nucleus accumbens (NAcc), midbrain, orbitofrontal cortex (OFC), anterior insula (INS), gustatory cortex (GC), lateral occipital cortex (LOC), and somatosensory cortex (SSC) (Giuliani et al., 2018). An increased activity was found in these brain regions when participants viewed high-caloric foods as compared to low-caloric foods or non-food images, and this was also predictive of the amount of food consumed (van der Laan et al., 2011; Smeets et al., 2012; Frankort et al., 2014; Giuliani et al., 2018; Hermann et al., 2019). However, a meta-analysis showed that these effects were quite inconsistent: the concurrence was moderate between studies in the activated clusters to food vs. non-food visual stimuli in healthy-weight participants (van der Laan et al., 2011). As CE intends to reduce food cue reactivity (Jansen et al., 2016), a decreased activity in food-cue-reactivity-related brain regions is expected in the current study.

Additionally, as a candidate-mechanism behind effective CE is inhibitory learning (Boutelle and Bouton, 2015), increased neural activity in inhibitory-control brain regions when processing palatable food stimuli is expected. Inhibitory-control-related brain regions include: dorso- and ventrolateral prefrontal cortex (dlPFC, vlPFC), parietal posterior cortex (PPC), dorsal anterior cingulate cortex (dACC), caudate, pre supplementary motor area (preSMA), and the globus pallidus (GP) (Kober et al., 2010; Giuliani et al., 2018).

In the current study, neural responses in food-cue-reactivity and in inhibitory-control brain regions to individually tailored high-caloric palatable food stimuli were examined pre- and post-CE or a healthy lifestyle (LS) intervention on subject-level (i.e., for each participant separately). During a functional magnetic resonance imaging (fMRI) session, participants were instructed to actively evaluate the taste of the visually presented food stimuli (hedonic focus) or to evaluate the colors of these food stimuli (neutral focus). We hypothesized that CE, as compared to LS, would lead to reduced neural activity in food-cue-reactivity-related brain regions and increased neural activity in inhibitory-control-related brain regions when viewing high-caloric food stimuli, mostly in the hedonic focus condition as this focus is aligned with the experience of craving (Roefs et al., 2018).

MATERIALS AND METHODS

Participants

Ten female overweight participants (BMI: M = 32.32 SD = 4.43 kg/m^2, age: M = 38.40 SD = 10.76 years) from a larger trial (n = 45) participated in this study, and were randomly assigned to CE (n = 5) or LS (n = 5) (van den Akker et al., 2016; Schyns et al., 2019). To overcome the problem of high heterogeneity in neural responses due to individual differences that could occur in small sample sizes (Roiser et al., 2016), data were analyzed on subject-level, as separate cases (for a similar approach see: Hubacher et al., 2015). All participants, except one, were right-handed. Participants were scanned within 2 weeks before and within 2 weeks after intervention.[1]

Inclusion criteria included: female, age between 18 and 60 years, BMI of at least 27 kg/m^2, no MRI contra-indications and no history of psychiatric or neurological illnesses. The study was approved by the local Ethical Committee. The participants gave written informed consent and were compensated for participation (€ 45).

Interventions

Interventions were provided by trained students, using a strict protocol, supervised by co-author GS. Both CE and LS

[1]Note that these pre-intervention fMRI data was also included in a previous study (Franssen et al., 2020).

consisted of eight individual sessions, scheduled twice per week, during ≈1 month.

During CE, participants performed several food cue exposures with a therapist. The exposure sessions were done in various overeating contexts (e.g., at the laboratory, at home watching television or work). Additionally, participants performed daily exposure exercises on their own at home or at other overeating-associated environmental contexts. LS consisted of four face-to-face sessions alternated with four telephone sessions. LS participants received healthy lifestyle advice, performed mindfulness and power posing exercises, and obtained psychoeducation on body image. For this intervention, daily homework exercises were given on mindfulness and on previous therapy session content. For a detailed description of both interventions see (van den Akker et al., 2016).

Behavioral Assessments

BMI Measurement

Weight and height were measured pre and post-intervention to compute BMI in kg/m^2.

Hunger Assessment

Participants were asked to refrain from eating or drinking (except water) for at least 1 h before the scan-sessions. To check compliance and have an indicative for subjective hunger, self-reported hunger was measured using a 100 mm visual analog scale (VAS), with the question: "How hungry do you feel at this moment?" ranging from 0 (not hungry at all) to 100 (very hungry) at the start of each session. Additionally, participants registered what and at what time they had eaten last.

Expectancy Violation

Eight food-cue-associated eating beliefs were rated on perceived expectancy if an associated cue would be followed by eating. Expectancies were measured pre- and post-intervention using 100 mm VAS, with a higher score reflecting a greater perceived expectancy of eating (see methodology paper for details: van den Akker et al., 2016).

Stimuli

Individual Stimulus Selection

Food stimuli used in the fMRI experiment were individually tailored. Each participant selected their five most palatable food items from a list of 33 high-caloric food items in an online questionnaire that was completed ≈1 week before the first scanning session. She then rated the selected stimuli on 10-point scales ranging from 1 (not palatable at all) to 10 (very palatable).

Stimulus Presentation

For each of the five chosen palatable food items, two different pictures were included in the fMRI stimulation protocol, to avoid visual adaptation by seeing the same picture too often. Pictures were presented as pop-out high-resolution colored images on a light gray background (RGB: 191 191 191; CKYM: 25 20 20 0) in the center of a black screen covering a visual angle of ≈12°.

Experimental Task

Attentional Focus Manipulation

The participant performed a fast-paced 1-back task in each functional run to induce an attentional focus (hedonic vs. neutral). During the 1-back task, the participant compared each presented food picture (starting from the 2nd presented picture) to the previously presented picture, and indicated whether the presented food was more or less palatable than the previous one (hedonic focus), or whether the picture contained more or fewer colors than the previous one (neutral focus). Each food stimulus was presented for 500 ms, with an inter-stimulus interval (ISI) as a response window of 1,500 ms. The participant's responses were registered using a buttonbox, with a right index finger press for "fewer" and a right middle finger press for "more."

fMRI Stimulation Protocol

The fMRI task consisted of four runs. In each run, six different conditions were presented, but for the current study only two conditions were relevant and included in the analyses: blocks with palatable high-caloric food stimuli – neutral focus (PAL-NEU) and blocks with palatable high-caloric food stimuli – hedonic focus (PAL-HED). Ten blocks were presented seven times in a randomized order with 12 stimuli each, across the four functional runs. Prior to each block, a cue-word "taste" or "color" was presented for 1 s to inform the participant which attentional focus to apply. Blocks lasted 24 s and were always followed by a 20 s rest block (fixation cross). Total functional scanning time was ≈35 min.

MRI Data Acquisition

Images were acquired on a 3 Tesla MRI scanner (Magnetom Prisma Fit, Siemens Medical Systems) using a 64-channel head/neck coil. Functional (T_2*-weighted) images were acquired using multiband gradient echo-planar imaging in an axial interleaved order (Feinberg et al., 2010) with the following settings: TR = 2,000 ms, TE = 30 ms, flip angle = 77°, FOV = 208 × 124 mm^2, and voxel size of 2 × 2 × 2 mm^3. To ensure whole brain coverage, slices were acquired in a backward tilted direction of ≈15 degrees to the transversal – coronal line. As anatomical scan, a high-resolution, three-dimensional (3D) T_1-weighted MPRAGE scan was acquired, with the following settings: TR = 2,250 ms, TE = 2.21 ms, flip angle = 9°, FOV = 256 × 192 mm^2, and voxel size 1 × 1 × 1 mmł and had a duration of ± 5 min.

fMRI Data Analysis

Preprocessing

Analyses were performed using SPM12 (Statistical Parametric Mapping, London, United Kingdom) and Matlab version 8.3.0.532 (R2014a). Functional images were slice-time corrected, realigned, co-registered, normalized using unified brain segmentation, and spatially smoothed using a Gaussian kernel of 6 mm full width at half-maximum (FWHM).

Preprocessed functional volume time series were used for statistical analysis.

Statistical Analysis

To compare the session differences on subject-level, a general linear model (GLM) design matrix was created including the two scan-sessions (pre- and post-intervention) as eight consecutive runs. Each experimental task condition was set as a predictor, which resulted in six predictors of interest per run (with two of interest for the current study). Additionally, six motion and eight run mean intensity predictors of no interest were added to the model as confound regressors. Predictor time courses were obtained using condition box-car shaped waves convolved with a two-gamma ideal hemodynamic response function (HRF).

Case Series Approach: First-Level Analysis

To investigate the effects of interest, we computed the following contrasts on subject-level for the high-caloric palatable food conditions: (1) main effect of session (*t*-contrasts A: pre-intervention > post-intervention and B: post-intervention > pre-intervention) and (2) session (pre-intervention vs. post-intervention) * attentional focus (neutral vs. hedonic) interaction *F*-contrasts. To extract beta values, each condition of interest was also contrasted against baseline.[2]

Region of Interest (ROI) Analysis

We defined a-priori ROI masks for food cue reactivity based on the review of Giuliani and colleagues (Giuliani et al., 2018), including: ventral striatum with NAcc, midbrain, OFC, anterior INS, GC, LOC, and SSC and for inhibitory control, including: dlPFC, vlPFC, PPC, dACC, caudate, preSMA and the GP. The ROI masks were manually generated by using the WFU Pickatlas tool (version 3.0.5) in SPM12.

To correct for multiple comparisons, family-wise error (FWE) correction based on Gaussian random field theory was applied to control for false positives at $\alpha = 0.05$ on subject-level (Eklund et al., 2016). This method was applied for the statistical maps of the main effects of session, and was combined with a clustersize threshold (k) of three contiguous voxels to only include more robust clusters. For the subtler session * attentional focus interaction, uncorrected statistical maps with $p < 0.001$ with $k = 3$ voxels were reported. The MarsBar toolbox[3] was used to extract beta values in SPM12. For localization and clustersize information of activated clusters, XJview[4] was used. Figures were created using the MNI brain template from MRIcroGL software package[5].

[2]For participant 2 of the LS group only three runs were acquired in the pre-intervention session due to set-up problems. Therefore, also only three runs of the post-intervention session were included for this participant. This was done to be able to balance the conditions in the GLM for defining contrasts. For the post-intervention session, we selected the three runs with best data quality (i.e., least movement of participant during scanning).

[3]http://marsbar.sourceforge.net/

[4]http://www.alivelearn.net/xjview/

[5]http://www.mccauslandcenter.sc.edu/mricro/mricrogl/

TABLE 1 | Participant characteristics and pre-post intervention behavioral measures and post – pre differences.

			Pre-intervention				Post-intervention				Difference post minus pre			
	Age	Palatability rating	BMI	Hunger	Not eaten (min)	Expectancies	BMI	Hunger	Not eaten (min)	Expectancies	BMI	Hunger	Not eaten (min)	Expectancies
CE1	18	10	38.69	0	110	65	38.94	11	120	16	0.26	11	10	−49
CE2	45	9.2	31.33	20	90	63	30.15	67	120	13	−1.18	47	30	−50
CE3	28	9	27.75	53	150	86	26.37	78	90	24	−1.38	25	−60	−62
CE4	33	9	37.42	12	120	88	37.99	29	105	33	0.57	17	−15	−55
CE5	42	9.2	29.19	9	90	80	28.76	36	195	16	−0.43	27	105	−64
Average	**33.2**	**9.28**	**32.88**	**18.8**	**112**	**76.4**	**32.44**	**44.2**	**126**	**20.4**	**−0.43**	**25.4**	**14**	**−56**
LS1	45	9.4	27.24	18	105	58	26.70	44	210	76	−0.54	26	105	18
LS2	46	9.6	37.91	9	120	83	37.27	2	150	48	−0.63	−7	30	−35
LS3	52	8.8	34.26	5	180	31	34.18	1	120	1	−0.07	−4	−60	−30
LS4	29	9	30.74	54	150	76	29.98	20	210	54	−0.76	−34	60	−22
LS5	46	9	34.09	36	300	78	34.15	66	510	51	0.06	30	210	−27
Average	**43.6**	**9.16**	32.85	**24.4**	**171**	**65.2**	**32.46**	**26.6**	**240**	**46**	**−0.39**	**2.2**	**69**	**−19.2**

BMI, body mass index; CE, Cue exposure intervention; LS, Lifestyle intervention. Hunger and expectancies were scored on a 0–100 mm visual analog scale a higher score reflecting more hunger or greater perceived expectancy. Not Eaten, time passed since eaten last meal.

RESULTS

Behavioral Assessments

An overview of behavioral assessments is provided in **Table 1**. The time between first and second scan session ranged for CE: 34–43 days and for LS: 36–58 days. Three CE and four LS participants lost weight after the intervention. Hunger-ratings were higher post-intervention than pre-intervention in all CE participants, whereas this was only true for two LS-participants (LS1 and LS5). However, 7 of the 10 participants reported relatively low hunger at post-intervention (scores $\leq$ 44 on a 0–100 VAS). All participants rated their selected foods as highly palatable (average scores $\geq$ 8.8 on 10-point scale). Expectancy violation changes (post-intervention – pre-intervention) differed between CE and LS participants. All CE participants showed a higher reduction of eating

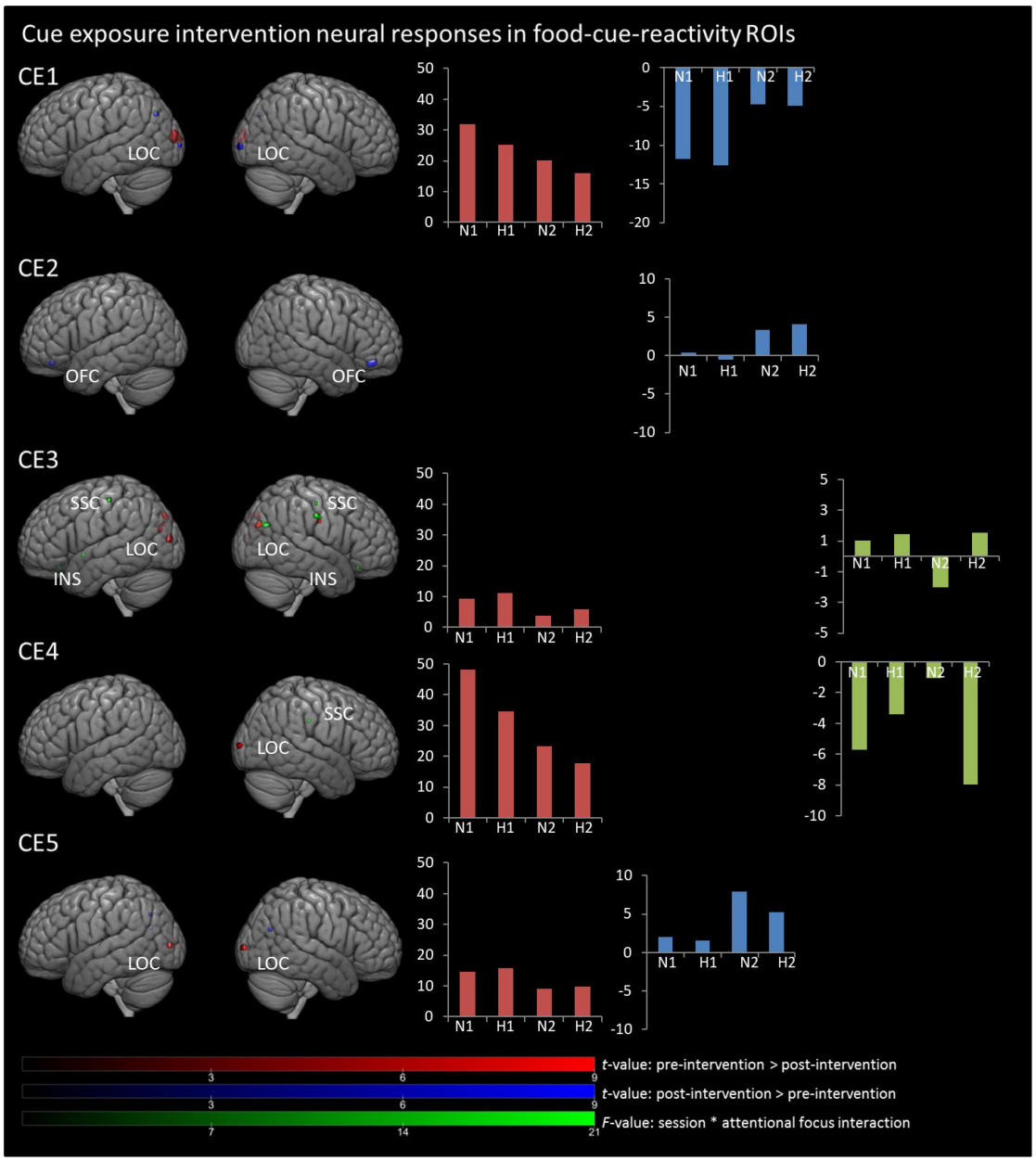

FIGURE 1 | Results from univariate analyses per participant for cue exposure intervention in food-cue-reactivity-ROIs. *t*-maps of significant main effects of session are shown in food-cue-reactivity-ROIs: pre > post-intervention in red, post > pre-intervention in blue ($p < 0.05$ FWE cor) and *F*-map of session * attentional focus interaction ($p < 0.001$ unc.) in green. Bar plots represents mean extracted beta values from the contributing clusters per condition per comparison. N1, neutral attentional focus pre-intervention; H1, hedonic attentional focus pre-intervention; N2, neutral attentional focus post-intervention; H2, hedonic attentional focus post-intervention; LOC, Lateral Occipital Complex; SSC, somatosensory cortex; OFC, orbitofrontal cortex, INS, Insula.

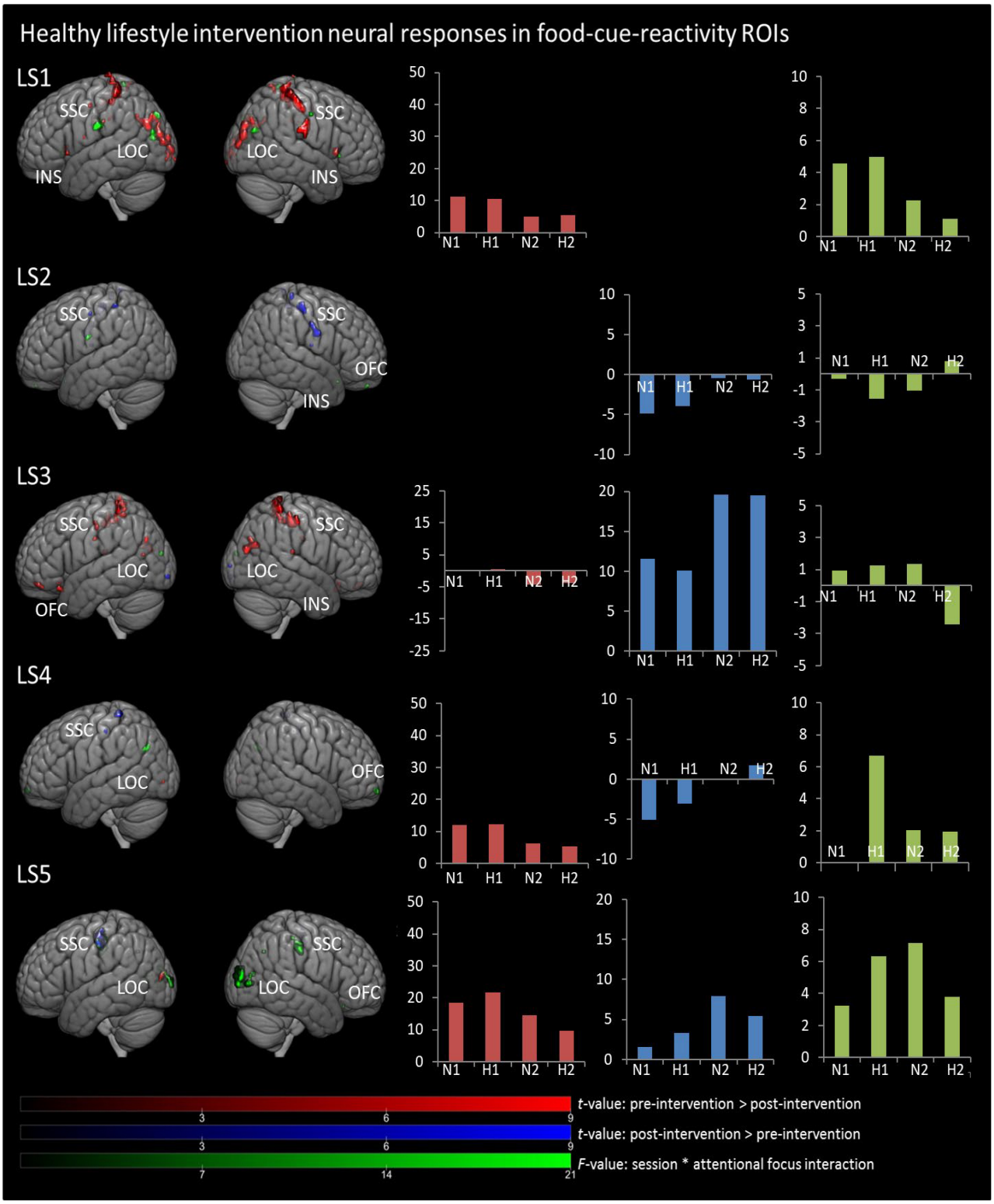

FIGURE 2 | Results from univariate analyses per participant for healthy lifestyle intervention in food-cue-reactivity-ROIs. *t*-maps of significant main effects of session are shown in food-cue-reactivity-ROIs: pre > post-intervention in red, post > pre-intervention in blue ($p < 0.05$ FWE cor) and *F*-map of session * attentional focus interaction ($p < 0.001$ unc.) in green. Bar plots represents mean extracted beta values from the contributing clusters per condition per comparison. N1, neutral attentional focus pre-intervention; H1, hedonic attentional focus pre-intervention; N2, neutral attentional focus post-intervention; H2, hedonic attentional focus post-intervention; LOC, Lateral Occipital Complex; SSC, somatosensory cortex; OFC, orbitofrontal cortex; INS, Insula.

expectancies after intervention as compared to the LS participants.

Neural Responses

In **Figures 1**, **2**, main effects of session are displayed, as well as the session * attentional focus interaction per participant in the food-cue-reactivity-ROIs. Details of each significant cluster can be found in **Tables 2**, **3**.

Main Effects Session

Contrary to our hypothesis, food-cue-reactivity-related activity was not substantially reduced after intervention for CE participants. In fact, LS participants showed reductions in more ROIs (e.g., SSC, INS, LOC, and OFC; see participants LS1 and LS3), and involved clusters were larger. However, reduction in beta values was larger in those clusters that changed significantly from pre- to post-intervention in CE participants. Note that these clusters were substantially smaller and localized in the LOC solely (see participants: CE1, CE3, CE4, and CE5). To examine opposite effects, we also compared post-intervention > pre-intervention contrasts. Here, unexpectedly, the CE participants showed also *in*creased activation in small clusters in the LOC (see: CE1 and CE5) and in the OFC (CE2) after intervention. LS participants showed an increase in activity in the SSC (LS2, LS4 and LS5) and in the LOC (LS3).

Session * Attentional Focus Interaction

As with the main effect of session, the interaction effect was also mainly observed in LS participants. Analyses of the interaction yielded significant clusters for all LS participants. Here, four LS participants (LS1, LS3, LS4, and LS5) showed a larger reduction from pre to post with the hedonic focus than with the neutral focus in the right INS and OFC and bilaterally in the SSC and LOC. For participant LS2 this was reversed, activity in food-cue-reactivity-ROIs (right OFC and left SSC) was increased from pre to post with the hedonic focus. Two CE participants showed an interaction effect, where participant CE4 showed a more reduced activation pre to post in the hedonic focus than in the neutral focus in a very small cluster in the right SCC. Participant CE3 showed more robust clusters, involving the INS and the SCC with an unexpectedly larger reduction in activation from pre to post in the neutral focus condition than the hedonic focus.

TABLE 2 | Significant clusters from univariate analyses per participant for cue exposure intervention in food-cue-reactivity-ROIs.

	Anatomical region	Hemisphere	Clustersize	Peak MNI coordinates			Peak
			(No. of voxels)	*x* (mm)	*y* (mm)	*z* (mm)	*F*/*t*-value
main effect session: Pre-intervention > Post-intervention							
CE1	LOC	L	105	−16	−100	10	6.57
	LOC	R	3	28	−92	20	5.34
CE3	LOC	L	23	−40	−90	12	7.06
	LOC	L	6	−38	−80	22	5.08
	LOC	L	3	−26	−84	28	5.31
	LOC	R	22	40	−78	28	5.54
	SSC	R	4	64	−12	32	5.21
	LOC	L	10	−24	−84	38	5.97
	LOC	R	4	34	−78	38	5.17
CE4	LOC	R	14	32	−100	8	6.26
CE5	LOC	R	25	30	−98	6	6.43
	LOC	L	17	−38	−90	6	7.09
Main effect session: Post-intervention > Pre-intervention							
CE1	LOC	R	21	30	−100	0	6.13
	LOC	L	6	−26	−100	2	5.15
	LOC	L	10	−38	−76	36	5.29
CE2	OFC	R	48	26	42	−16	7.07
	OFC	L	12	−20	38	−16	5.47
CE5	LOC	R	7	36	−68	24	5.48
	LOC	L	3	−26	−68	40	5.68
Interaction: Session * Attentional focus							
CE3	OFC	R	4	14	28	−18	11.76
	Insula	L	4	−40	4	−4	11.76
	LOC	R	22	46	−70	28	15.48
	SSC	R	13	64	−16	38	12.68
	SSC	R	5	58	−16	52	12.59
	SSC	L	9	−54	−24	54	14.24
CE4	SSC	R	3	66	−24	32	12.62

L, left; R, right; MNI, Montreal Neurological Institute; LOC, Lateral Occipital Complex; SSC, somatosensory cortex; OFC, orbitofrontal cortex.

TABLE 3 | Significant clusters from univariate analyses per participant for healthy lifestyle intervention in food-cue-reactivity-ROIs.

	Anatomical region	Hemisphere	Clustersize	Peak MNI coordinates			Peak
			(No. of voxels)	*x* (mm)	*y* (mm)	*z* (mm)	*F*/*t*-value
Main effect session: Pre-intervention > Post-intervention							
LS1	SSC	R	288	50	−28	58	8.19
	LOC	L	271	−26	−86	20	11.32
	LOC	R	188	28	−88	20	9.04
	SSC	L	156	−40	−40	68	9.75
	SSC	R	79	68	−18	24	8.11
	LOC	L	55	−20	−100	2	9.03
	LOC	L	34	−18	−96	14	11.49
	Insula	R	18	40	18	4	6.08
	SSC	R	17	12	−56	72	6.57
	LOC	R	14	38	−74	34	5.94
	SSC	L	14	−22	−30	82	7.00
	Insula	L	9	−40	18	−2	6.08
	LOC	L	8	−32	−95	−8	5.86
	SSC	L	8	−56	−18	26	5.15
	SSC	L	8	−4	−8	48	5.96
	SSC	L	8	−54	−32	52	6.61
	SSC	L	6	−58	−24	32	5.93
	LOC	L	4	−16	−104	−8	9.40
	LOC	L	3	−10	−96	0	5.72
	SSC	L	3	−54	−2	16	5.07
	SSC	L	3	−44	−32	36	5.13
LS3	SCC	R	200	32	−46	70	9.22
	LOC	R	109	44	−72	24	6.43
	SSC	L	105	−28	−48	68	8.51
	SSC	R	78	34	−28	54	7.72
	OFC	L	24	−34	48	16	6.44
	SSC	R	24	54	−24	54	6.11
	SSC	L	20	−56	−18	44	5.64
	OFC	L	19	−32	22	−20	6.56
	SSC	L	19	−18	−46	58	5.98
	SSC	R	14	6	−42	62	7.25
	SSC	R	14	8	−42	74	7.72
	SSC	R	11	6	−36	50	6.19
	LOC	L	10	−40	−72	32	5.40
	Insula	R	8	34	−26	20	5.43
	SSC	L	7	−40	−16	34	5.64
	SSC	L	6	−4	−48	62	5.68
	SSC	L	4	−14	−40	54	5.55
	SSC	L	4	−14	−44	74	6.80
	OFC	L	3	−34	24	−12	5.29
	LOC	L	3	−42	−68	16	5.67
LS4	LOC	L	3	−32	−88	−4	5.06
LS5	LOC	L	43	−28	−90	14	6.90
Main effect session: Post-intervention > Pre-intervention							
LS2	SSC	R	64	56	−2	−28	5.79
	SSC	R	37	42	−22	58	6.81
	SSC	L	11	−32	−38	58	5.29
	SSC	R	11	36	−32	68	5.67
	SSC	L	5	28	−26	−56	5.27
	SSC	R	4	28	−26	56	5.19

(Continued)

TABLE 3 | Continued

	Anatomical region	Hemisphere	Clustersize	Peak MNI coordinates			Peak
			(No. of voxels)	*x* (mm)	*y* (mm)	*z* (mm)	*F/t*-value
	Insula	R	3	40	−12	16	5.12
	SSC	L	3	−4	−44	72	5.26
LS3	LOC	L	6	−28	−98	−8	6.42
	LOC	R	4	24	98	4	5.07
LS4	SSC	L	33	−34	−36	68	5.51
	SSC	L	4	−52	−24	50	5.31
LS5	SSC	L	130	−50	−22	44	6.55
Interaction: Session * Attentional focus							
LS1	SSC	L	63	−66	−16	26	29.22
	LOC	L	26	−46	−78	22	15.85
	LOC	R	20	50	−72	26	19.03
	LOC	L	18	−26	−84	40	14.10
	SSC	L	8	−4	−46	70	23.43
	SSC	R	6	60	−10	44	15.61
	Insula	R	4	34	22	0	13.08
	SSC	L	3	−18	−26	80	15.45
LS2	SSC	L	9	−62	−6	24	12.60
	OFC	R	4	6	52	−26	12.74
	OFC	R	3	14	18	−22	13.18
LS3	LOC	L	7	−18	−90	18	12.87
LS4	OFC	R	18	18	64	−12	13.21
	LOC	L	17	−34	−70	34	12.15
LS5	LOC	R	224	36	−90	12	21.36
	SSC	R	68	48	−22	38	22.93
	LOC	L	47	−26	−100	10	15.41
	LOC	L	35	52	−78	6	16.79
	SSC	L	18	−38	−24	56	13.19
	SSC	L	17	−52	−20	44	13.48
	LOC	R	8	38	−76	14	11.73
	LOC	R	4	32	−62	38	12.11
	SSC	R	4	50	−32	52	12.65
	OFC	R	3	30	26	−18	11.06

L, left; R, right; MNI, Montreal Neurological Institute; LOC, Lateral Occipital Complex; SSC, somatosensory cortex; OFC, orbitofrontal cortex.

We also compared neural activity per participant in inhibitory-control-ROIs. Tests of the main- and interaction-effects did not lead to any meaningful results for the CE intervention either. The clusters of neural activity per participant can be found in **Supplementary Tables S1, S2**.

DISCUSSION

Contrary to our hypothesis, the results showed that for these cases a cue exposure intervention did not lead to a significantly stronger reduction in neural activity in brain regions related to food-cue-reactivity, in response to visual high-caloric palatable food stimuli, as compared to the participants that received a lifestyle intervention. In fact, most participants' reductions in neural activity in food-cue-reactivity-related brain regions were more pronounced and more widespread after a lifestyle intervention and mostly with a hedonic attentional focus. When comparing activity in inhibitory-control-related brain regions on subject-level, no meaningful results were observed.

Surprisingly, the expected reduced activity was more apparent in LS participants (in e.g., SSC, INS, OFC, and LOC). During the intervention, LS participants received education on dieting and healthy weight loss and on nutrients and energy balance (van den Akker et al., 2016). This could have raised awareness of negative health aspects of high caloric foods, which may have contributed to participants' reduced neural responses to high-caloric foods. This interpretation aligns well with previous studies, showing that focusing on negative health aspects can control reward-related activity to visually presented high-caloric food stimuli (Hollmann et al., 2012; Siep et al., 2012). Although participants were instructed during scanning to attend to the hedonic aspects of the foods presented, this lifestyle training may have interfered with this hedonic focus during the post-intervention scanning-session by increasing awareness of negative health aspects.

Unexpectedly, CE did not lead to a significant reduction of neural activity in most cases in food-cue-reactivity-related brain regions. Behavioral outcomes showed that self-reported expectancy violations did improve specifically for the CE participants. Also, hunger was higher for all CE participants at post-intervention measurement. However, these CE-related behavioral effects could not be meaningfully related to post-pre intervention patterns of neural activity. These neural pre-post intervention findings could be the consequence of participants learning a new inhibitory association (the cue does *not* predict intake) during food cue exposure, which then exists next to the original disinhibiting association (the cue does predicts intake) (Jansen et al., 2016). That is, the food-cue-intake association is not erased, and therefore food cues might still trigger neural activity in food-cue-reactivity-ROIs. However, also in inhibitory-control-related brain regions, no strong increased neural activity in CE participants was found after intervention in these inhibitory-control regions.

Important to realize is that inhibitory learning during extinction is context-dependent and food-specific (Bouton, 2004, 2011; Jansen et al., 2016). Both the context (fMRI scanner vs. a laboratory room, participants' home and other relevant contexts) and the food stimuli differed between the current fMRI measurement and the intervention setting. Furthermore, a CE intervention only led to reduced consumption of the exposed foods, but not of other foods (Schyns et al., 2016, 2018, 2019). So, there was no generalization to other foods. In an earlier study (Frankort et al., 2014), we did observe a reduction in neural activity in food-cue-reactivity-related brain regions after cue exposure. Importantly, here, the cue exposure and measurement of neural activity both took place in the scanner while using the same food stimuli throughout (i.e., chocolate) (Frankort et al., 2014). Taken together, these findings underline the importance of considering context and the food-specificity of cue exposure while examining neural responses.

In line with our hypothesis, the current study showed reduced activation in the lateral occipital complex (LOC) in four participants after CE. The LOC was identified, in a meta-analysis comparing visual food to non-food stimuli, as one of the main brain regions involved in visual food cue processing (van der Laan et al., 2011). The decreased LOC activity may reflect a decrease in visual saliency of the palatable high-caloric foods as a result of CE. As this decreased LOC activation was specifically found for the CE participants, it therefore might be a precursor for extinction.

A limitation of this study is that due to the inclusion of only female participants and the case-series analyses approach, it is hard to translate the current results to a group-intervention effect, or to a broader population (i.e., males). Results should be interpreted with caution. Data was analyzed with a-priori defined ROI masks, which reduces the between-subjects variability of activation locations (Ziauddeen et al., 2012) and makes interpreting and comparing findings more reliable. The scanning-protocol pre- and post-intervention was kept exactly the same, which made it a strong within-subject design, and therefore the current study might give interesting leads for conducting a group-level future study. Future research needs to replicate these findings, and investigate whether neural changes induced by a lifestyle intervention are related to concurrent and future weight change.

DATA AVAILABILITY STATEMENT

All datasets generated for this study are included in the article/**Supplementary Material**.

ETHICS STATEMENT

The studies involving human participants were reviewed and approved by the local Ethical Committee of the faculty of Psychology and Neuroscience, Maastricht University. The patients/participants provided their written informed consent to participate in this study.

AUTHOR CONTRIBUTIONS

SF, AR, and AJ designed the study. SF collected the data and analyzed the data. GS and KA designed and coordinated the interventions. SF and AR wrote the manuscript. AJ, GS, and KA gave feedback on the manuscript. All authors approved the final version.

FUNDING

This study was partly financed by the Netherlands Organization for Scientific Research (NWO) vici-grant (453.10.006) and the Maastricht University Interfaculty Program "Eatwell" awarded to AJ, and NWO vidi-grant (452.16.007) awarded to AR.

SUPPLEMENTARY MATERIAL

The Supplementary Material for this article can be found online at: https://www.frontiersin.org/articles/10.3389/fnbeh.2020.00046/full#supplementary-material

REFERENCES

Bish, C. L., Blanck, H. M., Serdula, M. K., Marcus, M., Kohl, H. W., and Khan, L. K. (2005). Diet and physical activity behaviors among americans trying to lose weight: 2000 behavioral risk factor surveillance system. *Obes. Res.* 13, 596–607. doi: 10.1038/oby.2005.64

Boswell, R. G., and Kober, H. (2016). Food cue reactivity and craving predict eating and weight gain: a meta-analytic review. *Obes. Rev.* 17, 159–177. doi: 10.1111/obr.12354

Boutelle, K. N., and Bouton, M. E. (2015). Implications of learning theory for developing programs to decrease overeating. *Appetite* 93, 62–74. doi: 10.1016/j.appet.2015.05.013

Bouton, M. E. (2004). Context and behavioral processes in extinction. *Learn. Mem.* 11, 485–494. doi: 10.1101/lm.78804

Bouton, M. E. (2011). Learning and the persistence of appetite: extinction and the motivation to eat and overeat. *Physiol. Behav.* 103, 51–58. doi: 10.1016/j.physbeh.2010.11.025

Craske, M. G., Treanor, M., Conway, C. C., Zbozinek, T., and Vervliet, B. (2014). Maximizing exposure therapy: an inhibitory learning approach. *Behav. Res. Ther.* 58, 10–23. doi: 10.1016/j.brat.2014.04.006

Eklund, A., Nichols, T. E., and Knutsson, H. (2016). Cluster failure: Why fMRI inferences for spatial extent have inflated false-positive rates. *Proc. Natl. Acad. Sci. U.S.A.* 113, 7900–7905. doi: 10.1073/pnas.1602413113

Feinberg, D. A., Moeller, S., Smith, S. M., Auerbach, E., Ramanna, S., Glasser, M. F., et al. (2010). Multiplexed echo planar imaging for sub-second whole brain fmri and fast diffusion imaging. *PLoS One* 5:e15710. doi: 10.1371/journal.pone.0015710

Ferriday, D., and Brunstrom, J. M. (2011). 'I just can't help myself': effects of food-cue exposure in overweight and lean individuals. *Int. J. Obes.* 35, 142–149. doi: 10.1038/ijo.2010.117

Frankort, A., Roefs, A., Siep, N., Roebroeck, A., Havermans, R., and Jansen, A. (2014). The craving stops before you feel it: neural correlates of chocolate craving during cue exposure with response prevention. *Cereb. Cortex* 24, 1589–1600. doi: 10.1093/cercor/bht016

Franssen, S., Jansen, A., den Hurk, J., Roebroeck, A., and Roefs, A. (2020). Power of mind: attentional focus rather than food palatability dominates neural responding to visual food stimuli in females with overweight. Appetite 148:104609. doi: 10.1016/j.appet.2020.104609

Giuliani, N. R., Merchant, J. S., Cosme, D., and Berkman, E. T. (2018). Neural predictors of eating behavior and dietary change. *Ann. N. Y. Acad. Sci.* 00, 1–13. doi: 10.1111/nyas.13637

Hall, K. D., Heymsfield, S. B., Kemnitz, J. W., Klein, S., Schoeller, D. A., and Speakman, J. R. (2012). Energy balance and its components: implications for body weight regulation. *Am. J. Clin. Nutr.* 95, 989–994. doi: 10.3945/ajcn.112.036350

Hermann, P., Gál, V., Kóbor, I., Kirwan, C. B., Kovács, P., Kitka, T., et al. (2019). Efficacy of weight loss intervention can be predicted based on early alterations of fMRI food cue reactivity in the striatum. *Neuroimage Clin.* 23:101803. doi: 10.1016/j.nicl.2019.101803

Hollmann, M., Hellrung, L., Pleger, B., Schlögl, H., Kabisch, S., Stumvoll, M., et al. (2012). Neural correlates of the volitional regulation of the desire for food. *Int. J. Obes.* 36, 648–655. doi: 10.1038/ijo.2011.125

Hubacher, M., Kappos, L., Weier, K., Stöcklin, M., Opwis, K., and Penner, I.-K. (2015). Case-based fMRI analysis after cognitive rehabilitation in MS: a novel approach. *Front. Neurol.* 6:78. doi: 10.3389/fneur.2015.00078

Jansen, A., Havermans, R. C., and Nederkoorn, C. (2011). "Cued Overeating," in *Handbook of Behavior, Food and Nutrition*, eds V. R. Preedy, R. R. Watson, and C. R. Martin (New York, NY: Springer), 1431–1443. doi: 10.1007/978-0-387-92271-3

Jansen, A., Schyns, G., Bongers, P., and van den Akker, K. (2016). From lab to clinic: extinction of cued cravings to reduce overeating. *Physiol. Behav.* 162, 174–180. doi: 10.1016/j.physbeh.2016.03.018

Kober, H., Mende-Siedlecki, P., Kross, E. F., Weber, J., Mischel, W., Hart, C. L., et al. (2010). Prefrontal-striatal pathway underlies cognitive regulation of craving. *Proc. Natl. Acad. Sci. U.S.A.* 107, 14811–14816. doi: 10.1073/pnas.1007779107

Mitchell, N. S., Catenacci, V. A., Wyatt, H. R., and Hill, J. O. (2011). Obesity: overview of an epidemic. *Psychiatr. Clin. North Am.* 34, 717–732. doi: 10.1016/j.psc.2011.08.005

Roefs, A., Franssen, S., and Jansen, A. (2018). The dynamic nature of food reward processing in the brain. *Curr. Opin. Clin. Nutr. Metab. Care* 21, 444–448. doi: 10.1097/MCO.0000000000000504

Roiser, J. P., Linden, D. E., Gorno-Tempinin, M. L., Moran, R. J., Dickerson, B. C., and Grafton, S. T. (2016). Minimum statistical standards for submissions to neuroimage: clinical. *Neuroimage Clin.* 12, 1045–1047. doi: 10.1016/j.nicl.2016.08.002

Schyns, G., Roefs, A., Mulkens, S., and Jansen, A. (2016). Expectancy violation, reduction of food cue reactivity and less eating in the absence of hunger after one food cue exposure session for overweight and obese women. *Behav. Res. Ther.* 76, 57–64. doi: 10.1016/j.brat.2015.11.007

Schyns, G., van den Akker, K., Roefs, A., Hilberath, R., and Jansen, A. (2018). What works better? Food cue exposure aiming at the habituation of eating desires or food cue exposure aiming at the violation of overeating expectancies? *Behav. Res. Ther.* 102, 1–7. doi: 10.1016/j.brat.2017.12.001

Schyns, G., van den Akker, K., Roefs, A., Houben, K., and Jansen, A. (2019). Exposure therapy vs lifestyle intervention to reduce food cue reactivity and binge eating in obesity: a pilot study. *J. Behav. Ther. Exp. Psychiatry* 67:101453. doi: 10.1016/j.jbtep.2019.01.005

Siep, N., Roefs, A., Roebroeck, A., Havermans, R., Bonte, M., and Jansen, A. (2012). Fighting food temptations: The modulating effects of short-term cognitive reappraisal, suppression and up-regulation on mesocorticolimbic activity related to appetitive motivation. *Neuroimage* 60, 213–220. doi: 10.1016/j.neuroimage.2011.12.067

Smeets, P. A. M., Charbonnier, L., van Meer, F., van der Laan, L. N., and Spetter, M. S. (2012). Food-induced brain responses and eating behaviour. *Proc. Nutr. Soc.* 71, 511–520. doi: 10.1017/S0029665112000808

van den Akker, K., Havermans, R. C., Bouton, M. E., and Jansen, A. (2014). How partial reinforcement of food cues affects the extinction and reacquisition of appetitive responses. New model for dieting success? *Appetite* 81, 242–252. doi: 10.1016/j.appet.2014.06.024

van den Akker, K., Schyns, G., and Jansen, A. (2016). Enhancing inhibitory learning to reduce overeating: design and rationale of a cue exposure therapy trial in overweight and obese women. *Contemp. Clin. Trials* 49, 85–91. doi: 10.1016/j.cct.2016.06.008

van der Laan, L. N., de Ridder, D. T. D., Viergever, M. A., and Smeets, P. A. M. (2011). The first taste is always with the eyes: a meta-analysis on the neural correlates of processing visual food cues. *Neuroimage* 55, 296–303. doi: 10.1016/j.neuroimage.2010.11.055

Wing, R. R., and Phelan, S. (2005). Long-term weight loss maintenance. *Am. J. Clin. Nutr* 82, 222–225. doi: 2005;82(suppl):222S-5S

World Health Organization (2018). Available online at: http://www.who.int/en/news-room/fact-sheets/detail/obesity-and-overweight Geneva. World Health Organization.

Ziauddeen, H., Farooqi, I. S., and Fletcher, P. C. (2012). Obesity and the brain: how convincing is the addiction model? *Nat. Rev. Neurosci.* 13, 279–286. doi: 10.1038/nrn3212

Conflict of Interest: The authors declare that the research was conducted in the absence of any commercial or financial relationships that could be construed as a potential conflict of interest.

frontiers in Behavioral Neuroscience

ORIGINAL RESEARCH
published: 03 June 2020
doi: 10.3389/fnbeh.2020.00091

Fight, Flight, – Or Grab a Bite! Trait Emotional and Restrained Eating Style Predicts Food Cue Responding Under Negative Emotions

Rebekka Schnepper[1], Claudio Georgii[1], Katharina Eichin[1], Ann-Kathrin Arend[1], Frank H. Wilhelm[2], Claus Vögele[3], Annika P. C. Lutz[3], Zoé van Dyck[3] and Jens Blechert[1]*

[1] Department of Psychology, Division of Health Psychology, Paris-Lodron-University of Salzburg, Salzburg, Austria, [2] Department of Psychology, Division of Clinical Psychology and Psychopathology, Paris-Lodron-University of Salzburg, Salzburg, Austria, [3] Department of Behavioural and Cognitive Sciences, Institute for Health and Behaviour, University of Luxembourg, Esch-sur-Alzette, Luxembourg

OPEN ACCESS

Edited by:
Kiyoshi Nakahara,
Kochi University of Technology, Japan

Reviewed by:
Maurizio Casarrubea,
University of Palermo, Italy
Agata Faron-Górecka,
Polish Academy of Sciences, Poland

****Correspondence:***
Rebekka Schnepper
rebekka.schnepper@sbg.ac.at

Specialty section:
This article was submitted to Motivation and Reward, a section of the journal Frontiers in Behavioral Neuroscience

Received: *08 April 2020*
Accepted: *14 May 2020*
Published: *03 June 2020*

Citation:
Schnepper R, Georgii C, Eichin K, Arend A-K, Wilhelm FH, Vögele C, Lutz APC, van Dyck Z and Blechert J (2020) Fight, Flight, – Or Grab a Bite! Trait Emotional and Restrained Eating Style Predicts Food Cue Responding Under Negative Emotions. Front. Behav. Neurosci. 14:91. doi: 10.3389/fnbeh.2020.00091

In today's society, obesity rates are rising as food intake is no longer only a response to physiological hunger signals that ensure survival. Eating can represent a reward, a response to boredom, or stress reduction and emotion regulation. While most people decrease food intake in response to stress or negative emotions, some do the opposite. Yet, it is unclear who shows emotional overeating under which circumstances. Emotion regulation theories describe emotional overeating as a learned strategy to down-regulate negative emotions. Cognitive theories, by contrast, attribute emotional overeating to perceived diet breaches in individuals who chronically attempt to diet. After consuming "forbidden foods", they eat more than individuals who do not restrict their food intake. This laboratory study investigated emotional overeating by exposing individuals to a personalized emotion induction while showing images of palatable foods. Outcome variables indexed cue reactivity to food images through picture ratings (valence, desire to eat), facial expressions (electromyography of the corrugator supercilii muscle), and brain reactivity by detecting event-related potentials (ERPs) by means of electroencephalography (EEG). The influence of emotion condition (negative, neutral) and individual differences (self-reported trait emotional and restrained eating) on outcome variables was assessed. Valence ratings and appetitive reactions of the corrugator muscle to food pictures showed a relative increase in the negative condition for individuals with higher emotional eating scores, with the opposite pattern in lower scores. Desire to eat ratings showed a similar pattern in individuals who showed a strong response to the emotion induction manipulation, indicative of a dose-response relationship. Although no differences between conditions were found for ratings or corrugator activity with restrained eating as a predictor, an ERP at P300 showed increased activation when viewing food compared to objects in the negative condition. Findings support emotion regulation theories: Emotional eaters showed an appetitive reaction in rating patterns and corrugator activity. EEG findings (increased P300)

suggest a motivated attention toward food in restrained eaters, which supports cognitive theories. However, this did not translate to other variables, which might demonstrate successful restraint. Future studies may follow up on these findings by investigating eating disorders with emotion regulation difficulties.

Keywords: emotional eating, restrained eating, mood induction, food cue reactivity, multilevel modeling, P300, corrugator supercilii

INTRODUCTION

While food search and metabolic energy balance represented a key challenge for the longest part of human evolution, today's modern, affluent societies secure the continued supply with energy dense, palatable and affordable foods. Eating has since assumed multiple roles and functions beyond energy homeostasis: it serves enjoyment, relief from boredom and sometimes, stress reduction and emotion regulation. Although such non-homeostatic roles of eating are natural, emotional eating is involved in difficulties with losing weight, linking it with the alarming rates of overweight and obesity worldwide (World Health Organization [WHO], 2018). Emotional eating has also been identified as a risk factor for developing binge eating and associated eating disorders as early as in middle school (Pearson et al., 2012). In the past three decades, these significant health concerns, along with interest in the basic science of emotions and eating behaviors motivated intense research into the connections between emotions and eating (Vögele et al., 2018). Different theories have attempted to explain emotional eating, including physiological theories on stress reactions, as well as psychological theories that consider individual traits.

From a physiological, evolutionary point of view, intense stress and negative emotions are expected to trigger a fight-or-flight response involving the sympathetic nervous system, resulting in increased alertness and energy provision from bodily stores and decreased appetite and food intake (Torres and Nowson, 2007). Yet, food cravings with subsequent overeating in response to stress can also be observed (Yau and Potenza, 2013) leading to the question what other processes override this basic, defensive mechanism. While physical stressors have become infrequent in the last centuries, emotional, chronic stressors are more present in daily life and have been linked to activation of the hypothalamic–pituitary–adrenal (HPA) axis. According to physiological theories, excessive "comfort food" consumption in response to emotional stress of this sort could be related to glucocorticoids (Bazhan and Zelena, 2013). Consequences of HPA axis dysregulation, e.g., excessive glucose release from the liver, have been shown to contribute to the development of unhealthy eating habits and obesity because of chronic environmental stress (Bose et al., 2009), albeit mechanisms are still unclear. Physiological theories predict that stronger responses to a stressor should alternate appetitive responding more (Vallès et al., 2000), possibly due to different stress axis activation and metabolic reaction.

Accompanying physiological adaptations to negative emotions and stress, several psychological theories and mechanisms of emotional overeating have been proposed. As early as 1955, Hilde Bruch ascribed emotional overeating to early breast-feeding experiences, conflating sensations of hunger relief with emotional caring. Booth (1994) proposed a learning model that predicts positive emotional effects of eating to counter negative emotions, thereby negatively reinforcing emotional overeating. Thus, trait emotional eating might serve as an emotion regulation strategy. Yet, there are rivaling theories, most prominently cognitive theories based on disinhibition of restraint. Research in the domain of trait restrained eating has shown that some individuals who chronically diet form relatively rigid diet rules. When violating such a diet rule, for example by having to consume high-calorie, "forbidden" foods in an experiment prior to a taste test, most restrained eaters disregard their diet rules on the taste test and thus disinhibit their suppressed eating desires (Herman and Mack, 1975). Crucially, emotions can disinhibit rigid restraint rules in restrained eaters in a similar fashion: Multiple studies have shown that restrained eaters do not only eat more in response to a "diet violation," but also when experiencing negative emotions, possibly because these emotions use up the cognitive resources needed for adhering to diet rules (Cardi et al., 2015). Taken together, on the one hand, learning theories suggest that emotional overeating primarily yields an emotional regulatory function – and individuals overeat to regulate negative emotions; on the other hand, cognitive theories suggest that emotional overeating does not necessarily have an emotional regulatory function but results from disinhibition in restrained eaters.

Departing from this theoretical debate, evidence for emotional overeating is surprisingly inconsistent and current debates revolve around several points that require clarification. First, recent reviews have yielded inconsistent results as of which theory best explains emotional overeating. Whereas Cardi et al. (2015) found evidence for emotional overeating in negative mood across studies and even more pronounced in restrained eaters and individuals with binge eating symptomatology, a more comprehensive and recent meta-analysis questioned that. Evers et al. (2018) showed emotional overeating only in trait restrained and not in trait emotional eating. Nevertheless, the authors note large variability in methodology and analytic strategies across studies and stress the importance of the method of emotion induction. Since trait emotional and restrained eating are operationalized with questionnaires, a cut-off debate of only including extreme scorers evolved (Van Strien et al., 2012) however, this contradicts dimensional models of psychopathology and personality (Cuthbert and Insel, 2013). Therefore, the current study applied a state of the art multilevel modeling (MLM) approach based on continuous trait emotional and restrained eating scores.

The present study investigates to what extent traits (emotional or restrained eating) and emotional states (negative compared to neutral emotions as well as individual strength of emotion reactivity) predict changes in appetitive responding to food images on experiential, autonomic, facial and neural outcome measures. Participants completed a previously validated experimental rating task (Blechert et al., 2014) consisting of food ratings in a neutral compared to a negative condition, which allowed for a high level of control over error variances. Preceding this task, negative emotions were induced with a validated procedure based on idiosyncratic autobiographic recall (Hilbert et al., 2011), this also ensured that emotional changes would cause changes in appetitive responding (and not the reverse, Adriaanse et al., 2011b). High density EEG was recorded, covering all relevant neural regions to reveal underlying mechanisms. As an indicator for a physiological appetitive reaction, corrugator supercilii activity was measured, a muscle that reacts with relaxation to positive stimuli and with contraction to negative stimuli (Larsen et al., 2003). As an indicator for general physiological arousal, heart rate (HR) and heart rate variability (HRV) data during the two conditions (neutral, negative) was collected. By including a sufficiently large sample with enough orthogonal variation on trait emotional and restrained eating, the present study was set up to model the relative predictive power of each of these traits on emotional overeating.

Measuring experiential, autonomic, facial and neural responses to induced negative emotions simultaneously allowed to get an overall picture for processes that lead to a motivational readiness to engage in emotional overeating. Under this approach, we addressed the following research questions. Based on (animal) literature suggesting appetite suppression due to activation of the sympathetic nervous system when experiencing stress (Vallès et al., 2000), we expected lower pleasantness and desire to eat rating scores for food pictures under negative emotion in individuals without a tendency for emotional overeating (that is, either low scores on emotional or restrained eating). This stress reaction should also be evident in increased facial frowning detected by the corrugator muscle. Individuals prone to emotional overeating should show opposite rating and corrugator reactivity patterns. Emotion regulation theories predict an emotional overeating effect in individuals with high emotional eating scores. Further, this might show in cortical activity in parietal-occipital, attentional areas, as indexed by the P300, particularly in emotional eaters as in Blechert et al. (2014). In contrast, disinhibition of restraint theories predict this effect only individuals with higher trait restrained eating. In addition, this elevated reactivity could be accompanied by decreased frontal brain activity due to the disinhibiting effects of negative emotions on regions that exert cognitive control over cravings (Kober et al., 2010; Blechert et al., 2014; Wood et al., 2016). Last, based on physiological theories, we investigated to what extent the relationship between appetitive responding and eating traits (emotional vs restrained) is modulated by individual differences in the strength of emotional reactivity (more suppression vs more emotional overeating). See **Figure 1** for a visualization of these research questions.

MATERIALS AND METHODS

Participants

Eighty female, right-handed participants aged between 16 and 50 years (M = 21.9, SD = 3.77) with normal average BMI (M = 22.3, SD = 3.09) were recruited in introductory psychology classes at the University of Salzburg, Austria, via newspapers and web portals. An all-female sample was chosen because women have a higher risk of eating disorders

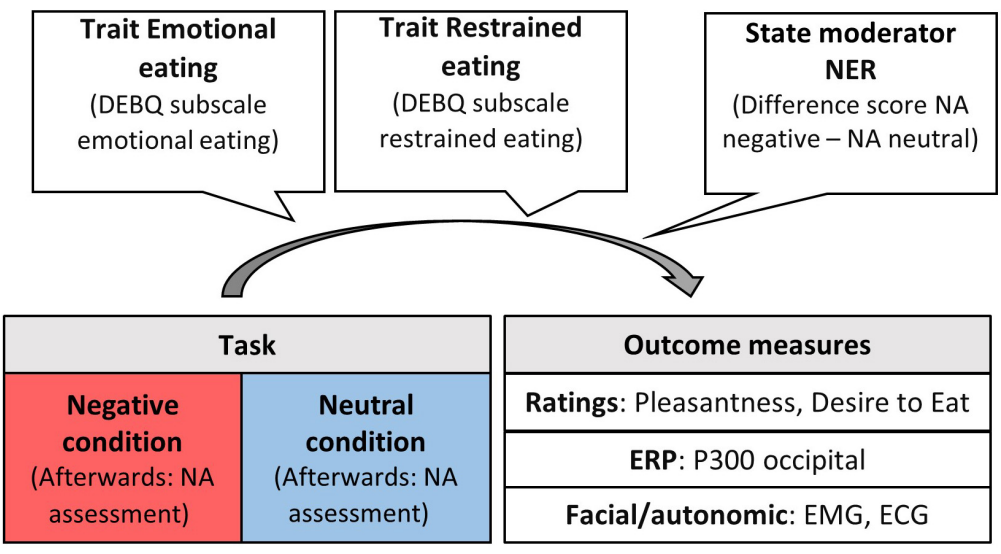

FIGURE 1 | Moderators, task conditions, and outcome measures for appetitive responding. NER, negative emotional reactivity; NA, negative affect; DEBQ, dutch eating behavior questionnaire; ERP, event-related potential; EMG, electromyography; ECG, electrocardiogram.

(Galmiche et al., 2019) and report eating more often as a coping mechanism when experiencing negative emotions or stress (Greeno and Wing, 1994). Further, the association between craving and eating pathology is stronger in women (Chao et al., 2016) and succumbing to cravings is more frequently related to negative feelings in women (Lafay et al., 2001). Sample size was based on Blechert et al. (2014), N = 45, and the additional consideration to include enough high and low restrained eaters. Emotional (M = 2.51, SD = 0.76) and restrained eating (M = 2.48, SD = 0.81) were known to correlate only weakly in the current sample (r = 0.120, p = 0.290, see scatterplot in **Supplementary Information A**), allowing independent, orthogonal modeling. Self-reported exclusion criteria were vegetarianism, food allergies, diabetes, and other disorders that affect digestion and eating behavior; a history of eating disorders; current substance abuse; and neurological disorders. One participant was excluded due to current substance abuse (final sample: n = 79). Due to poor data quality, six participants were excluded from EMG analyses (final sample: n = 73) and 10 from EEG analyses (final sample: n = 69). For participating in the lab part of the study, participants received either study credits or 30€ as compensation.

Procedure

Inclusion and Exclusion

Participants that met inclusion criteria first underwent a modified structural clinical interview for DSM-IV (SCID I; Wittchen et al., 1997) to assess current and lifetime mental disorders and current eating pathology according to criteria of the Diagnostic and Statistical Manual of Mental Disorders 5 (DSM-5; American Psychiatric Association, 2013). They further installed a smartphone app on their phone for a seven-day ecological momentary assessment (EMA) prior to the laboratory experiment (data reported elsewhere), and received a link to complete trait questionnaires and demographic information online during the EMA phase.

General Procedure and Idiosyncratic Emotional Script Generation

The laboratory session was scheduled after completing the EMA phase, always at 3 pm to avoid circadian variation. To limit variation in hunger, participants were instructed to consume one of five preset lunch options at noon, each containing ∼550 kcal. At the beginning of the testing session, compliance with these instructions was assessed verbally and hunger, appetite, and fullness were in the medium range for all participants on a scale from 1 = "not at all" to 9 = "very much" (M = 4.71, SD = 1.35). Laboratory testing started with informed consent (for n = 3 underage participants, parents' consent was obtained) and initial questionnaires, including negative affect at baseline. Further, recent situations were discussed, which had left the participant experiencing negative emotions like sadness or frustration (excluding traumatic events). Participants estimated how well they remembered the situations, how negative the situations were, and how much distress they felt when recalling the situation. The situation with the highest scores on all variables was chosen and further explored regarding what had happened, when, where, with whom, and which thoughts, emotions, physical sensations, behaviors, and consequences occurred. With this information, the experimenter then generated a script of eight sentences. These were then presented to the participant during the emotional eating task to induce negative emotions. Further, a script for the neutral condition in the emotional eating task was generated. Piloting showed that it was rather difficult for participants to recall a truly neutral situation, thus they chose one out of two pre-scripted situations (either brushing their teeth or going to work/school). These neutral scripts were of equal length as the negative scripts and participants were given the opportunity to adjust the sentences so that they best matched their memory of the situation. After this preparatory work for the emotional eating task, physiological sensors were attached (i.e., EEG, respiration, EMG, ECG), a rating of current hunger was taken, and an interoception task (∼10 min) (results reported elsewhere) completed.

Emotional Eating Task

The ∼40–50 min task comprised a neutral and negative condition, which were presented in alternating order across participants (**Figure 2**) enclosed by PANAS ratings as manipulation check. The eight scripted idiosyncratic sentences were first read out aloud by the experimenter prior to each condition. During each condition block, then, sentences were presented in written form on screen, interleaved with the presentation of food and object pictures (and picture rating prompts). Each of the eight negative and neutral sentences was repeated once within each condition block. Also, each of the 26 food and 26 object pictures were presented twice per condition, resulting in 104 image presentations per condition and a total of 208 image presentations for the study. In addition, each image was rated once per block for pleasantness (all images; 104 ratings) and current desire to eat (food images only; 52 ratings) on a visual analog scale ranging from 0 ("very unpleasant"/"no desire to eat") to 100 ("very pleasant"/"strong desire to eat"). Ratings were displayed either after the first or second picture presentation. A food choice task (Georgii et al., 2019) followed the emotional eating task. The University's ethics committee approved the study design; relevant guidelines and regulations were met during all experiments.

Measures

Dutch Eating Behavior Questionnaire (DEBQ German (FEV-I); 33 Items; Grunert, 1989)

The DEBQ is a 33-item measure consisting of three subscales. In this study, means of the subscales for trait emotional eating (13 items; e.g., "Do you have the desire to eat when you are irritated?"), and trait restrained eating (10 items; e.g., "Do you try to eat less than you would like to eat at mealtimes?") were included.

Positive and Negative Affective Schedule (PANAS State German; Krohne et al., 1996)

At the beginning of the experiment, after the negative condition, and after the neutral condition participants filled out the PANAS as an emotion induction check. It consists of 20 adjectives,

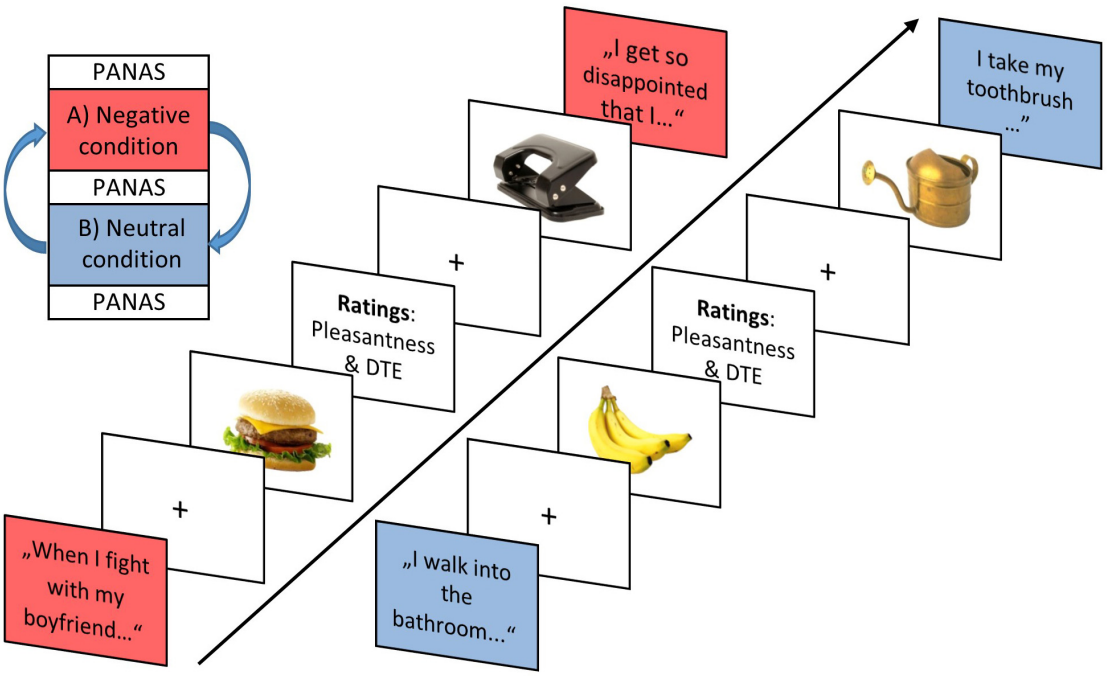

FIGURE 2 | Trial sequence exemplifying two idiosyncratic scripts of the negative and neutral condition with interleaved food/object image presentations alongside respective ratings in the negative condition (red box) and the neutral condition (blue box). The 52 different pictures were divided up evenly among the eight different sentences, resulting in six to seven picture presentations after a sentence presentation. DTE, desire to eat.

half of them inquiring positive and the other half inquiring negative affective states. Participants answer how much they experience a certain affective state described by an adjective on a 5 point Likert scale ranging from 1 = "just a little/not at all" to 5 = "very much". Analyses in this study focus on the negative affect (NA) subscale as a construct of interest in the context of emotional eating. PANAS scores assessed after the neutral emotion condition were subtracted from the scores taken after the negative emotion condition to create the "emotional reactivity score".

Electroencephalography (EEG)

Autonomic, facial, and neural measures were recorded with a 64-channel-amplifier (TMSi, Twente Medical Systems International, EJ Oldenzaal, Netherlands) at a sampling rate of 512 Hz. Online average reference EEG was recorded from 63 actively shielded, equidistant, and passive electrodes (sintered Ag/AgCl electrodes) and a ground electrode attached to the left wrist. Impedances were kept below 10 kΩ. Preprocessing in EEG lab (Delorme and Makeig, 2004) involved down-sampling (256 Hz), low-pass filtering (70 Hz), high-pass filtering (0.1 Hz), and notch filtering (45–55 Hz). Noisy channels were identified through visual inspection and removed, data was re-referenced to average and eye blinks and –movements were removed in an independent component analysis (ICA) using AMICA (Palmer, 2016). Then, 1500ms pre-stimulus to 2400 ms post-stimulus epochs were extracted unless large artifacts were evident upon visual inspection. Lastly, previously removed channels were interpolated.

Regions of interest were selected based on visual inspection of topography plots and difference waves (**Figure 5**). Other than in the previous report (Blechert et al., 2014), a P300 was evident between 200–400 ms at a parieto-occipital electrode cluster (5LB, 5LC, 7L, 8L, 9L, 7Z, 8Z, 9Z, 7R, 8R, 9R, 5RB, 5RC). Mean amplitudes were calculated and the ERP was indexed relative to a 300ms pre-stimulus baseline.

Corrugator Electromyography (EMG)

To record facial EMG activity, two 2 mm inner diameter Ag/AgCl electrodes were placed on the corrugator supercilii muscle region above the left eye, following established guidelines (Fridlund and Cacioppo, 1986). After 28 Hz high-pass filtering (removal of movement artifacts) and 50 Hz notch filtering, rectification and smoothing (50 ms moving average) was applied. After preprocessing, noisy signal segments were manually rejected through visual inspection. For visual inspection on picture level analyses, mean amplitudes of five 500 ms time segments, spanning 2500 ms picture presentation time were extracted before subtracting mean activation during a 500 ms pre-stimulus baseline.

Electrocardiogram (ECG)

Generalized emotional or arousal related effects of the conditions might also be evidenced in cardiac activity. Thus, ECG was recorded using disposable solid-gel snap electrodes placed on the upper sternum and distal end of the left costal arch. Data

were inspected offline and artifacts were corrected manually with ANSLAB 2.6 (Blechert et al., 2016). The number of heartbeats in each condition was automatically determined by detecting the number of R-spikes. Overall HR and HRV scores (natural logarithm of fast-Fourier transformation derived HRV for very low, low, and high frequency band power) for each condition were calculated. No picture level ECG responses were calculated due to the fast picture presentation mode and the resulting inability of the ECG to return to baseline. Furthermore, emotional reactivity can also be indexed on HR and HRV, similar to negative PANAS, by subtracting means of the neutral condition from means of the negative condition.

Multilevel Modeling

Statistical models that regressed food image reactivity on condition (negative, neutral) and eating traits (emotional eating, restrained eating) as well as individual differences in emotional reactivity (defined by a difference score of induced negative emotions) were built (see **Figure 1**). Person-level predictors (eating traits, emotional reactivity) were grand mean centered. To control for general mood effects on rating tendencies, mean pleasantness ratings of objects pictures were subtracted from mean pleasantness ratings of food pictures separately for each condition. These two difference scores were then submitted to an MLM with condition as a random intercept, testing for food specific effects. The same approach was used for autonomic, facial and neural measures.

Desire to eat ratings were treated differently: Since they were available for food images only, no difference score with object ratings could be calculated. This allowed to model ratings on single trial level without calculating a mean score for each condition. To test whether this more complex model would be a better fit to analyze data, intra-class correlation coefficients (ICCs) were calculated in a first step. Significant ICCs indicate that desire to eat as a dependent variable is nested within the crossed random predictors Condition, Participant and Picture Number (Bliese, 2000). This was the case for all predictors, all ps < 0.001, therefore a cross-classified, nested structure could be assumed. Thus, an MLM with desire to eat modeled on the single trial level (not averaged across trials) and both nested within Condition (Level-2) and within Participant (Level-2; crossed structure) was chosen as the best fitting model.

MLMs were analyzed in RStudio (Allaire, 2012) using lme4 (Bates et al., 2015) for linear mixed-effects models with crossed random effects structure (Bliese, 2013). Results were plotted using ggplot2 (Wickham, 2016). A hypothesis-driven, two-step, backward modeling approach was chosen. In a first step, all theoretically important predictors were included in the MLM (eating trait, emotional reactivity, Condition, and all their two- and three-way interactions) alongside covariates of no interest (condition order, i.e., whether the neutral or the negative condition came first, negative emotions at baseline, individual food picture, and trial position within a condition for effects of habituation). In a second step, models were reduced by stepwise exclusion of predictors that were not significant for each outcome variable. Akaike Information Criterion (AIC) served as an indicator of model fit, with lower AICs of the final model indicating a better fit. A random slope for participants was added, allowing the strength of relation between predictors and dependent variable to vary between participants.

RESULTS

Idiosyncratic Script Content Analysis

Idiosyncratic scripts were classified independently by two raters involved in the study. Most of the negative situations contained conflicts with other family members (25%), followed by friends (22%) and partners (16%). Fifteen percent were other interpersonal situations, 20% were various non-social situations. 42% of the situations mainly invoked anger, 34% induced sadness and 24% anxiety. As a neutral situation, 65% of participants chose brushing their teeth, the rest chose going to work/school by various means of transport. Participants indicated that they could visualize the scenarios well ($M = 7.49$, SD = 1.12, on scale from 1 = "not at all" to 9 = "very much").

Manipulation Check

Changes in NA scores (PANAS) confirmed effective emotion induction: the Condition (after negative-baseline, after neutral-baseline) × Order (negative first, neutral first) ANOVA with repeated measures on Condition revealed a main effect for Time, $F(2,77) = 44.6$, $p < 0.001$, $\eta p^2 = 0.367$ and no interaction effect with Order, $F(2,77) = 0.417$, $p = 0.598$, $\eta p^2 = 0.005$. Successful emotion induction was evident in more negative PANAS ratings after the negative, compared to the neutral condition, mean difference MD = −4.71, $p < 0.001$, 95% CI [−6.36, −3.06]. Relative to baseline, measured well before emotion induction, the neutral condition elicited less NA, MD = 1.75, $p = 0.034$, 95% CI [0.098, 3.40], and the negative condition elicited more NA, MD = –2.96, $p < 0.001$, 95% CI [−4.61, −1.31]. Trait emotional eating was not associated with altered negative affect at baseline, $r = 0.174$, $p = 0.124$; however, individuals with higher restrained eating reported slightly more negative affect at baseline, $r = 0.228$, $p = 0.044$; therefore, baseline negative affect was added as covariate of no interest in all analyses (fixed main effect, no interactions). No effects on the dependent variables were obtained when using a "physiological emotional reactivity score" (difference score of mean EMG or ECG activity for each condition) in all analyses. **Figure 3** shows PANAS scores for the three measurement points and illustrates the large individual variability in negative affect after the negative condition, which highlights the importance of including the (subjective) emotional reactivity variable in all analyses.

Food Picture Pleasantness Ratings

Modeling the effect of Condition, eating trait, and emotional reactivity on pleasantness ratings (for foods relative to objects) revealed a trend main effect of trait emotional eating that was moderated by Condition (**Table 2**). As can be seen in **Figure 4**, high emotional eaters rated food pleasantness higher than low emotional eaters specifically in the negative condition. The same model with trait restrained instead of emotional eating did not reveal main effects of restrained eating, an interaction

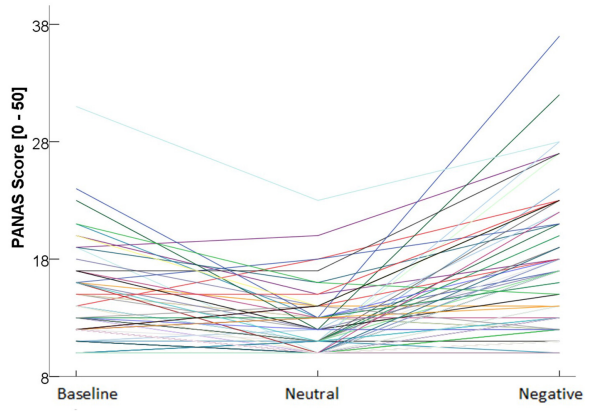

FIGURE 3 | Individual negative affect scores at different time points.

with emotional reactivity, but no interaction with Condition (**Supplementary Information B**).

Food Picture Desire to Eat Ratings

A Condition main effect on desire to eat (only obtained for food images) suggesting appetite suppression should be interpreted in the context of three two-way and the three-way interaction (**Table 1**). Inspection of **Figure 4** suggests a similar Condition × Emotional Eating two-way interaction as for pleasantness, with the clearest picture, however, emerging in individuals high in emotional reactivity (3-way interaction): among high-reacting individuals, low emotional eaters showed extreme appetite suppression under negative emotions, while this emotional suppression was attenuated in high emotional eaters. In other words, among strong responders, trait restrained eating went along with a relative increase in appetitive picture responding, our proxy measure for emotional overeating. By contrast, when investigating trait restrained instead of emotional eating in this model, we found no main effects or interactions (**Supplementary Information C**).

Electroencephalography (EEG)

The analysis of the parieto-occipital P300 activity (foods minus objects) showed no significant main effects or interactions as a function of trait emotional eating. The model with trait restrained eating as a predictor, however, revealed main effects for restrained eating and emotional reactivity, each interacting with Condition, but no three-way interaction. Inspection of the means in **Figure 5** suggest that high-reacting and low restrained individuals showed increased P300 amplitudes to food images (relative to object images) under negative (relative to neutral) emotion whereas their respective counterparts showed decreased food-specific P300 amplitudes under negative emotion. See **Supplementary Information D** for detailed predictor values.

A right frontal effect in the LPP time range (as in Blechert et al., 2014) was not visible upon inspection of difference waves. To test for potential higher order interactions, we extracted a broad bilateral frontal ERP cluster in the LPP time range (1LB, 1RB, 2LB, 2RB, 2L, 2R, 1Z, 2Z) and a right-frontal cluster (1R, 1RB, 2RB, 2RC, 1RD, as in previous report) between 300–600 ms. See **Supplementary Information E** for findings on frontal effects.

Corrugator Electromyography (EMG)

The EMG time course suggests a generalized increase in corrugator response within the first 500ms and a differentiated pattern thereafter, with food pictures inducing a decrease relative

FIGURE 4 | Picture responses with simple slopes illustrating different patterns in the two conditions between high and low emotional eaters for **(A)**, pleasantness ratings (difference score Food – Objects), **(B)**, desire to eat ratings (food only), and **(C)**, activity of corrugator supercilii (difference score Food – Objects). NER,negative emotional reactivity.

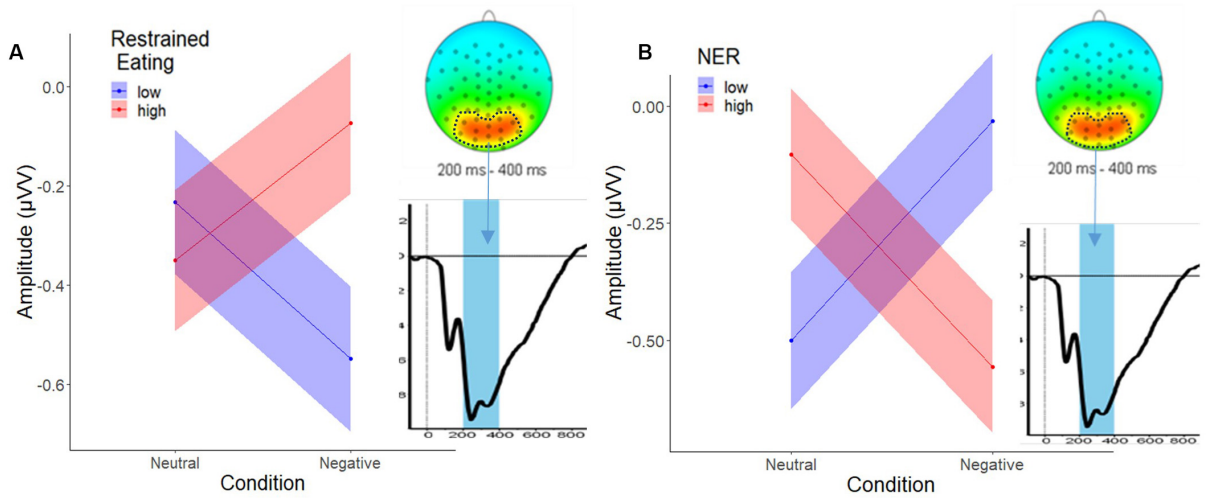

FIGURE 5 | Two-way interaction of **(A)**, restrained eating (±1SD) and condition, and **(B)**, NER (±1SD) and condition at P300. The circled area in the head plot shows the extracted cluster, the blue bar in the waveform graph illustrates the P300 peak observed in the 200–400 ms time window.

to objects, and condition effects mainly for foods. To capture this latter phase, averages over the segments covering activity between 500 and 2500 ms were calculated (**Figure 6**). Furthermore, to capture food specific effects only (and similar to pleasantness and ERP response scoring), object responses were subtracted from food responses prior to statistical analysis. An MLM predicting food-specific corrugator activity yielded main effects of Condition, Emotional Eating and their interaction (**Figure 4** and **Table 2**). Inspection of the slopes in **Figure 4** revealed a similar pattern as for pleasantness ratings: in low emotional eaters, corrugator activity increased from the neutral to the negative condition, indexing the negative affective state (or – by analogy – appetite suppression). This pattern reversed in high emotional eaters: corrugator attenuation – potentially indicative of positive and appetitive states – was seen in the negative relative to the neutral condition (**Figure 4** and **Table 2**). Again, there were no main effects or interactions of restrained instead of emotional

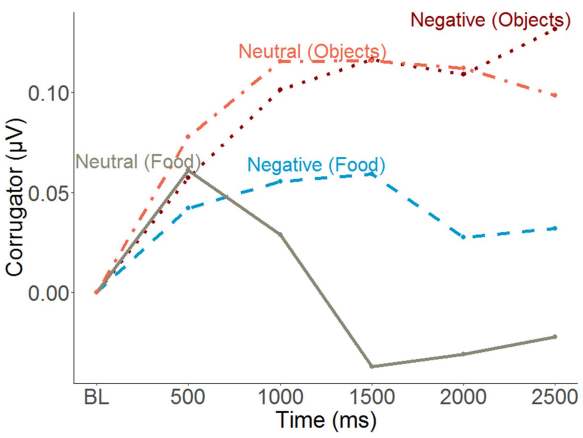

FIGURE 6 | Time course of the corrugator supercilii muscle responses to images as a function of conditions and picture type (mean amplitude of 500 ms segments). BL, Baseline.

TABLE 1 | Full and reduced Multilevel-Models for regression coefficients (*b*) of desire to eat rating for food only, modeled on trial level with trait emotional eating as a predictor (number of observations: *N* = 4108).

	Full model DTE	**Reduced model DTE**
Fixed effects	***b* (SE)**	***b* (SE)**
(Intercept)	51.77 (3.31)***	53.5 (2.57)***
Predictors		
Condition	7.04 (1.66)***	6.79 (1.65)***
Trial	0.03 (0.02)	
Condition order	0.12 (3.46)	
NA baseline	−0.21 (0.44)	
NER	−0.80 (0.36)*	−0.83 (0.36)*
tEE	7.00 (2.43)**	6.62 (2.33)**
Interactions		
Condition × NER	1.11 (0.34)**	1.11 (0.34)**
Condition × tEE	−6.00 (2.23)**	−5.52 (2.19)*
NER × tEE	1.26 (0.54)*	1.22 (0.53)*
Condition × NER × tEE	−1.78 (0.50)***	−1.73 (0.50)***
Random effects	**Variance (*SD*)**	**Variance (*SD*)**
Participant (Intercept)	198 (14.1)	196 (14.0)
Participant | Condition	135 (11.6)	133 (11.5)
Picture number (Intercept)	91.9 (9.58)	91.9 (9.59)
Residual	927 (30.4)	927 (30.4)
AIC	40094	40090
χ^2	0.592	

*DTE, desire to eat; NER, negative emotional reactivity; tEE, trait emotional eating; SE, standard error. Adding a random slope for participant significantly improved DTE predictions ($p < 0.001$). Significance codes: "***" = $p < 0.001$; "**" = $p < 0.01$; "*" = $p < 0.05$.*

TABLE 2 | Full and reduced Multilevel-Models for regression coefficients (*b*) of Pleasantness and Corrugator Electromyography for a food-object difference score with trait emotional eating as a predictor.

	Full model pleasantness	Reduced model pleasantness	Full model corrugator	Reduced model corrugator
Fixed Effects	***b* (SE)**	***b* (SE)**	***b* (SE)**	***b* (SE)**
(Intercept)	21.7 (2.03)***	21.8 (1.43)***	−0.15 (0.05)***	−0.10 (0.03)**
Predictors				
Condition	1.51 (1.26)		0.07 (0.05)	
Condition order	−1.55 (2.99)		0.05 (0.07)	
NA baseline	−0.43 (0.39)		0.01 (0.01)	
NER	−0.48 (0.33)		0.005 (0.008)	
tEE	4.90 (2.20)*	3.57 (2.05)$^{(*)}$	0.11 (0.06)	0.12 (0.05)*
Interactions				
Condition × NER	−4.21 (01.66)		−0.003 (0.01)	
Condition × tEE	0.32 (0.26)*	−3.48 (1.63)*	0.14 (0.07)*	−0.13 (0.06)*
NER × tEE	−0.24 (0.49)		0.008 (0.01)	
Condition × NER × tEE	−0.59 (0.38)		−0.02 (0.01)	
Random Effects	**Variance (*SD*)**	**Variance (*SD*)**	**Variance (*SD*)**	**Variance (*SD*)**
Participant (Intercept)	133 (11.6)	132 (11.5)	0.03 (0.17)	0.03 (0.17)
Residual	59.3 (7.70)	60.0 (7.75)	0.09 (0.30)	0.09 (0.30)
AIC	1242	1236	110	103
χ^2	0.363		0.504	

*NER, negative emotional reactivity; tEE, trait emotional eating; SE, standard error. Significance codes: "***" = p < 001; "**" = p < 0.01; "*" = p < 0.05; "$^{(*)}$" = p < 0.1.*

eating, ps > 0.168. See **Supplementary Information C** for trait restrained eating results.

Electrocardiogram (ECG)

Comparing HR and HRV during the neutral and negative condition revealed no significant main effects and no interaction with eating trait or emotional reactivity, all *ps* > 0.098. Modeling emotional reactivity through HR or HRV variables in the above analyses did not reveal significant interactions with the factors of interest.

DISCUSSION

This study addressed several core questions that have been debated in the emotional eating literature for decades and obscured its theoretical and clinical potential. To answer the question about who shows potentially problematic emotional overeating after experimental negative emotion induction, we contrasted emotional eating/emotion regulation theories with cognitive disinhibition /restrained eating theories by modeling trait restrained and emotional eating as predictors of appetitive food image responses. To answer the question of mechanisms, or the "how" of emotional overeating, a wide range of measures was taken, but particularly prefrontal brain activity allowed for contrasting these two models. Finally, the question of individual differences in emotional reactivity was assessed to uncover a possible dose-response relationship between emotion strength and emotional overeating ("fight or flight"). We based this study on Blechert et al. (2014) and sought to replicate findings and improve some design issues. First, we included neutral objects as an additional control to capture food-specific effects only. Second, we presented the same set of food pictures in both conditions. Third, we standardized starting time and lunch options. Last, we increased the sample size and variance in trait emotional and restrained eating. Results can be summarized as follows.

Evidence for Emotional Overeating in Trait Emotional Eating: Increase in Experiential and Facial Appetitive Responding in Negative Emotional States

As expected under the emotion regulation theory, pleasantness ratings of food pictures (compared to object pictures) were fully moderated by trait emotional eating (and not by restrained eating). Trait emotional eaters rated foods as more pleasant in the negative experimental condition compared to the neutral experimental condition, whereas individuals with lower scores conversely rated food as less pleasant when in a negative emotional state. This pattern replicated our results in the 2014 study, where we found similar opposing patterns in high and low emotional eaters for food craving ratings. Further, it extended to findings of the facial corrugator muscle: More emotional eaters showed a more appetitive reaction – less "frowning" – to food images (relative to object images) in the negative relative to the neutral condition. The relationship of corrugator EMG with bipolar pleasantness is relatively well established (Larsen et al., 2003) lending high validity to this result. The consistency of subjective pleasantness ratings and objective corrugator responses indicates that results are not a mere reflection of social

desirability or participants' self-concepts of their reactivity to food during negative emotions. Adding to that, desire to eat ratings as a measure with a more direct relationship to eating behavior (Boswell and Kober, 2016) generally confirmed the pattern in palatability and EMG measures, i.e., the moderation of emotional overeating by trait emotional eating. Yet, only individuals with a robust emotional response to the idiosyncratic emotion induction showed a relative increase in desire to eat in the negative condition.

Concluding, it seems that the "normative response" to negative emotional states in people reacting strongly to the emotion induction is appetite suppression (strong reductions in desire to eat in the negative condition). Only in highly emotional eaters, this suppressive effect reversed. Thus, on desire to eat, emotional overeating in high trait emotional eating is only relative in nature, i.e., when contrasted against the strong appetite suppression in low emotional eating. Hence, trait emotional eating can be defined as not showing the normative stress response of decreased food intake but rather an equal or increased intake compared to other situations (Van Strien, 2010).

Individual Differences in Emotional Reactivity: Rating and Neural Effects

Interestingly, in addition to interacting with emotional eating on desire to eat ratings, emotional reactivity also showed an independent effect: motivated attention to foods, as indexed by the P300, was increased under negative emotion in low responders, suggesting that their appetitive value counters mild negative affect (independent of emotional and restrained eating). This effect reversed in high responders: Their food-specific P300 decreased during negative emotions, maybe because immersive emotional recollection processes distracted from the foods or brain activity shifted to emotion-related or appetitive areas insufficiently measured in EEG. This resonates with physiological theories of emotional eating: low intensity emotional states seem to trigger compensatory appetitive attentional mechanisms, whereas high intensity emotional states ("fight or flight" mode) reverse this pattern. Thus, emotional reactivity should be seen as independent moderator of emotional overeating in addition to its interactive contribution to trait emotional eating, which has important methodological implications for future studies.

Restrained Eating Modulates Indices of Attention, but Not Experience or Facial Expression

In contrast to the predictions of the disinhibition theory, trait restrained eating did not moderate condition effects on rating and EMG indices. This contradicts cognitive models suggesting that restrained eaters are sensitive to emotional overeating (Evers et al., 2018; Ruderman, 1985). On a neural level, most dual process models of restrained eating assume an engagement of effortful top-down (prefrontal) mechanisms in following a weight control goal (Stroebe et al., 2013). However, in our study only the parieto-occipital P300 amplitude, a putative index of attention to motivationally salient stimuli, varied as a function of trait restrained eating. Individuals high in restraint showed increased activity to foods (relative to objects) in the negative (relative to the neutral) condition, which would indicate that they become susceptible to the foods (Papies et al., 2008; Werthmann et al., 2015). Yet, no "downstream" effects on ratings or facial responses were seen, suggestive of "successful" preparatory appetite regulation. Thus, instead of effortful, prefrontal, top-down control, they might have used more efficient means of regulation e.g., recurrence on habitual food choice rules (Adriaanse et al., 2011a). In addition, other than in emotional eating, restrained eating correlations with P300 did not depend on emotional reactivity and thus might be unrelated to the strength of negative states. Trait restrained eating can thus be conceptualized as an independent mechanism in emotional overeating centered on attentional control.

Limitations, Future Directions, and Conclusion

Our study included only women, mandating further research in men. Although disordered eating is more common among women, prevalence studies show that disordered eating in men most frequently expresses in binge eating without compensatory behavior and that compared to women, men are less likely to seek help (Kessler et al., 2013). Thus, the role of negative emotions on overeating and possible gender differences would add to the understanding of disordered eating in this understudied population. Additionally, food ratings on pleasantness and desire to eat represent a disposition to eat but remain inconsequential to the individual compared to real food intake. We intentionally opted against a taste-test to measure food intake after each condition because taste tests are consistently prone to effects of observation and social desirability considerations (Robinson et al., 2015) that cannot be excluded entirely. Furthermore, actual food intake can be modulated by self-regulatory processes such as meal planning, sensory specific satiety, diurnal food preferences, and effort-reward considerations (monetary value of foods), among others. Thus, we consider ratings (and to some degree EMG/EEG responses) as a propensity to consume respective foods upon availability and situational adequacy. However, the natural occurrence of emotional overeating in strong responders to the laboratory task might be followed up in daily life, e.g., by using EMA measures.

Although affective ratings (PANAS) confirmed a successful induction of negative emotion in the sample as a whole, 21.5% of the participants did not show the expected changes on PANAS ratings, i.e., they did not report more NA after the negative condition than after the neutral condition. Idiosyncratic scripts have been deemed as effective and used in patients (Cuthbert et al., 2003; Hilbert et al., 2011) and are consistent with capturing naturalistic stressors akin to EMA studies (Wilhelm and Grossman, 2010). However, they add variability compared to standardized emotion induction protocols such as affective picture or video exposure (Evers et al., 2010) and performance or social stressors (Van Strien et al., 2012) and might be less severe in sum. Effects of emotional reactivity did not go as far as altering

autonomic arousal systems: other than in Hilbert et al. (2011) no condition effects were detected on cardiac activity, which might be due to the much longer and rather passive emotion induction.

As emotional overeating might be a subclinical form of binge eating, an important future direction would be to apply the present paradigm to individuals with eating disorders like Anorexia Nervosa or Bulimia Nervosa. These disorders are characterized by emotion regulation difficulties (Naumann et al., 2016) and show both patterns of either emotional overeating (binging) or undereating/restricting (Meule et al., 2019). Further, explicit emotion regulation instructions (Svaldi et al., 2014) could be added to the present task to narrow down the role of emotional overeating and identify more adaptive alternatives that effectively abate negative emotions and their "spill over" effects on food cues. Cognitive disinhibition models require further investigation, maybe by inducing "diet breaches" (i.e., prior consumption of forbidden foods) in combination with emotion inductions (Herman and Polivy, 1975; Ruderman, 1986). To further assess subgroup differences within restrained eaters, different types of restraint could be classified in terms of cognitive resources, dieting success, rigidity, and other pathological eating styles (Papies et al., 2008; Meule et al., 2012). Future research might follow up on our P300 effects with more sophisticated EEG analyses (e.g., source level connectivity analyses) to elaborate the role of frontal/regulatory and occipito-parietal/attentional cue reactivity networks in emotional and restrained eating.

In conclusion, we were able to characterize a multi-layered emotional eating signature in trait emotional eaters and restrained eaters. Support for an emotion-regulation framework was found in trait emotional eating and emotional reactivity was identified as a potential boundary condition for the effect to emerge. Although recent work emphasizes the importance of restraint and failure in self-regulation as a cause for emotional overeating (Evers et al., 2018) our findings are more in line with emotional eating theories of food reducing negative affect, a negatively reinforced strategy probably learnt early on in life (Snoek et al., 2007). Restrained eaters attribute more attentional resources to food in negative emotional states but lack corresponding appetitive responses. Our findings might aid future theorizing and research on factors predicting emotional overeating.

DATA AVAILABILITY STATEMENT

The raw data supporting the conclusions of this article will be made available by the authors, without undue reservation.

ETHICS STATEMENT

The studies involving human participants were reviewed and approved by Ethics Committee of the University of Salzburg, Austria. Written informed consent to participate in this study was provided by the participant, or, if underage, by the participants' legal guardian/next of kin.

AUTHOR CONTRIBUTIONS

RS conducted data preparation and statistical analysis and drafted the manuscript. CG helped to writing the study protocol and to collect and structure data. KE helped with the preparation and analysis of the EEG data. A-KA helped with the preparation and analysis of the EMG data. FW contributed to the final draft. CV designed the study, acquired funding, helped writing the study protocol and contributed to the final draft. AL helped writing the study protocol and contributed to the final draft. ZD helped writing the study protocol and contributed to the final draft. JB designed the study, acquired funding, helped writing the study protocol and contributed to the final draft.

FUNDING

This work was supported by the Austrian Science Fund (FWF): (I02130-B27) and the European Research Council (ERC-StG-2014 639445 NewEat).

SUPPLEMENTARY MATERIAL

The Supplementary Material for this article can be found online at: https://www.frontiersin.org/articles/10.3389/fnbeh.2020.00091/full#supplementary-material

REFERENCES

Adriaanse, M. A., de Ridder, D. T. D., and Evers, C. (2011a). Emotional eating: eating when emotional or emotional about eating? *Psychol. Health* 26, 23–39. doi: 10.1080/08870440903207627

Adriaanse, M. A., Vinkers, C. D. W., De Ridder, D. T. D., Hox, J. J., and De Wit, J. B. F. (2011b). Do implementation intentions help to eat a healthy diet? A systematic review and meta-analysis of the empirical evidence. *Appetite* 56, 183–193. doi: 10.1016/j.appet.2010.10.012

Allaire, J. (2012). *RStudio: Integrated Development Environment for R*. Boston, MA: RStudio.

American Psychiatric Association (2013). *Diagnostic and Statistical Manual of Mental Disorders*, 5th Edn, Washington, DC: American Psychiatric Pub.

Bates, D., Maechler, M., Bolker, B., and Walker, B. (2015). Fitting linear mixed-effects models using lme4. *J. Statist. Softw.* 67, 1–48.

Bazhan, N., and Zelena, D. (2013). Food-intake regulation during stress by the hypothalamo-pituitary-adrenal axis. *Brain Res. Bull.* 95, 46–53. doi: 10.1016/j.brainresbull.2013.04.002

Blechert, J., Goltsche, J. E., Herbert, B. M., and Wilhelm, F. H. (2014). Eat your troubles away: electrocortical and experiential correlates of food image processing are related to emotional eating style and emotional state. *Biol. Psychol.* 96, 94–101. doi: 10.1016/j.biopsycho.2013.12.007

Blechert, J., Peyk, P., Liedlgruber, M., and Wilhelm, F. H. (2016). ANSLAB: integrated multi-channel peripheral biosignal processing in psychophysiological science. *Behav. Res. Methods* 48, 1528–1545. doi: 10.3758/s13428-015-0665-1

Bliese, P. D. (2000). "Within-group agreement, non-independence, and reliability: Implications for data aggregation and analysis," in *Multilevel Theory, Research, and Methods in Organizations*, eds K. J. Klein, and S. W. J. Kozlowski (San Francisco, CA: Jossey-Bass), 349–381.

Bliese, P. D. (2013). *Multilevel Modeling in R (2.5)*. Available online at: http://rsync.udc.es/CRAN/doc/contrib/Bliese_Multilevel (accessed September 3, 2013).

Booth, D. (1994). *The Psychology Of Nutrition*. Milton Park: Taylor & Francis.

Bose, M., Oliván, B., and Laferrère, B. (2009). Stress and obesity: the role of the hypothalamic-pituitary-adrenal axis in metabolic disease. *Curr. Opin. Endocrinol. Diabetes Obes.* 16, 340–346. doi: 10.1097/MED.0b013e32832fa137

Boswell, R. G., and Kober, H. (2016). Food cue reactivity and craving predict eating and weight gain: a meta-analytic review. *Obes. Rev.* 17, 159–177. doi: 10.1111/obr.12354

Cardi, V., Leppanen, J., and Treasure, J. (2015). The effects of negative and positive mood induction on eating behaviour: a meta-analysis of laboratory studies in the healthy population and eating and weight disorders. *Neurosci. Biobehav. Rev.* 57, 299–309. doi: 10.1016/j.neubiorev.2015.08.011

Chao, A. M., Grilo, C. M., and Sinha, R. (2016). Food cravings, binge eating, and eating disorder psychopathology: exploring the moderating roles of gender and race. *Eat. Behav.* 21, 41–47. doi: 10.1016/j.eatbeh.2015.12.007

Cuthbert, B. N., and Insel, T. R. (2013). Toward the future of psychiatric diagnosis: the seven pillars of RDoC. *BMC Med.* 11:126. doi: 10.1186/1741-7015-11-126

Cuthbert, B. N., Lang, P. J., Strauss, C., Drobes, D., Patrick, C. J., and Bradley, M. M. (2003). The psychophysiology of anxiety disorder: fear memory imagery. *Psychophysiology* 40, 407–422. doi: 10.1111/1469-8986.00043

Delorme, A., and Makeig, S. (2004). EEGLAB: an open source toolbox for analysis of single-trial EEG dynamics including independent component analysis. *J. Neurosci. Methods* 134, 9–21. doi: 10.1016/j.jneumeth.2003.10.009

Evers, C., Dingemans, A., Junghans, A. F., and Boevé, A. (2018). Feeling bad or feeling good, does emotion affect your consumption of food? A meta-analysis of the experimental evidence. *Neurosci. Biobehav. Rev.* 92, 195–208. doi: 10.1016/j.neubiorev.2018.05.028

Evers, C., Stok, M., and de Ridder, D. T. D. (2010). Feeding your feelings: emotion regulation strategies and emotional eating. *Pers. Soc. Psychol. Bull.* 36, 792–804. doi: 10.1177/0146167210371383

Fridlund, A. J., and Cacioppo, J. T. (1986). Guidelines for human electromyographic research. *Psychophysiology* 23, 567–589. doi: 10.1111/j.1469-8986.1986.tb00676.x

Galmiche, M., Déchelotte, P., Lambert, G., and Tavolacci, M. P. (2019). Prevalence of eating disorders over the 2000–2018 period: a systematic literature review. *Am. J. Clin. Nutr.* 109, 1402–1413. doi: 10.1093/ajcn/nqy342

Georgii, C., Schulte-Mecklenbeck, M., Richard, A., Van Dyck, Z., and Blechert, J. (2019). The dynamics of self-control: within-participant modeling of binary food choices and underlying decision processes as a function of restrained eating. *Psychol. Res.* doi: 10.1007/s00426-019-01185-3 [Epub ahead of print].

Greeno, C. G., and Wing, R. R. (1994). Stress-induced eating. *Psychol. Bull.* 115:444.

Grunert, S. C. (1989). Ein Inventar zur Erfassung von Selbstaussagen zum Ernährungsverhalten. [An inventory for determination of eating behaviors through self-reporting]. *Diagnostica* 35, 167–179.

Herman, C. P., and Mack, D. (1975). Restrained and unrestrained eating. *J. Pers.* 43, 647–660.

Herman, C. P., and Polivy, J. (1975). Anxiety, restraint, and eating behavior. *J. Abnorm. Psychol.* 84, 666–672. doi: 10.1037/0021-843x.84.6.666

Hilbert, A., Vögele, C., Tuschen-Caffier, B., and Hartmann, A. S. (2011). Psychophysiological responses to idiosyncratic stress in bulimia nervosa and binge eating disorder. *Physiol. Behav.* 104, 770–777. doi: 10.1016/j.physbeh.2011.07.013

Kessler, R. C., Berglund, P. A., Chiu, W. T., Deitz, A. C., Hudson, J. I., Shahly, V., et al. (2013). The prevalence and correlates of binge eating disorder in the world health organization world mental health surveys. *Biol. Psychiatry* 73, 904–914. doi: 10.1016/j.biopsych.2012.11.020

Kober, H., Mende-Siedlecki, P., Kross, E. F., Weber, J., Mischel, W., Hart, C. L., et al. (2010). Prefrontal-striatal pathway underlies cognitive regulation of craving. *PNAS* 107, 14811–14816. doi: 10.1073/pnas.1007779107

Krohne, H. W., Egloff, B., Kohlmann, C.-W., and Tausch, A. (1996). untersuchungen mit einer deutschen version der "positive and negative affect schedule" (PANAS). *Diagnostica* 42, 139–156.

Lafay, L., Thomas, F., Mennen, L., Charles, M. A., Eschwege, E., Borys, J. M., et al. (2001). Gender differences in the relation between food cravings and mood in an adult community: results from the fleurbaix laventie ville santé study. *Intern. J. Eat. Disord.* 29, 195–204. doi: 10.1002/1098-108x(200103)29:2<195::aid-eat1009>3.0.co;2-n

Larsen, J. T., Norris, C. J., and Cacioppo, J. T. (2003). Effects of positive and negative affect on electromyographic activity over zygomaticus major and corrugator supercilii. *Psychophysiology* 40, 776–785. doi: 10.1111/1469-8986.00078

Meule, A., Papies, E. K., and Kübler, A. (2012). Differentiating between successful and unsuccessful dieters. Validity and reliability of the perceived self-regulatory success in dieting scale. *Appetite* 58, 822–826. doi: 10.1016/j.appet.2012.01.028

Meule, A., Richard, A., Schnepper, R., Reichenberger, J., Georgii, C., Naab, S., et al. (2019). Emotion regulation and emotional eating in anorexia nervosa and bulimia nervosa. *Eat. Disord.* doi: 10.1080/10640266.2019.1642036 [Epub ahead of print].

Naumann, E., Tuschen-Caffier, B., Voderholzer, U., and Svaldi, J. (2016). Spontaneous emotion regulation in anorexia and bulimia nervosa. *Cogn. Ther. Res.* 40, 304–313. doi: 10.1007/s10608-015-9723-3

Palmer, J. (2016). *AMICA Algorithm*. Available at: http://sccn. ucsd. edu/∼jason/amica_web.html (accessed May 17, 2016).

Papies, E. K., Stroebe, W., and Aarts, H. (2008). Healthy cognition: processes of self-regulatory success in restrained eating. *Pers. Soc. Psychol. Bull.* 34, 1290–1300. doi: 10.1177/0146167208320063

Pearson, C. M., Combs, J. L., Zapolski, T. C. B., and Smith, G. T. (2012). A longitudinal transactional risk model for early eating disorder onset. *J. Abnorm. Psychol.* 121, 707–718. doi: 10.1037/a0027567

Robinson, E., Hardman, C. A., Halford, J. C. G., and Jones, A. (2015). Eating under observation: a systematic review and meta-analysis of the effect that heightened awareness of observation has on laboratory measured energy intake. *Am. J. Clin. Nutr.* 102, 324–337. doi: 10.3945/ajcn.115.111195

Ruderman, A. J. (1985). Dysphoric mood and overeating: a test of restraint theory's disinhibition hypothesis. *J. Abnorm. Psychol.* 94, 78–85. doi: 10.1037/0021-843x.94.1.78

Ruderman, A. J. (1986). Dietary restraint: a theoretical and empirical review. *Psychol. Bull.* 99, 247–262. doi: 10.1037/0033-2909.99.2.247

Snoek, H. M., Engels, R. C. M. E., Janssens, J. M. A. M., and van Strien, T. (2007). Parental behaviour and adolescents' emotional eating. *Appetite* 49, 223–230. doi: 10.1016/j.appet.2007.02.004

Stroebe, W., Van Koningsbruggen, G. M., Papies, E. K., and Aarts, H. (2013). Why most dieters fail but some succeed: a goal conflict model of eating behavior. *Psychol. Rev.* 120, 110–138. doi: 10.1037/a0030849

Svaldi, J., Tuschen-Caffier, B., Trentowska, M., Caffier, D., and Naumann, E. (2014). Differential caloric intake in overweight females with and without binge eating: effects of a laboratory-based emotion-regulation training. *Behav. Res. Ther.* 56, 39–46. doi: 10.1016/j.brat.2014.02.008

Torres, S. J., and Nowson, C. A. (2007). Relationship between stress, eating behavior, and obesity. *Nutrition* 23, 887–894. doi: 10.1016/j.nut.2007.08.008

Vallès, A., Martí, O., García, A., and Armario, A. (2000). Single exposure to stressors causes long-lasting, stress-dependent reduction of food intake in rats. *Am. J. Physiol. Regul. Integ. Compar. Physiol.* 279, R1138–R1144. doi: 10.1152/ajpregu.2000.279.3.R1138

Van Strien, T. (2010). Predicting distress-induced eating with self-reports: mission impossible or a piece of cake?[comment]. *Health Psychol.* 29, 343–343. doi: 10.1037/a0020329

Van Strien, T., Herman, C. P., Anschutz, D. J., Engels, R. C. M. E., and de Weerth, C. (2012). Moderation of distress-induced eating by emotional eating scores. *Appetite* 58, 277–284. doi: 10.1016/j.appet.2011.10.005

Vögele, C., Lutz, A., and Gibson, E. L. (2018). "Mood, emotions and eating disorders," in *Oxford Library Of Psychology. The Oxford Handbook Of Eating Disorders*, eds W. S. Agras, and A. Robinson (Oxford: Oxford University Press), 155–186.

Werthmann, J., Jansen, A., and Roefs, A. (2015). Worry or craving? A selective review of evidence for food-related attention biases in obese individuals, eating-disorder patients, restrained eaters and healthy samples. *Proc. Nutr. Soc.* 74, 99–114. doi: 10.1017/s0029665114001451

World Health Organization [WHO] (2018). *Obesity And Overweight, Fact Sheet N°311*. Geneva: WHO.

Wickham, H. (2016). *Ggplot2: Elegant Graphics For Data Analysis*. Berlin: Springer.

Wilhelm, F. H., and Grossman, P. (2010). Emotions beyond the laboratory: theoretical fundaments, study design, and analytic strategies for advanced ambulatory assessment. *Biol. Psychol.* 84, 552–569. doi: 10.1016/j.biopsycho.2010.01.017

Wittchen, H.-U., Wunderlich, U., Gruschwitz, S., and Zaudig, M. (1997). *SKID I. Strukturiertes Klinisches Interview für DSM-IV. Achse I: Psychische Störungen. Interviewheft und Beurteilungsheft. Eine deutschsprachige, Erweiterte Bearb. d. Amerikanischen Originalversion des SKID I.* Göttingen: Hogrefe.

Wood, S. M., Schembre, S. M., He, Q., Engelmann, J. M., Ames, S. L., and Bechara, A. (2016). Emotional eating and routine restraint scores are associated with activity in brain regions involved in urge and self-control. *Physiol. Behav.* 165, 405–412. doi: 10.1016/j.physbeh.2016.08.024

Yau, Y. H., and Potenza, M. N. (2013). Stress and eating behaviors. *Miner. Endocrinol.* 38:255.

Conflict of Interest: The authors declare that the research was conducted in the absence of any commercial or financial relationships that could be construed as a potential conflict of interest.

frontiers in Behavioral Neuroscience

MINI REVIEW
published: 24 July 2020
doi: 10.3389/fnbeh.2020.00131

Extrinsic Factors Underlying Food Valuation in the Human Brain

Kosuke Motoki[1,2]* *and Shinsuke Suzuki*[3]*

[1]Department of Food Management, School of Food, Agricultural and Environmental Sciences, Miyagi University, Sendai, Japan, [2]Institute of Development, Aging and Cancer, Tohoku University, Sendai, Japan, [3]Brain, Mind and Markets Laboratory, Department of Finance, Faculty of Business and Economics, The University of Melbourne, Parkville, VIC, Australia

Subjective values for food rewards guide our dietary choices. There is growing evidence that value signals are constructed in the brain by integrating multiple types of information about flavor, taste, and nutritional attributes of the foods. However, much less is known about the influence of food-extrinsic factors such as labels, brands, prices, and packaging designs. In this mini-review article, we outline recent findings in decision neuroscience, consumer psychology, and food science about the effect of extrinsic factors on food value computations in the human brain. To date, studies have demonstrated that, while the integrated value signal is encoded in the ventromedial prefrontal cortex, information on the extrinsic factors of the food is encoded in diverse brain regions previously implicated in a wide range of functions: cognitive control, memory, emotion and reward processing. We suggest that a comprehensive understanding of food valuation requires elucidation of the mechanisms behind integrating extrinsic factors in the brain to compute an overall subjective value signal.

Keywords: food, reward, value, preference, decision-making, consumer psychology, fMRI

OPEN ACCESS

Edited by:
Junichi Chikazoe, National Institute for Physiological Sciences (NIPS), Japan

Reviewed by:
Fabian Grabenhorst, University of Cambridge, United Kingdom
James Howard, Northwestern University, United States

***Correspondence:**
Kosuke Motoki
motokik@myu.ac.jp
Shinsuke Suzuki
shinsuke.szk@gmail.com

Specialty section:
This article was submitted to Motivation and Reward, a section of the journal Frontiers in Behavioral Neuroscience

Received: *09 May 2020*
Accepted: *02 July 2020*
Published: *24 July 2020*

Citation:
Motoki K and Suzuki S (2020) Extrinsic Factors Underlying Food Valuation in the Human Brain. Front. Behav. Neurosci. 14:131. doi: 10.3389/fnbeh.2020.00131

INTRODUCTION

The valuation of food is central in our daily decision-making about what to eat. Dysfunctional food valuation is often associated with the development of obesity and eating-disorders (Yokum et al., 2011; Carnell et al., 2012; Foerde et al., 2015). Human neuroimaging studies have begun to uncover the neural basis of food valuation (Rangel, 2013; Giuliani et al., 2018) by combining functional magnetic resonance neuroimaging (fMRI) with careful assessment of subjective values for food items. In a typical experimental design, participants inside the MRI scanner are shown images of food and are asked to report their subjective values for each of those food items (see **Figure 1A** for details). Accumulating evidence suggests that the ventromedial prefrontal cortex (vmPFC) encodes subjective value signals for various types of potential outcomes including food rewards (**Figure 1B**; Chib et al., 2009; Lebreton et al., 2009; Bartra et al., 2013; Chikazoe et al., 2014; Clithero and Rangel, 2014; Gross et al., 2014).

How is it the value signal for a food reward is constructed in the human brain? Previous studies suggest that individuals compute the value of a food item by integrating

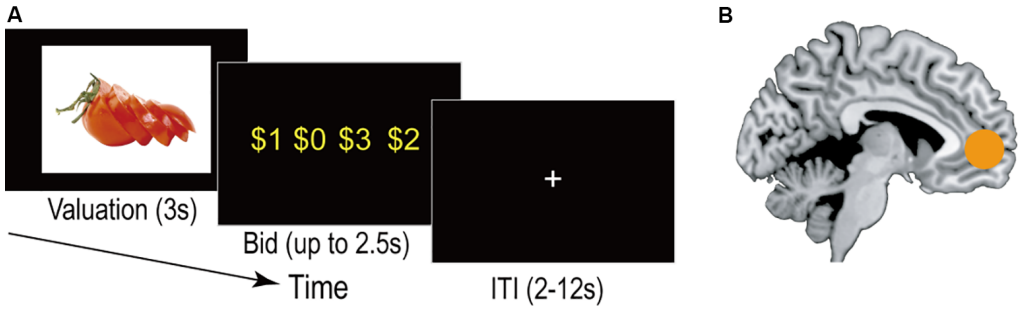

FIGURE 1 | Value signals in the brain. **(A)** Example timeline of the experimental task (called Becker-DeGroot-Marschak auction: Becker et al., 1964). In this task, participants report their "willingness to pay" (i.e., subjective value) for food items. On each trial, they make a bid for one item in the context of *auction*. Importantly, the auction mechanism is carefully designed so that the optimal strategy for the participants is to always bid the number closest to their true subjective value for obtaining that item. The food image is adopted from Food-pics (Blechert et al., 2014). **(B)** Neural correlates of value signals. Subjective value signals are correlated with neural activity (blood-oxygen-level-dependent signal) in the vmPFC. vmPFC, ventromedial prefrontal cortex.

information about multiple attributes from biologically relevant intrinsic factors (e.g., macronutrients, tastes, and flavors) to higher-order extrinsic factors (e.g., labels, brands, prices, and packaging designs; e.g., Steptoe et al., 1995; Satterthwaite and Fellows, 2018).

Researchers have examined the effects of nutrient factors with experimental designs using images of food as stimuli (**Figure 1A**; Tang et al., 2014; Suzuki et al., 2017; DiFeliceantonio et al., 2018). For example, food valuation is driven by the caloric content tracked in the vmPFC (Tang et al., 2014). Moreover, one study found that the subjective value of a food reward can be predicted by a linear combination of the constituent nutritive attributes (Suzuki et al., 2017). Multivariate decoding analyses on the neuroimaging data supported the possibility that information on the nutritive attributes of food is represented in the lateral orbitofrontal cortex (lOFC) and then integrated into the vmPFC to compute an overall subject value (Suzuki et al., 2017). Notably, an additional analysis in this study carefully ruled out the possibility that the lOFC contains information about low-level visual features of the food images (e.g., luminance and contrast). A subsequent study demonstrated supra-additive effects of fats and carbohydrates to food valuations beyond the linear combination (DiFeliceantonio et al., 2018), providing a potential account for overconsumption of high-fat/-carbohydrate food products (e.g., French fries).

Construction of the value signal through actual consumption/tasting (i.e., oral sensing) of the food has also been of considerable concern in human neuroscience. For instance, oral sensory representation of fat and sucrose have been found in the vmPFC, including the rostral anterior cingulate cortex (de Araujo and Rolls, 2004). Grabenhorst and colleagues further demonstrated that the vmPFC and lOFC track the pleasantness of oral fat texture *via* functional connectivity with the oral somatosensory cortex (Grabenhorst et al., 2010; Grabenhorst and Rolls, 2014).

Another line of study has attempted to characterize the neural encoding of quality, intensity, and preference for certain tastes and flavors (Small et al., 2007). One study demonstrated that pleasantness, or quality, of taste, is represented in the lOFC, while intensity is represented in the insular cortex and amygdala (Small et al., 2003). By combining careful experimental designs with multivariate analyses on neuroimaging data, recent studies have elaborated on how taste and flavor information is processed in the brain (e.g., Howard et al., 2015; Chikazoe et al., 2019; Avery et al., 2020). Chikazoe and colleagues showed taste qualities (sweet, salty, bitter, and sour) are represented in the insular cortex, which supports the notion that the insular is the primary gustatory cortex in humans (Small, 2010). Howard and colleagues revealed, by the careful manipulation of identities (qualities) of odor stimuli, that the lOFC encodes identity-specific values, while the vmPFC encodes subjective values independent of the identity. Although the extent to which taste and flavor contribute to the computation of subjective values beyond the nutritive and caloric contents remains elusive (de Araujo et al., 2020), these findings together suggest that the lOFC plays a pivotal role in representing multiple types of information about intrinsic factors of food (e.g., macronutrients, tastes, and flavors) which are then integrated in the vmPFC to compute an overall subjective value.

Despite the advancement in our understanding of the influences of intrinsic factors, much less is known about the effects of higher-order extrinsic factors on food valuation in the brain. Increasing evidence in consumer psychology and food science suggests that food valuation can be influenced by various factors outside of the food itself, such as labels, brands, prices, social information, and packaging designs (e.g., Okamoto and Dan, 2013; Higgs, 2015; Piqueras-Fiszman and Spence, 2015; Motoki et al., 2018, 2020). In this mini-review article, we discuss our current knowledge about how extrinsic factors affect food valuation in the brain while maintaining a focus on human neuroimaging (fMRI) studies. Although previous articles have discussed related issues (Plassmann et al., 2012; Okamoto and Dan, 2013; Stasi et al., 2018), the current review provides a new perspective by emphasizing how information about food-extrinsic factors gets integrated into the brain to compute an overall subjective value.

EXTRINSIC FACTORS OF FOOD VALUATION

Labels

In our everyday dietary choices, we often acquire a significant amount of information from the label attached to the food product (e.g., Piqueras-Fiszman and Spence, 2015; Motoki et al., 2020). A seminal study by de Araujo et al. (2005) examined how cognitive and semantic information modulates our food valuation. They exposed participants to an odor (isovaleric acid with cheddar cheese flavor) with different visual word labels, either "cheddar cheese" or "body odor." The participants were found to rate the subjective value of the odor as more unpleasant when labeled "body odor" than when labeled "cheddar cheese." Furthermore, the modulation of the unpleasantness rating was reflected in the neural activity in the vmPFC, suggesting that cognitive and semantic information can modulate food value signals in the vmPFC.

Enax et al. (2015a) compared two different ways of presenting the nutritional information in a food label. In the control condition, nutritional information was provided by a purely information-based textual label. Whereas, in the main condition, the same information was provided by a label with color codes: *green* and *red* signaling *healthy* and *unhealthy* foods, respectively. The behavioral data showed that the labeling method significantly affected participants' willingness to pay (WTP) for food items. Nutritional labels with color codes increased WTP for healthy foods compared with the purely information-based labels. The neuroimaging data revealed that consistent with the previous findings (Plassmann et al., 2007), WTP for each food item was significantly correlated with neural activity in the vmPFC, regardless of the type of nutritional label. Furthermore, the red signals, indicating unhealthiness, were found to increase neural activity in the dorsolateral prefrontal cortex (dlPFC), which has been implicated in self-control (Hare et al., 2009), and modulate its functional connectivity with the vmPFC. These results are consistent with the notion that top-down self-control signals in the dlPFC modulate the food value signals represented in the vmPFC to enable an overall decision.

Top-down modulation of the brain valuation region is potentially more prominent in obese female participants, compared to the healthy controls (Ng et al., 2011). Ng et al. (2011) scanned obese and normal females with fMRI while the participants were anticipating receiving a milkshake. Critically, in the experiment, identical milkshakes were delivered with a label indicating it was either "regular" or "low-fat." Relative to female participants with normal weight, obese participants showed greater activation in the vmPFC in response to receiving the regular labeled milkshake (vs. low-fat labeled one), which could contribute to excessive consumption of high-fat foods. A possible way to account for the result would be an excess top-down modulation of the food valuation in obese females, though the study did not provide neural evidence for the modulatory process (e.g., connectivity analyses).

Grabenhorst et al. (2008) examined the effects of labels including taste-related ("rich and delicious taste") descriptions on food valuation by using umami-taste stimuli. They found that pleasantness ratings from tasting the stimuli were increased by the taste-related labels, while intensity ratings were not. Consistent with the behavioral results, the neural representation of the pleasantness in the vmPFC was enhanced by the taste-related labels, while the representation of the taste intensity in the insular cortex was intact. The results suggest that food value signals represented in the vmPFC are modulated by top-down information about taste. The same research group also investigated how the inclusion of health-related properties (e.g., "high in calories"), as well as taste-related properties (e.g., "sweet and juicy") on labels, influenced food valuation and choice (Grabenhorst et al., 2013). The taste-related labels were found to enhance the neural representation of taste pleasantness in the amygdala, a core region in the emotional brain system (Pessoa, 2017). Similarly, the health-related labels enhanced activity in the amygdala, and the amygdala activity predicted the participant's behavioral shift towards healthier choices, highlighting a potential role of emotion in food. An explanation of these findings (Grabenhorst et al., 2008, 2013) could be that top-down information about taste and healthiness in the amygdala modulates food value signals in the vmPFC. An interesting avenue for future research would be to elucidate the modulation process by employing connectivity analyses and brain stimulation techniques (see "Discussion" section for details).

In today's society, many people are conscious about whether their food is produced ethically and sustainably. One study showed a positive effect of an "organic" label on food valuation (Linder et al., 2010). The authors found that participants' WTP was significantly higher for food items possessing an organic label rather than those without. Furthermore, the presentation of organically labeled foods increased the neural activity in the ventral striatum, and the increased striatal activity accounted for the individual differences in concern for natural food gradients and daily organic food buying behavior. Another study examined the effect of "fair-trade" labels highlighting the ethical sustainability of the food product (Enax et al., 2015b). In the neuroimaging experiment, participants were asked to report their WTP for food items presented with or without a fair-trade label. The behavioral and neuroimaging data revealed that the presence of the label increased WTP, while also increasing neural activity in brain regions such as ventral striatum, anterior cingulate cortex, and superior frontal gyrus. The presentation of the label was also found to modulate functional connectivity between these regions and the vmPFC, which signaled WTP. These results suggest that the fair-trade label influenced the valuation of food in the vmPFC through the functional connectivity with the regions that track the label information.

Price

Our daily purchasing behavior is guided not only by a preference for an item but also by the price (e.g., Jaeger, 2006). Underpriced goods are generally preferred, while overpriced goods are avoided. Hare et al. (2008) demonstrated in their neuroimaging experiment that both the WTP and the price of food determined participants' purchasing decisions. Furthermore, the decision value of food (defined as the WTP minus the price) was found to

be encoded in the lOFC, while WTP was encoded in the vmPFC. Another study (Knutson et al., 2007) suggests that, in purchasing various goods including food, the brain computes the decision value in the vmPFC, while the ventral striatum tracks WTP and the insular cortex tracks price.

In some cases, a high-priced item may be overvalued based on the belief that expensiveness implies enhanced quality. That is, the price information can reinforce the preference (i.e., WTP) for the item. For example, an expensive wine sometimes sells better than a comparable low-priced alternative. Plassmann et al. (2008) addressed this issue with a focus on the experienced pleasantness from consuming a glass a few drops of wine. In their neuroimaging experiment, participants were asked to sample different wines and report their experienced pleasantness. The critical manipulation was that, unknown to the participants, the identical wines were administered with different instructions about their retail price (i.e., a high price in half of the cases and a low price in the other cases). They found that price information about the wine was capable of manipulating participants' experienced pleasantness. That is, the expectation of higher-priced wine increased subjective reports of flavor pleasantness. Moreover, the change in the pleasantness reports was reflected in the neural activity of the vmPFC. A follow-up study formally tested the tripartite relationship among price, pleasantness, and neural activity (Schmidt et al., 2017). The results of a multilevel mediation analysis revealed that the effect of price information on experienced pleasantness of wine tasting was mediated by neural activity in the brain valuation system including the vmPFC, ventral striatum, and anterior prefrontal cortex.

Brand

Brand images can also influence our food choices. One study tested the effect of brand images by examining behavioral and neural responses to soft drink taste tests (McClure et al., 2004). In the experiment, the authors recruited participants who expressed either a preference for Coke or Pepsi. Within the experiment, participants were asked to choose between the two types of soda based on blind-tasting. The data analysis showed that participants' choice pattern was not significantly correlated with their self-reported preference, implying that our daily food choice is predominated by brand images rather than experienced tastes. Furthermore, the preference that was estimated from the choice data, but not the self-report, was found to be represented in the vmPFC. Moreover, they showed that disclosure of the brand information, Coke but not Pepsi, increased participants' preference for Coke and neural activity in dlPFC and hippocampus. A follow-up study (Koenigs and Tranel, 2008) examined the effect of the Coke brand cue in patients with lesions in the vmPFC. The authors demonstrated that the Coke label did not alter the patients' preference, suggesting a causal role of vmPFC in processing brand information for food valuation.

Another study (Kühn and Gallinat, 2013) prepared an artificial beverage that consisted of equal parts of Coca Cola, Pepsi Cola, and River Cola. The artificial beverage was delivered to participants with different brand name cues: Coca Cola, Pepsi Cola, River Cola, and T Cola. The participants exhibited a preference for drinks associated with the famous brands (i.e., Coca and Pepsi Cola) over the others (i.e., River and T Cola) despite the chemical composition being identical. Furthermore, neural activity in the vmPFC was more responsive to the pleasantness rating from consuming the beverage when the cue signaled famous brands compared to the others. These two studies (McClure et al., 2004; Kühn and Gallinat, 2013) together suggest that brand images, possibly encoded in the dlPFC and the hippocampus, modulate value signals in the vmPFC.

Social Information

Social information, such as the opinions of others, influences our judgment, preferences, and decision-making including food choice (e.g., Klucharev et al., 2009; Izuma, 2013; Higgs, 2015; Suzuki et al., 2016). Nook and Zaki (2015) investigated the social influence on food valuation. They conducted a neuroimaging experiment in which participants: (i) first rated how much they wanted to eat a series of foods; (ii) observed peer ratings for the foods; and (iii) again rated each of the food. As expected, the behavioral data showed a social conformity effect: that is, participants' ratings about the foods were conformed to the peers' ratings. At the neural level, an agreement between the participants' and the peers' ratings, as compared to disagreement, provoked neural activity in the ventral striatum, and the strength of the striatal activity predicted the individual differences in the degree of social conformity. Furthermore, the anterior prefrontal cortex was found to track information about the healthiness of the foods in the initial rating, but tracked popularity (i.e., information about peer ratings) in the second rating.

Packaging Design

Packaging design can also affect our flavor expectation and preference for food (e.g., Basso et al., 2014; Spence et al., 2019; Tijssen et al., 2019). One study (Van der Laan et al., 2012) asked participants to choose between two options of the same snack contained within different packaging designs. The neuroimaging data showed that several brain regions, including the striatum, encoded outcomes of the package-based choices. Reimann et al. (2010) investigated how aesthetic packages and well-known brands influence our purchasing behavior. Comparing the two packages (i.e., aesthetic and standardized) and the two brands (i.e., well-known and unknown) conditions, they found that food items in aesthetics packages were more likely to be chosen

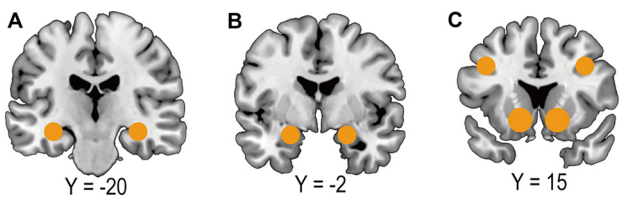

FIGURE 2 | Brain regions encoding extrinsic factors of food. **(A)** Hippocampus. **(B)** Amygdala. **(C)** The dorsolateral prefrontal cortex (*top*) and ventral striatum (*bottom*).

despite higher prices when compared to well-known brands in standardized packages. The preference for aesthetic packages was reflected in the neural activity of the vmPFC, striatum, and middle to posterior cingulate cortex.

DISCUSSION

Consumer psychology and food science have a long history of demonstrating that our preference for a food reward is modulated by higher-order extrinsic factors (e.g., labels, brand images, prices, social information, and packaging designs; e.g., Okamoto and Dan, 2013; Higgs, 2015; Piqueras-Fiszman and Spence, 2015). In this mini-review article, we have discussed recent advancements in decision neuroscience in our understanding of how extrinsic factors affect food value computation in the brain.

Accumulating evidence from human neuroimaging studies has consistently demonstrated that, while vmPFC encodes overall value signals by integrating information about the extrinsic factors of foods (e.g., Enax et al., 2015a; Schmidt et al., 2017), the various extrinsic factors are encoded in diverse brain regions such as the dlPFC (McClure et al., 2004; Enax et al., 2015a), the amygdala (Grabenhorst et al., 2013), the ventral striatum (Linder et al., 2010; Van der Laan et al., 2012; Nook and Zaki, 2015; Schmidt et al., 2017), and the hippocampus (McClure et al., 2004; see **Figure 2**). These regions cover a wide range of brain functions: cognitive control (dlPFC), emotion (amygdala), reward processing (ventral striatum), and memory (hippocampus). Interestingly, the involvement of these diverse brain regions contrasts the food value computation based on intrinsic factors, in which information about macronutrients, tastes, and flavors appear to be integrated with the lOFC and sent to the vmPFC where the overall subjective value is computed (e.g., Suzuki et al., 2017).

The findings discussed in this review are broadly consistent with the notion that extrinsic factors of food reward modulate the value signal in the vmPFC through functional connectivity with multiple brain regions that track information about each extrinsic factor. However, more evidence is needed to deepen the understanding of how the multiple types of information become integrated within the brain to compute an overall food value (see Suzuki et al., 2015; Suzuki and O'Doherty, 2020 for similar issues in social decision-making). For example, to elucidate the integration process, it would be helpful to examine the nature of functional and anatomical connectivity among the brain regions engaged in the food valuation (e.g., vmPFC and dlPFC). Although several studies to date have aimed to address the issue by employing psychophysiological interaction analysis (Friston et al., 1997), the regression-based connectivity analysis cannot test for the directionality of the connections. Future studies could provide a more comprehensive view by combining various approaches that allow examination of the causal and anatomical interactions among brain regions, such as dynamic causal modeling of the neuroimaging data (e.g., Stephan et al., 2010; Hare et al., 2011), transcranial magnetic stimulation of the neural activity (e.g., Hill et al., 2017; Polanía et al., 2018), and diffusion tensor imaging (e.g., Assaf and Pasternak, 2008).

AUTHOR CONTRIBUTIONS

KM and SS wrote the manuscript.

FUNDING

This work was supported by Japan Society for the Promotion of Science (JSPS) KAKENHI Grant Number 19K23384 (KM) and the Mishima Kaiun Memorial Foundation (SS).

REFERENCES

Assaf, Y., and Pasternak, O. (2008). Diffusion tensor imaging (DTI)-based white matter mapping in brain research: a review. *J. Mol. Neurosci.* 34, 51–61. doi: 10.1007/s12031-007-0029-0

Avery, J. A., Liu, A. G., Ingeholm, J. E., Riddell, C. D., Gotts, S. J., and Martin, A. (2020). Taste quality representation in the human brain. *J. Neurosci.* 40, 1042–1052. doi: 10.1523/jneurosci.1751-19.2019

Bartra, O., McGuire, J. T., and Kable, J. W. (2013). The valuation system: a coordinate-based meta-analysis of bold fMRI experiments examining neural correlates of subjective value. *NeuroImage* 76, 412–427. doi: 10.1016/j.neuroimage.2013.02.063

Basso, F., Robert-Demontrond, P., Hayek, M., Anton, J.-L., Nazarian, B., Roth, M., et al. (2014). Why people drink shampoo? Food imitating products are fooling brains and endangering consumers for marketing purposes. *PLoS One* 9:e100368. doi: 10.1371/journal.pone.0100368

Becker, G. M., DeGroot, M. H., and Marschak, J. (1964). Measuring utility by a single-response sequential method. *Behav. Sci.* 9, 226–232. doi: 10.1002/bs.3830090304

Blechert, J., Meule, A., Busch, N. A., and Ohla, K. (2014). *Food-pics*: an image database for experimental research on eating and appetite. *Front. Psychol.* 5:617. doi: 10.3389/fpsyg.2014.00617

Carnell, S., Gibson, C., Benson, L., Ochner, C. N., and Geliebter, A. (2012). Neuroimaging and obesity: current knowledge and future directions. *Obes. Rev.* 13, 43–56. doi: 10.1111/j.1467-789x.2011.00927.x

Chib, V. S., Rangel, A., Shimojo, S., and O'Doherty, J. P. (2009). Evidence for a common representation of decision values for dissimilar goods in human ventromedial prefrontal cortex. *J. Neurosci.* 29, 12315–12320. doi: 10.1523/JNEUROSCI.2575-09.2009

Chikazoe, J., Lee, D. H., Kriegeskorte, N., and Anderson, A. K. (2014). Population coding of affect across stimuli, modalities and individuals. *Nat. Neurosci.* 17, 1114–1122. doi: 10.1038/nn.3749

Chikazoe, J., Lee, D. H., Kriegeskorte, N., and Anderson, A. K. (2019). Distinct representations of basic taste qualities in human gustatory cortex. *Nat. Commun.* 10:1048. doi: 10.1038/s41467-019-08857-z

Clithero, J. A., and Rangel, A. (2014). Informatic parcellation of the network involved in the computation of subjective value. *Soc. Cogn. Affect. Neurosci.* 9, 1289–1302. doi: 10.1093/scan/nst106

de Araujo, I. E., and Rolls, E. T. (2004). Representation in the human brain of food texture and oral fat. *J. Neurosci.* 24, 3086–3093. doi: 10.1523/JNEUROSCI.0130-04.2004

de Araujo, I. E., Rolls, E. T., Velazco, M. I., Margot, C., and Cayeux, I. (2005). Cognitive modulation of olfactory processing. *Neuron* 46, 671–679. doi: 10.1016/j.neuron.2005.04.021

de Araujo, I. E., Schatzker, M., and Small, D. M. (2020). Rethinking food reward. *Annu. Rev. Psychol* 71, 139–164. doi: 10.1146/annurev-psych-122216-011643

DiFeliceantonio, A. G., Coppin, G., Rigoux, L., Thanarajah, S. E., Dagher, A., Tittgemeyer, M., et al. (2018). Supra-additive effects of combining fat and

carbohydrate on food reward. *Cell Metab.* 28, 33.e3–44.e3. doi: 10.1016/j.cmet.2018.05.018

Enax, L., Hu, Y., Trautner, P., and Weber, B. (2015a). Nutrition labels influence value computation of food products in the ventromedial prefrontal cortex. *Obesity* 23, 786–792. doi: 10.1002/oby.21027

Enax, L., Krapp, V., Piehl, A., and Weber, B. (2015b). Effects of social sustainability signaling on neural valuation signals and taste-experience of food products. *Front. Behav. Neurosci.* 9:247. doi: 10.3389/fnbeh.2015.00247

Foerde, K., Steinglass, J. E., Shohamy, D., and Walsh, B. T. (2015). Neural mechanisms supporting maladaptive food choices in anorexia nervosa. *Nat. Neurosci.* 18, 1571–1573. doi: 10.1038/nn.4136

Friston, K. J., Buechel, C., Fink, G. R., Morris, J., Rolls, E., and Dolan, R. J. (1997). Psychophysiological and modulatory interactions in neuroimaging. *NeuroImage* 6, 218–229. doi: 10.1006/nimg.1997.0291

Giuliani, N. R., Merchant, J. S., Cosme, D., and Berkman, E. T. (2018). Neural predictors of eating behavior and dietary change. *Ann. N Y Acad. Sci.* 1428, 208–220. doi: 10.1111/nyas.13637

Grabenhorst, F., and Rolls, E. T. (2014). The representation of oral fat texture in the human somatosensory cortex. *Hum. Brain Mapp.* 35, 2521–2530. doi: 10.1002/hbm.22346

Grabenhorst, F., Rolls, E. T., and Bilderbeck, A. (2008). How cognition modulates affective responses to taste and flavor: top-down influences on the orbitofrontal and pregenual cingulate cortices. *Cereb. Cortex* 18, 1549–1559. doi: 10.1093/cercor/bhm185

Grabenhorst, F., Rolls, E. T., Parris, B. A., and d'Souza, A. A. (2010). How the brain represents the reward value of fat in the mouth. *Cereb. Cortex* 20, 1082–1091. doi: 10.1093/cercor/bhp169

Grabenhorst, F., Schulte, F. P., Maderwald, S., and Brand, M. (2013). Food labels promote healthy choices by a decision bias in the amygdala. *NeuroImage* 74, 152–163. doi: 10.1016/j.neuroimage.2013.02.012

Gross, J., Woelbert, E., Zimmermann, J., Okamoto-Barth, S., Riedl, A., and Goebel, R. (2014). Value signals in the prefrontal cortex predict individual preferences across reward categories. *J. Neurosci.* 34, 7580–7586. doi: 10.1523/JNEUROSCI.5082-13.2014

Hare, T. A., Camerer, C. F., and Rangel, A. (2009). Self-control in decision-making involves modulation of the vmPFC valuation system. *Science* 324, 646–648. doi: 10.1126/science.1168450

Hare, T. A., O'Doherty, J., Camerer, C. F., Schultz, W., and Rangel, A. (2008). Dissociating the role of the orbitofrontal cortex and the striatum in the computation of goal values and prediction errors. *J. Neurosci.* 28, 5623–5630. doi: 10.1523/JNEUROSCI.1309-08.2008

Hare, T. A., Schultz, W., Camerer, C. F., O'Doherty, J. P., and Rangel, A. (2011). Transformation of stimulus value signals into motor commands during simple choice. *Proc. Natl. Acad. Sci. U S A* 108, 18120–18125. doi: 10.1073/pnas.1109322108

Higgs, S. (2015). Social norms and their influence on eating behaviours. *Appetite* 86, 38–44. doi: 10.1016/j.appet.2014.10.021

Hill, C. A., Suzuki, S., Polania, R., Moisa, M., O'Doherty, J. P., and Ruff, C. C. (2017). A causal account of the brain network computations underlying strategic social behavior. *Nat. Neurosci.* 20, 1142–1149. doi: 10.1038/nn.4602

Howard, J. D., Gottfried, J. A., Tobler, P. N., and Kahnt, T. (2015). Identity-specific coding of future rewards in the human orbitofrontal cortex. *Proc. Natl. Acad. Sci. U S A* 112, 5195–5200. doi: 10.1073/pnas.1503550112

Izuma, K. (2013). The neural basis of social influence and attitude change. *Curr. Opin. Neurobiol.* 23, 456–462. doi: 10.1016/j.conb.2013.03.009

Jaeger, S. R. (2006). Non-sensory factors in sensory science research. *Food Qual. Prefer.* 17, 132–144. doi: 10.1016/j.foodqual.2005.03.004

Klucharev, V., Hytönen, K., Rijpkema, M., Smidts, A., and Fernández, G. (2009). Reinforcement learning signal predicts social conformity. *Neuron* 61, 140–151. doi: 10.1016/j.neuron.2008.11.027

Knutson, B., Rick, S., Wimmer, G. E., Prelec, D., and Loewenstein, G. (2007). Neural predictors of purchases. *Neuron* 53, 147–156. doi: 10.1016/j.neuron.2006.11.010

Koenigs, M., and Tranel, D. (2008). Prefrontal cortex damage abolishes brand-cued changes in cola preference. *Soc. Cogn. Affect. Neurosci.* 3, 1–6. doi: 10.1093/scan/nsm032

Kühn, S., and Gallinat, J. (2013). Does taste matter? How anticipation of cola brands influences gustatory processing in the brain. *PLoS One* 8:e61569. doi: 10.1371/journal.pone.0061569

Lebreton, M., Jorge, S., Michel, V., Thirion, B., and Pessiglione, M. (2009). An automatic valuation system in the human brain: evidence from functional neuroimaging. *Neuron* 64, 431–439. doi: 10.1016/j.neuron.2009.09.040

Linder, N. S., Uhl, G., Fliessbach, K., Trautner, P., Elger, C. E., and Weber, B. (2010). Organic labeling influences food valuation and choice. *NeuroImage* 53, 215–220. doi: 10.1016/j.neuroimage.2010.05.077

McClure, S. M., Li, J., Tomlin, D., Cypert, K. S., Montague, L. M., and Montague, P. R. (2004). Neural correlates of behavioral preference for culturally familiar drinks. *Neuron* 44, 379–387. doi: 10.1016/j.neuron.2004.09.019

Motoki, K., Saito, T., Nouchi, R., Kawashima, R., and Sugiura, M. (2018). The paradox of warmth: ambient warm temperature decreases preference for savory foods. *Food Qual. Prefer.* 69, 1–9. doi: 10.1016/j.foodqual.2018.04.006

Motoki, K., Saito, T., Park, J., Velasco, C., Spence, C., and Sugiura, M. (2020). Tasting names: systematic investigations of taste-speech sounds associations. *Food Qual. Prefer.* 80:103801. doi: 10.1016/j.foodqual.2019.103801

Ng, J., Stice, E., Yokum, S., and Bohon, C. (2011). An fMRI study of obesity, food reward, and perceived caloric density. Does a low-fat label make food less appealing? *Appetite* 57, 65–72. doi: 10.1016/j.appet.2011.03.017

Nook, E. C., and Zaki, J. (2015). Social norms shift behavioral and neural responses to foods. *J. Cogn. Neurosci.* 27, 1412–1426. doi: 10.1162/jocn_a_00795

Okamoto, M., and Dan, I. (2013). Extrinsic information influences taste and flavor perception: a review from psychological and neuroimaging perspectives. *Semin. Cell Dev. Biol.* 24, 247–255. doi: 10.1016/j.semcdb.2012.11.001

Pessoa, L. (2017). A network model of the emotional brain. *Trends Cogn. Sci.* 21, 357–371. doi: 10.1016/j.tics.2017.03.002

Piqueras-Fiszman, B., and Spence, C. (2015). Sensory expectations based on product-extrinsic food cues: an interdisciplinary review of the empirical evidence and theoretical accounts. *Food Qual. Prefer.* 40, 165–179. doi: 10.1016/j.foodqual.2014.09.013

Plassmann, H., O'Doherty, J., and Rangel, A. (2007). Orbitofrontal cortex encodes willingness to pay in everyday economic transactions. *J. Neurosci.* 27, 9984–9988. doi: 10.1523/JNEUROSCI.2131-07.2007

Plassmann, H., O'Doherty, J., Shiv, B., and Rangel, A. (2008). Marketing actions can modulate neural representations of experienced pleasantness. *Proc. Natl. Acad. Sci. U S A* 105, 1050–1054. doi: 10.1073/pnas.0706929105

Plassmann, H., Ramsøy, T. Z., and Milosavljevic, M. (2012). Branding the brain: a critical review and outlook. *J. Consum. Psychol.* 22, 18–36. doi: 10.1016/j.jcps.2011.11.010

Polanía, R., Nitsche, M. A., and Ruff, C. C. (2018). Studying and modifying brain function with non-invasive brain stimulation. *Nat. Neurosci.* 21, 174–187. doi: 10.1038/s41593-017-0054-4

Reimann, M., Zaichkowsky, J., Neuhaus, C., Bender, T., and Weber, B. (2010). Aesthetic package design: A behavioral, neural, and psychological investigation. *J. Cons. Psychol.* 20:431–441. doi: 10.1016/j.jcps.2010.06.009

Rangel, A. (2013). Regulation of dietary choice by the decision-making circuitry. *Nat. Neurosci.* 16, 1717–1724. doi: 10.1038/nn.3561

Satterthwaite, M., and Fellows, L. K. (2018). Characterization of a food image stimulus set for the study of multi-attribute decision-making. *MNI Open Res.* 2:4. doi: 10.12688/mniopenres.12791.1

Schmidt, L., Skvortsova, V., Kullen, C., Weber, B., and Plassmann, H. (2017). How context alters value: the brain's valuation and affective regulation system link price cues to experienced taste pleasantness. *Sci. Rep.* 7:8098. doi: 10.1038/s41598-017-08080-0

Small, D. M. (2010). Taste representation in the human insula. *Brain Struct. Funct.* 214, 551–561. doi: 10.1007/s00429-010-0266-9

Small, D. M., Bender, G., Veldhuizen, M. G., Rudenga, K., Nachtigal, D., and Felsted, J. (2007). The role of the human orbitofrontal cortex in taste and flavor processing. *Ann. N Y Acad. Sci.* 1121, 136–151. doi: 10.1196/annals.1401.002

Small, D. M., Gregory, M. D., Mak, Y. E., Gitelman, D., Mesulam, M. M., and Parrish, T. (2003). Dissociation of neural representation of intensity and affective valuation in human gustation. *Neuron* 39, 701–711. doi: 10.1016/s0896-6273(03)00467-7

Spence, C., Velasco, C., and Petit, O. (2019). "The consumer neuroscience of packaging," in *Multisensory Packaging: Designing New Product Experiences*, eds C. Velasco and C. Spence (Cham: Springer International Publishing), 319–347.

Stasi, A., Songa, G., Mauri, M., Ciceri, A., Diotallevi, F., Nardone, G., et al. (2018). Neuromarketing empirical approaches and food choice: a systematic review. *Food Res. Int.* 108, 650–664. doi: 10.1016/j.foodres.2017.11.049

Stephan, K. E., Penny, W. D., Moran, R. J., den Ouden, H. E. M., Daunizeau, J., and Friston, K. J. (2010). Ten simple rules for dynamic causal modeling. *NeuroImage* 49, 3099–3109. doi: 10.1016/j.neuroimage.2009.11.015

Steptoe, A., Pollard, T. M., and Wardle, J. (1995). Development of a measure of the motives underlying the selection of food: the food choice questionnaire. *Appetite* 25, 267–284. doi: 10.1006/appe.1995.0061

Suzuki, S., Adachi, R., Dunne, S., Bossaerts, P., and O'Doherty, J. P. (2015). Neural mechanisms underlying human consensus decision-making. *Neuron* 86, 591–602. doi: 10.1016/j.neuron.2015.03.019

Suzuki, S., Cross, L., and O'Doherty, J. P. (2017). Elucidating the underlying components of food valuation in the human orbitofrontal cortex. *Nat. Neurosci.* 20, 1780–1786. doi: 10.1038/s41593-017-0008-x

Suzuki, S., Jensen, E. L., Bossaerts, P., and O'Doherty, J. P. (2016). Behavioral contagion during learning about another agent's risk-preferences acts on the neural representation of decision-risk. *Proc. Natl. Acad. Sci. U S A* 113, 3755–3760. doi: 10.1073/pnas.1600092113

Suzuki, S., and O'Doherty, J. P. (2020). Breaking human social decision making into multiple components and then putting them together again. *Cortex* 127, 221–230. doi: 10.1016/j.cortex.2020.02.014

Tang, D. W., Fellows, L. K., and Dagher, A. (2014). Behavioral and neural valuation of foods is driven by implicit knowledge of caloric content. *Psychol. Sci.* 25, 2168–2176. doi: 10.1177/0956797614552081

Tijssen, I. O. J. M., Smeets, P. A. M., Goedegebure, R. P. G., Zandstra, E. H., de Graaf, C., and Jager, G. (2019). Colouring perception: package colour cues affect neural responses to sweet dairy drinks in reward and inhibition related regions. *Appetite* 142:104378. doi: 10.1016/j.appet.2019.104378

Van der Laan, L. N., De Ridder, D. T. D., Viergever, M. A., and Smeets, P. A. M. (2012). Appearance matters: neural correlates of food choice and packaging aesthetics. *PLoS One* 7:e41738. doi: 10.1371/journal.pone.0041738

Yokum, S., Ng, J., and Stice, E. (2011). Attentional bias to food images associated with elevated weight and future weight gain: an fMRI study. *Obesity* 19, 1775–1783. doi: 10.1038/oby.2011.168

Conflict of Interest: The authors declare that the research was conducted in the absence of any commercial or financial relationships that could be construed as a potential conflict of interest.

frontiers in Human Neuroscience

ORIGINAL RESEARCH
published: 08 October 2020
doi: 10.3389/fnhum.2020.574148

Brain Responses to Food Odors Associated With BMI Change at 2-Year Follow-Up

Pengfei Han[1,2,3]*, *Hong Chen*[1,2] *and Thomas Hummel*[3]

[1]The Key Laboratory of Cognition and Personality, Ministry of Education, Chongqing, China, [2]Faculty of Psychology, Southwest University, Chongqing, China, [3]Interdisciplinary Center Smell and Taste, Department of Otorhinolaryngology, TU Dresden, Dresden, Germany

OPEN ACCESS

Edited by:
Björn H. Schott,
Leibniz Institute for Neurobiology (LG), Germany

Reviewed by:
Ayşe İkinci Keleş,
Niğde Ömer Halisdemir University, Turkey
Hüseyin Akan,
Ondokuz Mayıs University, Turkey
Samantha Jane Brooks,
Liverpool John Moores University, United Kingdom

***Correspondence:**
Pengfei Han
p.han@foxmail.com

Specialty section:
This article was submitted to Health, a section of the journal Frontiers in Human Neuroscience

Received: 19 June 2020
Accepted: 31 August 2020
Published: 08 October 2020

Citation:
Han P, Chen H and Hummel T (2020) Brain Responses to Food Odors Associated With BMI Change at 2-Year Follow-Up. Front. Hum. Neurosci. 14:574148. doi: 10.3389/fnhum.2020.574148

The understanding of food cue associated neural activations that predict future weight variability may guide the design of effective prevention programs and treatments for overeating and obesity. The current study investigated the association between brain response to different food odors with varied energy density and individual changes of body mass index (BMI) over 2 years. Twenty-five participants received high-fat (chocolate and peanut), low-fat (bread and peach) food odors, and a nonfood odor (rose) while the brain activation was measured using functional magnetic resonance imaging (fMRI). BMIs were calculated with participant's self-reported body weight and height collected at the time of the fMRI scan and again at 2 years later. Regression analyses revealed significant negative correlations between BMI increase over 2 years and brain activation of the bilateral precuneus and the right posterior cingulate cortex (PCC) in response to high-fat vs. low-fat food odors. Also, brain activation of the right supplementary motor area (SMA) in response to food vs. non-food odor was negatively correlated to subsequent BMI increase over 2 years. Taken together, the current findings suggest that individual differences in neural responsivity to (high calorie) food odors in brain regions of the default mode and motor control network serve as a neural marker for future BMI change.

Keywords: brain activation, food odor, fMRI, BMI change, 2-year follow-up

INTRODUCTION

Bodyweight variability in humans is usually regulated by many factors including diet and lifestyle (Mozaffarian et al., 2011). Bodyweight gain is the result of a long-term imbalance between energy consumption and energy expenditure, which is mainly triggered by excessive intake of high-calorie food and the dysfunction of the biological system for body weight regulation. External appetitive food cues are important drivers for eating behavior, with higher food cue reactivity and food craving predict weight gain (Boswell and Kober, 2016). Another key risk factor for weight gain is the motivation to eat, or food reinforcement (Epstein et al., 2014).

In recent years, brain activity as biological predictors for behavioral changes, especially in the area of food consumption and weight change, has been increasingly noted (Giuliani et al., 2018). Using functional magnetic resonance imaging (fMRI) and food cue-based stimulation paradigms, previous studies have found correlations between brain reactivity to food cues and long-term body weight change. For example, elevated brain activation of the reward-related regions (e.g., striatum, orbitofrontal cortex, anterior cingulate cortex, insula) in responses to food pictures (Yokum et al., 2011; Demos et al., 2012; Murdaugh et al., 2012; Hermann et al., 2019), food advertisements (Yokum et al., 2014), abstract cues that relate to palatable food (Stice et al., 2015) predicted later weight gain (Yokum et al., 2011, 2014; Demos et al., 2012; Stice et al., 2015) or less success in a weight-loss process (Murdaugh et al., 2012; Hermann et al., 2019). Apart from visual food cue, other studies have shown that an elevated reward brain activation in response to tastes of palatable food predicted future weight gain (Geha et al., 2013; Winter et al., 2017). Thus, the hyper brain responsivity involved in the incentive valuation of external food cues may act as a vulnerability factor that promotes food overconsumption and lead to long-term weight gain (Stice and Yokum, 2016). However, one recent research applying a bootstrapping sampling approach had suggested that only little reliable evidence regarding stronger reward brain responses to food images or food tastes predicted future weight gain (Stice and Yokum, 2018). Rather, the lower brain activation of the pre-supplementary motor area (SMA) in response to an oral tasting of high-fat/low-sugar milkshake and the increased activation of the precentral gyrus/Rolandic operculum in responses to palatable food images were moderately reliable predictors for future weight gain (Stice and Yokum, 2018). Noted that dietary macronutrients have different contributions to food intake and body weight, with dietary fat as a more potent factor related to excessive energy consumption and weight gain (Hu et al., 2018). A recent study investigated the neural response to a milkshake with varying levels of sugar or fat had found that individuals with greater activation in the postcentral gyrus, insula, and medial prefrontal cortex in response to high-fat vs. low-fat milkshake gained more weight in the later period (Yokum and Stice, 2019).

Appetitive food odors are powerful food stimuli that can trigger dopaminergic brain responses, and increase the motivation to eat (Boesveldt and de Graaf, 2017). Specifically, food odors steer appetite (Zoon et al., 2016; Proserpio et al., 2019) and craving for specific foods (Larsen et al., 2012), which largely determine food preference, selection, and consumption. Moreover, food odors can signal information including the calorie density, taste quality, and specific macronutrient content of the odor related food. Those odor-taste or odor-nutrient associations are developed through the learning process during repeated food consumption (Stevenson and Boakes, 2004). Therefore, food odors can be distinguished according to the taste quality or nutrient content (e.g., high or low fat; Boesveldt and de Graaf, 2017; Morquecho-Campos et al., 2019). Brain imaging studies showed that food odors compared to non-food odors mainly activate the reward-related brain regions (Bragulat et al., 2010; Eiler et al., 2012; Sorokowska et al., 2017). However, little research had been done on exploring the food odor elicited brain responsivity and future body weight changes.

The objective of the current study was to investigate the correlation between individual brain responses to food odors and future weight change. Using a sub-sample from a previous study (Han et al., 2020), brain activation in response to food (varied in fat content and sweetness) and nonfood odors were assessed among healthy adult participants. Body mass index (BMI) at the time of the fMRI test and again at 2-year later were calculated using self-reported height and body weight. Based on recent studies addressing similar research questions (Yokum and Stice, 2019), we tentative hypothesized that individual brain response to food odors correlate to subsequent BMI changes. Specifically, we hypothesized that greater activation of the taste and motor-related brain regions in response to high-fat vs. low-fat food odors would be associated with a larger BMI increase over 2 years.

MATERIALS AND METHODS

Participants

Of the 38 right-handed participants included in the initial study (Han et al., 2020), 25 of them were contacted *via* email or social networking tools (WeChat or Facebook) 2-years later and were included in the current analyses. Normal olfactory functions of them were ascertained using the threshold and identification test of the "Sniffin' Sticks" battery (Hummel et al., 1997). Also, all participants' behavior characteristics were measured using the Three-Factor Eating Questionnaire (Stunkard and Messick, 1985). Female participants were not at any stage of pregnancy at the time of the MRI scan and 2-years later according to their self-report. However, one female participant gave birth in May 2019. Self-reported height and body weight were recorded at the baseline session and 2 years later. BMI was calculated for each participant. BMI is a sensitive measure of adiposity that is adjusted for variation in height. The characteristics of included participants were shown in **Table 1**. The study was conducted according to the Declaration of Helsinki and was approved by the Ethics Board of the University of Dresden Medical School (#EK22012018). All participants signed an informed consent form prior to the tests.

Odor Stimuli

Odors that signaling food items with varied fat content and taste qualities were chosen as food-related odor stimuli, including a high-fat sweet chocolate odor (Fragrance Resources, Hamburg, Germany; Product code 51615/3), a high-fat non-sweet peanut odor (Symrise, GmbH, KG; Product code 10464774/3), a low-fat sweet peach odor (Frey und Lau, Henstedt-Ulzburg, Germany; Product code P0606040), and a low-fat non-sweet bread odor (Fragrance Resources, Hamburg, Germany; Product code PG93193). Also, a rose-like odor (Takasago, Paris, France; Product code DG FLO 792A) was chosen as non-food olfactory

TABLE 1 | Study participant characteristics (N = 25).

	M or %	SD	Range
Age	25.2	2.9	21–32
Sex			
Female	60%		
Male	40%		
BMI			
Baseline	21.5	1.7	18.5–26.7
At the 2-year follow-up	21.6	2.1	18.4–26.7
Sniffin' Sticks test			
Threshold (phenyl ethanol)	9.7	2.9	4–16
Identification	13.3	1.2	11–16
TFEQ			
Restraint	7.8	4	0–15
Disinhibition	6.2	3.2	0–11
Hunger level during fMRI	4.2	1.1	2–6

Abbreviations: TFEQ, three-factor eating questionnaire. Hunger level was assessed using 7-point scales.

stimuli. The odorants were diluted in propylene glycol to the following finalized concentrations to reach the proper and equal intensity according to daily life experiences: chocolate 1% (v/v) for chocolate odor; 20% (v/v) for peanut odor; 1% (v/v) for peach odor, 5% (v/v) for bread odor, and 0.5% (v/v) for rose odor.

fMRI Paradigm

All participants were refrained from consuming food or drinks (except water) for 2 h before taking part in the experiment. On arrival and before the fMRI test, participants rated their hunger/fullness levels on a 9-point scale (from 0 very hungry to 9 very full). The hunger ratings were used to check compliance with the fasting instructions and were used as a covariate during the correlation analysis between brain activation and future body weight changes, as suggested by a previous study (Winter et al., 2017). For the fMRI testing, food and non-food odors were embedded in a constant flow rate of clean air (2 liters/min) and were delivered to the bilateral nostrils of the participants using a portable olfactometer (Sommer et al., 2012). We used an "ON-OFF" block design paradigm for odor stimulation. Each block lasts 25 s, including a 15-s "odor ON" period followed by a 20-s "odor OFF" baseline period. To minimize odor habituation, participants received the odor stimuli intermittently during the "odor ON" period, with 1-s of odorized air (e.g., chocolate, peach, peanut, bread, or rose) and 2-s of odorless air. During the "odor OFF" baseline period, participants received only odorless air. This design permitted an assessment of brain activation in responses to each specific odor type with airflow being subtracted out (Small et al., 2005). There were 10 repeated blocks in each functional run (for a single odor) with the time duration 5 min and 50 s. The order of administration of the five odors (five runs) was randomized among participants. The total time for the fMRI test was about 35 min.

After each run, participants verbally rated the intensity (0–10; "not perceived" to "very strongly perceived"), pleasantness (0–10; "extremely unpleasant" to "extremely pleasant"), sweetness (0–10; "not sweet at all" to "very sweet") of the odor stimuli, and their desirability to eat food with a similar odor (0–10; "Do not want to eat at all" to "Want to eat very much") *via* the intercom. The participants were asked to keep their head still during the fMRI scan and also the verbal reporting. Before the fMRI test, participants took part in a training session where they practiced the velopharyngeal closure which enables breathing only through the mouth (Kobal, 1981), and were instructed to use this technique during the fMRI scanning. This technique can effectively eliminate the influences of the nasal breathing cycle (inhalation and exhalation) on brain activations, and had been used in multiple previous fMRI studies with a similar setup (Kareken et al., 2004; Croy et al., 2014; Wallrabenstein et al., 2015; Han et al., 2020).

Odor Ratings

To verify the significant differences regarding the energy density, taste quality, and major macronutrient content between the selected odors, participants completed an estimation task for the fat content and calorie density for the odor related food items after the fMRI session. We asked participants to rate the fat content and calorie density of the odor-associated food with the question "*Please estimate the fat content of the odor-associated food*," and the question "*Please estimate the calorie density of the odor-associated food*," respectively. Ratings were performed on a 9-point scale for macronutrient content (range from 1 = very low to 9 = a large amount) and calorie density (1 = very low-calorie density, to 9 = very high-calorie density). Notably, participants were not aware of the aforementioned rating task before and during the fMRI scan. This was meant to avoid biased brain activation results caused by any selective attention to such food attributes during the fMRI test.

Imaging Data Acquisition and Preprocessing

We collected the whole-brain functional and structural images with an 8-channel head coil on a 3 Tesla MRI scanner (Siemens Sonata, Erlangen, Germany). For each participant, functional images were collected using a T2-weighted echo-planar imaging (EPI) sequence (TR = 2,500 ms; TE = 40 ms; Flip Angle = 90°; voxel size = 3*3*3.75 mm; Field of View, FoV = 192 × 192 mm). A high-resolution T1-weighted anatomical image was acquired using a standard MPRAGE (magnetization prepared rapid acquisition gradient echo) sequence (TR = 2,530 ms; TE = 2.34 ms; Field of View, FoV = 256 × 256 mm; voxel size = 1*1*1 mm).

fMRI data were analyzed using SPM12 (Statistical Parametric Mapping; Welcome Department of Cognitive Neurology, London, UK) run with MATLAB (version 2014a, MathWorks, MA, USA). For image preprocessing, we used the standard pipeline batch in (\spm12\batches\preproc_fmri.m). In short, the preprocessing included realignment to the first image of the first run and unwrapped, co-registration with anatomical image, segmentation and spatial normalization of the standard EPI MNI template, and spatial smoothing with an 8-mm full width at half maximum (FWHM) isotropic Gaussian kernel. Finally, we used the ArtRepair tool (version 4, Stanford University) to examine the post-preprocessing brain volumes to detect and repair the artifact volumes due to excessive head motion. Brain volumes with image-to-image motion larger than 0.5 mm/TR and total

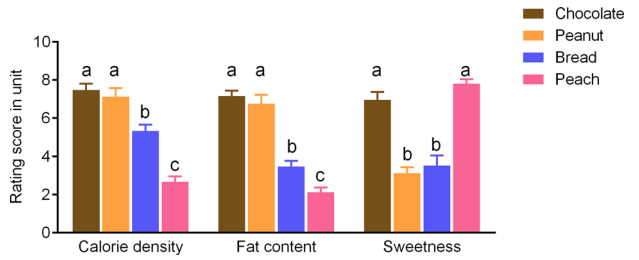

FIGURE 1 | Rating scores of the sweetness levels and estimated fat content or calorie density for food odors). Values are means with error bars (SEM), with different lowercase letters indicate significant differences ($p < 0.05$).

volumes repaired exceed 20% of the total volumes were excluded from the analysis. Data from 17 participants were repaired with no participant was excluded at this stage.

Imaging Data Analysis

For the baseline period, we discarded the first 5 s due to the potential carry-over effect from the odor period. We performed the analysis in a two-step manner. First, we modeled the following contrasts for each participant: food > nonfood odor; high-fat > nonfood odor; low-fat > nonfood odor; high-fat > low-fat odor; low-fat > high-fat odor, sweet > savory odor, savory > sweet odor. Then, on the group level, we entered the contrasts from all individual participants into a linear regression model to explore the association between brain responses and 2-year BMI changes. Subjective hunger ratings and baseline BMIs were entered as covariates as suggested in previous studies (Winter et al., 2017).

Statistical analyses were performed on a whole-brain level. To control for multiple statistical testing within the entire brain, we maintained a cluster-level false-positive detection rate at $p < 0.05$ using an initial voxel-level threshold of $p < 0.001$ in combination with a cluster extent (k) empirically determined by 1,000 Monte Carlo simulations, using AlphaSim as implemented in the REST toolbox[1] (Song et al., 2011). Simulation results indicated that a minimum cluster size of 66 contiguous voxels under the threshold of $p < 0.001$ would provide sufficient cluster-level Family-Wise Error correction of $p < 0.05$ across the whole brain. Mean responses (BOLD signals) of the significant clusters were extracted using the Marsbar toolbox. Specific brain regions were identified using the Automated Anatomical Labeling (AAL) toolbox (Tzourio-Mazoyer et al., 2002).

RESULTS

Psychophysical Odor Ratings

Participants rated the chocolate and peanut odors as significantly higher in terms of the fat content and calorie density as compared to bread and peach odors ($p < 0.05$; **Figure 1**). On the other hand, the chocolate and peach odors were rated as sweeter compared to the peanut and bread odors ($p < 0.05$; **Figure 1**). There was no intensity rating difference between odors ($p > 0.1$).

[1]http://www.restfmri.net/forum/REST_V1.7

Brain Response to High-Fat vs. Low-Fat Food Odor Correlates to BMI Increase Over 2 Years

Stronger BOLD responses to the contrast of high-fat > low-fat food odors in the right posterior cingulate cortex (PCC; peak $T = 6.92$, $k = 470$, corrected $p < 0.05$; **Figure 2A**; **Table 2**) and the bilateral precuneus (right hemisphere peak $T = 5.95$, $k = 462$; left hemisphere peak $T = 5.69$, $k = 145$, corrected $p < 0.05$; **Figures 2B,C**; **Table 2**) predicted lower BMI increase over 2 years. There was no observed significant correlation between the brain response to low fat > high-fat food odors and future BMI increase.

Brain Response to Food vs. Nonfood Odor Correlates to BMI Increase Over 2 Years

A negative correlation was found between brain response to food > nonfood odors in the SMA and BMI increase over 2 years (cluster size = 121 voxels, peak $T = 6.13$, corrected $p < 0.05$; **Table 2**; **Figure 3**). There is no significant brain response to sweet vs. savory odors and BMI change.

Correlation Between Psychometric Variables and BMI Increase Over 2 Years

No significant correlation was found between olfactory performance (odor threshold, odor identification scores), TFEQ scores, psychophysical odor ratings (pleasantness, intensity, sweetness, or desirability), and increases of BMI or body weight over the 2 years follow up (all $p > 0.1$).

DISCUSSION

In a group of healthy adult participants, individual variation of BMI changes over 2 years was related to the baseline brain responsivity to food odor cues. Specifically, a lower level of baseline brain activation in the bilateral precuneus and the right PCC in response to high-fat vs. low-fat food odors was correlated with BMI increase over 2 years. Both the precuneus and the PCC are key areas of the default mode network. The default mode network is active when participants are not focused on the external environment and attention is turned inward (Buckner et al., 2008). The precuneus was hypothesized to have a unifying function in self-mental representation and modulation of conscious processes (Cavanna and Trimble, 2006), and to play a role in olfactory related imagery or episodic memory retrieval (Plailly et al., 2012; Flohr et al., 2014). It had been argued that this region is related to self-referential processes, appetite control, or conscious suppression of food craving (Tuulari et al., 2015). For example, the precuneus have been implicated in evaluating the benefits of not eating compared with eating high-calorie palatable foods (Yokum and Stice, 2013), and assessing the healthiness of food items (Herwig et al., 2016). Stronger precuneus activation in response to palatable milkshake taste (Winter et al., 2017) or unhealthy food commercials (Gearhardt et al., 2020) was correlated to less weight gain over 3 years or less healthy food consumption, respectively. Oral taste of high vs. low-fat

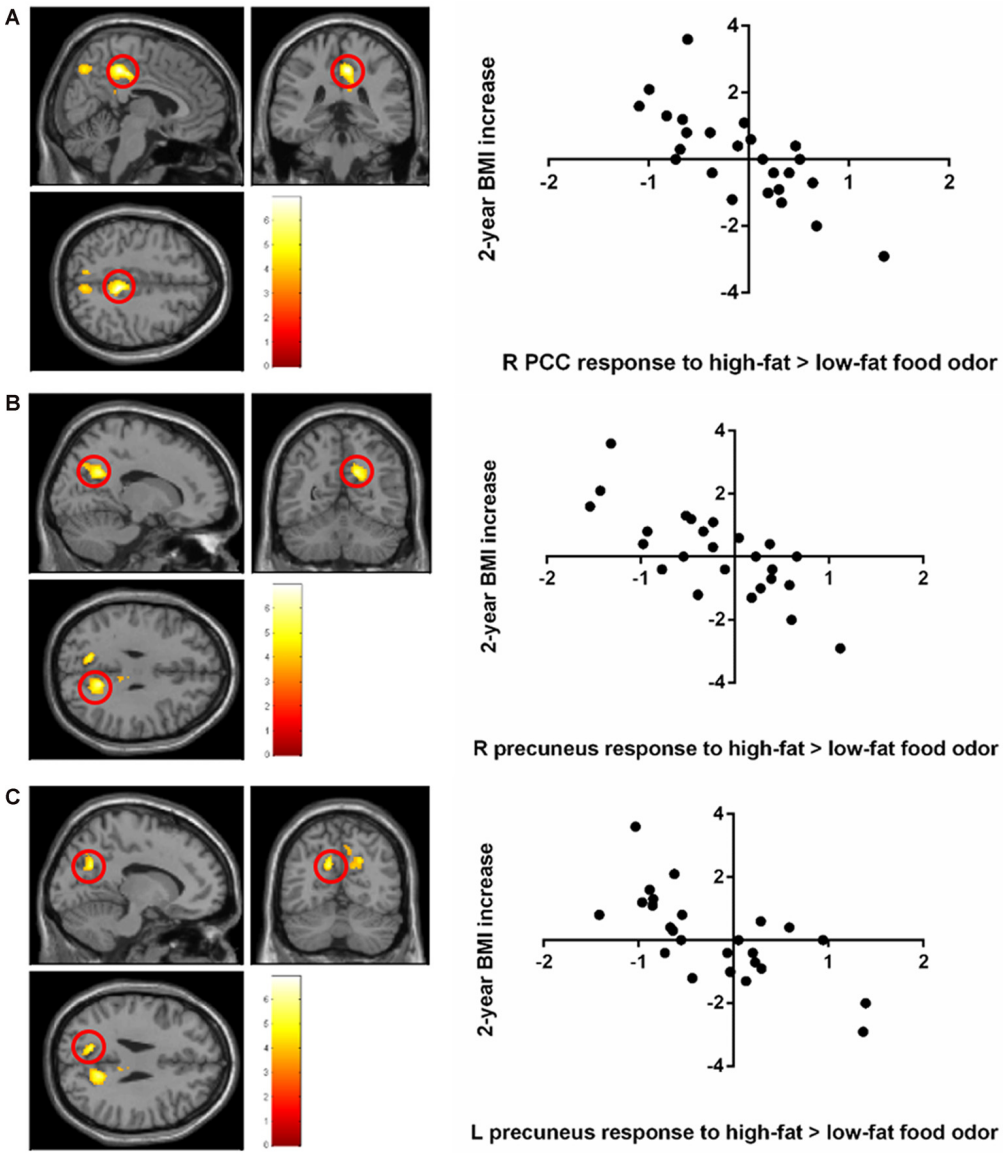

FIGURE 2 | Negative correlation between the 2-year body mass index (BMI) increase and baseline brain responses to high-fat vs. low-fat food odors in **(A)** the posterior cingulate cortex (PCC), **(B)** the left precuneus, and **(C)** the right precuneus. Brain activation was significant with corrected $p < 0.05$ and was illustrated on a template provided in SPM12 (single_sub_T1.nni).

TABLE 2 | Negative correlations between baseline brain response to High-calorie > Low-calorie odors and food > nonfood odors and BMI change over 2 years.

	Cluster size	Peak T	pFWEcorr.	MNI coordinates (xyz)			Region (AAL)
High-fat > low-fat odor	470	6.92	<0.001	6	−36	44	Posterior cingulate cortex R
	462	5.95	<0.001	16	−56	30	Precuneus R
	145	5.69	0.046	−12	−64	28	Precuneus L
Food > non-food odor	121	6.13	0.069	14	15	54	Supplementary motor area R

All reported results were significant at uncorrected $p < 0.001$ and cluster size of $k > 66$ contiguous voxels across the whole brain. Abbreviations: FWEcorr., Family-Wise Error corrected; AAL, Automated Anatomical Labeling; MNI, Montreal Neurological Institute.

milkshake independent of sugar content involved in the PCC activation difference that predicts future weight loss (Yokum and Stice, 2019). In a recent study, Roux-en-Y gastric bypass surgery-induced decreased liking of high-fat/high-sugar food odors was accompanied by an increased precuneus activation (Zoon et al., 2018). Taken together, the activation of the precuneus in responses to high-fat food odors may be protective against future weight gain. However, other studies had shown the precuneus

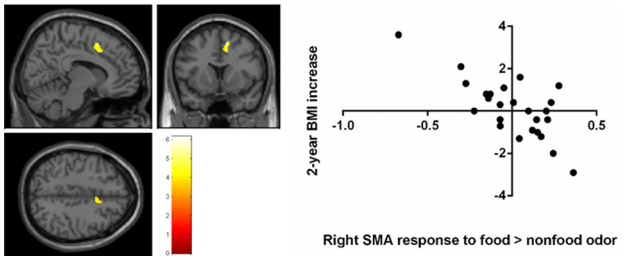

FIGURE 3 | Negative correlation between the 2-year BMI increase and the baseline brain responses to food vs. nonfood odors in the right supplementary motor area (SMA) Brain activation were significant with corrected $p < 0.05$ and were illustrated on a template provided in SPM12 (single_sub_T1.nni).

and PCC activation during imagination of eating (Yokum and Stice, 2013; Kiortsis et al., 2018) or reward/motivational processing of odors (Bragulat et al., 2008, 2010; Han et al., 2018b). Future work is necessary to elucidate the specific functioning mechanism of these regions behind the association between the activation during food cue processing and future weight changes.

Further, lower SMA activation in response to high-fat/low-sugar milkshake predicted later weight gain in adolescents (Stice and Yokum, 2018), which is in line with the current finding. The SMA had been frequently observed with food cue stimulation (Wagner et al., 2013), and was involved in cognitive reward control including food-related cues (Brandl et al., 2019). A recent meta-analysis of fMRI studies showed the recruitment of SMA activation when participants attempt to reduce their craving response to food cues (Han et al., 2018a). Besides, the SMA has been implicated in inhibitory processes (for meta-analyses, see Simmonds et al., 2008; Swick et al., 2011; Criaud and Boulinguez, 2013). To illustrate, Hollmann et al. (2012) found robust activation of the SMA during the downregulation of food desire using a cognitive reappraisal strategy compared to the "admit to food desire" condition. Stronger SMA activation was observed among successful vs. unsuccessful self-controllers during healthy food choices (van der Laan et al., 2014). An earlier study also showed increased SMA activation along with reduced pleasure during repeated food consumption (Small et al., 2001).

We did not observe significant activations of the reward-related brain regions (e.g., the striatum or insula) that predicted 2-year BMI or weight gain. A recent study using a bootstrap sampling approach had evaluated the reliability of the food-related neural responsivity as predictors for weight change among 10 bootstrap samples. An elevated response in the precentral gyrus/Rolandic operculum to images of appetizing foods turned out to be a moderately reliable predictor of future BMI gain (Stice and Yokum, 2018). However, the reward brain activation was less reliable (although one study found elevated responsivity of regions implicated in reward processing predicted future weight gain, see Geha et al., 2013). Our results further added to that by showing that brain activation of reward-related areas in response to appetitive food odors did not predict future BMI changes.

A major limitation of the current study was that important factors related to bodyweight alterations (e.g., regular physical activities, diet, stressors, metabolic alterations) were not followed during the 2-year follow-up, which affects the results cannot be ruled out. Besides, the dynamic changes of fat mass or lean tissues in the process of weight gain cannot be distinguished by the BMI values although BMI is widely used to assess excess adiposity and shows high test-retest reliability, it does not distinguish between increased fat mass and increased lean tissue mass, and hence can lead to significant misclassification (Prentice and Jebb, 2001). Moreover, the small sample size and motion artifacts during fMRI scanning may challenge the sensitivity and reliability of the current findings, longitudinal studies with larger sample size are warranted for looking into the structural and functional neural markers of weight change. Moreover, fMRI tasks such as the food odor Go/No-Go paradigm could further explore the neural predictors for future weight gain during specific processing of food odors (e.g., motivation or decision-making).

CONCLUSION

In sum, results from the current study suggest that 2-year BMI increase was associated with lower baseline brain activation of the precuneus and PCC in response to high-fat vs. low-fat food odor, and lower activation of the SMA in response to food vs. non-food odor. This research shows that there are long-term consequences of body weight changes in selective responsivity to odorous food cues.

DATA AVAILABILITY STATEMENT

The raw data supporting the conclusions of this article will be made available by the authors, without undue reservation.

ETHICS STATEMENT

The studies involving human participants were reviewed and approved by Ethics Board of the University of Dresden Medical School (#EK22012018). The patients/participants provided their written informed consent to participate in this study.

AUTHOR CONTRIBUTIONS

PH designed the study, performed the experiment, analyzed the data, and wrote the manuscript. TH and HC reviewed and revised the manuscript critically. All authors contributed to the article and approved the submitted version.

FUNDING

This work was supported by the fundamental research funds for the central universities (SWU019011) to PH.

REFERENCES

Boesveldt, S., and de Graaf, K. (2017). The differential role of smell and taste for eating behavior. *Perception* 46, 307–319. doi: 10.1177/0301006616685576

Boswell, R. G., and Kober, H. (2016). Food cue reactivity and craving predict eating and weight gain: a meta-analytic review. *Obes. Rev.* 17, 159–177. doi: 10.1111/obr.12354

Bragulat, V., Dzemidzic, M., Bruno, C., Cox, C. A., Talavage, T., Considine, R. V., et al. (2010). Food-related odor probes of brain reward circuits during hunger: a pilot FMRI study. *Obesity (Silver Spring)* 18, 1566–1571. doi: 10.1038/oby.2010.57

Bragulat, V., Dzemidzic, M., Talavage, T., Davidson, D., O'Connor, S. J., and Kareken, D. A. (2008). Alcohol sensitizes cerebral responses to the odors of alcoholic drinks: an fMRI study. *Alcohol Clin. Exp. Res.* 32, 1124–1134. doi: 10.1111/j.1530-0277.2008.00693.x

Brandl, F., Le Houcq Corbi, Z., Mulej Bratec, S., and Sorg, C. (2019). Cognitive reward control recruits medial and lateral frontal cortices, which are also involved in cognitive emotion regulation: a coordinate-based meta-analysis of fMRI studies. *NeuroImage* 200, 659–673. doi: 10.1016/j.neuroimage.2019.07.008

Buckner, R. L., Andrews-Hanna, J. R., and Schacter, D. L. (2008). The brain's default network: anatomy, function, and relevance to disease. *Ann. N Y Acad. Sci.* 1124, 1–38. doi: 10.1196/annals.1440.011

Cavanna, A. E., and Trimble, M. R. (2006). The precuneus: a review of its functional anatomy and behavioural correlates. *Brain* 129, 564–583. doi: 10.1093/brain/awl004

Criaud, M., and Boulinguez, P. (2013). Have we been asking the right questions when assessing response inhibition in go/no-go tasks with fMRI? A meta-analysis and critical review. *Neurosci. Biobehav. Rev.* 37, 11–23. doi: 10.1016/j.neubiorev.2012.11.003

Croy, I., Schulz, M., Blumrich, A., Hummel, C., Gerber, J., and Hummel, T. (2014). Human olfactory lateralization requires trigeminal activation. *NeuroImage* 98, 289–295. doi: 10.1016/j.neuroimage.2014.05.004

Demos, K. E., Heatherton, T. F., and Kelley, W. M. (2012). Individual differences in nucleus accumbens activity to food and sexual images predict weight gain and sexual behavior. *J. Neurosci.* 32, 5549–5552. doi: 10.1523/JNEUROSCI.5958-11.2012

Eiler, W. J. II., Dzemidzic, M., Case, K. R., Considine, R. V., and Kareken, D. A. (2012). Correlation between ventromedial prefrontal cortex activation to food aromas and cue-driven eating: an fMRI study. *Chemosens. Percept.* 5, 27–36. doi: 10.1007/s12078-011-9112-6

Epstein, L. H., Yokum, S., Feda, D. M., and Stice, E. (2014). Food reinforcement and parental obesity predict future weight gain in non-obese adolescents. *Appetite* 82C, 138–142. doi: 10.1016/j.appet.2014.07.018

Flohr, E. L., Arshamian, A., Wieser, M. J., Hummel, C., Larsson, M., Muhlberger, A., et al. (2014). The fate of the inner nose: odor imagery in patients with olfactory loss. *Neuroscience* 268, 118–127. doi: 10.1016/j.neuroscience.2014.03.018

Gearhardt, A. N., Yokum, S., Harris, J. L., Epstein, L. H., and Lumeng, J. C. (2020). Neural response to fast food commercials in adolescents predicts intake. *Am. J. Clin. Nutr.* 111, 493–502. doi: 10.1093/ajcn/nqz305

Geha, P. Y., Aschenbrenner, K., Felsted, J., O'Malley, S. S., and Small, D. M. (2013). Altered hypothalamic response to food in smokers. *Am. J. Clin. Nutr.* 97, 15–22. doi: 10.3945/ajcn.112.043307

Giuliani, N. R., Merchant, J. S., Cosme, D., and Berkman, E. T. (2018). Neural predictors of eating behavior and dietary change. *Ann. N Y Acad. Sci.* 142, 208–220. doi: 10.1111/nyas.13637

Han, J. E., Boachie, N., Garcia-Garcia, I., Michaud, A., and Dagher, A. (2018a). Neural correlates of dietary self-control in healthy adults: a meta-analysis of functional brain imaging studies. *Physiol. Behav.* 192, 98–108. doi: 10.1016/j.physbeh.2018.02.037

Han, J. E., Frasnelli, J., Zeighami, Y., Larcher, K., Boyle, J., McConnell, T., et al. (2018b). Ghrelin enhances food odor conditioning in healthy humans: an fMRI study. *Cell Rep.* 25, 2643–2652. doi: 10.1016/j.celrep.2018.11.026

Han, P., Mohebbi, M., Seo, H. S., and Hummel, T. (2020). Sensitivity to sweetness correlates to elevated reward brain responses to sweet and high-fat food odors in young healthy volunteers. *NeuroImage* 208:116413. doi: 10.1016/j.neuroimage.2019.116413

Hermann, P., Gál, V., Kóbor, I., Kirwan, C. B., Kovács, P., Kitka, T., et al. (2019). Efficacy of weight loss intervention can be predicted based on early alterations of fMRI food cue reactivity in the striatum. *Neuroimage Clin.* 23:101803. doi: 10.1016/j.nicl.2019.101803

Herwig, U., Dhum, M., Hittmeyer, A., Opialla, S., Scherpiet, S., Keller, C., et al. (2016). Neural signaling of food healthiness associated with emotion processing. *Front. Aging Neurosci.* 8:16. doi: 10.3389/fnagi.2016.00016

Hollmann, M., Hellrung, L., Pleger, B., Schlogl, H., Kabisch, S., Stumvoll, M., et al. (2012). Neural correlates of the volitional regulation of the desire for food. *Int. J. Obes.* 36, 648–655. doi: 10.1038/ijo.2011.125

Hu, S., Wang, L., Yang, D., Li, L., Togo, J., Wu, Y., et al. (2018). Dietary fat, but not protein or carbohydrate, regulates energy intake and causes adiposity in mice. *Cell Metab.* 28, 415.e4–431.e4. doi: 10.1016/j.cmet.2018.06.010

Hummel, T., Sekinger, B., Wolf, S. R., Pauli, E., and Kobal, G. (1997). 'Sniffin' Sticks': olfactory performance assessed by the combined testing of odor identification, odor discrimination and olfactory threshold. *Chem. Senses* 22, 39–52. doi: 10.1093/chemse/22.1.39

Kareken, D. A., Sabri, M., Radnovich, A. J., Claus, E., Foresman, B., Hector, D., et al. (2004). Olfactory system activation from sniffing: effects in piriform and orbitofrontal cortex. *NeuroImage* 22, 456–465. doi: 10.1016/j.neuroimage.2004.01.008

Kiortsis, D. N., Spyridonos, P., Margariti, P. N., Xydis, V., Alexiou, G., Astrakas, L. G., et al. (2018). Brain activation during repeated imagining of chocolate consumption: a functional magnetic resonance imaging study. *Hormones* 17, 367–371. doi: 10.1007/s42000-018-0053-1

Kobal, G. (1981). *Elektrophysiologische Untersuchungen des Menschlichen Geruchssinns.* Stuttgart: Thieme Verlag.

Larsen, J. K., Hermans, R. C., and Engels, R. C. (2012). Food intake in response to food-cue exposure. Examining the influence of duration of the cue exposure and trait impulsivity. *Appetite* 58, 907–913. doi: 10.1016/j.appet.2012.02.004

Morquecho-Campos, P., Bikker, F. J., Nazmi, K., de Graaf, K., Laine, M. L., and Boesveldt, S. (2019). Impact of food odors signaling specific taste qualities and macronutrient content on saliva secretion and composition. *Appetite* 143:104399. doi: 10.1016/j.appet.2019.104399

Mozaffarian, D., Hao, T., Rimm, E. B., Willett, W. C., and Hu, F. B. (2011). Changes in diet and lifestyle and long-term weight gain in women and men. *N. Engl. J. Med.* 364, 2392–2404. doi: 10.1056/NEJMoa1014296

Murdaugh, D. L., Cox, J. E., Cook, E. W. III., and Weller, R. E. (2012). fMRI reactivity to high-calorie food pictures predicts short- and long-term outcome in a weight-loss program. *NeuroImage* 59, 2709–2721. doi: 10.1016/j.neuroimage.2011.10.071

Plailly, J., Delon-Martin, C., and Royet, J. P. (2012). Experience induces functional reorganization in brain regions involved in odor imagery in perfumers. *Hum. Brain Mapp.* 33, 224–234. doi: 10.1002/hbm.21207

Prentice, A. M., and Jebb, S. A. (2001). Beyond body mass index. *Obes. Rev.* 2, 141–147. doi: 10.1046/j.1467-789x.2001.00031.x

Proserpio, C., Invitti, C., Boesveldt, S., Pasqualinotto, L., Laureati, M., Cattaneo, C., et al. (2019). Ambient odor exposure affects food intake and sensory specific appetite in obese women. *Front. Psychol.* 10:7. doi: 10.3389/fpsyg.2019.00007

Simmonds, D. J., Pekar, J. J., and Mostofsky, S. H. (2008). Meta-analysis of Go/No-go tasks demonstrating that fMRI activation associated with response inhibition is task-dependent. *Neuropsychologia* 46, 224–232. doi: 10.1016/j.neuropsychologia.2007.07.015

Small, D. M., Gerber, J. C., Mak, Y. E., and Hummel, T. (2005). Differential neural responses evoked by orthonasal versus retronasal odorant perception in humans. *Neuron* 47, 593–605. doi: 10.1016/j.neuron.2005.07.022

Small, D. M., Zatorre, R. J., Dagher, A., Evans, A. C., and Jones-Gotman, M. (2001). Changes in brain activity related to eating chocolate: from pleasure to aversion. *Brain* 124, 1720–1733. doi: 10.1093/brain/124.9.1720

Sommer, J. U., Maboshe, W., Griebe, M., Heiser, C., Hormann, K., Stuck, B. A., et al. (2012). A mobile olfactometer for fMRI-studies. *J. Neurosci. Methods* 209, 189–194. doi: 10.1016/j.jneumeth.2012.05.026

Song, X. W., Dong, Z. Y., Long, X. Y., Li, S. F., Zuo, X. N., Zhu, C. Z., et al. (2011). REST: a toolkit for resting-state functional magnetic resonance imaging data processing. *PLoS One* 6:e25031. doi: 10.1371/journal.pone.0025031

Sorokowska, A., Schoen, K., Hummel, C., Han, P., Warr, J., and Hummel, T. (2017). Food-related odors activate dopaminergic brain areas. *Front. Hum. Neurosci.* 11:625. doi: 10.3389/fnhum.2017.00625

Stevenson, R. J., and Boakes, R. A. (2004). "Sweet and sour smells: learned synesthesia between the senses of taste and smell," in *The Handbook of Multisensory Processes*, eds G. A. Calvert, C. Spence and B. E. Stein (Cambridge, MA: MIT Press), 69–83.

Stice, E., Burger, K. S., and Yokum, S. (2015). Reward region responsivity predicts future weight gain and moderating effects of the TaqIA allele. *J. Neurosci.* 35, 10316–10324. doi: 10.1523/JNEUROSCI.3607-14.2015

Stice, E., and Yokum, S. (2016). Neural vulnerability factors that increase risk for future weight gain. *Psychol. Bull.* 142, 447–471. doi: 10.1037/bul0000044

Stice, E., and Yokum, S. (2018). Relation of neural response to palatable food tastes and images to future weight gain: using bootstrap sampling to examine replicability of neuroimaging findings. *NeuroImage* 183, 522–531. doi: 10.1016/j.neuroimage.2018.08.035

Stunkard, A. J., and Messick, S. (1985). The three-factor eating questionnaire to measure dietary restraint, disinhibition and hunger. *J. Psychosom. Res.* 29, 71–83. doi: 10.1016/0022-3999(85)90010-8

Swick, D., Ashley, V., and Turken, U. (2011). Are the neural correlates of stopping and not going identical? Quantitative meta-analysis of two response inhibition tasks. *NeuroImage* 56, 1655–1665. doi: 10.1016/j.neuroimage.2011.02.070

Tuulari, J. J., Karlsson, H. K., Hirvonen, J., Salminen, P., Nuutila, P., and Nummenmaa, L. (2015). Neural circuits for cognitive appetite control in healthy and obese individuals: an fMRI study. *PLoS One* 10:e0116640. doi: 10.1371/journal.pone.0116640

Tzourio-Mazoyer, N., Landeau, B., Papathanassiou, D., Crivello, F., Etard, O., Delcroix, N., et al. (2002). Automated anatomical labeling of activations in SPM using a macroscopic anatomical parcellation of the MNI MRI single-subject brain. *NeuroImage* 15, 273–289. doi: 10.1006/nimg.2001.0978

van der Laan, L. N., de Ridder, D. T. D., Viergever, M. A., and Smeets, P. A. M. (2014). Activation in inhibitory brain regions during food choice correlates with temptation strength and self-regulatory success in weight—concerned women. *Front. Neurosci.* 8:308. doi: 10.3389/fnins.2014.00308

Wagner, D. D., Altman, M., Boswell, R. G., Kelley, W. M., and Heatherton, T. F. (2013). Self-regulatory depletion enhances neural responses to rewards and impairs top-down control. *Psychol. Sci.* 24, 2262–2271. doi: 10.1177/0956797613492985

Wallrabenstein, I., Gerber, J., Rasche, S., Croy, I., Kurtenbach, S., Hummel, T., et al. (2015). The smelling of Hedione results in sex-differentiated human brain activity. *NeuroImage* 113, 365–373. doi: 10.1016/j.neuroimage.2015.03.029

Winter, S. R., Yokum, S., Stice, E., Osipowicz, K., and Lowe, M. R. (2017). Elevated reward response to receipt of palatable food predicts future weight variability in healthy-weight adolescents. *Am. J. Clin. Nutr.* 105, 781–789. doi: 10.3945/ajcn.116.141143

Yokum, S., Gearhardt, A. N., Harris, J. L., Brownell, K. D., and Stice, E. (2014). Individual differences in striatum activity to food commercials predict weight gain in adolescents. *Obesity* 22, 2544–2551. doi: 10.1002/oby.20882

Yokum, S., Ng, J., and Stice, E. (2011). Attentional bias to food images associated with elevated weight and future weight gain: an fMRI study. *Obesity* 19, 1775–1783. doi: 10.1038/oby.2011.168

Yokum, S., and Stice, E. (2013). Cognitive regulation of food craving: effects of three cognitive reappraisal strategies on neural response to palatable foods. *Int. J. Obes.* 37, 1565–1570. doi: 10.1038/ijo.2013.39

Yokum, S., and Stice, E. (2019). Weight gain is associated with changes in neural response to palatable food tastes varying in sugar and fat and palatable food images: a repeated-measures fMRI study. *Am. J. Clin. Nutr.* 110, 1275–1286. doi: 10.1093/ajcn/nqz204

Zoon, H. F., de Graaf, C., and Boesveldt, S. (2016). Food odours direct specific appetite. *Foods* 5:12. doi: 10.1016/j.appet.2016.02.061

Zoon, H. F. A., de Bruijn, S. E. M., Smeets, P. A. M., de Graaf, C., Janssen, I. M. C., Schijns, W., et al. (2018). Altered neural responsivity to food cues in relation to food preferences, but not appetite-related hormone concentrations after RYGB-surgery. *Behav. Brain Res.* 353, 194–202. doi: 10.1016/j.bbr.2018.07.016

Conflict of Interest: The authors declare that the research was conducted in the absence of any commercial or financial relationships that could be construed as a potential conflict of interest.

frontiers in Human Neuroscience

ORIGINAL RESEARCH
published: 19 October 2020
doi: 10.3389/fnhum.2020.578578

Pancreatic Polypeptide but Not Other Members of the Neuropeptide Y Family Shows a Moderate Association With Perceived Anxiety in Obese Men

Selina Johanna Schaper[1]†, Tobias Hofmann[1†], Ellen Wölk[1], Elena Weibert[1], Matthias Rose[1,2] and Andreas Stengel[1,3]**

[1] Department for Psychosomatic Medicine, Charité Center for Internal Medicine and Dermatology, Charité-Universitätsmedizin, Corporate Member of Freie Universität Berlin, Humboldt-Universität zu Berlin, and Berlin Institute of Health, Berlin, Germany, [2] Department of Quantitative Health Sciences, University of Massachusetts Medical School, Worcester, MA, United States, [3] Department of Psychosomatic Medicine and Psychotherapy, Medical University Hospital Tübingen, Tübingen, Germany

OPEN ACCESS

Edited by:
Kiyoshi Nakahara,
Kochi University of Technology, Japan

Reviewed by:
Aitak Farzi,
Medical University of Graz, Austria
Nigel Irwin,
Ulster University, United Kingdom

***Correspondence:**
Selina Johanna Schaper
selina.schaper@charite.de
Andreas Stengel
andreas.stengel@med.uni-tuebingen.de

[†] These authors have contributed equally to this work

Specialty section:
This article was submitted to Health, a section of the journal Frontiers in Human Neuroscience

Received: 30 June 2020
Accepted: 22 September 2020
Published: 19 October 2020

Citation:
Schaper SJ, Hofmann T, Wölk E, Weibert E, Rose M and Stengel A (2020) Pancreatic Polypeptide but Not Other Members of the Neuropeptide Y Family Shows a Moderate Association With Perceived Anxiety in Obese Men. Front. Hum. Neurosci. 14:578578. doi: 10.3389/fnhum.2020.578578

Neuropeptide Y (NPY), peptide tyrosine tyrosine (PYY), and pancreatic polypeptide (PP) are important mediators in the bidirectional communication along the gut-brain-axis. Best known for their role in the regulation of appetite and food intake they are considered to play a crucial role in the development of obesity. Additionally, mounting evidence indicates a regulatory function in anxiety, mood and stress resilience with potential sex differences. In the present study, we examined the associations of NPY, PYY, and PP plasma levels with anxiety, depressiveness and perceived stress in obese patients. We analyzed 144 inpatients (90 female, 54 male, BMI mean: 49.4 kg/m^2) in a naturalistic treatment setting for obesity and its somatic and mental comorbidities. Fasting blood samples were taken, and patients completed psychometric self-assessment questionnaires (GAD-7, PHQ-9, PSQ-20) within the first week after admission and before discharge. Plasma concentrations of the peptides were measured by ELISA. Women showed significant higher anxiety (GAD-7: 8.13 ± 5.67 vs. 5.93 ± 5.42, $p = 0.04$) and stress scores (PSQ-20: 52.62 ± 23.5 vs. 41.23 ± 22.53, $p = 0.01$) than men. In the longitudinal analysis women with a clinically relevant improvement of anxiety (≥ 5 points on GAD-7, $p < 0.001$) also showed significant improvements in depression (PHQ-9: 38%, $p = 0.002$) and PSQ-20 scores (23%, $p = 0.005$) while anxiety-improved male patients only improved in the subscale *tension* of the PSQ-20 (34%, $p = 0.02$). In men we observed a positive correlation of PP with anxiety scores (GAD-7: $r = 0.41$, $p = 0.007$) and with age ($r = 0.49$, $p = 0.001$) on admission while NPY negatively correlated with age ($r = -0.38$, $p = 0.01$). In contrast, there were no significant associations ($p > 0.05$) in female subjects in the cross-sectional as well as in the longitudinal analysis. In conclusion, women suffering from morbid obesity showed

greater psychological comorbidity and considerable interactions among them. Despite that we solely observed associations of PP with anxiety and age with NPY and PP in men, suggesting a possible influence of sex hormones on the NPY system. However, improvement of anxiety scores did not lead to significant changes in NPY.

Keywords: brain-gut axis, depression, eating disorder, gut-brain axis, obesity, psychosomatic, stress, peptide YY

INTRODUCTION

Obesity, defined by the WHO as a body mass index (BMI) $\geq$ 30 kg/m^2 (World Health Organisation [WHO], 2020), is one of the major health problems of the 21st century. In recent years its prevalence has increased dramatically and thus became a global epidemic (NCDRF, 2016). Obesity is often accompanied by other health implications including a number of preventable chronic illnesses such as diabetes, cardiovascular diseases and cancer that are among the leading causes of death (GBD 2015 Obesity Collaborators Afshin et al., 2017). The concept of energy imbalance with excess dietary calories is considered to play a pivotal role in the development of obesity. In modern societies prevails the unrestricted availability of food and, therefore, human food consumption cannot solely be attributed to self-preservation. Emerging evidence suggests a strong impact of hedonic mechanisms in the control of food intake which involves cognitive, reward and emotional processes (Horwath et al., 2020).

Eating behavior is regulated by the gut-brain axis, the bidirectional communication between the central (CNS) and the enteric nervous system. Neural (Strandwitz, 2018), immunological (Fung et al., 2017), endocrine (Kuhne and Stengel, 2019) and gut microbiota-derived (Torres-Fuentes et al., 2017) messengers are closely interrelated in the regulation of appetite and food intake. Neuropeptide Y (NPY), peptide tyrosine tyrosine (PYY) and pancreatic polypeptide (PP) represent a family of peptide hormones consisting of 36 amino acids. In humans, these peptides act with particular affinities *via* four subtypes of G-protein-coupled receptors (Y1, Y2, Y4, Y5) (Pedragosa-Badia et al., 2013) as important mediators along the gut-brain axis. NPY is one of the most potent orexigenic peptides that is abundantly expressed within the central and peripheral nervous system (PNS) (Holzer et al., 2012). Centrally, NPY displays its highest expression within hypothalamic nuclei (Bai et al., 1985), particularly the arcuate nucleus (ARC) that plays a key role in the regulation of hunger and satiety (Myers and Olson, 2012). Within the gastrointestinal tract, the primary source of NPY originates from enteric neurons (Cox, 2007). NPY is known to influence several processes involved in energy homeostasis, including energy intake and expenditure, physical activity and adipose tissue function (Loh et al., 2015). PP and PYY are postprandially released gut-derived peptides that inhibit food intake (Field et al., 2010). PYY_{3-36}, the biologically active form accountable for its anorexigenic effects, is mainly produced by intestinal L cells, whereas PP is synthesized by endocrine F cells of the pancreatic islets (Ekblad and Sundler, 2002). The release of both peptides occurs proportionally to the preceding caloric intake (Adrian et al., 1976, 1985) and leads to the inhibition of orexigenic pathways in the hypothalamus (Shi et al., 2013). PYY inhibits the release of NPY in the ARC *via* Y2 receptors (Ghamari-Langroudi et al., 2005), while PP preferably binds to Y4 receptors to modulate vagal cholinergic pathways in the brainstem (McTigue et al., 1997) and the expression of several hypothalamic feeding-regulatory peptides (Asakawa et al., 2003; Lin et al., 2009). Reduced circulating PYY (Batterham et al., 2003) and PP (Marco et al., 1980) as well as elevated NPY (Baltazi et al., 2011) levels which can be found in obese subjects give rise to a role in the pathophysiology of obesity.

Besides controlling ingestion and energy homeostasis the NPY family also appears to have an impact on emotional-affective behavior. Chronic psychosocial stress is frequently linked to obesity and metabolic disorders (Scott et al., 2012). Mounting evidence indicates that NPY might promote some of the underlying pathomechanisms. Particularly, stress-induced sympathetic, glucocorticoid and hypothalamic activity leads to upregulated NPY expression which in turn results in increased food intake (Zakrzewska et al., 1999) and growth of abdominal fat (Kuo et al., 2007). In addition, postprandial PYY secretion is inhibited under conditions of psychological stress (Kiessl and Laessle, 2016). Moreover, NPY and its receptors are broadly expressed in brain areas, e.g., amygdala and the prefrontal cortex, that mediate stress resilience (Kask et al., 2002).

Anxiety is a fundamental response to stress. In rodents, NPY exerts anxiolytic effects in the amygdala, primarily *via* Y1 receptor activation (Sajdyk et al., 1999), although other receptors might be involved as well (Fendt et al., 2009). On the contrary, stimulation of the Y2 receptor promotes an anxiogenic response (Sajdyk et al., 2002) presumably due to presynaptic inhibition of NPY release (Caberlotto et al., 2000). In humans it was found that genetic variations with low-expression NPY genotypes display a maladaptive responsiveness to stress that predispose to major depression (Mickey et al., 2011) and anxiety disorders (Amstadter et al., 2010). Animal studies indicate an implication of PP and PYY in mediating regulation of emotion, however, the underlying pathways remain elusive. While the deletion of PYY increases depression-like behavior but does not affect anxiety (Painsipp et al., 2011), peripherally administered PP promotes extinction learning of cued fear by acting on central Y4 receptors in mice (Verma et al., 2016). However, intracerebroventricular (icv) injection of PP does not affect anxiety (Asakawa et al., 1999) and it is unclear whether PP is generally produced in the brain (DiMaggio et al., 1985).

Mood and anxiety disorders are common comorbidities among obese patients (Rajan and Menon, 2017) and their joint occurrence is related to poorer physical and mental quality of life (QoL) (Nigatu et al., 2016). The

exact mechanisms of this association still warrant further investigation of the signaling pathways involved. This is crucial to provide a better understanding and potential treatment options. Therefore, in the present study we investigated the relationship between circulating levels of the members of the NPY family (NPY, PYY, PP) and psychometrically evaluated anxiety, depressiveness and perceived stress in obese psychosomatic patients.

MATERIALS AND METHODS

Subjects

Within the course of a consecutive biosampling study 144 obese inpatients (54 male, 90 female) who received medical treatment for obesity-related somatic and mental comorbidities were recruited upon admission to the Department of Psychosomatic Medicine at Charité - Universitätsmedizin Berlin (between September 2010 and December 2015). All patients were at the age of $\geq$ 18 years and met the criteria for obesity with a body mass index (BMI) $\geq$ 30 kg/m^2. Their treatment consisted of biomedical therapy, individually adapted therapeutic exercise and both individual and group psychotherapy as well as music and art therapy. Patients with current pregnancy or malignant disease, psychotic disorders, somatoform disorders of the gastrointestinal system, preceding bariatric surgery, hypercortisolism and untreated hypothyroidism were excluded from the study.

All patients gave written informed consent. Investigations were conducted in accordance with the Declaration of Helsinki; the study was approved by the institutional ethics committee of the Charité - Universitätsmedizin Berlin (protocol number: EA1/114/10).

Laboratory Analyses

Venous blood samples were taken after an overnight fast between 7:00 and 8:00 AM within the first week after admission (T0) and at a second time point during treatment (Tx). Patients were advised not to smoke or exercise and only to have a small amount of water before blood withdrawal. Circulating glucose levels were determined by photometric measurement from blood collection tubes containing sodium fluoride that were kept at room temperature. Blood for measuring peptide concentrations was collected in pre-cooled standard EDTA tubes prepared with aprotinin (1.2 Trypsin Inhibitory Unit per 1 ml blood; ICN Pharmaceuticals, Costa Mesa, CA, United States) for peptidase inhibition. After blood withdrawal the tubes were stored on ice and centrifuged for 10 min at 3000 rpm at 4°C. Plasma was separated and samples were stored at −80°C until further processing. NPY, PYY and PP levels were determined using a commercial enzyme-linked immunosorbent assay (ELISA, catalog # EK-049-03, EK-059-02 and EK-054-02, Phoenix Pharmaceuticals, Inc., Burlingame, CA, United States). According to the manufacturer's information there is no cross-reactivity (0%) between the respective peptide antigens. All samples were processed in one batch; the intra-assay variability was 8, 5, and 5%, respectively.

Anthropometric Measurements

Body weight and height were assessed at the same day of blood withdrawal in patients wearing light underwear and BMI was calculated as kg/m^2. Medications and existence of comorbidities were recorded at admission and after hospital discharge.

Psychometric Parameters

For psychometric assessment patients were asked to complete the following questionnaires and results obtained between two days before and five days after the respective blood withdrawals were accepted. Two modules of the self-administered patient health questionnaire (PHQ) (Spitzer et al., 1999) were used for the assessment of anxiety (GAD-7) and depression (PHQ-9).

The generalized anxiety disorder questionnaire (GAD-7) consists of seven items with scores ranging from "0" (not at all) to "3" (nearly every day) with a maximum of 21 points (Spitzer et al., 1999). The GAD-7 is an efficient tool to measure general anxiety disorder and is also suited to detect symptoms of social anxiety, posttraumatic stress and panic disorder (Spitzer et al., 2006). In the present study we used the German version (Lowe et al., 2008) that showed an internal consistency (Cronbach's α) of 0.90.

The PHQ-9 depression scale is a 9-item screening instrument for the diagnosis of major depression and the evaluation of the severity of depressive symptoms. Total scores range from 0–27, while the nine items represent the DSM-IV diagnostic criteria for depressive disorders (Spitzer et al., 1999). Our patients were handed out the German version by Löwe et al. (2002). Cronbach's α in the present sample was determined as 0.88. In a meta-analysis of 17 validation studies in different languages including the German language translation, specificity was 0.92 and sensitivity 0.80 for the diagnosis of a major depressive disorder (Gilbody et al., 2007).

Evaluation of perceived stress was conducted by using the revised 20-item German version (PSQ-20) (Fliege et al., 2005) of the perceived stress questionnaire (PSQ; 30 items) (Levenstein et al., 1993). Providing four subscales the PSQ assesses "worries," "tension," "joy" as stress responses and "demands" as perception of external stressors and thereby emphasizes the subjective experience of stress. In the present sample Cronbach's alpha for the subscales ranged from 0.84 to 0.91.

Statistical Analyses

Data are expressed as mean ± standard deviation (SD). Normal distribution was evaluated by the Kolmogorov-Smirnov test. Differences between groups were calculated using t-tests and chi-square tests. Pearson's correlation was calculated to assess associations of two variables. Statistical differences and correlations were considered significant when $p < 0.05$. All statistical analyses were conducted using Sigma Stat 3.1 (Systat Software, San Jose, CA, United States).

RESULTS

Demographic, Socioeconomic and Medical Characteristics

The mean observation period between first (T0) and second (Tx) blood sample and psychometric assessment was 2.3 ± 1.2 weeks (range: 1–7 weeks). Demographic and socioeconomic characteristics as well as comorbidities and current medications of the study population are presented in **Table 1**. In the whole study sample mean age was 46.2 ± 13.4 with a range of 19–73 years and mean BMI was 49.1 ± 9.3 kg/m^2. Men and women did not differ regarding BMI (48.5 ± 9.3 vs. 49.5 ± 9.3 kg/m^2, $p = 0.528$), age (47.0 ± 14.1 vs. 45.7 ± 13.0 years, $p = 0.592$) and socioeconomic characteristics ($p > 0.050$; **Table 1**). However, significant sex differences were observed in the prevalence of obesity-related comorbid conditions and medication. More precisely, sleep-associated breathing disorder ($p = 0.011$), hypertriglyceridemia ($p = 0.007$), fatty liver disease ($p = 0.031$) and type 2 diabetes that requires insulin treatment ($p = 0.014$) were more frequent in men. Psychopharmacological medication was given to 33.3% of the study population with selective serotonin reuptake inhibitors (SSRI) and selective serotonin-norepinephrine reuptake inhibitors (SNRI) being the most frequent pharmaceuticals (19.4%).

Baseline Patient-Reported Outcomes

In the cross-sectional analysis women showed significant higher levels of anxiety (8.13 ± 5.67 vs. 5.93 ± 5.42, $p = 0.038$) and perceived stress total scores (52.62 ± 23.5 vs. 41.23 ± 22.53, $p = 0.010$) than men (**Table 2**). This also applied for the PSQ-20 subscales "worries" ($p = 0.005$), "tension" ($p = 0.015$) and "demands" ($p = 0.035$) but not for the subscale "joy" ($p = 0.110$), while all stress subscales highly correlated with each another in both sexes ($p < 0.001$).

Associations of Peptides With Age and Anxiety

We observed a positive correlation between PP and PYY in men ($r = 0.430$, $p = 0.004$) and women ($r = 0.843$, $p < 0.001$) while NPY and PYY ($r = 0.336$, $p < 0.030$) were associated solely in the male study population. On admission, in men age was negatively associated with NPY ($r = -0.378$, $p = 0.011$) and positively correlated with PP ($r = 0.492$, $p < 0.001$; data not shown). Male subjects also displayed a positive correlation of PP with GAD-7 scores ($r = 0.411$, $p < 0.007$), while NPY and PYY did not (**Figure 1**). In women neither NPY, PYY nor PP correlated with GAD-7 scores (**Figure 1**).

Potential Confounders

Fasting blood glucose did not significantly differ between male and female patients ($p = 0.200$). Moreover, we did not find any correlations between peptides and blood glucose levels in male (NPY: $r = -0.014$, $p = 0.375$; PYY: $r = 0.064$, $p = 0.688$; PP: $r = 0.131$, $p = 0.408$) nor female subjects (NPY: $r = 0.031$, $p = 0.804$; PYY: $r = 0.149$, $p = 0.225$; PP: $r = 0.182$, $p = 0.137$). In the whole sample 7 (4.68%) patients were taking dipeptidyl peptidase-4 (DPP4) antagonists as treatment for type 2 diabetes (**Table 1**). Male subjects taking DPP4-inhibitors displayed significantly lower NPY plasma concentrations ($p = 0.018$) compared to patients without. After exclusion of subjects taking

TABLE 1 | Demographic and socioeconomic characteristics, comorbidities and medication of study patients.

Parameter	Whole population ($n = 144$)	Women ($n = 90$)	Men ($n = 54$)	*P*
Age (years)	46.2 ± 13.4	45.7 ± 13.0	47.0 ± 14.1	0.592
BMI (kg/m^2)	49.1 ± 9.28	49.5 ± 9.28	48.5 ± 9.33	0.528
Socioeconomic characteristics				
Living in a partnership	66 (45.8%)	41 (45.6%)	25 (46.3%)	0.931
Level of education				0.76
University entrance diploma	27 (18.8%)	13 (14.4%)	14 (25.9%)	
Vocational diploma	9 (6.25%)	6 (6.67%)	3 (5.56%)	0.444
Secondary education certificate	58 (40.3%)	44 (48.9%)	14 (25.9%)	0.897
Basic school qualification	42 (29.2%)	23 (25.6%)	19 (35.2%)	
No school-leaving qualification	8 (5.56%)	4 (4.44%)	4 (7.41%)	
Currently employed	51 (35.4%)	34 (37.8%)	17 (31.5%)	
Unemployment during past 5 years	65 (45.1%)	41 (45.6%)	24 (44.4%)	
Comorbidities				
Binge eating disorder	21 (14.6%)	15 (16.7%)	6 (11.1%)	0.334
Sleep-associated breathing disorder	74 (51.4%)	38 (42.2%)	36 (66.7%)	**0.011**
Type 2 diabetes mellitus	49 (34.0%)	27 (30.0%)	22 (40.7%)	0.188
Arterial hypertension	96 (66.7%)	56 (62.2%)	40 (74.1%)	0.144
Hypercholesterinemia	87 (60.4%)	54 (60.0%)	33 (61.1%)	0.895
Hypertriglyceridemia	40 (27.8%)	18 (20.0%)	22 (40.7%)	**0.007**
Hyperuricemia	65 (45.1%)	37 (41.1%)	28 (51.9%)	0.21
Fatty liver disease	91 (63.2%)	53 (58.9%)	38 (70.4%)	**0.031**
Medication				
Insulin	15 (10.4%)	5 (5.56%)	10 (15.1%)	**0.014**
DPP4 inhibitors/GLP-1 analog	7 (4.86%)	3 (3.33%)	4 (7.41%)	0.271
Antidiabetics (other)	26 (18.1%)	16 (17.8%)	10 (18.5%)	0.911
Psychopharmacological treatment	48 (33.3%)	34 (37.8%)	14 (25.9%)	0.144
Neuroleptics	17 (11.8%)	11 (12.2%)	6 (11.1%)	0.841
SSRI/SNRI	28 (19.4%)	21 (23.3%)	7 (13.0%)	0.128
Tricyclic antidepressants	12 (8.33%)	10 (11.1%)	2 (3.70%)	0.12
Other antidepressants	10 (6.94%)	7 (7.78%)	3 (5.56%)	0.612
Tranquilizers, sedatives, hypnotics	3 (2.08%)	2 (2.22%)	1 (1.85%)	0.88
Other psychopharmacological medication	7 (4.86%)	4 (4.44%)	3 (5.56%)	0.764

Statistical analysis: Data are expressed as mean ± standard deviation. Differences between two groups were assessed using the t-test or chi-square test. Significant differences are displayed in bold. BMI, body mass index; DPP4, dipeptidyl peptidase-4; GLP-1, glucagon-like peptide-1; SNRI, serotonin-norepinephrine reuptake inhibitor; SSRI, selective serotonin reuptake inhibitor.

TABLE 2 | Endocrine and psychometric parameters in the cross-sectional analysis according to sex.

Parameter	Whole population (*n*= 122)	Women (*n*=77)	Men (*n*=45)	*P*
NPY (ng/ml)	1.31 ± 0.56	1.33 ± 0.57	1.29 ± 0.57	0.701
PP (ng/ml)	1.66 ± 0.72	1.66 ± 0.68	1.67 ± 0.78	0.929
PYY (ng/ml)	1.28 ± 0.40	1.31 ± 0.41	1.22 ± 0.37	0.244
Fasting glucose (mg/dl) (women: *n* = 68; men: *n* = 42)	113.8 ± 40.5	108.8 ± 35.7	121.8 ± 46.7	0.104
GAD-7	7.32 ± 5.66	8.13 ± 5.67	5.93 ± 5.42	**0.038**
PSQ-20 total	48.4 ± 23.7	52.6 ± 23.5	41.2 ± 22.5	**0.01**
- Worries	46.5 ± 28.6	52.0 ± 28.4	37.2 ± 26.7	**0.005**
- Tension	50.9 ± 28.1	55.6 ± 27.7	42.8 ± 27.3	**0.015**
- Joy	44.8 ± 26.5	41.8 ± 27.0	49.8 ± 25.3	0.11
- Demands	41.0 ± 23.7	44.8 ± 23.5	34.7 ± 24.6	**0.035**

Statistical analysis: Data are expressed as mean ± standard deviation. Differences between two groups were assessed using the t-test. Significant differences are displayed in bold. BMI, body mass index; GAD-7, Generalized Anxiety Disorder questionnaire; NPY, neuropeptide Y; PHQ-9, Patient Health Questionnaire; PP, pancreatic polypeptide; PSQ-20, Perceived Stress Questionnaire; PYY peptide $YY_{(3-36)}$.

DPP4-inhibitors the association of PP and anxiety in the male subgroup remained significant ($r = 0.427$, $p = 0.008$).

Psychometric Parameters and Peptides According to Changes of Anxiety

In the longitudinal analysis patients with a clinically relevant improvement of anxiety (≥ 5 points on GAD-7, $p < 0.001$) displayed significantly higher basal anxiety levels ($p < 0.001$) as well as higher PHQ-9 ($p < 0.001$) and PSQ-20 scores ($p < 0.001$) than patients with no change (± 1 point) or worsening of anxiety (≥ 5 points on GAD-7). Regarding baseline peptide levels, no significant differences in PP ($p = 0.47$) and PYY ($p = 0.09$) were observed in subjects with improvement *vs.* no improvement of anxiety.

Course of Psychometric Parameters, NPY and BMI During Treatment

Over the observation period, women with an improvement of anxiety also showed significant improvements in PHQ-9 (36%, $p = 0.002$) and PSQ-20 subscales "worries" (30%, $p < 0.002$), "tension" (27%, $p = 0.003$) as well as the total stress score (23%, $p = 0.005$), while "demands" showed a trend toward an improvement" (25%, $p = 0.052$; **Table 3**). Male patients only improved in the subscale "tension" (34%, $p = 0.024$; **Table 4**). In patients who did not show relevant alterations in anxiety scores (± 1 point on GAD-7) no significant changes in other psychometric measurements ($p > 0.050$) were observed. BMI did not significantly change during the observation period in women or men with or without an improvement of anxiety scores. Lastly, improvement of anxiety scores did not lead to significant changes in plasma NPY levels ($p > 0.050$).

DISCUSSION

While the three members of the NPY family are commonly known as potent hunger and satiety signals (Chee and Colmers, 2008; Field et al., 2010; Loh et al., 2015) their involvement in emotion regulatory processes has emerged as well. The aim of the presented study was to examine the association of circulating NPY, PYY, and PP with self-reported symptoms of anxiety, perceived stress and depression and in obese individuals as well as their alterations depending on the course of psychometric measures of anxiety during inpatient treatment.

We found higher symptom severity of anxiety and stress in female subjects compared to men, a finding in line with our previous studies (Hofmann et al., 2015, 2017) while another study found an increase in BMI among overweight women with high anxiety symptomatology in GAD-7 but not among men (Demmer et al., 2015). Additionally, women who achieved an improvement of anxiety scores also showed a significant reduction of depressiveness and perceived stress during treatment. These findings likely reflect the generally higher prevalence of depressive and anxiety disorders amongst women (Gater et al., 1998) as well as the frequent co-occurrence and mutual interference of these symptoms (Gros et al., 2013). Initial anxiety scores had to be high enough to enable their significant improvement in the first place. Consequently, patients with a clinically relevant improvement of anxiety presented with higher baseline levels of anxiety, depressiveness and perceived stress. These differences were not reflected in basal peptide concentrations.

The main finding of our study was a moderate positive correlation of PP and anxiety scores measured by GAD-7 which was solely observed in male subjects. The low strength of the relationship could be due to the small sample size of the male subgroup. In this context it is further worth mentioning that the male study cohort was more strongly affected by obesity-related diseases, particularly insulin dependency in type 2 diabetes (see **Table 1**). Since PP has been shown to mediate glucose homeostasis (Seymour et al., 1996) and circulating peptide concentrations are altered in type 2 diabetic patients (Floyd et al., 1976) we took fasting blood sugar levels as a confounding variable into consideration. However, we did not find any correlations between fasting blood glucose levels and PP or the other members of the NPY family. As mentioned in the introduction, Verma et al. (2016) described that peripheral injection of a selective Y4 agonist facilitates extinction learning of cued fear which could be interpreted as a contradiction to our own observations. On the other hand, PP did not affect fear acquisition and consolidation. A conceivable explanatory approach reconciling these findings with our own results could be that PP secretion is upregulated under the state of anxiety. From an evolutionary point of view anorexigenic effects of PP could benefit reduced risk-taking behavior in face of an acute threat. However, self-limitation of the underlying mechanisms would appear as important to assure long-term survival which could explain why PP simultaneously promotes extinction of conditioned fear but only in fasted and not in fed mice. Both findings reflect the hypothesis that PP is able to mediate anxiety-like behavior through mechanisms

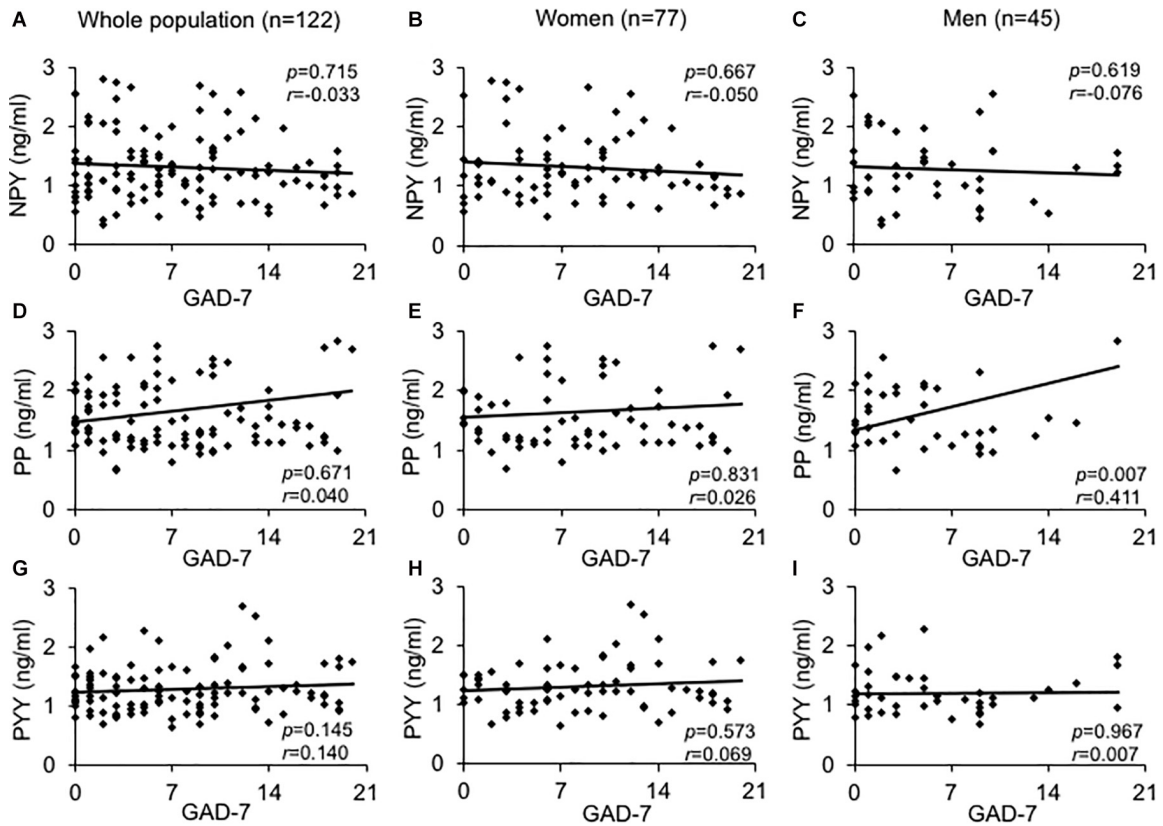

FIGURE 1 | Association between GAD-7 scores and baseline plasma levels of the neuropeptide Y family in obese psychosomatic inpatients. Correlations were assessed between plasma neuropeptide Y **(A–C)**, pancreatic polypeptide **(D–F)**, and peptide YY **(G–I)** in the obese population of both sexes **(A,D,G)** and separately for obese women **(B,E,H)** and men **(C,F,I)**. Values for *r* and *p* are indicated in the figure.

from the periphery since Y4 receptors are widely expressed in areas within reach of the peripheral blood circulation and its peripheral administration leads to an activation of regions critical to emotion regulation.

Laboratory analysis showed a negative correlation of age with NPY and a positive correlation with PP in men. Current literature suggests alterations in NPY system function with age, yet its precise role has not been completely clarified. Studies in rodents found age-related changes of NPY concentrations in brain and peripheral tissues, specifically an age-induced reduction in hypothalamic NPY (Pavia and Morris, 1994). Moreover, icv administered NPY stimulated food intake in young rats, while the effect diminished with increasing age up to its absence in old rats (Akimoto and Miyasaka, 2010). However, the attenuated responsiveness to NPY cannot be attributed to a decrease in number and expression of hypothalamic Y1 or Y5 receptors which are thought to mediate the orexigenic effects (Duhault et al., 2000) since older rats display lower Y1 and Y5 mRNA levels but an increased number of neurons transcribing Y1. This might be due to a compensatory mechanism (Coppola et al., 2004). In humans, NPY levels in the cerebrospinal fluid of women, but not men, increased significantly with aging (Taniguchi et al., 1994). It should be noted that in the present study NPY was measured peripherally which does not necessarily reflect its central expression. Nevertheless, consistent with our results a prior study investigating male subjects also demonstrated a decline of plasma NPY levels with increasing age as well as no correlation with BMI (Chiodera et al., 2000). Lastly, our observations match previous findings that found lower plasma PP in adults compared to children (Hanukoglu et al., 1990).

Contrary to our expectations, we did not find a significant association of NPY with depressiveness. In this case our results share a number of similarities with one previous study. Using the same tool for assessing depression (PHQ-9), Zheng et al. (2016) also did not detect a significant correlation with circulating NPY. However, these authors observed a positive association of DPP4 and depressiveness alongside an inverse correlation of NPY with increased DPP4 activity indicating their possible interaction in the pathogenesis of depression. DPP4-mediated proteolytic degradation of NPY and PYY results in altered signaling and functionality of respective peptides (Elmansi et al., 2019). A considerable proportion of our study population (34%) suffered from type 2 diabetes, a condition in which plasma DPP4 activity is altered (Mannucci et al., 2005; McKillop et al., 2008) and DPP4 inhibitors are commonly used oral antidiabetics. Male subjects taking DPP4 inhibitors displayed significantly decreased NPY levels ($p = 0.02$) compared with the remaining population while all psychometric parameters and other peptide values were

TABLE 3 | BMI, psychometric and endocrine parameters in the course of treatment according to the changes of anxiety in women.

	Before treatment	After treatment	% change	*p*
No change of anxiety (± 1 point, *n* = 20)				
GAD-7 score	6.85 ± 6.14	6.65 ± 6.12	−2.92	0.918
PHQ-9 score	8.56 ± 6.97	7.75 ± 7.03	−9.46	0.725
PSQ-20 score	50.8 ± 24.7	47.3 ± 22.5	−6.69	0.634
- Worries	47.7 ± 26.4	39.7 ± 29.9	−16.8	0.371
- Tension	52.7 ± 28.2	49.0 ± 26.9	−7.02	0.676
- Joy	47.0 ± 29.2	45.0 ± 23.9	−4.26	0.814
- Demands	50.0 ± 24.4	45.3 ± 22.8	−9.4	0.536
NPY (ng/ml)	1.11 ± 0.53	0.98 ± 0.45	−11.7	0.41
BMI (kg/m^2)	48.7 ± 8.57	47.8 ± 8.33	−1.85	0.744
Improvement of anxiety (≥ 5 points, *n* = 25)				
GAD-7 score	13.4 ± 4.46	5.88 ± 3.72	−56	**<0.001**
PHQ-9 score	13.4 ± 5.01	8.65 ± 4.99	−35.5	**0.002**
PSQ-20 score	68.1 ± 19.2	52.3 ± 18.6	−23.1	**0.005**
- Worries	72.8 ± 25.1	50.9 ± 19.8	−30	**0.001**
- Tension	73.9 ± 21.1	53.6 ± 24.7	−27.4	**0.003**
- Joy	30.4 ± 24.4	37.1 ± 20.3	+ 21.9	0.299
- Demands	56.0 ± 26.7	41.9 ± 23.5	−25.3	0.052
NPY (ng/ml)	1.15 ± 0.44	1.04 ± 0.35	−9.79	0.32
BMI (kg/m^2)	49.5 ± 9.51	48.5 ± 8.99	−2.12	0.691

It is to note that three patients showed a worsening of their anxiety (≥ 5 points); however, the n of this group was too small in order to perform meaningful comparisons; therefore these data are not shown in this table. Statistical analysis: Data are expressed as mean ± standard deviation. Differences between two measurements were assessed using the t-test. Significant differences are displayed in bold. BMI, body mass index; GAD-7, Generalized Anxiety Disorder questionnaire; NPY, neuropeptide Y; PHQ-9, Patient Health Questionnaire; PSQ-20, Perceived Stress Questionnaire.

TABLE 4 | BMI, psychometric and endocrine parameters in the course of treatment according to the changes of anxiety in men.

	Before treatment	After treatment	% change	*p*
No change of anxiety (± 1 point, *n* = 17)				
GAD-7 score	3.5 ± 3.30	3.00 ± 3.34	−13.6	0.676
PHQ-9 score	5.56 ± 5.01	4.35 ± 4.55	−21.8	0.451
PSQ-20 score	34.8 ± 20.9	31.9 ± 20.2	−8.46	0.687
-Worries	31.0 ± 22.5	25.5 ± 20.4	−17.7	0.414
-Tension	36.5 ± 25.5	31.0 ± 24.0	−15.1	0.553
-Joy	57.3 ± 24.4	58.8 ± 27.5	+ 2.74	0.861
-Demands	29.0 ± 22.5	29.8 ± 21.6	+ 2.70	0.877
NPY (ng/ml)	0.94 ± 0.41	0.83 ± 0.33	−11.1	0.425
BMI (kg/m^2)	48.1 ± 7.01	46.9 ± 6.59	−2.65	0.588
Improvement of anxiety (≥ 5 points, *n* = 12)				
GAD-7 score	10.8 ± 3.91	3.33 ± 2.93	−69	**<0.001**
PHQ-9 score	11.4 ± 6.92	7.40 ± 5.60	−35.2	0.156
PSQ-20 score	59.7 ± 24.8	43.5 ± 23.8	−27.2	0.116
- Worries	55.6 ± 30.4	34.4 ± 28.6	−38	0.093
- Tension	69.4 ± 23.9	45.6 ± 24.4	−34.4	**0.024**
- Joy	33.3 ± 20.9	41.1 ± 27.8	+23.3	0.447
- Demands	47.2 ± 34.9	35.0 ± 24.0	−25.9	0.328
NPY (ng/ml)	0.94 ± 0.36	0.74 ± 0.22	−21.4	0.114
BMI (kg/m^2)	50.8 ± 11.4	49.5 ± 11.3	−2.54	0.783

Statistical analysis: Data are expressed as mean ± standard deviation. Differences between two measurements were assessed using the t-test. Significant differences are displayed in bold. BMI, body mass index; GAD-7, Generalized Anxiety Disorder questionnaire; NPY, neuropeptide Y; PHQ-9, Patient Health Questionnaire; PSQ-20, Perceived Stress Questionnaire.

not affected. After excluding subjects taking DPP4 inhibitors association of PP and anxiety remained significant which concurs well with previous results that found PP secretion to be unaffected by DPP4 inhibition (Veedfald et al., 2015). However, DPP4 activity correlates with various parameters which are altered within the course of metabolic syndrome (Lamers et al., 2011). Therefore, we cannot exclude that lacking correlations between other peptides and psychometric measurements were caused by varying manifestations and severity of obesity-related disorders in the study population.

Another investigation indicated decreased NPY plasma concentrations in patients with major depressive disorder compared to healthy controls (Hashimoto et al., 1996). Incongruous evidence might be attributed to the co-occurrence of obesity and depression that are opposingly interrelated with NPY and conceivably offset one another. Indeed, the former study observed a positive association between NPY and BMI (Zheng et al., 2016) which has not been observed here, which might be due to antidepressants and concomitant diseases acting as confounding factors. Particularly, SSRI and SNRI which constituted the most frequent psychopharmacological medications taken by our study participants have been shown to interact with NPY (Lee et al., 2016).

NPY is known to be involved in the stress reaction (Reichmann and Holzer, 2016). Even though we did not find a significant correlation between NPY and perceived stress in our study population, a statistically significant negative association with the PSQ subscale "joy" was only narrowly missed in men. According to its validation study the subscale joy reflects individual resources and is positively correlated with QoL (Fliege et al., 2005). Thus, NPY may play a role in mediating stress resilience, a hypothesis to be further investigated.

Remarkably, female subjects did not show any correlation between peptides and other variables in the present study. Observed sex differences could be explained by disparities in hormonal status. Specifically, estradiol exhibits an inhibitory effect on NPY expression in the ARC of female rats (Reboucas et al., 2016), while increased NPY levels under estrogen deficiency, for instance during menopause, led to hyperphagia and body weight gain (Ainslie et al., 2001). In order to eliminate the impact of medical treatment as a potentially confounding factor in the cross-sectional analysis sample collection was carried out at the beginning of the hospital stay. Thus, an adjustment for menstrual cycle phase in female subjects was not feasible.

Contrary to our hypothesis, improvement of anxiety scores did not lead to significant changes in circulating NPY levels which was the main focus of this study. Other members of the NPY family were not determined in the longitudinal analysis which should be further investigated in the future with respect to the observed association of PP with anxiety scores in men.

Further limitations of the present study are noteworthy. First, all psychometric measurements used self-assessment

questionnaires. Despite the substantial advantages of reflecting the subjectively perceived state of emotional aspects and their easy implementation, self-report data bears the risk of inaccuracy due to recall bias, social desirability and difficulties in introspective ability. Secondly, the study population predominantly consisted of morbidly obese patients, a condition that frequently entails a considerable number of comorbidities that in turn might act as confounding variables. Third, since we chose a naturalistic study design that usually does not provide a control group, therefore no healthy normal weight subjects were included. The naturalistic design can either be seen as a limitation or a strength. The low degree of standardization in return favors a higher ecological validity. Compared with randomized controlled trials (RCTs) our investigations allow a more comprehensive picture which fits the biopsychosocial approach that is widely acknowledged in the field of psychosomatic medicine. However, it is important to note that no causality can be drawn from our findings since the influence of confounding and interaction effects cannot be entirely eliminated. Lastly, it cannot be excluded that the employed immunoassays recognized certain degradation products of the targeted peptides next to their biologically active forms. Especially with regard to PYY, C-terminal truncation of PYY_{3-36} to PYY_{3-34} entails the loss of its bioactivity in regulating energy homeostasis (Lafferty et al., 2018). Nonetheless, in the event of an upregulation as observed in PP associated with anxiety, we would expect increased levels of both active as well as inactive forms. Besides, psychometric assessment tools for anxiety and depression used in the present study evaluate symptom severity during the past two weeks while PSQ-20 assesses the patients general experience of stress. As we did not aim to examine acute emotional responses the exact determination of biologically active forms would not appear to be of utmost importance.

Taken together, current data support the concept of the gut-brain axis as bidirectional interplay of peripheral and central signals in the regulation of behavioral patterns essential for survival. In this case the role of the gut-derived PP in the regulation of anxiety is particularly noteworthy, although other factors are very likely to affect this association as well. Peptides of the NPY family are involved in multiple physiological pathways and thus being influenced by many different variables. Our findings emphasize especially age and conceivably sex hormones as distinct contributing factors. Further research employing normal-weight controls as well as the consideration of hormonal status or menstrual cycle phase are required to better understand the role of NPY, PYY and PP in the pathophysiology of obesity and the emotional response to stress.

DATA AVAILABILITY STATEMENT

The raw data supporting the conclusions of this article will be made available by the authors, without undue reservation, to any qualified researcher.

ETHICS STATEMENT

The studies involving human participants were reviewed and approved by the Ethikkommission – Charité – Universitätsmedizin Berlin. The patients/participants provided their written informed consent to participate in this study.

AUTHOR CONTRIBUTIONS

EWö, EWe, and SS collected the samples. SS analyzed the data and wrote the first draft of the manuscript. TH and AS designed the study and gave critical input throughout the work. AS analyzed the data. All authors finalized and agreed on the final version of the manuscript.

FUNDING

This study was supported by the German Research Foundation STE 1765/3-2 (AS) and Charité University Funding UFF 89/441-176 (AS and TH).

ACKNOWLEDGMENTS

We further acknowledged support from the German Research Foundation (DFG) and the Open Access Publication Fund of the Charité Universitätsmedizin Berlin.

REFERENCES

Adrian, T. E., Bloom, S. R., Bryant, M. G., Polak, J. M., Heitz, P. H., and Barnes, A. J. (1976). Distribution and release of human pancreatic polypeptide. *Gut* 17, 940–944. doi: 10.1136/gut.17.12.940

Adrian, T. E., Ferri, G. L., Bacarese-Hamilton, A. J., Fuessl, H. S., Polak, J. M., and Bloom, S. R. (1985). Human distribution and release of a putative new gut hormone, peptide YY. *Gastroenterology* 89, 1070–1077. doi: 10.1016/0016-5085(85)90211-2

Ainslie, D. A., Morris, M. J., Wittert, G., Turnbull, H., Proietto, J., and Thorburn, A. W. (2001). Estrogen deficiency causes central leptin insensitivity and increased hypothalamic neuropeptide Y. *Int. J. Obes Relat. Metab. Disord.* 25, 1680–1688. doi: 10.1038/sj.ijo.0801806

Akimoto, S., and Miyasaka, K. (2010). Age-associated changes of appetite-regulating peptides. *Geriatr. Gerontol. Int.* 10(Suppl. 1), S107–S119.

Amstadter, A. B., Koenen, K. C., Ruggiero, K. J., Acierno, R., Galea, S., Kilpatrick, D. G., et al. (2010). NPY moderates the relation between hurricane exposure and generalized anxiety disorder in an epidemiologic sample of hurricane-exposed adults. *Depress Anxiety* 27, 270–275. doi: 10.1002/da.20648

Asakawa, A., Inui, A., Ueno, N., Fujimiya, M., Fujino, M. A., and Kasuga, M. (1999). Mouse pancreatic polypeptide modulates food intake, while not influencing anxiety in mice. *Peptides* 20, 1445–1448. doi: 10.1016/s0196-9781(99)00155-2

Asakawa, A., Inui, A., Yuzuriha, H., Ueno, N., Katsuura, G., Fujimiya, M., et al. (2003). Characterization of the effects of pancreatic polypeptide in the regulation of energy balance. *Gastroenterology* 24, 1325–1336. doi: 10.1016/s0016-5085(03)00216-6

Bai, F. L., Yamano, M., Shiotani, Y., Emson, P. C., Smith, A. D., Powell, J. F., et al. (1985). An arcuato-paraventricular and -dorsomedial hypothalamic neuropeptide Y-containing system which lacks noradrenaline in the rat. *Brain Res.* 331, 172–175. doi: 10.1016/0006-8993(85)90730-9

Baltazi, M., Katsiki, N., Savopoulos, C., Iliadis, F., Koliakos, G., and Hatzitolios, A. I. (2011). Plasma neuropeptide Y (NPY) and alpha-melanocyte stimulating hormone (a-MSH) levels in patients with or without hypertension and/or obesity: a pilot study. *Am. J. Cardiovasc. Dis.* 1, 48–59.

Batterham, R. L., Cohen, M. A., Ellis, S. M., Le Roux, C. W., Withers, D. J., Frost, G. S., et al. (2003). Inhibition of food intake in obese subjects by peptide YY3-36. *N. Engl. J. Med.* 49, 941–948. doi: 10.1056/nejmoa030204

Caberlotto, L., Fuxe, K., and Hurd, Y. L. (2000). Characterization of NPY mRNA-expressing cells in the human brain: co-localization with Y2 but not Y1 mRNA in the cerebral cortex, hippocampus, amygdala, and striatum. *J. Chem. Neuroanat.* 20, 327–337. doi: 10.1016/s0891-0618(00)00107-1

Chee, M. J., and Colmers, W. F. (2008). Y eat? *Nutrition* 24, 869–877.

Chiodera, P., Volpi, R., Pilla, S., Cataldo, S., and Coiro, V. (2000). Decline in circulating neuropeptide Y levels in normal elderly human subjects. *Eur. J. Endocrinol.* 143, 715–716. doi: 10.1530/eje.0.1430715

Coppola, J. D., Horwitz, B. A., Hamilton, J., and McDonald, R. B. (2004). Expression of NPY Y1 and Y5 receptors in the hypothalamic paraventricular nucleus of aged Fischer 344 rats. *Am. J. Physiol. Regul. Integr. Comp. Physiol.* 287, R69–R75.

Cox, H. M. (2007). Neuropeptide Y receptors; antisecretory control of intestinal epithelial function. *Auton. Neurosci.* 133, 76–85.

Demmer, R. T., Gelb, S., Suglia, S. F., Keyes, K. M., Aiello, A. E., Colombo, P. C., et al. (2015). Sex differences in the association between depression, anxiety, and type 2 diabetes mellitus. *Psychosom. Med.* 77, 467–477. doi: 10.1097/psy.0000000000000169

DiMaggio, D. A., Chronwall, B. M., Buchanan, K., and O'Donohue, T. L. (1985). Pancreatic polypeptide immunoreactivity in rat brain is actually neuropeptide Y. *Neuroscience* 15, 1149–1157. doi: 10.1016/0306-4522(85)90259-3

Duhault, J., Boulanger, M., Chamorro, S., Boutin, J. A., Della Zuana, O., Douillet, E., et al. (2000). Food intake regulation in rodents: Y5 or Y1 NPY receptors or both? *Can. J. Physiol. Pharmacol.* 78, 173–185. doi: 10.1139/y99-131

Ekblad, E., and Sundler, F. (2002). Distribution of pancreatic polypeptide and peptide YY. *Peptides* 23, 251–261. doi: 10.1016/s0196-9781(01)00601-5

Elmansi, A. M., Awad, M. E., Eisa, N. H., Kondrikov, D., Hussein, K. A., Aguilar-Perez, A., et al. (2019). What doesn't kill you makes you stranger: dipeptidyl peptidase-4 (CD26) proteolysis differentially modulates the activity of many peptide hormones and cytokines generating novel cryptic bioactive ligands. *Pharmacol. Ther.* 198, 90–108. doi: 10.1016/j.pharmthera.2019.02.005

Fendt, M., Burki, H., Imobersteg, S., Lingenhohl, K., McAllister, K. H., Orain, D., et al. (2009). Fear-reducing effects of intra-amygdala neuropeptide Y infusion in animal models of conditioned fear: an NPY Y1 receptor independent effect. *Psychopharmacology* 06, 291–301. doi: 10.1007/s00213-009-1610-8

Field, B. C., Chaudhri, O. B., and Bloom, S. R. (2010). Bowels control brain: gut hormones and obesity. *Nat. Rev. Endocrinol.* 6, 444–453. doi: 10.1038/nrendo.2010.93

Fliege, H., Rose, M., Arck, P., Walter, O. B., Kocalevent, R. D., Weber, C., et al. (2005). The perceived stress questionnaire (PSQ) reconsidered: validation and reference values from different clinical and healthy adult samples. *Psychosom. Med.* 67, 78–88. doi: 10.1097/01.psy.0000151491.80178.78

Floyd, J. C. Jr., Fajans, S. S., Pek, S., and Chance, R. E. (1976). A newly recognized pancreatic polypeptide; plasma levels in health and disease. *Recent Prog. Horm. Res.* 33, 519–570. doi: 10.1016/b978-0-12-571133-3.50019-2

Fung, T. C., Olson, C. A., and Hsiao, E. Y. (2017). Interactions between the microbiota, immune and nervous systems in health and disease. *Nat. Neurosci.* 20, 145–155. doi: 10.1038/nn.4476

Gater, R., Tansella, M., Korten, A., Tiemens, B. G., Mavreas, V. G., and Olatawura, M. O. (1998). Sex differences in the prevalence and detection of depressive and anxiety disorders in general health care settings: report from the World Health Organization Collaborative Study on psychological problems in general health care. *Arch. Gen. Psychiatry* 55, 405–413. doi: 10.1001/archpsyc.55.5.405

GBD 2015 Obesity Collaborators Afshin, A., Forouzanfar, M. H., Reitsma, M. B., Sur, P., Estep, K., et al. (2017). Health effects of overweight and obesity in 195 countries over 25 Years. *N. Engl. J. Med.* 377, 13–27. doi: 10.1056/nejmoa1614362

Ghamari-Langroudi, M., Colmers, W. F., and Cone, R. D. (2005). PYY3-36 inhibits the action potential firing activity of POMC neurons of arcuate nucleus through postsynaptic Y2 receptors. *Cell Metab.* 2, 191–199.

Gilbody, S., Richards, D., Brealey, S., and Hewitt, C. (2007). Screening for depression in medical settings with the patient health questionnaire (PHQ): a diagnostic meta-analysis. *J. Gen. Intern. Med.* 22, 1596–1602. doi: 10.1007/s11606-007-0333-y

Gros, D. F., McCabe, R. E., and Antony, M. M. (2013). Using a hybrid model to investigate the comorbidity and symptom overlap between social phobia and the other anxiety disorders and unipolar mood disorders. *Psychiatry Res.* 210, 188–192. doi: 10.1016/j.psychres.2013.05.005

Hanukoglu, A., Chalew, S., and Kowarski, A. A. (1990). Human pancreatic polypeptide in children and young adults. *Horm. Metab. Res.* 22, 41–43. doi: 10.1055/s-2007-1004845

Hashimoto, H., Onishi, H., Koide, S., Kai, T., and Yamagami, S. (1996). Plasma neuropeptide Y in patients with major depressive disorder. *Neurosci. Lett.* 216, 57–60. doi: 10.1016/0304-3940(96)13008-1

Hofmann, T., Elbelt, U., Ahnis, A., Rose, M., Klapp, B. F., and Stengel, A. (2015). Sex-specific regulation of NUCB2/nesfatin-1: differential implication in anxiety in obese men and women. *Psychoneuroendocrinology* 60, 130–137. doi: 10.1016/j.psyneuen.2015.06.014

Hofmann, T., Weibert, E., Ahnis, A., Obbarius, A., Elbelt, U., Rose, M., et al. (2017). Alterations of circulating NUCB2/nesfatin-1 during short term therapeutic improvement of anxiety in obese inpatients. *Psychoneuroendocrinology* 79, 107–115. doi: 10.1016/j.psyneuen.2017.02.021

Holzer, P., Reichmann, F., and Farzi, A. (2012). Neuropeptide Y, peptide YY and pancreatic polypeptide in the gut-brain axis. *Neuropeptides* 46, 261–274. doi: 10.1016/j.npep.2012.08.005

Horwath, C. C., Hagmann, D., and Hartmann, C. (2020). The power of food: self-control moderates the association of hedonic hunger with overeating, snacking frequency and palatable food intake. *Eat. Behav.* 38:101393. doi: 10.1016/j.eatbeh.2020.101393

Kask, A., Harro, J., von Horsten, S., Redrobe, J. P., Dumont, Y., and Quirion, R. (2002). The neurocircuitry and receptor subtypes mediating anxiolytic-like effects of neuropeptide Y. *Neurosci. Biobehav. Rev.* 26, 259–283. doi: 10.1016/s0149-7634(01)00066-5

Kiessl, G. R., and Laessle, R. G. (2016). Stress inhibits PYY secretion in obese and normal weight women. *Eat Weight Disord.* 21, 245–249. doi: 10.1007/s40519-015-0231-y

Kuhne, S. G., and Stengel, A. (2019). Alteration of peptidergic gut-brain signaling under conditions of obesity. *J. Physiol. Pharmacol.* 70, 651–665.

Kuo, L. E., Kitlinska, J. B., Tilan, J. U., Li, L., Baker, S. B., Johnson, M. D., et al. (2007). Neuropeptide Y acts directly in the periphery on fat tissue and mediates stress-induced obesity and metabolic syndrome. *Nat. Med.* 13, 803–811. doi: 10.1038/nm1611

Lafferty, R. A., Flatt, P. R., and Irwin, N. (2018). C-terminal degradation of PYY peptides in plasma abolishes effects on satiety and beta-cell function. *Biochem. Pharmacol,* 158, 95–102. doi: 10.1016/j.bcp.2018.10.004

Lamers, D., Famulla, S., Wronkowitz, N., Hartwig, S., Lehr, S., Ouwens, D. M., et al. (2011). Dipeptidyl peptidase 4 is a novel adipokine potentially linking obesity to the metabolic syndrome. *Diabetes* 60, 1917–1925. doi: 10.2337/db10-1707

Lee, S. H., Paz-Filho, G., Mastronardi, C., Licinio, J., and Wong, M. L. (2016). Is increased antidepressant exposure a contributory factor to the obesity pandemic? *Transl. Psychiatry* 6:e759. doi: 10.1038/tp.2016.25

Levenstein, S., Prantera, C., Varvo, V., Scribano, M. L., Berto, E., Luzi, C., et al. (1993). Development of the perceived stress questionnaire: a new tool for psychosomatic research. *J. Psychosom. Res.* 37, 19–32. doi: 10.1016/0022-3999(93)90120-5

Lin, S., Shi, Y. C., Yulyaningsih, E., Aljanova, A., Zhang, L., Macia, L., et al. (2009). Critical role of arcuate Y4 receptors and the melanocortin system in pancreatic polypeptide-induced reduction in food intake in mice. *PLoS One* 4:e8488. doi: 10.1371/journal.pone.0008488

Loh, K., Herzog, H., and Shi, Y. C. (2015). Regulation of energy homeostasis by the NPY system. *Trends Endocrinol. Metab.* 26, 125–135. doi: 10.1016/j.tem.2015.01.003

Lowe, B., Decker, O., Muller, S., Brahler, E., Schellberg, D., Herzog, W., et al. (2008). Validation and standardization of the Generalized Anxiety Disorder Screener (GAD-7) in the general population. *Med. Care* 46, 266–274. doi: 10.1097/mlr.0b013e318160d093

Löwe, B., Spitzer, R., Zipfel, S., and Herzog, W. (2002). *Gesundheitsfragebogen für Patienten (PHQ-D). Manual und Testunterlagen. 2. Auflage (PRIME MD Patient Health Questionnaire (PHQ) — German Version Manual and Materials*, 2nd Edn. Karlsruhe: Pfizer.

Mannucci, E., Pala, L., Ciani, S., Bardini, G., Pezzatini, A., Sposato, I., et al. (2005). Hyperglycaemia increases dipeptidyl peptidase IV activity in diabetes mellitus. *Diabetologia* 48, 1168–1172. doi: 10.1007/s00125-005-1749-8

Marco, J., Zulueta, M. A., Correas, I., and Villanueva, M. L. (1980). Reduced pancreatic polypeptide secretion in obese subjects. *J. Clin. Endocrinol. Metab.* 0, 744–747. doi: 10.1210/jcem-50-4-744

McKillop, A. M., Duffy, N. A., Lindsay, J. R., O'Harte, F. P., Bell, P. M., and Flatt, P. R. (2008). Decreased dipeptidyl peptidase-IV activity and glucagon-like peptide-1(7-36)amide degradation in type 2 diabetic subjects. *Diabetes Res. Clin. Pract.* 79, 79–85. doi: 10.1016/j.diabres.2007.08.001

McTigue, D. M., Hermann, G. E., and Rogers, R. C. (1997). Effect of pancreatic polypeptide on rat dorsal vagal complex neurons. *J. Physiol.* 99(Pt 2), 475–483. doi: 10.1113/jphysiol.1997.sp021942

Mickey, B. J., Zhou, Z., Heitzeg, M. M., Heinz, E., Hodgkinson, C. A., Hsu, D. T., et al. (2011). Emotion processing, major depression, and functional genetic variation of neuropeptide Y. *Arch. Gen. Psychiatry* 68, 158–166. doi: 10.1001/archgenpsychiatry.2010.197

Myers, M. G. Jr., and Olson, D. P. (2012). Central nervous system control of metabolism. *Nature* 491, 357–363. doi: 10.1038/nature11705

NCDRF (2016). Collaboration NCDRF. Trends in adult body-mass index in 200 countries from 1975 to 2014: a pooled analysis of 1698 population-based measurement studies with 19.2 million participants. *Lancet* 387, 1377–1396. doi: 10.1016/s0140-6736(16)30054-x

Nigatu, Y. T., Reijneveld, S. A., de Jonge, P., van Rossum, E., and Bultmann, U. (2016). The combined effects of obesity, abdominal obesity and major Depression/Anxiety on health-related quality of life: the lifelines cohort study. *PLoS One* 11:e0148871. doi: 10.1371/journal.pone.0148871

Painsipp, E., Herzog, H., Sperk, G., and Holzer, P. (2011). Sex-dependent control of murine emotional-affective behaviour in health and colitis by peptide YY and neuropeptide Y. *Br. J. Pharmacol.* 163, 1302–1314. doi: 10.1111/j.1476-5381.2011.01326.x

Pavia, J. M., and Morris, M. J. (1994). Age-related changes in neuropeptide Y content in brain and peripheral tissues of spontaneously hypertensive rats. *Clin. Exp. Pharmacol. Physiol.* 21, 335–338. doi: 10.1111/j.1440-1681.1994.tb02523.x

Pedragosa-Badia, X., Stichel, J., and Beck-Sickinger, A. G. (2013). Neuropeptide Y receptors: how to get subtype selectivity. *Front. Endocrinol.* 4:5. doi: 10.3389/fendo.2013.00005

Rajan, T. M., and Menon, V. (2017). Psychiatric disorders and obesity: a review of association studies. *J. Postgrad. Med.* 63, 182–190. doi: 10.4103/jpgm.jpgm_712_16

Reboucas, E. C., Leal, S., and Sa, S. I. (2016). Regulation of NPY and alpha-MSH expression by estradiol in the arcuate nucleus of Wistar female rats: a stereological study. *Neurol. Res.* 38, 740–747. doi: 10.1080/01616412.2016.1203124

Reichmann, F., and Holzer, P. (2016). Neuropeptide Y: a stressful review. *Neuropeptides* 55, 99–109. doi: 10.1016/j.npep.2015.09.008

Sajdyk, T. J., Schober, D. A., Smiley, D. L., and Gehlert, D. R. (2002). Neuropeptide Y-Y2 receptors mediate anxiety in the amygdala. *Pharmacol. Biochem. Behav.* 71, 419–423. doi: 10.1016/s0091-3057(01)00679-7

Sajdyk, T. J., Vandergriff, M. G., and Gehlert, D. R. (1999). Amygdalar neuropeptide Y Y1 receptors mediate the anxiolytic-like actions of neuropeptide Y in the social interaction test. *Eur. J. Pharmacol.* 368, 143–147. doi: 10.1016/s0014-2999(99)00018-7

Scott, K. A., Melhorn, S. J., and Sakai, R. R. (2012). Effects of chronic social stress on obesity. *Curr. Obes Rep.* 1, 16–25. doi: 10.1007/s13679-011-0006-3

Seymour, N. E., Volpert, A. R., and Andersen, D. K. (1996). Regulation of hepatic insulin receptors by pancreatic polypeptide in fasting and feeding. *J. Surg. Res.* 65, 1–4. doi: 10.1006/jsre.1996.9999

Shi, Y. C., Lin, Z., Lau, J., Zhang, H., Yagi, M., Kanzler, I., et al. (2013). PYY3-36 and pancreatic polypeptide reduce food intake in an additive manner via distinct hypothalamic dependent pathways in mice. *Obesity* 21, E669–E678. doi: 10.1016/j.yfrne.2014.12.003

Spitzer, R. L., Kroenke, K., and Williams, J. B. (1999). Validation and utility of a self-report version of PRIME-MD: the PHQ primary care study. Primary care evaluation of mental disorders. Patient health questionnaire. *JAMA* 282, 1737–1744. doi: 10.1001/jama.282.18.1737

Spitzer, R. L., Kroenke, K., Williams, J. B., and Lowe, B. (2006). A brief measure for assessing generalized anxiety disorder: the GAD-7. *Arch. Intern. Med.* 166, 1092–1097. doi: 10.1001/archinte.166.10.1092

Strandwitz, P. (2018). Neurotransmitter modulation by the gut microbiota. *Brain Res.* 1693(Pt B), 128–133. doi: 10.1016/j.brainres.2018.03.015

Taniguchi, S., Yanase, T., Kurimoto, F., Takayanagi, R., Haji, M., Kurose, S., et al. (1994). Age-related increase in neuropeptide Y-like immunoreactivity in cerebrospinal fluid in women. *Fukuoka Igaku Zasshi* 85, 361–365.

Torres-Fuentes, C., Schellekens, H., Dinan, T. G., and Cryan, J. F. (2017). The microbiota-gut-brain axis in obesity. *Lancet Gastroenterol. Hepatol.* 2, 747–756.

Veedfald, S., Plamboeck, A., Hartmann, B., Svendsen, L. B., Vilsboll, T., Knop, F. K., et al. (2015). Pancreatic polypeptide responses to isoglycemic oral and intravenous glucose in humans with and without intact vagal innervation. *Peptides* 71, 229–231. doi: 10.1016/j.peptides.2015.07.020

Verma, D., Hormer, B., Bellmann-Sickert, K., Thieme, V., Beck-Sickinger, A. G., Herzog, H., et al. (2016). Pancreatic polypeptide and its central Y4 receptors are essential for cued fear extinction and permanent suppression of fear. *Br. J. Pharmacol.* 173, 1925–1938. doi: 10.1111/bph.13456

World Health Organisation [WHO] (2020). *Obesity and Overweight Factsheet*. Geneva: World Health Organisation.

Zakrzewska, K. E., Cusin, I., Stricker-Krongrad, A., Boss, O., Ricquier, D., Jeanrenaud, B., et al. (1999). Induction of obesity and hyperleptinemia by central glucocorticoid infusion in the rat. *Diabetes* 48, 365–370. doi: 10.2337/diabetes.48.2.365

Zheng, T., Liu, Y., Qin, S., Liu, H., Yang, L., Zhang, X., et al. (2016). Increased dipeptidyl peptidase-4 activity is associated with high prevalence of depression in middle-aged and older adults: a cross-sectional study. *J. Clin. Psychiatry* 77, e1248–e1255.

Conflict of Interest: The authors declare that the research was conducted in the absence of any commercial or financial relationships that could be construed as a potential conflict of interest.

frontiers in Neural Circuits

ORIGINAL RESEARCH
published: 05 November 2020
doi: 10.3389/fncir.2020.595783

Activation of the ARC^{POMC}→MeA Projection Reduces Food Intake

Eunjin Kwon[1,2] *and Young-Hwan Jo*[1,2,3]*

[1]The Fleischer Institute for Diabetes and Metabolism, Bronx, NY, United States, [2]Division of Endocrinology, Department of Medicine, Bronx, NY, United States, [3]Department of Molecular Pharmacology, Albert Einstein College of Medicine, Bronx, NY, United States

Proopiomelanocortin (POMC) neurons in the arcuate nucleus of the hypothalamus (ARC) plays an essential role in the control of food intake and energy expenditure. Melanocortin-4 receptors (MC4Rs) are expressed in key areas that are implicated in regulating energy homeostasis. Although the importance of MC4Rs in the paraventricular hypothalamus (PVH) has been well documented, the role of MC4Rs in the medial amygdala (MeA) on feeding remains controversial. In this study, we specifically examine the role of a novel ARC^{POMC}→MeA neural circuit in the regulation of short-term food intake. To map a local melanocortinergic neural circuit, we use monosynaptic anterograde as well as retrograde viral tracers and perform double immunohistochemistry to determine the identity of the neurons receiving synaptic input from POMC neurons in the ARC. To investigate the role of the ARC^{POMC}→MeA projection on feeding, we optogenetically stimulate channelrhodopsin-2 (ChR2)-expressing POMC fibers in the MeA. Anterograde viral tracing studies reveal that ARC POMC neurons send axonal projections to estrogen receptor-α (ER-α)- and MC4R-expressing neurons in the MeA. Retrograde viral tracing experiments show that the neurons projecting to the MeA is located mainly in the lateral part of the ARC. Optogenetic stimulation of the ARC^{POMC}→MeA pathway reduces short-term food intake. This anorectic effect is blocked by treatment with the MC4R antagonist SHU9119. In addition to the melanocortinergic local circuits within the hypothalamus, this extrahypothalamic ARC^{POMC}→MeA neural circuit would play a role in regulating short-term food intake.

Keywords: melanocortin, estrogen, stress, POMC (proopiomelanocortin), anorexia, amygdala

OPEN ACCESS

Edited by:
Anne Roefs,
Maastricht University, Netherlands

Reviewed by:
Qingchun Tong,
University of Texas Health Science Center at Houston, United States
Jong-Woo Sohn,
Korea Advanced Institute of Science and Technology, South Korea
Pingwen Xu,
University of Illinois at Chicago, United States

***Correspondence:**
Young-Hwan Jo
young-hwan.jo@einsteinmed.org

Received: *17 August 2020*
Accepted: *09 October 2020*
Published: *05 November 2020*

Citation:
Kwon E and Jo Y-H (2020) Activation of the ARC^{POMC}→MeA Projection Reduces Food Intake. Front. Neural Circuits 14:595783. doi: 10.3389/fncir.2020.595783

INTRODUCTION

Melanocortin-4 receptors (MC4Rs) play a critical role in regulating food intake and energy expenditure and in preventing obesity (Huszar et al., 1997; Balthasar et al., 2005; Rossi et al., 2011; Liu et al., 2013; Berglund et al., 2014; Shah et al., 2014). MC4Rs are expressed throughout the brain (Kishi et al., 2003), including several areas that are implicated in the control of energy balance (Kishi et al., 2003; Liu et al., 2003). In particular, MC4Rs in the paraventricular hypothalamus (PVH) appear to be responsible for

melanocortin-mediated regulation of food intake (Balthasar et al., 2005). Selective restoration of MC4Rs in single-minded 1 (SIM1) neurons in mice lacking MC4Rs (i.e., *Sim-Cre*; loxTB *Mc4r* mice) results in significantly reduced body weight gain and food intake, compared with loxTB *Mc4r* mice (Balthasar et al., 2005). Detailed neuroanatomical studies further demonstrate that MC4R-expressing SIM1 neurons in the PVH, but not the medial amygdala (MeA), are necessary for MC4R-mediated anorectic effects (Shah et al., 2014). Additionally, it has been shown that these MC4R-expressing neurons are glutamatergic and send projections to the lateral parabrachial nucleus (PBN; Shah et al., 2014), an area that mediates the suppression of appetite (Carter et al., 2013; Garfield et al., 2015). Thus, MC4R-expressing glutamatergic neurons in the PVH and the neurons in the PBN appear to be a functionally important circuit for regulating food intake.

Outside the hypothalamus, the MeA that controls emotional behaviors, including stress-induced anxiety (Liu et al., 2013) and male social behavior (Cushing et al., 2008; Sano et al., 2016) highly expresses MC4Rs (Kishi et al., 2003; Liu et al., 2003). Importantly, it has been shown that MC4Rs in the MeA regulate feeding (Liu et al., 2013). For instance, local infusion of a selective MC4R agonist into the MeA decreases food intake in rodents (Liu et al., 2013). Early studies demonstrate the presence of melanocortinergic input to the MeA (Jacobowitz and O'Donohue, 1978; Watson et al., 1978). The central melanocortin system such as pro-opiomelanocortin (POMC) neurons and agouti-related peptide (AgRP)/neuropeptide Y (NPY) neurons in the arcuate nucleus of the hypothalamus (ARC) appears to project to the MeA (Jacobowitz and O'Donohue, 1978; Padilla et al., 2016). In particular, AgRP neurons send inhibitory input to NPY 1 receptor (NPY1R)-expressing neurons, and activation of NPY1R-expressing neurons in the MeA reduces food intake (Padilla et al., 2016). Therefore, both the MeA and the PVH would be downstream targets of the central melanocortin system.

The MeA contains estrogen receptor-α (ER-α)-expressing cells (Xu et al., 2015; Saito et al., 2016). Importantly, it has been well described that estrogen receptor-α (ER-α) activity in the MeA controls energy balance as well (Liu et al., 2013; Estrada et al., 2018). For example, local implantation of estradiol in the MeA or treatment with estradiol reduces food intake, body weight, and adiposity observed in ovariectomized female rodents (Xu et al., 2017; Estrada et al., 2018). Specific deletion of ER-α in SIM1 neurons in the MeA causes obesity in both male and female mice, while overexpression of ER-α prevents diet-induced obesity (DIO) in male mice (Xu et al., 2015). As the MeA receives dense α-melanocyte-stimulating hormone (α-MSH)-positive fibers (Jacobowitz and O'Donohue, 1978) and SIM1 neurons in the MeA express both ER-α and MC4Rs (Balthasar et al., 2005; Xu et al., 2015), we examined the role of this $ARC^{POMC}\rightarrow$MeA projection in the control of feeding. Antero- and retrograde viral tracing studies revealed that ARC POMC neurons sent direct axonal projections to the MeA. In particular, ER-α- and MC4R-expressing neurons in the MeA were innervated by ARC POMC neurons. Optogenetic stimulation of this $ARC^{POMC}\rightarrow$MeA projection reduced short-term food intake. Therefore, the $ARC^{POMC}\rightarrow$MeA pathway that we identified would be an important melanocortinergic circuit for regulating feeding.

MATERIALS AND METHODS

Ethics Statement

All mouse care and experimental procedures were approved by the Institutional Animal Care Research Advisory Committee of the Albert Einstein College of Medicine and were performed following the guidelines described in the NIH guide for the care and use of laboratory animals. Stereotaxic surgery and viral injections were performed under isoflurane anesthesia.

Animals

Mice used in this study included POMC-Cre (Stock #005965), floxed-stop GFP (Stock #004077), and floxed-stop ChR2-tdTomato (Stock #012567) transgenic mice (The Jackson Laboratory). Both female and male mice of mixed C57BL/6J, FVB, and 129 strain backgrounds were used. Animals were housed in groups in cages under conditions of controlled temperature (22°C) with a 12:12 h light-dark cycle and fed a standard chow diet with *ad libitum* access to water.

Stereotaxic Surgery and Viral Injections

Six to seven-week-old mice were anesthetized deeply with 3% isoflurane. A deep level of anesthesia was maintained throughout the surgical procedure. Under isoflurane anesthesia (2%), a Cre-inducible anterograde viral tracer AAV1.CAG.FLEX.GFPsm_myc.WPRE.SV40 (AAV1-Flex-GFPsm; UPenn Vector core; Viswanathan et al., 2015) was bilaterally injected to the ARC of POMC-Cre mice (AP, −1.75 mm, ML, ±0.15 mm, DV, −5.8 mm; 150 nl of 1.36×10^{13} pfu/ml per side, $n = 6$ mice). This viral tracer has been shown to label long-range axonal projections (Viswanathan et al., 2015), which permits the mapping of neural circuits. We also used a Cre-dependent retrograde virus retroAAV.CAG.FLEX.tdTomato (retroAAV-FLEX-tdTomato, Addgene). This viral vector was unilaterally injected to the MeA (AP, −1.58 mm; ML, −2.0 mm; DV, −5.0 mm; 200 nl of 1.3×10^{13} pfu/ml, $n = 8$ mice). Animals were sacrificed and perfused at 3–4 weeks post-viral injections to perform immunohistochemistry.

Optogenetic Stimulation of the $ARC^{POMC}\rightarrow$MeA Projection

We crossbred the POMC-Cre strain with the floxed-stop ChR2-tdTomato strain to generate POMC-Cre; ChR2-tdTomato mice. To stimulate the $ARC^{POMC}\rightarrow$MeA projection, a mono fiber-optic cannula of 230 μm diameter (MFC_200/230–0.48_5 mm, Doric Lenses) was implanted into the MeA (AP, −1.58 mm; ML, −2.0 mm; DV, −5.0 mm) and coupled to a 473 nm diode-pumped solid-state (DPSS) laser (Laserglow Technologies). Animals were allowed at least a week to recover from surgery. ChR2-expressing POMC fibers in the MeA were illuminated at 20 Hz (25 ms pulse duration, 20 Hz pulses per 1 s, 3 s interval between events).

Stimulation pulses were generated with Doric Neuroscience Studio software (Doric Lenses). Light illumination started 30 min before food presentation. To measure liquid food intake (Ensure Plus, Abbott), animals were separated individually in single cages for 5 days and fasted for 6 h (from 12 PM to 6 PM). The MC4R antagonist SHU-9119 (1 mg/kg) was intraperitoneally injected 30 min before food presentation.

Immunofluorescence Staining

Mice were anesthetized with isoflurane (3%) and transcardially perfused with the pre-perfusion solution (9 g NaCl, 5 g sodium nitrate, 10,000 U heparin in 1 L distilled water). Brains were post-fixed in 4% paraformaldehyde overnight at cold room and sectioned with a vibratome in 40 μm on the following day. The sections were blocked in 0.1 M PBS buffer containing 0.2 M glycine, 0.1% Triton X-100, 10% normal donkey serum, and 5% bovine serum albumin for 2 h at room temperature and then incubated with mouse anti-GFP (1:200, Invitrogen, cat# A-11120), rabbit anti-POMC (1:1,000, Phoenix pharmaceuticals, cat# H-029-30), mouse anti-ACTH (1:100, Santa Cruz, cat# sc-57021), sheep anti-α-MSH (1:10,000, Millipore, cat# AB5087), rabbit anti-MC4R (1:250, Alomone labs, cat# AMR-024), and rabbit anti-ER-α (1:40,000, Millipore, cat# 06-935) antibodies for 72 h at cold room. The sections were washed three times in PBS and incubated with Alexa 488 anti-mouse IgG (1:200; Invitrogen, cat# A11001), Alexa 568 anti-rabbit IgG (1:500, Life Technologies, cat# A10042), or Alexa 568 anti-mouse IgG (1:500, Life Technologies, cat# A10037) for 2 h at room temperature. For co-labeling of ER-α and MC4Rs, we used an Alexa 488 conjugated MC4R antibody (1:200, G-Biosciences, cat#ITA 5860) as both ER-α and MC4R antibodies are from the same species. Tissues were washed, dried, and mounted with VECTASHIELD media containing DAPI. Images were acquired using a Leica SP8 confocal microscope.

Statistics

All statistical results are presented as mean ± SEM. Statistical analyses were performed using Graphpad Prism 7.0. Two-tailed Student's *t*-tests were used to calculate *p*-values of pair-wise comparisons. Data for comparisons across more than two groups were analyzed using a one-way ANOVA with *post hoc* Tukey's multiple comparisons. Data were considered significantly different when the probability value was less than 0.05.

RESULTS

ARC POMC Neurons Send Axonal Projections to the MeA

As it has been shown that the MeA exhibits dense α-MSH-positive fibers (Jacobowitz and O'Donohue, 1978), we first sought to determine if the MeA is innervated by ARC POMC neurons. To examine this possibility, we used a Cre-dependent anterograde viral tracer AAV1-FLEX-GFPsm (Viswanathan et al., 2015). This viral tracer was stereotaxically injected into the ARC of the POMC-Cre animals (**Figure 1A**). Three to four weeks after such viral injections, we conducted immunohistochemistry with an anti-GFP antibody. Under these experimental conditions, Cre-mediated recombination resulted in the expression of GFP in ARC POMC neurons (**Figure 1A**). Also, we observed abundant GFP-positive fibers and terminals in the MeA (**Figure 1B**), indicating that ARC^{POMC} neurons send axonal projections to the MeA. Double immunostaining with an anti-adrenocorticotropic hormone (ACTH) antibody revealed that GFP-positive fibers in the MeA were co-labeled with ACTH (**Figure 1C**), consistent with early studies describing the presence of α-MSH and ACTH-positive fibers in the MeA (Jacobowitz and O'Donohue, 1978; Watson et al., 1978).

We further examined this $ARC^{POMC} \rightarrow$ MeA projection with a Cre-dependent retrograde virus retroAAV-FLEX-tdTomato. RetroAAV-FLEX-tdTomato viruses were stereotaxically injected into the MeA of the POMC-Cre; eGFP mice (**Figure 1D**). Under these experimental conditions, mice injected with these viral tracers displayed tdTomato-positive fibers in the MeA (**Figure 1D**), indicating that these are POMC fibers. We found that there were retrogradely labeled tdTomato-positive cells in the ipsilateral, but not contralateral, ARC (**Figure 1E**). Most tdTomato-positive cells in the ARC co-expressed GFP (**Figure 1F**), supporting the interpretation that these cells are MeA-projecting POMC neurons in the ARC. Interestingly, the retrogradely identified POMC cells were located mainly in the lateral part of the ARC (**Figures 1E,G**).

ARC POMC Neurons Innervate ER-α-Expressing Neurons in the MeA

We then asked what neurons in the MeA receive melanocortinergic input from ARC POMC neurons. As the MeA contains abundant ER-α-expressing neurons (Merchenthaler et al., 2004; Xu et al., 2015; Saito et al., 2016) that control energy homeostasis (Xu et al., 2015), we examined if ER-α-expressing neurons is a downstream target of ARC POMC neurons by performing immunostaining with an anti-ER-α antibody. Anterograde AAV1-FLEX-GFPsm viruses were injected into the ARC of the POMC-Cre mice. Three to four weeks after viral injections, brain sections were double-stained with anti-ER-α and GFP antibodies (**Figure 2A**). As described in the prior studies (Merchenthaler et al., 2004; Xu et al., 2015; Saito et al., 2016), abundant ER-α-positive cells were detected in the MeA (**Figure 2B**). Double immunostaining revealed that GFP-positive fibers and terminals were close to ER-α-expressing neurons (**Figures 2B,C**).

We further investigated if these ER-α-positive cells express MC4Rs. Double immunostaining with anti-ER-α and anti-MC4R antibodies exhibited that ER-α-positive cells were positive for MC4Rs (**Figure 2D**). In our preparations, we found that about 90% of ER-α-positive cells coexpress MC4Rs (88.5 ± 1.7%; n = 220/249 ER-α-positive cells). These immunohistochemical results support the interpretation that ER-α-positive cells receiving direct synaptic input from ARC POMC neurons in the MeA express MC4Rs, consistent with

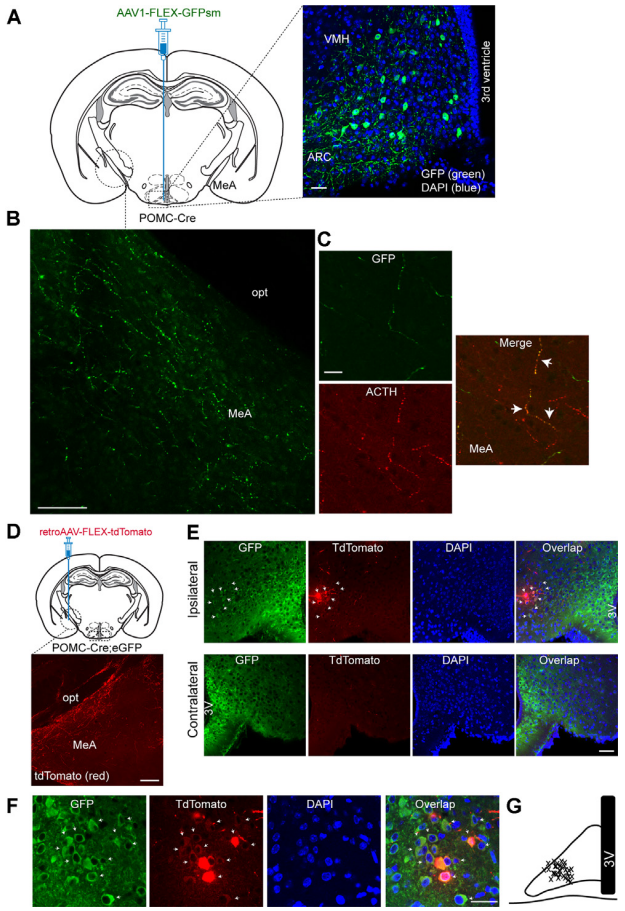

FIGURE 1 | Proopiomelanocortin neurons in the arcuate nucleus of the hypothalamus project to the medial amygdala (MeA). **(A)** Schematic illustration showing our experimental configurations (left panel). A Cre recombinase-inducible anterograde viral tracer AAV1-FLEX-GFPsm was injected into the ARC of the POMC-Cre mice. Right panel: The ARC of the POMC-Cre mice injected with AAV1-FLEX-GFPsm exhibited GFP-positive cells in the ARC. Scale bar: 30 μm. **(B)** Image of fluorescence confocal microscopy showing GFP-positive fibers and terminals in the MeA of the POMC-Cre mice injected with AAV1-FLEX-GFPsm. opt, optic tract, Scale bar: 100 μm. **(C)** Images of fluorescence confocal microscopy showing co-expression of GFP and ACTH in axonal fibers in the MeA (white arrow). Scale bar: 20 μm. **(D)** Schematic illustration showing our experimental configurations (top panel). POMC-Cre; eGFP mice were stereotaxically injected with a Cre-inducible retrograde viral tracer retroAAV-FLEX-tdTomato into the MeA. TdTomato-positive fibers were observed in the MeA (bottom panel). Scale bar: 200 μm. **(E)** Images of fluorescence confocal microscopy showing retrogradely identified ARC POMC neurons projecting to the MeA. Retrogradely identified cells (white arrow) were found in the ipsilateral, but not contralateral, ARC of the POMC-Cre; eGFP mice injected with retroAAV-FLEX-tdTomato. Importantly, most tdTomato-positive cells were found in the lateral part of the ARC. Scale bar: 50 μm. **(F)** Images of fluorescence confocal microscopy showing retrogradely labeled ARC POMC neurons. Most tdTomato neurons co-expressed GFP in the POMC-Cre; eGFP mice injected with retroAAV-FLEX-tdTomato into the MeA (white arrow). Scale bar: 30 μm. **(G)** Schematic drawing showing the location of retrogradely identified cells (x) in the ARC. 3V, 3rd ventricle.

prior studies showing SIM1 neurons in the MeA express ER-α as well as MC4Rs (Balthasar et al., 2005; Xu et al., 2015).

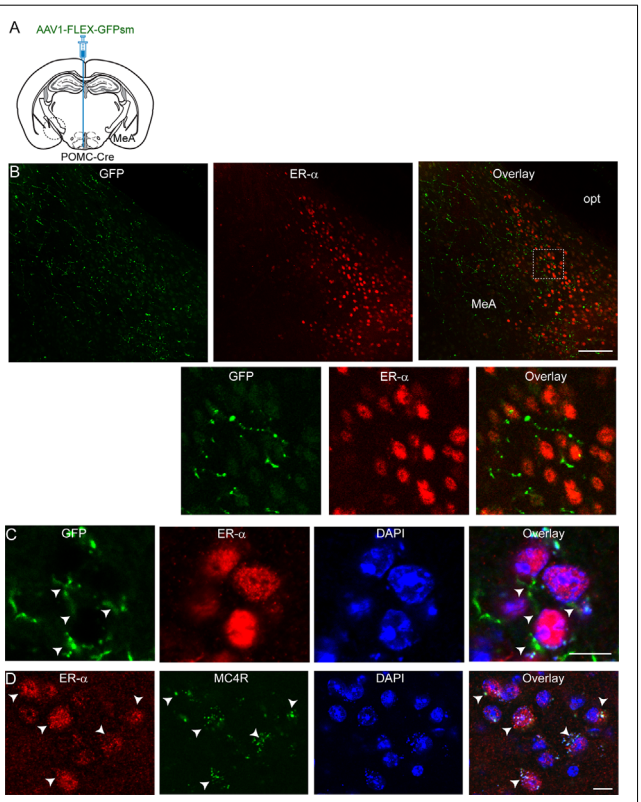

FIGURE 2 | ARC POMC neurons project to ER-α-expressing cells in the MeA. **(A)** Schematic illustration of our experimental configurations. AAV1-FLEX-GFPsm was stereotaxically injected into the ARC of the POMC-Cre mice. **(B)** Images of fluorescence confocal microscopy showing that ARC POMC neurons send projections to ER-α-positive cells (top panel). GFP-positive fibers and axonal terminals were observed in the MeA where ER-α-positive cells were located. Scale bar: 100 μm. Bottom panel: images on the expanded scale (white square area in the top panel). **(C)** Images of fluorescence confocal microscopy showing that ER-α-positive cells receive POMC input from the ARC. GFP-positive fibers and axonal terminals made synaptic contacts with a subset of ER-α-positive cells (white arrowheads). Scale bar: 10 μm. **(D)** Images of fluorescence confocal microscopy showing co-expression of ER-α and MC4Rs (white arrows). Scale bar: 10 μm.

Optogenetic Stimulation of the ARC^{POMC} → MeA Projection Reduces Short-Term Food Intake

As both MC4Rs and ER-α in the MeA play a role in the control of feeding (Liu et al., 2013; Xu et al., 2015), we investigated the effect of activation of the ARC^{POMC}→MeA projection on feeding. To selectively stimulate POMC fibers in the MeA, we expressed light-activated proteins in POMC neurons by crossbreeding the POMC-Cre mice with the floxed-stop channelrhodopsin-2 (ChR2)-tdTomato mice (**Figure 3A**). In this mouse model, the MeA exhibited tdTomato-positive fibers and some tdTomato-positive fibers in the MeA were positive for α-MSH, further supporting the presence of the ARC^{POMC}→MeA pathway (**Figures 3A,B**).

We next examined if the neurons receiving POMC input in the MeA express MC4Rs. We microinjected AAV1-FLEX-GFPsm to the ARC of POMC-Cre mice. In

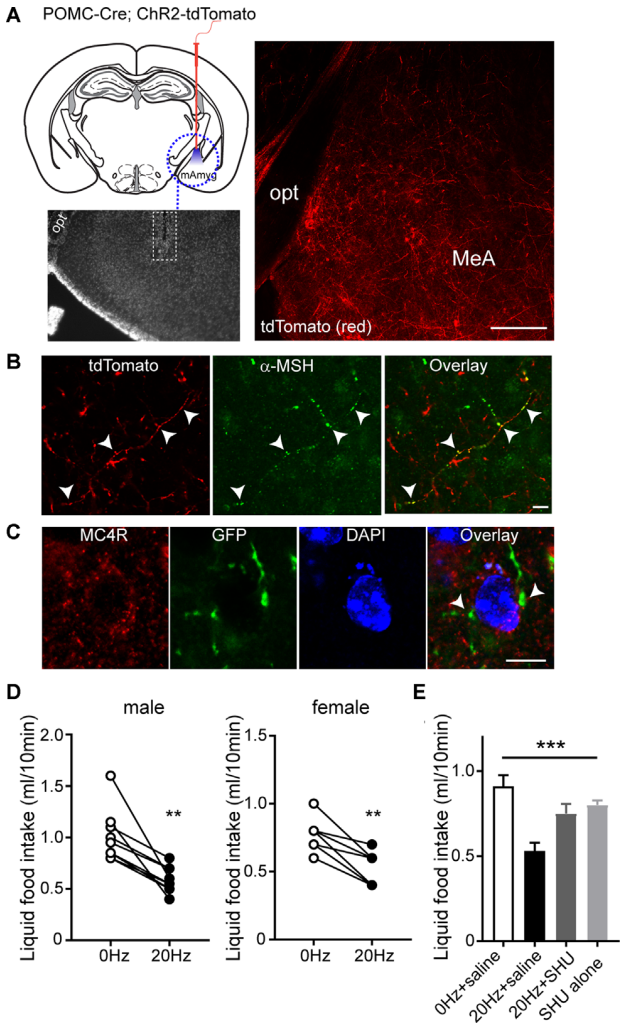

FIGURE 3 | Activating the ARC^{POMC}→MeA projection leads to an acute reduction in food intake. **(A)** Schematic drawing of our experimental configurations. A mono fiber-optic cannula was implanted into the MeA of the POMC-Cre; ChR2-tdTomato mice (top panel). The bottom panel shows the implantation site. tdTomato-positive fibers were observed in the MeA of POMC-Cre; ChR2-tdTomato mice. Scale bar: 200 μm. **(B)** Images of fluorescence confocal microscopy showing that tdTomato-positive fibers were positive for α-MSH in the MeA (white arrowheads). Scale bar: 10 μm. **(C)** Images of fluorescence confocal microscopy showing that MC4R-positive cells receive POMC input from the ARC. GFP-positive fibers and axonal terminals made synaptic contacts with MC4R-positive cells (white arrowheads). Scale bar: 10 μm. **(D)** Pooled data from nine male and seven female mice. Twenty hertz stimulation of the ARC^{POMC}→MeA pathway significantly reduced liquid food intake (males, 1.0 ± 0.08 ml vs. 0.6 ± 0.04 ml, $^{**}p < 0.01$, $n = 9$ mice; females, 0.8 ± 0.05 ml vs. 0.5 ± 0.05 ml, $^{**}p < 0.01$, $n = 7$ mice). **(E)** Plot showing blockade of the effect of optogenetic stimulation of the ARC^{POMC}→MeA pathway by the MC4R antagonist SHU9119 [1 mg/kg, $n = 5$ mice, SHU9119 alone, $n = 8$ mice, Treatment (between groups), $F_{(3,9)} = 10.3$, $^{***}p < 0.001$, 0 Hz + saline vs. 20 Hz + saline, $p < 0.001$, 20 Hz + saline vs. 20 Hz + SHU9119, $p < 0.05$, 20 Hz + saline vs. SHU9119 alone, $p < 0.01$].

the MeA of POMC-Cre mice injected with these viruses, we found that GFP-positive fibers and terminals were close to MC4R-expressing cells (**Figure 3C**), suggesting that MC4R-expressing cells are a downstream target of ARC POMC neurons.

To measure short-term food intake, mice were mildly fasted from 12 PM to 6 PM and then given liquid food. Under these experimental conditions, ChR2-expressing POMC fibers in the MeA were illuminated with light 30 min before liquid food presentation. Bursts of light pulses (20 Hz) were applied for 1 s followed by a 3 s break that repeats continuously for 40 min as described in our recent studies (Jeong et al., 2015, 2017, 2018a,b). We found that activating the ARC^{POMC}→MeA pathway significantly reduced short-term liquid food intake in both male and female mice (**Figure 3D**).

We examined if the anorexigenic effect of optogenetic stimulation of the ARC^{POMC}→MeA pathway is due in part to MC4R activation. We intraperitoneally injected the melanocortin 3/4 receptor antagonist SHU9119 30 min before optogenetic stimulation of the ARC^{POMC}→MeA pathway. SHU9119 alone did not change liquid food intake (**Figure 3E**). Optogenetic stimulation of POMC fibers in the MeA did not affect liquid food intake in mice treated with SHU9119 (**Figure 3E**). Therefore, our results support the interpretation that the ARC^{POMC}→MeA projection contributes to the control of short-term feeding, and ER-α- and MC4R-expressing cells are a potential downstream target of the pathway.

DISCUSSION

In the present study, we provide physiological evidence that in addition to the ARC^{POMC}→PVH and ARC^{POMC}→DMH^{NPY} circuits within the hypothalamus (Balthasar et al., 2005; Shah et al., 2014; Trotta et al., 2020), the ARC^{POMC}→MeA pathway is another important neural circuit that mediates MC4R-mediated anorexic effects. We found that ARC POMC neurons sent axonal projections to the MeA. Interestingly, the projection neurons were located mainly in the lateral part of the ARC. ER-α-positive neurons as well as MC4R-expressing neurons in the MeA received direct synaptic input from ARC POMC neurons. A subset of ER-α-expressing cells was positive for MC4Rs, indicating that these ER-α- and MC4R-positive neurons were a downstream target of this projection. Optogenetic activation of the ARC^{POMC}→MeA pathway caused a reduction in short-term liquid food intake in both female and male mice. This anorectic effect was blocked by the MC4R antagonist. As stress increases the activity of ARC POMC neurons (Liu et al., 2007; Qu et al., 2020) and MC4Rs in the MeA contribute to stress-induced behavior and hypophagia (Liu et al., 2013), the ARC^{POMC}→MeA pathway that we identified may contribute to stress-induced short-term hypophagia.

Accumulating evidence has demonstrated heterogeneity of ARC POMC neurons (Parton et al., 2007; Hentges et al., 2009; Williams et al., 2010; Sohn et al., 2011; Jarvie and Hentges, 2012; Shi et al., 2013; Qiu et al., 2014; Dodd et al., 2018; Jones et al., 2019; Trotta et al., 2020). ARC POMC neurons are neurochemically, anatomically, and functionally heterogeneous (Parton et al., 2007; Hentges et al., 2009; Williams et al., 2010; Sohn et al., 2011; Jarvie and Hentges, 2012; Shi et al., 2013; Qiu et al., 2014; Dodd et al., 2018;

Wei et al., 2018; Jones et al., 2019; Trotta et al., 2020). It has been recently shown that re-expression of the *Pomc* gene in ARC glutamatergic neurons in ARC specific *Pomc* KO mice completely normalizes body weight and body composition (Jones et al., 2019), although it is unknown if these effects are attributed to decreased food intake or increased energy expenditure, or both. Interestingly, POMC rescues exclusively in ARC GABAergic neurons are also able to normalize food intake and significantly reduce body weight. This anorectic effect is mediated by the $ARC^{POMC} \rightarrow DMH^{NPY}$ projection (Trotta et al., 2020). The DMH is innervated largely by GABAergic POMC neurons and NPY expression in the DMH is inversely regulated by POMC expression in ARC GABAergic neurons (Trotta et al., 2020). These prior studies suggest that fast-acting neurotransmitters (i.e., glutamate and GABA) released from ARC POMC neurons are essential in regulating feeding and body weight.

Interestingly, it has been also described that ARC^{POMC} neurons do not release either glutamate or GABA to MC4R-expressing neurons in the PVH (Fenselau et al., 2017), a structure that relays information from the ARC to other brain areas including the lateral parabrachial nucleus. Instead, α-MSH released from ARC^{POMC} neurons post-synaptically regulates the strength of glutamatergic transmission in the PVN (Fenselau et al., 2017). This short-term synaptic plasticity by α-MSH appears to play a role in reducing feeding. In contrast to these well-known anorectic effects of α-MSH, it has been documented that activation of ARC POMC neurons can promote feeding by releasing β-endorphin (Koch et al., 2015; Wei et al., 2018). Therefore, it seems likely that both distinct axonal projections and neurotransmitters/neuropeptides released from ARC POMC neurons determine the net balance between anorexigenic melanocortin POMC and orexigenic opioid POMC neurons as suggested in our prior studies (Lee et al., 2015; Jeong et al., 2018b).

The MeA highly expresses MC4Rs (Kishi et al., 2003; Liu et al., 2003). Restoration of MC4Rs in the PVH as well as in the MeA in MC4R-deficient mice reduces food intake and body weight without changing energy expenditure compared with the loxTB MC4R mice (Balthasar et al., 2005). However, selective re-expression of MC4Rs in the MeA does not affect the body weight gain in mice lacking MC4Rs, suggesting that the PVH is the major site through which MC4Rs restrain feeding (Shah et al., 2014). However, the MeA receives synaptic input from ARC^{AgRP} neurons (Padilla et al., 2016). Stimulation of the $ARC^{AgRP} \rightarrow$MeA pathway drives feeding *via* inhibition of NPY 1 receptor-expressing neurons in the MeA (Padilla et al., 2016), suggesting that the central melanocortin system can control feeding *via* the neurons in the MeA. In our present study, we found that ARC^{POMC} neurons sent axonal projections to ER-α-expressing neurons in the MeA. The neurons receiving melanocortinergic input also expressed MC4Rs. These results suggest that the neurons receiving POMC input would be SIM1 neurons as SIM1 neurons express both receptors (Balthasar et al., 2005; Xu et al., 2015). Importantly, optogenetic activation of this pathway was able to acutely reduce food intake. Therefore, in addition to the PVH (Balthasar et al., 2005; Fenselau et al., 2017) and the DMH (Trotta et al., 2020), the MeA appears to be an important downstream target of both orexigenic AgRP and anorexigenic POMC neurons in the ARC.

The MeA is a brain region implicated in innate social behavior such as responses to a sexual partner, an aggressive intruder, or a predator (Cushing et al., 2008; Sano et al., 2016) and is critical for the processing of emotional stress (Ebner et al., 2004; Liu et al., 2013). It is known that fear and stress actively suppress eating. Chronic stress results in reduced body weight and anorexia that is associated with increased ARC POMC neuron activity (Qu et al., 2020). This anorectic effect in response to stress appears to be mediated through inhibition by opioids of dopamine-expressing neurons in the ventral tegmental area (VTA; Qu et al., 2020). As the MeA can respond to stress, it is plausible that the $ARC^{POMC} \rightarrow$MeA circuit that we identified would also contribute to stress-induced hypophagia. As stress promotes the activity of ARC POMC neurons (Liu et al., 2007; Qu et al., 2020), the increased POMC neuron activity would release α-MSH into the MeA and in turn activate ER-α-expressing neurons in the MeA, resulting in a short-term reduction in food intake. In this case, α-MSH and β-endorphin released by ARC POMC neurons would control feeding through the two distinct pathways (i.e., $ARC^{POMC} \rightarrow$MeA and $ARC^{POMC} \rightarrow VTA^{DA}$). These findings further support the idea that both distinct neuronal projections and neurotransmitters/neuropeptides released from ARC POMC neurons are crucial in determining the net balance between anorexigenic and orexigenic POMC neurons.

ER-α-expressing neurons in the MeA control metabolic homeostasis in both female and male mice (Xu et al., 2015) and in stress-induced pressor responses in females (Hinton et al., 2016). For instance, over-expression of ER-α in the MeA prevents DIO in male mice (Xu et al., 2015). Specific deletion of ER-α in the MeA causes obesity in male and female mice fed regular chow (Xu et al., 2015). These effects appear to be due in part to ER-α-induced activation of SIM1 neurons in the MeA (Xu et al., 2015). Activation of ER-α excites SIM1 neurons in the MeA. However, chemogenetic activation of SIM1 neurons changes neither food intake nor body temperature (Xu et al., 2015). These findings are somewhat inconsistent with prior findings (Xu et al., 2017; Estrada et al., 2018). Both local administration of estrogen to the MeA and subcutaneous estradiol treatment abolishes hyperphagia and body weight gain in ovariectomized female rodents (Xu et al., 2017; Estrada et al., 2018), suggesting that ER-α-expressing neurons in the MeA may have the ability to control feeding at least in female animals. Indeed, our present results support this possibility. Stimulation of the $ARC^{POMC} \rightarrow$MeA pathway significantly reduced feeding that is consistent with the feeding-regulating effects of MC4Rs in the MeA (Liu et al., 2013). Like melanocortinergic local circuits such as $ARC^{POMC} \rightarrow$PVH and $ARC^{POMC} \rightarrow DMH^{NPY}$ neural circuits, this extrahypothalamic $ARC^{POMC} \rightarrow$MeA neural circuit would play a critical role in regulating feeding and possibly stress-mediated anorexia.

DATA AVAILABILITY STATEMENT

The raw data supporting the conclusions of this article will be made available by the authors, without undue reservation.

ETHICS STATEMENT

The animal study was reviewed and approved by Institutional Animal Care Research Advisory Committee of the Albert Einstein College of Medicine.

AUTHOR CONTRIBUTIONS

EK performed the immunocytochemistry. Y-HJ designed the research, performed viral injection, immunocytochemistry, optogenetics, analyzed the data, and wrote the manuscript. All authors contributed to the article and approved the submitted version.

FUNDING

This work was supported by the National Institute of Diabetes and Digestive and Kidney Diseases (NIDDK; RO1 DK092246, R03 TR003313, and P30 DK020541) to Y-HJ.

ACKNOWLEDGMENTS

We thank Tae-Sik Yoo who had initiated this study and Hye-Young Joung for viral injections.

REFERENCES

Balthasar, N., Dalgaard, L. T., Lee, C. E., Yu, J., Funahashi, H., Williams, T., et al. (2005). Divergence of melanocortin pathways in the control of food intake and energy expenditure. *Cell* 123, 493–505. doi: 10.1016/j.cell.2005.08.035

Berglund, E. D., Liu, T., Kong, X., Sohn, J. W., Vong, L., Deng, Z., et al. (2014). Melanocortin 4 receptors in autonomic neurons regulate thermogenesis and glycemia. *Nat. Neurosci.* 17, 911–913. doi: 10.1038/nn.3737

Carter, M. E., Soden, M. E., Zweifel, L. S., and Palmiter, R. D. (2013). Genetic identification of a neural circuit that suppresses appetite. *Nature* 503, 111–114. doi: 10.1038/nature12596

Cushing, B. S., Perry, A., Musatov, S., Ogawa, S., and Papademetriou, E. (2008). Estrogen receptors in the medial amygdala inhibit the expression of male prosocial behavior. *J. Neurosci.* 28, 10399–10403. doi: 10.1523/JNEUROSCI.1928-08.2008

Dodd, G. T., Michael, N. J., Lee-Young, R. S., Mangiafico, S. P., Pryor, J. T., Munder, A. C., et al. (2018). Insulin regulates POMC neuronal plasticity to control glucose metabolism. *eLife* 7:e38704. doi: 10.7554/eLife.38704

Ebner, K., Rupniak, N. M., Saria, A., and Singewald, N. (2004). Substance P in the medial amygdala: emotional stress-sensitive release and modulation of anxiety-related behavior in rats. *Proc. Natl. Acad. Sci. U S A* 101, 4280–4285. doi: 10.1073/pnas.0400794101

Estrada, C. M., Ghisays, V., Nguyen, E. T., Caldwell, J. L., Streicher, J., and Solomon, M. B. (2018). Estrogen signaling in the medial amygdala decreases emotional stress responses and obesity in ovariectomized rats. *Horm. Behav.* 98, 33–44. doi: 10.1016/j.yhbeh.2017.12.002

Fenselau, H., Campbell, J. N., Verstegen, A. M., Madara, J. C., Xu, J., Shah, B. P., et al. (2017). A rapidly acting glutamatergic ARC→PVH satiety circuit postsynaptically regulated by α-MSH. *Nat. Neurosci.* 20, 42–51. doi: 10.1038/nn.4442

Garfield, A. S., Li, C., Madara, J. C., Shah, B. P., Webber, E., Steger, J. S., et al. (2015). A neural basis for melanocortin-4 receptor-regulated appetite. *Nat. Neurosci.* 18, 863–871. doi: 10.1038/nn.4011

Hentges, S. T., Otero-Corchon, V., Pennock, R. L., King, C. M., and Low, M. J. (2009). Proopiomelanocortin expression in both GABA and glutamate neurons. *J. Neurosci.* 29, 13684–13690. doi: 10.1523/JNEUROSCI.3770-09.2009

Hinton, A. O. Jr., He, Y., Xia, Y., Xu, P., Yang, Y., Saito, K., et al. (2016). Estrogen receptor-α in the medial amygdala prevents stress-induced elevations in blood pressure in females. *Hypertension* 67, 1321–1330. doi: 10.1161/HYPERTENSIONAHA.116.07175

Huszar, D., Lynch, C. A., Fairchild-Huntress, V., Dunmore, J. H., Fang, Q., Berkemeier, L. R., et al. (1997). Targeted disruption of the melanocortin-4 receptor results in obesity in mice. *Cell* 88, 131–141. doi: 10.1016/s0092-8674(00)81865-6

Jacobowitz, D. M., and O'Donohue, T. L. (1978). Alpha-melanocyte stimulating hormone: immunohistochemical identification and mapping in neurons of rat brain. *Proc. Natl. Acad. Sci. U S A* 75, 6300–6304. doi: 10.1073/pnas.75.12.6300

Jarvie, B. C., and Hentges, S. T. (2012). Expression of GABAergic and glutamatergic phenotypic markers in hypothalamic proopiomelanocortin neurons. *J. Comp. Neurol.* 520, 3863–3876. doi: 10.1002/cne.23127

Jeong, J. H., Chang, J. S., and Jo, Y. H. (2018a). Intracellular glycolysis in brown adipose tissue is essential for optogenetically induced nonshivering thermogenesis in mice. *Sci. Rep.* 8:6672. doi: 10.1038/s41598-018-25265-3

Jeong, J. H., Lee, D. K., and Jo, Y.-H. (2017). Cholinergic neurons in the dorsomedial hypothalamus regulate food intake. *Mol. Metab.* 6, 306–312. doi: 10.1016/j.molmet.2017.01.001

Jeong, J. H., Lee, D. K., Blouet, C., Ruiz, H. H., Buettner, C., Chua, S., et al. (2015). Cholinergic neurons in the dorsomedial hypothalamus regulate mouse brown adipose tissue metabolism. *Mol. Metab.* 4, 483–492. doi: 10.1016/j.molmet.2015.03.006

Jeong, J. H., Lee, D. K., Liu, S. M., Chua, S. C. Jr., Schwartz, G. J., and Jo, Y. H. (2018b). Activation of temperature-sensitive TRPV1-like receptors in ARC POMC neurons reduces food intake. *PLoS Biol.* 16:e2004399. doi: 10.1371/journal.pbio.2004399

Jones, G. L., Wittmann, G., Yokosawa, E. B., Yu, H., Mercer, A. J., Lechan, R. M., et al. (2019). Selective restoration of *pomc* expression in glutamatergic POMC neurons: evidence for a dynamic hypothalamic neurotransmitter network. *eNeuro* 6:ENEURO.0400-18.2019. doi: 10.1523/ENEURO.0400-18.2019

Kishi, T., Aschkenasi, C. J., Lee, C. E., Mountjoy, K. G., Saper, C. B., and Elmquist, J. K. (2003). Expression of melanocortin 4 receptor mRNA in the central nervous system of the rat. *J. Comp. Neurol.* 457, 213–235. doi: 10.1002/cne.10454

Koch, M., Varela, L., Kim, J. G., Kim, J. D., Hernandez-Nuno, F., Simonds, S. E., et al. (2015). Hypothalamic POMC neurons promote cannabinoid-induced feeding. *Nature* 519, 45–50. doi: 10.1038/nature14260

Lee, D. K., Jeong, J. H., Chun, S. K., Chua, S. Jr., and Jo, Y. H. (2015). Interplay between glucose and leptin signalling determines the strength of GABAergic synapses at POMC neurons. *Nat. Commun.* 6:6618. doi: 10.1038/ncomms7618

Liu, H., Kishi, T., Roseberry, A. G., Cai, X., Lee, C. E., Montez, J. M., et al. (2003). Transgenic mice expressing green fluorescent protein under the control of the melanocortin-4 receptor promoter. *J. Neurosci.* 23, 7143–7154. doi: 10.1523/JNEUROSCI.23-18-07143.2003

Liu, J., Garza, J. C., Li, W., and Lu, X. Y. (2013). Melanocortin-4 receptor in the medial amygdala regulates emotional stress-induced anxiety-like behaviour, anorexia and corticosterone secretion. *Int. J. Neuropsychopharmacol.* 16, 105–120. doi: 10.1017/S146114571100174X

Liu, J., Garza, J. C., Truong, H. V., Henschel, J., Zhang, W., and Lu, X.-Y. (2007). The melanocortinergic pathway is rapidly recruited by emotional stress and contributes to stress-induced anorexia and anxiety-like behavior. *Endocrinology* 148, 5531–5540. doi: 10.1210/en.2007-0745

Merchenthaler, I., Lane, M. V., Numan, S., and Dellovade, T. L. (2004). Distribution of estrogen receptor alpha and beta in the mouse central nervous system: *in vivo* autoradiographic and immunocytochemical analyses. *J. Comp. Neurol.* 473, 270–291. doi: 10.1002/cne.20128

Padilla, S. L., Qiu, J., Soden, M. E., Sanz, E., Nestor, C. C., Barker, F. D., et al. (2016). Agouti-related peptide neural circuits mediate adaptive behaviors in the starved state. *Nat. Neurosci.* 19, 734–741. doi: 10.1038/nn.4274

Parton, L. E., Ye, C. P., Coppari, R., Enriori, P. J., Choi, B., Zhang, C. Y., et al. (2007). Glucose sensing by POMC neurons regulates glucose homeostasis and is impaired in obesity. *Nature* 449, 228–232. doi: 10.1038/nature06098

Qiu, J., Zhang, C., Borgquist, A., Nestor, C. C., Smith, A. W., Bosch, M. A., et al. (2014). Insulin excites anorexigenic proopiomelanocortin neurons *via* activation of canonical transient receptor potential channels. *Cell Metab.* 19, 682–693. doi: 10.1016/j.cmet.2014.03.004

Qu, N., He, Y., Wang, C., Xu, P., Yang, Y., Cai, X., et al. (2020). A POMC-originated circuit regulates stress-induced hypophagia, depression and anhedonia. *Mol. Psychiatry* 25, 1006–1021. doi: 10.1038/s41380-019-0506-1

Rossi, J., Balthasar, N., Olson, D., Scott, M., Berglund, E., Lee, C. E., et al. (2011). Melanocortin-4 receptors expressed by cholinergic neurons regulate energy balance and glucose homeostasis. *Cell Metab.* 13, 195–204. doi: 10.1016/j.cmet.2011.01.010

Saito, K., He, Y., Yan, X., Yang, Y., Wang, C., Xu, P., et al. (2016). Visualizing estrogen receptor-alpha-expressing neurons using a new ERα-ZsGreen reporter mouse line. *Metabolism* 65, 522–532. doi: 10.1016/j.metabol.2015.12.011

Sano, K., Nakata, M., Musatov, S., Morishita, M., Sakamoto, T., Tsukahara, S., et al. (2016). Pubertal activation of estrogen receptor α in the medial amygdala is essential for the full expression of male social behavior in mice. *Proc. Natl. Acad. Sci. U S A* 113, 7632–7637. doi: 10.1073/pnas.1524907113

Shah, B. P., Vong, L., Olson, D. P., Koda, S., Krashes, M. J., Ye, C., et al. (2014). MC4R-expressing glutamatergic neurons in the paraventricular hypothalamus regulate feeding and are synaptically connected to the parabrachial nucleus. *Proc. Natl. Acad. Sci. U S A* 111, 13193–13198. doi: 10.1073/pnas.1407843111

Shi, X., Zhou, F., Li, X., Chang, B., Li, D., Wang, Y., et al. (2013). Central GLP-2 enhances hepatic insulin sensitivity *via* activating PI3K signaling in POMC neurons. *Cell Metab.* 18, 86–98. doi: 10.1016/j.cmet.2013.06.014

Sohn, J.-W., Xu, Y., Jones, J. E., Wickman, K., Williams, K. W., and Elmquist, J. K. (2011). Serotonin 2C receptor activates a distinct population of arcuate pro-opiomelanocortin neurons *via* TRPC channels. *Neuron* 71, 488–497. doi: 10.1016/j.neuron.2011.06.012

Trotta, M., Bello, E. P., Alsina, R., Tavella, M. B., Ferran, J. L., Rubinstein, M., et al. (2020). Hypothalamic pomc expression restricted to GABAergic neurons suppresses Npy overexpression and restores food intake in obese mice. *Mol. Metab.* 37:100985. doi: 10.1016/j.molmet.2020.100985

Viswanathan, S., Williams, M. E., Bloss, E. B., Stasevich, T. J., Speer, C. M., Nern, A., et al. (2015). High-performance probes for light and electron microscopy. *Nat. Methods* 12, 568–576. doi: 10.1038/nmeth.3365

Watson, S. J., Akil, H., Richard, C. W. III, and Barchas, J. D. (1978). Evidence for two separate opiate peptide neuronal systems. *Nature* 275, 226–228. doi: 10.1038/275226a0

Wei, Q., Krolewski, D. M., Moore, S., Kumar, V., Li, F., Martin, B., et al. (2018). Uneven balance of power between hypothalamic peptidergic neurons in the control of feeding. *Proc. Natl. Acad. Sci. U S A* 115, E9489–E9498. doi: 10.1073/pnas.1802237115

Williams, K. W., Margatho, L. O., Lee, C. E., Choi, M., Lee, S., Scott, M. M., et al. (2010). Segregation of acute leptin and insulin effects in distinct populations of arcuate proopiomelanocortin neurons. *J. Neurosci.* 30, 2472–2479. doi: 10.1523/JNEUROSCI.3118-09.2010

Xu, P., Cao, X., He, Y., Zhu, L., Yang, Y., Saito, K., et al. (2015). Estrogen receptor-alpha in medial amygdala neurons regulates body weight. *J. Clin. Invest.* 125, 2861–2876. doi: 10.1172/JCI80941

Xu, P., Zhu, L., Saito, K., Yang, Y., Wang, C., He, Y., et al. (2017). Melanocortin 4 receptor is not required for estrogenic regulations on energy homeostasis and reproduction. *Metabolism* 70, 152–159. doi: 10.1016/j.metabol.2016.12.004

Conflict of Interest: The authors declare that the research was conducted in the absence of any commercial or financial relationships that could be construed as a potential conflict of interest.

frontiers in Neural Circuits

MINI REVIEW
published: 11 November 2020
doi: 10.3389/fncir.2020.577880

Hypothetical Roles of the Olfactory Tubercle in Odor-Guided Eating Behavior

Koshi Murata[1,2]*

[1] Division of Brain Structure and Function, Faculty of Medical Sciences, University of Fukui, Fukui, Japan, [2] Life Science Innovation Center, Faculty of Medical Science, University of Fukui, Fukui, Japan

Olfaction plays an important role in the evaluation, motivation, and palatability of food. The chemical identity of odorants is coded by a spatial combination of activated glomeruli in the olfactory bulb, which is referred to as the odor map. However, the functional roles of the olfactory cortex, a collective region that receives axonal projections from the olfactory bulb, and higher olfactory centers in odor-guided eating behaviors are yet to be elucidated. The olfactory tubercle (OT) is a component of the ventral striatum and forms a node within the mesolimbic dopaminergic pathway. Recent studies have revealed the anatomical domain structures of the OT and their functions in distinct odor-guided motivated behaviors. Another component of the ventral striatum, the nucleus accumbens, is well known for its involvement in motivation and hedonic responses for foods, which raises the possibility of functional similarities between the OT and nucleus accumbens in eating. This review first summarizes recent findings on the domain- and neuronal subtype-specific roles of the OT in odor-guided motivated behaviors and then proposes a model for the regulation of eating behaviors by the OT.

Keywords: olfaction, olfactory tubercle, eating, dopamine, motivation, palatability, attractive behavior, aversive behavior

OPEN ACCESS

Edited by:
Masahiro Yamaguchi, Kōchi University, Japan

Reviewed by:
Daniel W. Wesson, University of Florida, United States
Fuqiang Xu, Chinese Academy of Sciences (CAS), China

***Correspondence:**
Koshi Murata
kmurata@u-fukui.ac.jp

Received: *30 June 2020*
Accepted: *21 October 2020*
Published: *11 November 2020*

Citation:
Murata K (2020) Hypothetical Roles of the Olfactory Tubercle in Odor-Guided Eating Behavior. Front. Neural Circuits 14:577880. doi: 10.3389/fncir.2020.577880

INTRODUCTION

The smell of food stimulates appetite, especially during states of hunger. Conversely, the smell of rotten foods incites a sense of discomfort and promotes arousal. The sense of olfaction is also involved in mastication. Volatile flavor compounds move through the nasopharynx and reach the olfactory mucosa, a process termed as retronasal olfaction. Therefore, the sense of "taste" and pleasure of palatable tastes is attenuated if the nose is pinched during chewing or drinking. Gustatory, tactile, and olfactory inputs of foods are integrated during "tasting" and create a sense of "flavor," subsequently resulting in the palatability of foods. Thus, olfaction is involved in the evaluation, appetite, and palatability of food before and during eating (Lawless, 1991; Shepherd, 2013).

Odorants are volatile chemical molecules that can be detected by olfactory sensory neurons in the olfactory epithelium. Each olfactory sensory neuron expresses a single type of odorant receptor that has a particular molecular receptive range and sends axons to a specific glomerulus in the olfactory bulb, the first relay center of the central olfactory system (Mori and Sakano, 2011). Odorants are coded by specific combinations of activated glomeruli, termed "odor maps," in the olfactory bulb (Uchida et al., 2000). The brain regions that receive synaptic inputs from projection

neurons in the olfactory bulb (mitral and tufted cells) are collectively referred to as the olfactory cortex (Neville and Haberly, 2004). The olfactory cortex includes the anterior olfactory nucleus, tenia tecta, piriform cortex, olfactory tubercle (OT), cortical amygdala, and entorhinal cortex. In contrast to that in the olfactory bulb, the spatial combination of activated neurons in the piriform cortex does not seem to represent the chemical identities of odorants (Stettler and Axel, 2009). Axonal projections from the olfactory bulb to the olfactory cortex are diffused and dispersed (Ghosh et al., 2011; Sosulski et al., 2011). To date, the nature of the information encoded by neural activity in the olfactory cortex has not been elucidated. Furthermore, the neural mechanisms underpinning odor-guided evaluation, appetite, and palatability of foods remain unclear.

The OT is a component of the olfactory cortex based on the definition that it receives direct inputs from the olfactory bulb and has been observed in every mammal studied including humans and rodents to date. The term "olfactory tubercle" is used to designate the region on the basal surface of the frontal lobe between the olfactory tract and the nucleus of the diagonal band in humans (Crosby and Humphrey, 1941; Allison, 1954). The OT also forms the ventral striatum, is anatomically bridged to the nucleus accumbens (NAc), and is a component of the mesolimbic dopaminergic pathway (Heimer, 1978; Heimer et al., 1987; Ikemoto, 2010). The OT can efficiently induce intracranial self-administration of addictive drugs (Ikemoto, 2003; Ikemoto et al., 2005; Shin et al., 2008), which are hallmarks of reward processing in the brain (Berridge and Kringelbach, 2015). Recent studies have revealed the involvement of the OT in motivated behaviors, including eating. In this review, I first outline how anatomical maps of the OT match the functional domains of distinct motivated behaviors. I then propose hypothetical roles of the OT in eating behaviors based on the sense of olfaction.

Functional Domains of the Olfactory Tubercle and Odor-Guided Motivated Behaviors

The principal neurons in most areas of the olfactory cortex are pyramidal-type glutamatergic neurons. By contrast, the majority of neurons in the OT, as a component of the striatum, are small to medium-sized spiny GABAergic neurons (Millhouse and Heimer, 1984; Neville and Haberly, 2004). The cytoarchitecture of the OT comprises three major neuronal types: medium spiny neurons distributed in layer II of the cortex-like region; dwarf cells, which are small spiny neurons constituting the cap regions (Hosoya and Hirata, 1974); and granule cells, which are also small GABAergic neurons constituting the Islands of Calleja (Fallon et al., 1978; de Vente et al., 2001). These structural divisions can be observed based on the mRNA expression levels of the dopamine receptors D1 and D2 (**Figure 1**; Murata et al., 2015). Medium spiny neurons in the cortex-like region express either *Drd1* or *Drd2* mRNA (**Figures 1A,B**). The dwarf cells in the cap region express *Drd1* but not *Drd2* mRNA (**Figures 1B,C**). The granule cells in the Islands of Calleja are characterized by weak expression of *Drd1* mRNA and the absence of *Drd2* mRNA (**Figures 1B,C**). The cap region and Islands of

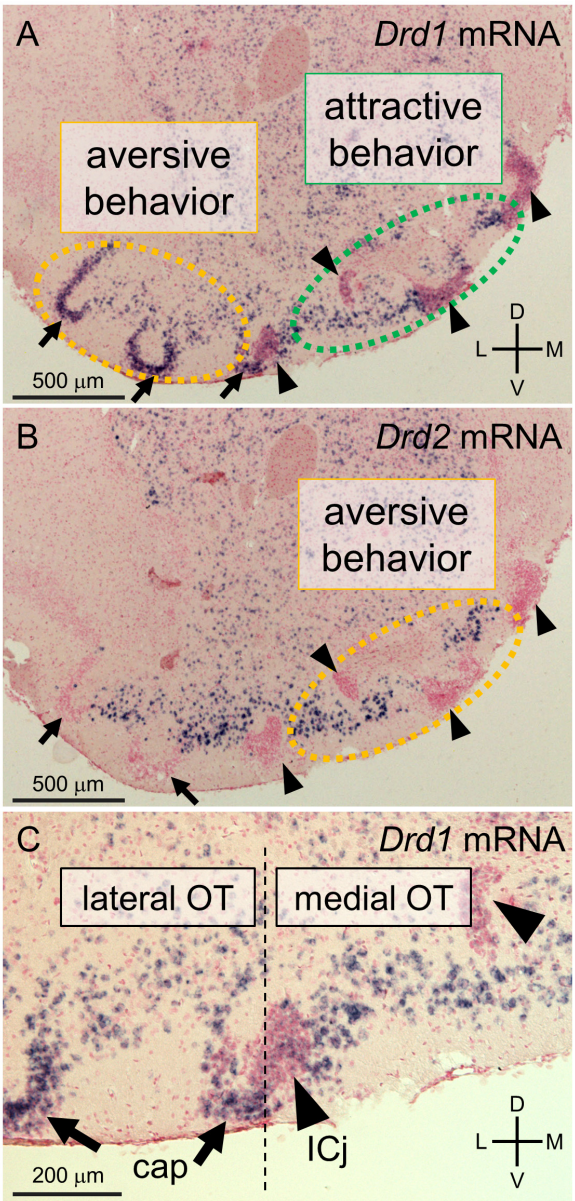

FIGURE 1 | Cytoarchitectonically defined-domains of the mouse olfactory tubercle (OT). **(A–C)** *In situ* hybridization for dopamine receptor D1 (*Drd1*, **A,C**) and D2 (*Drd2*, **B**) mRNA in the anterior OT of mouse counterstained with Nuclear Fast Red. *c-fos* expression mapping revealed that D1 receptor-expressing neurons in the anteromedial OT were activated by sugar-associated cue odors, which accompanied attractive behavior **(A)** and that D1 receptor-expressing neurons in the lateral OT **(A)** and D2 receptor-expressing neurons in the anteromedial OT **(B)** were activated by electrical shock-associated cue odors which accompanied aversive behavior. In the cap regions (arrows), the dwarf cells are densely packed and express *Drd1* but not *Drd2* mRNA **(B,C)**. The granule cells in the Islands of Calleja (arrowheads) are also densely packed but exhibit weak expression of *Drd1* and no *Drd2* mRNA **(B,C)**. Medium spiny neurons are mainly distributed in the layer II of the cortex-like regions, which are interposed between the cap regions and Islands of Calleja in these coronal sections, and express either *Drd1* or *Drd2* **(A,B)**. The cap region and Islands of Calleja serve as anatomical landmarks for the lateral and medial domains of the OT, respectively. ICj, Islands of Calleja; D, dorsal; V, ventral; M, medial; L, lateral. The Figures are modified from (Murata et al., 2015).

Calleja are also distinguishable by the expression of DARPP-32, as the cap regions are immunopositive and the Islands of Calleja are immunonegative for DARPP-32, respectively (Ouimet et al., 1984; Murata et al., 2015). The cap regions run in an anteroposterior direction through the lateral part of the OT. In contrast, the Islands of Calleja run in an anteroposterior direction through the anteromedial superficial layer to the posteromedial deep layer (Murata et al., 2015; Xiong and Wesson, 2016).

A recent study revealed that spatially segregated domains of the OT are involved in distinct motivated behaviors. Learned odor-induced attractive and aversive behaviors accompanied *c-fos* expression in distinct domains of the OT (Murata et al., 2015). When mice exhibited attractive behaviors to a cue odor paired with the presence of sugar, *c-fos* expression increased in D1 receptor-expressing medium spiny neurons in the anteromedial domain. Conversely, when mice exhibited aversive behaviors to a cue odor paired with an electrical foot shock, *c-fos* expression was increased in D1 receptor-expressing medium spiny neurons and dwarf cells in the lateral domain and D2 receptor-expressing medium spiny neurons in the anteromedial domain. These findings suggest that the spatial pattern of neural activation in the OT encodes odor-induced attractive or aversive behaviors, in contrast to the odor map of the olfactory bulb. Consistent with this, electrophysiological recordings in behaving mice revealed that the firing activity of the OT flexibly encoded the valence of conditioned odors over odorant identity (Gadziola et al., 2015, 2020). These studies suggest that OT neurons evaluate odorants in an experience-dependent manner and that spatially segregated domains and neuronal subtypes play distinct roles in inducing appropriate motivated behaviors.

The involvement of the medial domain of the OT in attractive behaviors has been demonstrated in several reports. The anteromedial OT was the most effective region that elicited intracranial self-administration of cocaine among a range of distinct striatal regions including the anteromedial OT, anterolateral OT, posteromedial OT, NAc shell and core, and dorsal striatum (Ikemoto, 2003). Silencing of the medial OT in estrous female mice with the inhibitory designer receptor exclusively activated by designer drug (DREADD) hM4Di prevented attractive behavior to chemosignals of the opposite sex (DiBenedictis et al., 2015). Notably, chemogenetic silencing of the medial OT did not suppress attractive behaviors to peanut butter odor in pre-fed mice, implying that the medial OT is dispensable and is not the sole neural circuit that facilitates attraction to food-related odors. The medial OT receives dopaminergic inputs from the medial part of the ventral tegmental area (VTA) (Ikemoto, 2007). Optogenetic stimulation of dopaminergic axon terminals of the VTA-medial OT pathway promoted place preference and odor preference (Zhang et al., 2017a). Neuronal subtype-specific activation of D1 or D2 receptor-expressing neurons has provided further insight into the functions of the anteromedial OT. Optogenetic stimulation of D1 receptor-expressing neurons and D2 receptor-expressing neurons in the anteromedial OT elicited place preference and place aversion, respectively (Murata et al., 2019b). The effects of manipulating the lateral domain of the OT on aversive behaviors are yet to be reported. Neuroanatomical tracing has revealed that the cap regions in the lateral OT receive axonal projections from tufted cells in the dorsal part of the olfactory bulb, which respond to predator fox odor trimethylthiazoline and rotten food odor 2-methylbutyric acid (Igarashi et al., 2012). Further experiments are required to elucidate the spatially segregated domain- and neuronal subtype-specific functional roles of the OT in odor-guided motivated behaviors.

Involvement of the Olfactory Tubercle and Nucleus Accumbens in Motivated and Hedonic Eating

Another component of the ventral striatum, the NAc, constitutes a critical node within mesocorticolimbic circuits that mediate "wanting" and "liking" (Richard et al., 2013; Morales and Berridge, 2020). Pharmacological functional mapping revealed that local microcircuits of the NAc medial shell differentially regulate food intake of palatable chocolate and hedonic reactions to taste stimulation. Microinjections of the $GABA_A$ receptor agonist muscimol into the rostral medial shell elicited increased food intake and hedonic reactions to the taste of sucrose. In contrast, microinjections of muscimol into the caudal medial shell induced defensive behavior and aversive reactions to sucrose or quinine tastants (Reynolds and Berridge, 2002). Microinjections of agonists of opioid receptor subtypes (mu, delta, and kappa) have revealed the anatomical heterogeneity of the NAc in the regulation of motivated and hedonic eating behaviors (Castro and Berridge, 2014). The anatomical similarity between the OT andNAc, both of which contain GABAergic neurons that project to the ventral pallidum, raises the possibility of similar functional maps of motivated and hedonic behaviors in the OT (Zahm and Heimer, 1985; Heimer et al., 1987; Zhou et al., 2003). Optogenetic self-stimulation experiments suggested that the excitation of D1 receptor-expressing neurons in the medial shell of the NAc supports strong incentive motivation to self-stimulate (Cole et al., 2018). However, neural pathways from the OT are not identical to those from the NAc. For instance, D1 receptor-expressing medium spiny neurons in the NAc provide synaptic inputs onto GABAergic neurons in the lateral hypothalamus, which are involved in the downregulation of feeding behavior (O'Connor et al., 2015). Retrograde tracing from the lateral hypothalamus revealed a substantially larger number of labeled cells in the NAc than in the OT (Murata et al., 2019a). Future studies should address whether and how distinct OT domains regulate motivated and hedonic eating behaviors.

The development of OT neural circuits during weaning has implications for the involvement of the OT in eating. Neurogenesis of the OT in the embryonic mouse and rat occurs in a lateral-to-medial gradient (Bayer, 1985; Martin-Lopez et al., 2019). Early postnatal development of the mouse OT is consistent with this gradient (Martin-Lopez et al., 2019). *Drd1* mRNA and DARPP-32 expression in the lateral OT precedes the corresponding expression that in the anteromedial OT at postnatal days 3-8 (P3-8) (Murofushi et al., 2018). Mapping of c-fos expression after search and consumption of food pellets indicated widespread neural activation across diffuse OT domains at P15, whereas the anteromedial domain

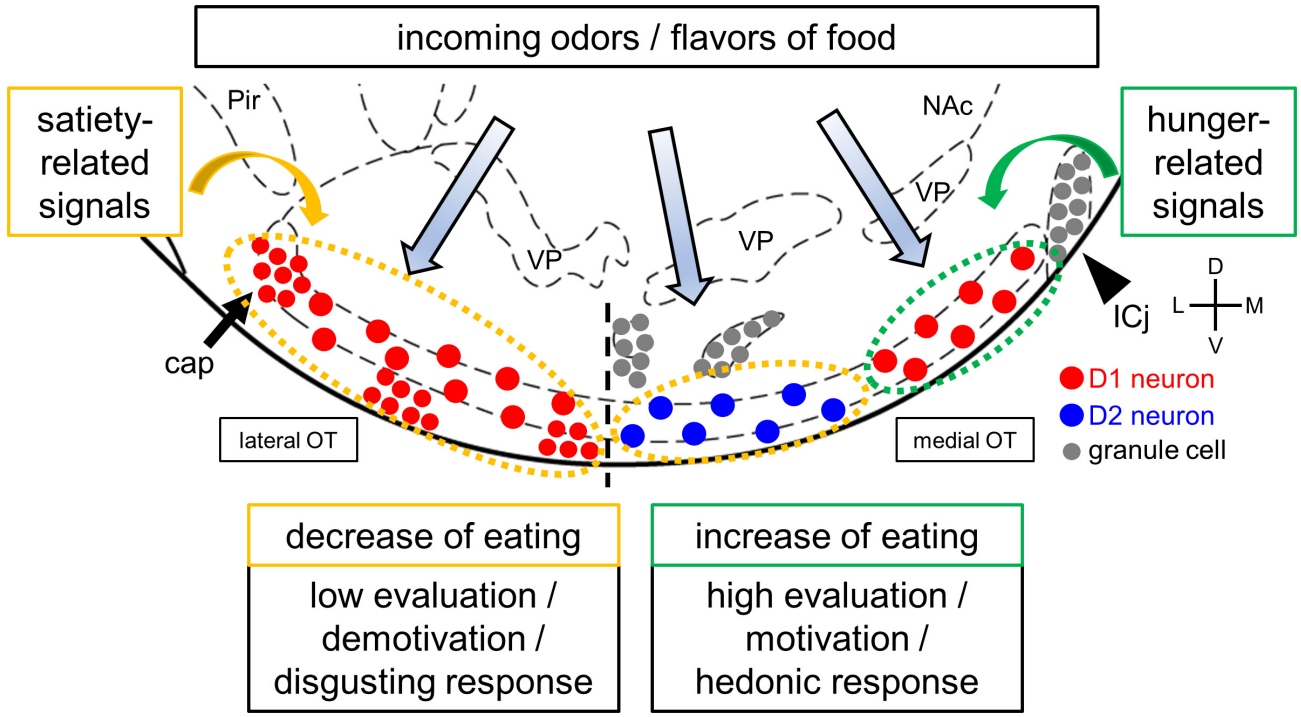

FIGURE 2 | A hypothetical model of the OT and eating. The OT receives and may integrate olfactory inputs and feeding-related hormonal signals, as well as other sensory modalities, visceral, and neuromodulatory inputs. The hypothesis is that activation of the D1 receptor-expressing neurons in the anteromedial OT increases food intake, whereas activation of the D2 receptor-expressing neurons in the anteromedial OT and D1 receptor-expressing neurons in the lateral OT decreases food intake based on their involvement in attractive and aversive behaviors, respectively. Feeding-related hormonal signals, such hunger and satiety, may regulate the activity of OT neurons in a domain- and cell type-specific manner. These signals result in homeostatic evaluation, motivation, and hedonic responses to food odors and flavors. D1 and D2 receptor-expressing neurons in layer II of the cortex-like region were noted to be intermingled in both the anteromedial and lateral OT domains, as shown in **Figure 1** but simplified here in this figure. Red circles, D1 receptor-expressing medium spiny neurons in layer II of cortex-like regions and dwarf cells in the cap regions (arrows); blue circles, D2 receptor-expressing medium spiny neurons in layer II of cortex-like regions; gray circles, granule cells in the Islands of Calleja (arrowheads). Pir, piriform cortex; NAc, nucleus accumbens; VP, ventral pallidum; ICj, Islands of Calleja. D, dorsal; V, ventral; M, medial; L, lateral. Stereotaxic atlas from Paxinos and Franklin (2008).

was preferentially activated at P21 and later ages (Murofushi et al., 2018). Acquisition of food-eating habits including consumption of laboratory animal pellets is a form of learning during weaning which involves evaluation, motivation, and palatability of foods, which may be associated with the functional maturation of OT domains.

The OT receives multimodal sensory inputs alongside olfaction (Wesson and Wilson, 2011). Odor information can be conveyed to the OT directly from the olfactory bulb or via other areas of the olfactory cortex (Heimer, 1978). Whole-brain mapping of input pathways has indicated that the medial OT receives synaptic inputs from widespread areas of the brain including the isocortex, septum, striatum, pallidum, amygdala, thalamus, hypothalamus, olfactory areas, and VTA (Zhang et al., 2017b). The VTA-medial OT dopaminergic pathway is activated by rewarding experiences such as sucrose-licking (Zhang et al., 2017a). Axonal projections from the nucleus of the solitary tract to the OT suggest that visceral signals are directly transferred to the OT via this pathway (Ruggiero et al., 1998). The OT expresses various receptors of neuromodulatory inputs, opioids, hormones, and neurosteroids (Cansler et al., 2020). In the anteromedial OT, various orexigenic peptides (orexin and prodynorphin) and receptors (orexin receptors 1 and 2, ghrelin receptor, and opioid receptor kappa 1) were highly expressed compared to those in the lateral OT. This trend was also seen in anorexigenic peptides (CART peptide) and receptors (melanocortin four receptor and arginine-vasopressin receptor 1a) (Nogi et al., 2020). Odor cues may influence the release and expression of these feeding-related peptides and receptors in the anteromedial OT and the subsequent ingestive behaviors. Indeed, the expression levels of the orexigenic peptide (ghrelin) and receptors (cannabinoid receptor 1, opioid receptor delta 1, and opioid receptor kappa 1) were increased in the anteromedial OT by odor-guided food-seeking behavior. A similar increase was noted in the levels of the anorexigenic peptide (arginine-vasopressin) and receptors (leptin receptor and melanocortin four receptor) in the anteromedial OT (Nogi et al., 2020). Cell-type identification will assist in determining how specific neural circuits in the OT function in eating behaviors by elucidating which neurons (D1 receptor or D2 receptor-expressing neurons and other types of neurons) express the aforementioned peptides and receptors.

A Hypothetical Neural Model Relating the OT and Eating Behavior

In summary, the OT has the following neuroanatomical and neurochemical similarities with the NAc: dense dopaminergic inputs from the VTA, high expression of the dopamine receptors, and GABAergic outputs to the ventral pallidum (Heimer et al., 1987; Ikemoto, 2007). A notable difference between the OT and NAc is that the OT receives abundant synaptic inputs from the olfactory bulb and olfactory cortical areas (Zhang et al., 2017b), which convey olfactory sensory cues of food in the environment and olfactory components of flavors during mastication via the retronasal pathway to the OT. Indeed, the OT is considered the "striatum with olfactory function" (Wesson and Wilson, 2011; Martin-Lopez et al., 2019) and may drive olfaction-based "wanting" and "liking" behaviors (Richard et al., 2013; Morales and Berridge, 2020).

As previously mentioned, the cytoarchitectonically defined-domains of the mouse OT play distinct roles in attractive and aversive responses to odor cues (**Figure 1**). These domains raise the possibility that D1 receptor-expressing neurons in the anteromedial domain facilitate eating by high evaluation, motivation, and hedonic response to food-related odors and flavors. In contrast, D2 receptor-expressing neurons in the anteromedial domain and D1 receptor-expressing neurons in the lateral domain may suppress eating by low evaluation, demotivation, and disgusting response to food-related odors and flavors. The OT also expresses orexigenic and anorexigenic peptides and their receptors (Cansler et al., 2020; Nogi et al., 2020), which may endow OT domains with homeostatic control over odor-guided eating behaviors (Aime et al., 2007; Palouzier-Paulignan et al., 2012). For instance, hunger state and its orexigenic hormonal signals such as orexin and ghrelin might upregulate the responses of D1 receptor-expressing neurons in the anteromedial OT to food odors and flavors, resulting in increase of food intake. Satiety state and its anorexigenic hormonal signals such as leptin, in contrast, might upregulate responses to food odors and flavors of D2 receptor-expressing neurons in the anteromedial OT and D1 receptor-expressing neurons in the lateral OT, resulting in food intake suppression (**Figure 2**). Future studies should address whether and how the OT integrates olfaction, other sensory modalities, and visceral and feeding-related endocrine signals during and after eating. Specific domains and neuronal subtypes of the OT may be activated by incoming environmental odors and flavors of food when evaluating the decision to eat, appetitive or aversive motivation, and hedonic palatability.

AUTHOR CONTRIBUTIONS

KM wrote the manuscript.

FUNDING

KM was supported by JSPS KAKENHI Grant Numbers 16H01671, 16K18377, 17KK0190, and 18H05005, and by the Takeda Science Foundation.

REFERENCES

Aime, P., Duchamp-Viret, P., Chaput, M. A., Savigner, A., Mahfouz, M., and Julliard, A. K. (2007). Fasting increases and satiation decreases olfactory detection for a neutral odor in rats. *Behav. Brain Res.* 179, 258–264. doi: 10.1016/j.bbr.2007.02.012

Allison, A. C. (1954). The secondary olfactory areas in the human brain. *J. Anat.* 88, 481–488.

Bayer, S. A. (1985). Neurogenesis in the olfactory tubercle and islands of Calleja in the rat. *Int. J. Dev. Neurosci.* 3, 135–147. doi: 10.1016/0736-5748(85)90004-8

Berridge, K. C., and Kringelbach, M. L. (2015). Pleasure systems in the brain. *Neuron* 86, 646–664. doi: 10.1016/j.neuron.2015.02.018

Cansler, H. L., Wright, K. N., Stetzik, L. A., and Wesson, D. W. (2020). Neurochemical organization of the ventral striatum's olfactory tubercle. *J. Neurochem.* 152, 425–448. doi: 10.1111/jnc.14919

Castro, D. C., and Berridge, K. C. (2014). Opioid hedonic hotspot in nucleus accumbens shell: mu, delta, and kappa maps for enhancement of sweetness "liking" and "wanting". *J. Neurosci.* 34, 4239–4250. doi: 10.1523/JNEUROSCI.4458-13.2014

Cole, S. L., Robinson, M. J. F., and Berridge, K. C. (2018). Optogenetic self-stimulation in the nucleus accumbens: D1 reward versus D2 ambivalence. *PLoS One* 13:e0207694. doi: 10.1371/journal.pone.0207694

Crosby, E. C., and Humphrey, T. (1941). Studies of the vertebrate telencephalon. II. The nuclear pattern of the anterior olfactory nucleus, tuberculum olfactorium and the amygdaloid complex in adult man. *J. Comp. Neurol.* 74, 309–352. doi: 10.1002/cne.900740209

de Vente, J., Hani, L., Steinbusch, H. E., and Steinbusch, H. W. (2001). The three dimensional structure of the islands of Calleja: a single heterogenous cell complex. *Neuroreport* 12, 565–568. doi: 10.1097/00001756-200103050-00026

DiBenedictis, B. T., Olugbemi, A. O., Baum, M. J., and Cherry, J. A. (2015). DREADD-induced silencing of the medial olfactory tubercle disrupts the preference of female mice for opposite-sex chemosignals(1,2,3). *eNeuro* 2:ENEURO.0078-15.2015. doi: 10.1523/ENEURO.0078-15.2015

Fallon, J. H., Riley, J. N., Sipe, J. C., and Moore, R. Y. (1978). The islands of Calleja: organization and connections. *J. Comp. Neurol.* 181, 375–395. doi: 10.1002/cne.901810209

Gadziola, M. A., Stetzik, L. A., Wright, K. N., Milton, A. J., Arakawa, K., Del Mar Cortijo, M., et al. (2020). A neural system that represents the association of odors with rewarded outcomes and promotes behavioral engagement. *Cell. Rep.* 32:107919. doi: 10.1016/j.celrep.2020.107919

Gadziola, M. A., Tylicki, K. A., Christian, D. L., and Wesson, D. W. (2015). The olfactory tubercle encodes odor valence in behaving mice. *J. Neurosci.* 35, 4515–4527. doi: 10.1523/JNEUROSCI.4750-14.2015

Ghosh, S., Larson, S. D., Hefzi, H., Marnoy, Z., Cutforth, T., Dokka, K., et al. (2011). Sensory maps in the olfactory cortex defined by long-range viral tracing of single neurons. *Nature* 472, 217–220. doi: 10.1038/nature09945

Heimer, L. (1978). "The olfactory cortex and the ventral striatum," in *Limbic Mechanisms: The Continuing Evolution of the Limbic System Concept*, eds K. E. Livingston and O. Hornykiewicz (Boston, MA: Springer), 95–187. doi: 10.1007/978-1-4757-0716-8_7

Heimer, L., Zaborszky, L., Zahm, D. S., and Alheid, G. F. (1987). The ventral striatopallidothalamic projection: I. The striatopallidal link originating in the striatal parts of the olfactory tubercle. *J. Comp. Neurol.* 255, 571–591. doi: 10.1002/cne.902550409

Hosoya, Y., and Hirata, Y. (1974). The fine structure of the "dwarf-cell cap" of the olfactory tubercle in the rat's brain. *Arch. Histol. Jpn.* 36, 407–423. doi: 10.1679/aohc1950.36.407

Igarashi, K. M., Ieki, N., An, M., Yamaguchi, Y., Nagayama, S., Kobayakawa, K., et al. (2012). Parallel mitral and tufted cell pathways route distinct odor

information to different targets in the olfactory cortex. *J. Neurosci.* 32, 7970–7985. doi: 10.1523/JNEUROSCI.0154-12.2012

Ikemoto, S. (2003). Involvement of the olfactory tubercle in cocaine reward: intracranial self-administration studies. *J. Neurosci.* 23, 9305–9311. doi: 10.1523/jneurosci.23-28-09305.2003

Ikemoto, S. (2007). Dopamine reward circuitry: two projection systems from the ventral midbrain to the nucleus accumbens-olfactory tubercle complex. *Brain Res. Rev.* 56, 27–78. doi: 10.1016/j.brainresrev.2007.05.004

Ikemoto, S. (2010). Brain reward circuitry beyond the mesolimbic dopamine system: a neurobiological theory. *Neurosci. Biobehav. Rev.* 35, 129–150. doi: 10.1016/j.neubiorev.2010.02.001

Ikemoto, S., Qin, M., and Liu, Z. H. (2005). The functional divide for primary reinforcement of D-amphetamine lies between the medial and lateral ventral striatum: is the division of the accumbens core, shell, and olfactory tubercle valid? *J. Neurosci.* 25, 5061–5065. doi: 10.1523/JNEUROSCI.0892-05.2005

Lawless, H. (1991). The sense of smell in food quality and sensory evaluation. *J. Food Qual.* 14, 33–60. doi: 10.1111/j.1745-4557.1991.tb00046.x

Martin-Lopez, E., Xu, C., Liberia, T., Meller, S. J., and Greer, C. A. (2019). Embryonic and postnatal development of mouse olfactory tubercle. *Mol. Cell. Neurosci.* 98, 82–96. doi: 10.1016/j.mcn.2019.06.002

Millhouse, O. E., and Heimer, L. (1984). Cell configurations in the olfactory tubercle of the rat. *J. Comp. Neurol.* 228, 571–597. doi: 10.1002/cne.902280409

Morales, I., and Berridge, K. C. (2020). 'Liking' and 'wanting' in eating and food reward: brain mechanisms and clinical implications. *Physiol. Behav.* 227:113152. doi: 10.1016/j.physbeh.2020.113152

Mori, K., and Sakano, H. (2011). How is the olfactory map formed and interpreted in the mammalian brain? *Annu. Rev. Neurosci.* 34, 467–499. doi: 10.1146/annurev-neuro-112210-112917

Murata, K., Kanno, M., Ieki, N., Mori, K., and Yamaguchi, M. (2015). Mapping of learned odor-induced motivated behaviors in the mouse olfactory tubercle. *J. Neurosci.* 35, 10581–10599. doi: 10.1523/JNEUROSCI.0073-15.2015

Murata, K., Kinoshita, T., Fukazawa, Y., Kobayashi, K., Kobayashi, K., Miyamichi, K., et al. (2019a). GABAergic neurons in the olfactory cortex projecting to the lateral hypothalamus in mice. *Sci. Rep.* 9:7132. doi: 10.1038/s41598-019-43580-1

Murata, K., Kinoshita, T., Fukazawa, Y., Kobayashi, K., Yamanaka, A., Hikida, T., et al. (2019b). Opposing roles of dopamine receptor D1- and D2-expressing neurons in the anteromedial olfactory tubercle in acquisition of place preference in mice. *Front. Behav. Neurosci.* 13:50. doi: 10.3389/fnbeh.2019.00050

Murofushi, W., Mori, K., Murata, K., and Yamaguchi, M. (2018). Functional development of olfactory tubercle domains during weaning period in mice. *Sci. Rep.* 8:13204. doi: 10.1038/s41598-018-31604-1

Neville, K. R., and Haberly, L. B. (2004). Olfactory cortex. *Synapt. Organ. Brain* 5, 415–454.

Nogi, Y., Ahasan, M. M., Murata, Y., Taniguchi, M., Sha, M. F. R., Ijichi, C., et al. (2020). Expression of feeding-related neuromodulatory signalling molecules in the mouse central olfactory system. *Sci. Rep.* 10:890. doi: 10.1038/s41598-020-57605-7

O'Connor, E. C., Kremer, Y., Lefort, S., Harada, M., Pascoli, V., Rohner, C., et al. (2015). Accumbal D1R neurons projecting to lateral hypothalamus authorize feeding. *Neuron* 88, 553–564. doi: 10.1016/j.neuron.2015.09.038

Ouimet, C. C., Miller, P. E., Hemmings, H. C. Jr., Walaas, S. I., and Greengard, P. (1984). DARPP-32, a dopamine- and adenosine 3':5'-monophosphate-regulated phosphoprotein enriched in dopamine-innervated brain regions. III. Immunocytochemical localization. *J. Neurosci.* 4, 111–124. doi: 10.1523/jneurosci.04-01-00111.1984

Palouzier-Paulignan, B., Lacroix, M. C., Aime, P., Baly, C., Caillol, M., Congar, P., et al. (2012). Olfaction under metabolic influences. *Chem. Senses* 37, 769–797. doi: 10.1093/chemse/bjs059

Paxinos, G., and Franklin, K. (2008). *The Mouse Brain in Stereotaxic Coordinates, Compact: The Coronal Plates and Diagrams*. London, UK: Academic press .

Reynolds, S. M., and Berridge, K. C. (2002). Positive and negative motivation in nucleus accumbens shell: bivalent rostrocaudal gradients for GABA-elicited eating, taste "liking"/"disliking" reactions, place preference/avoidance, and fear. *J. Neurosci.* 22, 7308–7320. doi: 10.1523/jneurosci.22-16-07308.2002

Richard, J. M., Castro, D. C., Difeliceantonio, A. G., Robinson, M. J., and Berridge, K. C. (2013). Mapping brain circuits of reward and motivation: in the footsteps of Ann Kelley. *Neurosci. Biobehav. Rev.* 37(9 Pt A), 1919–1931. doi: 10.1016/j.neubiorev.2012.12.008

Ruggiero, D. A., Anwar, S., Kim, J., and Glickstein, S. B. (1998). Visceral afferent pathways to the thalamus and olfactory tubercle: behavioral implications. *Brain Res.* 799, 159–171. doi: 10.1016/s0006-8993(98)00442-9

Shepherd, G. M. (2013). *Neurogastronomy : How the Brain Creates Flavor and Why It Matters*. New York, NY: Columbia University Press.

Shin, R., Qin, M., Liu, Z. H., and Ikemoto, S. (2008). Intracranial self-administration of MDMA into the ventral striatum of the rat: differential roles of the nucleus accumbens shell, core, and olfactory tubercle. *Psychopharmacology* 198, 261–270. doi: 10.1007/s00213-008-1131-x

Sosulski, D. L., Bloom, M. L., Cutforth, T., Axel, R., and Datta, S. R. (2011). Distinct representations of olfactory information in different cortical centres. *Nature* 472, 213–216. doi: 10.1038/nature09868

Stettler, D. D., and Axel, R. (2009). Representations of odor in the piriform cortex. *Neuron* 63, 854–864. doi: 10.1016/j.neuron.2009.09.005

Uchida, N., Takahashi, Y. K., Tanifuji, M., and Mori, K. (2000). Odor maps in the mammalian olfactory bulb: domain organization and odorant structural features. *Nat. Neurosci.* 3, 1035–1043. doi: 10.1038/79857

Wesson, D. W., and Wilson, D. A. (2011). Sniffing out the contributions of the olfactory tubercle to the sense of smell: hedonics, sensory integration, and more? *Neurosci. Biobehav. Rev.* 35, 655–668. doi: 10.1016/j.neubiorev.2010.08.004

Xiong, A., and Wesson, D. W. (2016). Illustrated review of the ventral striatum's olfactory tubercle. *Chem. Senses* 41, 549–555. doi: 10.1093/chemse/bjw069

Zahm, D. S., and Heimer, L. (1985). Synaptic contacts of ventral striatal cells in the olfactory tubercle of the rat: correlated light and electron microscopy of anterogradely transported Phaseolus vulgaris-leucoagglutinin. *Neurosci. Lett.* 60, 169–175. doi: 10.1016/0304-3940(85)90239-3

Zhang, Z., Liu, Q., Wen, P., Zhang, J., Rao, X., Zhou, Z., et al. (2017a). Activation of the dopaminergic pathway from VTA to the medial olfactory tubercle generates odor-preference and reward. *eLife* 6:e25423. doi: 10.7554/eLife.25423

Zhang, Z., Zhang, H., Wen, P., Zhu, X., Wang, L., Liu, Q., et al. (2017b). Whole-brain mapping of the inputs and outputs of the medial part of the olfactory tubercle. *Front. Neural Circ.* 11:52. doi: 10.3389/fncir.2017.00052

Zhou, L., Furuta, T., and Kaneko, T. (2003). Chemical organization of projection neurons in the rat accumbens nucleus and olfactory tubercle. *Neuroscience* 120, 783–798. doi: 10.1016/s0306-4522(03)00326-9

Conflict of Interest: The author declares that the research was conducted in the absence of any commercial or financial relationships that could be construed as a potential conflict of interest.

frontiers in Human Neuroscience

ORIGINAL RESEARCH
published: 12 November 2020
doi: 10.3389/fnhum.2020.577669

Brain Activity Associated With Regulating Food Cravings Predicts Changes in Self-Reported Food Craving and Consumption Over Time

Nicole R. Giuliani[1], Danielle Cosme[2], Junaid S. Merchant[3], Bryce Dirks[4] and Elliot T. Berkman[5]*

[1] Department of Special Education and Clinical Sciences, Prevention Science Institute, University of Oregon, Eugene, OR, United States, [2] Communication Neuroscience Lab, Annenberg School for Communication, University of Pennsylvania, Philadelphia, PA, United States, [3] Developmental Social Cognitive Neuroscience Lab, Neuroscience and Cognitive Science Program, Department of Psychology, University of Maryland, College Park, College Park, MD, United States, [4] Brain Connectivity and Cognition Lab, Department of Psychology, University of Miami, Miami, FL, United States, [5] Social and Affective Neuroscience Lab, Department of Psychology, Center for Translational Neuroscience, University of Oregon, Eugene, OR, United States

OPEN ACCESS

Edited by:
Masahiro Yamaguchi, Kôchi University, Japan

Reviewed by:
Kyle S. Burger, University of North Carolina at Chapel Hill, United States
Joe Jacques Simon, Heidelberg University, Germany

***Correspondence:**
Nicole R. Giuliani
giuliani@uoregon.edu

Specialty section:
This article was submitted to Health, a section of the journal Frontiers in Human Neuroscience

Received: *29 June 2020*
Accepted: *28 October 2020*
Published: *12 November 2020*

Citation:
Giuliani NR, Cosme D, Merchant JS, Dirks B and Berkman ET (2020) Brain Activity Associated With Regulating Food Cravings Predicts Changes in Self-Reported Food Craving and Consumption Over Time. Front. Hum. Neurosci. 14:577669. doi: 10.3389/fnhum.2020.577669

Neural patterns associated with viewing energy-dense foods can predict changes in eating-related outcomes. However, most research on this topic is limited to one follow-up time point, and single outcome measures. The present study seeks to add to that literature by employing a more refined assessment of food craving and consumption outcomes along with a more detailed neurobiological model of behavior change over several time points. Here, a community sample of 88 individuals (age: M = 39.17, SD = 3.47; baseline BMI: M = 31.5, SD = 3.9, range 24–42) with higher body mass index (BMI) performed a food craving reactivity and regulation task while undergoing functional magnetic resonance imaging. At that time—and 1, 3, and 6 months later—participants reported craving for and consumption of healthy and unhealthy foods via the Food Craving Inventory (FCI) and ASA24 (N at 6 months = 52–55 depending on the measure). *A priori* hypotheses that brain activity associated with both viewing and regulating personally desired unhealthy, energy-dense foods would be associated with self-reported craving for and consumption of unhealthy foods at baseline were not supported by the data. Instead, regression models controlling for age, sex, and BMI demonstrated that brain activity across several regions measured while individuals were regulating their desires for unhealthy food was associated with the self-reported craving for and consumption of healthy food. The hypothesis that vmPFC activity would predict patterns of healthier eating was also not supported. Instead, linear mixed models controlling for baseline age and sex, as well as changes in BMI, revealed that more regulation-related activity in the dlPFC, dACC, IFG, and vmPFC at baseline predicted decreases in the craving for and consumption of healthy foods over the course of 6 months.

Keywords: food cue reactivity, food craving regulation, healthy food, unhealthy food, food craving, food consumption, brain activity

INTRODUCTION

For many of us, simply seeing or smelling something that reminds us of a favorite food can elicit a strong desire for that food. Strong desires, called cravings, often lead to the consumption of that food (e.g., Fedoroff et al., 2003). This frequently occurs for unhealthy or energy-dense foods like snacks and desserts (Massicotte et al., 2019). Consumption of such energy-dense foods is associated with increased risk for overweight [25 kg/m^2 $\leq$ body mass index (BMI) $<$ 30 kg/m^2], obesity (BMI $\geq$ 30 kg/m^2), and health consequences associated with higher body weight (Pereira et al., 2005; Duffey et al., 2007; Centers for Disease Control and Prevention, 2011).

Cravings are a form of "food cue reactivity," or conditioned responses to food that are frequently accompanied by a suite of experiential, physiological, and neural responses (Boswell and Kober, 2016). However, people also work to regulate the cravings they experience, such that they don't automatically lead to consuming the craved food (Giuliani and Berkman, 2015). A growing body of research has focused on brain activity associated with food cue reactivity and the regulation of these responses, with the goal of explaining how these neural responses predict subsequent health outcomes. At present, this research is mostly limited to studies with one follow-up time point, or a single outcome measure (e.g., BMI, snack consumption; Yokum et al., 2011; Lawrence et al., 2012). The present study seeks to extend this work by (1) employing a more refined assessment of food preference, craving, and consumption outcomes above and beyond BMI, (2) interrogating these patterns for both healthy and unhealthy foods, and (3) creating a more detailed model of behavior change over multiple time points.

Behavior Change From Food Cue Reactivity

The subjective experience of craving predicts subsequent eating behavior in the presence (Cornell et al., 1989; Fedoroff et al., 1997, 2003; Nederkoorn et al., 2000) and absence of actual food cues (Gilhooly et al., 2007; Martin et al., 2008; Batra et al., 2013; Cleobury and Tapper, 2014; Crowley et al., 2014). Recent work suggests that this effect is specific to highly palatable energy-dense foods (Massicotte et al., 2019), which are also those that individuals most often report craving (Chao et al., 2014). Craving is related to but separable from liking; where craving implies a motivational state, liking is the hedonic reaction to the pleasure of the reward (Berridge, 2009). As such, a full investigation of the patterns of behavior change from food cue reactivity should interrogate both subjective liking for foods as well as craving for and intake of those foods.

Similarly, physiological and neural responses to food cues are also prospectively associated with both eating behavior and weight gain (Rogers and Hill, 1989; Nederkoorn et al., 2000; Nederkoorn and Jansen, 2002; Jansen et al., 2003; Stice et al., 2010; Yokum et al., 2011, 2014; Demos et al., 2012; Lawrence et al., 2012; Mehta et al., 2012; Murdaugh et al., 2012; Lopez et al., 2014; Winter et al., 2017; Versace et al., 2018). This literature, while robust, is not uniform; several studies investigating measures of food cue reactivity have failed to demonstrate associations with eating behavior and/or weight, or found an association with physiological cue reactivity but not self-reported reactivity (see Boswell and Kober, 2016). A recent meta-analysis by Boswell and Kober (2016) found a medium effect of food cue reactivity and craving on food consumption and weight (r = 0.33), which did not vary based on the presence or absence of an actual food cue to induce the craving.

Interestingly, the bulk of the neurobehavioral work in this area has focused on brain regions associated with reward processing and incentive valuation, including the ventral striatum (VS), ventromedial prefrontal cortex (vmPFC), and amygdala (Giuliani et al., 2018). Craving is thought to recruit more of this reward network than liking, but the overlapping neural structures make experimentally separating the two processes quite difficult (Havermans, 2011). Recent evidence suggests that liking may be more associated with BMI than craving (Polk et al., 2017), and that food cue reactivity in the VS may be more strongly associated with food consumption than the vmPFC, which tracks with craving (Lawrence et al., 2012). Past work from our lab found that, independent of an individual's motivational state, activity in a broad network of regions involved in food cue reactivity, including the parahippocampal gyrus, cingulate, inferior occipital gyrus, and anterior insula, predicted consumption of a personally desired unhealthy food, but only in individuals who were not dieting (Giuliani et al., 2015). Other studies have found that activity in the inferior frontal gyrus (IFG, a lateral prefrontal region typically implicated in inhibitory control) while viewing food cues was positively associated with weight loss several months later (Neseliler et al., 2019). Therefore, the field's dominant focus on the mesolimbic dopamine system as the neural seat of food cue reactivity, craving, and consumption may be obscuring the roles of other brain regions and complementary cognitive processes such as liking in predicting these behaviors.

Behavior Change From Food Craving Regulation

Another complementary cognitive process is regulation. When individuals view energy-dense foods that they crave, they often don't passively follow those temptations. People use a variety of methods to regulate cravings for things that aren't in line with their long term goals (Giuliani et al., 2018). In the face of a tempting food, individuals engage in a variety of food craving regulation strategies. One popular strategy is reappraisal, which entails recontextualizing the food stimulus to change one's response to it (e.g., focusing on the negative consequences of eating a desired but unhealthy food; Giuliani and Berkman, 2015). Indeed, the tendency and capacity to engage in food craving regulation varies substantially among individuals (Lowe et al., 2019), supporting the notion that obesity, overweight, and the consumption of unhealthy foods is much more complex than differences in cue reactivity and craving. Behavioral measures of food craving regulation have been found to predict changes in the consumption of both healthy and unhealthy food over time (Giuliani et al., 2015; Reader et al., 2018).

Regulating the motivation to consume a desired unhealthy food relies heavily on the prefrontal cortex (PFC), which is implicated in the control over human behaviors, actions, and thoughts. When individuals are instructed to reappraise or suppress their cravings for food, increased activity in the

dorsolateral PFC (dlPFC), dorsal anterior cingulate cortex (dACC), and inferior temporal lobe is regularly observed (Giuliani et al., 2014; Han et al., 2018). A recent meta-analysis found that BMI is negatively associated with activity in the left dlPFC, right ventrolateral PFC (vlPFC), and IFG during regulation, which suggests that individuals with higher BMIs may be less able to recruit the lateral PFC to regulate their food choices (Han et al., 2018). Indeed, it is believed that lateral regions like the dlPFC modulate incentive valuation and reward processing within medial regions like the vmPFC and ventral striatum, which then affects the likelihood that individuals will select food items on the basis of healthiness compared to taste (Hare et al., 2009; Maier et al., 2015, though see Tusche and Hutcherson, 2018). Of these regions, the vmPFC is uniquely thought to support value-based decision-making (Berkman et al., 2017), in which choice options are assigned subjective values and a decision is made through a dynamic integration process of gains and costs. Assessments of vmPFC activation during decision-making, including in this study, typically take place before consumption as people consider their degree of motivation to approach (e.g., eat or purchase) the food stimuli. As such, vmPFC activation as measured by tasks such as the one used in this study can be considered an index of "wanting" as opposed to "liking."

Moving laterally, further evidence for the role of the lateral PFC in regulation comes from experimental manipulation of dlPFC activity. Stimulation of this region attenuates food cravings and the consumption of energy-dense foods in individuals who report strong food cravings, and inhibiting dlPFC activity is associated with overconsumption of energy-dense foods via changes in inhibitory control (Lowe et al., 2019). While there is considerable evidence linking eating behavior to brain activity (see Giuliani et al., 2018), additional evidence supports the effect of weight on brain function. Recent work on individuals who underwent bariatric surgery revealed that weight loss resulted in significant increases in dlPFC activity during food appraisal (Holsen et al., 2018). As such, this literature suggests a strong but bidirectional association between lateral PFC activity and eating behavior. Thus, according to Lowe et al. (2019), weaker lateral PFC responses to food cues may increase individual susceptibility to the rewarding properties of energy-dense foods, which prompts overconsumption, which then, over time, leads to lateral PFC dysregulation, exacerbated sensitivity to food rewards, and increased adiposity. While this model is intriguing, few studies have attempted to reconcile this PFC-centered model with the large literature implicating mesolimbic food cue reactivity in predicting food craving and consumption or the recent work indicating that both reactivity and regulation information are integrated in the vmPFC.

The Present Study

The present study aimed to address this gap by measuring brain activity associated with both food cue reactivity and regulation, and prospectively investigating how it predicted changes in self-reported liking of, craving for, and consumption of both healthy and unhealthy foods over the course of 6 months in a sample of middle-aged adults with higher BMIs.

First, we hypothesized that brain activity associated with both viewing and regulating personally desired unhealthy, energy-dense foods would be associated with self-reported craving and consumption of unhealthy foods at baseline. We also explored the association between brain activity and liking of, craving for, and consumption of healthy foods in order to examine the specificity of this effect to unhealthy food. Second, we hypothesized that activity in the vmPFC during the viewing of unhealthy foods would mediate the association between regulation-related brain activity and self-reported craving for and/or consumption of these foods. Third, we hypothesized that value-related brain activity in the vmPFC during food craving regulation at baseline would predict a decrease in the consumption of unhealthy food and an increase in the consumption of healthy food over 6 months. We also explored the role of other brain regions in predicting eating behavior change.

MATERIALS AND METHODS

Participants

A community sample of 105 middle-aged individuals with higher BMIs who intended to eat more healthfully were screened and enrolled into a larger project investigating a text message-based intervention aimed to improve eating habits. Inclusion criteria for the overarching study included (1) an approximate BMI between 25–40; (2) early, middle-age (i.e., approximately 35–45 years old); (3) no psychiatric, neurological, or eating disorders; (4) no fMRI contraindications; (5) not actively enrolled in a diet program or any other type of eating intervention; and (6) self-reported desire to eat more healthfully. Ten participants were excluded for non-compliance or repeatedly missing appointments, or decided to drop out before completion of the baseline session. A further 7 participants were excluded from the MRI analyses because they had excessive motion artifacts (defined below; n = 2), were not compliant with enrollment criteria (n = 2), had structural anomalies (n = 1), or for whom timing data were lost due to a technical error (n = 2). Therefore, analyses for this study are from the 88 individuals who provided useable MRI data (age: M = 39.2, SD = 3.57, range 33–46; baseline BMI: M = 31.5, SD = 3.9, range 24–42); they did not differ with regard to age or BMI from those who provided MRI data that were not useable. These participants were 81.91% female, and 79.5% identified as Caucasian, 8% Hispanic, 3.4% Black (not of Hispanic origin), 2.3% Middle Eastern, 1.1% each South Asian and American Indian/Alaskan Native, and 3.4% other.

An *a priori* power analysis was not conducted for this study; sample size was determined by budget and the duration of the grant award period. A *post hoc* power analysis in G*Power (Faul et al., 2009) indicated that we were adequately powered to test for medium-sized brain-behavior associations at baseline (f^2 = 0.156, with power = 0.8, α = 0.05, 5 predictors). With regard to change over time, we achieved up to 89% power (time x dlPFC interaction predicting craving for healthy foods) according to *post hoc* power simulations using simr (Green and MacLeod, 2016). However, many of the other findings were underpowered

and should be interpreted accordingly. Hypotheses and analytical procedures for this study were preregistered at the Open Science Framework[1].

Protocol

Participants were recruited for this study using a combination of online, newspaper, and public advertising. Interested individuals were screened for exclusion criteria via phone, and eligible participants were sent a battery of measures to complete before arriving for their baseline session. Participants were scheduled for their baseline lab visit, and asked to complete the pre-baseline measures within 24 h of the visit. Pre-baseline measures included demographic information, assessments of eating behavior, self-reported food craving and liking, and a set of psychometric measures not presented here. Participants were instructed to not eat anything for at least an hour before the baseline visit. During the baseline (T1) visit, participants provided informed consent, after which they were screened for MRI contraindications and instructed on the requirements of the study. Weight and height were measured, after which participants took part in an MRI session (described below). After the MRI session, they were randomized into intervention and control groups. The intervention, in which participants received self-authored text messages aligning healthy eating with personal values for 28 days after T1, did not have a significant effect on changes in BMI, healthy eating, or food craving compared to the control condition, where participants received standardized healthy eating messages. For the purposes of the analyses pursued here of measures acquired after randomization to condition, individuals were collapsed across groups, with group assignment controlled in the statistical models as a dummy-coded variable.

After the 28 days follow-up period, participants returned to the lab where they repeated all baseline measures with the exception of demographics and the MRI session (T2). Eating behavior was assessed over two separate days in advance of the visit. Three months after baseline (T3), participants were emailed instructions as to how to provide information on eating behavior and self-reported food craving and liking online. Six months after baseline (T4), participants returned to the lab where they repeated the procedures of the T2 visit.

Measures

Body Mass Index (BMI)

Weight and height were measured using a commercially available weight scale and wall ruler, and BMI was calculated by dividing the participant's weight in kilograms by height in square meters. These measures were collected in the laboratory at T1, T2, and T4. The number of participants from whom we collected this information at each time point is listed in **Table 1**.

Food Craving Inventory (FCI)

The FCI (White et al., 2002) is a 67-item self-report measure of cravings for and liking of specific foods. Craving was defined as "an intense desire for a specific food that is difficult to resist." Participants were asked to rate the frequency of cravings for the past 30 days on a 5-point Likert scale (1 = "not at all," 5 = "nearly every day"). They were also asked to rate how much they liked each food on a 4-point Likert scale (1 = "dislike," 4 = "love").

Foods were grouped into categories and ratings in each category were averaged for craving and liking separately. The foods included in each category are listed in the **Supplementary Materials**. We created composite measures of liking of and craving for unhealthy foods by averaging across ratings in the following categories: processed meats, fried foods, red meats, sugary foods, and empty calories. The same procedure was followed for healthy foods with the following categories: vegetables, fruits, lean proteins, whole grains, and olive oil.

ASA24

Eating behavior was assessed via the Automated Self-Administered 24 h (ASA24®) Dietary Assessment Tool (Subar et al., 2012) which allows for the calculation of the Healthy Eating Index (HEI; Guenther et al., 2013) using calculations provided by the developers of the ASA[2]. Following the recommendations proposed by the developers of this measure, participants completed the ASA twice at each time point to obtain a more representative estimate of daily eating behavior. We used the HEI as our measure of healthy eating as it quantifies how well a person's eating behavior aligns with recommended dietary guidelines for Americans. We also created an average of HEI indices 1–4, which captured daily consumption of total vegetables, greens and beans, total fruit, and whole fruit. In addition, we used the ASA24's calculation of total kilocalories consumed and empty calories consumed. All data were averaged across the 2 days of data collection at each time point.

Regulation of Craving (ROC) Task

Participants were trained to decrease their desire to consume personally-desired (for task purposes these are referred to as "craved" foods) foods using cognitive reappraisal (Giuliani et al., 2014; Giuliani and Pfeifer, 2015). Participants viewed unhealthy craved foods ("Craved" condition), unhealthy not-craved foods ("Not Craved" condition), or healthy vegetables ("Neutral" condition). For unhealthy craved foods, participants either actively viewed the foods ("Look" condition) or reappraised their craving for them ("Regulate" condition). On "Look" trials, participants imagined how they would interact with the food if it were in front of them. On "Regulate" trials, participants reappraised the foods by focusing on the short- or long-term negative health consequences associated with consumption (e.g., stomach aches, weight gain, cavities, etc.). Participants generated several negative health consequences with the help of the experimenter, to ensure they had multiple reappraisals they could use during the task. To minimize demand characteristics (e.g., reduced craving ratings on regulate trials), participants were reassured they were not expected to be able to regulate well on every trial and were told that it was important to rate their cravings honestly. Neutral stimuli were only viewed under "Look" instructions, and are not used in the present analyses. To keep

[1]https://osf.io/uvrkj/

[2]https://epi.grants.cancer.gov/asa24/resources/hei.html

TABLE 1 | Demographic and self-report information.

Measure	T1—0 months		T2—1 month		T3—3 months (online)		T4—6 months	
	M (*SD*)/% (*n*)	N	*M* (*SD*)	N	*M* (*SD*)	N	*M* (*SD*)	N
Age	39.2 (3.57)	88						
Gender (# female)	83.9% (73)							
BMI	31.5 (3.9)	88	31.57 (3.92)	78			31.18 (4.48)	52
FCI—healthy like rating	2.67 (0.46)	86	2.61 (0.45)	74	2.55 (0.47)	57	2.53 (0.50)	53
FCI—healthy crave rating	2.14 (0.73)	88	1.97 (0.68)	77	1.99 (0.68)	59	1.90 (0.63)	56
FCI—unhealthy like rating	2.70 (0.39)	86	2.61 (0.41)	74	2.63 (0.41)	57	2.61 (0.45)	53
FCI—unhealthy crave rating	2.47 (0.57)	88	2.20 (0.58)	77	2.26 (0.55)	59	2.16 (0.57)	56
ASA24—total kcal consumed	2087.94 (790.44)	87	1827.13 (688.58)	78	1805.44 (680.91)	55	1790.07 (797.25)	55
ASA24—HEI	52.86 (12.75)	87	50.75 (11.99)	77	50.38 (13.20)	55	54.24 (11.92)	55
ASA24—fruit/vegetable consumption	2.61 (1.28)	87	2.63 (1.28)	77	2.47 (1.26)	55	2.88 (1.09)	55
ASA24—empty calorie consumption	11.67 (5.22)	87	11.48 (5.73)	78	11.68 (5.19)	55	12.91 (5.45)	55

Age and gender were only collected at baseline; BMI was collected in person at baseline, T2, and T4; all other variables were collected at every time point. BMI = Body Mass Index; FCI = Food Craving Inventory; HEI = Healthy Eating Index.

task time to a minimum, only craved foods were viewed under "Regulate" instructions.

To maximize craving, participants selected their most craved and least craved food from the following menu of unhealthy food categories for the "Crave" and "Not Craved" conditions respectively: chocolate, cookies, donuts, French fries, ice cream, pasta, pizza. Stimuli were independently rated for desirability, such that the mean desirability of stimuli within each unhealthy food category did not differ significantly across categories (Giuliani et al., 2013). As such, each participant viewed a set of individually adapted unhealthy food stimulus categories; across all participants, the only domain on which the "Craved" and "Not Craved" conditions differed was with regard to individual food preferences. Each condition (Look Neutral, Look Craved, Look Not Craved, and Regulate Craved) had 20 trials, presented across two task runs. On each trial (see **Figure 1**), participants are presented with an instruction (2 s; Look or Regulate), viewed a food image while following the instruction (5 s), and rated their craving for the food on a 5-point Likert scale (4 s; 1 = not at all, 5 = very much). Each 11s trial of this event-related design was followed by a jittered fixation cross (M = 1 s) and trial order is optimized using a genetic algorithm (Wager and Nichols, 2003). Stimuli were presented using Psychtoolbox 3 (Brainard, 1997), and participants responded using a five-button box.

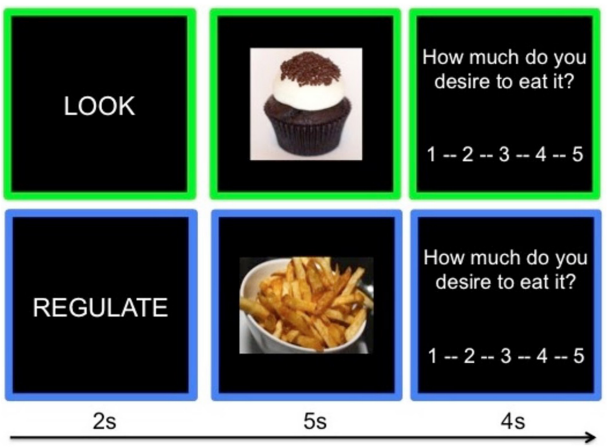

FIGURE 1 | Example trials from the ROC task.

Neuroimaging Data Acquisition and Preprocessing

Neuroimaging data were acquired on a 3T Siemens Skyra scanner at the University of Oregon Lewis Center for Neuroimaging. We acquired a high-resolution anatomical T1-weighted MP-RAGE scan (TR/TE = 2,500.00/3.43 ms, 256 × 256 matrix, 1 mm thick, 176 sagittal slices, FOV = 208 × 208 mm), functional images with a T2*- weighted echo-planar sequence (72 axial slices, TR/TE = 2,000.00/27.00 ms, 90-degree flip angle, 100 × 100 matrix, 2 mm thick, FOV = 208 × 208 mm, multiband acceleration factor = 3), and opposite phase encoded echo-planar images to correct for magnetic field inhomogeneities (72 axial slices, TR/TE = 6,390.00/47.80 ms, 90-degree flip angle, 104 × 104 matrix, 2 mm thick, FOV = 208 × 208 mm).

Neuroimaging data were preprocessed using fMRIPrep 1.1.4 (Esteban et al., 2019). A detailed account of the preprocessing pipeline appears in **Supplementary Material**, but briefly, anatomical images were segmented and normalized to MNI space using FreeSurfer (Fischl, 2012); functional images were susceptibility distortion corrected, realigned, and coregistered to the normalized anatomical images. Normalized functional data were then smoothed (6 mm FWHM) in SPM12 (Wellcome Department of Cognitive Neurology[3]).

Neuroimaging Analysis

Event-related condition effects were estimated in first-level analyses using a fixed-effects general linear model and convolving a canonical hemodynamic response function to stimulus events

[3]http://www.fil.ion.ucl.ac.uk/spm

using SPM12. Regressors were entered for each experimental condition (regulate craved, look craved, look not-craved, look neutral) and were modeled during stimulus presentation (5 s). Additional regressors of no interest were added for the instruction and rating periods. Five motion regressors were modeled as covariates of no interest. Realignment parameters were transformed into Euclidean distance for translation and rotation separately; we also included the displacement derivative of each, resulting in a total of four motion regressors. Another regressor of no interest indicated images with motion artifacts (e.g., striping) identified via automated motion assessment (Cosme et al., 2018) or visual inspection. Data were high-pass filtered at 128s and temporal autocorrelation was modeled using FAST (Corbin et al., 2018). Task runs with > 10% of volumes contaminated with motion artifacts were excluded (n = 8) or if they were missing 80% or more responses (n = 5). Participants were excluded completely if both task runs were excluded (N = 4). For each participant, we computed the following linear contrasts: Look Craved > Look Not Craved (LC > LNC, called "reactivity") and Regulate Crave > Look Crave (RC > LC, called "regulation") using SPM12.

We estimated second-level random effects for each contrast using a one-sample t-test in SPM12. Multiple comparisons were corrected using cluster-extent thresholding implemented in AFNI version 18.2.04 (Cox, 1996). In accordance with recent guidelines (Cox et al., 2017), the spatial autocorrelation function was first estimated for each subject and task run separately using AFNI's 3dFWHMx, and then averaged across subjects. To determine probability estimates of false-positive clusters given a random field of noise, Monte-Carlo simulations were conducted with AFNI's 3dClustSim using the average autocorrelation across subjects (ACF = 0.70, 4.27, 8.63). For each model, a voxel-wise threshold of $p < 0.001$ and cluster extent of k = 61 was estimated (voxel dimensions = 2 × 2 × 2 mm) to achieve a whole-brain familywise error rate of $\alpha = 0.05$.

ROI Definition and Extraction

Region of interests were defined anatomically due to the *a priori* nature of our hypotheses. The VS and vmPFC ROIs were from Bartra and colleagues' (2013) publicly available database of ROIs based on a 200 paper meta-analysis of subjective value (Bartra et al., 2013)[4]. The dlPFC, IFG, and dACC ROIs were all created using the WFU PickAtlas (Tzourio-Mazoyer et al., 2002; Maldjian et al., 2003). For the dlPFC ROI, we selected Brodmann areas 8 and 9, and dilated the mask by 1mm. The IFG ROI was defined using the WFU PickAtlas TD Labels inferior frontal gyrus ROI. The dACC ROI was created by bounding the WFU PickAtlas TD Labels anterior cingulate ROI on the y-axis at 0–32. Per our hypotheses, we extracted individual parameter estimates from the VS and vmPFC ROIs from the LC > LNC contrast, and dlPFC, IFG, and dACC ROIs from the RC > LC contrast. These three regulation ROIs were averaged and combined into a composite for analysis purposes, and also explored separately.

In addition, we explored associations between regulation-related brain activity and food craving (from the FCI) and consumption (from the ASA24) by creating 6 mm^3 spherical ROIs around the peaks from the RC > LC contrast (listed in **Table 2**, labeled with an *). The purpose of these ROIs was to explore the association of regulation-related brain activity with longitudinal patterns of healthy and unhealthy food liking, craving, and consumption orthogonal to the contrast that defined the ROIs. These seven ROIs were averaged and combined into a composite to reduce the number of statistical tests run, and also explored separately.

Statistical Analyses

Statistical analyses were conducted in R (version 3.6.1; R Core Team, 2019). First, variables were investigated for skewness and kurtosis; all exhibited acceptable distributions and were retained for further analysis. We then created a series of multilevel models predicting liking, craving, and intake of healthy and unhealthy foods with time at Level 1 and person at Level 2 using lmer in R (Bates et al., 2015). Because the models failed to converge when including the linear effect of time (month slope) as a random effect, only participant intercepts were modeled as random effects. The time variable (number of months since T1) was centered at 0, and the rest of the variables were grand mean centered. These models included main effects of brain activity, BMI, age, gender, and condition at baseline, as well as the main effect of time and the interaction between time and brain activity. Lastly, we investigated the pattern of missingness in this data set using the non-parametric MCAR (Missing Completely at Random) test proposed by Jamshidian and Jalal (2010, as implemented in the MissMech R package, Jamshidian et al., 2014). Here, a significant result for the Hawkins test of normality and homoscedasticity indicates that the hypothesis of MCAR would be rejected, and results should be interpreted accordingly.

To interrogate hypothesis 1, that food craving reactivity and regulation brain activity would be associated with self-reported craving for and consumption of unhealthy food at baseline, we assessed these models for main effects of brain activity on FCI-reported craving for unhealthy foods and ASA24-reported consumption of empty calories. Because eight separate models (4 ROIs × 2 dependent variables) were run to address this hypothesis, a Bonferroni correction was used to correct for multiple comparisons. The corrected alpha was therefore set at $p < 0.0063$. Additional models assessing self-reported liking of unhealthy foods were also included, in order to separate out the motivational state (craving) from the hedonic response (liking). We also explored the associations between brain activity and the liking of, craving for, and consumption of healthy foods at baseline, in order to examine the specificity of previously reported brain-behavior associations by food type. Because these analyses were exploratory, we only report estimates and 95% confidence intervals for effects that surpass $\alpha < 0.05$ in the text; all results are included in supplementary material available online[5]. To interrogate hypothesis 2, that vmPFC activity would mediate the relation between regulation-related brain activity and unhealthy food craving and/or consumption, we planned to run mediation models in R using lavaan (Rousseel, 2012)

[4]https://www.sas.upenn.edu/$\sim$mcguirej/meta-analysis.html

[5]https://github.com/UOSAN/regulation-craving-consumption

TABLE 2 | Correlations at baseline (T1).

Variable	1	2	3	4	5	6	7	8
1. BMI								
2. FCI—healthy like rating	−0.040							
3. FCI—healthy crave rating	0.207	0.467**						
4. FCI—unhealthy like rating	0.052	0.335**	0.154					
5. FCI—unhealthy crave rating	0.260**	0.005	0.488**	0.592**				
6. ASA24—total kcal consumed	−0.070	−0.010	−0.169	0.263*	0.077			
7. ASA24—HEI	0.031	0.128	0.075	−0.141	−0.093	−0.071		
8. ASA24—fruit/vegetable consumption	0.035	0.148	0.088	−0.071	−0.078	−0.056	0.680**	
9. ASA24—empty calorie consumption	0.168	−0.038	−0.003	−0.221*	−0.088	−0.322*	0.578**	0.160

*BMI, body mass index; FCI, Food Craving Inventory; HEI, healthy eating index. *Indicates $p < 0.05$. ** indicates $p < 0.01$.*

for any and all significant associations between regulation-related brain activity and behavior at baseline. These models would be constructed as follows: regulation-related brain activity would be the independent variable; reactivity-related vmPFC activity would be the mediator; the craving or consumption variable associated with regulation-related activity would be the dependent variable; and BMI, age, gender, and condition included as covariates. Lastly, to interrogate hypothesis 3, that vmPFC brain activity associated with regulating the desire for personally desired energy-dense foods at baseline would predict an increase in the consumption of healthy food and a decrease in unhealthy food over 6 months, we examined the time x brain interaction terms from the multilevel models. We additionally explored other reactivity- and regulation-related brain activity in other regions for this interaction on liking of, craving for, and consumption of both food types.

RESULTS

Baseline

Baseline data from the FCI and the ASA24 are presented in **Table 1**, along with relevant demographic information. Correlations among non-brain variables at baseline are presented in **Table 2**. BMI was significantly positively correlated with self-reported craving for unhealthy [$r(88) = 0.260$, $p = 0.014$] foods. Liking and craving were significantly correlated for both healthy [$r(88) = 0.467$, $p < 0.001$] and unhealthy [$r(88) = 0.592$, $p < 0.001$] foods. Total calories consumed was positively correlated with self-reported liking of unhealthy foods [$r(87) = 0.263$, $p = 0.015$], and negatively correlated with consumption of empty calories [$r(87) = -0.322$, $p = 0.002$]. The ASA24's HEI was positively correlated with fruit and vegetable consumption [$r(87) = 0.680$, $p < 0.001$] and empty calories [$r(87) = 0.578$, $p < 0.001$]; it was not significantly associated with liking or craving of healthy foods (p-values > 0.24). Consumption of empty calories was significantly negatively associated with self-reported liking of unhealthy foods [$r(85) = -0.221$, $p = 0.042$] and total calories consumed [$r(87) = -0.322$, $p = 0.002$].

As shown in **Figure 2A**, whole brain results for the main effect of food cue reactivity revealed significant clusters in the left postcentral gyrus, right lingual gyrus, right fusiform gyrus, and right inferior temporal gyrus. Peaks and cluster sizes are listed in **Table 3**. The main effect of regulation was associated with a very large cluster of activity with subpeaks in the left supramarginal gyrus, right post-medial frontal gyrus, and left inferior gyrus. Additional peaks were located in the right supramarginal gyrus, midbrain, left cerebellum, and left parahippocampal gyrus (**Figure 2B** and **Table 3**).

In contrast to Hypothesis 1, reactivity-related activity in neither the VS ROI nor the vmPFC ROI was significantly associated with self-reported craving for or consumption of unhealthy foods at baseline. Average regulation-related brain activity in neither the *a priori* ROIs nor the peak ROIs were significantly associated with self-reported craving for or consumption of unhealthy foods. Full models are available in the supplementary material available online (see footnote).

Regulation-related activity in the average of the *a priori* ROIs was positively associated with consumption of fruits and vegetables, $B = 0.73$, 95% CI [0.08, 1.37], SE = 0.33, $t(108.06) = 2.24$, $p = 0.027$. Exploration of the individual ROIs revealed that this effect was only statistically significant in the dlPFC, $B = 0.68$, 95% CI [0.07, 1.28], SE = 0.31, $t(108.96) = 2.21$, $p = 0.029$. In addition, regulation-related activity in the vmPFC *a priori* ROI was positively associated with craving for healthy foods, $B = 0.27$, 95% CI [0.02, 0.52], SE = 0.13, $t(90.80) = 2.11$, $p = 0.037$. While the average of the peak ROIs from the RC > LC contrast was not significantly associated with liking, craving, or consumption, individual peaks showed intriguing associations with behavior at baseline. Left cerebellum activity (−6, −56, −44) was positively associated with the HEI, $B = 4.18$, 95% CI [0.64, 7.72], SE = 1.79, $t(124.12) = 2.34$, $p = 0.021$, and fruit and vegetable intake, $B = 0.58$, 95% CI [0.21, 0.95], SE = 0.18, $t(109.81) = 3.13$, $p = 0.002$. This pattern was also observed in the right supramarginal gyrus [64, −46, 36; HEI: $B = 4.07$, 95% CI [0.63, 7.52], SE = 1.74, $t(123.28) = 2.34$, $p = 0.021$; fruit and vegetable intake: $B = 0.49$, 95% CI [0.13, 0.85], SE = 0.18, $t(110.40) = 2.72$, $p = 0.008$]. Lastly, activity in the right post-medial frontal peak (6, 12, 70) showed an inverse relationship with the consumption of empty calories, $B = -1.80$, 95% CI [−3.50, −0.09], SE = 0.86, $t(136.97) = -2.08$, $p = 0.039$. Because Hypothesis 1 was not supported by the data, the criteria for assessing the mediation outlined in Hypothesis 2 was also not met.

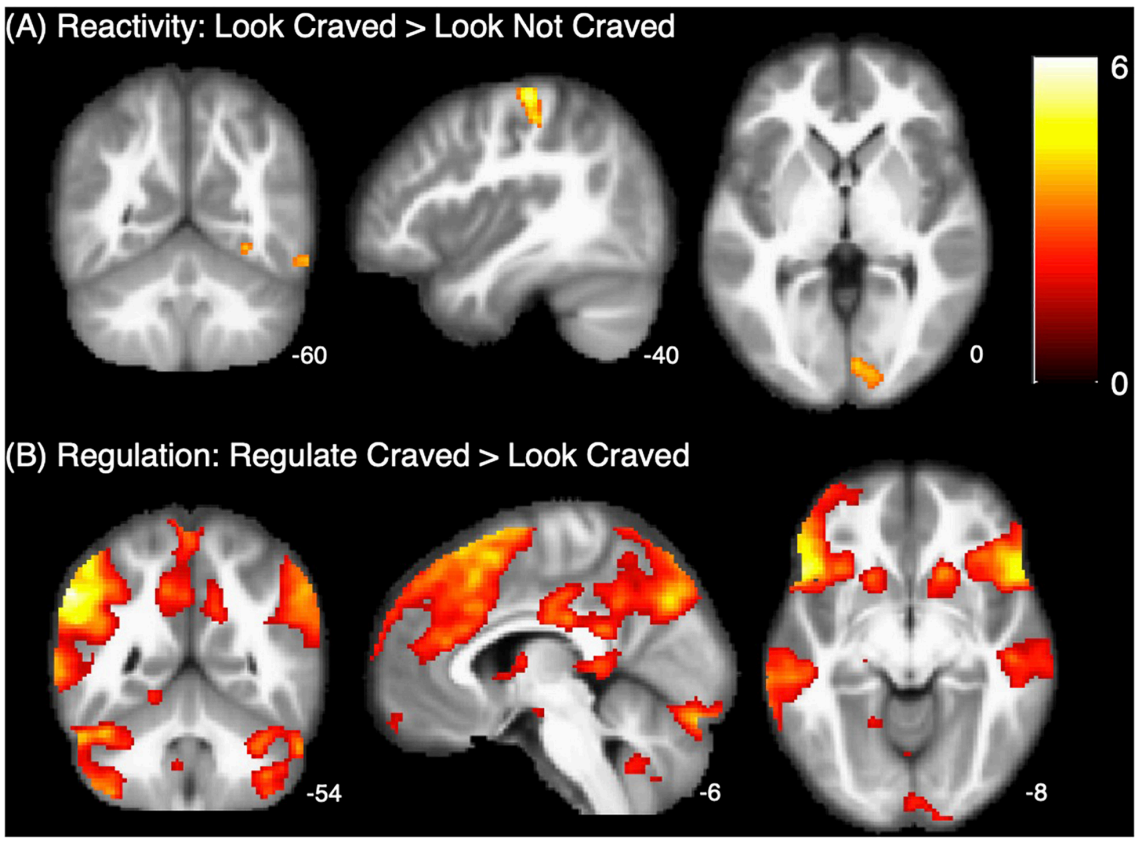

FIGURE 2 | Whole brain maps of **(A)** reactivity and **(B)** regulation. $p > 0.001$, $k = 61$.

Change Over Time

As shown in **Table 1**, there was notable attrition over time. A test for the nature of the missing data revealed that these data were not Missing Completely At Random (Hawkins Test $p < 0.001$). However, follow-up group comparisons between participants who provided data at all three follow-up time points compared to those who did not indicated that these groups did not significantly differ with regard to age, gender, intervention condition, reactivity or regulation-related brain activity, or baseline BMI, healthy eating (both HEI and fruit/vegetable consumption), or liking/craving for healthy and unhealthy foods. The individuals who provided complete data did, however, report consuming significantly fewer calories per day at baseline compared to those who provided incomplete data, $F(1, 85) = 4.61$, $p = 0.035$. As such, the following results should be interpreted with this limitation in mind.

With regard to Hypothesis 3, linear mixed models controlling for changes in BMI and age, gender, and intervention condition indicated that regulation-related activity in the vmPFC ROI was not associated with changes in the consumption of unhealthy food over time, operationalized as self-reported intake of empty calories via the ASA24. It was, however, significantly associated with changes in fruit and vegetable intake over time, $B = -0.11$, 95% CI [−0.21, −0.00], SE = 0.05, $t(137.64) = -2.03$, $p = 0.045$. A visual interrogation of this effect revealed a crossover interaction (**Figure 3**), such that individuals who recruited more vmPFC activity during the regulation of the desire to consume unhealthy food reported consuming fewer fruits and vegetables

TABLE 3 | Regions, MNI coordinates, cluster sizes, and peak t values for the Look Craved > Look Not Craved and Regulate Craved > Look Craved main effects ($p < 0.001$, $k = 61$ threshold used for all contrasts).

Contrast and region	MNI Coordinates (x, y, z)	Cluster size	Peak t
Reactivity: Look Craved > Look Not Craved			
Left postcentral gyrus	(−46, −26, 64)	285	6.42
Right lingual gyrus	(6, −86, −2)	165	4.37
Right fusiform gyrus	(30, −60, −10)	84	4.14
Right inferior temporal gyrus	(58, −58, −16)	75	4.08
Regulation: Regulate Craved > Look Craved			
Left supramarginal gyrus*	(−60, −52, 40)	46,121	12.03
Right post-medial frontal gyrus*	(6, 12, 70)		10.83
Left inferior frontal gyrus*	(−52, 20, −6)		10.8
Right supramarginal gyrus*	(64, −46, 36)	3,180	8.34
Right middle temporal gyrus	(48, −30, −2)		7.89
Midbrain	(0, −18, −26)	79	5.61
Left cerebellum (IX)*	(−6, −56, −44)	149	4.49
Left parahippocampal gyrus*	(−10, −12, −18)	71	3.97

* *mm^3 sphere ROI created at that location.*

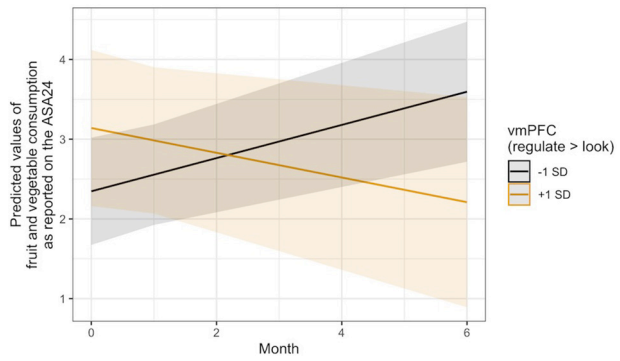

FIGURE 3 | Visualization of the time x vmPFC activity interaction predicting changes in self-reported fruit and vegetable intake over time via the ASA24. Lines indicate the association at −1 (black) and + 1 (gold) SD from the mean vmPFC activity during Regulate Craved > Look Craved.

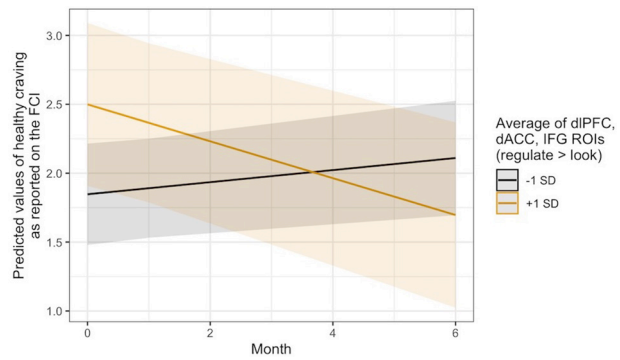

FIGURE 4 | Visualization of the time x activity interaction predicting changes in self-reported craving for healthy foods over time via the ASA24. Lines indicate the association at −1 (black) and + 1 (gold) SD from the mean activity in the dlPFC, dACC, and IFG ROIs during Regulate Craved > Look Craved.

over time, whereas those who displayed less vmPFC activity during regulation reported eating more fruits and vegetables.

Exploratory analyses revealed that this same pattern occurred in the vmPFC with regard to changes in self-reported craving for healthy foods, $B = -0.04$, 95% CI [−0.08, −0.01], SE = 0.02, $t(124.48) = -2.36$, $p = 0.020$. It was also seen in the average regulation-related brain activity across the three *a priori* ROIs for changes in healthy food craving, $B = -0.08$, 95% CI [−0.14, −0.02], SE = 0.03, $t(124.50) = -2.84$, $p = 0.005$, and only in the dlPFC ROI with regard to changes in the consumption of fruits and vegetables, $B = -0.14$, 95% CI [−0.27, −0.00], SE = 0.07, $t(134.70) = -2.00$, $p = 0.047$. Visual inspection of the healthy craving interaction across all three ROIs (**Figure 4**) indicated that people who recruited these brain regions more during regulation showed a decrease in their self-reported craving for healthy food over time, which was not seen in individuals who did not recruit these regulation network regions as strongly. Additional model results that did not pass the significance threshold are included in the **Supplementary Material** online.

DISCUSSION

The present study sought to investigate the associations between food craving reactivity and regulation-related brain activity and measures of craving for and consumption of healthy and unhealthy foods in a community sample of middle-aged adults with higher BMIs, as well as how this brain activity at baseline predicted changes in food craving and consumption over the course of 6 months.

Baseline

Reactivity

Our analyses did not reveal any significant associations between food cue reactivity in the brain and self-reported liking of, craving for, or consumption of unhealthy—or healthy—food at baseline. This is surprising, given that the bulk of the brain-behavior research in this area has focused on food cue reactivity, and that a recent meta-analysis of this literature demonstrated a medium effect of food cue reactivity on food consumption and weight (Boswell and Kober, 2016). Because we controlled for BMI in our analyses in order to focus on brain-behavior associations, we may have obscured any weight-related effects. However, *post hoc* analyses showed that there was also no association between baseline BMI and reactivity-related brain activity in the present sample [$r(88)$-values = 0.024–0.087, $p > 0.41$]. As such, removing variance associated with BMI most likely did not obscure any weight-driven brain-behavior associations at baseline. It is also possible that these null results could be related to the contrast we used to operationalize reactivity in the brain. As evident in **Figure 2A**, there were very few clusters that differed significantly between the craved (LC) and not craved (LNC) foods, indicating that reactivity was similar across conditions, despite substantial differences in self-reported craving ratings for craved and not craved foods (**Supplementary Table S1**). Because this measure of cue reactivity does not appear to have been specific to craved foods here, it may account for not observing the expected relationships. Lastly, these null findings may also be due to limitations inherent to the self-report measures we used to assess food craving and consumption (e.g., self-presentation bias, imperfect memory recall). Accurate measurement of food consumption is notoriously challenging, and while the ASA24 retrospective food intake measure used in the present study is the measure of choice for the National Cancer Institute, a recent paper documented several usability challenges with this tool that may have led to reporting errors (Kupis et al., 2019).

Regulation

We also did not see any significant baseline associations between regulation-related activity and self-reported liking of, craving for, or consumption of unhealthy foods in our *a priori* ROIs. However, exploratory analyses revealed that regulation-related brain activity was positively associated with the craving for and consumption of healthy foods. Specifically, activity in an average of our three *a priori* ROIs (dlPFC, dACC, IFG) was significantly positively associated with fruit and vegetable consumption, which appeared to be driven by dlPFC activity. We also saw this effect with regard to healthy food craving in the vmPFC, and

general healthy eating as well as fruit/vegetable intake in the left cerebellum and right supramarginal gyrus. We also found that right post-medial frontal activity was negatively associated with empty calorie consumption.

Together, these data demonstrate that greater engagement of these regions during the regulation of the desire for unhealthy food was associated with concurrent healthier eating. Activation in these regions could also be indexing health goals representations (Tusche and Hutcherson, 2018), motivation to change, or effort on and engagement with the task of down-regulating craving for unhealthy foods. While we expected to see this pattern in the traditional lateral prefrontal regions like the dlPFC, we were somewhat surprised that the cerebellum and supramarginal gyrus also showed such a consistent pattern of associations with healthy eating. These two regions are generally thought to underlie mentalizing and other types of social cognition (Van Overwalle and Mariën, 2016), yet some studies have found them to be significantly involved in cognitive control (e.g., Żurawska vel Grajewska et al., 2011). Therefore, it may be that individuals who engage these regions during regulation may be—consciously or subconsciously—using more socially-relevant regulation strategies, which may be associated with greater healthy food intake. While we have explored different types of craving regulation strategies in past work (see Giuliani et al., 2013), these have not yet included social strategies (Nook and Zaki, 2015).

The fact that almost all of the baseline associations we observed were in the domain of healthy eating also supports the assertion that our present lack of reactivity-consumption findings—which are traditionally seen in the domain of unhealthy food (e.g., Lopez et al., 2014)—may be due to the increased motivation of our participants to eat better. The specificity of the results to the healthy food domain may also be why we found relatively few effects on craving for these foods, as there are not as frequently craved as unhealthy foods (Massicotte et al., 2019). Interestingly, we also found no brain-behavior associations regarding the self-reported liking of healthy foods, which suggests that this pattern is specific to the motivational and ingestive aspects of eating behavior, and not the more subjective process of liking.

Change Over Time

Reactivity

With regard to baseline levels of brain activity predicting overall changes in food liking, craving, and consumption over the course of the 6 month follow-up period, we did not find any evidence that brain activity during food cue reactivity predicted behavior changes in the domains of unhealthy or healthy foods. These results are contrary to much of the previous findings in this domain, which have shown relatively consistent associations between food cue reactivity and behavior change using dependent variables such as weight gain/loss, cue-induced eating, or snack consumption (e.g., Demos et al., 2012; Lawrence et al., 2012; Murdaugh et al., 2012; Versace et al., 2018). The present null result may be due to the paradigm we used to index food cue reactivity, which contrasted two energy-dense foods that only differed based on participant preference. This is quite different from most other studies in this domain, which usually contrast high energy-dense foods with low-density foods, if a contrasting condition is used at all. In addition, these results may be due to the sample, which consisted of community adults who were selected because they had BMIs between 25 and 40 but were also highly motivated to improve their eating habits. As such, the increased motivation of the subjects may have negated any hypothesized reactivity-consumption associations by influencing both brain reactivity to pictures of unhealthy foods and consumption of those foods.

Regulation

In contrast to the reactivity results, we did find that brain activity associated with regulating the desire for unhealthy foods was significantly associated with changes in craving for and consumption of healthy foods. Specifically, we found that increased regulation-related activity in the dlPFC, IFG, dACC, and vmPFC significantly predicted decreases in healthy food craving over time. Regulation-related activity in the dlPFC and vmPFC also predicted a decrease in self-reported fruit and vegetable consumption. Across all of these regions, greater engagement during regulation predicted less craving for and consumption of healthy foods over time. While the brain regions implicated here are those we expected would track with real-world regulation success, we found an opposite pattern than predicted: *less* brain activity during regulation was associated with *more* craving for and consumption of healthy foods.

This pattern of brain-as-predictor results is complex and somewhat contradictory, with more regulation-related activity associated with healthier eating at baseline, which then waned over the course of 6 months. One possible explanation is simply that craving regulation is multifaceted, reflecting many psychological processes including effort, attentional control, motivation, desire, meta-cognition and planning, among others. As such, simply asking people to indicate their food desire ratings via a button press after attempting to down-regulate their desire for a food may not get at the complexity of the process (e.g., effort, conflict, etc.). In addition, we used mean-level activation within ROIs as brain-based indices of reactivity and regulation, but because they are not specific indicators of these psychological processes, they likely represent integrated engagement of numerous cognitive functions. Future studies should investigate multivariate measures of reactivity and regulation to improve sensitivity and potentially predictive utility (Cosme et al., 2020). Regardless, the present findings suggest that the health neuroscience literature may benefit from an increased interrogation of the factors predicting healthy food consumption, instead of continuing to focus primarily on reducing the consumption of unhealthy food.

As mentioned earlier, some features of the sample itself are worth considering and might provide clues that help interpret the observed pattern of response. The sample consisted of community adults who were selected because they had higher BMIs, and also highly motivated to improve their eating habits. Indeed, it may be that this increased motivation to eat better upon study entry was reflected in both greater effort during

regulation—which resulted in more brain activity—and healthier baseline eating behavior. Cognitive reappraisal, the regulation strategy employed in the present study, is thought to be relatively less effortful compared to more response-focused regulation strategies like suppression (Gross, 2002). However, this work was done using negative images; neural reactions to unhealthy food cues have been found to occur early and are relatively automatic (Meule et al., 2013). As such, reappraising the desire for a delicious-looking unhealthy food may actually be a form of late reappraisal, which has been shown to engage substantial inhibitory control resources (Sheppes et al., 2009). This level of effort is hard to maintain in the long run, which is why greater recruitment of these brain regions at baseline ultimately resulted in a downward trajectory of healthy eating over 6 months. These results suggest that targeting less effortful food craving regulation strategies may be more successful in helping people meet their healthy eating goals over longer periods of time. Recent work by Reader et al. (2018) supports this idea, showing that greater success at up-regulating the desire for healthy foods was associated with increased craving strength for low-calorie foods as well as decreased consumption of high-calorie foods in their daily lives.

Limitations

The present findings should be interpreted in light of several limitations of the present study. First, the sample was majority female and Caucasian. We did employ broad recruitment in the community of a mid-sized city in the Pacific Northwest, United States, but the limited gender and racial makeup of the present sample may limit the generalizability of the present findings to other samples. In addition, the sample was entirely higher BMI, with no comparison group. As such, the patterns of results in this study may be reflective of this specific group, who may also process stimuli and approach food in ways different from lower-weight individuals. Second, while we excluded individuals who were actively enrolled in a diet program, we did not collect information about past diet attempts or weight fluctuations. Because previous studies have found an influence of dietary behavior on brain activity (e.g., Ely et al., 2014), this is an important caveat to the present results that should be addressed in future work. Third, while we worked hard to retain our sample throughout the full 6 month study protocol, we experienced substantial attrition, with only 52 of the original 88 participants providing BMI data at T4. A comparison of the participants who provided data throughout the study versus those who did not revealed that they did not differ significantly with regard to age, gender, or ethnicity. However, we cannot assess how this attrition may have impacted our longitudinal outcome measures, as we do not have follow-up data from participants who did not return to the lab at T4. Relatedly, participants reported that inventorying their 24-h food consumption using the ASA24 twice at each time point was cumbersome, which may have led to loss of follow-up data and perhaps also contributed to careless or more inaccurate reporting among those who did complete the follow-up assessments (Kupis et al., 2019). While accurately measuring actual food consumption is notoriously difficult, future work would benefit from employing a measure of food intake that participants are more likely to complete at multiple time points (i.e., taking photos of meals). Lastly, half of the participants in these analyses were enrolled in an intervention designed to increase their motivation to engage in healthier eating behaviors. While we collapsed across groups and included intervention condition as a covariate in all analyses, the fact that half of the participants had received this intervention between baseline and T2 may have affected the self-reported food craving and consumption data we collected at all three time points.

CONCLUSION

Overall, this study demonstrated that brain activity associated with regulating desires for unhealthy food predicted meaningful changes in the craving for and consumption of healthy food over the course of 6 months in a population of middle-aged adults with higher BMIs. These nuanced findings add to the growing body of research on the neuroscience of eating, which has predominantly focused on the consumption of unhealthy foods and/or body weight, and highlights the importance of studying healthy eating behavior as well.

DATA AVAILABILITY STATEMENT

The datasets presented in this study can be found in online repositories. The names of the repository/repositories and accession number(s) can be found below: https://github.com/UOSAN/regulation-craving-consumption.

ETHICS STATEMENT

The studies involving human participants were reviewed and approved by the Institutional Review Board of the University of Oregon. The patients/participants provided their written informed consent to participate in this study.

AUTHOR CONTRIBUTIONS

NG and EB designed the study. JM, BD, and NG collected the data. NG, JM, and DC analyzed the data. NG wrote the manuscript and created the figures. DC created the supplementary tables. DC, JM, BD, and EB provided edits. All authors contributed to the article and approved the submitted version.

FUNDING

This research was supported by the grants from the National Cancer Institute CA211224 and CA175241.

ACKNOWLEDGMENTS

We would like to thank the participants, as well as Anthony Fager, Michael Morrison, Aidan Boese, and David Esquivel for their help on this study.

SUPPLEMENTARY MATERIAL

The Supplementary Material for this article can be found online at: https://www.frontiersin.org/articles/10.3389/fnhum.2020.577669/full#supplementary-material

REFERENCES

Bartra, O., McGuire, J. T., and Kable, J. W. (2013). The valuation system: a coordinate-based meta-analysis of BOLD fMRI experiments examining neural correlates of subjective value. *Neuroimage* 76, 412–427. doi: 10.1016/j.neuroimage.2013.02.063

Bates, D., Mächler, M., Bolker, B. M., and Walker, S. C. (2015). Fitting linear mixed-effects models using lme4. *J. Stat. Softw.* 67, 1–48. doi: 10.18637/jss.v067.i01

Batra, P., Das, S. K., Salinardi, T., Robinson, L., Saltzman, E., Scott, T., et al. (2013). Relationship of cravings with weight loss and hunger. Results from a 6 month worksite weight loss intervention. *Appetite* 69, 1–7. doi: 10.1016/j.appet.2013.05.002

Berkman, E. T., Hutcherson, C. A., Livingston, J. L., Kahn, L. E., and Inzlicht, M. (2017). Self-control as value-based choice. *Curr. Direct. Psychol. Sci.* 26, 422–428. doi: 10.1177/0963721417704394

Berridge, K. C. (2009). "Liking" and "wanting" food rewards: brain substrates and roles in eating disorders. *Physiol. Behav.* 97, 537–550. doi: 10.1016/j.physbeh.2009.02.044

Boswell, R. G., and Kober, H. (2016). Food cue reactivity and craving predict eating and weight gain: a meta-analytic review. *Obesity Rev.* 17, 159–177. doi: 10.1111/obr.12354

Brainard, D. H. (1997). The psychophysics toolbox. *Spatial Vis.* 10, 433–436.

Centers for Disease Control and Prevention (2011). *About BMI forAdults*. Available online at: http://www.cdc.gov/healthyweight/assessing/bmi/adult_bmi/ (accessed November 2, 2020).

Chao, A., Grilo, C. M., White, M. A., and Sinha, R. (2014). Food cravings, food intake, and weight status in a community-based sample. *Eating Behav.* 15, 478–482. doi: 10.1016/J.EATBEH.2014.06.003

Cleobury, L., and Tapper, K. (2014). Reasons for eating "unhealthy" snacks in overweight and obese males and females. *J. Hum. Nutr. Dietetics* 27, 333–341. doi: 10.1111/jhn.12169

Corbin, N., Todd, N., Friston, K. J., and Callaghan, M. F. (2018). Accurate modeling of temporal correlations in rapidly sampled fMRI time series. *Hum. Brain Mapp.* 39, 3884–3897. doi: 10.1002/hbm.24218

Cornell, C. E., Rodin, J., and Weingarten, H. (1989). Stimulus-induced eating when satiated. *Physiol. Behav.* 45, 695–704. doi: 10.1016/0031-9384(89)90281-3

Cosme, D., Flournoy, J. C., and Vijayakumar, N. (2018). *Auto-Motion-Fmriprep: A Tool for Automated Assessment of Motion Artifacts (Version v1.0)*. Zenodo. doi: 10.5281/zenodo.1412131

Cosme, D., Zeithamova, D., Stice, E., and Berkman, E. T. (2020). Multivariate neural signatures for health neuroscience: assessing spontaneous regulation during food choice. *Soc. Cogn. Affect. Neurosci.* nsaa002. doi: 10.1093/scan/nsaa002 [Epub ahead of print].

Cox, R. W. (1996). AFNI: software analysis and visualization of functional magnetic resonance neuroimages. *Comp. Biomed. Res.* 29, 162–173.

Cox, R. W., Chen, G., Glen, D. R., Reynolds, R. C., and Taylor, P. A. (2017). FMRI clustering in AFNI: false-positive rates Redux. *Brain Connect.* 7, 152–171. doi: 10.1089/brain.2016.0475

Crowley, N., Madan, A., Wedin, S., Correll, J. A., Delustro, L. M., Borckardt, J. J., et al. (2014). Food cravings among bariatric surgery candidates. *Eating Weight Disord.* 19, 371–376. doi: 10.1007/s40519-013-0095-y

Demos, K. E., Heatherton, T. F., and Kelley, W. M. (2012). Individual differences in nucleus accumbens activity to food and sexual images predict weight gain and sexual behavior. *J. Neurosci.* 32, 5549–5552. doi: 10.1523/JNEUROSCI.5958-11.2012

Duffey, K. J., Gordon-Larsen, P., Jacobs, D. R., Williams, O. D., and Popkin, B. M. (2007). Differential associations of fast food and restaurant food consumption with 3-y change in body mass index: the coronary artery risk development in young adults study. *Am. J. Clin. Nutr.* 85, 201–208. doi: 10.1093/ajcn/85.1.201

Ely, A. V., Childress, A. R., Jagannathan, K., and Lowe, M. R. (2014). Differential reward response to palatable food cues in past and current dieters: a fMRI study. *Obesity* 22, E38–E45. doi: 10.1002/oby.20599

Esteban, O., Markiewicz, C. J., Blair, R. W., Moodie, C. A., Isik, A. I., Erramuzpe, A., et al. (2019). fMRIPrep: a robust preprocessing pipeline for functional MRI. *Nat. Methods* 16, 111–116. doi: 10.1038/s41592-018-0235-4

Faul, F., Erdfelder, E., Buchner, A., and Lang, A.-G. (2009). Statistical power analyses using G*Power 3.1: tests for correlation and regression analyses. *Behav. Res. Methods* 41, 1149–1160.

Fedoroff, I. C., Polivy, J., and Herman, C. P. (1997). The effect of pre-exposure to food cues on the eating behavior of restrained and unrestrained eaters. *Appetite* 28, 33–47. doi: 10.1006/appe.1996.0057

Fedoroff, I. C., Polivy, J., and Herman, C. P. (2003). The specificity of restrained versus unrestrained eaters' responses to food cues: general desire to eat, or craving for the cued food? *Appetite* 41, 7–13. doi: 10.1016/S0195-6663(03)00026-6

Fischl, B. (2012). FreeSurfer. *Neuroimage* 62, 774–781. doi: 10.1016/j.neuroimage.2012.01.021

Gilhooly, C. H., Das, S. K., Golden, J. K., McCrory, M. A., Dallal, G. E., Saltzman, E., et al. (2007). Food cravings and energy regulation: the characteristics of craved foods and their relationship with eating behaviors and weight change during 6 months of dietary energy restriction. *Int. J. Obesity* 31, 1849–1858. doi: 10.1038/sj.ijo.0803672

Giuliani, N. R., and Berkman, E. T. (2015). Craving is an affective state and its regulation can be understood in terms of the extended process model of emotion regulation. *Psychol. Inquiry* 26, 48–53. doi: 10.1080/1047840X.2015.955072

Giuliani, N. R., Calcott, R. D., and Berkman, E. T. (2013). Piece of cake. Cognitive reappraisal of food craving. *Appetite* 64, 56–61. doi: 10.1016/j.appet.2012.12.020

Giuliani, N. R., Mann, T., Tomiyama, A. J., and Berkman, E. T. (2014). Neural systems underlying the reappraisal of personally craved foods. *J. Cogn. Neurosci.* 26, 1390–1402. doi: 10.1162/jocn_a_00563

Giuliani, N. R., Merchant, J. S., Cosme, D., and Berkman, E. T. (2018). Neural predictors of eating behavior and dietary change. *Ann. N. Y. Acad. Sci.* 1428, 208–220. doi: 10.1111/nyas.13637

Giuliani, N. R., and Pfeifer, J. H. (2015). Age-related changes in reappraisal of appetitive cravings during adolescence. *Neuroimage* 108, 173–181. doi: 10.1016/j.neuroimage.2014.12.037

Giuliani, N. R., Tomiyama, A. J., Mann, T., and Berkman, E. T. (2015). Prediction of daily food intake as a function of measurement modality and restriction status. *Psycho. Med.* 77, 583–590. doi: 10.1097/PSY.0000000000000187

Green, P., and MacLeod, C. J. (2016). SIMR?: an R package for power analysis of generalized linear mixed models by simulation. *Methods Ecol. Evol.* 7, 493–498. doi: 10.1111/2041-210X.12504

Gross, J. J. (2002). Emotion regulation: affective, cognitive, and social consequences. *Psychophysiology* 39, 281–291.

Guenther, P. M., Casavale, K. O., Reedy, J., Kirkpatrick, S. I., Hiza, H. A. B., Kuczynski, K. J., et al. (2013). Update of the healthy eating index: HEI-2010. *J. Acad. Nutr. Dietetics* 113, 569–580. doi: 10.1016/j.jand.2012.12.016

Han, J. E., Boachie, N., Garcia-Garcia, I., Michaud, A., and Dagher, A. (2018). Neural correlates of dietary self-control in healthy adults: a meta-analysis of functional brain imaging studies. *Physiol. Behav.* 192, 98–108. doi: 10.1016/j.physbeh.2018.02.037

Hare, T. A., Camerer, C. F., and Rangel, A. (2009). Self-control in decision-making involves modulation of the vmPFC valuation system. *Science* 324, 646–648. doi: 10.1126/science.1168450

Havermans, R. C. (2011). "You Say it's Liking, I Say it's Wanting .". On the difficulty of disentangling food reward in man. *Appetite* 57, 286–294. doi: 10.1016/j.appet.2011.05.310

Holsen, L. M., Davidson, P., Cerit, H., Hye, T., Moondra, P., Haimovici, F., et al. (2018). Neural predictors of 12-month weight loss outcomes following bariatric surgery. *Int. J. Obesity* 42, 785–793. doi: 10.1038/ijo.2017.190

Jamshidian, M., and Jalal, S. J. (2010). Tests of homoscedasticity, normality, and missing completely at random for incomplete multivariate data. *Psychometrika* 75, 649–674.

Jamshidian, M., Jalal, S. J., and Jansen, C. (2014). MissMech: an R package for testing homoscedasticity, multivariate normality, and missing completely at random (MCAR). *J. Stat. Softw.* 56, 1–31.

Jansen, A., Theunissen, N., Slechten, K., Nederkoorn, C., Boon, B., Mulkens, S., et al. (2003). Overweight children overeat after exposure to food cues. *Eating Behav.* 4, 197–209. doi: 10.1016/S1471-0153(03)00011-4

Kupis, J., Johnson, S., Hallihan, G., and Olstad, D. L. (2019). Assessing the usability of the automated self-administered dietary assessment tool (Asa24) among low-income adults. *Nutrients* 11:132. doi: 10.3390/nu11010132

Lawrence, N. S., Hinton, E. C., Parkinson, J. A., and Lawrence, A. D. (2012). Nucleus accumbens response to food cues predicts subsequent snack consumption in women and increased body mass index in those with reduced self-control. *Neuroimage* 63, 415–422. doi: 10.1016/j.neuroimage.2012.06.070

Lopez, R. B., Hofmann, W., Wagner, D. D., Kelley, W. M., and Heatherton, T. F. (2014). Neural predictors of giving in to temptation in daily life. *Psychol. Sci.* 25, 1337–1344. doi: 10.1177/0956797614531492

Lowe, C. J., Reichelt, A. C., and Hall, P. A. (2019). The prefrontal cortex and obesity: a health neuroscience perspective. *Trends Cogn. Sci.* 23, 349–361. doi: 10.1016/j.tics.2019.01.005

Maier, S. U., Makwana, A. B., and Hare, T. A. (2015). Acute stress impairs self-control in goal-directed choice by altering multiple functional connections within the Brain's decision circuits. *Neuron* 87, 621–631. doi: 10.1016/j.neuron.2015.07.005

Maldjian, J. A., Laurienti, P. J., Kraft, R. A., and Burdette, J. H. (2003). An automated method for neuroanatomic and cytoarchitectonic atlas-based interrogation of fMRI data sets. *Neuroimage* 19, 1233–1239.

Martin, C. K., O'Neil, P. M., Tollefson, G., Greenway, F. L., and White, M. A. (2008). The association between food cravings and consumption of specific foods in a laboratory taste test. *Appetite* 51, 324–326. doi: 10.1016/j.appet.2008.03.002

Massicotte, E., Deschênes, S. M., and Jackson, P. L. (2019). Food craving predicts the consumption of highly palatable food but not bland food. *Eating Weight Disord.* 24, 693–704. doi: 10.1007/s40519-019-00706-8

Mehta, S., Melhorn, S. J., Smeraglio, A., Tyagi, V., Grabowski, T., Schwartz, M. W., et al. (2012). Regional brain response to visual food cues is a marker of satiety that predicts food choice. *Am. J. Clin. Nutr.* 96, 989–999. doi: 10.3945/ajcn.112.042341

Meule, A., Kübler, A., and Blechert, J. (2013). Time course of electrocortical food-cue responses during cognitive regulation of craving. *Front. Psychol.* 4:669. doi: 10.3389/fpsyg.2013.00669

Murdaugh, D. L., Cox, J. E., Cook, E. W., and Weller, R. E. (2012). fMRI reactivity to high-calorie food pictures predicts short- and long-term outcome in a weight-loss program. *Neuroimage* 59, 2709–2721. doi: 10.1016/j.neuroimage.2011.10.071

Nederkoorn, C., and Jansen, A. (2002). Cue reactivity and regulation of food intake. *Eating Behav.* 3, 61–72. doi: 10.1016/S1471-0153(01)00045-9

Nederkoorn, C., Smulders, F. T. Y., and Jansen, A. (2000). Cephalic phase responses, craving and food intake in normal subjects. *Appetite* 35, 45–55. doi: 10.1006/appe.2000.0328

Neseliler, S., Hu, W., Larcher, K., Zacchia, M., Dadar, M., Scala, S. G., et al. (2019). Neurocognitive and hormonal correlates of voluntary weight loss in humans. *Cell Metab.* 29, 39–49.e4. doi: 10.1016/j.cmet.2018.09.024

Nook, E. C., and Zaki, J. (2015). Social norms shift behavioral and neural responses to foods. *J. Cogn. Neurosci.* 27, 1412–1426. doi: 10.1162/jocn_a_00795

Pereira, M. A., Kartashov, A. I., Ebbeling, C. B., Van Horn, L., Slattery, M. L., Jacobs, D. R., et al. (2005). Fast-food habits, weight gain, and insulin resistance (the CARDIA study): 15-year prospective analysis. *Lancet* 365, 36–42. doi: 10.1016/S0140-6736(04)17663-0

Polk, S. E., Schulte, E. M., Furman, C. R., and Gearhardt, A. N. (2017). Wanting and liking: separable components in problematic eating behavior? *Appetite* 115, 45–53. doi: 10.1016/j.appet.2016.11.015

R Core Team (2019). *R: A Language and Environment for Statistical Computing*. Vienna, Austria: R Foundation for Statistical Computing. Available online at: https://www.R-project.org/

Reader, S. W., Lopez, R. B., and Denny, B. T. (2018). Cognitive reappraisal of low-calorie food predicts real-world craving and consumption of high- and low-calorie foods in daily life. *Appetite* 131, 44–52. doi: 10.1016/j.appet.2018.08.036

Rogers, P. J., and Hill, A. J. (1989). Breakdown of dietary restraint following mere exposure to food stimuli: interrelationships between restraint, hunger, salivation, and food intake. *Addictive Behav.* 14, 387–397. doi: 10.1016/0306-4603(89)90026-9

Rousseel, Y. (2012). lavaan: an R package for structural equation modeling. *J. Stat. Softw.* 48, 1–36.

Sheppes, G., Catran, E., and Meiran, N. (2009). Reappraisal (but not distraction) is going to make you sweat: physiological evidence for self-control effort. *Int. J. Psychophysiol.* 71, 91–96. doi: 10.1016/j.ijpsycho.2008.06.006

Stice, E., Yokum, S., Blum, K., and Bohon, C. (2010). Weight gain is associated with reduced striatal response to palatable food. *J. Neurosci.* 30, 13105–13109. doi: 10.1523/JNEUROSCI.2105-10.2010

Subar, A. F., Kirkpatrick, S. I., Mittl, B., Zimmerman, T. P., Thompson, F. E., Bingley, C., et al. (2012). The automated self-administered 24-hour dietary recall (ASA24): a resource for researchers, clinicians, and educators from the national cancer institute. *J. Acad. Nutr. Dietetics* 112, 1134–1137. doi: 10.1016/j.jand.2012.04.016

Tusche, A., and Hutcherson, C. A. (2018). Cognitive regulation alters social and dietary choice by changing attribute representations in domain-general and domain-specific brain circuits. *eLife* 7:e31185. doi: 10.7554/eLife.31185

Tzourio-Mazoyer, N., Landeau, B., Papathanassiou, D., Crivello, F., Etard, O., Delcroix, N., et al. (2002). Automated anatomical labeling of activations in SPM using a macroscopic anatomical parcellation of the MNI MRI single-subject brain. *Neuroimage* 15, 273–289. doi: 10.1006/nimg.2001.0978

Van Overwalle, F., and Mariën, P. (2016). Functional connectivity between the cerebrum and cerebellum in social cognition: a multi-study analysis. *Neuroimage* 124, 248–255. doi: 10.1016/J.NEUROIMAGE.2015.09.001

Versace, F., Frank, D. W., Stevens, E. M., Deweese, M. M., Guindani, M., and Schembre, S. M. (2018). The reality of "food porn": larger brain responses to food−related cues than to erotic images predict cue−induced eating. *Psychophysiology* 56:e13309. doi: 10.1111/psyp.13309

Wager, T. D., and Nichols, T. E. (2003). Optimization of experimental design in fMRI: a general framework using a genetic algorithm. *Neuroimage* 18, 293–309. doi: 10.1016/S1053-8119(02)00046-0

White, M. A., Whisenhunt, B. L., Williamson, D. A., Greenway, F. L., and Netemeyer, R. G. (2002). Development and validation of the food-craving inventory. *Obesity* 10, 107–114. doi: 10.1038/oby.2002.17

Winter, S. R., Yokum, S., Stice, E., Osipowicz, K., and Lowe, M. R. (2017). Elevated reward response to receipt of palatable food predicts future weight variability in healthy-weight adolescents. *Am. J. Clin. Nutr.* 105, 781–789. doi: 10.3945/ajcn.116.141143

Yokum, S., Gearhardt, A. N., Harris, J. L., Brownell, K. D., and Stice, E. (2014). Individual differences in striatum activity to food commercials predict weight gain in adolescents. *Obesity* 22, 2544–2551. doi: 10.1002/oby.20882

Yokum, S., Ng, J., and Stice, E. (2011). Attentional bias to food images associated with elevated weight and future weight gain: an fMRI study. *Obesity* 19, 1775–1783. doi: 10.1038/oby.2011.168

Żurawska vel Grajewska, B., Sim, E.-J., Hoenig, K., Herrnberger, B., and Kiefer, M. (2011). Mechanisms underlying flexible adaptation of cognitive control: behavioral and neuroimaging evidence in a flanker task. *Brain Res.* 1421, 52–65. doi: 10.1016/J.BRAINRES.2011.09.022

Conflict of Interest: EB was manager of Berkman Consultants, a boutique consulting firm specializing in goals, motivation, and behavior change.

The remaining authors declare that the research was conducted in the absence of any commercial or financial relationships that could be construed as a potential conflict of interest.

frontiers in Human Neuroscience

ORIGINAL RESEARCH
published: 16 November 2020
doi: 10.3389/fnhum.2020.587763

Caudate Functional Connectivity Associated With Weight Change in Adolescents

Yuko Nakamura[1], Sachiyo Ozawa[1] and Shinsuke Koike[1,2,3,4]*

[1] UTokyo Center for Integrative Science of Human Behavior, The University of Tokyo, Tokyo, Japan, [2] International Research Center for Neurointelligence, Tokyo, Japan, [3] University of Tokyo Institute for Diversity and Adaptation of Human Mind, Tokyo, Japan, [4] Center for Evolutionary Cognitive Sciences, Graduate School of Arts and Sciences, University of Tokyo, Tokyo, Japan

Background: Childhood obesity has become a global epidemic and the etiology of maladaptive ingestive behavior in children warrants further research. Mounting evidence suggests that the caudate is associated with body weight gain and obesity in adults. In adolescents, however, how caudate-related neural networks are associated with body weight gain is unclear because their central nervous systems are still developing.

Objectives: The current longitudinal resting-state functional magnetic resonance imaging (rs-fMRI) study was conducted to investigate the hypothesis that caudate-related neural networks have a role in weight gain in adolescents.

Methods: The study included 20 healthy adolescents with a mean age of 17.5 ± 2.0 years and a mean body mass index of 20.6 ± 2.1 who underwent baseline rs-fMRI then follow-up rs-fMRI approximately 1 year later. Body mass index (BMI) was measured at both timepoints. Seed-based functional connectivity analysis was utilized to analyze caudate-related functional connectivity (FC) using the caudate as a seed. Associations between caudate-related FC and BMI at baseline were assessed, as were associations between change in BMI and caudate-related FC between baseline and follow-up.

Results: At baseline, greater caudate-lateral prefrontal cortex FC was correlated with lower BMI (family wise error-corrected $p < 0.05$). Compared to the baseline, increased FC in the caudate-lateral prefrontal cortex at follow up were negatively associated with increased BMI ($p < 0.05$).

Conclusion: Given that the lateral prefrontal cortex and caudate are associated with inhibitory control, the caudate-lateral prefrontal cortex FC may have a preventive effect on weight gain in adolescents. The results of the current study suggest that developing inhibitory control would lead to the prevention of childhood obesity.

Keywords: adolescents, caudate, lateral prefrontal cortex, resting-state functional connectivity, weight management

OPEN ACCESS

Edited by:
Kiyoshi Nakahara, Kochi University of Technology, Japan

Reviewed by:
Yi Zhang, Xidian University, China
Chiara Begliomini, University of Padua, Italy

****Correspondence:***
Yuko Nakamura
nakamura.yuko0707@mail.u-tokyo.ac.jp

Specialty section:
This article was submitted to Health, a section of the journal Frontiers in Human Neuroscience

Received: *27 July 2020*
Accepted: *27 October 2020*
Published: *16 November 2020*

Citation:
Nakamura Y, Ozawa S and Koike S (2020) Caudate Functional Connectivity Associated With Weight Change in Adolescents. Front. Hum. Neurosci. 14:587763. doi: 10.3389/fnhum.2020.587763

INTRODUCTION

Childhood obesity has become a global epidemic in the last three decades (Abarca-Gómez et al., 2017), and it may cause deficits in structural and functional brain development (Laurent et al., 2019; Ronan et al., 2020) as well as various non-communicable diseases such as diabetes and cardiovascular conditions (Sahoo et al., 2015). A better understanding of the neuropathology of childhood obesity is thus needed to improve strategies for its prevention and treatment.

Weight change is reportedly associated with structural and functional alterations in reward regions of the brain such as the midbrain, pallidum, orbitofrontal cortex (Stice and Yokum, 2016), and especially the caudate. In one study, reduced caudate responses to palatable liquid consumption were correlated with increased body mass index (BMI), and this caudate response was associated with weight gain at a 1-year follow-up timepoint (Stice et al., 2008a). In another study, reduced caudate responses to sugary liquid consumption were correlated with increased BMI at a 6-month follow-up timepoint in women (Stice et al., 2010). In adolescents, altered caudate responses to food cues were reportedly associated with body fat gain at a 3-year follow-up timepoint (Stice et al., 2015) and BMI gain at an 1-year follow-up (Yokum et al., 2014). In a weight loss trial, greater reduction in brain responses to high-calorie food cues at a 1-month follow-up timepoint predicted greater weight loss at a 6-month follow-up timepoint (Hermann et al., 2019). In addition, altered caudate-related functional connectivity is reportedly predictive of increased BMI 6-months later (Gao et al., 2018) and 1 year later (Contreras-Rodríguez et al., 2017). Collectively, these observations suggest that aberrant functions or connectivity in the caudate are likely to be linked to disrupted weight maintenance.

The caudate is deep inside the brain near the thalamus, and is connected to parts of the brain associated with nearly all of its facets, including cognition, emotion, perception, and action-related structures and networks (Grahn et al., 2008; Robinson et al., 2012). The caudate responses to various food stimuli (van der Laan et al., 2011; Huerta et al., 2014; Arsalidou et al., 2020; Chen and Zeffiro, 2020) and caudate-related networks are changed by internal states (e.g., hunger or fullness) or food consumption in adults (Siep et al., 2009; Contreras-Rodriguez et al., 2019; Chen and Zeffiro, 2020) and adolescents (Page et al., 2013; Jastreboff et al., 2016). The caudate is connected to basal ganglia (e.g., substantia nigra and globus pallidus) as well as the prefrontal cortex, and is involved in reward processing, learning, goal-directed behavior, and decision-making (Balleine et al., 2007). In concert with the prefrontal cortex, it is also involved in inhibitory control (Guo et al., 2018; Cai et al., 2019) and cognitive appetite control (Tuulari et al., 2015). Given that the caudate and related neural networks are associated with perception of food stimuli, reward processing, and cognitive appetite control, it is likely to have an important role in ingestive behavior and weight change.

It has been repeatedly reported that impulsivity is associated with binge eating that could be a cause of excessive weight gain (Meule, 2013) in young adults (Claes et al., 2005; Oliva et al., 2019, 2020) and adolescents (Stice et al., 2013). In addition, increased impulsivity is associated with altered caudate function or connectivity (Babbs et al., 2013; Davis et al., 2013; Oliva et al., 2019) and obstruct function or structure in the prefrontal cortex, which is a key region for inhibitory or self-control behavior (Lowe et al., 2019). Given that adolescents exhibit greater impulsivity than adults because their inhibitory control mechanisms are still developing (Romer, 2010), and they are evidently more prone to over consumption of rewarding high-calorie food (van Meer et al., 2016). It is thus important to elucidate the associations between caudate-related neural networks and body weight change in adolescents, but these associations have not been well characterized. In the current longitudinal study resting-state functional magnetic resonance imaging (rs-fMRI) and seed-based functional connectivity (FC) analysis were used to examine associations between caudate-related FC and BMI change in adolescents. We hypothesized that increased BMI or BMI change would be associated with reduced caudate-related FC in the inhibitory region and increased caudate-related FC in reward processing or motivation regions, which were associated with food reward processing and weight gain (e.g., striatum, midbrain, amygdala, insula, pre-/postcentral gyrus, and orbitofrontal cortex) (García-García et al., 2014; Stice and Yokum, 2016).

MATERIALS AND METHODS

Participants

The study included 20 adolescents (seven male, 13 female) with a mean age of 17.5 years [standard deviation (SD) 2.0, range 14–19 years] and a mean BMI of 20.6 (SD 2.1, range 17.2–25.7) at baseline who were recruited from the metropolitan area of Tokyo. All participants and parents/guardians of the high school or middle school participants provided written informed consent, and the study was approved by the Ethics Committee of the Graduate School of Arts and Sciences at the University of Tokyo (approval number 513-2). All participants were healthy and had no history of psychological or neurological disorders or head injury. Detailed demographic data are shown in **Table 1**.

Experimental Timepoints

All participants underwent rs-fMRI at baseline and approximately 1 year or more thereafter (mean 12.95 ± 3.02 months, range 11–22 months). Within 1 month before or after each rs-fMRI session, each participant visited the laboratory and their weight and height were measured by trained experimenters (YN or SO) using a multi-frequency body composition meter (MC-780A, TANITA CORPORATION, Tokyo, Japan) to calculate BMI (kg/m^2). We also collected self-reported weight and height on the scanning day. We calculate BMI using self-reported weight and height. There was no significant difference between self-reported BMI and measured BMI ($p = 0.86$, $t = -0.18$ at baseline; $p = 0.79$, $t = -0.27$ at follow-up). Therefore, we assumed that the participants'

TABLE 1 | Demographics.

	Baseline	1-year follow-up	Change	*p* value
Sex (male/female)	7/13			
Age (mean ± SD) (range)	17.5 ± 2.0 (14.1–19.9)	18.6 ± 2.0 (15.1–20.8)	1.1 ± 0.3 (0.9–1.8)	<0.001
BMI (mean ± SD) (range)	20.6 ± 2.1 (17.2–25.7)	20.8 ± 1.6 (17.6–23.8)	0.25 ± 2.53 (−4.3 – 6.5)	0.68

BMI, Body mass index.

BMI did not significantly change within a month from the rs-fMRI scanning day.

At this visit, participants also completed the Japanese version Barratt Impulsiveness Scale Version 11 (BIS-11) (Patton et al., 1995; Someya et al., 2001; Kobashi and Ida, 2013), which was a questionnaire designed to assess the personality/behavioral construct of impulsiveness (Someya et al., 2001). This self-reported questionnaire has been adapted to assess impulsivity in adolescents (Pechorro et al., 2016; Huang et al., 2017). The BIS-11 contains a total of 30 items scored on a Likert scale (ranging from never = 1 point to very frequently = 6 points) yielding impulsivity measures on three scales: attentional (inability to focus or concentrate), motor (tendency to act without thinking), and non-planning impulsivity (lack of future planning and forethought). The total score ranges from 30 to 180, with a higher score indicating greater impulsivity.

Rs-fMRI Procedure

Approximately three to 4 h after a meal, the level of appetite generally returns to almost the same level as that of the pre-meal appetite (Leidy et al., 2010; Gibbons et al., 2013; DeBenedictis et al., 2020). Since caudate-related functional connectivity could be changed by internal states (e.g., hunger or fullness) (Siep et al., 2009; Page et al., 2013; Jastreboff et al., 2016; Contreras-Rodriguez et al., 2019; Chen and Zeffiro, 2020), the participants were instructed to abstain from food or drink except for water for at least 3 h before their visit to the laboratory to avoid the effect of the meal on caudate FC. In an effort to standardize participants' internal states, they were instructed to consume pre-fixed snacks (280 kcal) approximately 30 min before rs-fMRI scanning (**Figure 1**). The participant was then escorted to the fMRI room to undergo rs-fMRI scanning. Approximately 10 min before rs-fMRI scanning, each participant rated their internal states (e.g., hunger and fullness) using an 8-point Likert scale, where 1 equated to "not at all" and 8 equated to "more than ever." Before rs-fMRI scanning, each participant underwent an fMRI experiment to measure brain responses to food cues. After the food cue fMRI experiment, we asked all participants if they felt any fatigue or anxiety. All participants responded that they were comfortable to continue scanning. The participant underwent rs-fMRI scanning (10 min 10 s, 244 volumes).

The participant was instructed to relax and lie still in the scanner while remaining calm and awake. During rs-fMRI scanning, the participant was instructed to fix their gaze on a white cross on the black screen, which was projected on a mirror attached to the head-coil from the monitor that was set behind the bore of the MRI machine.

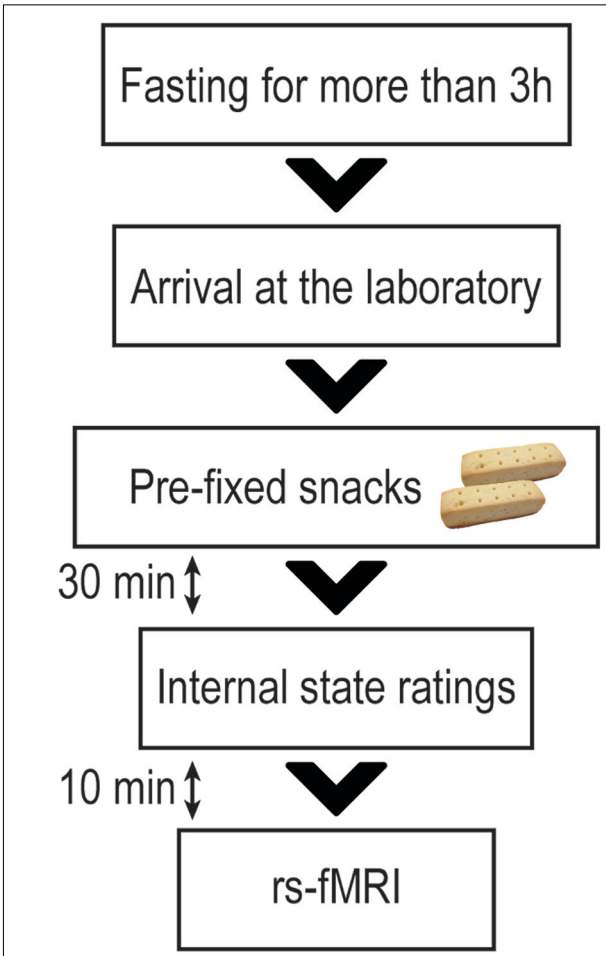

FIGURE 1 | Resting-state functional magnetic resonance imaging session. All participants were instructed to abstain from any food or drinks apart from water for at least 3 h before their visit to the laboratory. Approximately 30 min before the resting-state functional magnetic resonance imaging (rs-fMRI) scanning, each participant was instructed to consume pre-prepared snacks (280 kcal) to standardize their internal states of hunger and fullness. Approximately 10 min before the rs-fMRI scanning, participants rated their levels of hunger and fullness.

Image Acquisition

Images were acquired on a 3 Tesla MRI scanner (Magnetom Prisma Fit, Siemens Medical Systems, Munich, Germany) using a 64-channel head/neck coil. T2*-weighted images reflecting blood oxygen level-dependent signals were acquired using gradient-echo echo-planar imaging (repetition time 2500 ms, echo time 30 ms, 38 slices, flip angle 80°, field of view 212 mm × 212 mm,

and resolution 3.3 mm × 3.3 mm × 4.0 mm) in ascending order (10 min and 10 s). Anatomical images were acquired using a T1-weighted 3D MPRAGE protocol (repetition time 1900 ms, echo time 2.53 ms, flip angle 9°, field of view 256 mm × 256 mm, resolution 1.0 mm × 1.0 mm × 1.0 mm).

Rs-fMRI Data Preprocessing

Resting-state functional magnetic resonance imaging data were preprocessed using FSL (version 6.0) (Jenkinson et al., 2012) and AFNI (version 20.0.05 "Galba") (Cox, 1996) software. The first four volumes of each functional time series were excluded from the analysis to allow for magnetization equilibrium. Conventional preprocessing was conducted as follows: (1) Head-motion correction via realignment of the time-series to the middle volume; (2) fieldmap-based distortion-correction; (3) slice-timing correction; (4) non-brain tissue removal using the brain extraction tool; (5) spatial smoothing with a 5-mm full-width at half maximum Gaussian kernel; (6) high-pass temporal filtering (1/150 Hz cutoff); and (7) linear detrending. The exclusion criterion for head-motion was greater than one voxel size (3.3 mm × 3.3 mm × 4.0 mm). No participant met this exclusion criterion, thus data from all participants were included in further rs-fMRI analyses in which head-motion in rs-fMRI scanning was calculated. In baseline rs-fMRI, the mean head-motion values (x, y, z) were 0.16 ± 0.09, 0.38 ± 0.27, and 0.88 ± 0.63, and at follow-up, they were 0.17 ± 0.11, 0.34 ± 0.15, and 0.72 ± 0.48. Derivative or root mean square variance over voxels (DVARS) were also calculated, quantifying the mean change in image intensity between timepoints (Power et al., 2012). Time-series were then extracted from white matter and cerebrospinal fluid from preprocessed time-series data. Motion-regressors, DVARS, and white matter and cerebrospinal fluid time-series were included in a confounder matrix.

Caudate-Related Connectivity Maps

Based on a previous report (Contreras-Rodríguez et al., 2017), 3-mm spheres were placed centered on (x, y, z) = (13, 15, 9) and (x, y, z) = (−13, 15, 9) as right and left caudate seeds. Right and left seeds were then merged and regions outside the anatomical caudate area were cut out and binarized to create the caudate seed (**Figure 2**). A time-series was extracted from unsmoothed preprocessed rs-fMRI data using the caudate seed. To create individual caudate connectivity maps, the extracted time-series from the seed was included in a general linear model using FSL's fMRI Expert Analysis Tool. This model also included a confounder matrix as a nuisance covariate.

Statistical Analysis

The Effect of Gender on BMI

We tested for gender differences in BMI at baseline and follow-up, and in the change in BMI, using a two-sample *t*-test.

Association Between Caudate-Related Connectivity and BMI

First, paired *t*-tests were conducted on individual connectivity maps derived from baseline and follow-up data to compare caudate-related FC.

Then, to assess the correlation between BMI and individual connectivity maps at baseline and follow-up, a group-level voxel-wise linear regression analysis with BMI as a covariate of interest was performed on individual caudate-related connectivity maps. To control for variance in age, age was included as a covariate of no-interest in the regression analysis. The cluster-forming threshold was set at $z > 3.1$. Clusters were then formed, associated p values were calculated, and p values that were > 0.05 (family wise error (FWE) corrected) were disregarded.

From brain regions in which there was a significant correlation between caudate-related FC and BMI at baseline, FC values (z-values) were extracted from connectivity maps at baseline and follow-up and compared. Further, correlation coefficients between extracted FC values and BMI were compared at baseline and follow-up using the "cocor" package version 1.1-3 in R (Diedenhofen and Musch, 2015).

Association Between Change in BMI and Change in Caudate-Related Connectivity

Changes in extracted FC values between baseline and follow-up (follow-up > baseline) were calculated, and the correlations

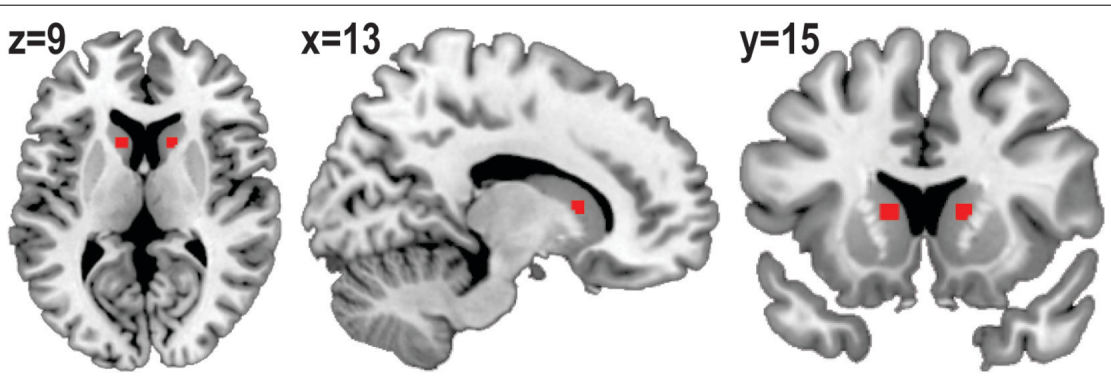

FIGURE 2 | Binarized caudate seed. Three-millimeter spheres were placed centered on (x, y, z) = (13, 15, 9) and (x, y, z) = (–13, 15, 9). Right and left seeds were merged and regions outside of the anatomical caudate area were cut out.

between changes in extracted FC values and change in BMI (follow-up > baseline) were calculated using the Robust Correlation Toolbox in MATLAB R2020a (MathWorks, Inc., Natick, MA, United States) (Pernet et al., 2012). Robust correlation methods could provide better estimates of true associations, with accurate false-positive control and without loss of power by removing or down-weighting outliers and accounting for them in significance testing. To calculate skipped Pearson's correlational coefficient, first the robust center of the data cloud was estimated using the minimum covariance determinant. Outliers were then identified using a projection technique. Lastly, Pearson's correlation and associated t values were calculated using the remaining data. For correlational coefficients (r), 95% confidence intervals (CI) were calculated based on 1000 samples with the percentile bootstrap method implemented in the toolbox.

RESULTS

Change in BMI and the Effect of Gender on BMI

The mean change in BMI was 0.25 ± 2.53 (range −4.33 to 6.53), and there was no significant difference in the change in BMI between male and female participants ($p = 0.74$, $t = -0.34$). The change in BMI was not significantly associated with the change in age ($p = 0.09$, $r = 0.39$).

There was no significant gender difference in BMI at baseline ($p = 0.81$, $t = -0.24$) or at follow-up ($p = 0.36$, $t = -0.95$).

Internal State at the Rs-fMRI Sessions

The mean hunger rating at baseline was 4.6 ± 1.2, and at the follow-up timepoint, it was 4.1 ± 1.3. The mean fullness rating at baseline was 4.2 ± 1.2, and at the follow-up timepoint, it was 4.8 ± 1.2. Ratings for hunger and fullness at baseline did not differ significantly from the corresponding ratings at follow-up ($p = 0.25$, $t = 1.18$ for hunger and $p = 0.17$, $t = -1.43$ for fullness). There were no significant differences between ratings for hunger and fullness at baseline ($p = 0.38$, $t = 0.89$) or follow-up ($p = 0.15$, $t = -1.51$), suggesting that participants were neither hungry nor full at either of their rs-fMRI sessions.

Association Between Caudate-Related Connectivity and BMI

There was no significant difference in caudate-related connectivity maps between baseline and follow-up.

Body mass index was inversely correlated with caudate-related FC in the inferior frontal gyrus (IFG), the opercular part [(x, y, z) = (−44, 10, 14), $z = 4.07$, $P_{FWE\text{-}corrected} = 0.0014$, cluster size = 187 voxels], and the superior frontal gyrus (SFG) [(x, y, z) = (−22, 56, 16), $z = 4.09$, $P_{FWE\text{-}corrected} = 0.0048$, cluster size = 154 voxels] (**Figure 3**). After controlling for age, the correlation between BMI and caudate-related FC in the IFG and SFG still remained significant [IFG: (x, y, z) = (−44, 10, 14), $z = 3.94$, $P_{FWE\text{-}corrected} = 0.0089$, cluster size = 137 voxels, SFG: (x, y, z) = (−22, 56, 16), $z = 4.09$, $P_{FWE\text{-}corrected} = 0.0030$, cluster size = 165 voxels].

There was no significant positive nor negative correlation between caudate-related FC and BMI at follow-up.

The linear relationship between caudate-related connectivity maps and BMI did not differ between baseline and follow-up.

Extracted caudate-related FCs in the IFG or SFG at baseline did not differ from those at follow-up ($p = 0.61$, $t = -0.94$ for FC in the IFG and $p = 0.34$, $t = -0.97$ for FC in the SFG).

Correlations between extracted FCs in the IFG or SFG and BMI at baseline were greater than those at follow-up ($p = 0.030$, $z = -2.17$ for the IFG and $p = 0.039$, $z = -2.07$ for the SFG).

Time of intervals between baseline and follow-up rs-fMRI sessions were not significantly correlated with caudate-related FC in IFG ($p = 0.18$, $r = 0.31$) or SFG ($p = 0.41$, $r = 0.20$), but change in BMI ($p = 0.047$, $r = 0.45$).

Association Between Change in BMI and Change in Caudate-Related Connectivity

There were significant negative correlations between the change in BMI and change in FC values (z values) from the IFG (skipped Pearson's r [15] = −0.65, $p = 0.002$, 95% CI = [−0.90 to −0.19], number of outliers (NO) = 3) and from the SFG (skipped Pearson's r [16] = −0.54, $p = 0.015$, 95% CI = [−0.80 to −0.10], NO = 2) (**Figure 4**). These results indicated that increased connectivity was correlated with reduced BMI gain.

Associations Between Impulsivity and Age, Caudate-Related Connectivity, and BMI

Associations between each subscale of impulsivity and age at baseline and follow-up were tested. Increased attentional and motor subscales were positively correlated with age at baseline ($p = 0.003$, $r = 0.63$ for attentional subscale; $p = 0.033$, $r = 0.48$ for motor subscale) and increased attentional subscale with age at follow-up ($p = 0.018$, $r = 0.52$).

There was no significant difference in the correlation between age and attentional subscale between baseline and follow-up ($p = 0.42$, $z = 0.81$).

Associations between each subscale of impulsivity and caudate-prefrontal cortex connectivity in the IFG and SFG at baseline and follow-up were tested. Motor subscale was negatively correlated with FC in the IFG ($p = 0.047$, $r = -0.45$) at baseline and in the SFG at follow-up ($p = 0.032$, $r = -0.48$). Change in motor subscale was negatively associated with FC in the SFG ($p = 0.030$, $r = -0.49$).

Associations between each subscale of impulsivity and BMI at baseline and follow-up were tested. A significant association was not observed ($p > 0.07$ for all).

After the Bonferroni adjustment was performed for a multiple-comparison correction, the positive correlation between attentional impulsivity and age at baseline remained significant (significant level: $p < 0.0125$).

There was no significant gender difference in any subscales ($p > 0.12$ for all).

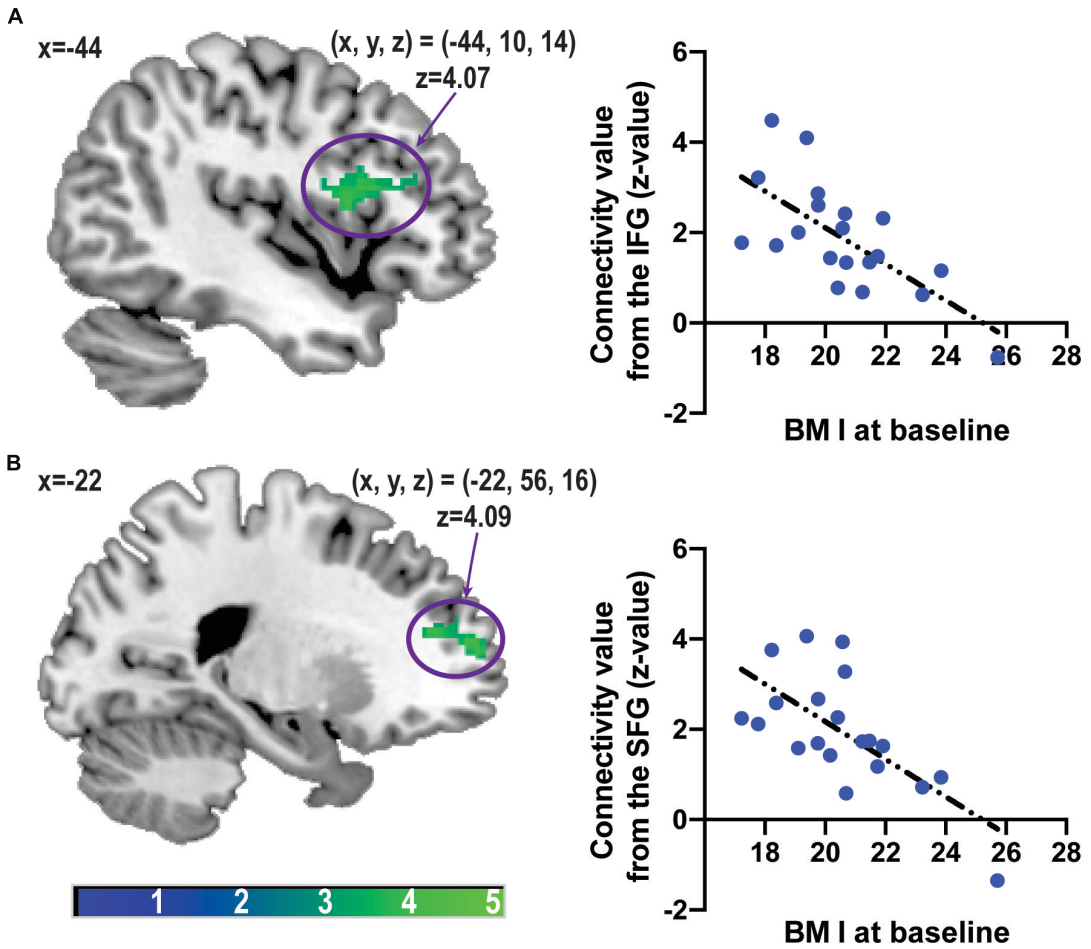

FIGURE 3 | Associations between caudate-related functional connectivity and body mass index at baseline. Scatter plots depict associations between body mass index and caudate-related functional connectivity in the inferior frontal gyrus **(A)** and superior frontal gyrus **(B)**. The color bar depicts the *z*-value. IFG, inferior frontal gyrus; SFG, superior frontal gyrus.

DISCUSSION

In the current study, greater caudate-IFG and caudate-SFG FCs were associated with lower BMI at baseline, and increased FC was negatively correlated with BMI gain at follow-up. Further, increased caudate-prefrontal cortex FC was associated with decreased impulsivity. To the best of our knowledge, the current longitudinal study is the first to show the association among the change in caudate-prefrontal cortex FC, BMI, and impulsivity in adolescents. The IFG, SFG, and caudate are involved in inhibitory control in adults (Guo et al., 2018; Cai et al., 2019) and children (Cai et al., 2019). Alterations in the IFG and SFG are involved in obesity, and gray matter reduction in the IFG has been reported in people with obesity (Herrmann et al., 2019). In adolescents, reduced cortical thickness in the IFG and SFG is reportedly associated with increased BMI and reduced cognitive function (Ronan et al., 2020). The IFG and SFG are involved in cognitive appetite control in adults (Tuulari et al., 2015) and attenuated caudate activation was observed during appetite control in middle aged people with obesity (Tuulari et al., 2015). Moreover, lower caudate responses to palatable liquid consumption in people with increased BMI are associated with elevated impulsivity (Babbs et al., 2013). Both caudate-IFG and caudate-SFG FC may be involved in cognitive appetite control and increases in these FCs may have preventive effects on excessive weight gain in adolescents.

In the present study, caudate-related FC at follow-up was not significantly associated with BMI, and the correlations between BMI and caudate-related FC in the prefrontal cortex were attenuated at follow-up. In young adolescents with healthy weight, increased impulsivity is associated with increased local FC in the caudate and decreased FC between the prefrontal cortex and caudate (Davis et al., 2013). Further, decreased caudate response to the inhibitory task was associate with increased impulsivity (Oliva et al., 2019). Given that age was positively associated with impulsivity at baseline in the current study, and the immature or obstruct PFC is involved with weight gain as well as elevated impulsivity (Lowe et al., 2019), attenuated FC between caudate-prefrontal cortex could be linked to increased impulsivity and lead to gained BMI at baseline. However, as the

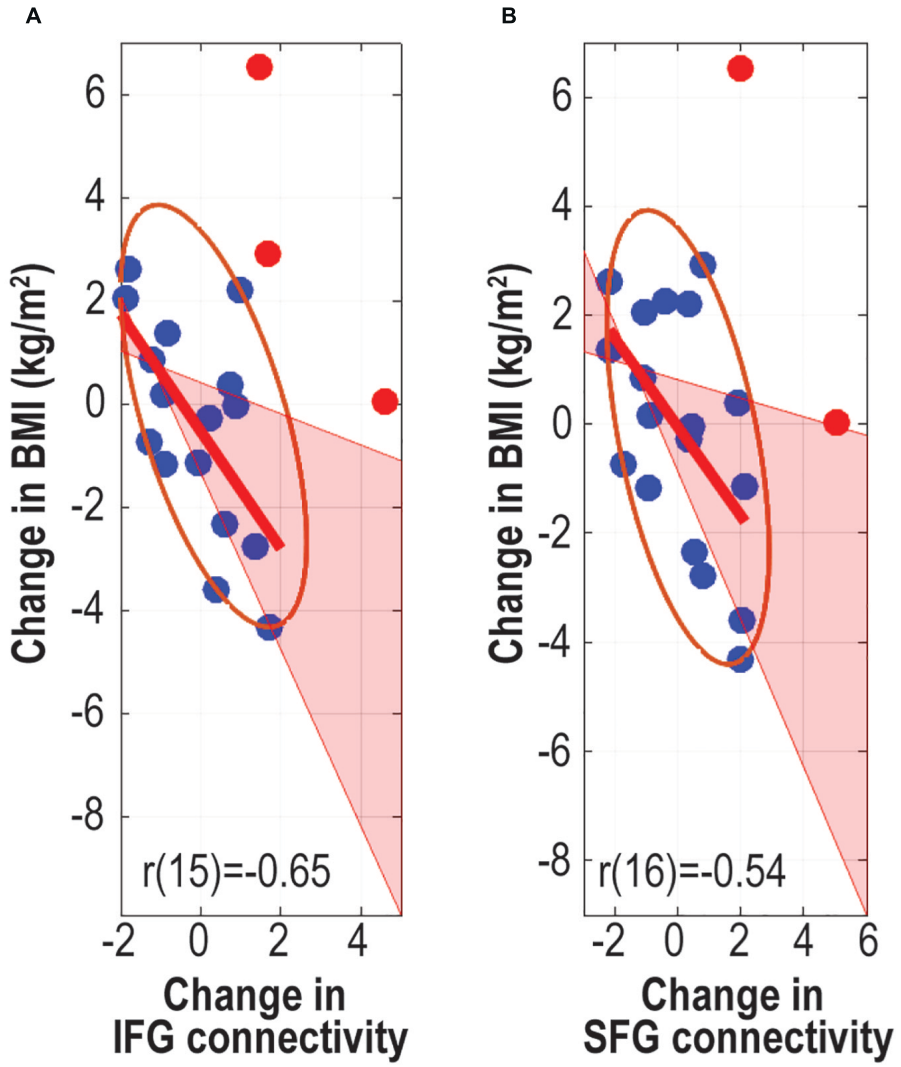

FIGURE 4 | Associations between change in body mass index and change in caudate-related connectivity. Scatter plots depict associations between change in body mass index and caudate-related functional connectivity in the inferior frontal gyrus **(A)** and superior frontal gyrus **(B)**. *r* values are skipped Pearson's correlational coefficients. Red data-points indicate outliers. IFG, inferior frontal gyrus; SFG, superior frontal gyrus.

results showing that the associations between age and subscales of impulsivity at baseline differed from those at follow-up, the balance between sensation-seeking activation in the striatum and inhibitory control in the prefrontal cortex changes during adolescence (Romer, 2010), and this biological change may alter associations between caudate-related FC and BMI at follow-up compared to that at baseline. To examine this hypothesis, it is necessary to perform further follow-up observations.

Contrary to the study hypothesis, BMI was not significantly associated with caudate-related FC in reward regions, such as the striatum, midbrain, amygdala, insula, and orbitofrontal cortex (García-García et al., 2014; Stice and Yokum, 2016). Reward regions are related to weight gain and obesity (Stice and Yokum, 2016) and people with obesity reportedly have different caudate-related FC in reward-related regions (Lips et al., 2014). Therefore, associations between caudate-related FC in reward regions and BMI or BMI change may have been non-significant in the present study because almost all of the participants were of healthy weight.

The current study had several limitations. One is that it did not include obese adolescents. Compared with healthy weight adolescents, obese adolescents showed a greater caudate response to high calorie food images (Jastreboff et al., 2014), and a decreased caudate response following consumption of a milkshake (Stice et al., 2008b); therefore, caudate functional connectivity in adolescents with obesity is predicted to be different from that in healthy weight adolescents. While further investigation is needed to test this hypothesis, the current study provides insights into neural involvement in weight gain in adolescents. Second, not all participants' BMI were measured on the day of the rs-fMRI session; however, all participants' BMI were measured within 1 month before or after each rs-fMRI

session. We assumed that their BMI did not change significantly within 1 month from the day of the rs-fMRI session because their self-reported BMI on the day of the rs-fMRI session were not significantly different from the measured BMI. However, since self-reported BMI is not reliable, small differences between the actual BMI on the day of the rs-fMRI session and that measured within a month from the day of the rs-fMRI session could potentially affect the association between BMI and caudate FC. Third, there was variation in the intervals between baseline and follow-up rs-fMRI sessions (mean 12.95 ± 3.02 months, range 11–22 months). Since there was no significant association between time of intervals and change in caudate FCs, this variation in the interval time appeared to have little effect on our analysis. However, as variance in the interval time could affect the correlation between the change in BMI and caudate FC, further studies should be conducted with fixed follow-up intervals. The fourth is that our sample size is not large. Although a preferable sample size for rs-fMRI studies has not been addressed in the literature to date, for a task-based fMRI experiment, Thirion et al. (2007) showed that a minimum sample size of 20 was necessary to ensure acceptable reliability. In addition, our sample is relatively homogeneous because all participants are Asian adolescents from similar residential areas, and we controlled the internal state for each participant. In addition, the effect size of correlation analysis between the connectivity values and BMI at baseline was calculated using G*Power (Faul et al., 2007). All effect sizes were greater than 0.8. Therefore, the current results would be acceptable. However, it is preferable to perform further studies with greater sample size. Fifth, the results of the study do not demonstrate that there is a causal relationship between change in BMI and change in FC. Given that BMI gain is predicted by altered caudate function in adolescents, however (Stice et al., 2015), disrupted caudate-related FC may cause excessively increased BMI. Additional longitudinal studies are needed to investigate associations between development and the neuropathology of aberrant ingestive behavior in adolescents.

In conclusion, caudate-related FC in the inhibitory control regions has a preventive effect on excessive weight gain in adolescents. In the present longitudinal study, increased caudate-related FC in the prefrontal cortex – the inhibitory control region – was associated with lower BMI and impulsivity at baseline, and strengthened FC was inversely correlated with BMI gain and increment of impulsivity at follow-up in adolescents. These results suggest that developing inhibitory control may lead to successful prevention of childhood obesity.

DATA AVAILABILITY STATEMENT

The original contributions presented in the study are included in the article/supplementary material, further inquiries can be directed to the corresponding author.

ETHICS STATEMENT

The studies involving human participants were reviewed and approved by the Ethics Committee of the Graduate School of Arts and Sciences at the University of Tokyo (approval number 513-2). Written informed consent to participate in this study was provided by the participants' legal guardian/next of kin.

AUTHOR CONTRIBUTIONS

YN and SK: conceptualization and design, reviewing and editing the manuscript. YN and SO: data acquisition. YN: data analysis and writing the manuscript. All authors contributed to the article and approved the submitted version.

FUNDING

This study was supported by the 12th Hakuho Research Grant for Child Education from the Hakuho Foundation, Grants-in-Aid for Early-Career Scientists from the Japan Society for the Promotion of Science (grant ID 17K13931), and UTokyo Center for Integrative Science of Human Behavior (CiSHuB).

ACKNOWLEDGMENTS

We thank Naoko Aoki and Tomoko Kawashima for their help with conducting the study.

REFERENCES

Abarca-Gómez, L., Abdeen, Z. A., Hamid, Z. A., Abu-Rmeileh, N. M., Acosta-Cazares, B., Acuin, C., et al. (2017). Worldwide trends in body-mass index, underweight, overweight, and obesity from 1975 to 2016: a pooled analysis of 2416 population-based measurement studies in 128.9 million children, adolescents, and adults. *Lancet* 390, 2627–2642.

Arsalidou, M., Vijayarajah, S., and Sharaev, M. (2020). Basal ganglia lateralization in different types of reward. *Brain Imaging Behav. [Internet]*. doi: 10.1007/s11682-019-00215-3 [Epub ahead of print].

Babbs, R. K., Sun, X., Felsted, J., Chouinard-Decorte, F., Veldhuizen, M. G., and Small, D. M. (2013). Decreased caudate response to milkshake is associated with higher body mass index and greater impulsivity. *Physiol. Behav.* 121, 103–111. doi: 10.1016/j.physbeh.2013.03.025

Balleine, B. W., Delgado, M. R., and Hikosaka, O. (2007). The role of the dorsal striatum in reward and decision-making. *J. Neurosci. Off. J. Soc. Neurosci.* 27, 8161–8165. doi: 10.1523/jneurosci.1554-07.2007

Cai, W., Duberg, K., Padmanabhan, A., Rehert, R., Bradley, T., Carrion, V., et al. (2019). Hyperdirect insula-basal-ganglia pathway and adult-like maturity of global brain responses predict inhibitory control in children. *Nat. Commun.* 10:4798.

Chen, E. Y., and Zeffiro, T. A. (2020). Hunger and BMI modulate neural responses to sweet stimuli: fMRI meta-analysis. *Int. J. Obes.* 44, 1636–1652. doi: 10.1038/s41366-020-0608-5

Claes, L., Vandereycken, W., and Vertommen, H. (2005). Impulsivity-related traits in eating disorder patients. *Personal Individ. Differ.* 39, 739–749. doi: 10.1016/j.paid.2005.02.022

Contreras-Rodriguez, O., Burrows, T., Pursey, K. M., Stanwell, P., Parkes, L., Soriano-Mas, C., et al. (2019). Food addiction linked to changes in ventral

striatum functional connectivity between fasting and satiety. *Appetite* 133, 18–23. doi: 10.1016/j.appet.2018.10.009

Contreras-Rodríguez, O., Martín-Pérez, C., Vilar-López, R., and Verdejo-Garcia, A. (2017). Ventral and dorsal striatum networks in obesity: link to food craving and weight gain. *Biol. Psychiatry* 81, 789–796. doi: 10.1016/j.biopsych.2015.11.020

Cox, R. W. (1996). AFNI: software for analysis and visualization of functional magnetic resonance neuroimages. *Comput. Biomed. Res. Int. J.* 29, 162–173. doi: 10.1006/cbmr.1996.0014

Davis, F. C., Knodt, A. R., Sporns, O., Lahey, B. B., Zald, D. H., Brigidi, B. D., et al. (2013). Impulsivity and the modular organization of resting-state neural networks. *Cereb. Cortex N. Y. N 1991* 23, 1444–1452. doi: 10.1093/cercor/bhs126

DeBenedictis, J. N., Nymo, S., Ollestad, K. H., Boyesen, G. A., Rehfeld, J. F., Holst, J. J., et al. (2020). Changes in the homeostatic appetite system after weight loss reflect a normalization toward a lower body weight. *J. Clin. Endocrinol. Metab.* 105, e2538–e2546.

Diedenhofen, B., and Musch, J. (2015). cocor: a comprehensive solution for the statistical comparison of correlations. *PLoS One* 10:e0121945. doi: 10.1371/journal.pone.0121945

Faul, F., Erdfelder, E., Lang, A.-G., and Buchner, A. G. (2007). *Power 3: a flexible statistical power analysis program for the social, behavioral, and biomedical sciences. *Behav. Res. Methods* 39, 175–191. doi: 10.3758/bf03193146

Gao, X., Liang, Q., Wu, G., She, Y., Sui, N., and Chen, H. (2018). Decreased resting-state BOLD regional homogeneity and the intrinsic functional connectivity within dorsal striatum is associated with greater impulsivity in food-related decision-making and BMI change at 6-month follow up. *Appetite* 127, 69–78. doi: 10.1016/j.appet.2018.04.024

García-García, I., Horstmann, A., Jurado, M. A., Garolera, M., Chaudhry, S. J., Margulies, D. S., et al. (2014). Reward processing in obesity, substance addiction and non-substance addiction. *Obes. Rev. Off. J. Int. Assoc. Study Obes.* 15, 853–869. doi: 10.1111/obr.12221

Gibbons, C., Caudwell, P., Finlayson, G., Webb, D.-L., Hellström, P. M., Näslund, E., et al. (2013). Comparison of postprandial profiles of ghrelin, active GLP-1, and total PYY to meals varying in fat and carbohydrate and their association with hunger and the phases of satiety. *J. Clin. Endocrinol. Metab.* 98, E847–E855.

Grahn, J. A., Parkinson, J. A., and Owen, A. M. (2008). The cognitive functions of the caudate nucleus. *Prog. Neurobiol.* 86, 141–155. doi: 10.1016/j.pneurobio.2008.09.004

Guo, Y., Schmitz, T. W., Mur, M., Ferreira, C. S., and Anderson, M. C. (2018). A supramodal role of the basal ganglia in memory and motor inhibition: meta-analytic evidence. *Neuropsychologia* 108, 117–134. doi: 10.1016/j.neuropsychologia.2017.11.033

Hermann, P., Gál, V., Kóbor, I., Kirwan, C. B., Kovács, P., Kitka, T., et al. (2019). Efficacy of weight loss intervention can be predicted based on early alterations of fMRI food cue reactivity in the striatum. *Neuroimage Clin.* 23:101803. doi: 10.1016/j.nicl.2019.101803

Herrmann, M. J., Tesar, A.-K., Beier, J., Berg, M., and Warrings, B. (2019). Grey matter alterations in obesity: a meta-analysis of whole-brain studies. *Obes. Rev. Off. J. Int. Assoc. Study Obes.* 20, 464–471. doi: 10.1111/obr.12799

Huang, Y.-H., Liu, H.-C., Tsai, F.-J., Sun, F.-J., Huang, K.-Y., Chiu, Y.-C., et al. (2017). Correlation of impulsivity with self-harm and suicidal attempt: a community study of adolescents in Taiwan. *BMJ Open* 7:e017949. doi: 10.1136/bmjopen-2017-017949

Huerta, C. I., Sarkar, P. R., Duong, T. Q., Laird, A. R., and Fox, P. T. (2014). Neural bases of food perception: coordinate-based meta-analyses of neuroimaging studies in multiple modalities. *Obes. Silver Spring Md.* 22, 1439–1446. doi: 10.1002/oby.20659

Jastreboff, A. M., Lacadie, C., Seo, D., Kubat, J., Van Name, M. A., Giannini, C., et al. (2014). Leptin is associated with exaggerated brain reward and emotion responses to food images in adolescent obesity. *Diabetes Care* 37, 3061–3068. doi: 10.2337/dc14-0525

Jastreboff, A. M., Sinha, R., Arora, J., Giannini, C., Kubat, J., Malik, S., et al. (2016). Altered brain response to drinking glucose and fructose in obese adolescents. *Diabetes* 65, 1929–1939. doi: 10.2337/db15-1216

Jenkinson, M., Beckmann, C. F., Behrens, T. E. J., Woolrich, M. W., and Smith, S. M. (2012). FSL. *Neuroimage* 62, 782–790.

Kobashi, M., and Ida, M. (2013). Making the revised version of barratt impulsiveness scale 11th in Japanese: a study on reliability and validity. *J. Psychol. Rissho. Univ.* 4, 53–61.

Laurent, J. S., Watts, R., Adise, S., Allgaier, N., Chaarani, B., Garavan, H., et al. (2019). Associations among body mass index, cortical thickness, and executive function in children. *JAMA Pediatr.* 174, 170–177. doi: 10.1001/jamapediatrics.2019.4708

Leidy, H. J., Apolzan, J. W., Mattes, R. D., and Campbell, W. W. (2010). Food form and portion size affect postprandial appetite sensations and hormonal responses in healthy, nonobese, older adults. *Obes. Silver Spring Md.* 18, 293–299. doi: 10.1038/oby.2009.217

Lips, M. A., Wijngaarden, M. A., van der Grond, J., van Buchem, M. A., de Groot, G. H., Rombouts, S. A. R. B., et al. (2014). Resting-state functional connectivity of brain regions involved in cognitive control, motivation, and reward is enhanced in obese females. *Am. J. Clin. Nutr.* 100, 524–531. doi: 10.3945/ajcn.113.080671

Lowe, C. J., Reichelt, A. C., and Hall, P. A. (2019). The prefrontal cortex and obesity: a health neuroscience perspective. *Trends Cogn. Sci.* 23, 349–361. doi: 10.1016/j.tics.2019.01.005

Meule, A. (2013). Impulsivity and overeating: a closer look at the subscales of the barratt impulsiveness scale. *Front. Psychol. [Internet]* 4:177. doi: 10.3389/fpsyg.2013.00177/full

Oliva, R., Morys, F., Horstmann, A., Castiello, U., and Begliomini, C. (2019). The impulsive brain: neural underpinnings of binge eating behavior in normal-weight adults. *Appetite* 136, 33–49. doi: 10.1016/j.appet.2018.12.043

Oliva, R., Morys, F., Horstmann, A., Castiello, U., and Begliomini, C. (2020). Characterizing impulsivity and resting-state functional connectivity in normal-weight binge eaters. *Int. J. Eat. Disord.* 53, 478–488. doi: 10.1002/eat.23212

Page, K. A., Chan, O., Arora, J., Belfort-Deaguiar, R., Dzuira, J., Roehmholdt, B., et al. (2013). Effects of fructose vs glucose on regional cerebral blood flow in brain regions involved with appetite and reward pathways. *JAMA* 309, 63–70. doi: 10.1001/jama.2012.116975

Patton, J. H., Stanford, M. S., and Barratt, E. S. (1995). Factor structure of the barratt impulsiveness scale. *J. Clin. Psychol.* 51, 768–774. doi: 10.1002/1097-4679(199511)51:6<768::aid-jclp2270510607>3.0.co;2-1

Pechorro, P., Ayala-Nunes, L., Ray, J. V., Nunes, C., and Gonçalves, R. A. (2016). The barratt impulsiveness scale-11 among a school sample of portuguese male and female adolescents. *J. Child. Fam. Stud.* 25, 2753–2764. doi: 10.1007/s10826-016-0453-2

Pernet, C. R., Wilcox, R., and Rousselet, G. A. (2012). Robust correlation analyses: false positive and power validation using a new open source matlab toolbox. *Front. Psychol.* 3:606.

Power, J. D., Barnes, K. A., Snyder, A. Z., Schlaggar, B. L., and Petersen, S. E. (2012). Spurious but systematic correlations in functional connectivity MRI networks arise from subject motion. *Neuroimage* 59, 2142–2154. doi: 10.1016/j.neuroimage.2011.10.018

Robinson, J. L., Laird, A. R., Glahn, D. C., Blangero, J., Sanghera, M. K., Pessoa, L., et al. (2012). The functional connectivity of the human caudate: an application of meta-analytic connectivity modeling with behavioral filtering. *Neuroimage* 60, 117–129. doi: 10.1016/j.neuroimage.2011.12.010

Romer, D. (2010). Adolescent risk taking, impulsivity, and brain development: implications for prevention. *Dev. Psychobiol.* 52, 263–276.

Ronan, L., Alexander-Bloch, A., and Fletcher, P. C. (2020). Childhood obesity, cortical structure, and executive function in healthy children. *Cereb. Cortex N. Y. N 1991* 30, 2519–2528. doi: 10.1093/cercor/bhz257

Sahoo, K., Sahoo, B., Choudhury, A. K., Sofi, N. Y., Kumar, R., and Bhadoria, A. S. (2015). Childhood obesity: causes and consequences. *J. Fam. Med. Prim Care* 4, 187–192.

Siep, N., Roefs, A., Roebroeck, A., Havermans, R., Bonte, M. L., and Jansen, A. (2009). Hunger is the best spice: an fMRI study of the effects of attention, hunger and calorie content on food reward processing in the amygdala and orbitofrontal cortex. *Behav. Brain Res.* 198, 149–158. doi: 10.1016/j.bbr.2008.10.035

Someya, T., Sakado, K., Seki, T., Kojima, M., Reist, C., Tang, S. W., et al. (2001). The Japanese version of the barratt impulsiveness scale, 11th version (BIS-11): its reliability and validity. *Psychiatry Clin. Neurosci.* 55, 111–114. doi: 10.1046/j.1440-1819.2001.00796.x

Stice, E., Burger, K. S., and Yokum, S. (2015). Reward region responsivity predicts future weight gain and moderating effects of the TaqIA allele. *J. Neurosci. Off. J. Soc. Neurosci.* 35, 10316–10324. doi: 10.1523/jneurosci.3607-14.2015

Stice, E., Marti, C. N., and Rohde, P. (2013). Prevalence, incidence, impairment, and course of the proposed DSM-5 eating disorder diagnoses in an 8-year prospective community study of young women. *J. Abnorm. Psychol.* 122, 445–457. doi: 10.1037/a0030679

Stice, E., Spoor, S., Bohon, C., and Small, D. M. (2008a). Relation between obesity and blunted striatal response to food is moderated by TaqIA A1 allele. *Science* 322, 449–452. doi: 10.1126/science.1161550

Stice, E., Spoor, S., Bohon, C., Veldhuizen, M. G., and Small, D. M. (2008b). Relation of reward from food intake and anticipated food intake to obesity: a functional magnetic resonance imaging study. *J. Abnorm. Psychol.* 117, 924–935. doi: 10.1037/a0013600

Stice, E., and Yokum, S. (2016). Neural vulnerability factors that increase risk for future weight gain. *Psychol. Bull.* 142, 447–471. doi: 10.1037/bul0000044

Stice, E., Yokum, S., Blum, K., and Bohon, C. (2010). Weight gain is associated with reduced striatal response to palatable food. *J. Neurosci. Off. J. Soc. Neurosci.* 30, 13105–13109. doi: 10.1523/jneurosci.2105-10.2010

Thirion, B., Pinel, P., Mériaux, S., Roche, A., Dehaene, S., and Poline, J.-B. (2007). Analysis of a large fMRI cohort: statistical and methodological issues for group analyses. *Neuroimage* 35, 105–120. doi: 10.1016/j.neuroimage.2006.11.054

Tuulari, J. J., Karlsson, H. K., Hirvonen, J., Salminen, P., Nuutila, P., and Nummenmaa, L. (2015). Neural circuits for cognitive appetite control in healthy and obese individuals: an fMRI study. *PLoS One* 10:e0116640. doi: 10.1371/journal.pone.0116640

van der Laan, L. N., de Ridder, D. T. D., Viergever, M. A., and Smeets, P. A. M. (2011). The first taste is always with the eyes: a meta-analysis on the neural correlates of processing visual food cues. *Neuroimage* 55, 296–303. doi: 10.1016/j.neuroimage.2010.11.055

van Meer, F., Charbonnier, L., and Smeets, P. A. M. (2016). Food decision-making: effects of weight status and age. *Curr. Diab. Rep.* 16:84.

Yokum, S., Gearhardt, A. N., Harris, J. L., Brownell, K. D., and Stice, E. (2014). Individual differences in striatum activity to food commercials predict weight gain in adolescents. *Obes. Silver Spring Md.* 22, 2544–2551.

Conflict of Interest: The authors declare that the research was conducted in the absence of any commercial or financial relationships that could be construed as a potential conflict of interest.

frontiers in Human Neuroscience

ORIGINAL RESEARCH
published: 27 November 2020
doi: 10.3389/fnhum.2020.586998

Reduced Olfactory Bulb Volume in Obesity and Its Relation to Metabolic Health Status

Maria Poessel[1,2†], Nora Breuer[1,2†], Akshita Joshi[3], André Pampel[4], Arno Villringer[1,5,6,7,8,9], Thomas Hummel[3] and Annette Horstmann[1,2,10,11]*

[1] Department of Neurology, Max Planck Institute for Human Cognitive and Brain Sciences, Leipzig, Germany, [2] Integriertes Forschungs- und Behandlungszentrum (IFB) Adiposity Diseases, Leipzig University Medical Center, Leipzig, Germany, [3] Smell and Taste Clinic, Department of Otorhinolaryngology, University of Dresden Medical School, Dresden, Germany, [4] Department of Neurophysics, Max Planck Institute for Human Cognitive and Brain Sciences, Leipzig, Germany, [5] Day Clinic for Cognitive Neurology, University Hospital at the University of Leipzig, Leipzig, Germany, [6] Berlin School of Mind and Brain, Mind Brain Body Institute, Humboldt-Universität zu Berlin, Berlin, German, [7] Charité – Universitätsmedizin Berlin, Berlin, Germany, [8] International Max Planck Research School on the Life Course, Max Planck Institute for Human Development, Berlin, Germany, [9] International Max Planck Research School on the Neuroscience of Communication, Max Planck Institute for Human Cognitive and Brain Sciences, Leipzig, Germany, [10] Department of Psychology and Logopedics, Faculty of Medicine, University of Helsinki, Helsinki, Finland, [11] Leipzig University Medical Center, Collaborative Research Council (CRC) 1052A5 'Obesity Mechanisms', Leipzig, Germany

OPEN ACCESS

Edited by:
Suleyman Kaplan,
Ondokuz Mayıs University, Turkey

Reviewed by:
Hirac Gurden,
Université de Paris, France
Debra Ann Fadool,
Florida State University, United States
Tara Sankar Roy,
All India Institute of Medical Sciences, India

***Correspondence:**
Maria Poessel
poessel@cbs.mpg.de

[†] These authors have contributed equally to this work and share first authorship

Specialty section:
This article was submitted to Health, a section of the journal Frontiers in Human Neuroscience

Received: 24 July 2020
Accepted: 03 November 2020
Published: 27 November 2020

Citation:
Poessel M, Breuer N, Joshi A, Pampel A, Villringer A, Hummel T and Horstmann A (2020) Reduced Olfactory Bulb Volume in Obesity and Its Relation to Metabolic Health Status. Front. Hum. Neurosci. 14:586998. doi: 10.3389/fnhum.2020.586998

Smell perception plays an important role in eating behavior and might be involved in body weight gain. Since a body of literature implies that olfactory perception and function is hampered in obesity, we here investigate neuroanatomical correlates of this phenomenon. We assessed olfactory bulb (OB) volume with magnetic resonance imaging in 67 healthy participants with a body mass index (BMI) from 18.9 to 45.4 kg/m^2 (mean = 28.58 ± 6.64). Moreover, we obtained psychophysiological data on olfactory ability (Sniffin' Sticks, Food associated odor test) and self-report measurements on eating behavior. Additionally, we collected parameters associated with metabolic health in obesity (waist-hip ratio, waist-height ratio, leptin levels, body fat percentage, fat mass index, insulin resistance) to investigate recently proposed mechanistic explanatory models of why olfaction may be altered in obesity. We showed that OB volume was significantly lower in participants with obesity when compared to those of normal weight. Moreover, we found weak to moderate negative correlations between OB volume and BMI and related measures of metabolic health, especially leptin, body fat percentage, waist-height ratio and insulin resistance. However, neither OB volume nor BMI were related to olfactory function in our young and healthy sample. Nevertheless, our results provide first indications that obesity is associated with brain anatomical changes in the OBs.

Keywords: olfactory bulb, obesity, olfaction, smell perception, HOMA-IR, metabolic health

INTRODUCTION

Obesity has become a worldwide epidemic with an increased risk for major individual health consequences and a severe burden to the healthcare system (Stevens et al., 2012). Since obesity is a risk factor for many diseases such as diabetes type 2, cardiovascular diseases, certain forms of cancer and stroke (Rosenthal et al., 2017), it is essential to understand the factors that accompany

excessive accumulation of body weight and its maintenance. One major factor driving the rapid increase of obesity is our obesogenic environment that encourages overconsumption of energy-dense foods even without physiological needs (Berthoud, 2012; Lopez-Gonzalez et al., 2020). Especially external cues, such as the smell of foods, can trigger appetite and intensify food cravings (Firmin et al., 2016). Thus, the olfactory system came into focus as an important contributor to unintentional weight gain.

In recent years, it has been shown that smell perception plays a significant role in the enjoyment of food and the control of food intake (Ramaekers et al., 2014, 2016; Proserpio et al., 2017). More specifically, olfaction influences food selection and meal size (Gaillet-Torrent et al., 2014) and triggers cephalic phase responses and cravings (Kitamura et al., 2010; Firmin et al., 2016; Proserpio et al., 2017). Hence, changes in olfactory perception might be involved in unhealthy eating and potentially lead to weight gain. On this notion, it has been shown that individuals with obesity show several alterations in the olfactory system. First, they have a higher hedonic response to palatable food odors when compared to people of normal weight (Stafford and Whittle, 2015). Second, it is widely accepted that individuals with obesity have decreased olfactory function (Richardson et al., 2004; Skrandies and Zschieschang, 2015; Fernández-Aranda et al., 2016; Fernandez-Garcia et al., 2017; Peng et al., 2019). Especially odor sensitivity, which reflects perceptual function (Hedner et al., 2010), is decreased in individuals with obesity when compared to people with normal weight (Skrandies and Zschieschang, 2015; Fernandez-Garcia et al., 2017).

The mechanisms behind these alterations remain unclear, however, it has been suggested that decreased olfactory function may be caused by hormonal and metabolic changes that are associated with obesity (Peng et al., 2019). This is supported by a recent finding of our working group, where we could show that high insulin resistance has a negative effect on food odor sensitivity in obesity (Poessel et al., 2020). Moreover, these hormonal changes might lead to altered function of the olfactory bulbs (Lacroix et al., 2015). Notably, the OBs have a high density of insulin and leptin receptors (Havrankova et al., 1981; Baskin et al., 1983; Marks et al., 1990; Thanarajah et al., 2019), hormones that are elevated in obesity and involved in homeostatic signaling (Murphy and Bloom, 2006; Durham, 2016; Lean and Malkova, 2016) as well as in modulating odor sensitivity (Tong et al., 2011; Brunner et al., 2013).

Interestingly, not all individuals with obesity show significant alterations in their metabolic and endocrine systems, referring to the concept of metabolically "healthy" obesity (Blüher, 2020). Those individuals are characterized by preserved insulin sensitivity and beta cell function, better cardiorespiratory fitness and lower visceral fat. In this respect, we believe that the olfactory system of metabolically healthy individuals with obesity might be less affected by these alterations. Consequently, we not only focus on body mass index (BMI) criteria for weight status, but additionally examine waist-height ratio (WHtR), waist-hip ratio (WHR), and leptin as proxies of body fat (Münzberg and Heymsfield, 2015; Christen et al., 2018; Landecho et al., 2019) and insulin resistance as assessed by homeostatic model assessment (HOMA-IR) (Gutch et al., 2015) and total body fat percentage as well as fat mass index (FMI).

The olfactory performance in standard tests (identification, discrimination and threshold tests) is reflected in the size of the olfactory bulb (OB) in participants with and without olfactory dysfunction (Buschhüter et al., 2008; Mazal et al., 2016). OB volume is reduced in various diseases that are associated with low olfactory performance, such as Parkinson's disease, Alzheimer's disease, schizophrenia, and depression (Turetsky et al., 2000; Thomann et al., 2009; Negoias et al., 2010; Liu et al., 2017). However, olfactory function was in most, but not in all cases negatively related to OB volume (Turetsky et al., 2000; Schriever et al., 2013). It is discussed that an insufficient afferent input of olfactory information from the olfactory receptor neurons to the OB causes the reduction in bulb volume (Gudziol et al., 2009). In addition, animal studies have reliably demonstrated that obesity leads to structural and functional changes in the olfactory system (Fadool et al., 2011; Thiebaud et al., 2014; Rivière et al., 2016). Since brain anatomical correlations to altered smell perception in human obesity have not been studied yet, we here investigate whether OB volume is associated with BMI and associated metabolic and hormonal markers of obesity, such as WHR, WHtR, body fat percentage, FMI, plasma level of leptin and insulin resistance. Further, we assessed olfactory function with the Sniffin' Sticks test battery. Moreover, we explore whether eating behavior as assessed by subjective reporting via questionnaires correlates with brain anatomical changes in the olfactory primary pathways.

MATERIALS AND METHODS

Participants

The sample consisted of 67 participants (33 women, 34 men), 28 participants had normal weight (BMI = 18.5 − 24.9 kg/m^2), 28 participants were obese (BMI > 30 kg/m^2), and 11 participants were overweight (BMI = 25 − 29.9 kg/m^2) (see **Table 1** for details). All participants were recruited from the Max Planck Institute for Human Cognitive and Brain Sciences database in Leipzig, Germany. They were aged between 21 and 41 years (28.5 ± 4.6 years) to minimize the impact of age on olfactory performance (Hummel et al., 2007). We excluded current or recent smokers (<3 years of abstinence) and subjects with allergies, history of nose surgery (except childhood adenoidectomy) and metabolic diseases (e.g., thyroid diseases or diabetes mellitus). Further exclusion criteria were vegetarian/vegan diet, history of neurological or psychiatric disorders, current use of medication (except oral contraceptives), drug use within the last 4 weeks and alcoholism. Pregnant and currently breastfeeding women were excluded for ethical reasons and because smell perception is altered in these conditions. All participants were previously screened by means of telephone interviews and had to meet our inclusion criteria (age between 18 and 45 years). After inclusion, participants provided written informed consent. The study was carried out in accordance with the Declaration of Helsinki and was approved by the Ethics

TABLE 1 | Sample characteristics.

	Total	Normal weight	Obese		Overweight
	Mean ± SD (range)			*p*-value/*F*-value between NW and OBE	
Characteristics					
n	67	28	28		11
Sex	33 ♀, 34 ♂	14 ♀, 14 ♂	14 ♀, 14 ♂		5 ♀, 6 ♂
Age (years)	28.5 ± 4.6 (21 – 41)	27.1 ± 4.3 (21 – 35)	29.5 ± 5.1 (21 – 41)	0.109/2.3[a]	29.5 ± 3.0
BMI (kg/m^2)	28.4 ± 6.6 (18.9 – 45.4)	22.3 ± 1.6 (18.9 – 24.9)	35.1 ± 4.3 (30.1 – 45.4)	<0.001***/212.834[a]	26.9 ± 1.4
WHR	0.89 ± 0.08 (0.75 – 1.05)	0.84 ± 0.06 (0.75 – 0.98)	0.93 ± 0.08 (0.80 – 1.05)	<0.001***/23.875[b]	0.88 ± 0.06
WHtR	0.52 ± 0.09 (0.38 – 0.71)	0.43 ± 0.04 (0.38 – 0.53)	0.61 ± 0.05 (0.51 – 0.71)	<0.001***/222.22[b]	0.51 ± 0.03 (0.45 – 0.55)
Body fat percentage (%)	28.43 ± 11.60 (8.21 – 60.60)	20.56 ± 6.02 (8.21 – 30.51)	37.50 ± 10.65 (11.99 – 60.60)	<0.001***/53.658[b]	25.39 ± 8.31
FMI	0.15 ± 0.09 (0.03 – 0.43)	0.08 ± 0.02 (0.03 – 0.11)	0.23 ± 0.08 (0.07 – 0.43)	<0.001***/92.03[b]	0.12 ± 0.50 (0.07 – 0.18)
BDI sum score	3.0 ± 3.3 (0 – 13)	2.0 ± 2.8 (0 – 11)	4.2 ± 3.8 (0 – 13)	0.018*/5.905[a]	2.5 ± 2.5
Passive smoking hours	1.5 ± 2.7 (0 – 15)	1.5 ± 2.9 (0 – 15)	1.5 ± 3.0 (0 – 15)	0.964/0.002[a]	1.5 ± 1.5
Hormonal profile					
HOMA-IR	1.14 ± 0.91 (0.10 – 5.10)	0.69 ± 0.38 (0.10 – 1.80)	1.73 ± 1.10 (0.60 – 5.10)	<0.001***/21.903[a]	0.78 ± 0.37
Leptin (ng/ml)	15.41 ± 13.91 (0.10 – 61.90)	8.13 ± 6.23 (0.10 – 27.70)	24.04 ± 15.95 (3.40 – 61.90)	<0.001***/21.878[b]	9.97 ± 8.04
Insulin (pmol/l)	60.18 ± 49.36 (7.00 – 278.30)	36.36 ± 19.82 (7.00 – 92.60)	91.68 ± 60.37 (30.40 – 278.30)	<0.001***/21.222[a]	40.59 ± 19.74
Glucose (mmol/l)	5.32 ± 0.43 (4.58 – 6.45)	5.15 ± 0.45 (4.58 – 6.16)	5.54 ± 0.39 (4.62 – 6.45)	0.001**/11.777[a]	5.18 ± 0.18

*Data are presented as mean values, standard deviations, and minimum and maximum values. [a]One-way analysis of variance (ANOVA). [b]One-way analysis of variance with the covariate sex (ANCOVA). BMI, body mass index; WHR, waist-hip ratio; WHtR, waist-height ratio; FMI, fat mass index; BDI sum score, sum score of Beck's Depression inventory; HOMA-IR, homeostatic model assessment of insulin resistance. *p ≤ 0.05; **p ≤ 0.01; ***p ≤ 0.001.*

Committee of the University of Leipzig (Reference number 387/17-ek, date of vote: 2017-10-17).

Study Design

The data presented here are part of a larger, multi-centered study in Saxony, Germany. We here only present the data of participants that were tested in one location at the Max Planck Institute for Human Cognitive and Brain Sciences in Leipzig. Participants were tested on 2 consecutive days. On the first test day, we collected a blood sample after an overnight fasting period of approximately 12 h. All participants were screened for normal olfactory function with the short form of the Sniffin' Sticks odor identification test (Mueller and Renner, 2006). They further underwent a medical examination to assess body weight, height, waist and hip circumference and body fat percentage (measured by body impedance analysis). We conducted several questionnaires and interviews to assess eating behavior, past and present smoking behavior, including passive smoking, as well as information about the menstrual cycle phase of female participants. Moreover, we conducted a computer-based behavioral task and saliva tests on the first test day that are not part of the present data presentation in this manuscript. On the second test day, participants underwent after a 2 h fasting period a 50-min MRI scan, consisting of an anatomical and a functional part. After scanning, participants completed another set of questionnaires. In this manuscript, we only focus on the anatomical scan, the fMRI experiment is part of another subproject.

Materials

Olfactory Tests

Olfactory testing was performed with the commercially available Sniffin' Sticks® test battery (Sniffin' Sticks; Burghart Instruments, Wedel, Germany). It is a well-validated instrument to assess olfactory performance in the clinical and research context (Hummel et al., 1997). It includes subtests for odor threshold, odor discrimination and odor identification. In the threshold test, 16 triplets of felt-tip like pens are presented to the participant (Kobal et al., 1996; Hummel et al., 1997). In each triplet, one pen contains n-butanol, diluted in aqua conservans and concentrated from 1.22 ppm in pen number 16 up to 4% in pen number 1, whereas the other two pens contain only the solvent and serve

as blanks. The odorized pen of each triplet must be identified correctly, starting with the lowest concentration. Participants are blindfolded to avoid visual identification. In a single staircase procedure, a higher concentration is presented following an incorrect choice, and a lower concentration following two correct identifications in a row. This procedure is repeated until seven staircase reversals are reached. The threshold is defined as the mean of the four last reversals of the staircase. A higher score signals higher capacity to pick up odors from the environment. The odor discrimination test assesses the participant's ability to discriminate between different odorants. The task is to identify from three pens which one smells different than the other two pens. The odor identification test assesses the participant's ability to correctly identify commonly known odors from a list of four descriptors for each odorized pen. The odors are similar in intensity and include: orange, peppermint, turpentine, cloves, leather, banana, garlic, rose, fish, lemon, coffee, anise, cinnamon, liquorice, apple, pineapple. In each test the sum of correct answers can range from 0 to 16. The sum of all three subtests results in the composite TDI-score and reflects general olfactory capacity, it can range from 0 to 48. Hereby, a TDI score of $\geq$30.5 is defined as normosmia (=normal smell function), a score between 16.5 and 30 hyposmia (=reduced smell function) and $\leq$16.5 anosmia (=functional smell impairment) (Hummel et al., 2007). Additionally, we obtained odor identification data from a newly developed food associated odor test (FAOT), here the participants had to identify the correct odor from a list of four descriptors. The test was developed to examine how naturalistic food odors are perceived. It includes the following odors: cinnamon, vanilla, coconut, bell pepper, caraway, peppermint, marzipan, butter, peach, liquorice, grape juice, cacao, cooked beef, bread, chicken, and fish (Denzer-Lippmann et al., 2017). Questionnaires and Interviews.

We initially screened for inclusion and exclusion criteria and education, using a self-developed screening questionnaire assessing smoking and drinking behavior, health status and subjective olfactory function. Depressive symptoms were assessed with the Beck Depression Inventory (BDI) (Beck et al., 1961) in a paper pencil form at the beginning of the first test day to control for acute suicidal tendencies and exclude participants with a sum-score >18 since depression is a confounding factor for smell impairment (Negoias et al., 2010). Additionally, participants were face to face interviewed about their smoking status by means of a smoking interview that was previously implemented in the Leipzig LIFE study (Loeffler et al., 2015). The interview contains questions about their past and present smoking behavior as well as passive smoking. Eating behavior was assessed by means of the German version (Nagl et al., 2016) of the Three factor Eating Questionnaire (TFEQ) (Stunkard and Messick, 1985). The TFEQ describes three dimensions of human eating behavior: cognitive restraint of eating, disinhibition and hunger. Dietary Fat and Free Sugar Short Questionnaire (DFS) (Fromm and Horstmann, 2019) that obtains data about monthly intake of saturated fat and free sugar within the last year. Moreover, we used the German versions of the Food Craving Questionnaires for food (FCQ) (Meule et al., 2014) and chocolate (FCQ-C) (Meule and Hormes, 2015). Both scales obtain information about experienced food cravings. The FCQ collects information about general state and trait cravings for food while the FCQ-C assesses craving and hunger for chocolate specifically. Furthermore, we obtained information on the menstrual cycle of women to assess cycle phase, since odor sensitivity is higher in follicular phase of the cycle / under oral contraception and lower in the luteal phase (Derntl et al., 2013; McNeil et al., 2013).

Blood Collection

Venous blood samples were collected after a fasting period of approximately 12 h, using 5.5 ml Sarstedt S-Monovette containers prepared with clotting activator for serum leptin and insulin and 2.7 ml Fluoride/EDTA preparations for glucose. Glucose tubes were immediately centrifuged at 3500 r.p.m. at 10°C and serum after standing at room temperature for 30 min. Both, serum and glucose were separated in two 1 ml tubes (Eppendorf Safe-Lock Tubes) and immediately after centrifugation frozen at -80°C.

Neuroimaging

Brain imaging data were acquired using a 3 Tesla Siemens SKYRA scanner equipped with a 20-channel head coil. An MPRAGE (Mugler and Brookeman, 1990) dataset was acquired to create a T1-weighted (T1w) image. *TR* = 2,300 ms, echo time; *TE* = 2.98 ms, inversion times; *TI* = 900 ms (non-selective inversion recovery), flip angle; *FA* = 9°, nominal resolution = 1 mm isotropic. Right and left OB volume were determined using multislice T2-weighted turbo spin-echo images, with *TR*/*TE*/*FA* = 6,630 ms/126 ms/160°, acquired spatial resolution = 0.5 × 0.5 (in-plane), 1 mm slice thickness, 30 slices (no slice gap), and signal averages = 2.

Data Analysis

R version 3.4.3. within RStudio (RStudio Team, 2016) was used for statistical evaluation. We used BMI as a continuous variable or as a grouping variable (normal weight: BMI 18.4 — 24.99 kg/m^2, obese: BMI > 30 kg/m^2). We used WHR, WHtR, circulating leptin levels, body fat percentage and FMI as additional measures of weight status, that are more related to metabolic health. Especially, WHtR and FMI have been identified as reliable predictors of metabolic risk in obesity (Łopatyński et al., 2003; Liu et al., 2013). Homeostasis Model Assessment of insulin resistance (HOMA-IR score) (Matthews et al., 1985), an index that serves as a proxy of insulin resistance, was then calculated from insulin and glucose by means of the HOMA2 Calculator[1], applying the formula: HOMA-IR = glucose [mmol/l] × insulin [pmol/l]/135.

The α-level was set at 0.05. Bonferroni correction was applied to adjust the α-level for multiple testing. Whenever statistical assumptions for parametric testing were violated, we applied non-parametric robust tests. We defined outliers as values below or above 2.2 interquartile range from the samples lower or upper quartile (Hoaglin and Iglewicz, 1987).

Olfactory bulb size was assessed with 3D Slicer software (Fedorov et al., 2012), version 4.10.2[2]. We employed the

[1]https://www.dtu.ox.ac.uk/homacalculator/index.php

[2]https://www.slicer.org/

planimetric contouring method (Rombaux et al., 2009). The examiner manually delineates the OBs in the coronal slices and multiplies each surface area (mm^2) by slice thickness (1 mm). The posterior end of the OBs is reached when encountering two equal sized, narrower surface areas in a row. Finally, all obtained volumes are added up for the total volume of each bulb. OB measurements were performed by three independent experimenters who were blinded for the weight status and sex of the participants. The mean of their results serves as the OB volume.

First, we applied a group design to display differences between BMI groups as defined by international standards on OB volume while controlling for sex. Assumption tests showed homogeneity of variances/covariances, as assessed by Box's M test. There were no univariate/multivariate outliers, as assessed by standardized residuals greater than ±3 standard deviations/Mahalanobis distance. Second, the relationship between OB volume and measures that reflect body weight status (BMI, WHR, body fat percentage, leptin) was assessed by correlation analysis. We performed partial Spearman's rank correlation for not normally distributed variables (BMI, WHR, leptin, insulin, HOMA-IR, age, TDI score, odor identification, odor discrimination, craving questionnaires, eating behavior questionnaires, olfaction questionnaires) with OB volume. Since OB volume is smaller in women when compared to men, we used sex as a covariate. Additionally, we used partial Pearson's product moment correlation to depict the relation between normally distributed variables (body fat percentage, odor threshold, DFS data). We interpreted the strength of the correlation according to Cohen's conventions (Cohen, 1988).

We further used SPSS (version 22.0, SPSS Inc., Chicago, IL) for the replication of a mediation analysis to disentangle the effect of insulin resistance on the relationship between obesity and olfactory function. Unstandardized indirect effects were computed for each of 10,000 bootstrapped samples, and the 95% confidence interval was computed by determining the indirect effects at the 2.5th and 97.5th percentiles.

RESULTS

Sample Characteristics

Participant characteristics are given in **Table 1**. Descriptive values for the total sample as well as for BMI subgroups are listed. **Table 1** contains general characteristics (age, depressive symptoms, information about passive smoking), metabolic health parameters (BMI, WHR, body fat percentage) and hormonal parameters (plasma insulin, glucose and leptin, HOMA-IR score). BDI scores indicated no or only mild depressive symptoms in all subjects (mean = 3.01, *SD* = 3.35, range: 0–13), however, participants with obesity had significantly more depressive symptoms than participants with normal weight. As expected participants significantly differed in BMI, WHR, and body fat percentage. Participants with normal weight had also significantly lower HOMA-IR scores as well as lower levels of plasma insulin, glucose and leptin when compared to obese participants.

Psychophysical Function

Olfactory function assessed by Sniffin' Sticks and food associated odor test (FAOT) are given in **Table 2**. A one-way multivariate analysis of variance was run to determine the effect of weight status (normal weight vs. obese) on olfactory performance (Odor identification, odor discrimination, odor identification, TDI sum score) while controlling for sex. There was no statistically significant difference between weight groups in all olfactory tests, $F(3, 51) = 0.389$, $p = 0.761$ (**Table 2**).

In addition, none of the olfactory tests was associated with OB volume or BMI as determined by Pearson's product moment correlation and Spearman's rank-order correlation (**Table 2**).

Relationship Between OB Volume and BMI/Other Measures That Are Associated With Metabolic Health (WHR, WHtR, Body Fat Percentage, FMI, Leptin, Insulin Resistance)

Means, range and standard deviations of OB volume and whole brain volume grouped by weight status and in total are depicted in **Table 3**. Firstly, we explored group differences in OB volume between participants with obesity and normal weight, we found a significant group effect as determined by one-way ANCOVA [$F(1, 52) = 8.119$, $p = 0.004$] with smaller volume in individuals with obesity (**Figure 1**). Additionally, we checked whole brain volume to control the specificity of this effect. There was no difference in whole brain volume in the weight groups [$F(1, 52) = 1,691$, $p = 0.682$].

Additionally, we investigated the relationship between OB volume and BMI as a continuous variable as well as other measures of metabolic health in obesity using correlation analysis. A partial Spearman's rank-order correlation was run to determine the relationship between BMI and OB volume whilst controlling for sex. There was a weak, negative correlation between OB volume and BMI, which was statistically significant ($r = -0.278$, $n = 65$, $p = 0.028$) (**Figure 2**). Further, we assessed other measures that are associated with metabolic health status in obesity: HOMA-IR, leptin, body fat percentage, WHtR, WHR, and FMI (**Figure 2**). A partial Pearson's product moment correlation was run to determine the relationship between body fat percentage and OB volume. There was a weak, negative correlation between OB volume and body fat percentage, which was statistically significant ($r = -0.273$, $n = 65$, $p = 0.031$). A partial Spearman's rank-order correlation was run to determine the relationship between OB volume and HOMA-IR/leptin/WHtR/WHR/FMI whilst controlling for sex. There were statistically significant weak to moderate, negative correlations for HOMA-IR and OB volume ($r = -0.258$, $n = 65$, $p = 0.041$), leptin and OB volume ($r = -0.253$, $n = 65$, $p = 0.045$) as well as for WHtR and OB volume ($r = -0.321$, $n = 65$, $p = 0.010$). However, there were no statistically significant correlations between OB volume and WHR ($r = -0.199$, $n = 65$, $p = 0.118$) or FMI ($r = -0.216$, $n = 65$, $p = 0.089$) whilst controlling for sex.

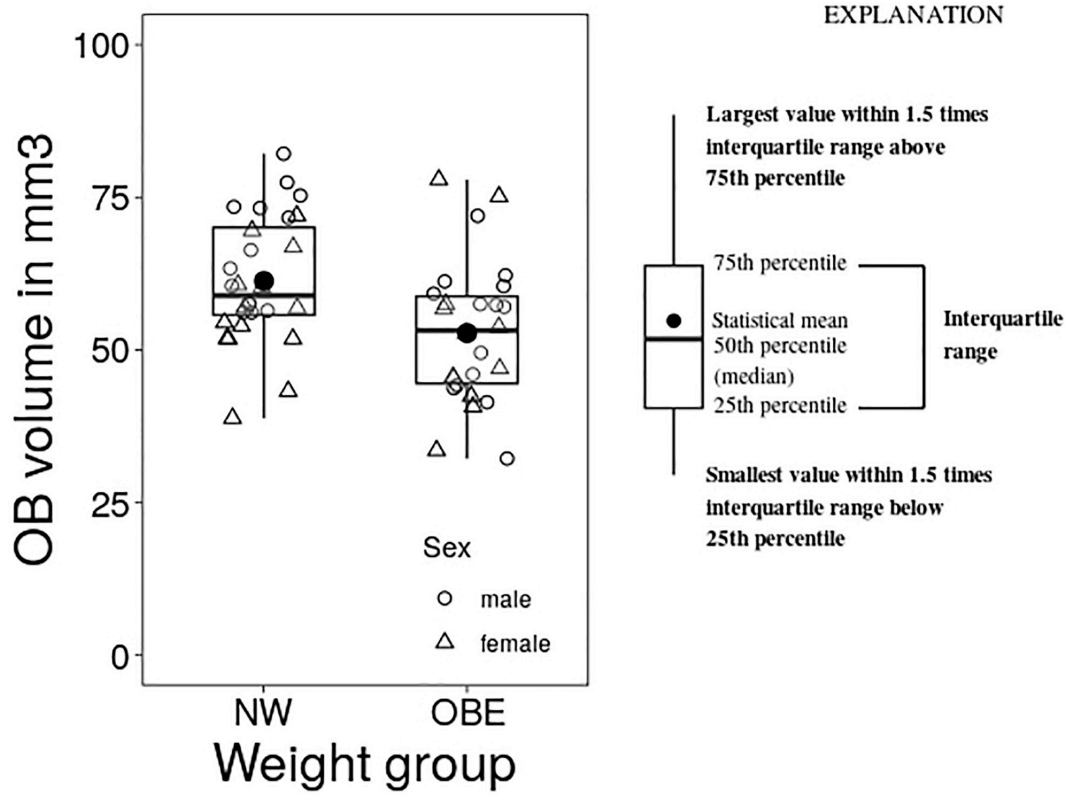

FIGURE 1 | Group differences between normal weight (NW) and obese (OBE) participants in OB volume as assessed by one-way analysis of variance with the covariate sex (ANCOVA).

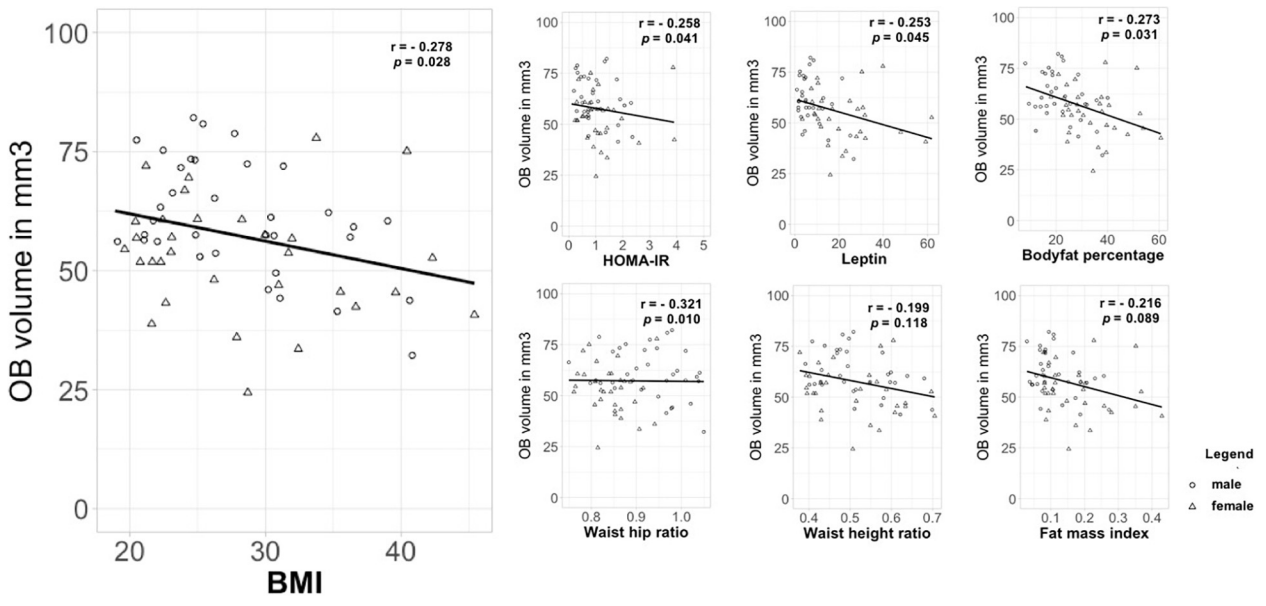

FIGURE 2 | Correlation between OB volume and measures that are associated with metabolic health status in obesity. OB volume in mm^3; BMI in kg/m^2; HOMA-IR, homeostatic model assessment of insulin resistance; leptin in ng/ml; body fat in percentage; WHtR, waist-height ratio; WHR, waist-hip ratio in cm; FMI, fat mass index.

TABLE 2 | Olfactory performance assessed with the Sniffin' Sticks battery and FAOT.

	Total (n = 67)	Correlation with BMI	Correlation with OB volume	Normal weight (n = 28)	Obese (n = 28)	p-value/F-value between NW and OB	Overweight (n = 11)
	Mean ± SD (range)	p-value/r		Mean ± SD (range)			
Smell tests							
Threshold	7.63 ± 1.85 (1.75 – 11.00)	0.393/ – 0.109[a]	0.348/0.120[a]	7.65 ± 2.19 (1.75 – 11.00)	7.56 ± 1.61 (4.25 – 10.50)	0.959/0.030[b]	7.75 ± 1.65
Discrimination	12.45 ± 2.12 (6 – 16)	0.938/0.010[a]	0.505/0.086[a]	12.11 ± 2.67 (6 – 16)	12.64 ± 1.66 (10 – 16)	0.863/0.812[b]	12.82 ± 1.54
Identification	13.55 ± 1.51 (9 – 16)	0.268/-0.142[a]	0.807/0.003[a]	13.54 ± 1.17 (11 – 15)	13.43 ± 1.91 (9 – 16)	0.801/0.064[b]	13.91 ± 1.14
TDI sumscore	33.63 ± 3.90 (22.75 – 40.25)	0.230/-0.133[a]	0.244/0.149[a]	33.29 ± 4.60 (22.75 – 40.25)	33.63 ± 3.54 (26.25 – 38.50)	0.758/0.096[b]	34.48 ± 2.85
FAOT	13.4 ± 1.47 (9 – 16)	0.272/-0.141[a]	0.854/0.024[a]	13.29 ± 1.27 (10 – 15)	13.39 ± 1.50 (11 – 16)	0.774/0.083[b]	13.73 ± 1.90

Data are presented as mean values, standard deviations, and minimum and maximum values. [a]Spearman's rank-order correlation. [b]One-way analysis of variance with the covariate sex (ANCOVA). BMI, body mass index; TDI sumscore, sumscore of odor threshold, odor discrimination, and odor identification; FAOT, food associated odor test.

TABLE 3 | Olfactory bulb (OB) and whole brain volume (WBV) overall participants and for weight groups.

	Total	Normal weight (n = 28)	Obese (n = 26)	p-value/F-value between NW and OBE	Overweight
	Mean ± SD (range)				
OB volume right	56.95 ± 12.83 (26.21 – 82.47)	61.01 ± 10.67 (26.21 – 82.47)	52.05 ± 10.94 (30.59 – 74.87)	**0.002**/9.272[a]**	58.19 ± 18.33
OB volume left	57.59 ± 13.35 (22.59 – 84.25)	61.58 ± 11.25 (22.59 – 82.74)	53.51 ± 13.07 (32.44 – 80.90)	**0.016*/5.959[a]**	57.07 ± 16.83
Mean OB volume	57.27 ± 12.64 (24.40 – 82.13)	61.29 ± 10.33 (24.40 – 80.83)	52.78 ± 11.64 (32.30 – 77.89)	**0.004**/8.119[a]**	57.63 ± 17.27
WBV	1.20 ± 0.10 (0.96 – 1.39)	1.21 ± 0.10 (1.04 – 1.33)	1.20 ± 0.10 (1.00 – 1.39)	0.682/.169[a]	1.18 ± 0.08

*[a]One-way analysis of variance with the covariate sex (ANCOVA). OB volume in mm^3, WBV in liter; NW, normal weight; OBE, obese. *$p \leq 0.05$; **$p \leq 0.01$; Bold font indicates statistical significance.*

Replication: Mediation Effect of HOMA-IR on the Relation Between BMI and Smell Function

The relationship between BMI and olfactory function, as assessed by TDI score, was mediated by HOMA-IR. The standardized regression coefficient was significant between BMI and the mediator HOMA-IR (r = 0.625, p = 0.001) and between TDI score and the mediator HOMA-IR (r = 0.348, p = 0.042). The standardized indirect effect between BMI and TDI score via HOMA-IR was -0.154 (CI -0.268 and -0.036). There was no significant direct effect for BMI and TDI score (r = 0.126, p = 0.164, CI: -0.053 and 0.304).

Relation Between Eating Behavior and BMI/OB Volume

A Spearman' rank-order correlation was applied to investigate the relationship between BMI and eating behavior questionnaires. We found a weak, positive correlation between BMI and cognitive restraint as well as hunger scale of the TFEQ (r = 0.258, n = 61, p = 0.041; r = 0.249, n = 61, p = 0.049).

A partial Spearman's rank-order correlation was run to determine the relationship between eating behavior questionnaire data and OB volume whilst controlling for sex. There was a weak, positive correlation between OB volume and chocolate craving (sum score from the FCQ-Trait Chocolate questionnaire), which was statistically significant (r = 0.278, n = 59, p = 0.033). All correlational data of BMI and OB volume with eating behavior questionnaires are given in **Supplementary Table 1**.

Yet we treat these findings with caution, since they would not survive alpha level correction for multiple testing.

DISCUSSION

In this study, we demonstrate for the first time that OB volume is reduced in individuals with obesity when compared to those with normal weight. Additionally, we found weak to moderate negative correlations between OB volume and BMI as well as

other measures of metabolic health in obesity, such as body fat percentage, WHtR, leptin levels and insulin resistance. Our results imply that, similar to other diseases such as depression and Parkinson's disease (Negoias et al., 2010; Li et al., 2016), obesity also involves a neuroanatomical change in the OBs compared to healthy participants with normal weight.

Since we could show that whole brain volume was not associated with BMI and weight status in our sample, we conclude that our observation is not related to a general atrophy in our obese sample but might be specific to the olfactory system. However, since we have not measured the volume of other sensory regions, such as the gustatory, visual or auditory cortex, we cannot conclude with certainty that our results are specific to this one sensory system or might also affect other sensory areas. Additionally, as our study groups did not differ in age, we can exclude a frequently observed effect of age on the sense of smell in obesity due to older obese study populations when compared to those of normal weight, as discussed in a recent review paper by Peng and colleagues (Peng et al., 2019).

Yet, what might be the underlying causes for smaller OB volume in obesity? Our observation poses the question whether OB volume reduction is involved in the development of obesity or a consequence of this condition. First, it might be possible that altered olfactory processing leads to changes in eating behavior and consequently favors weight gain. Second, it might be possible that reduction in OB volume is a consequence of obesity and is for instance caused by metabolic and endocrine impairments. Both questions cannot be fully addressed by the design of our study. Nonetheless, we assume that the latter point of view is more likely, since it has been shown that olfactory dysfunction is more pronounced in severe obesity when compared to overweight or moderate obesity (Richardson et al., 2004; Pastor et al., 2016; Fernandez-Garcia et al., 2017).

Surprisingly, we could not find a relationship between OB volume or BMI and psychophysiological measures of olfactory ability, respectively. This is striking for two reasons: (1) obesity is commonly associated with low olfactory ability and (2) we expected that lower OB volume in obesity is associated with lower olfactory function. As to the first point, we think that our very young and healthy obese sample may be the reason for the preserved olfactory ability. As discussed by the authors of this paper it is plausible that individuals with obesity that are metabolically healthy may have normal olfactory function (Poessel et al., 2020). This point of view is in line with another finding that especially people that are morbidly obese when compared to moderately obese are affected from limitations in olfactory function (Richardson et al., 2004). In this regard, proposed explanatory models of impaired olfactory function in obesity might explain this phenomenon: They point to an important role of metabolic and hormonal changes in obesity that may cause altered smell perception (Fernandez-Garcia et al., 2017; Peng et al., 2019). For instance, leptin, which is often increased in obesity while their brain is insensitive to this hormone, has an inhibitory role on olfactory function in mice (Getchell et al., 2006). In line with this reasoning, it is interesting that we could replicate our results from Poessel et al. (2020) in this sample. We find a strong mediating effect of insulin resistance as assessed by HOMA-IR score on the relationship between BMI and olfactory function as assessed by TDI score. This implies that high BMI is associated with lower olfactory function via IR. As to the second point, one can speculate that reduced OB volume in obesity is an early sign of the pathophysiological changes in olfactory function. Therefore, obesity and associated metabolic changes might have negative effects on the olfactory system before hampering obvious psychophysical function. Especially, young age, short duration of obesity and being metabolically healthy might protect against decline of olfactory function (Attems et al., 2015; Lacroix et al., 2015; Riera and Dillin, 2016). Yet, it is unexpected that the alteration of smell perception does not first manifest itself in behavior, but in the brain anatomy. Typically, a bottom-up mechanism is discussed as the cause of decreasing OB volume, for instance in chronic rhinosinusitis (Han et al., 2017) and smoking (Schriever et al., 2013). In those conditions, lower afferent input is thought to reduce OB volume because of inflammatory processes in the nose or due to toxic effect of smoke-associated products on the olfactory epithelium. This bottom-up mechanism of olfactory dysfunction has been shown in animal models: deprivation of olfactory function leads to decreased OB volume (Cummings et al., 1997). Interestingly, this effect is reversible after restoring olfactory function. In line with that result is an observation in humans, where surgical treatment of patients with chronic rhinosinusitis results in increasing OB volume (Gudziol et al., 2009). However, since we detect a low OB volume without obvious olfactory dysfunction in our obese sample, it might be possible that function is preserved due to redundant information processing: the specific anatomy and physiology of the olfactory system with its parallel processing pathways could ensure that olfactory function is maintained. Olfactory sensory neurons project to homologous glomeruli on the level of the olfactory bulb, in a way that odor information is represented and processed in two mirror maps (Nagao et al., 2002; Sato et al., 2020). From there, the olfactory information is transferred to higher order olfactory brain regions in a parallel manner (Savic et al., 2000; Nagayama et al., 2010; Payton et al., 2012). With regard to our data, we assume that based on the parallel circuitry of odor information processing at the level of the olfactory bulb, a reduction in the volume of OBs does not necessarily lead to behavioral deficits.

Secondly, a top-down process explanation seems also probable, as for instance discussed in Parkinson's Disease (Li et al., 2016) and depression (Negoias et al., 2010). Here, neurodegenerative processes or disrupted salience processing in the brain with a bias toward internal thoughts disregarding the exteroceptive sensory system may lead to a reduction of OB volume (Rottstädt et al., 2018). Especially, the loss of sensory neurons in obesity (O'Brien et al., 2017) might result in a decrease of sensory function. This has been shown in various sensory systems, such as the auditory (Hwang et al., 2013) and olfactory system. More specifically, Thiebaud et al. (2014) reported that hyperlipidemic diet in mice and associated obesity leads to a loss of olfactory sensory neurons and a decrease in olfactory function (Thiebaud et al., 2014). Moreover, it might be possible that the neural response to sensory input is blunted as it has been shown in taste processing (Weiss et al., 2019).

It has recently been shown that hormones whose homeostatic signaling may be impaired in obesity (Baly et al., 2007; Aime et al., 2012; Russo et al., 2018), modulate olfactory performance in humans. More specifically, intranasally applied insulin as well as intravenously applied ghrelin improve olfactory function (Tong et al., 2011; Thanarajah et al., 2019). Interestingly, the OBs have a high density of receptors for these hormones. Thus, the OBs might be directly affected by these alterations. In this respect, we think that another approach to explain diminished OB volume in the absence of olfactory dysfunction might be plausible: metabolic and hormonal dysfunction in obesity might directly affect the neurogenesis and synaptogenesis of the OB. Interestingly, chronic inflammation, as observed in obesity, is associated with the disruption of hippocampal neurogenesis (Chesnokova et al., 2016) and lower hippocampal and gray matter volumes (Tsai et al., 2019). Especially, body fat percentage, leptin and insulin resistance are among other indicators of increased fat mass and might thus be associated with chronic low-grade inflammation in obesity (Jung and Choi, 2014; Chen et al., 2015; Saad et al., 2016; La Cava, 2017; Reilly and Saltiel, 2017). Interestingly, it has been found in rats that diet induced type 2 diabetes leads to a decreased electrophysiological response of olfactory neurons (Rivière et al., 2016). Moreover, obesity and chronically high levels of insulin disrupt the metabolic sensing of the OBs in mice (Fadool et al., 2011). In the light of these findings, one can speculate that the negative correlation between OB volume and markers of metabolic health might be a hint that neurogenesis of the OBs might be affected by obesity associated inflammatory processes.

Another, albeit highly speculative, possibility could be that smells might be differently processed in individuals with obesity. Following the observation of Weiss et al. (2020) that people without apparent OBs can still smell, one can speculate that other structures in the brain might take over the processing of olfactory information by the formation of a glomerular space somewhere else in the cortex. In this respect, we assume that although the OB volume might be lower in our obese sample, the olfactory ability might be preserved by other structures.

Since the OBs are structures that respond directly to odors and play an important role in the processing and dissemination of olfactory information to higher order brain regions (Rombaux et al., 2009), they may also play a crucial role in homeostatic signaling and eating behavior. Thus, we examined the relationship between OB volume and eating behavior as assessed by subjective questionnaires on cravings (FCQ), actual food intake (DFS) and eating style (TFEQ). We found weak positive correlations between OB volume and chocolate craving whilst controlling for sex and BMI. This means that the higher chocolate craving the bigger are the OBs. These results should be interpreted prudently since this correlation would not survive alpha level correction for multiple testing. However, we think this is a first interesting link between brain anatomy in the olfactory system and eating behavior.

Although we have planned our study carefully, there are limitations to consider. First, in the context of eating behavior and obesity we would encourage researchers to develop or use further instruments to assess olfactory perception. Albeit the standard olfactory Sniffin' Sticks test battery is a well-validated measure of olfactory function, it might not be as sensitive to depict subtle differences in healthy subjects, because it was primarily developed for the evaluation of olfactory loss. Moreover, the investigation of eating behavior can be extended in future studies. Especially, we would suggest that direct and implicit measurements of eating behavior should be carried out to avoid bias through subjective reporting. In addition, we consider it necessary to determine the onset and duration of obesity in future studies in order to make a more reliable statement about the influence of obesity associated changes in the metabolic and endocrine systems on olfactory function. In this context, we think an extension of the hormonal profile and collecting inflammatory markers would be compelling. Additionally, we think that our results only provide first indications that the olfactory system is neuroanatomically altered in people with obesity. Further studies should also look at other structures of the primary and secondary olfactory pathways to understand whether reduction in OB volume also affects higher regions of olfactory processing.

In sum, our study finds solid evidence that OB volume is decreased in obesity while sensory function appears to be preserved. Furthermore, we show negative correlations between OB volume and insulin resistance, leptin levels and body fat. This might provide a mechanistic link between changes in the olfactory system in obesity.

DATA AVAILABILITY STATEMENT

The raw data supporting the conclusions of this article will be made available by the authors, without undue reservation.

ETHICS STATEMENT

The studies involving human participants were reviewed and approved by the Ethics Committee of the University of Leipzig (Reference number 387/17-ek, date of vote: 2017–10–17). The patients/participants provided their written informed consent to participate in this study.

AUTHOR CONTRIBUTIONS

MP, TH, and AH: conceptualization. MP, NB, and AH: methodology. MP and NB: software, investigation, and writing—original draft preparation. MP: validation, data curation, and visualization. MP, AJ, and NB: formal analysis. AH and AV: resources. MP, AH, TH, NB, and AV: writing—review and editing. AH, TH, and AV: supervision. MP and AH: project administration and funding acquisition. All authors have read and agreed to the published version of the manuscript.

FUNDING

This work was supported by the Roland-Ernst-Stiftung für Gesundheitswesen (project 2/18). The work of AH was funded by the German Research Foundation (DFG), within the framework

of the CRC 1052 'Obesity Mechanisms' with the project number 209933838. The work of AH and NB was supported by the IFB Adiposity Diseases, Federal Ministry of Education and Research (BMBF), Germany, FKZ: 01EO1501.

ACKNOWLEDGMENTS

We would like to thank Suse Prejawa for her practical and energetic support throughout the whole study. We thank Ramona Menger for recruiting participants and her motivational support. We thank Marie Meemken and Veronica Witte for inspiring discussions on the study design. We thank Jessica Freiherr for her passionate support and advice on how to purchase and use the food associated odor test.

SUPPLEMENTARY MATERIAL

The Supplementary Material for this article can be found online at: https://www.frontiersin.org/articles/10.3389/fnhum.2020.586998/full#supplementary-material

Supplementary Table 1 | Correlation analysis of eating behavior questionnaires and BMI/OB volume.

REFERENCES

Aime, P., Hegoburu, C., Jaillard, T., Degletagne, C., Garcia, S., Messaoudi, B., et al. (2012). A physiological increase of insulin in the olfactory bulb decreases detection of a learned aversive odor and abolishes food odor-induced sniffing behavior in rats. *PLoS One* 7:e51227. doi: 10.1371/journal.pone.0051227

Attems, J., Walker, L., and Jellinger, K. A. (2015). Olfaction and aging: a mini-review. *Gerontology* 61, 485–490. doi: 10.1159/000381619

Baly, C., Aioun, J., Badonnel, K., Lacroix, M.-C., Durieux, D., Schlegel, C., et al. (2007). Leptin and its receptors are present in the rat olfactory mucosa and modulated by the nutritional status. *Brain Res.* 1129, 130–141. doi: 10.1016/j.brainres.2006.10.030

Baskin, D. G., Porte, D., Guest, K., and Dorsa, D. M. (1983). Regional concentrations of insulin in the rat brain. *Endocrinology* 112, 898–903. doi: 10.1210/endo-112-3-898

Beck, A. T., Ward, C. H., Mendelson, M., Mock, J., and Erbaugh, J. (1961). An inventory for measuring depression. *Arch Gen Psychiatry* 4, 561–571. doi: 10.1001/archpsyc.1961.01710120031004

Berthoud, H. R. (2012). The neurobiology of food intake in an obesogenic environment. *Proc. Nutr. Soc.* 71, 478–487. doi: 10.1017/S0029665112000602

Blüher, M. (2020). Metabolically healthy obesity. *Endocr. Rev.* 41, 405–420. doi: 10.1210/endrev/bnaa004

Brunner, Y. F., Benedict, C., and Freiherr, J. (2013). Intranasal insulin reduces olfactory sensitivity in normosmic humans. *J. Clin. Endocrinol. Metab.* 98, E1626–E1630. doi: 10.1210/jc.2013-2061

Buschhüter, D., Smitka, M., Puschmann, S., Gerber, J. C., Witt, M., Abolmaali, N. D., et al. (2008). Correlation between olfactory bulb volume and olfactory function. *Neuroimage* 42, 498–502. doi: 10.1016/j.neuroimage.2008.05.004

Chen, L., Chen, R., Wang, H., and Liang, F. (2015). Mechanisms linking inflammation to insulin resistance. *Int. J. Endocrinol.* 2015, 1–9. doi: 10.1155/2015/508409

Chesnokova, V., Pechnick, R. N., and Wawrowsky, K. (2016). Chronic peripheral inflammation, hippocampal neurogenesis, and behavior. *Brain Behav. Immun.* 58, 1–8. doi: 10.1016/j.bbi.2016.01.017

Christen, T., Trompet, S., Noordam, R., van Klinken, J. B., van Dijk, K. W., Lamb, H. J., et al. (2018). Sex differences in body fat distribution are related to sex differences in serum leptin and adiponectin. *Peptides* 107, 25–31. doi: 10.1016/j.peptides.2018.07.008

Cohen, J. (1988). *Statistical Power Analysis for the Behavioral Sciences*, 2 Edn. Hillsdale, NJ: L. Erlbaum Associates, doi: 10.4324/9780203771587

Cummings, D. M., Henning, H. E., and Brunjes, P. C. (1997). Olfactory bulb recovery after early sensory deprivation. *J. Neurosci.* 17, 7433–7440. doi: 10.1523/jneurosci.17-19-07433.1997

Denzer-Lippmann, M. Y., Beauchamp, J., Freiherr, J., Thuerauf, N., Kornhuber, J., and Buettner, A. (2017). Development and validation of a food-associated olfactory test (FAOT). *Chem. Senses* 42, 47–57. doi: 10.1093/chemse/bjw099

Derntl, B., Schopf, V., Kollndorfer, K., and Lanzenberger, R. (2013). Menstrual cycle phase and duration of oral contraception intake affect olfactory perception. *Chem. Senses* 38, 67–75. doi: 10.1093/chemse/bjs084

Durham, A. E. (2016). Insulin dysregulation and obesity: you are what you eat. *Vet. J.* 213:90. doi: 10.1016/j.tvjl.2016.03.010

Fadool, D. A., Tucker, K., and Pedarzani, P. (2011). Mitral cells of the olfactory bulb perform metabolic sensing and are disrupted by obesity at the level of the Kv1.3 ion channel. *PLoS One* 6:e24921. doi: 10.1371/journal.pone.0024921

Fedorov, A., Beichel, R., Kalpathy-Cramer, J., Finet, J., Fillion-Robin, J.-C., Pujol, S., et al. (2012). 3D Slicer as an image computing platform for the Quantitative Imaging Network. *Magn. Reson. Imaging* 30, 1323–1341. doi: 10.1016/j.mri.2012.05.001

Fernández-Aranda, F., Agüera, Z., Fernández-García, J. C., Garrido-Sanchez, L., Alcaide-Torres, J., Tinahones, F. J., et al. (2016). Smell-taste dysfunctions in extreme weight/eating conditions: Analysis of hormonal and psychological interactions. *Endocrine* 51, 256–267. doi: 10.1007/s12020-015-0684-9

Fernandez-Garcia, J. C., Alcaide, J., Santiago-Fernandez, C., Roca-Rodriguez, M. M., Aguera, Z., Baños, R., et al. (2017). An increase in visceral fat is associated with a decrease in the taste and olfactory capacity. *PLoS One* 12:e0171204. doi: 10.1371/journal.pone.0171204

Firmin, M. W., Gillette, A. L., Hobbs, T. E., and Wu, D. (2016). Effects of olfactory sense on chocolate craving. *Appetite* 105, 700–704. doi: 10.1016/j.appet.2016.07.004

Fromm, S. P., and Horstmann, A. (2019). Psychometric evaluation of the German version of the dietary fat and free sugar–short questionnaire. *Obes. Facts* 12, 518–528. doi: 10.1159/000501969

Gaillet-Torrent, M., Sulmont-Rosse, C., Issanchou, S., Chabanet, C., and Chambaron, S. (2014). Impact of a non-attentively perceived odour on subsequent food choices. *Appetite* 76, 17–22. doi: 10.1016/j.appet.2014.01.009

Getchell, T. V., Kwong, K., Saunders, C. P., Stromberg, A. J., and Getchell, M. L. (2006). Leptin regulates olfactory-mediated behavior in ob/ob mice. *Physiol. Behav.* 87, 848–856. doi: 10.1016/j.physbeh.2005.11.016

Gudziol, V., Buschhuter, D., Abolmaali, N., Gerber, J., Rombaux, P., and Hummel, T. (2009). Increasing olfactory bulb volume due to treatment of chronic rhinosinusitis–A longitudinal study. *Brain* 132, 3096–3101. doi: 10.1093/brain/awp243

Gutch, M., Kumar, S., Razi, S. M., Gupta, K. K., and Gupta, A. (2015). Assessment of insulin sensitivity/resistance. *Indian J. Endocrinol. Metab.* 19, 160–164. doi: 10.4103/2230-8210.146874

Han, P., Whitcroft, K. L., Fischer, J., Gerber, J., Cuevas, M., Andrews, P., et al. (2017). Olfactory brain gray matter volume reduction in patients with chronic rhinosinusitis: gray matter loss in CRS. *Int. Forum Allergy Rhinol.* 7, 551–556. doi: 10.1002/alr.21922

Havrankova, J., Brownstein, M., and Roth, J. (1981). Insulin and insulin receptors in rodent brain. *Diabetologia* 20, 268–273. doi: 10.1007/BF00254492

Hedner, M., Larsson, M., Arnold, N., Zucco, G. M., and Hummel, T. (2010). Cognitive factors in odor detection, odor discrimination, and odor identification tasks. *J. Clin. Exp. Neuropsychol.* 32, 1062–1067. doi: 10.1080/13803391003683070

Hoaglin, D. C., and Iglewicz, B. (1987). Fine-tuning some resistant rules for outlier labeling. *J. Am. Stat. Assoc.* 82, 1147–1149. doi: 10.1080/01621459.1987.10478551

Hummel, T., Kobal, G., Gudziol, H., and Mackay-Sim, A. (2007). Normative data for the „Sniffin' Sticks" including tests of odor identification, odor discrimination, and olfactory thresholds: An upgrade based on a group of more

than 3,000 subjects. *Eur. Arch. Otorhinolaryngol.* 264, 237–243. doi: 10.1007/s00405-006-0173-0

Hummel, T., Sekinger, B., Wolf, S. R., Pauli, E., and Kobal, G. (1997). „Sniffin" sticks': Olfactory performance assessed by the combined testing of odor identification, odor discrimination and olfactory threshold. *Chem. Senses* 22, 39–52.

Hwang, J.-H., Hsu, C.-J., Yu, W.-H., Liu, T.-C., and Yang, W.-S. (2013). Diet-induced obesity exacerbates auditory degeneration via hypoxia, inflammation, and apoptosis signaling pathways in CD/1 Mice. *PLoS One* 8:e60730. doi: 10.1371/journal.pone.0060730

Jung, U. J., and Choi, M. S. (2014). Obesity and its metabolic complications: The role of adipokines and the relationship between obesity, inflammation, insulin resistance, dyslipidemia and nonalcoholic fatty liver disease. *Int. J. Mol. Sci.* 15, 6184–6223. doi: 10.3390/ijms15046184

Kitamura, A., Torii, K., Uneyama, H., and Niijima, A. (2010). Role played by afferent signals from olfactory, gustatory and gastrointestinal sensors in regulation of autonomic nerve activity. *Biol. Pharm. Bull.* 33, 1778–1782. doi: 10.1248/bpb.33.1778

Kobal, G., Hummel, T., Sekinger, B., Barz, S., Roscher, S., Wolf, S., et al. (1996). "Sniffin' sticks": screening of olfactory performance. *Rhinology* 34, 222–226.

La Cava, A. (2017). Leptin in inflammation and autoimmunity. *Cytokine* 98, 51–58. doi: 10.1016/j.cyto.2016.10.011

Lacroix, M.-C., Caillol, M., Durieux, D., Monnerie, R., Grebert, D., Pellerin, L., et al. (2015). Long-lasting metabolic imbalance related to obesity alters olfactory tissue homeostasis and impairs olfactory-driven behaviors. *Chem. Senses* 40, 537–556. doi: 10.1093/chemse/bjv039

Landecho, M. F., Tuero, C., Valentí, V., Bilbao, I., de la Higuera, M., and Frühbeck, G. (2019). Relevance of leptin and other adipokines in obesity-associated cardiovascular risk. *Nutrients* 11:2664. doi: 10.3390/nu11112664

Lean, M. E. J., and Malkova, D. (2016). Altered gut and adipose tissue hormones in overweight and obese individuals: cause or consequence? *Int. J. Obes.* 40, 622–632. doi: 10.1038/ijo.2015.220

Li, J., Gu, C., Su, J., Zhu, L., Zhou, Y., Huang, H., et al. (2016). Changes in olfactory bulb volume in parkinson's disease: a systematic review and meta-analysis. *PLoS One* 11:e0149286. doi: 10.1371/journal.pone.0149286

Liu, H., Hang, W., Liu, G., and Han, T. (2017). [Olfactory bulb volume in patients with posttraumatic olfactory dysfunction]. *Zhonghua Er Bi Yan Hou Tou Jing Wai Ke Za Zhi* 52, 273–277. doi: 10.3760/cma.j.issn.1673-0860.2017.04.007

Liu, P., Ma, F., Lou, H., and Liu, Y. (2013). The utility of fat mass index vs. Body mass index and percentage of body fat in the screening of metabolic syndrome. *BMC Public Health* 13:629. doi: 10.1186/1471-2458-13-629

Loeffler, M., Engel, C., Ahnert, P., Alfermann, D., Arelin, K., Baber, R., et al. (2015). The LIFE-Adult-Study: Objectives and design of a population-based cohort study with 10,000 deeply phenotyped adults in Germany. *BMC Public Health* 15:691. doi: 10.1186/s12889-015-1983-z

Łopatyński, J., Mardarowicz, G., and Szcześniak, G. (2003). A comparative evaluation of waist circumference, waist-to-hip ratio, waist-to-height ratio and body mass index as indicators of impaired glucose tolerance and as risk factors for type-2 diabetes mellitus. *Ann. Univ. Mariae Curie Sklodowska Med.* 58, 413–419.

Lopez-Gonzalez, D., Partida-Gaytán, A., Wells, J. C., Reyes-Delpech, P., Avila-Rosano, F., Ortiz-Obregon, M., et al. (2020). Obesogenic lifestyle and its influence on adiposity in children and adolescents, evidence from Mexico. *Nutrients* 12:819. doi: 10.3390/nu12030819

Marks, J. L., Porte, D., Stahl, W. L., and Baskin, D. G. (1990). Localization of insulin receptor mRNA in rat brain by in situ hybridization. *Endocrinology* 127, 3234–3236. doi: 10.1210/endo-127-6-3234

Matthews, D. R., Hosker, J. P., Rudenski, A. S., Naylor, B. A., Treacher, D. F., Turner, R. C., et al. (1985). Homeostasis model assessment: insulin resistance and β-cell function from fasting plasma glucose and insulin concentrations in man. *Diabetologia* 28, 412–419. doi: 10.1007/BF00280883

Mazal, P. P., Haehner, A., and Hummel, T. (2016). Relation of the volume of the olfactory bulb to psychophysical measures of olfactory function. *Eur. Arch. Oto Rhino Laryngol.* 273, 1–7. doi: 10.1007/s00405-014-3325-7

McNeil, J., Cameron, J. D., Finlayson, G., Blundell, J. E., and Doucet, E. (2013). Greater overall olfactory performance, explicit wanting for high fat foods and lipid intake during the mid-luteal phase of the menstrual cycle. *Physiol. Behav.* 112–113, 84–89. doi: 10.1016/j.physbeh.2013.02.008

Meule, A., Teran, C. B., Berker, J., Gründel, T., Mayerhofer, M., Platte, P., et al. (2014). On the differentiation between trait and state food craving: Half-year retest-reliability of the *Food Cravings Questionnaire-Trait-reduced* (FCQ-T-r) and the *Food Cravings Questionnaire-State* (FCQ-S). *J. Eat. Disord.* 2. doi: 10.1186/s40337-014-0025-z

Meule, A., and Hormes, J. M. (2015). Chocolate versions of the *Food Cravings Questionnaires*. Associations with chocolate exposure-induced salivary flow and ad libitum chocolate consumption. *Appetite* 91, 256–265. doi: 10.1016/j.appet.2015.04.054

Mueller, C., and Renner, B. (2006). A new procedure for the short screening of olfactory function using five items from the „Sniffin' Sticks" identification test kit. *Am. J. Rhinol.* 20, 113–116.

Mugler, J. P., and Brookeman, J. R. (1990). Three-dimensional magnetization-prepared rapid gradient-echo imaging (3D MP RAGE). *Magn. Reson. Med.* 15, 152–157. doi: 10.1002/mrm.1910150117

Münzberg, H., and Heymsfield, S. B. (2015). "Leptin, obesity, and leptin resistance," in *Leptin—Regulation and Clinical Applications*, ed. M. D. Sam Dagogo-Jack (Cham: Springer International Publishing), 67–78. doi: 10.1007/978-3-319-09915-6_6

Murphy, K. G., and Bloom, S. R. (2006). Gut hormones and the regulation of energy homeostasis. *Nature* 444, 854–859. doi: 10.1038/nature05484

Nagl, M., Hilbert, A., de Zwaan, M., Braehler, E., and Kersting, A. (2016). The German version of the dutch eating behavior questionnaire: psychometric properties, measurement invariance, and population-based norms. *PLOS ONE* 11:e0162510. doi: 10.1371/journal.pone.0162510

Nagao, H., Yamaguchi, M., Takahash, Y., and Mori, K. (2002). Grouping and representation of odorant receptors in domains of the olfactory bulb sensory map. *Microsc. Res. Tech.* 58:168. doi: 10.1002/jemt.10146

Nagayama, S., Enerva, A., Fletcher, M. L., Masurkar, A. V., Igarashi, K. M., Mori, K., et al. (2010). Differential axonal projection of mitral and tufted cells in the mouse main olfactory system. *Front. Neural Circuits* 4:120. doi: 10.3389/fncir.2010.00120

Negoias, S., Croy, I., Gerber, J., Puschmann, S., Petrowski, K., Joraschky, P., et al. (2010). Reduced olfactory bulb volume and olfactory sensitivity in patients with acute major depression. *Neuroscience* 169, 415–421. doi: 10.1016/j.neuroscience.2010.05.012

O'Brien, P. D., Hinder, L. M., Callaghan, B. C., and Feldman, E. L. (2017). Neurological consequences of obesity. *Lancet Neurol.* 16, 465–477. doi: 10.1016/S1474-4422(17)30084-4

Pastor, A., Fernandez-Aranda, F., Fito, M., Jimenez-Murcia, S., Botella, C., Fernandez-Real, J. M., et al. (2016). A lower olfactory capacity is related to higher circulating concentrations of Endocannabinoid 2-arachidonoylglycerol and higher body mass index in women. *PLoS One* 11:e0148734. doi: 10.1371/journal.pone.0148734

Payton, C. A., Wilson, D. A., and Wesson, D. W. (2012). Parallel odor processing by two anatomically distinct olfactory bulb target structures. *PLoS One* 7:e34926. doi: 10.1371/journal.pone.0034926

Peng, M., Coutts, D., Wang, T., and Cakmak, Y. O. (2019). Systematic review of olfactory shifts related to obesity. *Obes. Rev.* 20, 325–338. doi: 10.1111/obr.12800

Poessel, M., Freiherr, J., Wiencke, K., Villringer, A., and Horstmann, A. (2020). Insulin resistance is associated with reduced food odor sensitivity across a wide range of body weights. *Nutrients* 12:2201. doi: 10.3390/nu12082201

Proserpio, C., de Graaf, C., Laureati, M., Pagliarini, E., and Boesveldt, S. (2017). Impact of ambient odors on food intake, saliva production and appetite ratings. *Physiol. Behav.* 174, 35–41. doi: 10.1016/j.physbeh.2017.02.042

Ramaekers, M. G., Boesveldt, S., Gort, G., Lakemond, C. M., van Boekel, M. A., and Luning, P. A. (2014). Sensory-specific appetite is affected by actively smelled food odors and remains stable over time in normal-weight women. *J. Nutr.* 144, 1314–1319. doi: 10.3945/jn.114.192567

Ramaekers, M. G., Verhoef, A., Gort, G., Luning, P. A., and Boesveldt, S. (2016). Metabolic and sensory influences on odor sensitivity in humans. *Chem. Senses* 41, 163–168. doi: 10.1093/chemse/bjv068

Reilly, S. M., and Saltiel, A. R. (2017). Adapting to obesity with adipose tissue inflammation. *Nat. Rev. Endocrinol.* 13, 633–643. doi: 10.1038/nrendo.2017.90

Richardson, B. E., Vander Woude, E. A., Sudan, R., Thompson, J. S., and Leopold, D. A. (2004). Altered olfactory acuity in the morbidly obese. *Obes. Surg.* 14, 967–969. doi: 10.1381/0960892041719617

Riera, C. E., and Dillin, A. (2016). Emerging role of sensory perception in aging and metabolism. *Trends Endocrinol. Metab.* 27, 294–303. doi: 10.1016/j.tem.2016.03.007

Rivière, S., Soubeyre, V., Jarriault, D., Molinas, A., Léger-Charnay, E., Desmoulins, L., et al. (2016). High Fructose Diet inducing diabetes rapidly impacts olfactory epithelium and behavior in mice. *Sci. Rep.* 6:34011. doi: 10.1038/srep34011

Rombaux, P., Duprez, T., and Hummel, T. (2009). Olfactory bulb volume in the clinical assessment of olfactory dysfunction. *Rhinology* 47, 3–9.

Rosenthal, R. J., Morton, J., Brethauer, S., Mattar, S., De Maria, E., Benz, J. K., et al. (2017). Obesity in America. *Surg. Obes. Relat. Dis.* 13, 1643–1650. doi: 10.1016/j.soard.2017.08.002

Rottstädt, F., Han, P., Weidner, K., Schellong, J., Wolff-Stephan, S., Strauß, T., et al. (2018). Reduced olfactory bulb volume in depression-A structural moderator analysis. *Hum. Brain Mapp.* 39, 2573–2582. doi: 10.1002/hbm.24024

RStudio Team (2016). *RStudio: Integrated Development Environment for R*. Boston, MA: RStudio Team.

Russo, C., Russo, A., Pellitteri, R., and Stanzani, S. (2018). Ghrelin-containing neurons in the olfactory bulb send collateralized projections into medial amygdaloid and arcuate hypothalamic nuclei: neuroanatomical study. *Exp. Brain Res.* 236, 2223–2229. doi: 10.1007/s00221-018-5298-z

Saad, M. J. A., Santos, A., and Prada, P. O. (2016). Linking gut microbiota and inflammation to obesity and insulin resistance. *Physiology* 31, 283–293. doi: 10.1152/physiol.00041.2015

Sato, T., Homma, R., and Nagayama, S. (2020). Direct comparison of odor responses of homologous glomeruli in the medial and lateral maps of the mouse olfactory bulb. *eNeuro* 7, doi: 10.1523/ENEURO.0449-19.2020

Savic, I., Gulyas, B., Larsson, M., and Roland, P. (2000). Olfactory functions are mediated by parallel and hierarchical processing. *Neuron* 26, 735–745. doi: 10.1016/S0896-6273(00)81209-X

Schriever, V. A., Reither, N., Gerber, J., Iannilli, E., and Hummel, T. (2013). Olfactory bulb volume in smokers. *Exp. Brain Res.* 225, 153–157. doi: 10.1007/s00221-012-3356-5

Skrandies, W., and Zschieschang, R. (2015). Olfactory and gustatory functions and its relation to body weight. *Physiol. Behav.* 142, 1–4. doi: 10.1016/j.physbeh.2015.01.024

Stafford, L. D., and Whittle, A. (2015). Obese individuals have higher preference and sensitivity to odor of chocolate. *Chem. Senses* 40, 279–284. doi: 10.1093/chemse/bjv007

Stevens, G. A., Singh, G. M., Lu, Y., Danaei, G., Lin, J. K., Finucane, M. M., et al. (2012). National, regional, and global trends in adult overweight and obesity prevalences. *Popul. Health Metr.* 10:22. doi: 10.1186/1478-7954-10-22

Stunkard, A. J., and Messick, S. (1985). The three-factor eating questionnaire to measure dietary restraint, disinhibition and hunger. *J. Psychosom. Res.* 29, 71–83. doi: 10.1016/0022-3999(85)90010-8

Thanarajah, S., Hoffstall, V., Rigoux, L., Hanssen, R., Brüning, J. C., and Tittgemeyer, M. (2019). The role of insulin sensitivity and intranasally applied insulin on olfactory perception. *Sci. Rep.* 9:7222. doi: 10.1038/s41598-019-43693-7

Thiebaud, N., Johnson, M. C., Butler, J. L., Bell, G. A., Ferguson, K. L., Fadool, A. R., et al. (2014). Hyperlipidemic diet causes loss of olfactory sensory neurons, reduces olfactory discrimination, and disrupts odor-reversal learning. *J. Neurosci.* 34, 6970–6984. doi: 10.1523/JNEUROSCI.3366-13.2014

Thomann, P. A., Dos Santos, V., Toro, P., Schönknecht, P., Essig, M., and Schröder, J. (2009). Reduced olfactory bulb and tract volume in early Alzheimer's disease–A MRI study. *Neurobiol. Aging* 30, 838–841. doi: 10.1016/j.neurobiolaging.2007.08.001

Tong, J., Mannea, E., Aime, P., Pfluger, P. T., Yi, C. X., Castaneda, T. R., et al. (2011). Ghrelin enhances olfactory sensitivity and exploratory sniffing in rodents and humans. *J. Neurosci.* 31, 5841–5846. doi: 10.1523/JNEUROSCI.5680-10.2011

Tsai, S.-Y., Gildengers, A. G., Hsu, J.-L., Chung, K.-H., Chen, P.-H., and Huang, Y.-J. (2019). Inflammation associated with volume reduction in the gray matter and hippocampus of older patients with bipolar disorder. *J. Affect. Disord.* 244, 60–66. doi: 10.1016/j.jad.2018.10.093

Turetsky, B. I., Moberg, P. J., Yousem, D. M., Doty, R. L., Arnold, S. E., and Gur, R. E. (2000). Reduced olfactory bulb volume in patients with schizophrenia. *Am. J. Psychiatry* 157, 828–830. doi: 10.1176/appi.ajp.157.5.828

Weiss, M. S., Hajnal, A., Czaja, K., and Di Lorenzo, P. M. (2019). Taste responses in the nucleus of the solitary tract of awake obese rats are blunted compared with those in lean rats. *Front. Integr. Neurosci.* 13:35. doi: 10.3389/fnint.2019.00035

Weiss, T., Soroka, T., Gorodisky, L., Shushan, S., Snitz, K., Weissgross, R., et al. (2020). Human olfaction without apparent olfactory bulbs. *Neuron* 105, 35–45.e5. doi: 10.1016/j.neuron.2019.10.006

Conflict of Interest: The authors declare that the research was conducted in the absence of any commercial or financial relationships that could be construed as a potential conflict of interest.

frontiers in Behavioral Neuroscience

ORIGINAL RESEARCH
published: 04 December 2020
doi: 10.3389/fnbeh.2020.578676

Neural Substrates of Food Valuation and Its Relationship With BMI and Healthy Eating in Higher BMI Individuals

Junaid S. Merchant[1], Danielle Cosme[2], Nicole R. Giuliani[3], Bryce Dirks[4] and Elliot T. Berkman[5]*

[1] Neuroscience and Cognitive Science Program (NACS), Department of Psychology, University of Maryland, College Park, MD, United States, [2] Annenberg School for Communication, University of Pennsylvania, Philadelphia, PA, United States, [3] Prevention Science Institute, Department of Special Education and Clinical Sciences, University of Oregon, Eugene, OR, United States, [4] Department of Psychology, University of Miami, Coral Gables, FL, United States, [5] Center for Translational Neuroscience, Department of Psychology, University of Oregon, Eugene, OR, United States

Considerable evidence points to a link between body mass index (BMI), eating behavior, and the brain's reward system. However, much of this research focuses on food cue reactivity without examining the subjective valuation process as a potential mechanism driving individual differences in BMI and eating behavior. The current pre-registered study (https://osf.io/n4c95/) examined the relationship between BMI, healthy eating, and subjective valuation of healthy and unhealthy foods in a community sample of individuals with higher BMI who intended to eat more healthily. Particularly, we examined: (1) alterations in neurocognitive measures of subjective valuation related to BMI and healthy eating; (2) differences in the neurocognitive valuation for healthy and unhealthy foods and their relation to BMI and healthy eating; (3) and whether we could conceptually replicate prior findings demonstrating differences in neural reactivity to palatable vs. plain foods. To this end, we scanned 105 participants with BMIs ranging from 23 to 42 using fMRI during a willingness-to-pay task that quantifies trial-by-trial valuation of 30 healthy and 30 unhealthy food items. We measured out of lab eating behavior via the Automated Self-Administered 24 H Dietary Assessment Tool, which allowed us to calculate a Healthy Eating Index (HEI). We found that our sample exhibited robust, positive linear relationships between self-reported value and neural responses in regions previously implicated in studies of subjective value, suggesting an intact valuation system. However, we found no relationship between valuation and BMI nor HEI, with Bayes Factor indicating moderate evidence for a null relationship. Separating the food types revealed that healthy eating, as measured by the HEI, was inversely related to subjective valuation of unhealthy foods. Imaging data further revealed a stronger linkage between valuation of healthy (compared to unhealthy) foods and corresponding response in the ventromedial prefrontal cortex (vmPFC), and that the interaction between healthy and unhealthy food valuation in this region is related to HEI. Finally, our results did not replicate reactivity differences demonstrated in prior work, likely due to differences in the mapping between food healthiness and palatability. Together, our findings point to disruptions in the

OPEN ACCESS

Edited by:
Junichi Chikazoe, National Institute for Physiological Sciences (NIPS), Japan

Reviewed by:
Shinsuke Suzuki, The University of Melbourne, Australia
Ahmad Jezzini, Washington University in St. Louis, United States

****Correspondence:***
Junaid S. Merchant
merchantjs@gmail.com

Specialty section:
This article was submitted to Motivation and Reward, a section of the journal Frontiers in Behavioral Neuroscience

Received: *30 June 2020*
Accepted: *10 November 2020*
Published: *04 December 2020*

Citation:
Merchant JS, Cosme D, Giuliani NR, Dirks B and Berkman ET (2020) Neural Substrates of Food Valuation and Its Relationship With BMI and Healthy Eating in Higher BMI Individuals. Front. Behav. Neurosci. 14:578676. doi: 10.3389/fnbeh.2020.578676

valuation of unhealthy foods in the vmPFC as a potential mechanism influencing healthy eating.

Keywords: subjective valuation, food-cue reactivity, healthy eating, BMI—body mass index, willingness-to-pay, fMRI

INTRODUCTION

Global obesity rates have increased nearly 3-fold since 1975 (Abarca-Gómez et al., 2017), and current estimates indicate that middle-aged adults have the highest prevalence of obesity (Hales et al., 2020). Body mass index (BMI) during the early middle-age years (i.e., ages 35–45; Medley, 1980) predicts life expectancy (Peeters et al., 2003), and research suggests that prolonged life-style changes during this period have the ability to reverse the deleterious effects of poor health (Howden et al., 2018). A confluence of factors has been examined to understand the development of overweight and obesity status during early middle-age adulthood, but one factor that has received relatively little attention is the change in neural circuitry underlying decision-making during this stage of life (Samanez-Larkin and Knutson, 2015). In particular, recent work points to the promise of examining subjective valuation as an underlying process involved in dietary choice and changes in eating behavior that contribute to higher BMI (Rangel, 2013; Giuliani et al., 2018).

Subjective valuation is the neurocognitive process by which an individual assigns value to an item, which is used to guide decision making (Rangel, 2013; Berkman et al., 2017a). When applied to food-based decision making, this framework allows for the integration of motivational and self-relevant factors contributing to the subjective valuation process when making choices about healthy and unhealthy foods (Rangel, 2013; Berkman et al., 2017b; Berkman, 2018). Despite the promise of the value-based approach to understanding the neurocognitive mechanisms contributing to weight and eating behavior, much of the health neuroscience research has focused on the link between food-cue reactivity in the brain, and its relation to eating behavior and BMI (Tetley et al., 2009; Yokum et al., 2011; Gunes et al., 2012; Murdaugh et al., 2012; Verdejo-Román et al., 2017; Harding et al., 2018; Contreras-Rodriguez et al., 2020). Thus, the current pre-registered study (https://osf.io/n4c95/) aims to expand health neuroscience research in this area by examining the relationship between BMI, healthy eating, and the brain regions involved in subjective valuation of healthy and unhealthy foods in a sample of early middle-aged adults with higher BMI.

Food-Cue Reactivity, Self-Regulation, and the Relationship With BMI and Eating Behavior

Much of our understanding of the relationship between higher BMI, eating behavior, and the brain's reward system has been examined through the lens of the "food addiction" model (Smith and Robbins, 2013). The reward system is comprised of dopamine producing neurons in the ventral tegmental area (VTA) that project to the nucleus accumbens (NAcc) and prefrontal cortex, which are involved in motivation and pleasure, but show dysregulated activity in individuals with higher BMI similar to what has been observed in individuals with substance addictions (Volkow et al., 2013a). The food addiction model proposes that the heightened reactivity to food cues in individuals with higher BMI leads to an inability to regulate food intake, thereby leading to overeating and weight gain (Volkow et al., 2013b). Neuroimaging research has confirmed heightened reactivity to food-cues in the brain's reward system, as well as brain regions associated with attention and emotional salience in relation to BMI and eating behavior (Yokum et al., 2011; Smeets et al., 2012; Verdejo-Román et al., 2017). For instance, Lawrence and colleagues (2012) demonstrated that food-cue reactivity in the NAcc predicts the amount of subsequent food consumption, and interactions between NAcc reactivity and self-reported self-control predicted BMI (Lawrence et al., 2012). Moreover, this work has shown that the relationship between food-cue reactivity and eating behavior and weight is specific to desirable foods (e.g., high-calorie foods; Yokum et al., 2011; Stice and Yokum, 2018; Yokum and Stice, 2019; Verdejo-Román et al., 2017), and can prospectively predict later consummatory behavior and outcomes in weight-loss programs (Demos et al., 2012; Murdaugh et al., 2012; Kroemer et al., 2016). Together, these findings suggest that biases in the subjective valuation system, particularly for unhealthy, desirable foods might be the process linking brain reactivity, BMI, and eating behavior.

Self-regulation research provides a complementary framework for health neuroscience research by providing neurocognitive mechanisms leading to healthier behavior. In the context of eating behavior, self-regulation involves the reduction of food cravings through cognitive regulation strategies that engage executive control regions of the brain, which is thought to break the link between food-cue reactivity and eating behavior (Giuliani et al., 2018). For instance, the process of reappraising personally craved foods to make them a less desirable elicited relatively greater activity in the dorsolateral prefrontal cortex (dlPFC) and dorsal anterior cingulate cortex (dACC), and this activity was negatively correlated with BMI in a sample of young adults (Giuliani et al., 2014). Importantly, self-regulation, with respect to eating, can be trained (Boswell and Kober, 2016), and greater self-regulatory ability protects against developing obesity (Duckworth, 2011). Indeed, recent studies using this framework have targeted the brain's self-regulation system using real-time neurofeedback, and demonstrated measurable reductions in palatability ratings and consumption of unhealthy foods after neurofeedback training (Spetter et al., 2017; Kohl et al., 2019). For purposes of the current study, healthy eating goals are another top-down factor integrated during valuation. If health goals are active during valuation, they may be indexed by activation in cognitive control brain regions (Tusche and Hutcherson, 2018).

Subjective Valuation as a Mechanism Driving BMI and Eating

Subjective valuation is the neurocognitive process wherein an individual assigns value to items in order to help guide decision-making, and can be measured as the correspondence between self-reported value and level of activity in brain regions commonly associated with reward processing (Bartra et al., 2013; Berkman et al., 2017a). Examining weight and eating behavior within this framework provides a means to incorporate findings from the food-cue reactivity and self-regulation research, and better operationalizes the neurocognitive mechanism involved in food-based decision making as it relates to BMI and eating behavior (Giuliani et al., 2018). Particularly, a value-based approach posits that the brain's reward, salience, and self-regulation networks comprise general-purpose value systems that assign subjective value during decision making, and suggests a special role for the ventromedial prefrontal cortex (vmPFC) in integrating disparate value signals (Chib et al., 2009; Hare et al., 2011; Berkman, 2018). This neurocognitive mechanism has been supported by a meta-analysis of over 200 studies that established a highly reliable, positive relationship between subjective value (i.e., how much one is willing to pay for an object, or "willingness-to-pay") and the blood-oxygenation-level-dependent (BOLD) response in the brain's reward centers, particularly the vmPFC and anterior ventral striatum (aVS; Bartra et al., 2013). Within this framework, multiple factors, such as healthy eating goals and food desirability, are integrated into a common value signal that guides choices (Berkman et al., 2017b; Berkman, 2018). For example, research has demonstrated that the value signal in the vmPFC is modulated by activity in the dlPFC that responds to immediate task demands, such as focusing on food healthiness, which in turn drives the selection of food-based decisions (Hare et al., 2011; Hutcherson et al., 2012).

To date, few studies have utilized willingness-to-pay paradigms, in which subjective values of foods are measured directly via bids in a food auction, to examine the relationship between eating behavior, BMI, and brain responses to the food cues (Verdejo-Román et al., 2017; Contreras-Rodriguez et al., 2020). The two studies that have examined the relationship between willingness-to-pay and BMI did not model the linear relationship between BOLD response and bid amount for the food items, but instead examined differences in the overall brain activation for different food categories. Thus, the previous approach is more akin to food-cue reactivity paradigms, which compare average activation to discrete categories of stimuli, rather than to the approach used in subjective valuation paradigms, because the continuously-rated self-reported values (i.e., bids) were disregarded.

Current Study

The current pre-registered analyses aim to extend our understanding of the relationship between the neurocognitive process of subjective valuation, eating behavior, and BMI by utilizing data collected for a larger intervention study. The project was pre-registered after data were collected, but before any of the registered analyses were conducted (https://osf.io/n4c95/). The original study targeted adults who were at-risk for developing weight-related health consequences—a community sample of early middle-aged adults (i.e., 35–45 years old) with higher BMI (i.e., BMI = 25–40) who had explicit healthy eating goals, but were not actively enrolled in any dietary intervention during the time of testing. Recent estimates indicate that middle-aged adults have the highest prevalence of obesity (Esteban et al., 2019), but research suggests that life-style changes during the early middle-age years have the ability to reverse the negative impacts of poor health (Howden et al., 2018). The current analyses were conducted on data collected at the baseline session before any intervention took place. To elucidate brain regions supporting valuation, participants completed the willingness-to-pay paradigm—which provides an explicit measure of self-reported value for different food types—while in the MRI scanner.

First, we examined the functioning of the valuation system using neuroimaging, and its relationship to BMI and healthy eating. That is, we assessed the degree to which our sample showed the expected relationship between self-reported value and BOLD response in the brain's valuation system during food choices, and whether valuation was related to BMI and healthy food consumption. Due to the relative novelty of this analysis, we did not have *a priori* hypotheses about the existence or direction of this relationship. However, if vmPFC activity tracked value *and* was related to BMI or healthy eating, we could infer that the valuation process may drive some of the individual differences for these measures. Second, we compared the valuation of healthy and unhealthy foods separately, and how they related to BMI and healthy eating. Specifically, we compared the coupling of self-reported value and BOLD response between decisions made for healthy vs. unhealthy food items, and examined if this predicted BMI and/or healthy eating. Based on studies of food-cue reactivity that suggest an overreactivity bias to unhealthy foods in higher BMI individuals (Yokum et al., 2011; Verdejo-Román et al., 2017), we expected to see differences in the valuation process between food categories, but did not have strong predictions as to the nature or direction of the relationship with BMI and healthy eating. Finally, we aimed to provide a conceptual replication of Verdejo-Román et al. (2017) who also used the willingness-to-pay paradigm, but disregarded self-reported value. Specifically, we examined if activation differences between healthy and unhealthy foods (i.e., ignoring self-reported value) showed a similar pattern of results as when Verdejo-Roman and colleagues contrasted unpalatable and palatable foods.

METHODS

Participants

A sample of 105 higher BMI, middle-aged individuals who had explicit goals to eat more healthily were screened and enrolled into a larger, longitudinal project investigating the neural predictors of dietary change. Inclusion criteria for the overarching study included (1) overweight or obese status as defined by the Center for Disease Control and Prevention

(i.e., approximate BMI between 25 and 40); (2) early, middle-age (i.e., 33–45 years old); (3) no psychiatric, neurological, or eating disorders; (4) no fMRI contraindications; (5) not actively enrolled in a diet program or any other type of eating intervention; and (6) self-reported desire to eat more healthily. The current analysis included all participants that completed baseline measures of eating behavior, BMI and usable fMRI data during the willingness-to-pay experiment. Ten participants were excluded for non-compliance, not showing up, or the decision to drop out before completion of the baseline session. Two participants were excluded because of technical error during the willingness-to-pay task, and one participant was excluded from analyses of healthy eating because of technical error. A final sample of 93 participants (77 female, mean (SD) age = 39.25 (3.50); mean (SD) BMI = 31.41 (3.91) were included in all analyses, except for analyses of healthy eating, which had a sample 92 participants. Results from this sample were reported in a separate paper comparing alternative neurocognitive models of self-control using trial-level data (Cosme et al., 2019). However, the current analyses are unique in that they relate the valuation process to real world measures of health (i.e., BMI and eating behavior) using participant-level data. Importantly, the analytic plan in our pre-registration was not based on results from the previous analyses, and what was known about the data at the time of registering was included in the pre-registration document for complete transparency.

Protocol and Measures

Participants were recruited from the community through a combination of online, newspaper, and public advertising. Interested participants were screened for exclusion criteria via phone, and eligible participants were sent a package of materials to complete before arriving for their baseline session. Participants were scheduled for their baseline lab visit, and asked to complete the package of measures within 24 h of the visit. Pre-baseline measures included demographic information, assessments of eating behavior, and a battery of psychometric measures assessing self-control, impulsivity, and other relevant affective and motivational factors (see https://osf.io/n4c95/ for full list of measures). Participants were instructed to not eat anything for at least an hour before the baseline visit. During the baseline visit, participants were consented, screened for MRI contraindications, and instructed on the requirements of the study. Weight and height were measured using a commercially available weight scale and wall ruler, and BMI was calculated by dividing the participant's weight in kilograms by squared height in meters. Eating behavior was assessed via the Automated Self-Administered 24-Hour (ASA24®) Dietary Assessment Tool (Subar et al., 2012) which allows for the calculation of the Healthy Eating Index (HEI; Guenther et al., 2013) using equations provided by the developers of the ASA (https://epi.grants.cancer.gov/asa24/resources/hei.html). The HEI quantifies healthy eating behavior based on the dietary guidelines for Americans. Following the recommendations proposed by the developers of this measure, participants completed the ASA within a few days prior to and during the baseline visit to obtain a more representative estimate of daily eating behavior.

The current study examined performance during the scanner-compatible willingness-to-pay task that quantifies trial-by-trial valuation of 30 healthy and 30 unhealthy snack food items, the healthiness of which was determined based on caloric density (Hutcherson et al., 2012), thereby providing both the self-report and BOLD responses used to index subjective valuation. Participants were given $2 prior to scanning for the purpose of bidding, and told that they would be bidding on snack food items during the scan for a chance to win one of the snacks. For each item, they were required to make bids on a scale from $0 to $2 dollars in increments of $0.50 based on how willing they are to pay to obtain the snack (**Figure 1**). To ensure truthful bids, we employed the rules of a Becker-DeGroot-Marschak auction (Becker et al., 1964; Plassmann et al., 2007). Briefly, they were instructed to treat each trial as if they had a fresh $2, and told that one of the snack items would be chosen at random at the end of the scan as the actual auction item they may win. If the bid they made for the selected item was higher than a randomly generated bid amount, they won the snack and were given the remainder of the $2 if the bid was below $2. If their bid was equal to or lower than the randomly generated bid, they did not win the snack item, and were refunded the full $2. All food stimuli were presented on black backgrounds, and the food item was centered such that the food stimulus took up most of the image space without crossing the margins. The task was presented using the PsychToolBox package for MATLAB (Brainard, 1997), and responses were made using a five-button button-box provided by the Lewis Center for Neuroimaging at the University of Oregon.

MRI Data and Processing

Neuroimaging data were acquired on a 3T Siemens Skyra scanner at the University of Oregon Lewis Center for Neuroimaging. We acquired a high-resolution anatomical T1-weighted MP-RAGE scan (TR/TE = 2500.00/3.43 ms, 256 × 256 matrix, 1 mm thick, 176 sagittal slices, FOV = 208 × 208 mm), functional images with a T2*–weighted echo-planar sequence (72 axial slices, TR/TE = 2000.00/27.00 ms, 90-degree flip angle, 100 × 100 matrix, 2 mm thick, FOV = 208 × 208 mm, multiband acceleration factor = 3), and opposite phase encoded echo-planar images to correct for magnetic field inhomogeneities (72 axial slices, TR/TE = 6390.00/47.80 ms, 90-degree flip angle, 104 ×104 matrix, 2 mm thick, FOV = 208 × 208 mm). The willingness-to-pay task was acquired over 357 functional volumes scanned as one run.

Neuroimaging data were preprocessed using fMRIPrep 1.1.4 (Esteban et al., 2019). Briefly, anatomical images were segmented and normalized to MNI space; functional images were skull-stripped, susceptibility distortion corrected, realigned, slice-time corrected, co-registered and warped to the normalized anatomical image (see https://osf.io/n4c95/ for full report of the preprocessing pipeline). Normalized functional data were then smoothed (6 mm FWHM) in SPM12 (http://www.fil.ion.ucl.ac.uk/spm). Subject-level, voxel-wise multiple linear regression was calculated using AFNI's 3dREMLfit (Cox, 1996), using functions representing each condition convolved with a standard hemodynamic response function, each condition convolved with a standard hemodynamic response function with the amplitude modulated by trial-wise bid amount (in the case of research

FIGURE 1 | Task schematic for the willingness-to-pay task. On each trial, a snack food was presented for 4 s, followed by a 4 s bid period, and jittered fixation period between trials (M = 4.38 s). Snack foods were healthy (e.g., fruit) or unhealthy (e.g., candy) items.

questions 1 and 2), motion regressors, and a "trash" regressor indicating images with motion artifacts (e.g., striping) identified via automated motion assessment (Cosme et al., 2018). For all group-level, whole-brain analyses, the cluster correction value was calculated automatically by using the -Clustsim option in AFNI's 3dttest++, which sends the input volumes directly to the 3dClustSim program after simulating the noise volumes by randomizing and permuting the input datasets. This model-free approach is more accurate at controlling the false positive rate compared to simulating noise using a mixed-model estimation of the autocorrelation function. This yielded a voxel-wise threshold of $p < 0.001$ and cluster extent of $k = 119$ to achieve a whole-brain familywise error rate of $\alpha = 0.05$ when nearest neighbor cluster definitions are set to 3 (i.e., voxel faces, edges, and corners touching count as part of a contiguous cluster). Despite using the 3dttest++ program to determine cluster thresholds, we used AFNI's 3dMEMA program for group-level statistics because it better accounts for subject-level variance. All code used for neuroimaging analysis available (https://github.com/UOSAN/CHIVES_WTP_scripts).

Overall Valuation

To address our first research question regarding neural function during the valuation process and its relation to BMI and healthy eating, we conducted a series of ROI and whole-brain analyses. First, we calculated subject-level whole-brain maps comprised of voxel-wise beta values that quantify the linear relationship between bid value for each food item and the corresponding BOLD response during the decision making period. Because prior research has established a set of brain regions comprising the valuation system, we first explored the valuation process within *a priori* regions of interest (ROIs) obtained from the Bartra et al. (2013) meta-analysis that best mapped on to our task parameters. Specifically, we used the vmPFC and anterior ventral striatum (aVS) ROIs from Figure 9 (Bartra et al., 2013, page 423) that reliably demonstrated a positive relationship with subjective value for primary and monetary rewards, and the anterior cingulate cortex (ACC) and bilateral anterior insulae (AI) from **Figure 3C** (Bartra et al., 2013, page 417) that showed a conjunction between positive and negative relationships with subjective value (available here: https://www.sas.upenn.edu/~mcguirej/meta-analysis.html).

Within each ROI, we averaged the voxel-wise parameter estimates from each participant, and used a one-sample *t*-test against zero to assess if our sample showed evidence of neurocognitive valuation. We then used the parameter estimates from the vmPFC and aVS ROIs to assess their relationship with BMI using linear regression, and similarly regressed HEI on the same parameter estimates in a separate linear regression model. We focused on the vmPFC and aVS because of the reliability with which they have been implicated in prior studies of subjective valuation (Bartra et al., 2013). Lastly, we conducted whole-brain searches to confirm the results of the ROI analysis, and to elucidate unpredicted brain regions involved in the subjective valuation process. The whole-brain search of subjective valuation was conducted by entering subject-level beta- and *t*-maps into AFNI's 3dMEMA program, which calculates a group-level mixed effects meta-analysis map that accounts for subject-level variance. Separate whole-brain searches for clusters relating valuation to BMI and HEI were calculated similarly in two separate analyses, but with the added covariates of interest (i.e., BMI and HEI, respectively).

Valuation by Food Type

To address the second research question regarding differences in the valuation process between healthy and unhealthy foods, we conducted a series of behavioral and neuroimaging analyses. First, we assessed if self-reported value for healthy and unhealthy foods, or the interaction between the two, was related to BMI and healthy eating. To this end, we regressed BMI on subject-averaged bid amounts for healthy and unhealthy foods as separate independent variables in the first step of a linear regression model, and the interaction term between the two in the second

step. This procedure was then repeated with HEI in a separate step-wise, linear regression model.

To compare the neurocognitive valuation between food types, we calculated a new set of subject-level models that separated healthy and unhealthy foods, and generated separate whole-brain maps for each food category comprised of voxel-wise beta values that quantified the linear relationship between bid amount and BOLD response. We then contrasted these maps (i.e., neurocognitive valuation for healthy > unhealthy foods) within subjects to evaluate differences in valuation across food categories across our sample. To examine differences in valuation for the food category within the vmPFC and aVS ROIs, we averaged the voxel-wise contrast value within each, and used a one-sample *t*-test against zero to examine if the coupling of self-reported value and corresponding BOLD amount was greater for one food category.

To assess the relationship between the neurocognitive valuation of healthy and unhealthy foods with individual differences in BMI and healthy eating, we calculated a set of regression models similar to the behavioral regression models above. We first combined the ROIs by averaging the parameter estimates across the vmPFC and aVS within subjects to use as our measure of neurocognitive valuation for healthy and unhealthy foods. We then regressed BMI on our neurocognitive measures of healthy and unhealthy foods as separate independent variables in the first step of linear regression model, and the interaction term between the two as in the second step. This procedure was repeated for HEI in a separate step-wise, linear regression model. Lastly, we conducted a set of whole-brain searches to confirm the results of our ROI analyses, and elucidate unpredicted brain clusters distinguishing the valuation for the food categories. Whole-brain search for differences in the neurocognitive valuation of healthy and unhealthy foods was calculated by entering subject-level contrast beta- and *t*-maps into AFNI's 3dMEMA program. Separate whole-brain searches for clusters relating this difference in valuation to BMI and HEI were calculated similarly in two separate analyses, but with the added covariates of interest (i.e., BMI and HEI, respectively).

Replication Analysis

Finally, we attempted to conceptually replicate the findings from Verdejo-Román et al. (2017). In their paper, they similarly used the willingness-to-pay task, but categorized the foods into palatable (e.g., chocolate) and unpalatable (e.g., plain yogurt) conditions based on previously obtained ratings of palatability. Instead of modeling the relationship between bid amount and BOLD response, they contrasted overall activations for food categories (i.e., palatable > unpalatable) and found greater activation in "[bilateral] dorsal caudate, nucleus accumbens, ventral putamen, ventral tegmental area, intraparietal, ventromedial and dorsolateral prefrontal and anterior cingulate cortices, and the anterior insula extending to the lateral orbitofrontal gyrus" (p. 671; Verdejo-Román et al., 2017). Further, they demonstrated greater activation in striatal regions for obese compared to overweight individuals when comparing this contrast between groups.

Toward the goal of a conceptual replication, we examined if our unhealthy > healthy reactivity contrast showed a similar pattern of activation to their palatable > unpalatable contrast, as well as the between group differences they report. To this end, we calculated a third set of subject-level models that ignored bid values, and examined the reactivity to healthy and unhealthy foods. In particular, we generated separate whole-brain maps for each food category comprised of voxel-wise beta values that quantified the amplitude of the BOLD response, disregarding its relationship with self-reported value. We contrasted these maps at the subject level, and entered the resulting contrast beta- and *t*-maps into AFNI's 3dMEMA program for a whole-brain search of activation differences between food categories. Lastly, we split our sample into overweight (BMI < 30; $N = 37$) and obese groups (BMI > 30; $N = 56$) in an attempt to replicate Verdejo-Román and colleagues (2017) between group contrast (obese > overweight, for the unhealthy > healthy contrast), and entered the corresponding beta- and *t*-maps into AFNI's 3dMEMA program for a between group analysis.

Deviations From the Pre-registration

We conducted exploratory, follow up analyses that were intended to clarify the pattern of results of any significant results as needed, none of which were pre-registered. Also, when possible, we assessed the evidence in favor of the null hypothesis by calculating Bayes Factor for non-significant findings. We calculated Bayes Factor (BF_{10}) as the ratio of the likelihood of the alternative hypothesis to the likelihood of the null hypothesis, and followed Lee and Wagenmakers (2014) heuristics for interpreting this value as the strength of evidence in favor of the null hypothesis: 1–1/3 = anecdotal evidence, 1/3–1/10 = moderate evidence, 1/10–1/30 = strong evidence, 1/30> = very strong evidence. Given that these relationships had not been previously explored, BF_{10} was calculated to clarify the nature of null results, and provide a possible explanation as to why such findings have not been reported in prior work.

RESULTS

Overall Valuation

ROI Analyses

Each of the ROIs showed a positive, linear relationship between self-reported value and corresponding BOLD response, even after Bonferroni correction, suggesting that our sample displayed normative functioning of the valuation system: vmPFC (M = 5.93, SD = 7.70, 95% CI [4.34, 7.51]), $t(92) = 7.42$, $p < 0.001$; aVS (M = 4.56, SD = 5.53, 95% CI [3.42, 5.70]), $t(92) = 7.95$, $p < 0.001$; ACC (M = 4.74, SD = 8.49, 95% CI [2.99, 6.49]), $t(92) = 5.38$, $p < 0.001$; Left AI (M = 2.71, SD = 6.43, 95% CI [1.38, 4.03]), $t(92) = 4.06$, $p < 0.001$; Right AI (M = 2.32, SD = 5.47, 95% CI [1.19, 3.44]), $t(92) = 4.08$, $p < 0.001$. However, when regressing BMI and HEI on the parameter estimates from the vmPFC and aVS ROIs, we did not find a significant model fit, nor were any of the individual partial regression coefficients significantly related to BMI or HEI, even when controlling for hunger level and time since the last meal (all $p > 0.14$; **Table 1A**). Bayes Factor for each model overall indicated moderate evidence in favor of the null hypothesis, $BF_{10} = 0.15$ and.18 for BMI and HEI, respectively, suggesting that BMI and HEI may not be

TABLE 1 | Regression tables for **(A)** the relationship between overall neurocognitive valuation in the vmPFC and aVS with BMI and HEI, respectively; **(B)** the relationship between self-reported bids for healthy foods, unhealthy foods, and their interaction with BMI and HEI, respectively; **(C)** the relationship between neurocognitive valuation in the vmPFC and aVS combined parameter estimates for healthy foods, unhealthy foods, and their interaction with BMI and HEI, respectively.

Model	Variable	B	SE	95% CI	β	*t*	*p*
A) RELATIONSHIP WITH OVERALL NEUROCOGNITIVE FOOD VALUATION							
BMI = vmPFC + aVS							
0	Intercept	30.989	0.554	29.89, 32.09		55.958	<0.001
	vmPFC	0.073	0.061	−0.05, 0.19	0.143	1.199	0.234
	aVS	−0.002	0.084	−0.17, 0.17	−0.003	−0.028	0.978
Model summary: $F_{(2, 90)} = 0.92$, $p = 0.40$, R squared = 0.02							
HEI = vmPFC + aVS							
0	Intercept	58.5	1.88	54.77, 62.23		31.19	<0.001
	vmPFC	0.16	0.21	−0.25, 0.56	0.09	0.76	0.45
	aVS	−0.42	0.29	−0.99, 0.14	−0.18	−1.48	0.14
Model summary: $F_{(2, 89)} = 1.10$, $p = 0.34$, R squared = 0.024							
B) RELATIONSHIP WITH SELF-REPORTED VALUE (BIDS) BY FOOD TYPE							
BMI = Healthy + Unhealthy + Interaction							
0	Intercept	30.43	1.43	27.60, 33.27		21.31	<0.001
	Healthy	−0.21	1.4	−2.99, 2.58	−0.016	−0.15	0.88
	Unhealthy	1.82	1.26	−0.69, 4.32	0.16	1.44	0.15
Model summary: $F_{(2, 90)} = 1.07$, $p = 0.35$, R squared = 0.023							
1	Intercept	29.53	3.25	23.07, 35.98		9.09	<0.001
	Healthy	0.71	3.26	−5.78, 7.19	0.05	0.22	0.83
	Unhealthy	3.23	4.73	−6.15, 12.62	0.28	0.69	0.5
	Interaction	−1.38	4.42	−10.15, 7.40	−0.16	−0.31	0.76
Model summary: $F_{(3, 89)} = 0.74$, $p = 0.53$, R squared = 0.024							
R squared change = 0.001, $p = 0.76$							
HEI = Healthy + Unhealthy + Interaction							
0	Intercept	59.62	4.61	50.45, 68.78		12.92	<0.001
	Healthy	6.89	4.52	−2.09, 15.87	0.16	1.53	0.13
	Unhealthy	−13.48	4.08	−21.60, −5.37	−0.34	−3.30	0.001
Model summary: $F_{(2, 89)} = 5.68$, $p = 0.005$, R squared = 0.113							
1	Intercept	57.47	10.49	36.62, 78.31		5.48	<0.001
	Healthy	9.07	10.54	−11.87, 30.01	0.21	0.86	0.39
	Unhealthy	−10.12	15.27	−40.46, 20.22	−0.26	−0.66	0.51
	Interaction	−3.26	14.26	−31.60, 25.08	−0.11	−0.23	0.82
Model summary: $F_{(3, 88)} = 3.76$, $p = 0.014$, R squared = 0.114							
R squared change = 0.001, $p = 0.82$							
C) RELATIONSHIP WITH NEUROCOGNITIVE VALUATION BY FOOD TYPE							
BMI = Healthy + Unhealthy + Interaction							
0	Intercept	30.86	0.57	29.73, 31.99		54.39	<0.001
	Healthy	0.04	0.04	−0.05, 0.13	0.1	0.91	0.37
	Unhealthy	0.06	0.03	−0.02, 0.14	0.16	1.53	0.13
Model summary: $F_{(2, 90)} = 1.37$, $p = 0.26$, R squared = 0.03							
1	Intercept	31.14	0.62	29.90, 32.38		49.99	<0.001
	Healthy	0.01	0.05	−0.09, 0.11	0.03	0.24	0.81
	Unhealthy	0.03	0.05	−0.06, 0.13	0.09	0.68	0.5
	Interaction	0.004	0.003	−0.003, 0.01	0.14	1.08	0.28
Model summary: $F_{(3, 89)} = 1.30$, $p = 0.28$, R squared = 0.04							
R squared change = 0.013, $p = 0.28$							

(Continued)

TABLE 1 | Continued

Model	Variable	B	SE	95% CI	β	*t*	*p*
HEI = Healthy + Unhealthy + Interaction							
0	Intercept	57.17	1.96	54.28, 61.06		29.22	<0.001
	Healthy	0.03	0.15	−0.26, 0.33	0.02	0.22	0.83
	Unhealthy	0.02	0.14	−0.25, 0.29	0.02	0.14	0.89
Model summary: $F_{(2, 89)} = 0.03$, $p = 0.97$, R squared = 0.001							
1	Intercept	54.78	2.07	50.66, 58.90		26.43	<0.001
	Healthy	0.27	0.17	−0.06, 0.58	0.19	1.6	0.11
	Unhealthy	0.26	0.16	−0.05, 0.57	0.21	1.65	0.1
	Interaction	−0.032	0.01	−0.06, −0.009	−0.37	−2.78	0.007
Model summary: $F_{(3, 88)} = 2.60$, $p = 0.057$, R squared = 0.081							
R squared change = 0.285, $p = 0.007$							

related to the functioning of the valuation system when making decisions about foods in general.

Whole-Brain Analyses

The whole-brain search for regions linearly related to subjective value confirmed the involvement of our *a priori* ROIs, and additionally revealed an extended network of brain regions that showed a positive linear relationship with self-reported value. These included a cluster traversing much of the cingulate cortex, large swaths of medial and lateral PFC, dorsal attention network regions, the ventral visual stream, and dorsal and ventral portions of the striatum. We also observed negative relationships between subjective value and the BOLD response in the left visual cortex and bilateral somatosensory cortices (**Figure 4A**, **Table 2A**). Finally, a whole-brain search of brain areas showing a relationship with BMI and HEI revealed no significant clusters.

Valuation by Food Type

Behavioral

Behaviorally, we did not find a significant relationship when regressing BMI on the averaged bid value for healthy and unhealthy foods, nor when the interaction was included, $p >$ 0.35. Bayes Factor suggested strong evidence in favor of the null hypothesis for the model including the interaction term, $BF_{10} = 0.07$, indicating that it is quite likely that there truly is no relationship. When regressing HEI on the averaged bid values for healthy and unhealthy foods, we did find a significant relationship, $F_{(2, 89)} = 5.68$, $p = 0.005$, $R^2 = 0.11$. Partial model coefficients indicate that this effect was driven by a negative relationship between HEI and unhealthy food bids, B = −13.48, SE = 4.08, 95% CI [−21.60, −5.37], $t = -3.30$, $p = 0.001$ (**Figure 2**; **Table 1B**), suggesting that participants who bid higher for unhealthy foods ate less healthily in the real world. The inclusion of the interaction term in the second step of this model did not significantly add to the variance explained, $p = 0.82$, further suggesting that this effect is specific just to bids for unhealthy foods.

ROI Analyses

When comparing the parameter estimates for valuation of healthy > unhealthy foods within each of our *a priori* ROIs, the vmPFC showed a stronger relationship (i.e., larger beta value) for healthy compared to unhealthy foods, $M_{diff} = 5.31$, SD = 21.53, 95% CI [0.88, 9.75], $t(92) = 2.38$, $p = 0.02$ (**Figure 3A**), while there was no such difference in the aVS, $p = 0.12$ (**Figure 3B**). This suggests that, while the aVS tracked value for both food categories relatively equally, the coupling of self-reported value and corresponding BOLD response in the vmPFC was stronger for healthy foods, possibly due to the integration of non-desire related value inputs.

We did not find a significant relationship when regressing BMI on our neurocognitive measures of valuation for healthy and unhealthy foods, even when including the interaction term, $p >$0.26. Bayes Factor of the model including the interaction term suggested moderate evidence in favor of the null hypothesis, $BF_{10} = 0.13$. When regressing HEI on these measures, the model including the interaction term to predict HEI showed a trending effect, $F_{(3, 88)} = 2.60$, $p = 0.057$, $R^2 = 0.08$. Partial model coefficients indicated that this effect was driven by the interaction term, B = −0.03, SE = 0.01, 95% CI [−0.06, −0.01], $t = -2.78$, $p = 0.007$ (**Table 1C**). Using median split to probe the direction of the interaction revealed that participants who exhibited high parameter estimates (i.e., stronger coupling between self-reported value and corresponding BOLD response) for healthy foods *and* low parameter estimates for unhealthy foods reported eating healthier in the real world than participants who had high parameter estimates for both food categories, while participants exhibiting low parameter estimates for healthy foods did not show differences in their healthy eating regardless (**Figure 3C**). Follow-up, exploratory regression models that separated out the ROIs suggested that valuation of the food types in the vmPFC largely contributed to this effect, $F_{(3, 88)} = 2.20$, $p = 0.094$, $R^2 = 0.07$, again driven by the interaction term, B = −0.01, SE = 0.01, 95% CI [−0.02, −0.002], $t = -2.29$, $p = 0.024$, while the regression model of just aVS showed no such effect, p =0.7. Together, these results suggest that, rather than either food category alone, it is the neurocognitive valuation of both healthy *and* unhealthy foods that relates to real world eating behavior.

TABLE 2 | Clusters from whole-brain results for a) overall valuation, and b) reactivity by food type.

Region	Side	Cluster *k*	Peak *t*	MNI Coordinates (center)		
				x	y	z
A) ALL FOODS VALUATION, $p < 0.001$, k = 119						
Positive relationship w/self-reported value						
Postcentral gyrus (peak)*	L	29,602	8.92	−42	−24	58
Inferior parietal lobule-angular gyrus	R	1,950	6.11	43.2	−50.6	49.4
Inferior temporal gyrus	L	1,175	9.25	−59.8	−49.2	−13.2
Cerebellum	L	1,070	5.57	−38.3	−66	−41.5
Inferior temporal gyrus	R	921	6.66	59.5	−46.1	−15.2
Middle frontal gyrus	R	659	7.58	45.8	42.6	14.7
Inferior frontal gyrus-opercularis	R	449	5.89	51.1	10.1	20.3
Superior frontal gyrus	R	402	4.31	29.9	15.2	57.3
Anterior insula	R	135	6.14	36.5	20.1	−0.2
Negative relationship w/self-reported value						
Lingual gyrus, visual cortex	L	1,426	−10.58	−10.9	−85.5	−8.5
Precentral gyrus	R	505	−6.91	51.7	−11.2	46.8
Postcentral gyrus	L	501	−12.96	−48.2	−16.8	48.3
Postcentral gyrus	R	162	−4.33	24.8	−37.2	67.5
B) FOOD-CUE REACTIVITY, $p < 0.001$, k = 119						
Healthy > Unhealthy						
Superior-inferior parietal lobule	L	2,681	5.81	−32.7	−65.7	46.3
Dorsolateral prefrontal cortex	L	2,535	5.35	−52	12	30
Inferior temporal gyrus	L	1,256	7.76	−55.7	−57.5	−10
Angular gyrus	R	1,239	3.84	34.3	−63	44.4
Inferior temporal gyrus	R	1,168	7.04	54.7	−56.8	−12.7
Inferior frontal gyrus-opercularis	R	440	5.01	45.6	9.7	27.9
Supplementary motor area	L	427	5.05	−1	18.2	51.7
Inferior frontal gyrus-triangularis	R	281	4.68	47.2	36.3	15.1
Cerebellum	R	246	5.97	35.9	−70.3	−51.7
Precuneus	L	205	5.75	−5.5	−55.1	9.8
Cerebellum	R	121	5.29	34.3	−64.8	−29.6
Unhealthy > Healthy						
Calcarine gyrus, visual cortex	L	8,119	−16	−4.1	−90.4	−4.4
Middle cingulate	R	289	−4.95	2.1	−20.4	42
Postcentral gyrus	L	267	−6.09	−46.9	−17.1	47.3
Middle frontal gyrus	R	215	−4.24	26.4	56	23.2
Temporal pole	R	150	−4.44	58	14	−4
Middle temporal gyrus	R	135	−3.71	63.6	−23.2	−6.7

**One contiguous cluster that spans most of the left parietal lobe, most of the cingulate gyrus, much of the mPFC, left dlPFC, left AI, most of the striatum, parts of the hippocampus, and brain stem.*

Whole-Brain Analyses

The whole-brain contrast between the valuation of healthy vs. unhealthy foods revealed no significant clusters at our predetermined threshold of $p < 0.001$, k = 119. However, when relaxing the threshold to an uncorrected $p < 0.005$, k = 300, we found clusters in the vmPFC and pre-SMA, which provide converging evidence with our ROI analysis that the vmPFC shows a stronger relationship for healthy vs. unhealthy foods (**Figure 3A**, green). A whole-brain search looking for relationships between this contrast and BMI revealed no significant clusters, nor did the whole-brain search for HEI.

Replication Attempt

In our attempt to provide a conceptual replication of Verdejo-Román and colleagues (2017) who contrasted reactivity to palatable > unpalatable foods, we contrasted reactivity to unhealthy > healthy foods, but we did not find similar results. The unhealthy > healthy contrast showed considerable activation in the visual cortex, posterior to mid-cingulate, central sulcus, and anterior portion of the right middle frontal gyrus. The healthy > unhealthy contrast revealed extended activation traversing the dorsal attention network into bilateral dlPFC and IFG, bilateral regions of the dorsal and ventral visual

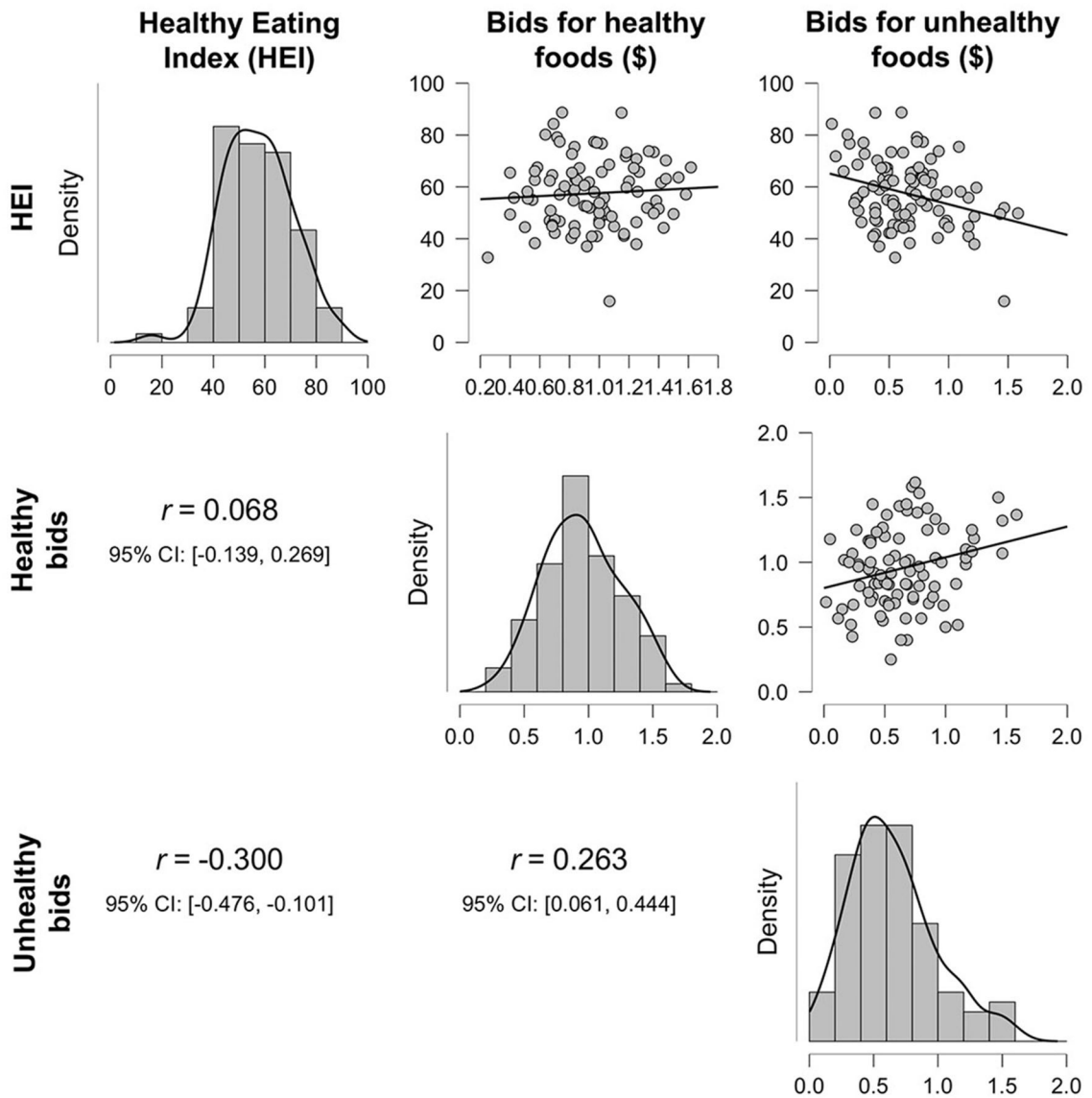

FIGURE 2 | Density plots and correlations between the healthy eating index (HEI), average bid amounts for healthy foods, and average bid amounts for unhealthy foods.

streams, supplementary motor area, and precuneus (**Figure 4B**; **Table 2B**). While lateral prefrontal activation was reported by Verdejo-Román et al. (2017), our result is in the opposite direction of what would qualify as a conceptual replication, such that they reported this cluster for the unpalatable > palatable contrast, while we found this for the healthy > unhealthy contrast. We also were unable to replicate their findings when comparing obese > overweight individuals for this contrast, such that we found no significant clusters, even when using very liberal thresholds. Moreover, we conducted an exploratory whole-brain search of BMI on the healthy > unhealthy contrast, and still found no significant clusters.

DISCUSSION

The current study provides the first examination of how subjective valuation of food items relates to BMI and healthy eating in a sample of early middle-aged, higher BMI adults motivated to eat more healthily. Our findings suggest normative functioning in the brain's valuation system during food-based decision making, such that there were robust linear relationships between self-reported value of food items and the corresponding BOLD response in the vmPFC, aVS, bilateral AI, and the ACC when making decisions about snack food items. Further, we found moderate evidence in favor of a null relationship between

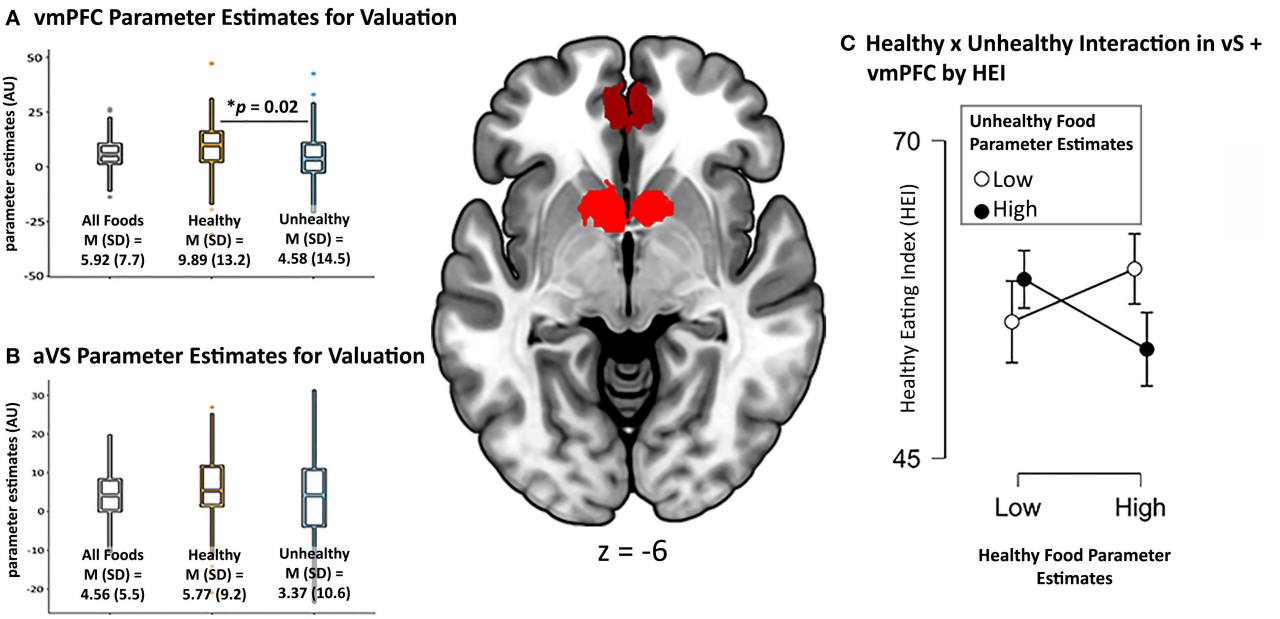

FIGURE 3 | vmPFC and aVS ROIs used in analysis pictured in center image. Parameter estimates in arbitrary units (AU) of overall valuation of all foods, healthy foods, and unhealthy foods from **(A)** vmPFC and **(B)** aVS. The interaction between valuation for healthy and unhealthy foods, and its relation to healthy eating **(C)** plotted using median split of the vmPFC + VS combined parameter estimates of healthy and unhealthy foods (even though data are continuous).

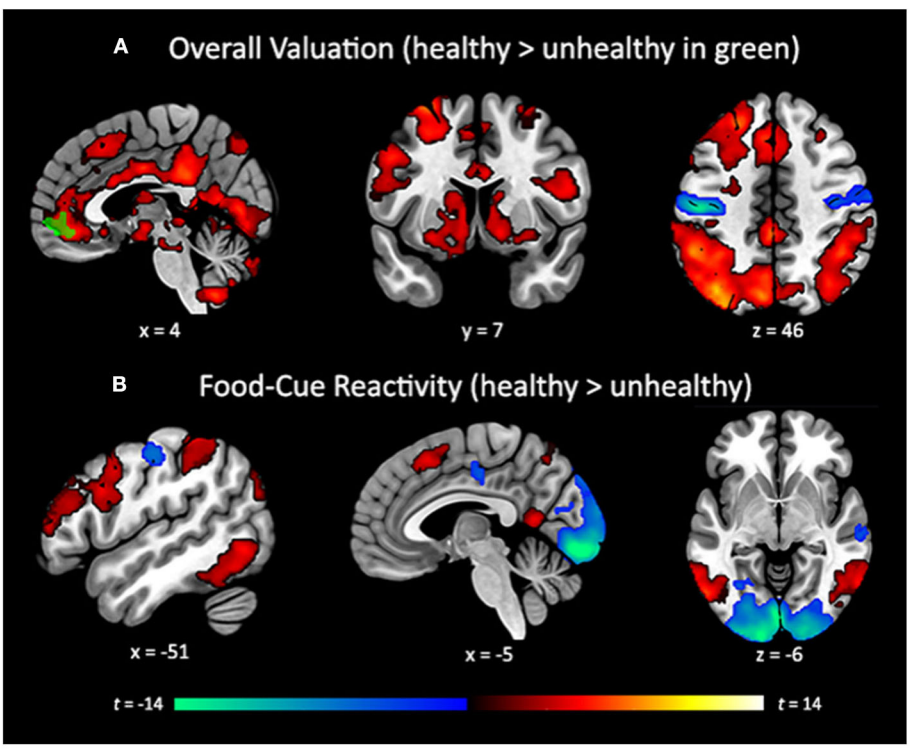

FIGURE 4 | (A) Whole-brain search of subjective valuation for all foods with positive (hot colors) and negative (cold colors) coupling between bid value and corresponding BOLD response (cluster corrected $p < 0.05$). vmPFC cluster (green) showing greater coupling for healthy than unhealthy foods ($p < 0.005$, k = 300, uncorrected). **(B)** Whole-brain contrast between reactivity for healthy (hot colors) and unhealthy foods (cold colors) not accounting for bid value (cluster corrected $p <$ 0.05). Cluster correction of $p < 0.001$, k = 119 to achieve a whole-brain familywise error rate of $\alpha = 0.05$.

our estimates of overall valuation with both BMI and HEI. Together, these findings add to the health neuroscience literature by suggesting that higher BMI individuals do not display biases in the neurocognitive substrates of subjective valuation, and that the general functioning of this system may not relate to BMI or healthy eating. When examining differences in the self-reported valuation of healthy and unhealthy foods, our results indicate that self-reported valuation of unhealthy foods is inversely related to real world healthy eating, but we found no relationship for the valuation of either food type with BMI. This finding echoes prior work demonstrating a relationship between unhealthy eating behavior and reactivity to unhealthy food cues (Tetley et al., 2009), and suggests that valuation may be an important factor underlying this relationship (Cosme and Lopez, 2020). Moreover, this highlights the importance of regulation strategies that target the devaluation of unhealthy foods, whether by reappraisal or other down-regulation strategies (Giuliani et al., 2014).

Interestingly, despite reporting higher overall value for healthy compared to unhealthy foods (Cosme et al., 2019), we found no relationship with the self-reported valuation of healthy foods and real-world healthy eating behavior or BMI. One possibility is that the motivation of people in this sample, who volunteered for a healthy eating study, to eat more healthily might have contributed to higher self-reported value for healthy foods, whereas the self-reported value of unhealthy foods tracked with an elevated craving for unhealthy foods that more strongly predict real-world eating behavior when considering only self-report data. This interpretation is in line with the value-based models of health-oriented behavior that point to the vmPFC as a hub where various motivational factors are integrated (Berkman, 2018), and is partially supported by our neuroimaging findings that demonstrate a stronger coupling between self-reported value and BOLD response in the vmPFC for healthy compared to unhealthy foods overall. Importantly, the interaction between the valuation process for healthy and unhealthy foods in this region is related to healthy eating, such that the participants who show higher neurocognitive coupling for healthy foods *and* lower coupling for unhealthy foods exhibited the healthiest eating. However, these findings need to be validated by future work given that our full model was only marginally significant. Nonetheless, these findings suggest that the vmPFC may integrate health motivations during the subjective valuation of healthy foods, and the interaction between valuation of healthy and unhealthy foods predicts healthy eating. Future research should also obtain quantitative measures of health motivation to better test the value integration model.

We were unable to replicate the findings of Verdejo-Román et al. (2017), which showed greater activation in subcortical reward circuitry, and medial and lateral portions of the prefrontal cortex when contrasting palatable vs. unpalatable foods. The motivation for this replication attempt relied on the assumption that palatability is inversely related to healthiness, such that unhealthy foods are more palatable (e.g., pizza), while healthy foods are less palatable (e.g., whole-grain oats). However, it is not necessarily the case that food healthiness relates to its palatability. Indeed, many of the healthy food items used as stimuli in the willingness-to-pay task were pictured in appealing ways (e.g., a bunch of fresh grapes), while some of the unhealthy items were less so (e.g., a bag of chips). A better approach would have been to re-categorize our stimuli based on palatability ratings rather than using our existing categories of healthy and unhealthy foods. Another promising direction for future research would be to examine the nutritional content of food stimuli as it relates to food-cue reactivity and the subjective valuation process. Recent work has demonstrated that different areas of the prefrontal cortex can track caloric density (Tang et al., 2014) and represent macro-nutrients (Suzuki et al., 2017), while the combination of fat and carbohydrates have supra-additive effects on striatal response (DiFeliceantonio et al., 2018). By quantifying the various dimensions of food stimuli that are encoded by the brain, we can gain a more complete picture of the neural mechanisms underlying weight and eating behavior. Thus, while we were unable to provide converging evidence for the neural systems that are sensitive to palatability as reported by Verdejo-Román and colleagues (2017), it is likely due to a mismatch the dimensions of health and palatability.

Our healthy food-cue reactivity contrast did demonstrate greater activity in lateral prefrontal, dorsal attention, and higher order visual processing regions, while unhealthy foods elicited greater activity in primary visual and somatosensory regions. These findings suggest that healthy foods engaged higher order, top-down processing networks, while unhealthy foods caused reactivity in bottom-up perceptual systems. The engagement of top-down processing may be due to the fact that our sample was motivated to eat more healthily, and therefore engaged more effortful deliberation when making decisions about healthy foods. This interpretation is line with studies showing the engagement of these regions during regulatory processes (see Buhle et al., 2014 for meta-analysis). The pattern of activation for unhealthy foods mirrors the results from traditional studies of food-cue reactivity (Murdaugh et al., 2012).

It is noteworthy that, throughout all our analyses, we found no relationships between brain activity and BMI, which is similar to results from other experiments in this sample (Giuliani et al., 2020). While researchers have argued for better measures of obesity as it relates to health (Ahima and Lazar, 2013), there are a number of reasons we do not see a relationship between BMI and brain response in the valuation system as reported in other studies (e.g., Petit et al., 2016). First, this may be due entirely to the fact that we were studying a sample that desired to eat more healthily, thus the self-reported and neural responses we observed might not be comparable to what has been reported in prior literature. This interpretation is supported by research showing that when individuals attend to the health aspects of food, it improves dietary choice and modulates the neural responses associated with the valuation process (Hare et al., 2011). Thus, it is likely that people in our sample—who were motivated to eat more healthily and who enrolled in a healthy eating study—were more attentive to food

healthiness. However, there are no studies to our knowledge that have examined healthy eating motivation as mediator between BMI and brain response to food cues, so this interpretation requires further investigation. Another major shortcoming that may have contributed to this null result is the fact that the current study did not include healthy-weight controls. Thus, the restricted range of BMI we investigated may have reduced the variability needed to uncover the relationship with BMI reported in previous literature. Relatedly, it is possible that there are categorical differences between healthy-weight and higher BMI individuals in how they process food stimuli, as suggested by the food addiction model (Volkow et al., 2013b), which may further obscure a relationship with weight. Finally, it is possible that these null results were due to measurement error, since we measured participant weight in the lab. Because we did not have a clinical setting to provide lightweight scrubs to all participants, combined with the fact that these data were collected on a rolling basis over the course of 2 years, differences in clothing weight across the seasons may have contributed unsystematic noise to our measurement of weight, and, consequently, BMI.

Taken together, the current study adds to the health neuroscience literature by demonstrating both significant *and* null findings across a set of well-motivated, pre-registered analyses. We provide evidence that higher BMI individuals exhibit normative coupling between self-reported value and corresponding BOLD response. These individuals also show meaningful relations between value-related brain activation and eating patterns. These results add to the knowledge base on how people with higher BMI process and relate to food stimuli. The null results are equally informative to the literature in this area. Interestingly, the neurocognitive measures of food valuation do not relate to BMI or healthy eating behaviors. The lack of a relation provides a possible explanation for why such a relationship has not been reported in prior work. Moreover, we demonstrated a potential mechanism that contributes to real-world eating behavior—the valuation of healthy and unhealthy foods. These findings direct future research toward further examinations of motivational factors and food-cue information that are integrated in the vmPFC during food-based decision making, and suggest that interventions should target both the up-valuation of healthy foods and down-valuation of unhealthy foods, rather than focusing on one or the other exclusively.

DATA AVAILABILITY STATEMENT

The datasets generated for this study can be found in online repositories. The names of the repository/repositories and accession number(s) can be found at: https://neurovault.org/collections/GDNZHILR/.

ETHICS STATEMENT

The studies involving human participants were reviewed and approved by Institutional Review Board at the University of Oregon. The patients/participants provided their written informed consent to participate in this study.

AUTHOR CONTRIBUTIONS

NG and EB designed the study. JM, BD, and NG collected the data. JM and DC analyzed the data. JM wrote the manuscript and created the figures. NG, DC, BD, and EB provided edits. All authors contributed to the article and approved the submitted version.

FUNDING

This research was supported by grants from the National Cancer Institute CA211224 and CA175241.

REFERENCES

Abarca-Gómez, L., Abdeen, Z. A., Hamid, Z. A., Abu-Rmeileh, N. M., Acosta-Cazares, B., Acuin, C., et al. (2017). Worldwide trends in body-mass index, underweight, overweight, and obesity from 1975 to 2016: a pooled analysis of 2416 population-based measurement studies in 128·9 million children, adolescents, and adults. *Lancet* 390, 2627–2642. doi: 10.1016/S0140-6736(17)32129-3

Ahima, R. S., and Lazar, M. A. (2013). The health risk of obesity—better metrics imperative. *Science* 341, 856–858. doi: 10.1126/science.1241244

Bartra, O., McGuire, J. T., and Kable, J. W. (2013). The valuation system: a coordinate-based meta-analysis of BOLD fMRI experiments examining neural correlates of subjective value. *Neuroimage* 76, 412–427. doi: 10.1016/j.neuroimage.2013.02.063

Becker, G. M., Degroot, M. H., and Marschak, J. (1964). Measuring utility by a single-response sequential method. *Behav. Sci.* 9, 226–232. doi: 10.1002/bs.3830090304

Berkman, E. T. (2018). Value-based choice: an integrative, neuroscience-informed model of health goals. *Psychol. Health* 33, 40–57. doi: 10.1080/08870446.2017.1316847

Berkman, E. T., Hutcherson, C. A., Livingston, J. L., Kahn, L. E., and Inzlicht, M. (2017a). Self-control as value-based choice. *Curr. Dir. Psychol. Sci.* 26, 422–428. doi: 10.1177/0963721417704394

Berkman, E. T., Livingston, J. L., and Kahn, L. E. (2017b). Finding the "self" in self-regulation: the identity-value model. *Psychol. Inquiry* 28, 77–98. doi: 10.1080/1047840X.2017.1323463

Boswell, R. G., and Kober, H. (2016). Food cue reactivity and craving predict eating and weight gain: a meta-analytic review. *Obes. Rev.* 17, 159–177. doi: 10.1111/obr.12354

Brainard, D. H. (1997). The psychophysics toolbox. *Spat. Vis.* 10, 433–436. doi: 10.1163/156856897X00357

Buhle, J. T., Silvers, J. A., Wager, T. D., Lopez, R., Onyemekwu, C., Kober, H., et al. (2014). Cognitive reappraisal of emotion: a meta-analysis of human neuroimaging studies. *Cereb. Cortex* 24, 2981–2990. doi: 10.1093/cercor/bht154

Chib, V. S., Rangel, A., Shimojo, S., and O'Doherty, J. P. (2009). Evidence for a common representation of decision values for dissimilar goods in human ventromedial prefrontal cortex. *J. Neurosci.* 29, 12315–12320. doi: 10.1523/JNEUROSCI.2575-09.2009

Contreras-Rodriguez, O., Mata, F., Verdejo-Román, J., Ramírez-Bernabé, R., Moreno, D., Vilar-Lopez, R., et al. (2020). Neural-based valuation of functional foods among lean and obese individuals. *Nutr. Res.* 78, 27–35. doi: 10.1016/j.nutres.2020.03.006

Cosme, D., Flournoy, J. C., and Vijayakumar, N. (2018). *Auto-Motion-Fmriprep: A Tool for Automated Assessment of Motion Artifacts (v1.0) [Computer Software]*. Zenodo. doi: 10.5281/zenodo.1412131

Cosme, D., and Lopez, R.B., (2020). Neural indicators of food cue reactivity, regulation, and valuation and their associations with body composition and daily eating behavior. *Soc. Cogn. Affect. Neurosci.* nsaa155. doi: 10.31234/osf.io/23mu5

Cosme, D., Ludwig, R. M., and Berkman, E. T. (2019). Comparing two neurocognitive models of self-control during dietary decisions. *Soc. Cogn. Affect. Neurosci.* 14, 957–966. doi: 10.1093/scan/nsz068

Cox, R. W. (1996). AFNI: software for analysis and visualization of functional magnetic resonance neuroimages. *Comput. Biomed. Res.* 29, 162–173. doi: 10.1006/cbmr.1996.0014

Demos, K. E., Heatherton, T. F., and Kelley, W. M. (2012). Individual differences in nucleus accumbens activity to food and sexual images predict weight gain and sexual behavior. *J. Neurosci.* 32, 5549–5552. doi: 10.1523/JNEUROSCI.5958-11.2012

DiFeliceantonio, A. G., Coppin, G., Rigoux, L., Edwin Thanarajah, S., Dagher, A., Tittgemeyer, M., et al. (2018). Supra-additive effects of combining fat and carbohydrate on food reward. *Cell Metab.* 28, 33–44.e3. doi: 10.1016/j.cmet.2018.05.018

Duckworth, A. L. (2011). The significance of self-control. *Proc. Natl. Acad. Sci. U.S.A.* 108, 2639–2640. doi: 10.1073/pnas.1019725108

Esteban, O., Markiewicz, C. J., Blair, R. W., Moodie, C. A., Isik, A. I., Erramuzpe, A., et al. (2019). fMRIPrep: a robust preprocessing pipeline for functional MRI. *Nat. Methods* 16, 111–116. doi: 10.1038/s41592-018-0235-4

Giuliani, N. R., Cosme, D., Merchant, J. S., Dirks, B., and Berkman, E. T. (2020). Brain activity associated with regulating food cravings predicts changes in self-reported food craving and consumption over time. *Front. Hum. Neurosci.* 14:577669. doi: 10.3389/fnhum.2020.577669

Giuliani, N. R., Mann, T., Tomiyama, A. J., and Berkman, E. T. (2014). Neural systems underlying the reappraisal of personally craved foods. *J. Cogn. Neurosci.* 26, 1390–1402. doi: 10.1162/jocn_a_00563

Giuliani, N. R., Merchant, J. S., Cosme, D., and Berkman, E. T. (2018). Neural predictors of eating behavior and dietary change. *Ann. N. Y. Acad. Sci.* 1428, 208–220. doi: 10.1111/nyas.13637

Guenther, P. M., Casavale, K. O., Reedy, J., Kirkpatrick, S. I., Hiza, H. A. B., Kuczynski, K. J., et al. (2013). Update of the healthy eating index: HEI-2010. *J. Acad. Nutr. Diet* 113, 569–580. doi: 10.1016/j.jand.2012.12.016

Gunes, F. E., Bekiroglu, N., Imeryuz, N., and Agirbasli, M. (2012). Relation between eating habits and a high body mass index among freshman students: a cross-sectional study. *J. Am. Coll. Nutr.* 31, 167–174. doi: 10.1080/07315724.2012.10720024

Hales, C. M., Carroll, M. D., Fryar, C. D., and Ogden, C. L. (2020). Prevalence of obesity and severe obesity among adults: United States, 2017-2018. *NCHS Data Brief* 360, 1–8.

Harding, I. H., Andrews, Z. B., Mata, F., Orlandea, S., Martínez-Zalacaín, I., Soriano-Mas, C., et al. (2018). Brain substrates of unhealthy versus healthy food choices: influence of homeostatic status and body mass index. *Int. J. Obes.* 42, 448–454. doi: 10.1038/ijo.2017.237

Hare, T. A., Malmaud, J., and Rangel, A. (2011). Focusing attention on the health aspects of foods changes value signals in vmPFC and improves dietary choice. *J. Neurosci.* 31, 11077–11087. doi: 10.1523/JNEUROSCI.6383-10.2011

Howden, E. J., Sarma, S., Lawley Justin, S., Opondo, M., Cornwell, W., Stoller, D., et al. (2018). Reversing the cardiac effects of sedentary aging in middle age—a randomized controlled trial. *Circulation* 137, 1549–1560. doi: 10.1161/CIRCULATIONAHA.117.030617

Hutcherson, C. A., Plassmann, H., Gross, J. J., and Rangel, A. (2012). Cognitive regulation during decision making shifts behavioral control between ventromedial and dorsolateral prefrontal value systems. *J. Neurosci.* 32, 13543–13554. doi: 10.1523/JNEUROSCI.6387-11.2012

Kohl, S. H., Veit, R., Spetter, M. S., Günther, A., Rina, A., Lührs, M., et al. (2019). Real-time fMRI neurofeedback training to improve eating behavior by self-regulation of the dorsolateral prefrontal cortex: a randomized controlled trial in overweight and obese subjects. *Neuroimage* 191, 596–609. doi: 10.1016/j.neuroimage.2019.02.033

Kroemer, N. B., Sun, X., Veldhuizen, M. G., Babbs, A. E., de Araujo, I. E., and Small, D. M. (2016). Weighing the evidence: variance in brain responses to milkshake receipt is predictive of eating behavior. *Neuroimage* 128, 273–283. doi: 10.1016/j.neuroimage.2015.12.031

Lawrence, N. S., Hinton, E. C., Parkinson, J. A., and Lawrence, A. D. (2012). Nucleus accumbens response to food cues predicts subsequent snack consumption in women and increased body mass index in those with reduced self-control. *Neuroimage* 63, 415–422. doi: 10.1016/j.neuroimage.2012.06.070

Lee, M. D., and Wagenmakers, E.-J. (2014). *Bayesian Cognitive Modeling: A Practical Course*. Cambridge: Cambridge University Press.

Medley, M. L. (1980). Life satisfaction across four stages of adult life. *Int. J. Aging Hum. Dev.* 11, 193–209. doi: 10.2190/D4LG-ALJQ-8850-GYDV

Murdaugh, D. L., Cox, J. E., Cook, E. W., and Weller, R. E. (2012). FMRI reactivity to high-calorie food pictures predicts short- and long-term outcome in a weight-loss program. *Neuroimage* 59, 2709–2721. doi: 10.1016/j.neuroimage.2011.10.071

Peeters, A., Barendregt, J. J., Willekens, F., Mackenbach, J. P., Al Mamun, A., Bonneux, L., et al. (2003). Obesity in adulthood and its consequences for life expectancy: a life-table analysis. *Ann. Intern. Med.* 138, 24–32. doi: 10.7326/0003-4819-138-1-200301070-00008

Petit, O., Merunka, D., Anton, J.-L., Nazarian, B., Spence, C., Cheok, A. D., et al. (2016). Health and pleasure in consumers' dietary food choices: individual differences in the brain's value system. *PLoS ONE* 11:e0156333. doi: 10.1371/journal.pone.0156333

Plassmann, H., O'Doherty, J., and Rangel, A. (2007). Orbitofrontal cortex encodes willingness to pay in everyday economic transactions. *J. Neurosci.* 27, 9984–9988. doi: 10.1523/JNEUROSCI.2131-07.2007

Rangel, A. (2013). Regulation of dietary choice by the decision-making circuitry. *Nat. Neurosci.* 16, 1717–1724. doi: 10.1038/nn.3561

Samanez-Larkin, G. R., and Knutson, B. (2015). Decision making in the ageing brain: changes in affective and motivational circuits. *Nat. Rev. Neurosci.* 16, 278–289. doi: 10.1038/nrn3917

Smeets, P. A. M., Charbonnier, L., van Meer, F., van der Laan, L. N., and Spetter, M. S. (2012). Food-induced brain responses and eating behaviour. *Proc. Nutr. Soc.* 71, 511–520. doi: 10.1017/S0029665112000808

Smith, D. G., and Robbins, T. W. (2013). The neurobiological underpinnings of obesity and binge eating: a rationale for adopting the food addiction model. *Biol. Psychiatry* 73, 804–810. doi: 10.1016/j.biopsych.2012.08.026

Spetter, M. S., Malekshahi, R., Birbaumer, N., Lührs, M., van der Veer, A. H., Scheffler, K., et al. (2017). Volitional regulation of brain responses to food stimuli in overweight and obese subjects: a real-time fMRI feedback study. *Appetite* 112, 188–195. doi: 10.1016/j.appet.2017.01.032

Stice, E., and Yokum, S. (2018). Relation of neural response to palatable food tastes and images to future weight gain: using bootstrap sampling to examine replicability of neuroimaging findings. *Neuroimage* 183, 522–531. doi: 10.1016/j.neuroimage.2018.08.035

Subar, A. F., Kirkpatrick, S. I., Mittl, B., Zimmerman, T. P., Thompson, F. E., Bingley, C., et al. (2012). The automated self-administered 24-hour dietary recall (ASA24): a resource for researchers, clinicians, and educators from the National Cancer Institute. *J. Acad. Nutr. Diet.* 112, 1134–1137. doi: 10.1016/j.jand.2012.04.016

Suzuki, S., Cross, L., and O'Doherty, J. P. (2017). Elucidating the underlying components of food valuation in the human orbitofrontal cortex. *Nat. Neurosci.* 20, 1780–1786. doi: 10.1038/s41593-017-0008-x

Tang, D. W., Fellows, L. K., and Dagher, A. (2014). Behavioral and neural valuation of foods is driven by implicit knowledge of caloric content. *Psychol. Sci.* 25, 2168–2176. doi: 10.1177/0956797614552081

Tetley, A., Brunstrom, J., and Griffiths, P. (2009). Individual differences in food-cue reactivity. The role of BMI and everyday portion-size selections. *Appetite* 52, 614–620. doi: 10.1016/j.appet.2009.02.005

Tusche, A., and Hutcherson, C. A. (2018). Cognitive regulation alters social and dietary choice by changing attribute representations in domain-general and domain-specific brain circuits. *Elife* 7:e31185. doi: 10.7554/eLife.31185.030

Verdejo-Román, J., Vilar-López, R., Navas, J. F., Soriano-Mas, C., and Verdejo-García, A. (2017). Brain reward system's alterations in response to food and

monetary stimuli in overweight and obese individuals. *Hum. Brain Mapp.* 38, 666–677. doi: 10.1002/hbm.23407

Volkow, N. D., Wang, G.-J., Tomasi, D., and Baler, R. D. (2013a). Obesity and addiction: neurobiological overlaps. *Obes. Rev.* 14, 2–18. doi: 10.1111/j.1467-789X.2012.01031.x

Volkow, N. D., Wang, G.-J., Tomasi, D., and Baler, R. D. (2013b). The addictive dimensionality of obesity. *Biol. Psychiatry* 73, 811–818. doi: 10.1016/j.biopsych.2012.12.020

Yokum, S., Ng, J., and Stice, E. (2011). Attentional bias to food images associated with elevated weight and future weight gain: an fMRI study. *Obesity* 19, 1775–1783. doi: 10.1038/oby.2011.168

Yokum, S., and Stice, E. (2019). Weight gain is associated with changes in neural response to palatable food tastes varying in sugar and fat and palatable food images: a repeated-measures fMRI study. *Am. J. Clin. Nutr.* 110, 1275–1286. doi: 10.1093/ajcn/nqz204

Conflict of Interest: EB is manager of Berkman Consultants, a boutique consulting firm specializing in goals, motivation, and behavior change.

The remaining authors declare that the research was conducted in the absence of any commercial or financial relationships that could be construed as a potential conflict of interest.

frontiers in Behavioral Neuroscience

ORIGINAL RESEARCH
published: 12 January 2021
doi: 10.3389/fnbeh.2020.600920

Involvement of Peripheral Opioid Receptors in the Realization of Food Motivation Into Eating Behavior

Sergey Sudakov and Natalia Bogdanova*

Laboratory of Physiology of Reinforcement, P.K. Anokhin Research Institute of Normal Physiology, Moscow, Russia

The involvement of peripheral opioid receptors in the mechanisms of eating behavior is still unclear. The aim of this work was to study the role of peripheral, predominantly gastric mu and delta opioid receptors in the realization of food motivation in conditions of different energy costs for eating behavior. Experiments were performed under a between-sessions progressive ratio schedule of reinforcement in food-deprived rats. The level of food motivation was calculated using a self-developed method. Food intake, motor activity, and metabolic rate were recorded in fed and hungry animals. Results showed that intragastric administration of the mu opioid receptor agonist DAMGO led to an increase in the level of food motivation in the light variant of operant feeding behaviors. Food consumption did not change. At high costs for feeding behavior, the administration of DAMGO did not alter food motivation; however, food consumption and motor activity were reduced. Intragastric administration of the delta opioid receptor agonist DADLE did not lead to changes in the level of food motivation and physical activity, but inhibition of feeding behavior was observed in all reinforcement schedules. Three regulatory pathways of eating behavior in difficult food conditions by peripheral, predominantly gastric opioid receptors are hypothesized: environmental-inhibitory afferentations and suppression of the realization of food motivation into behavior; homeostatic-inhibitory action on food motivation; and rewarding-suppression of the anticipatory reinforcement.

Keywords: metabolism, motor activity, operant eating behavior, gastric opioid receptors, food motivation, DAMGO, DADLE

OPEN ACCESS

Edited by:
Masahiro Yamaguchi, Kōchi University, Japan

Reviewed by:
Maurizio Casarrubea, University of Palermo, Italy
Masaaki Yoshikawa, Kyoto University, Japan

****Correspondence:***
Sergey Sudakov
s-sudakov@nphys.ru

Specialty section:
This article was submitted to Motivation and Reward, a section of the journal Frontiers in Behavioral Neuroscience

Received: *31 August 2020*
Accepted: *09 December 2020*
Published: *12 January 2021*

Citation:
Sudakov S and Bogdanova N (2021) Involvement of Peripheral Opioid Receptors in the Realization of Food Motivation Into Eating Behavior. Front. Behav. Neurosci. 14:600920. doi: 10.3389/fnbeh.2020.600920

INTRODUCTION

The endogenous opioid system plays an important role in the organization of feeding motivation and eating behavior (Holtzman, 1979; Morley et al., 1983; Gosnell et al., 1986; Drewnowski et al., 1992; Selleck et al., 2018; Bodnar, 2019). It has been shown that activation of mu opioid receptors in a number of brain structures leads to activation of eating behavior in rodents (Zhang et al., 1998), but inhibits food intake in birds (Bungo et al., 2004). Activation of delta opioid receptors of the brain, as a rule, leads to hyperphagia (Majeed et al., 1986; Bakshi and Kelley, 1993). However, the role of delta opioid signaling in modulating feeding is not fully understood, as administration of delta opioid antagonists in the nucleus accumbens also causes an increase in food consumption (Kelley et al., 1996). The effect of opioids on food motivation is difficult to evaluate since most studies rely on measurements of the amount of food eaten. Classical breakpoint can be used to gauge the level of motivation and this method incorporates within- and between-sessions progressive ratio schedules and is defined as the last fixed ratio response in the increasing

fixed ratio progression. For example, in rodent studies, this can be both the number of the lever presses (Spear and Katz, 1991) and the holding time of the pressed lever (Gulotta and Byrne, 2015). However, this approach is most often used to assess the severity of the reinforcer effect and does not allow separation of such systemic mechanisms of eating behavior as motivation, anticipation, and the actual behavioral act of eating. It was shown that the opioid system of the brain mainly takes part in the anticipatory component of eating behavior and does not participate in the mechanisms of motivational and consummative components (Barbano and Cador, 2006). However, for such a study, a separate series of experiments are needed, using different methods to study the corresponding components of eating behavior. The method we developed (Sudakov et al., 2015) made it possible, using the same animals in the same environment, to study the effect of opioid agonists both on food motivation and on its implementation in nutritional behavior.

The endogenous opioid system consists of central and peripheral divisions which share the same receptors, endogenous peptide ligands, and enzymes for their formation and degradation. The divisions are separated by a blood-brain barrier that restricts opioid peptides. A large number of peripheral opioid receptors are located in the gastrointestinal tract (Holzer, 2009). Their activation can take place when eating certain foods which contain substances with opioid activity such as casomorphin produced from milk casein (Brantl et al., 1979, 1982), exorphins and gliadorphine from gluten (Fukudome and Yoshikawa, 1993; Takahashi et al., 2000), soymorphin from soybean (Yamada et al., 2012), and rubiscolin from spinach (Yang et al., 2001). Theoretically, the formation of other peptides with opioid activity from food protein products under the action of pepsin is possible. Under normal conditions, in an adult mammal, opioid peptides from the gastrointestinal tract do not penetrate into the central nervous system. Opioid receptors located in the wall of the stomach and intestines can bind to these opioid ligands to induce local and behavioral effects (Dubynin et al., 2004, 2007; Belyaeva et al., 2008; Yoshikawa, 2015). Thus, orally ingested soymorphin has been found to suppress food intake by activating mu opioid receptors in the gastrointestinal tract (Kaneko et al., 2010). Orally administered rubiscolin-6 suppressed high-fat diet intake (Kaneko et al., 2014) and enhanced memory consolidation in a step-through type passive avoidance test (Yang et al., 2003). These effects were blocked by centrally administered naltrindole, an antagonist for the delta receptor.

In our previous studies, it was shown that activation of mu opioid receptors of the gastrointestinal tract leads to a decrease in the intercellular content of beta-endorphin, as well as to a decrease in the density and affinity of mu opioid receptors in the brain (Proskuryakova et al., 2009; Sudakov et al., 2010). The administration of opioid peptides into the stomach of rats caused a change in the level of motor activity, anxiety, and pain sensitivity (Alexeeva et al., 2012; Sudakov et al., 2017). Based on the obtained data, the hypothesis of reciprocal interaction of the peripheral and central parts of the endogenous opioid system was formulated (Sudakov and Trigub, 2008). This hypothesis implies that activation of peripheral, and gastric in particular, opioid receptors will lead to suppression of the central part of the endogenous opioid system (Sudakov, 2019). Thus, the effects on peripheral opioid receptors, altering the activity of central opioid mechanisms, could lead to some changes in eating behavior.

In our preliminary experiments we found that activation of peripheral, predominantly gastric opioid receptors may influence the operant feeding behavior in rat (Bogdanova et al., 2015). Other information on the participation of gastric opioid receptors in the mechanisms of regulation of eating behavior is currently not available. The aim of this work was to study the role of mu and delta opioid receptors on the implementation of feeding motivation into eating behavior in varying conditions of energy costs for this behavior. The objectives of the study were to examine the effect of intragastric administration of peptide agonists of mu and delta opioid receptors on: (I) food intake, metabolic rate, and motor activity in conditions of free access to food in home cages; and (II) food intake, the level of food motivation, and metabolism in test cages where conditions of instrumental feeding behavior were regulated under a between-sessions progressive ratio schedule of reinforcement.

MATERIALS AND METHODS

Animals

The experiments were performed on 30 Wistar male rats with an average weight of about 230 g before the start of the experiment. The animals were kept in individually ventilated cages of eight animals each, with free access to water and a rat chow (3 kcal/g; Profgryzun, Russia) at a temperature of 21°C in the presence of light from 08:00 to 20:00. All behavioral tests were conducted during the light portion of the cycle. The general scheme of the experiment is shown in **Figure 1**.

Training

Experiments were performed using PhenoMaster modular equipment with an integrated operant wall (TSE Systems, Bad Homburg, Germany). One day prior to training, animals were subjected to 24-h food deprivation. Deprivation was carried out to speed up the training process, as we showed earlier (Chumakova et al., 2011; Sudakov et al., 2015). Training was performed in the tool chamber equipped with feeder, lever, and light stimulus. The two metal response levers were located 7.0 cm above the cage floor on either side of the food tray. During lever press training, 1 food pellet (44 mg; 3.6 kcal/g; Bio-Serv®, Flemington, NJ, USA) was presented in a recessed food receptacle after the active lever was pressed. Individual rats were placed in a chamber every 3 days for 1 h. Subsequently, only those animals that produced at least 10 lever pressings within 1 h were chosen to participate in the experiment. Three groups of eight animals were formed from trained animals. Groups were normalized such that the average number of lever pressings from the last training session were equivalent. After training, rats were placed in a home cage with free access to standard feed and water.

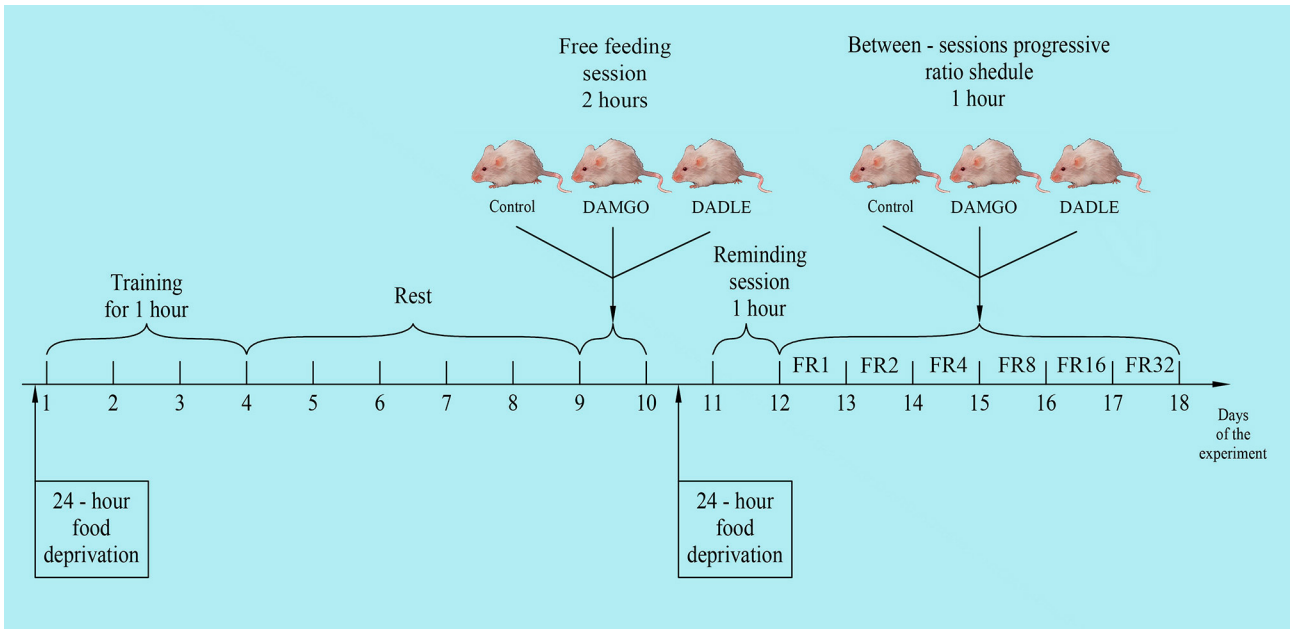

FIGURE 1 | The general scheme of the experiment.

TABLE 1 | The total amount of food eaten, motor activity, and average metabolism during 2 h of free access to food.

	Food eaten (pellets)	Motor activity (units)	Metabolism (kkal/h/kg)
Control	18.9 ± 1.6	3290 ± 115.4	6.79 ± 0.6
DAMGO	25.0 ± 1.8	3624 ± 121.7	7.05 ± 0.7
DADLE	24.7 ± 1.7	2174 ± 110.1	6.63 ± 0.5

Free Feeding Session

After 5 days the animals were individually placed into PhenoMaster cages in the same environmental conditions as the standard home cages. Animals were recorded every 40 min for 2 h for motor activity by the number of squares crossed, the amount of food eaten and water drunk, as well as oxygen consumption and carbon dioxide production. Thirty minutes before the start of experiments, test solutions were injected directly into the stomach with a special metallic probe in a volume of 0.1 ml per 100 g of body weight. A peptide agonist of mu opioid receptors DAMGO [(D-Ala^2, *N*-MePhe^4, Gly-ol)-enkephalin] and a peptide agonist of delta opioid receptors DADLE [(D-Ala^2, D-Leu^5)-enkephalin] were used. Peptides rapidly degrade in the gastrointestinal tract and, when introduced directly into the stomach, have no systemic or central effect. The first (control) group of animals ($n = 10$) was administered vehicle alone (water); the second group ($n = 10$) was administered 200 mg/kg DAMGO (Tocris Bioscience, Bristol, UK); and the third group ($n = 10$) was administered 200 mg/kg DADLE (Tocris Bioscience). The dose of the administered substances was selected on the basis of our previous experiments (Trigub et al., 2014; Bogdanova et al., 2015).

Reminding Session

One day before the start of the next series of experiments, animals were subjected to 24-h food deprivation. On this and following days outside of the 1-h experimental procedure, animals were kept under conditions of limited feeding (8 g of standard feed daily).

On the following day, rats were placed in a modular PhenoMaster unit for a 1 h reminding session where rats received one food pellet after each pressing on the lever. There were no intragastric administrations during the reminding session.

Between-Sessions Progressive Ratio Schedule

The next day, rats were again placed in experimental cages for 1 h. They received one feed pellet after each pedal press. The number of lever presses to obtain one feed pellet was increased daily to 2, 4, 8, 16, and 32 times during five experimental days, respectively (between-sessions progressive ratio schedule). Thirty minutes before daily placement of the animal in the experimental chamber, the above substances were intragastrically administered. The amount of pellet eaten, feed rate, and locomotor activity were measured. Metabolic rate was

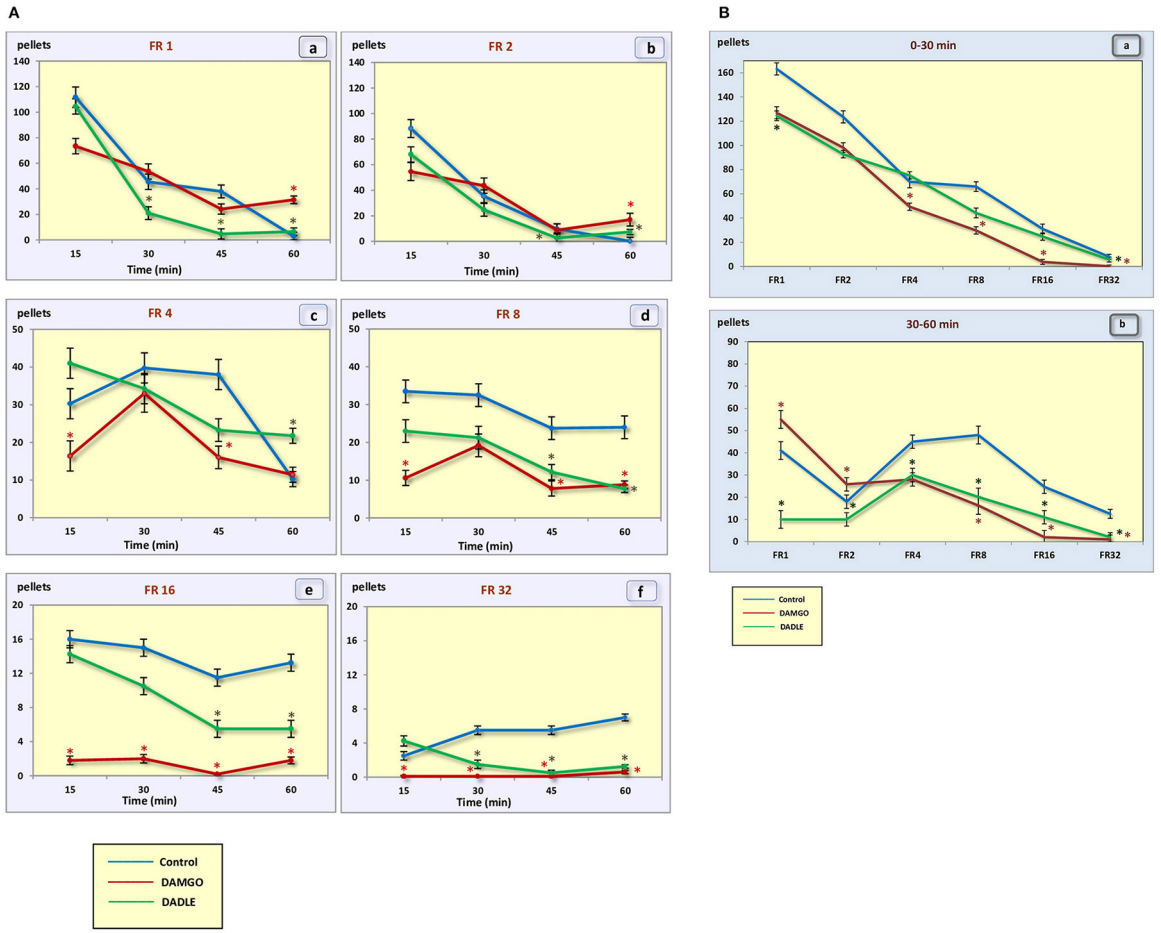

FIGURE 2 | (A) Number of pellets eaten during a 1 h session. (a) – FR 1 reinforcement schedule; (b) – FR 2 reinforcement schedule; (c) – FR 4 reinforcement schedule; (d) – FR 8 reinforcement schedule; (e) – FR 16 reinforcement schedule; (f) – FR 32 reinforcement schedule; *$p < 0.05$ compared to control. **(B)** Number of pellets eaten during 0–30 min (a) and 30–60 min (b) of 1 h session. *$p < 0.05$ compared to control.

calculated by indirect calorimetry by monitoring concentration of oxygen and carbon dioxide in the experimental cages with electrochemical sensors. All parameters were measured at 15 min intervals for 1 h.

Determination of The Level of Food Motivation

The rate of response shows the number of feed pellets eaten per time interval and reflects the magnitude of the food motivation of the animal. Thus, the level of food motivation can be estimated by the number of lever presses to receive food at each 15 min timepoint of the experiment. The more intense the rate of response, the higher the level of motivation. So, if the motivational level of a hungry animal is normalized to 100%, then under the condition of fixed ratio (FR) 1, in 45 min the rats completely satisfy the food motivation. In the last 15 min of the hourly session, most rats have never pressed the lever and the level of food motivation can be considered equal to zero (**Figure 1**). Intermediate states can be expressed as a percentage of the initial motivation according to the formula: M15 = 100% – (P15/Ptotal * 100%) (for the level of motivation after 15 min of eating behavior); M30 = 100% – (P15 + P30/Ptotal * 100%) (for the level of motivation after 30 min of eating behavior); M45 = 100% – (P15 + P30 + P45/Ptotal * 100%) (for the level of motivation after 45 min of eating behavior); and M60 = 100% – (P15 + P30 + P45 + P60/Ptotal * 100%) (for the level of motivation after 60 min of eating behavior). For these calculations, M is the level of motivation, P15, P30, P45, and P60 are the number of food pellets eaten for the corresponding period of time (0–15, 15–30, 30–45, or 45–60 min, respectively), and Ptotal is the total amount of eaten granules necessary for full satiation. In general, Ptotal during FR 1 averaged 152 ± 25 granules. Since rats on different FR reinforcement schedules needed to pay different energy costs for food-producing behavior, animals could not fully satisfy food motivation during the hour-long experiment and the number of pellets eaten could not accurately reflect the magnitude of motivation. The level of motivation can be

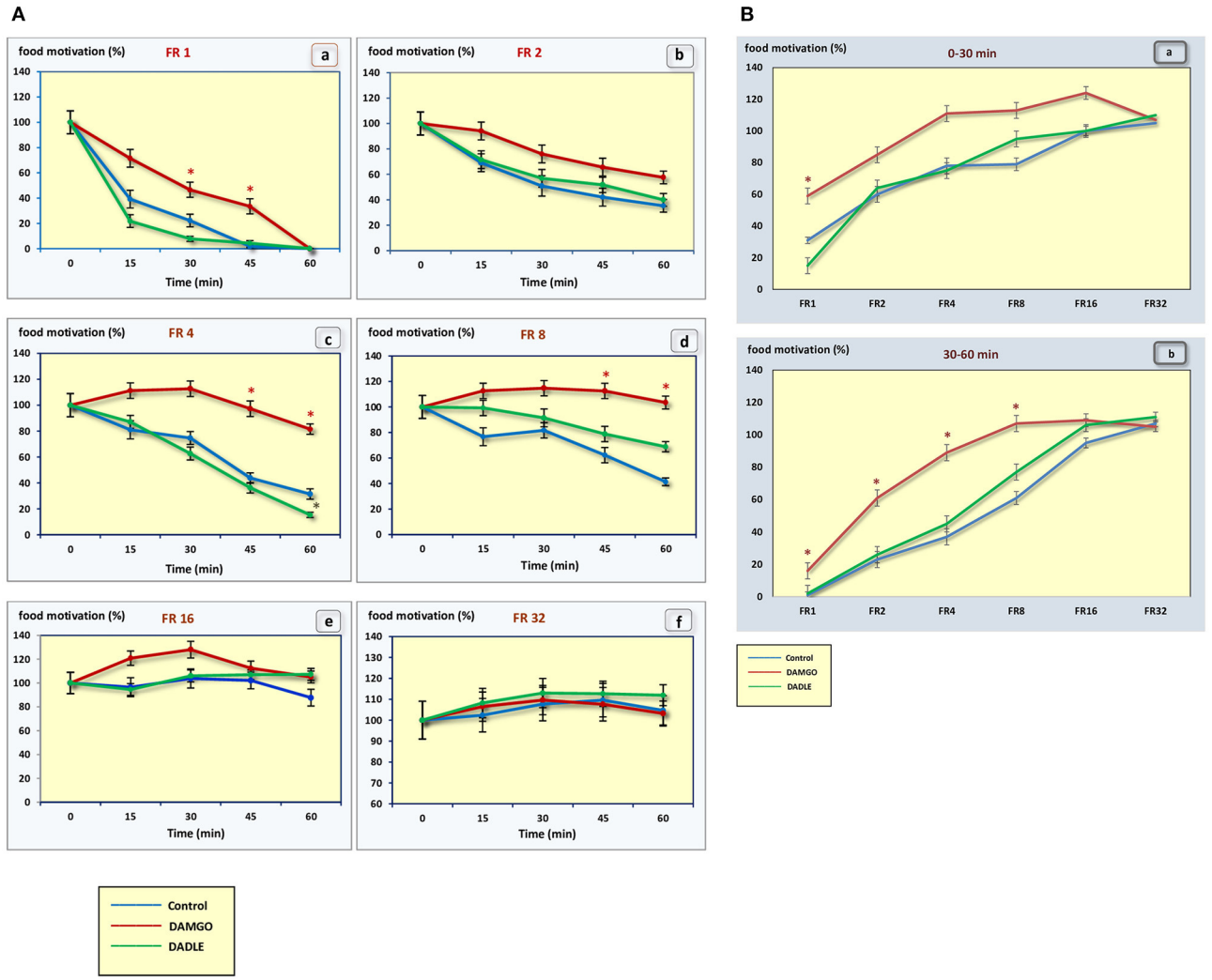

FIGURE 3 | (A) The level of food motivation as a percentage of the basal level during a 1 h session. (a) – FR 1 reinforcement schedule; (b) – FR 2 reinforcement schedule; (c) – FR 4 reinforcement schedule; (d) – FR 8 reinforcement schedule; (e) – FR 16 reinforcement schedule; (f) – FR 32 reinforcement schedule; *$p < 0.05$ compared to control. **(B)** The level of food motivation as a percentage of the basal level during 0–30 min (a) and 30–60 min (b) of 1 h session. *$p < 0.05$ compared to control.

very high whereas the number of pellets eaten can be small due to the large energy costs for their procurement. In this regard, we used a correction coefficient which reflected the activating effect of food motivation on metabolism (Sudakov et al., 2015). The coefficient is equal to the current energy consumption in kcal/h/kg divided by the average basal level of rat metabolism in each corresponding time interval. The average level of Wistar rat metabolism according to our previous experiments (Sudakov and Bashkatova, 2013; Sudakov et al., 2017) is 6.0 kcal/h/kg. Thus, for an animal in conditions of limited feeding, at the beginning of instrumental eating behavior, the level of food motivation can be adjusted to 100%, after *n* minutes it can be calculated as Mn * kn, where kn is the metabolic coefficient determined for the interval 0–15, 15–30, 30–45, or 45–60 min.

Statistics

Since the measured variable did not meet normality, non-parametric statistical methods were applied. The Kruskal–Wallis test showed that the mean ranks of the groups were not equal. As a result, two groups comparison was applied using the Mann–Whitney U test. The results were considered significant at $p < 0.05$. All results are presented as mean ± standard deviation.

Ethical Statement

The protocols and procedures for this study were ethically reviewed and approved by the Animal Care and Use Committee of the P.K. Anokhin Research Institute of Normal Physiology (Permission number 328) and conform to Directive 2010/63/EU.

TABLE 2 | Statistical analysis data.

		15 min	30 min	45 min	60 min
Food eaten	FR1	$U = 22.00, Z = 0.99, p = 0.328$	$U = 23.00, Z = 0.63, p = 0,505$	$U = 23.00, Z = 0.57, p = 0.573$	$U = 8.00, Z = 2.72, p = 0.002$
	FR2	$U = 25.00, Z = 0.50, p = 0.645$	$U = 22.00, Z = 0.88, p = 0.382$	$U = 22.00, Z = 0.68, p = 0.541$	$U = 8.00, Z = 2.76, p = 0.001$
	FR4	$U = 10.00, Z = 2.50, p = 0.011$	$U = 23.00, Z = 0.82, p = 0.452$	$U = 8.00, Z = 2.74, p = 0.001$	$U = 24.00, Z = 0.50, p = 0.696$
	FR8	$U = 13.00, Z = 2.04, p = 0.035$	$U = 19.00, Z = 1.14, p = 0.244$	$U = 10.00, Z = 2.52, p = 0.011$	$U = 10.0, Z = 2.25, p = 0.017$
	FR16	$U = 8.00, Z = 2.76, p = 0.001$	$U = 8.00, Z = 2.72, p = 0.002$	$U = 8.00, Z = 2.74, p = 0.001$	$U = 8.00, Z = 2.76, p = 0.001$
	FR32	$U = 7.50, Z = 2.78, p = 0.001$	$U = 7.50, Z = 2.76, p = 0.001$	$U = 7.50, Z = 2.78, p = 0.001$	$U = 7.50, Z = 2.78, p = 0.001$
Food motivation	FR1	$U = 15.00, Z = 2.42, p = 0.059$	$U = 13.00, Z = 2.08, p = 0.037$	$U = 8.00, Z = 2.71, p = 0.002$	$U = 20.50, Z = 0.88, p = 0.374$
	FR2	$U = 21.00, Z = 0.84, p = 0.378$	$U = 21.00, Z = 0.92, p = 0.364$	$U = 18.00, Z = 1.18, p = 0.237$	$U = 18.00, Z = 1.19, p = 0.233$
	FR4	$U = 19.00, Z = 1.06, p = 0.289$	$U = 19.00, Z = 1.12, p = 0.257$	$U = 10.00, Z = 2.24, p = 0.012$	$U = 10.00, Z = 2.36, p = 0.011$
	FR8	$U = 18.00, Z = 1.56, p = 0.163$	$U = 18.00, Z = 1.44, p = 0.189$	$U = 13.00, Z = 1.96, p = 0.048$	$U = 13.00, Z = 2.06, p = 0.033$
	FR16	$U = 20.00, Z = 0.98, p = 0.325$	$U = 20.50, Z = 0.90, p = 0.347$	$U = 20.00, Z = 1.01, p = 0.310$	$U = 19.00, Z = 1.10, p = 0.267$
	FR32	$U = 22.00, Z = 0.68, p = 0.543$	$U = 23.00, Z = 0.52, p = 0.674$	$U = 25.00, Z = 0.34, p = 0.731$	$U = 27.00, Z = 0.25, p = 0.754$
Motor activity	FR1	$U = 11.00, Z = 2.20, p = 0.021$	$U = 11.00, Z = 2.00, p = 0.044$	$U = 11.00, Z = 2.10, p = 0.032$	$U = 8.00, Z = 2.76, p = 0.001$
	FR2	$U = 18.00, Z = 1.18, p = 0.238$	$U = 22.00, Z = 0.72, p = 0.448$	$U = 22.00, Z = 0.70, p = 0.460$	$U = 22.00, Z = 0.68, p = 0.520$
	FR4	$U = 11.00, Z = 2.08, p = 0.036$	$U = 8.00, Z = 2.60, p = 0.005$	$U = 21.00, Z = 0.88, p = 0.376$	$U = 21.00, Z = 0.86, p = 0.348$
	FR8	$U = 22.00, Z = 0.86, p = 0.416$	$U = 23.00, Z = 0.80, p = 0.488$	$U = 22.00, Z = 0.86, p = 0.420$	$U = 10.00, Z = 2.00, p = 0.043$
	FR16	$U = 21.00, Z = 1.04, p = 0.314$	$U = 22.00, Z = 0.88, p = 0.386$	$U = 11.00, Z = 2.04, p = 0.041$	$U = 8.00, Z = 2.64, p = 0.003$
	FR32	$U = 8.00, Z = 2.72, p = 0.002$	$U = 8.00, Z = 2.70, p = 0.002$	$U = 8.00, Z = 2.76, p = 0.001$	$U = 8.00, Z = 2.78, p = 0.001$

Comparison of food eaten, motivation level and motor activity between control and DAMGO groups.

RESULTS

Free Feeding Session

It was found that the administration of neither DAMGO nor DADLE affects eating behavior, motor activity, and metabolism of well-fed rats with free access to food (**Table 1**).

Between-Sessions Progressive Ratio Schedule

In the control group of hungry, trained rats, when the fixed ratio reinforcement schedule was FR 1 and FR 2, approximately the same rates of response and dynamics of lever pressing were observed. In this regard, the rats were able to eat almost two times less food when the fixed ratio reinforcement schedule became FR 2 (**Figures 2A,B**). At the beginning of the experimental session, the rate of response was 7.6 and 12 times per minute, respectively. Then the rate gradually decreased, reaching two and three presses per minute by 45 min, respectively, and by 60 min it was near 0. For the FR 4 reinforcement schedule (medium difficulty), the initial rate of 10.5 lever presses remained practically unchanged for 45 min, and it decreased to 3.8 presses per minute only in the last 15 min. With FR 8, the initial rate of response was 19.5 per minute, and in the last 15 min it decreased to 15.6 presses per minute. The same initial rate was observed for FR 16, however, by the end of the session the rate of response did not decrease, and even increased slightly, reaching an average value of 20.8. With a "high difficulty" in food-producing behavior at FR 32, the rat's rate of response increased throughout the session.

In the "light" variants of operant feeding behavior (FR 1, FR 2), the high food motivation at the beginning of the session gradually decreased over the course of an hour, and by the end of the session the animals were completely satiated.

With an increase in difficulty for obtaining food, at the beginning of the experiment, food motivation remains at approximately the same level, and then begins to increase (**Figures 3A,B**). The effectiveness of operant feeding behavior as the number of pellets eaten decreases with increasing complexity (**Figure 2**).

Intragastric administration of a mu opioid receptor agonist DAMGO led to an increase in the level of food motivation in "light" operant feeding behaviors (FR 1, FR 4, and FR 8) (**Figure 3A**a, c, d). Most of differences were obtained in the second half of the sessions (**Figure 3B**; **Table 2**). Feed consumption did not change (**Figure 2A**a,b; **Table 1**). At high costs for feeding behavior (FR 16, FR 32), administration of DAMGO did not lead to a change in food motivation (**Figure 3A**e,f; **Table 2**), however feed consumption and motor activity were reduced (**Figure 2A**c–f; **Figure 2B**b; **Figure 4A**e, f; **Figure 4B**b; **Table 2**). Significant differences were observed throughout the experiment (**Table 2**).

Intragastric administration of delta opioid receptors agonist DADLE did not lead to changes in levels of feeding motivation and physical activity, but inhibition of feeding behavior was observed for all reinforcement schedules (**Figure 2A**). Significant changes were observed, mainly in the second half of the hourly session (**Figure 2B**; **Table 3**).

The administration of neither DAMGO nor DADLE led to changes in the level of animal metabolism during instrumental eating behavior (**Figures 5A,B**).

DISCUSSION

Our results showed significant differences in the mechanisms of implementation of food motivation in behavior, which depended

FIGURE 4 | (A) The motor activity (square crossings) during 1 h sessions. (a) – FR 1 reinforcement schedule; (b) – FR 2 reinforcement schedule; (c) – FR 4 reinforcement schedule; (d) – FR 8 reinforcement schedule; (e) – FR 16 reinforcement schedule; (f) – FR 32 reinforcement schedule; *$p < 0.05$ compared to control. **(B)** The motor activity (square crossings) during 0–30 min (a) and 30–60 min (b) of 1 h session. *$p < 0.05$ compared to control.

TABLE 3 | Statistical analysis data.

	15 min	30 min	45 min	60 min
FR1	$U = 17.00, Z = 1.62, p = 0.132$	$U = 11.00, Z = 2.20, p = 0.024$	$U = 8.00, Z = 2.74, p = 0.001$	$U = 10.00, Z = 2.46, p = 0.011$
FR2	$U = 18.00, Z = 1.12, p = 0.256$	$U = 19.00, Z = 1.10, p = 0.274$	$U = 11.00, Z = 2.25, p = 0.022$	$U = 8.00, Z = 2.76, p = 0.001$
FR4	$U = 18.00, Z = 1.14$, p = 0.244	$U = 18.00, Z = 1.18, p = 0.212$	$U = 19.00, Z = 1.06, p = 0.296$	$U = 11.00, Z = 2.15, p = 0.027$
FR8	$U = 19.00, Z = 1.02, p = 0.302$	$U = 20.00, Z = 1.04, p = 0.310$	$U = 11.00, Z = 2.25, p = 0.022$	$U = 10.00, Z = 2.32, p = 0.016$
FR16	$U = 18.00, Z = 1.14, p = 0.248$	$U = 17.00, Z = 1.58, p = 0.144$	$U = 10.00, Z = 2.34$, p = 0.015	$U = 10.00, Z = 2.36, p = 0.014$
FR32	$U = 17.00, Z = 1.64, p = 0.130$	$U = 8.00, Z = 2.70, p = 0.002$	$U = 8.00, Z = 2.74, p = 0.001$	$U = 8.00, Z = 2.76, p = 0.001$

Comparison of food eaten between control and DADLE groups.

upon the conditions for achieving the result. With free access to food and weak food motivation, gastric opioid receptors were not involved in regulation of feeding behavior. However, their activation can significantly change the processes of organizing eating behavior in the presence of increasing levels of food motivation and energy costs to satisfy it. The same data was obtained earlier with the introduction of DAMGO into the subthalamic nucleus. DAMGO microinfusions had no effect on

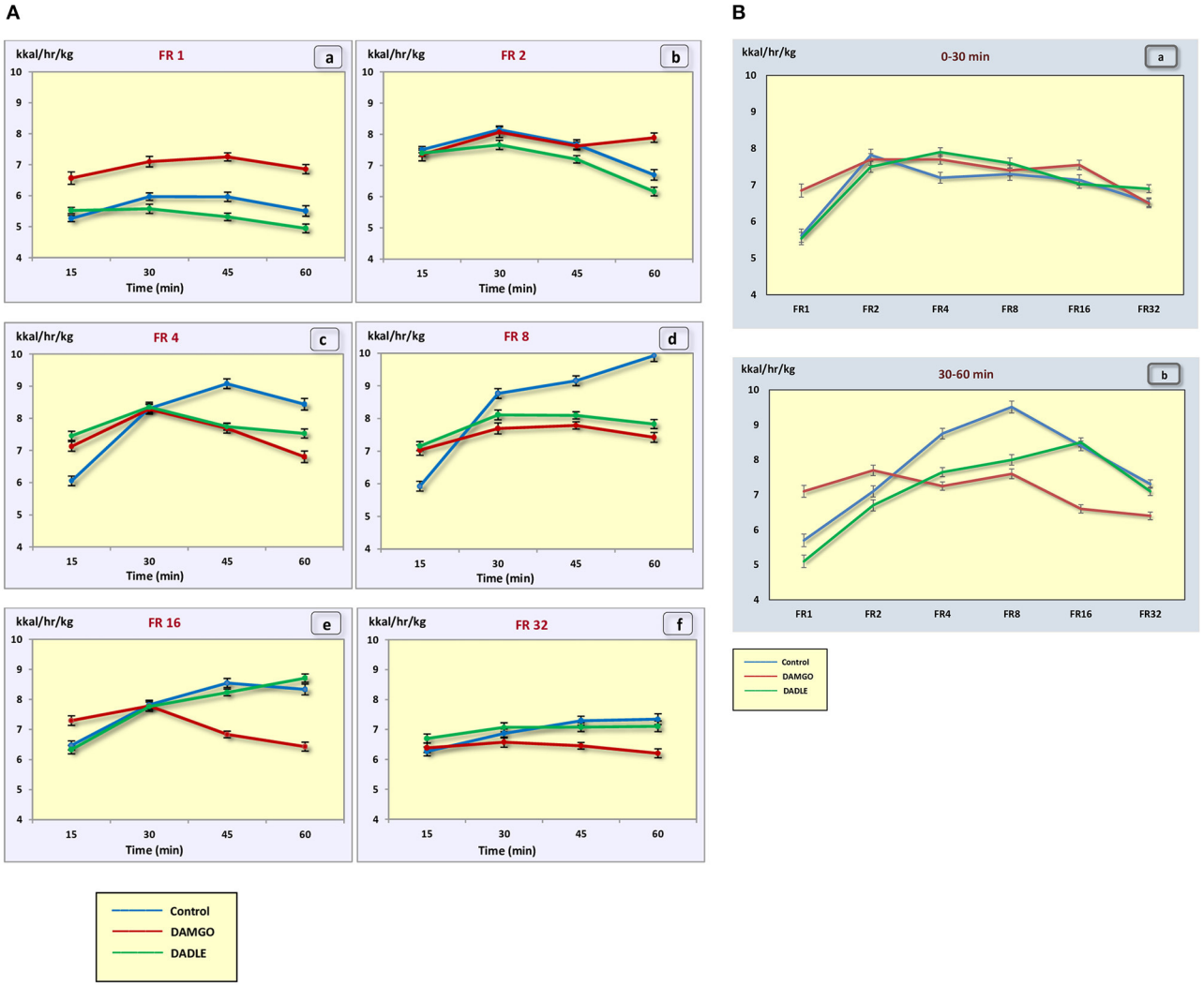

FIGURE 5 | (A) The metabolic rate (kcal/h/kg) during 1 h sessions. (a) – FR 1 reinforcement schedule; (b) – FR 2 reinforcement schedule; (c) – FR 4 reinforcement schedule; (d) – FR 8 reinforcement schedule; (e) – FR 16 reinforcement schedule; (f) – FR 32 reinforcement schedule; *$p < 0.05$ compared to control. **(B)** The metabolic rate (kcal/h/kg) during 0–30 min (a) and 30–60 min (b) of 1 h session. *$p < 0.05$ compared to control.

FR 2 performance. Nevertheless, mu opioid receptor stimulation significantly increased feeding on a palatable diet and reduced the reinforcers earned on a DRL20 schedule (Pratt et al., 2012). We observed the opposite effect. The introduction of DAMGO into the stomach led to a suppression of food intake. This is fully consistent with our hypothesis of a reciprocal relationship between the central and peripheral opioid systems (Sudakov and Trigub, 2008). Earlier, Levine and colleagues demonstrated that involvement of the opioid system in feeding behavior may depend on the level of motivation. The efficacy of naloxone at reducing food intake was inversely related to the level of food deprivation that the animal was subjected to Rudski et al. (1994), Levine et al. (1995), Weldon et al. (1996).

The disappearance of the DAMGO effect on days 5 and 6 outwardly looks like the development of tolerance. In fact, an increase in the effect of DAMGO on feed intake is observed precisely on days 5 and 6. However, it is possible, but unlikely, that on the 5th and 6th day of DAMGO administration, tolerance to the effect on motivation and sensitization to the effect on food intake develops. Additional experiments are needed to verify this assumption.

According to the theory of functional systems by P.K. Anokhin (Anokhin and Serzhantov, 1973), nutritional needs form a motivation that, at the stage of afferent synthesis, extracts from the memory genetic and individually acquired information about the program of eating behavior that is optimal in a particular environment. The decision to start eating behavior is based on the integration of motivational arousal, memory, and afferent situational arousal, which can either activate the decision or slow it down (**Figure 6**).

Our data suggest that afferentation from gastric receptors can affect both the level of food motivation and the processes

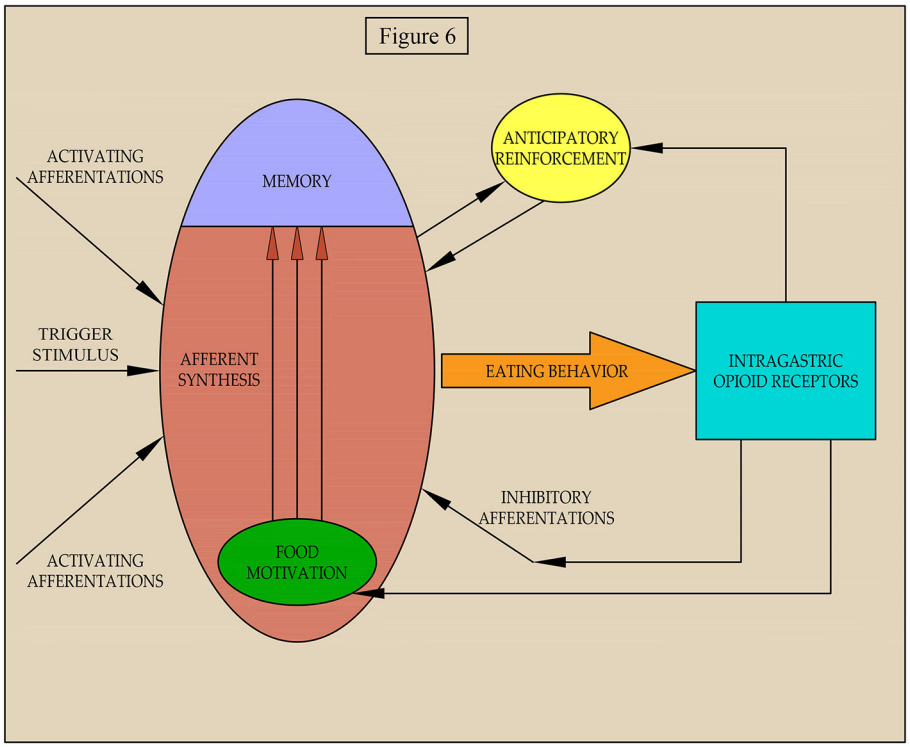

FIGURE 6 | Scheme of regulation of the implementation of food motivation into eating behavior.

of its implementation in food behavior whenever there is a pronounced food motivation that requires some effort to satisfy. It is possible that both in our experiment and in a natural setting for eating of food, the activation of mu opioid receptors in the stomach by peptides with opioid activity leads to simultaneous increases of inhibitory afferentations food motivation. This balances the impact on afferent synthesis and eating behavior and is not affected by weak inhibitory afferentations. With further activation of the inhibitory afferentations, despite increased motivation, eating behavior is suppressed.

As our earlier data suggests, activation of mu opioid receptors of the stomach leads to vagal afferentation (Sudakov et al., 2012) causing a decrease in release of beta-endorphin and reducing the affinity of mu opioid receptors in the midbrain and cortex (Proskuryakova et al., 2009; Sudakov et al., 2010). It is known that nutritional reinforcement is due to the activation of the mesocorticolimbic dopamine system, which occurs with the direct participation of beta-endorphin in the ventral tegmentum area. If the amount of beta-endorphin is decreased by activation of the gastric mu opioid receptor, then food reinforcement should change. We propose a two-stage mechanism of positive reinforcement. The first stage, anticipatory reinforcement, is formed when the result is still not achieved. At this stage, the importance of the planned result and the probability of its achievement are assessed. The greater these indices are, the stronger the anticipatory reinforcement becomes. Hypothetically, anticipatory reinforcement is mediated by dopamine release from nerve terminals in the mesencephalon (Sudakov, 2019). If the likelihood of achieving a result decreases, for example, with an increase in energy expenditure for eating behavior, the intensity of anticipatory reinforcement will also decrease. Since, anticipatory reinforcement stimulates the implementation of food motivation in behavior, when it is suppressed, the behavior will also be inhibited.

Thus, we hypothesize that central and peripheral mechanisms are involved in regulating the implementation of food motivation into eating behavior under conditions of varying difficulty to achieve a result. With poor food motivation and free access to food, the peripheral regulation mechanism is not involved.

We propose three pathways of regulation of eating behavior in difficult food conditions by gastric opioid receptors: (I) environmental-inhibitory afferentations and suppression of the implementation of food motivation in behavior; (II) homeostatic-inhibitory action on food motivation; and (III) rewarding-suppression of the anticipatory reinforcement. We hypothesize that excitation from opioid receptors in the stomach is transmitted through vagal afferentation to the nucleus tractus solitaries. There are anatomical evidence shows mRNA expression of serotonin receptors on GLP-1-producing preproglucagon (PPG) neurons in the medial nucleus tractus solitarius by fluorescent *in situ* hybridization, suggesting that PPG neurons are likely to express these receptors (Leon et al., 2019). GLP-1 is an anorectic hormone involved in the control of food intake (Barrera et al., 2011). Thus, the first pathway

can be realized through the release of serotonin and glucagon in hindbrain, which can cause hypophagia. The second pathway follows from the well-known facts about suppression of food motivation when food enters the stomach. This causes the release of glucose from the depot and the effect on glucose-sensitive neurons of the hypothalamus (Balagura and Kanner, 1971; Oomura, 1981). The third pathway is based upon data from a number of studies on mechanisms of reward (Majeed et al., 1986; Bakshi and Kelley, 1993; Kelley et al., 1996; Zhang et al., 1998) and anticipation (Barbano and Cador, 2006) and the participation of opioids in the mesocorticolimbic system of the brain, and our early studies showing the possibility of gastric opioid receptors acting on these central processes (Proskuryakova et al., 2009; Sudakov et al., 2010, 2012; Sudakov, 2019). Of course, the above neurochemical mechanisms of the effect of opioid receptors on eating behavior are still speculative and will be the subject of our further research.

Thus, our data indicates experimental confirmation of the mechanism of peripheral regulation of the implementation of food motivation in behavior. This result opens up the possibility for influencing this process with relatively safe peripherally acting drugs, nutritional supplements, and foods with opioid activity.

DATA AVAILABILITY STATEMENT

The raw data supporting the conclusions of this article will be made available by the authors, without undue reservation.

ETHICS STATEMENT

The animal study was reviewed and approved by Animal Care and Use Committee of the P.K. Anokhin Research Institute of Normal Physiology (Permission number 328).

AUTHOR CONTRIBUTIONS

SS wrote the article. NB processed the data and carried out the technical design of the article. All authors have read and agreed to the published version of the manuscript and contributed equally to the data collection for this work.

ACKNOWLEDGMENTS

Editorial assistance, in the form of language editing and correction, was provided by XpertScientific Editing and Consulting Services.

REFERENCES

Alexeeva, E. V., Nazarova, G. A., and Sudakov, S. K. (2012). Effects of peripheral μ, δ, and?-opioid receptor agonists on the levels of anxiety and motor activity of rats. *Bull. Exp. Biol. Med.* 153, 720–721. doi: 10.1007/s10517-012-1809-2

Anokhin, P. K., and Serzhantov, V. F. (1973). Some trends in modern theoretical biology and the conception of a functional system. Usp. Fiziol. *Nauk* 4, 3–18.

Bakshi, V. P., and Kelley, A. E. (1993). Feeding induced by opioid stimulation of the ventral striatum: role of opiate receptor subtypes. *J. Pharmacol. Exp. Ther.* 265, 1253–1260.

Balagura, S., and Kanner, M. (1971). Hypothalamic sensitivity to 2-deoxy-D-glucose and glucose: effects on feeding behavior. *Physiol. Behav.* 7, 251–255. doi: 10.1016/0031-9384(71)90292-7

Barbano, M. F., and Cador, M. (2006). Differential regulation of the consummatory, motivational and anticipatory aspects of feeding behavior by dopaminergic and opioidergic drugs. *Neuropsychopharmacology* 31, 1371–1381. doi: 10.1038/sj.npp.1300908

Barrera, J. G., Sandoval, D. A., D'Alessio, D. A., and Seeley, R. J. (2011). GLP-1 and energy balance: an integrated model of short-term and long-term control GLP-1 and energy balance: an integrated model of short-term and long-term control GLP-1 and energy balance: an integrated model of short-term and long-term control. *Nat Rev Endocrinol.* 7, 507–516. doi: 10.1038/nrendo.2011.77

Belyaeva, Y.u,., A., Dubynin, V. A., Stovolosov, I. S., and Kamensky, A. A. (2008). Neurotropic activity of exorphins with different affinity to m- and d-types of opioid receptors. *Neurohemical* 2, 47–52. doi: 10.1007/s11710-008-1010-8

Bodnar, R. J. (2019). Endogenous opioid modulation of food intake and body weight: implications for opioid influences upon motivation and addiction. *Peptides* 116, 42–62. doi: 10.1016/j.peptides.2019.04.008

Bogdanova, N. G., Kolpakov, A. A., and Sudakov, S. K. (2015). Effect of peptide agonists of peripheral opioid receptors on operant feeding behavior and food motivation in rats. *Bull. Exp. Biol. Med.* 158, 589–591. doi: 10.1007/s10517-015-2812-1

Brantl, V., Pfeiffer, A., Herz, A., Henschen, A., and Lottspeich, F. (1982). Antinociceptive potencies of beta-casomorphin analogs as compared to their affinities towards mu and delta opiate receptor sites in brain and periphery. *Peptides* 3, 793–797. doi: 10.1016/0196-9781(82)90017-1

Brantl, V., Teshemacher, H., Henschen, A., and Lottspeich, F. (1979). Novel opioid peptides derived from casein (beta-casomorphins). I. Isolation from bovine casein peptone. Hoppe Seylers Z. *Physiol. Chem.* 360, 1211–1216. doi: 10.1515/bchm2.1979.360.2.1211

Bungo, T., Kawamura, K., Izumi, T., Dodo, K., and Ueda, H. (2004). Feeding responses to mu-, delta- and kappa-opioid receptor agonists in the meat-type chick. *Pharmacol. Biochem. Behav.* 78, 707–710. doi: 10.1016/j.pbb.2004.05.015

Chumakova, Y. A., Bashkatova, V. G., and Sudakov, S. K. (2011). Changes in feeding behavior after peripheral loperamide administration in rats. *Bull. Exp. Biol. Med.* 150, 398–400. doi: 10.1007/s10517-011-1151-0

Drewnowski, A., Krahn, D. D., Demitrack, M. A., Nairn, K., and Gosnell, B. A. (1992). Taste responses and preferences for sweet high-fat foods: evidence for opioid involvement. *Physiol. Behav.* 51, 371–379. doi: 10.1016/0031-9384(92)90155-U

Dubynin, V. A., Ivleva, Y.u,., A., and Kamensky, A. A. (2004). The neurotropic activity of b-casomorphins, food-derived opioid peptides. Usp. physiol. *nauk* 35, 83–101.

Dubynin, V. A., Ivleva, Y.u,., A., Stovolosov, I. S., Belyaeva, Yu,. A., Dobryakova, Y.u,., V., Andreeva, L. A., et.al. (2007). Effect of β-casomorphines on mother-oriented ("childs") behavior of white rats. *Dokl. Biol. Sci.* 412, 1–4. doi: 10.1134/S0012496607010012

Fukudome, S., and Yoshikawa, M. (1993). Gluten exorphin c. A novel opioid peptide derived from wheat gluten. *FEBS Lett.* 316, 17–19. doi: 10.1016/0014-5793(93)81727-H

Gosnell, B. A., Levine, A. S., and Morley, J. E. (1986). The stimulation of food intake by selective agonists of mu, kappa and delta opioid receptors. *Life Sci.* 38, 1081–1088. doi: 10.1016/0024-3205(86)90243-2

Gulotta, K. B., and Byrne, T. (2015). A progressive-duration schedule of reinforcement. *Behav. Processes* 121, 93–97. doi: 10.1016/j.beproc.2015.10.022

Holtzman, S. G. (1979). Suppression of appetitive behavior in the rat by naloxone: lack of effect of prior morphine dependence. *Life Sci.* 24, 219–226. doi: 10.1016/0024-3205(79)90222-4

Holzer, P. (2009). Opioid receptors in the gastrointestinal tract. *Regul. Pept.* 155, 11–17. doi: 10.1016/j.regpep.2009.03.012

Kaneko, K., Iwasaki, M., and Yoshikawa M/, Ohinata, K. (2010). Orally administered soymorphins, soy-derived opioid peptides, suppress feeding and intestinal transit via gut mu(1)-receptor coupled to 5-HT(1A), D(2), and

GABA(B) systems. *Am. J. Physiol. Gastrointest. Liver Physiol*. 299, 799–805. doi: 10.1152/ajpgi.00081.2010

Kaneko, K., Mizushige, T., Miyazaki, Y., Lazarus, M., Urade, Y., Yoshikawa, M., Kanamoto, R., and Ohinata, K. (2014). δ-Opioid receptor activation stimulates normal diet intake but conversely suppresses high-fat diet intake in mice. *Am. J. Physiol. Regul. Integr. Comp. Physiol*. 306, R265–72. doi: 10.1152/ajpregu.00405.2013

Kelley, A. E., Bless, E. P., and Swanson, C. J. (1996). Investigation of the effects of opiate antagonists infused into the nucleus accumbens on feeding and sucrose drinking in rats. *J. Pharmacol. Exp. Ther*. 278, 1499–1507.

Leon, R. M., Borner, T., Reiner, D. J., Stein, L. M., Lhamo, R., De Jonghe, B. C., and Hayes, M. R. (2019). Hypophagia induced by hindbrain serotonin is mediated through central GLP-1 signaling and involves 5-HT2C and 5-HT3 receptor activation. *Neuropsychopharmacology* 44, 1742–1751. doi: 10.1038/s41386-019-0384-x

Levine, A. S., Weldon, D. T., Grace, M., Cleary, J. P., and Billington, C. J. (1995). Naloxone blocks that portion of feeding driven by sweet taste in food-restricted rats. *Am. J. Physiol*. 268, 248–252. doi: 10.1152/ajpregu.1995.268.1.R248

Majeed, N. H., Przewlocka, B., Wedzony, K., and Przewłocki, R. (1986). Stimulation of food intake following opioid microinjection into the nucleus accumbens septi in rats. *Peptides* 7, 711–716. doi: 10.1016/0196-9781(86)90083-5

Morley, J. E., Levine, A. S., Yim, G. K., and Lowy, M. T. (1983). Opioid modulation of appetite. *Neurosci. Biobehav. Rev*. 7, 281–305. doi: 10.1016/0149-7634(83)90020-9

Oomura, Y. (1981). Chemosensitive neuron in the hypothalamus related to food intake behavior. *Jpn. J. Pharmacol* 31(Suppl.1), P—12P. doi: 10.1016/S0021-5198(19)54826-0

Pratt, W. E., Choi, E., and Guy, E. G. (2012). An examination of the effects of subthalamic nucleus inhibition or μ-opioid receptor stimulation on food-directed motivation in the non-deprived rat. *Behav. Brain Res*. 230, 365–373. doi: 10.1016/j.bbr.2012.02.031

Proskuryakova, T. V., Shokhonova, V. A., Chumakova, Y.u,., A., Bashkatova, V. G., and Sudakov, S. K. (2009). Modulation of peripheral opioid receptors affects the concentration of mu-opioid receptors in rat brain. *Bull. Exp. Biol. Med*. 148, 357–359. doi: 10.1007/s10517-010-0711-z

Rudski, J. M., Billington, C. J., and Levine, A. S. (1994). Naloxone's effects on operant responding depend upon level of deprivation. *Pharmacol. Biochem. Behav*. 49, 377–383. doi: 10.1016/0091-3057(94)90437-5

Selleck, R. A., Giacomini, J., Buchholtz, B. D., Lake, C., Sadeghian, K., and Baldo, B. A. (2018). Modulation of appetitive motivation by prefrontal cortical mu-opioid receptors is dependent upon local dopamine D1 receptor signaling. *Neuropharmacology* 140, 302–309. doi: 10.1016/j.neuropharm.2018.07.033

Spear, D. J., and Katz, J. L. (1991). Cocaine and food as reinforcers: effects of reinforcer magnitude and response requirement under second-order fixed-ratio and progressive-ratio schedules. *J. Exp. Anal. Behav*. 56, 261–275. doi: 10.1901/jeab.1991.56-261

Sudakov, S. K. (2019). Physiology and pharmacology of positive reinforcement. *Bull. Exp. Biol. Med*. 166, 709–713. doi: 10.1007/s10517-019-04423-1

Sudakov, S. K., Alekseeva, E. V., and Nazarova, G. A. (2017). Effect of peripheral μ-, δ-, and κ-opioid ligands on the development of tolerance to ethanol-induced analgesia. *Bull. Exp. Biol. Med*. 163, 177–179. doi: 10.1007/s10517-017-3760-8

Sudakov, S. K., and Bashkatova, V. G. (2013). Effect of peripheral D_2 dopamine receptor antagonist domperidone on metabolism, feeding behavior, and locomotor activity of rats. *Bull. Exp. Biol. Med*. 155, 705–707. doi: 10.1007/s10517-013-2231-0

Sudakov, S. K., Bashkatova, V. G., Kolpakov, A. A., and Chernyaeva, N. N. (2012). Loperamide effects on anxiety level and feeding behavior in rats. Role of vagal afferentation. *Bull. Exp. Biol. Med*. 153, 717–719. doi: 10.1007/s10517-012-1808-3

Sudakov, S. K., Bogdanova, N. G., and Kolpakov, A. A. (2015). Method for determining the level of food motivation in rats. *Bull. Exp. Biol. Med*. 158, 401–403. doi: 10.1007/s10517-015-2772-5

Sudakov, S. K., Sotnikov, S. V., Chekmareva, N., Yu., Kolpakov, A. A., Chumakova, Y.u,., A., and Umryukhin, A. E. (2010). Changes in β-endorphin level in the cingulate cortex in rats after peripheral loperamide and methylnaloxone administration at rest and during emotional stress. *Bull. Exp. Biol. Med*. 149, 167–169. doi: 10.1007/s10517-010-0898-z

Sudakov, S. K., and Trigub, M. M. (2008). Hypothesis on reciprocal interactions between the central and peripheral components of the endogenous opioid system. *Bull. Exp. Biol. Med*. 146, 663–666. doi: 10.1007/s10517-009-0368-7

Takahashi, M., Fukunaga, H., Kaneto, H., Fukudome, S., and Yoshikawa, M. (2000). Behavioral and pharmacological studies on gluten exorphin A5, a newly isolated bioactive food protein fragment, in mice. *Jpn. J. Pharmacol*. 84, 259–265. doi: 10.1254/jjp.84.259

Trigub, M. M., Bogdanova, N. G., Kolpakov, A. A., Bashkatova, V. G., and Sudakov, S. K. (2014). Effect of peripheral opioid receptor agonists on depressive activity of ethanol. *Bull. Exp. Biol. Med*. 156, 778–780. doi: 10.1007/s10517-014-2448-6

Weldon, D. T., Hare, E. O., Cleary, J., Billington, C. J., and Levine, A. S. (1996). Effect of naloxone on intake of cornstarch, sucrose, and polycose diets in restricted and nonrestricted rats. *Am. J. Physiol*. 270, R1183–1188. doi: 10.1152/ajpregu.1996.270.6.R1183

Yamada, Y., Muraki, A., Oie, M., Kanegawa, N., Oda, A., Sawashi, Y., et al. (2012). Soymorphin-5, a soy-derived μ-opioid peptide, decreases glucose and triglyceride levels through activating adiponectin and PPARα systems in diabetic KKAy mice. *Am. J. Physiol. Endocrinol. Metab*. 302, E433–440. doi: 10.1152/ajpendo.00161.2011

Yang, S., Kawamura, Y., and Yoshikawa, M. (2003). Effect of rubiscolin, a delta opioid peptide derived from Rubisco, on memory consolidation. *Peptides* 24, 325–328. doi: 10.1016/S0196-9781(03)00044-5

Yang, S., Yunden, J., Sonoda, S., Doyama, N., Lipkowski, A. W., Kawamura, Y., et al. (2001). Rubiscolin, a delta selective opioid peptide derived from plant Rubisco. *FEBS Lett*. 509, 213–217. doi: 10.1016/S0014-5793(01)03042-3

Yoshikawa, M. (2015). Bioactive peptides derived from natural proteins with respect to diversity of their receptors and physiological effects. *Peptides* 72, 208–225. doi: 10.1016/j.peptides.2015.07.013

Zhang, M., Gosnell, B. A., and Kelley, A. E. (1998). Intake of high-fat food is selectively enhanced by mu opioid receptor stimulation within the nucleus accumbens. *J. Pharmacol. Exp. Ther*. 285, 908–914.

Conflict of Interest: The authors declare that the research was conducted in the absence of any commercial or financial relationships that could be construed as a potential conflict of interest.

frontiers in Human Neuroscience

SYSTEMATIC REVIEW
published: 20 January 2021
doi: 10.3389/fnhum.2020.596381

Animal Models for Anorexia Nervosa—A Systematic Review

Sophie Scharner[1] *and Andreas Stengel*[1,2]*

[1] Department for Psychosomatic Medicine, Charité Center for Internal Medicine and Dermatology, Berlin Institute of Health, Charité-Universitätsmedizin Berlin, Humboldt-Universität zu Berlin, Berlin, Germany, [2] Department of Psychosomatic Medicine and Psychotherapy, University Hospital Tübingen, Tübingen, Germany

Anorexia nervosa is an eating disorder characterized by intense fear of gaining weight and a distorted body image which usually leads to low caloric intake and hyperactivity. The underlying mechanism and pathogenesis of anorexia nervosa is still poorly understood. In order to learn more about the underlying pathophysiology of anorexia nervosa and to find further possible treatment options, several animal models mimicking anorexia nervosa have been developed. The aim of this review is to systematically search different databases and provide an overview of existing animal models and to discuss the current knowledge gained from animal models of anorexia nervosa. For the systematic data search, the Pubmed—Medline database, Embase database, and Web of Science database were searched. After removal of duplicates and the systematic process of selection, 108 original research papers were included in this systematic review. One hundred and six studies were performed with rodents and 2 on monkeys. Eighteen different animal models for anorexia nervosa were used in these studies. Parameters assessed in many studies were body weight, food intake, physical activity, cessation of the estrous cycle in female animals, behavioral changes, metabolic and hormonal alterations. The most commonly used animal model (75 of the studies) is the activity-based anorexia model in which typically young rodents are exposed to time-reduced access to food (a certain number of hours a day) with unrestricted access to a running wheel. Of the genetic animal models, one that is of particular interest is the *anx/anx* mice model. Animal models have so far contributed many findings to the understanding of mechanisms of hunger and satiety, physical activity and cognition in an underweight state and other mechanisms relevant for anorexia nervosa in humans.

Keywords: activity, brain-gut axis, food restriction, psychosomatic, reward, stress

OPEN ACCESS

Edited by:
Masahiro Yamaguchi, Kōchi University, Japan

Reviewed by:
Emilio Gutierrez, Universidad de Santiago de Compostela, Spain
Moïse Coëffier, Normandie Université, France

***Correspondence:**
Andreas Stengel
andreas.stengel@med.uni-tuebingen.de

Specialty section:
This article was submitted to Health, a section of the journal Frontiers in Human Neuroscience

Received: *19 August 2020*
Accepted: *16 December 2020*
Published: *20 January 2021*

Citation:
Scharner S and Stengel A (2021) Animal Models for Anorexia Nervosa—A Systematic Review. Front. Hum. Neurosci. 14:596381. doi: 10.3389/fnhum.2020.596381

INTRODUCTION

Anorexia nervosa is an eating disorder characterized by an intense fear of gaining weight and a distorted body image which usually leads to low caloric intake and hyperactivity (American-Psychiatric-Association, 2013). Women and girls are nine-times more often affected than men or boys (Nagl et al., 2016). Frequent comorbidities are depression, obsessive-compulsive disorder and suicidality (Treasure et al., 2015). Somatic sequelae are various: electrolyte abnormalities, osteoporosis, cardiac abnormalities, or brain atrophy, to name just a few (Ghadirian et al., 1993). These comorbidities and somatic complications are one of the reasons why anorexia nervosa is the psychiatric disorder with the highest mortality rate (Arcelus et al., 2011). The underlying

mechanism and pathogenesis of anorexia nervosa is still poorly understood. The treatment options are still quite limited to mainly nutritional support and psychotherapy, and treatment success is hampered by high relapse rates (Zipfel et al., 2015).

Scientists often try to develop animal models of a disease to understand basic neurobiological processes that are either conserved across species or if not—at least provide conceptual insight on the subject. In order to learn more about the underlying pathophysiology of the eating disorder anorexia nervosa and to find further possible treatment options, several animal models mimicking anorexia nervosa have been employed (Mequinion et al., 2015a). Some of these animal models have been developed and some have been discovered out of coincidence. The aim of this review is to systematically search different databases and provide an overview of existing animal models and to compare them with each other. The purpose is also to discuss advantages and disadvantages to identify which might be the most suited model. We will also highlight the current knowledge gained from the different animal models concerning anorexia nervosa. Lastly, we also discuss gaps in knowledge to highlight where more research is necessary.

METHODS

For the systematic data search, the three commonly used scientific databases, Pubmed—Medline database, Embase database and Web of Science database, were searched using the following search terms: "Anorexia nervosa" and "Animal model". The search was performed on April 2nd, 2020. The search provided 945 results. Afterwards, duplicates were removed which were around a third (312). Selection criteria applied were original publications (reviews $n = 214$, conference abstracts and book chapters $n = 46$ were removed), animal studies (human studies $n = 157$ were removed), animal studies of anorexia nervosa (animal studies of other diseases than anorexia nervosa $n = 73$ were removed), full text availability (20 papers were removed) and English language (different language than English papers were removed $n = 21$). During the manual screening all publications were selected which study animal models that mimic the eating disorder anorexia nervosa. After selection, 108 publications were included in this systematic review (**Figure 1**).

RESULTS

The initial search of the three scientific databases that we chose gave 945 results. About a third of the papers were duplicates (312 papers), which shows that these three chosen databases do have some overlap in results. The 633 records that were left after removal of duplicates were manually screened for eligibility according to our criteria (**Figure 1**). The resulting 108 studies that we included in our quantitative synthesis were then analyzed for species, animal model protocol and important findings (**Table 1**).

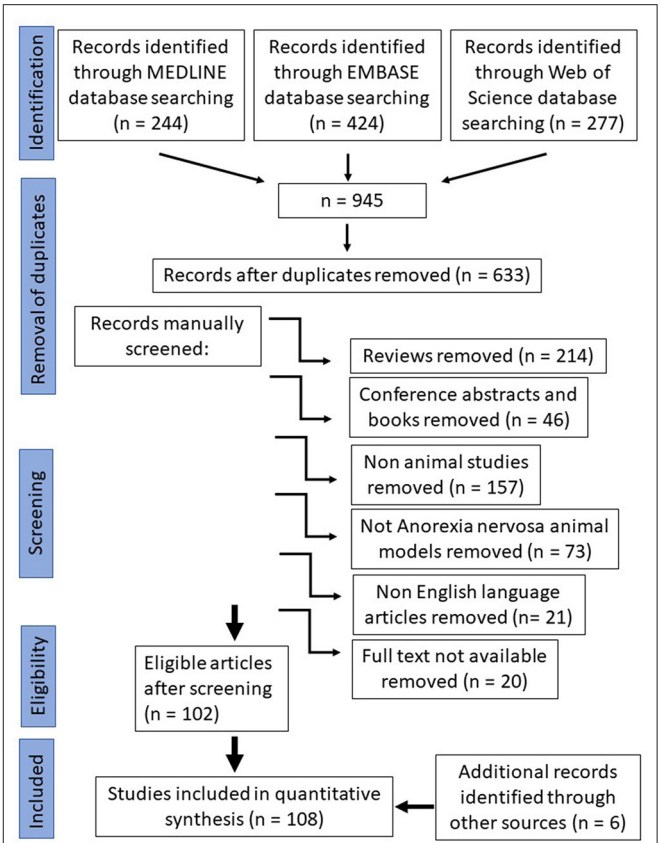

FIGURE 1 | Prisma flow chart.

Species

Of the 108 included studies, 106 used rodents as their experimental species—of these, 64 studies were performed in rats, 40 in mice and 2 in rats and mice. Two studies were performed in monkeys (marmoset and rhesus monkey, respectively).

Sex

The majority of studies was performed in experimental animals of female sex. Not all authors gave a reason for their sex choice, but if they did, it was always the much higher prevalence of anorexia nervosa in women compared to men. When male animals were used and an explanation was given, it stated that male animals were chosen because they do not have an estrous cycle that could interfere with the experiments. In rats, 43 studies used females and 13 studies used males. In mice, 21 studies used females and 10 males. One of the two monkey studies used females and the other used males and females. A few rodent studies used animals of both sexes and looked specifically for sex differences (8 studies in rats and 7 in mice).

Abbreviations: 5HT4, serotonin receptor 4; ABA, Activity-based anorexia; BDNF, brain derived neurotrophic factor; CART, Cocaine- and amphetamine-regulated transcript; CTA, conditioned taste aversion; GABA, Gamma aminobutyric acid; GH/IGF-1 axis, growth hormone/insulin-like growth factor 1 axis; HPA axis, hypothalamus pituitary adrenal axis; icv, intracerebroventricular; ip, intraperitoneal; NAc, Nucleus accumbens; NMDA, N-Methyl-D-Aspartat; POMC, Pro-opiomelanocortin; THC, tetrahydrocannabinol; zg, zeptogram.

TABLE 1 | Overview of the 108 selected studies in alphabetical order.

References	Year	Species	Model	Strain	*N*	Methods: Anorexia protocol	Topic and important findings
Achamrah et al. (2016b)	2016	Mice	ABA	C57Bl/6	72 m	Progressive limited food access from 6 h/day (day 6) to 3 h/day (day 9), wheel 24 h	Access to running wheel during refeeding from ABA in mice improves body composition, intestinal hyperpermeability and behavior
Achamrah et al. (2016a)	2017	Mice	ABA	C57Bl/6	24 m 16 f	Progressive limited food access from 6 h/day (day 6) to 3 h/day (day 9), wheel 24 h	Sex differences in response to ABA: male mice more susceptible and higher mortality rate
Adams et al. (2009)	2009	Rats	Activity	SD	40 m	Rats have running wheel access and on third day get injection, voluntary food reduction	Drug treatment: Chlorpromazine prevents running induced feeding suppression
Altemus et al. (1996)	1996	Rats	ABA	SD	66 f	1.5 h food, 22.5 h wheel	Drug treatment: Fluoxetine prevented ABA, imipramine no effect; PCPA aggravated ABA
Aoki et al. (2012)	2012	Rats	ABA		24 f	1 h food, 24 h wheel	Brain changes in adolescent ABA: more GABA receptors in hippocampus
Aoki et al. (2014)	2014	Rats	ABA	SD	∼24 f	1 h food, 24 h wheel	Resilience and susceptibility to ABA: resilient animals have lower alpha 4 GABA receptors in hippocampus
Aravich et al. (1995)	1993	Rats	ABA	SD	80 m	1.5 h food, 22.5 h wheel	Intervention in ABA: 2-deoxy-D-glucose (2DG) injection reduced food intake
Atchley and Eckel (2005)	2005	Rats	ABA	Long Evans	24 f	2 h food, 24 h wheel	Fenfluramine (serotonin agonist) treatment in ABA: increases weight loss
Atchley and Eckel (2006)	2006	Rats	ABA	Long Evans	17 f	2 h food, 24 h wheel	8-OH-DPAT treatment (reduces serotonin) in ABA: prevents weight loss
Avraham et al. (1996)	1996	Mice	Reduced calories	Sabra	103 f	60 and 40% of daily calories	Specific diet: tyrosine high food improved cognitive function
Avraham et al. (2017)	2017	Mice	Reduced time	Sabra	50 f	2.5 h food	Injection treatment: 2-arachidonylglycerol increases food intake
Barbarich-Marsteller et al. (2013a)	2013	Rats	ABA	SD	32 f	1 h food, 24 h wheel	Brain changes in ABA: ABA reduces cell proliferation in hippocampus
Barbarich-Marsteller et al. (2005)	2005	Rats	ABA	Wistar	9 f	40% of baseline food intake, 24 h wheel	Imaging in ABA: first study using micro PET imaging of rats
Barbarich-Marsteller et al. (2013b)	2013	Rats	ABA	SD	80 f	1 h food, 24 h wheel	Susceptibility to ABA: defining vulnerability subtypes
Belmonte et al. (2016)	2016	Mice	ABA	C57BL/6	48 f	3 h food, 24 h wheel	Immune system in ABA: TLR4 upregulated in ABA
Breton et al. (2020)	2019	Mice	ABA	C57BL/6	32 f	3 h food, 24 h wheel	Metabolic changes in ABA: analysis of fecal metabolite changes in ABA
Brown et al. (2008)	2008	Rats	ABA	SD	66 m	1 h food, 24 h wheel	Special diet: high fat diet prevents ABA
Campos et al. (2019)	2019	Rats	Food restriction	Fischer	84 f	40% of control animal food intake	Anxiety and behavior: Estrogen receptor beta activation reverses anxiety like behavior
Carrera et al. (2009)	2009	Rats	ABA	SD	144 (72 m, 72 f)	1.5 h food, 22.5 h wheel	Female rats that had longer times of maternal separation are more resilient to ABA
Casteels et al. (2014)	2014	Rats	ABA	Wistar	80 (23 m, 57 f)	1.5 h food, 24 h wheel	Endocannabinoid system: changes in endocannabinoid transmission in PET imaging
Chen et al. (2018)	2018	Mice	ABA	C57Bl/6J wild-type and α4-subunit of GABA A receptors (α4) KO	90 (35 m, 36 f WT and 9 m KO and 10 f KO)	2 h food, 24 h wheel	Resilience to ABA: female mice with upregulation of alpha4 GABA A receptors were more resilient, but not male

(Continued)

TABLE 1 | Continued

References	Year	Species	Model	Strain	*N*	Methods: Anorexia protocol	Topic and important findings
Chen et al. (2017)	2017	Rats	ABA	SD	32 f	1 h food, 24 h wheel	Susceptibility to ABA: NR2A-NMDA receptors correlate with physical activity in ABA
Cerrato et al. (2012)	2012	Rats	ABA	SD	48 f	1.5 h food, 22.5 h wheel	Heat (ambient temperature 32°C) helps rats reverse ABA and maintain body weight
Chowdhury et al. (2013a)	2013	Rats	ABA	SD	16 f	1 h food, 24 h wheel	Brain changes in ABA: apical dendritic branching in dorsal and ventral hippocampal CA1 might explain anxiety
Chowdhury et al. (2014)	2014	Rats	ABA	SD	30 f	1 h food, 24 h wheel	Brain changes in ABA: hippocampal changes depend on whether ABA was started during adolescence or adulthood
Chowdhury et al. (2013b)	2013	Mice	ABA	C57BL/6	23 f	1 h food, 24 h wheel ($n = 13$, only 1 in 5 survived 3 days), 2 h food 24 h wheel ($n = 10$, all 10 survived 3 days)	Resilience to ABA: Mice with hippocampal CA1 pyramidal cells that receive more glutamic contacts are more resilient
Collu et al. (2020)	2020	Rats	ABA	SD	64 f	1.5 h food, 22.5 h wheel	Inflammatory processes: ABA altered central inflammatory pathways
Collu et al. (2019)	2019	Rats	ABA	SD	36 f	1.5 h food, 22.5 h wheel	Hormonal changes: Impaired brain endocannabinoid tone in ABA
Duclos et al. (2005)	2005	Rats	ABA	Fischer 344, Brown Norway and Lewis	72 m	1.5 h food, 22.5 h wheel	Rat strain differences in ABA and HPA axis involvement in running activity
Endou et al. (2001)	2001	Rats	ABA	SD	36 m	1.5 h food, 22.5 h or 24 h wheel	Neurotransmitters: ABA decreased histaminergic neuron system activity
Farinetti et al. (2020)	2019	Rats	ABA	SD	48 (24 m 24 f)	1 h food, 2 h running wheel (just before food)	Maternal separation and ABA: maternally separated female ABA rats were more hyperactive, male not
Filaire et al. (2009)	2009	Rats	ABA	Wistar	56 m	1 h food, 23 h wheel	Lipid peroxidation and antioxidant status in ABA rats
Fraga et al. (2020)	2020	Rats	ABA	SD	74 m	60% of baseline food, 24 h wheel	Heat/increased room temperature is better at preventing ABA than leptin effects
Francois et al. (2015)	2015	Mice	ABA	C57Bl/6	32 m	3 h food, 24 h wheel	Ghrelin in ABA: ABA mice have more preproghrelin mRNA expressing cells in the stomach
Frintrop et al. (2018a)	2018	Rats	Chronic ABA	Wistar	41 f	40% of baseline food intake until 25% body weight loss (acute starvation), then stable weight with adjusted food (chronic starvation), 24 h wheel	Brain changes: reduced astrocyte density might be cause of brain volume reduction in ABA
Frintrop et al. (2019)	2019	rats	Chronic ABA	Wistar	47 f	40% of baseline food intake until 25% body weight loss (acute starvation), then stable weight with adjusted food (chronic starvation), 24 h wheel	Imaging in ABA: longitudinal MRI and post mortem study of brain volume loss in ABA
Frintrop et al. (2018b)	2018	Rats	Chronic ABA	Wistar	53 f	40% of baseline food intake until 25% body weight loss (acute starvation), then stable weight with adjusted food (chronic starvation), 24 h wheel	ABA protocol: development of a more chronic ABA model
Gelegen et al. (2007)	2007	Mice	ABA	C57BL/6J and DBA/2J	C57BL/6J ($n = 14$) and DBA/2J ($n = 15$) all f	2 h food, 24 h wheel	Mice strain differences in susceptibility to ABA

(Continued)

TABLE 1 | Continued

References	Year	Species	Model	Strain	*N*	Methods: Anorexia protocol	Topic and important findings
Gelegen et al. (2010)	2010	Mice	ABA	Each strain in the panel has a chromosome pair substituted from the A/J strain on to a host C57BL/6J background	321 f	2 h food, 24 h wheel	Mice strain differences in susceptibility to ABA and chromosomal mapping of susceptibility to ABA (excessive running)
Gelegen et al. (2008)	2008	Mice	ABA	36 C57BL/6J and 21 A/J, some dopamine transporter knockout	57 f	2 h food, 24 h wheel	Neurotransmitters: dopamine receptor D2 expression in the caudate putamen increased in ABA and BDNF expression in the hippocampus reduced
Giles et al. (2016)	2016	Rats	ABA	SD	f	1 h food, 23 h wheel	Refeeding after ABA: ABA rats had more hepatic lipid accumulation
Gilman et al. (2019)	2019	Rats	ABA	SD	73 f/m	1 h food, 24 h wheel	Neurotransmitter: ABA modulates dopamine transporter functional plasticity during adolescence
Gutiérrez et al. (2006)	2006	Rats	ABA	Wistar	32 m	1.5 h food, 22.5 h wheel	High ambient temperature (27–29°C) decreases rate of body weight loss in ABA
Gutierrez et al. (2008)	2008	Rats	ABA	SD	48 m	1.5 h food, 22.5 h wheel	Heat prevents ABA
Gutierrez et al. (2009)	2009	Rats	ABA	SD	24 m	1.5 h food, 22.5 h wheel	Heat prevents ABA and reverses hypothalamic MC4 overexpression in ABA animals
Hancock and Grant (2009)	2009	Rats	ABA	SD	94 (48 m, 46 f) half adolescent and half adult	2 h wheel followed by 1 h food	Maternal separation: maternally separated adolescent ABA rats ran more and ate less
Hao et al. (2001)	2001	Mice	separation induced	Sabra	70 f	Separation into single cage	Tyrosine improves separation induced body weight loss and impairment in cognitive behavior
Hata et al. (2019)	2019	Mice	Stool transplant by AN patient	Germ-free BALB/c	80 f	Food intake *ad libitum*	Intervention: stool transplant of anorexic patient stool leads to anorexia in mice
Hillebrand et al. (2006b)	2006	Rats	ABA	Wistar	29 f	1 h food, 24 h wheel	Neurotransmitter: MSH and Agouti related peptide involvement in ABA
Hillebrand et al. (2005b)	2005	Rats	ABA	Wistar	64 f	1 h food, 24 h wheel	Hormonal treatment: leptin treatment aggravates ABA
Hillebrand et al. (2005c)	2005	Rats	ABA	Wistar	30 f	1 h food, 24 h wheel	Drug treatment in: olanzapine treatment reduced physical activity
Hillebrand et al. (2005a)	2005	Rats	ABA	Wistar	13 f	1 h food, 24 h wheel	Warm plate access reduced running in ABA and weight loss
Hillebrand et al. (2006a)	2006	Rats	ABA	Wistar	30 f	1 h food, 24 h wheel	Treatment with appetite suppressant d-fenfluramine reduced water intake, but not food intake
Ho et al. (2016)	2016	Mice	ABA	Balb/cJ	28 f	6 h food, 24 h wheel	Neurotransmitter: BDNF expression in mesocorticolimbic reward circuit
Hurel et al. (2019)	2019	Mice	ABA	C57BL/6N	32 m/f	50% amount of food, 24 h wheels	Post-weaning isolation trauma in mice
Jean et al. (2012)	2012	Mice	ABA	Male KO1B, KO4 and WT 129/SvPas	40 m	80% amount of food, 24 h wheel	Neurotransmitter: MDMA in mice with ABA

(Continued)

TABLE 1 | Continued

References	Year	Species	Model	Strain	*N*	Methods: Anorexia protocol	Topic and important findings
Jean et al. (2017)	2017	Mice	Restraint-stress induced hypophagia and Overexpression of 5-HT4Rs in the mPFC	129SvPas WT, 129SvTer 5-HT4R KO, and WT mice	60 m	Restraint-stress and Overexpression of 5-HT4Rs in the medial prefrontal cortex	5-HT4 receptor expression in the medial prefrontal cortex rescues hypophagia
Jesus et al. (2014)	2014	Mice	ABA	C57Bl/6	40 m	3 h food, 24 h wheel	Intestinal barrier dysfunction in ABA mice
Johansen et al. (2000)	2000	Mice	anx/anx	anx mice	30 m/f	Genetic aberration	anx mouse model: hypothalamic CART anx and serum leptin are reduced in anx mice
Johnson et al. (1996)	1996	Marmot-set prima-tes	Social isolation	*Callithrix jacchus* jacchus	36 m/f	2 weeks complete social isolation from peers	Social isolation leads to body weight loss in small monkeys
L'Huillier et al. (2019)	2019	Mice	ABA	C57BL/6	58 m	3 h food, 24 h wheel	Glutamine restores colonic permeability in ABA
Kim et al. (2017)	2017	Mice	anx/anx	anx/+ mice and anx/anx	111	anx	anx mouse model: tyrosine kinase receptor Tyro3 enhances lifespan and Npy neuron survival in anx mice
Kinzig and Hargrave (2010)	2010	Rats	ABA	Long Evans	39 f	1 h food, 24 h wheel	Behavior: ABA in adolescence increases anxiety in adults
Klenotich et al. (2015)	2015	Mice	ABA	Balb/cJ	98 f	6 h food, 24 h wheel	Drug treatment: amisulpride (D2 antagonism) reduces ABA
Klenotich et al. (2012)	2012	Mice	ABA	Balb/cJ and A/J	102 f	6 h food, 24 h wheel	Drug treatment: olanzapine treatment increases survival in ABA
Koh et al. (2000)	2000	Rats	ABA with alley	SD	24 m	1 h food, 24 h alley or wheel	Circular alley does not work like wheel running activity in ABA
Kumar and Kaur (2013)	2013	Rats	Wistar	Intermittent fasting 24 h on/24 h off	24 m/f	24 h food *ad lib*, 24 h no food, alternating	Intermittent fasting negatively effects on estrous cycle in rats
Legrand et al. (2016)	2016	Mice	C57Bl/6	ABA	59 m	3 h food 24 h wheel	Ghrelin: ghrelin treatment prevents ABA
Lewis and Brett (2010)	2010	Mice	C57/BL6	ABA	112 m	3 h food 21 h wheel	Endocannabinoid system: THC decreased survival in ABA, but increased feeding in survivors
Liang et al. (2011)	2011	Rats	SD	ABA	43 f	1. group 2 h food, 2. group 1 h food, 24 h wheel	Food aversion learning is stronger in rats after recovery of ABA
Lindfors et al. (2015)	2015	mice	anx/anx	anx	47 (21 anx) m/f	anx	anx mouse model: glucose intolerance in anx mice
Lujan et al. (2006)	2006	Rhesus monkey	Reduced food intake		5 f	Dietary restriction in calories	Caloric restriction leads to amenorrhea in rhesus monkeys
Lutter et al. (2017b)	2017	Mice	Original mice were B6/CBA F1 hybrid mice and 87.5% C57BL/6, then heterozygous for HDAC4A778T		64 m/f	HDAC4A778T mutation	Female mice heterozygous for HDAC4A778T display several eating disorder related feeding and behavioral deficits
Madra and Zeltser (2016)	2016	Mice	Val66Met genotype	Genotype, social isolation, juvenile caloric restriction	40 f	20–30% dietary restriction, genetic susceptibility	Female mice with genetic susceptibility to anxiety, decrease food intake on social isolation
Mequinion et al. (2015b)	2015	Mice	C57BL/6J	ABA	82 f	Quantitative food restriction comprising 30%/day for 3 days and then 50%/day until the end of protocol, 24 h wheel	Physical activity in ABA

(Continued)

TABLE 1 | Continued

References	Year	Species	Model	Strain	*N*	Methods: Anorexia protocol	Topic and important findings
Mequinion et al. (2017)	2017	Mice	C57BL/6J	Food restriction	24 f	Gradually restricted to 2 h a day	Persistent hypoleptinemia in mice after recovery from decreased body weight
Mercader et al. (2008)	2008	Mice	anx/anx	anx	6 m	anx	anx mouse model: hypothalamus transcriptome profile
Nakahara et al. (2012)	2012	Mice	C57BL/6 J	Valine deficient diet	36 m	Valine deficient diet	Specific diet: valine deficient diet leads to weight loss
Nobis et al. (2018a)	2018	Mice	C57Bl/6	ABA	48f	3 h food, 24 h wheel	Intestinal barrier: analysis of colonic mucosal proteome
Nobis et al. (2018c)	2018	Mice	C57Bl/6	ABA	24 f	3 h food, 24 h wheel	ABA mice have delayed gastric emptying
Nobis et al. (2018b)	2018	Mice	C57Bl/6	ABA	48 f	Progressive limited food access from 6 h/day (day 6) to 3 h/day (day 9), wheel 24 h	ABA mice show changes in proteome, mitochondrial dynamic and signs of autophagy in the hypothalamus
Paulukat et al. (2016)	2016	Rats	Wistar	ABA	47 f	40% food intake, until 20% weight loss, then 2 weeks maintenance	Memory impairment in ABA is associated with decrease in estrogen
Perez-Leighton et al. (2014)	2014	Rats	SD	ABA	57 m/f	1 h food, 24 h wheel	Spontaneous physical activity predicts susceptibility to ABA in rats
Petrovich and Lougee (2011)	2011	Rats	SD	ABA	25 m, 32f	1 h food, 24 h wheel	Prolonged effects of fear induced feeding cessation in females compared to males
Pjetri et al. (2012)	2012	Mice and rats	11 inbred mouse strains (A/J, AKR/J, BALB/cByJ, C3H/HeJ, C57BL/6J, CAST/EiJ, DBA/2J, FVB/NJ, KK/HlJ, NZW/LacJ, WSB/EiJ, and Wistar	ABA	98 mice, 34 rats	2 h food for mice, 1.5 h food for rats, 24 h wheel	Susceptibility to ABA in 11 inbred mouse strains
Reyes-Haro et al. (2015)	2015	Rats	Wistar	Dehydration induced anorexia	27 f	Dehydration-induced anorexia (DIA) group received a 2.5% NaCl solution as their sole drinking liquid with no food restriction; food-restricted group, a positive control to distinguish between starvation and dehydration effects, received tap water *ad libitum* and the same amount of food consumed by the DIA animals	Dehydration induced anorexia reduces astrocyte density
Reyes-Haro et al. (2016)	2016	Rats	Wistar	Dehydration induced anorexia	24 f	Dehydration-induced anorexia (DIA) group received a 2.5% NaCl solution as their sole drinking liquid with no food restriction; food-restricted group, a positive control to distinguish between starvation and dehydration effects, received tap water *ad libitum* and the same amount of food consumed by the DIA animals	Dehydration induced anorexia reduce astrocyte density in the hippocampus

(Continued)

TABLE 1 | Continued

References	Year	Species	Model	Strain	*N*	Methods: Anorexia protocol	Topic and important findings
Rieg and Aravich (1994)	1994	Rats	SD	ABA	30 m	1.5 h food, 22.5 wheel	Drug treatment: Clonidine increases feeding in ABA but not body weight
Scharner et al. (2018)	2018	Rats	SD	ABA	24 f	1.5 h food, 24 h wheel	Neurotransmitter: CRF immunoreactive neurons activated in ABA
Scharner et al. (2016)	2016	Rats	SD	ABA	44 f	1.5 h food, 24 h wheel	Brain changes: mapping of ABA brain with cFOS immunohistochemistry
Scharner et al. (2017)	2017	Rats	SD	ABA	24 f	1.5 h food, 24 h wheel	Brain changes: nesfatin-1 immunoreactive neurons in ABA
Scherma et al. (2017)	2017	Rats	SD	ABA	42 f	1.5 h food, 24 h wheel	Cannabinoid receptor agonists in ABA reduce hyperactivity
Schroeder et al. (2018)	2018	Mice	ICR/CD1	ABA	60 m/f	?	Placental miR-340 mediates vulnerability to ABA in mice
Skowron et al. (2018)	2018	Rats	Wistar	ABA	16 f	?	ABA's rats' weight of their uterus decreased and the number of follicles in the ovaries too
van Kuyck et al. (2007)	2007	Rats	Wistar	ABA	19 m	1.5 h food, 24 h wheel	Micro PET study of ABA
Verhagen et al. (2011a)	2011	Rats and mice	Wistar rats, C57Bl/6 ghrelin receptor knockout	ABA	77 rats 24 mice, all f	2 h food, 24 h wheel	Ghrelin levels are highly associated with activity n ABA
Verhagen et al. (2011b)	2011	Rats	Wistar	ABA	64 f	1.5 h food, 24 h wheel	Leptin reduces hyperactivity
Verhagen et al. (2009a)	2009	Rats	Wistar	ABA	56 f	1.5 h food, 24 h wheel	Dopamine antagonism inhibits ABA
Verhagen et al. (2009b)	2009	Rats	Wistar	ABA	24 f	1.5 h food, 24 h wheel	Dopamine in the NAc was increased during feeding in ABA
Verty et al. (2011)	2011	Rats	SD	ABA	28 f	1.5 h food, 24 h wheel	Cannabinoid system: THC reduces weight loss
Wable et al. (2014)	2014	Rats	SD	ABA	8 f	1 h food, 24 h wheel	Neurotransmitter: changes in GABA A receptors in amygdala in ABA
Wable et al. (2015a)	2015	Mice	C57BL6	ABA	23 f	2 h food, 24 h wheel	Exogenous progesterone aggravates running in adolescent female mice
Wable et al. (2015b)	2015	Mice	C57BL6	ABA	36 f	2 h food, 24 h wheel	Anxiety is correlated with running in female mice in ABA
Welch et al. (2019)	2019	Mice	D2-Cre BAC transgenic mice	D2 Receptor overexpression	40 m/f		D2 overexpression leads to increased weight loss during restrictive feeding schedule
Welkenhuysen et al. (2008)	2008	Rats	Wistar	ABA	26 f	1.5 h food, 24 h wheel	Intervention: Electrical stimulation in the lateral hypothalamus in ABA did not have significant effects
Wojciak (2014)	2014	Rats	Wistar	Intermittent fasting	48 f	1 group (half the food intake of control group). 2 group 1 day *ad lib*, 1 day starvation, 3 group 2 day *ad lib*, 2 day starvation, etc 4 days on (*ad lib*), 4 days starvation	Intermittent fasting decreased hemoglobin in rats
Wu et al. (2014)	2014	Rats	Wistar	ABA	56 f	1.5 h food, 24 h wheel	Behavior: Investigations of food anticipatory activity
Zgheib et al. (2014)	2014	Mice	C57Bl/6	Separation-based anorexia	48 f	2 h food, separation	Separation based anorexia

?, unclear; ad lib, ad libitum; f, female; m, male.

Animal Models

Different animal models and experimental protocols were used in the 108 included studies (**Table 1**). We assessed and divided them into 18 groups. One overall common finding is that most study protocols state that after a 25 or 30% weight loss, animals are taken out of the experiment for ethical reasons. Some studies had additional parameters for termination of the experiment: food intake in rodents below 2 g/24 h or signs of stress.

Environmental Models

Activity-Based Anorexia (ABA)

In total, 81 of the 108 analyzed studies used the ABA model. Therefore, the ABA model is by far the most used animal model to mimic anorexia nervosa. The ABA model is a rodent model that combines food restriction (usually time restricted to a few hours daily) with the possibility for the rodents to run in a running wheel. The combination of these two factors leads, in rodents, to significant weight loss. The extent of the weight loss is mainly dependent on the length of the time period that the animals have access to food. There are two opposing ideas among ABA researchers whether the animals should have constant access (24 h) to the running wheel or whether during the period of feeding the running wheel should be blocked. Usually, studies in which the running wheel gets blocked during the feeding time reason that they do not want to bring the animals in a conflict of whether they prefer running or eating; but in studies that do not block the running wheel, it is often argued that bringing the animals in this conflict is an interesting aspect of this model.

In the ABA studies included in this review, rats and mice were used. Younger animals (adolescents) are more susceptible to developing ABA, but the model works with adult animals as well. Both, in rats and mice, animals usually get a time period in which they get food a*d libitum* but are already in the cage in which they have access to the running wheel. This habituation period usually provides a baseline for running activity and for food intake for each animal. Depending on the experimental protocol, the habituation period lasts between 3 to 10 days with 7 days being a very commonly used time. The period is followed by food restriction. In rats, animals usually have access to food for either 1, 1.5, or 2 h per day. In mice it is more common to have a gradual food restriction from *ad libitum* 24 h access to food to 6 h a day for 3 days for example, and then a further decrease to 3 h a day.

ABA With Circular Alley Instead of Wheel

Koh et al. tested whether activity in a flat circular alley also produces the ABA syndrome (Koh et al., 2000). They compared animals that had 24 h access to a wheel with animals that had 24 h access to a circular alley. Both groups had access to food for 1 h per day. The animals with the alley did not develop ABA and in contrast to wheel running, their amount of activity in the alley decreased over days (Koh et al., 2000). The researchers hypothesized that alley activity, in contrast to wheel running, may not be reinforcing and that most likely a physical activity must be reinforcing in order to lead to ABA development (Koh et al., 2000).

Chronic ABA in Rats

The ABA model has evolved to be the most commonly used animal model for anorexia nervosa. The chronic ABA model has a changed protocol and tries to address one of the common critique points of the ABA model: that ABA is a very acute model and does not reflect the chronicity of the disease anorexia nervosa. Three studies used the chronic ABA model developed by the research group of Frintrop et al. (2018b). In the chronic ABA model, animals also have access to a running wheel the whole day and receive 40% of their individual baseline food intake (Frintrop et al., 2018b). This regimen is maintained until a 20 to 25% body weight reduction has been reached, which in ABA is the typical period of acute starvation (Frintrop et al., 2018b). Afterwards, rats receive a daily adjusted amount of food to maintain their lower body weight for 14 more days which is the period of chronic starvation (Frintrop et al., 2018b). Female rats experience a complete cessation of the estrous cycle in this model (Frintrop et al., 2018b).

Chronic ABA in Mice

Mequinion et al. established a mouse model in C57Bl/6 mice for chronic ABA (Mequinion et al., 2015b). They used a quantitative food restriction comprising 30%/day of baseline food intake for 3 days and then 50%/day of baseline food intake until the end of protocol (Mequinion et al., 2015b). The mice had 24 h access to a wheel. In this protocol, the mice with a running wheel reached a crucial point of body weight loss (especially fat mass) faster than mice with food restriction only (Mequinion et al., 2015b). However, in contrast to the food-restricted control mice, their body weight stabilized, giving rise to a protective effect of moderate, regular physical activity (Mequinion et al., 2015b). The long-term nature of the protocol induced alterations in bone parameters similar to those observed in anorexia patients. Both food-restricted groups differentially adapted their energy metabolism in the short and long term, with less fat oxidation in food-restricted mice with a running wheel and a preferential use of glucose to compensate for the chronic energy imbalance (Mequinion et al., 2015b). Similar to patients with restrictive anorexia nervosa, mice exhibited low leptin levels, high plasma concentrations of corticosterone and ghrelin as well as a disruption of the estrous cycle (Mequinion et al., 2015b).

Activity

Adams et al. used a model of voluntary activity in rats that led to food intake suppression (Adams et al., 2009). Rats had 24 h *ad libitum* access to a running wheel which led to an average food intake suppression of 5 g per day (from 30 g to 25 g daily) (Adams et al., 2009).

Reduced Calories

Two studies used caloric restriction as a mean to investigate cognitive and behavioral effects of the reduced body weight in animals. The caloric intake was reduced to 60 and 40% of baseline caloric intake in mice in one study (Avraham et al., 1996) and to

40% of control animals' food intake in the second study (Campos et al., 2019). Cognitive function was evaluated using a modified eight-arm maze with rewards. Animals fed to 60% of controls showed improved maze performance while this was significantly impaired in animals on food restriction to 40% (Avraham et al., 1996). However, in these animals, injections of tyrosine restored performance (Avraham et al., 1996). The second study showed that animals with food restriction showed more anxiety- like behavior than controls (Campos et al., 2019).

Reduced Calories in Rhesus Monkeys

Lujan et al. investigated in four normal-weight and one obese female rhesus monkeys the relationship between caloric intake and amenorrhea (Lujan et al., 2006). The weight loss required to inhibit ovulation ranged from 2 to 11% in the four normal-weight animals and was achieved with a 23% reduction in dietary intake (Lujan et al., 2006). The animals were provided a healthy diet with low caloric food. From the first day of reduced food intake to first missed ovulation was on average 62 $\pm$ 13 days. In the obese monkey only after 10 months of food reduction and a weight loss of 46% body weight lead to inhibition of ovulation (Lujan et al., 2006). The onset of anovulation was not preceded by changes in menstrual cycle length or progesterone secretion (Lujan et al., 2006). When animals were allowed free access to food again, ovulation restarted typically at a body weight close to the animal's weight at the time of the last ovulatory cycle during dietary restriction (Lujan et al., 2006). By contrast, caloric intake at the return of ovulation during realimentation was 28% greater than before amenorrhea (Lujan et al., 2006).

Reduced Time of Food Access per Day

Two studies initiated weight loss in mice by reducing their access time to food to 2.5 h per day (Avraham et al., 2017) or a gradual reduction down to 2 h per day (Mequinion et al., 2017).

Intermittent Fasting

Two studies used intermittent fasting schedules in rats. Kumar et al. investigated the effects on the HPA axis of an intermittent fasting schedule with 24 h *ad libitum* access to food alternating with 24 h without access to food in female and male rats (Kumar and Kaur, 2013). They observed significant changes in body weight, blood glucose, estrous cyclicity and serum estradiol, testosterone and LH level indicating a negative role of the intermittent fasting regimen on reproduction in these young animals (Kumar and Kaur, 2013).

Wojciak et al. examined the effect of five different feeding regimens on iron and hemoglobin levels in the blood of rats (Wojciak, 2014). They had one group that received 50% of the food intake of a control group. The second group had 1 day *ad libitum* access to food alternating with 1 day of no access to food. The third group had 2 days *ad libitum* access to food alternating with 2 days of no access to food. The fourth group had 3 days *ad libitum* access alternating with 3 days of no access to food. The fifth group had 4 days *ad libitum* access to food and 4 days no access to food (Wojciak, 2014). They found that the longer the starvation the stronger the negative effect on blood concentrations of hemoglobin, hematocrit, RBC, serum ferritin and iron levels in different organs (but even in rats with acute starvation a decrease in these parameters was observable) (Wojciak, 2014).

Valine-Deficient Diet

Nakahara et al. fed mice a special diet that was deficient in the essential amino acid valine (Nakahara et al., 2012). The ingestion of this diet results in a significant reduction of food intake and body weight within 24 h, and this phenomenon continues throughout the period over which such a diet is supplied (Nakahara et al., 2012). Nakahara et al. investigated the mechanisms that lead to this weight loss and found that the expression of somatostatin mRNA is increased in the hypothalamus in the mice that received a Valine-deficient diet (Nakahara et al., 2012). They reported, too, that when somatostatin was administered intracerebroventricularly (icv) to normal weight animals that were fed a control diet, their 24 h food intake decreased significantly (Nakahara et al., 2012).

Dehydration-Induced Anorexia

Reyes-Haro et al. used dehydration-induced anorexia to examine specific effects of this model on the brain in Wistar rats (Reyes-Haro et al., 2015, 2016). The dehydration-induced anorexia group received a 2.5% NaCl solution as their sole drinking liquid with no food restriction (Reyes-Haro et al., 2015, 2016). Additionally, they had a food-restricted group which served as positive control to distinguish between starvation and dehydration effects. The food-restricted group received tap water *ad libitum* and the same amount of food consumed by the dehydration-induced anorexia animals. The authors described that in dehydration-induced anorexia rats the astrocyte density was significantly reduced (∼34%) in the body of the corpus callosum (but no changes in the genu and the splenium callosum) (Reyes-Haro et al., 2015) and the glia cell density was about 20% reduced in all regions of the hippocampus, except in CA1 (Reyes-Haro et al., 2016).

Separation-Induced Anorexia in Mice

Hao et al. separated mice into single cages (Hao et al., 2001) which led to self-induced weight loss caused by separation stress. Separation significantly decreased body weight in mice (Hao et al., 2001). They showed in their study, that tyrosine-rich food in mice with separation-induced weight loss and decreased cognitive function, restored their cognitive function and restored their separation-induced low dopamine levels (Hao et al., 2001).

Separation-Induced Anorexia in Monkeys

Johnson et al. investigated body weight loss in marmoset primates. The animals were in complete social isolation from peers for 2 weeks (Johnson et al., 1996). All animals (male and female) lost close to 10% (around 25 g) of their body weight after 2 weeks of social isolation (Johnson et al., 1996).

Separation Combined With Reduced Time Access to Food

Zgheib et al. combined a reduced access time to food of 2 h per day and separation into single cages in mice (Zgheib et al., 2014). The animals displayed marked alterations in body weight, fat

mass, lean mass, bone mass acquisition, reproductive function, GH/IGF-1 axis and circulating leptin levels (Zgheib et al., 2014). All these alterations were corrected during the recovery phase, except for the hypoleptinemia that persisted despite full recovery of fat mass (Zgheib et al., 2014).

Procedure-Induced Models

Stool Transplantation of Patients With Anorexia Nervosa to Mice

Hata et al. investigated the effects of stool transplantation from human patients with restrictive anorexia nervosa in germ-free mice (Hata et al., 2019). The female offspring of the anorexia patient-stool transplanted mice showed a decrease in body weight gain, concomitant with reduced food intake compared to the female offspring of mice that received stool from healthy individuals (Hata et al., 2019). Food efficiency ratio (body weight gain/food intake) was also significantly lower in the female offspring of anorexia patient-stool transplanted mice than in the female offspring of healthy individuals-stool transplanted mice, suggesting that decreased appetite as well as the capacity to convert ingested food to unit of body substance may contribute to poor weight gain (Hata et al., 2019).

Genetic Models

Anx/anx

Four of the 108 included articles used the anx/anx genetic mouse model. The anorexia *(anx)* mutation is an autosomal recessive mutation detected in 1984 by Maltais et al. that causes starvation in mice. *anx/anx* mice appear normal at birth, but develop growth failure and low body weight, even appearing emaciated, as well as neurological motor disturbances (e.g., head weaving (head moving up and down), gait abnormalities and hyperactivity) (Maltais et al., 1984). Usually, they die early, between the age of 3–5 weeks, due to severe malnutrition. The amount of milk consumed by *anx*/*anx* mice is significantly lower than for littermate controls and leads to a caloric deficit. Researchers have made differing statements about how similar this model is to anorexia nervosa, but many stated that this mutation might play an important role as a model system for the study of basic feeding drive (Maltais et al., 1984).

Mercader et al. performed an expression profiling in the hypothalamus of the *anx/anx* mice (Mercader et al., 2008). Their results show enrichment in deregulated genes involved in cell death, cell morphology and cancer, as well as an alteration of several signaling circuits involved in energy balance including neuropeptide Y and melanocortin signaling (Mercader et al., 2008).

Johansen et al. showed that in mice with the genetic aberration *anx/anx* levels of CART mRNA and peptide-immunoreactive cell bodies and fibers in the arcuate nucleus were decreased and additionally a lower number of detectable CART-expressing cells in the dorsomedial hypothalamic nucleus/lateral hypothalamic area was observed (Johansen et al., 2000). Moreover, serum leptin levels were significantly lower in *anx/anx* mice compared to normal littermates (Johansen et al., 2000).

Kim et al. identified a mutation (C19T) that converts arginine to tryptophan (R7W) in the TYRO3 protein tyrosine kinase 3 (*Tyro3*) gene, which resides within the *anx* critical interval, likely contributing to the severity of the *anx* phenotype (Kim et al., 2017). *Tyro3* is expressed in the hypothalamus and other brain regions affected by the *anx* mutation, and its mRNA localization appeared abnormal in *anx/anx* brains by postnatal day 19 (Kim et al., 2017). The presence of wild-type *Tyro3* transgenes, but not an *R7W-Tyro3* transgene, doubled the weight and lifespans of *anx/anx* mice and near-normal numbers of hypothalamic neuropeptide Y expressing neurons were present in *Tyro3*-transgenic *anx/anx* mice (hypothalamic neuropeptide Y expressing neurons are reduced in anx/anx mice) (Kim et al., 2017). Further analyses indicated that the C19T *Tyro3* mutation is present in a few other mouse strains, and hence is not the causative *anx* mutation, but rather an *anx* modifier (Kim et al., 2017).

Lindfors et al. investigated glucose tolerance in *anx*/*anx* mice (Lindfors et al., 2015). *anx/anx* exhibit marked glucose intolerance associated with reduced insulin release following an intraperitoneal (ip) injection of glucose (Lindfors et al., 2015). In contrast, insulin release from isolated *anx*/*anx* islets is increased after stimulation with glucose or KCl (Lindfors et al., 2015). In addition, they show elevated concentrations of free fatty acids in *anx*/*anx* serum and increased macrophage infiltration (indicative of inflammation) in *anx*/*anx* islets (Lindfors et al., 2015).

Heterozygous for HDAC4A778T

Lutter et al. found that a rare missense mutation in the gene for the transcriptional repressor histone deacetylase 4 (HDAC4) is associated with the risk of developing an eating disorder in humans (Lutter et al., 2017a). To investigate further the biological consequences of this missense mutation, the authors created transgenic mice carrying this mutation by introducing the alanine to threonine mutation at position 778 of mouse Hdac4 (corresponding to position 786 of the human protein) (Lutter et al., 2017b). Female mice heterozygous for HDAC4A778T displayed several eating disorder-related feeding and behavioral deficits depending on housing condition, whereas male mice did not show any behavioral differences (Lutter et al., 2017b). Individually housed HDAC4A778T female mice exhibited reduced effortful responding for high-fat diet and compulsive grooming, whereas group-housed female mice displayed increased weight gain on a high-fat diet, reduced behavioral despair and increased anxiety-like behavior (Lutter et al., 2017b).

D2-Cre BAC Transgenic Mice—Overexpression of Dopamine 2 Receptors on Nucleus Accumbens Core Neurons

Welch et al. investigated mice that overexpressed dopamine-2 receptors on nucleus accumbens core (D2R-OENA mice) neurons that endogenously express D2 receptors, and tested mice of both sexes in the open field test, ABA paradigm and the ip glucose tolerance test (Welch et al., 2019). D2R-OENAc did not alter baseline body weight but increased locomotor activity in the open field across both sexes. During constant access to food and running wheels, D2R-OENAc mice of both sexes increased food intake and ran more than controls. However, when food

was available only 7 h a day, only female D2R-OENAc mice rapidly lost 25% of their initial body weight, reduced food intake, and substantially increased wheel running (Welch et al., 2019). Surprisingly, female D2R-OENAc mice also rapidly lost 25% of their initial body weight during scheduled fasting without wheel access and showed no changes in food intake. In contrast, male D2R-OENAc mice maintained body weight during scheduled fasting (Welch et al., 2019). D2R-OENAc mice of both sexes also showed glucose intolerance in the IGTT. The findings implicate that the overexpression of D2 receptors in the nucleus accumbens core neurons alters glucose metabolism in both sexes but drives robust weight loss only in females during scheduled fasting (Welch et al., 2019).

Overexpression of 5-HT4Rs in the Medial Prefrontal Cortex Neurons + Restraint Stress

Restraint-stress can induce transient hypophagia in mice. In this study by Jean et al., they examined the effects of restraint stress on transgenic mice that overexpressed 5-HT4 receptors in the medial prefrontal cortex (Jean et al., 2017) which is involved in goal-directed behavior (decision making). They showed that mice with this overexpression displayed restraint stress-induced hypophagia that was more persistent than in wild type mice (Jean et al., 2017).

Val66Met Genotype + Social Isolation + Juvenile Caloric Restriction

In this study Madra et al. examined mice that were genetically more susceptible to anxiety (Madra and Zeltser, 2016). Female mice with the *hBDNF*-Val66Met allele were exposed to social isolation stress during adolescence and a restricted caloric intake by 20–30% for 11 days (Madra and Zeltser, 2016). Approximately 40% of the female *hBDNF*-Val66Met carriers exposed to early social isolation stress and caloric reduction during adolescence exhibited severe self-imposed dietary restriction, sometimes to the point of death (Madra and Zeltser, 2016).

Important Findings in ABA (Table 1)

Sex Differences

Achamrah et al. reported greater susceptibility of male mice to develop ABA leading to a higher mortality rate in male mice and slightly different physical activity patterns (Achamrah et al., 2016a).

ABA rats of both sexes display hyperactive behavior associated with reduced anxiety-like behavior when compared to controls in tests like open field and elevated plus maze (Hancock and Grant, 2009; Farinetti et al., 2020). Farinetti et al. further investigated this phenomenon and found a sexually dimorphic effect of early maternal separation in ABA rats: female rats exposed to maternal separation+ ABA were even more hyperactive with further diminished anxiety-related behaviors compared to females of ABA group, while in male rats maternal separation did not exert an additional effect to their behavior (Farinetti et al., 2020). Hancock et al. examined sex differences in early separation and ABA as well and found age-specific sex differences: compared to handled females, maternally separated females demonstrated greater increases in wheel running and a more pronounced running-induced suppression of food intake during adolescence, but not in adulthood (Hancock and Grant, 2009). In contrast, it was only in adulthood that wheel running produced more prolonged anorexic effects in maternally separated males than in handled males (Hancock and Grant, 2009).

Petrovich et al. tested the phenomenon of fear induced-food cessation in ABA rats (by combining electro shocks to one foot with a tone and then playing just that tone during food intake) (Petrovich and Lougee, 2011). They found that female rats showed sustained fear-cue induced feeding inhibition compared to males during the extinction (the period in which the rats "unlearn" that the tone is associated with pain (Petrovich and Lougee, 2011).

One study by Skowron et al. looked specifically at the effect of ABA on female reproductive organs during the cessation of the estrous cycle (Skowron et al., 2018). They reported that in the ABA group the weight of the uteri and the number of follicles in the ovaries decreased significantly (Skowron et al., 2018).

Rodent Strain Differences

The most commonly used rat strains were Sprague-Dawley or Wistar rats, which are known to be rather physically active. However, a few studies used other rat strains like Long Evans, which is known to be less active. All rat strains included in this review developed ABA.

Most studies involved Wistar and Sprague Dawley strains. Duclos et al. tested Brown Norway, Lewis and Fischer rats in the ABA model (Duclos et al., 2005). They found that Brown Norway and Lewis rats lost 25% of body weight faster than Fischer rats (Duclos et al., 2005). Additionally, they tested daily the prefeeding corticosterone levels in the blood of the rats which were increased in the two more susceptible rat strains under ABA conditions, while no rise was observed in Fischer rats (Duclos et al., 2005).

In mice by far most studies were performed on C57BL/6J mice (Gelegen et al., 2007). Gelegen et al. tested the differences between C57BL/6J and DBA/2J inbred mouse strains because they have been previously reported as having low and high anxiety, respectively (Gelegen et al., 2007). C57BL/6J mice during ABA reduced their wheel activity, in contrast to DBA/2J mice which exhibited increased physical activity (Gelegen et al., 2007). Food restriction induced hypoleptinemia in both strains, but the decline in plasma leptin was stronger in DBA/2J mice and correlated with increased activity only in that strain (Gelegen et al., 2007). In a further study they investigated a panel of mouse chromosome substitution strains derived from C57BL/6J and A/J strains and their reaction to ABA (Gelegen et al., 2010). They showed that A/J chromosomes 4, 12, and 13 contribute to the development of excessive running wheel activity in response to daily restricted feeding and hence, accelerated weight loss (Gelegen et al., 2010). Gelegen et al. mentioned that regions on mouse chromosomes 4, 12, and 13 display homology with regions on human chromosomes linked with anxiety and obsessionality in anorexia cohorts (Gelegen et al., 2010).

Pjetri et al. tested the ABA model on 11 different strains of mice (A/J, AKR/J, BALB/cByJ, C3H/HeJ, C57BL/6J, CAST/EiJ, DBA/2J, FVB/NJ, KK/HlJ, NZW/LacJ, and WSB/EiJ) and Wistar rats and found that baseline wheel running activity levels preceding the scheduled food restriction phase strongly predicted activity-based anorexia susceptibility compared to other baseline parameters (Pjetri et al., 2012).

Vulnerability/Susceptibility to ABA

Perez-Leighton et al. reported that baseline spontaneous physical activity before ABA (voluntary in a cage without a running wheel) can predict the baseline running activity and the probability of high weight loss in rats (Perez-Leighton et al., 2014).

The research group of Chen et al. examined gender-specific vulnerability to ABA in mice (Chen et al., 2018). ABA led to an overall suppression of wheel running (compared to baseline) but there was a sex-specific effect: suppression of wheel running occurred during the food-anticipatory hours in males, while in females suppression was observed during food-access hours. Correspondingly, only females adaptively increased food intake (Chen et al., 2018). Another study reported that rats with the highest body weight loss had the lowest level of food-anticipatory activity (running in the wheel during the time period of 4 h before feeding) and that postprandial activities are more directly predictive of weight loss (Wu et al., 2014). Barbarich-Marsteller et al. tried to identify vulnerable subtypes to ABA and found that rats with maximal hyperactivity, minimal food intake, and the shortest time to experimental exit were most vulnerable, while those with minimal activity and the longest time to experimental exit were more resistant (Barbarich-Marsteller et al., 2013b).

As infant/adolescent trauma is a risk factor for the development of anorexia nervosa, the study by Hurel et al. analyzed the impact of post-weaning isolation on body weight and wheel-running performance in female mice exposed to an ABA protocol (Hurel et al., 2019). Post-weaning isolation amplified ABA-elicited body weight reduction and stimulated wheel-running activities in anticipation of feeding in female mice compared to controls (Hurel et al., 2019).

Schroeder et al. found that by screening placental microRNA expression of naive and prenatally stressed fetuses and assessing vulnerability to ABA that miR-340 might be a sexually dimorphic regulator involved in prenatal programming of ABA (Schroeder et al., 2018). Prenatal stress caused hypermethylation of placental miR-340, which is associated with reduced miR-340 expression and increased protein levels of several target transcripts linked to the expression of several nutrient transporters both in mice and human placentas (Schroeder et al., 2018).

Carrera et al. showed that female rats that were exposed to longer times of maternal separation (180 min) during their first 20 days of their life were more resilient to ABA (Carrera et al., 2009). Interestingly, they did not see this effect of longer survival times in male rats, neither in rats that experienced only short times of maternal separation (15 min) (Carrera et al., 2009).

Effects of Different Diets

Brown et al. examined the effect of a high-fat diet in ABA rats (1 h food access/day, 24 h running wheel) (Brown et al., 2008). Access to the sweet high-fat chow both reversed and prevented the weight loss typical for activity-based anorexia (Brown et al., 2008). Vegetable fat reduced body weight loss, but to a lesser degree than the sweet high-fat diet (Brown et al., 2008). In contrast, addition of saccharin or sucrose solutions to the standard lab chow diet had no effect (Brown et al., 2008).

Giles et al. found that weight restoration on a high carbohydrate refeeding diet promotes rapid weight regain in ABA compared to rats that were food restricted without a running wheel (Giles et al., 2016). Further, they reported that after refeeding ABA rats had higher hepatic lipid accumulation compared to food restricted rats which had more lipid accumulation in visceral adipose tissue despite maintaining the same total body weight in both groups (Giles et al., 2016).

Neurocognitive and Behavioral Changes

Some studies show that food-restricted animals display more anxiety behavior (Campos et al., 2019), while others show that they have less anxiety behavior (Wable et al., 2015b) giving rise to other contributing factors. Campos et al. described that estrogen receptor beta activation within the dorsal raphe nucleus reversed anxiety-like behavior induced by food restriction in rats (Campos et al., 2019). This points into the direction that decreased estrogen levels in food-restricted animals lead to anxiety behavior (Campos et al., 2019). Another study reported that food restriction, with or without exercise, reduced anxiety as measured by the proportion of entries into the open arms of the elevated plus maze (Wable et al., 2015b). Moreover, the authors found a correlation that individual ABA animals with less entries (more anxious) displayed more running behavior in the wheel (Wable et al., 2015b).

In Hata et al.'s study of stool transplantation of patients with anorexia nervosa in germ-free mice both anxiety-related behavior measured by open-field tests and compulsive behavior measured by a marble-burying test were increased only in female offspring of mice that received the human anorexia nervosa stool transplantation, but not in the female offspring of the healthy human stool-transplanted mice (Hata et al., 2019).

Kinzig et al. wanted to investigate whether experience with ABA produced enduring effects on brain and behavior (Kinzig and Hargrave, 2010). They tested adult female rats that had experienced ABA during adolescence for anxiety-like behavior and also showed in elevated plus maze and open field test increased anxiety behavior compared to adult rats with only food restriction experience in adolescence (Kinzig and Hargrave, 2010). Lastly, in chronic ABA, starvation disrupted menstrual cycle and impaired memory function (object recognition memory) which became statistically significant in the chronic state compared to control rats (Paulukat et al., 2016). 17 β-estradiol level reduction correlated with the loss of memory in the chronic condition (Paulukat et al., 2016) suggesting a role of estrogens in cognitive functions as well.

Neuroendocrine and Cerebral Changes

Aoki et al. showed that female ABA rats exhibit a rise of α4 and δ subunits of α4βδ GABA receptors at puberty onset compared to control animals (Aoki et al., 2012) and that animals that

do not develop ABA have lower α4 GABA receptors in CA1 hippocampus than rats that develop ABA (Aoki et al., 2014). They demonstrated that exogenous progesterone exacerbates the running response of adolescent female mice to repeated food restriction stress by increasing alpha4-GABA A receptor expression on hippocampal CA1 pyramid neurons (Wable et al., 2015a). The same research group examined effects of ABA on GABA receptors in the amygdala, too, and found that in ABA mice excitatory synapses on dendritic shafts of the caudal basal amygdala exhibit elevated levels of GABA A receptor α4 subunit (Wable et al., 2014).

The group around Chowdhury examined the effects of ABA on cells in the hippocampus. They showed that cell proliferation was acutely reduced in the hippocampus after 3 days of ABA and that this effect was mainly on gliogenesis and not on neurogenesis (Barbarich-Marsteller et al., 2013a). In the dorsal hippocampus, which preferentially mediates spatial learning and cognition, cells of ABA animals had less total dendritic length and fewer dendritic branches in stratum radiatum than in controls (Chowdhury et al., 2013a). In the ventral hippocampus, which preferentially mediates anxiety, ABA evoked more branching in stratum radiatum than in control animals (Chowdhury et al., 2013a). The authors state that these results may indicate that ABA elicits pathway-specific changes in the hippocampus that may explain the increased anxiety and reduced behavioral flexibility observed in ABA (Chowdhury et al., 2013a). In another study they reported that ABA during adolescence disrupts normal development of the CA1 pyramidal cells in the ventral hippocampus (increased branching), which did not occur in ABA during adulthood suggesting an age-dependent effect on structural plasticity (Chowdhury et al., 2014). They reported, too, that hippocampal CA1 pyramidal cells of ABA-resilient mice receive enhanced glutamic acid decarboxylase contacts compared to the pyramidal cells of ABA-susceptible mice (Chowdhury et al., 2013b). Furthermore, NR2A- and NR2B-NMDA receptors and drebrin within postsynaptic spines of the hippocampus correlated with hunger-evoked exercise and a rat's individual ABA severity (Chen et al., 2017).

Two studies in chronic ABA rats observed the volumes of the cerebral cortex and corpus callosum to be significantly reduced compared to controls by 6 and 9%, respectively (Frintrop et al., 2018a). The number of GFAP-positive astrocytes in these regions decreased, but no changes in neurons were observed (Frintrop et al., 2018a). Furthermore, mean astrocytic GFAP mRNA expression was similarly reduced in ABA animals, as was the mean cell proliferation rate, whereas the mean apoptosis rate did not increase (Frintrop et al., 2019). Longitudinal animal MRI confirmed a reduction in the mean brain volumes of ABA animals compared to controls (Frintrop et al., 2019). After refeeding, the starvation-induced effects were almost completely reversed (Frintrop et al., 2019).

Nobis et al. examined the hypothalamus of ABA mice with proteomic analysis and found changes in the proteome, mitochondrial signaling (increase in fission, no change in fusion) and signs of autophagy (increased dynamin-1, and LC3II/LC3I ratio) (Nobis et al., 2018b) which shows adaptation of the hypothalamic protein synthesis to ABA.

Barbarich-Marsteller et al. performed the first study with micro PET imaging in ABA in 2005 and found increased intake of 18-fluorodeoxyglucose (FDG) in the cerebellum, and decreased in the hippocampus and striatum compared to control animals (Barbarich-Marsteller et al., 2005). In a study from 2007 increased uptake was once again found in the cerebellum and additionally in the mediodorsal thalamus and the ventral pontine nuclei, while decreased uptake was seen in the striatum again and in the left rhinal and bilateral insular cortex (van Kuyck et al., 2007).

In a PET imaging of the type 1 cannabinoid receptor in ABA animals, widespread transient disturbance of the endocannabinoid transmission was shown compared to control animals (Casteels et al., 2014). Another study indicated that cannabinoid receptor 1 density was decreased in the dentate gyrus of the hippocampus and in the lateral hypothalamus (Collu et al., 2019). After recovery, the density was partially normalized in some areas (Collu et al., 2019).

Endou et al. reported that ABA in rats decreased the activity of the histaminergic neuron system and intraventricular administration of histamine significantly reduced the hyperactivity caused by ABA (Endou et al., 2001).

Brain-derived neurotrophic factor (BDNF), an activity-dependent modulator of neuronal plasticity, is reduced in the serum of AN patients, and is a known regulator of feeding and weight maintenance (Ho et al., 2016). Gelegen et al. described reduced BDNF expression in the hippocampus of ABA mice (Gelegen et al., 2008). Ho et al. examined the effects of scheduled feeding and running wheel access on the expression of BDNF transcripts within the mesocorticolimbic pathway (Ho et al., 2016). Conversely, they found that scheduled feeding increased the levels of BDNF mRNA in the hippocampus and decreased BDNF mRNA levels in the medial prefrontal cortex (Ho et al., 2016). In addition, wheel running increased BDNF mRNA expression in the ventral tegmental area (Ho et al., 2016).

Gelegen et al. described increased dopamine receptor D2 expression in the caudate putamen of ABA mice (Gelegen et al., 2008). Gilman et al. studied dopamine transporters in ABA and suggest that ABA modulates dopamine transporter functional plasticity during adolescence in a sex-dependent and age-specific manner (Gilman et al., 2019).

Activation of the melanocortin system leads to hypophagia and increased energy expenditure in *ad libitum* fed rats (Hillebrand et al., 2006b). Pro-opiomelanocortin (POMC) gene expression is normally decreased during negative energy balance (Hillebrand et al., 2006b). Hillebrand et al. reported a transient up-regulation of POMC mRNA levels in the arcuate nucleus during the development of ABA, giving rise to a hyperactive melanocortin system (Hillebrand et al., 2006b). However, ABA development was not influenced by treating ABA rats with the competitive melanocortin antagonist SHU9119 (Adan et al., 2011). Instead, treatment with the inverse agonist Agouti related peptide (AgRP) did ameliorate signs of ABA (Adan et al., 2011) pointing toward constitutive signaling of the receptor.

Jean et al. investigated the addictive facet of anorexia by studying the nucleus accumbens (NAc) (Jean et al., 2012). They found that nucleus accumbens 5-HT_4 receptor overexpression upregulated NAc-cocaine and amphetamine related transcript

(CART) and provoked anorexia and hyperactivity (Jean et al., 2012). NAc-5-HT_4 knockdown or blockade reduced ecstasy-induced hyperactivity (Jean et al., 2012). Finally, NAc-CART knockdown suppressed hyperactivity upon stimulation of the NAc-5-HT_4 (Jean et al., 2012).

Verhagen et al. examined the dopamine and serotonin levels in the NAc upon development of ABA (Verhagen et al., 2009b). Surprisingly, the release of dopamine and serotonin in the NAc were not increased during wheel running in the time period just before scheduled feeding time (Verhagen et al., 2009b). Dopamine release in the NAc was increased while eating in ABA rats (Verhagen et al., 2009b). During ABA, levels of serotonin were low and circadian activity was blunted (Verhagen et al., 2009b).

In an investigation of c-Fos expression in the brain of ABA rats, our research group found neuronal activation in several brain nuclei such as the supraoptic nucleus, arcuate nucleus, locus coeruleus and nucleus of the solitary tract of ABA compared to *ad libitum* fed rats, indicating neuronal activation in brain areas involved in the regulation of several functions such as motor activity, stress response, food intake and thermogenesis (Scharner et al., 2016).

Our research group also examined CRF immunohistochemistry in brains of ABA rats (Scharner et al., 2018). ABA increased the number of c-Fos/CRF double labeled neurons in the paraventricular nucleus and the dorsomedial hypothalamic nucleus compared to *ad libitum* fed animals but not to restricted fed rats, pointing toward brain CRF playing a role in the development and maintenance of ABA possibly by activation of nuclei involved in food intake, thermogenesis and circadian rhythms regulation (Scharner et al., 2018).

In another study, we tried to further determine the role of the anorexigenic hormone nesfatin-1 in ABA (Scharner et al., 2017). ABA increased the number of nesfatin-1 immunopositive neurons in the paraventricular nucleus, arcuate nucleus, dorsomedial hypothalamic nucleus, locus coeruleus and in the rostral part of the nucleus of the solitary tract compared to *ad libitum* fed rats but not to restricted fed rats (Scharner et al., 2017). Moreover, we observed significantly more c-Fos and nesfatin-1 double-labeled cells in ABA rats compared to all control groups in the supraoptic nucleus and compared to *ad libitum* fed animals in the paraventricular nucleus, arcuate nucleus, dorsomedial hypothalamic nucleus, dorsal raphe nucleus and the rostral raphe pallidus (Scharner et al., 2017). These results indicate that the observed changes of brain nesfatin-1 might play a role in the pathophysiology and symptomatology under conditions of ABA, since nesfatin-1 plays a role in the inhibition of food intake and the response to stress (Scharner et al., 2017).

Induction of and recovery from ABA altered central COX, LOX and CYP pathways in rats (Collu et al., 2020). Arachidonic acid and arachidonic acid derived eicosanoids levels were altered in corticolimbic brain areas of female rats displaying an ABA phenotype (Collu et al., 2020). mRNA expression of PLA2, ALOX-5 and ALOX-15 enzymes was altered in the nucleus accumbens and caudate putamen regions in ABA rats (Collu et al., 2020).

Metabolic System

Filaire et al. showed that food-restricted rats had higher plasma antioxidant concentrations and higher alpha-tocopherol concentrations in the liver when compared to animals fed *ad libitum* (Filaire et al., 2009). They also showed that food restriction coupled to wheel running decreased antioxidant parameters in liver, and plasmatic lipid peroxidation parameters and increased antioxidant plasma concentrations when compared to the *ad libitum* sedentary situation (Filaire et al., 2009). Thus, ABA might have a different effect on antioxidant parameters than food restriction without physical activity, but further research on the different effects and pathways is necessary.

Gut-Brain Axis

Intestinal Barrier

Intestinal barrier alterations in ABA were reported by Jesus et al. Colonic histology showed decreased thickness of the muscularis layer in ABA and colonic permeability was increased in ABA compared to control animals, while jejunal permeability was not affected (Jesus et al., 2014). ABA mice exhibited increased paracellular permeability and reduced protein synthesis in the colonic mucosa (L'Huillier et al., 2019). Oral glutamine supplementation restored colonic paracellular permeability and protein synthesis and increased the mucin-2 mRNA level without affecting body weight (L'Huillier et al., 2019). Colonic mucosal proteome is altered during ABA suggesting a downregulation of energy metabolism (Nobis et al., 2018a). A decrease of protein synthesis and an activation of autophagy were also observed to be mediated by mTOR pathway (Nobis et al., 2018a).

Fecal Metabolites

Physical activity altered the abundance of 14 fecal metabolites involved in gut microbial metabolism and proteolysis (Breton et al., 2020). Food restriction only and ABA both disrupted a wide range of metabolic pathways including gut microbial metabolism, proteolysis and fatty acid breakdown (24 urinary and 6 plasma metabolites), but there were no differences between food restricted or ABA animals (Breton et al., 2020) giving rise to food restriction driving the changes in microbiota.

Intestinal Inflammatory Status

ABA seems to affect intestinal inflammatory status and the hypothalamic response (Belmonte et al., 2016). Belmonte et al. found that TLR4 was upregulated both on colonic epithelial cells and intestinal macrophages, leading to elevated downstream mucosal cytokine production (Belmonte et al., 2016). Paradoxically, TLR4-deficient mice exhibited greater vulnerability to ABA with increased mortality rate, suggesting a major contribution of TLR4-mediated responses during ABA-induced weight loss (Belmonte et al., 2016).

Gastric Emptying

Both food restricted and ABA mice exhibited a delayed gastric emptying compared with controls (Nobis et al., 2018c). ABA mice specifically exhibited an increased rate of gastric oxidized proteins (Nobis et al., 2018c).

Ghrelin

Preproghrelin mRNA expressing cells were studied by *in situ* hybridization in mice (Francois et al., 2015). ABA increased their number in the stomach proportionally to body weight loss (Francois et al., 2015). Verhagen et al. described that plasma ghrelin levels were highly associated with food anticipatory behavior, measured by running wheel activity in rats (Verhagen et al., 2011a). Furthermore, they showed that ghrelin receptor (GHS-R1A) knockout mice do not anticipate food when exposed to the ABA model, unlike their wild type littermate controls (Verhagen et al., 2011a). Likewise, food anticipatory activity in the ABA model was suppressed by a GHS-R1A antagonist administered either by acute central (icv) injection in rats or by chronic peripheral treatment in mice (Verhagen et al., 2011a). The GHS-R1A antagonist treatment did not alter food intake in any of these models (Verhagen et al., 2011a). Legrand et al. examined the effects of a single daily intraperitoneal injection of ghrelin together from obese or lean mice before access to food in ABA mice (Legrand et al., 2016). They found that ghrelin from obese, but not lean mice, prevented the hyperactivity typical in ABA, however, they were not able to diminish body weight loss (Legrand et al., 2016).

Leptin

Hillebrand et al. examined the effects of chronic leptin treatment (icv, 4 μg/day over 5 days) (Hillebrand et al., 2005b). Leptin treatment decreased running wheel activity in ABA rats and reduced food intake as well as increased energy expenditure by thermogenesis in ABA rats (Hillebrand et al., 2005b). Altogether, this resulted in a stronger negative energy balance and body weight loss in leptin-treated ABA rats (Hillebrand et al., 2005b). Verhagen et al. showed, too, that icv leptin injections and local injections of leptin into the ventral tegmental area suppress running wheel activity (Verhagen et al., 2011b) pointing toward an important role of leptin/hypoleptinemia in physical (hyper)activity.

Interventions

Drug Treatment

Aravic et al. showed that 2-deoxy-D-glucose (2DG) injections paradoxically reduced food intake in ABA (as also seen in human anorexia nervosa where it is associated with decreased subjective hunger ratings) (Aravich et al., 1995). Avraham et al. examined the effects of intraperitoneal 2-arachidonoylglycerol injections in restricted fed mice (Avraham et al., 2017). 2-Arachidonoylglycerol administered 10 min before food intake increased food intake and improved cognition by elevating norepinephrine and L-DOPA in the hippocampus (Avraham et al., 2017).

Deep Brain Stimulation

In an experiment of electrical stimulation in the lateral hypothalamus in ABA rats, Welkenhuysen et al. could not show any differences between the ABA animals receiving the stimulation and control animals (Welkenhuysen et al., 2008).

Temperature Increase in the Experimental Room

Gutierrez et al. examined the effects of increased ambient temperature in the experimental room on the development of ABA since ABA often leads to hypothermia (Gutiérrez et al., 2006; Gutierrez et al., 2008; Cerrato et al., 2012). They found that increased ambient temperature reduced running rates and led to weight gain in female and male ABA rats (Gutiérrez et al., 2006; Gutierrez et al., 2008; Cerrato et al., 2012). The effect of increasing ambient temperature on food intake in food restricted rats was dependent on whether they had access to a running wheel (ABA) or not (Gutierrez et al., 2008). In their 2006 study they showed that male rats had less weight loss when kept at high ambient temperatures (27–29°C), but even less if their running wheel access was additionally reduced to only 3 h a day (compared to 22.5 h in their normal ABA protocol) (Gutiérrez et al., 2006). In their 2008 study they showed that although warming reduced food intake in the food restricted sedentary rats their body weight remained stable, whereas in ABA rats increased ambient temperature did not reduce food intake and weight gain gradually rose (Gutierrez et al., 2008). Female sedentary food-restricted rats at 32°C ambient temperature were able to maintain the same body weight as the sedentary food-restricted rats at 21°C ambient temperature, but ate 20% less food (Cerrato et al., 2012). Moreover, hypothalamic melanocortin 4 receptors were increased in ABA rats, but reduced in ABA rats at high ambient temperature (32°C) (Gutierrez et al., 2009). Fraga et al. showed that room temperature increase was better at preventing hyperactivity in ABA than leptin infusion, which led to a decrease in hyperactivity too, but less pronounced (Fraga et al., 2020). Lastly, Hillebrand et al. examined whether a warm plate that was installed in the cage of the rats would influence development of ABA (Hillebrand et al., 2005a). They reported that during ABA, rats preferred the warm plate and hypothermia was prevented, accompanied by reduced hyperactivity and body weight loss when compared to ABA rats without a plate (Hillebrand et al., 2005a).

Medication Trials in ABA

Chlorpromazine

Adams et al. reported that chlorpromazine prevented running induced feeding suppression in rats (Adams et al., 2009). Rats that were treated with the first generation antipsychotic medication, chlorpromazine, had a significantly higher food intake than controls (Adams et al., 2009).

Fluoxetine, 8-OH-DPAT and Fenfluramine

Altemus et al. examined drugs with serotonergic effects in ABA (Altemus et al., 1996). They found that ABA rats with daily fluoxetine treatment (SSRI increasing serotonin) ate most and ran least, rats with imipramine (TCA increasing serotonin) ran and ate similar to saline rats and rats with para-chlorophenylalanine (PCPA, tryptophan hydroxylase inhibitor that depletes serotonin) ate least and ran most (Altemus et al., 1996). In another study by Klenotich et al., it was shown that fluoxetine in ABA mice increased food intake and reduced food anticipatory activity, but did not alter survival (Klenotich et al., 2012). Conversely, Atchley et al. found that treatment with

8-OH-DPAT (which reduces serotonergic activity) attenuates weight loss in ABA female rats by reducing hyperactivity (but food intake was similar) (Atchley and Eckel, 2006).

Two studies examined the effects of fenfluramine in ABA: Fenfluramine is an appetite suppressant drug in humans and acts agonistic on 5-HT2C receptors located on pro-opiomelanocortin (POMC) neurons in the arcuate nucleus of the hypothalamus (Atchley and Eckel, 2005; Hillebrand et al., 2006a). Atchley et al. showed that treatment with fenfluramine in female Long Evans ABA rats accelerates the weight loss (Atchley and Eckel, 2005). Hillebrand et al. reported 1 year later in a study in Wistar rats that unexpectedly, fenfluramine treated ABA rats did not reduce food intake or increase wheel running as compared with vehicle-treated ABA rats (Hillebrand et al., 2006a). However, fenfluramine treated ABA rats showed hypodypsia and increased plasma osmolality and arginine-vasopressin expression levels in the hypothalamus (Hillebrand et al., 2006a).

Dopamine 2/3 Receptor Antagonists (Antipsychotics)

Rats were chronically infused with the atypical antipsychotic drug olanzapine and exposed to the ABA model or *ad libitum* feeding (Hillebrand et al., 2005c). Olanzapine treatment reduced development of ABA in rats by reducing running wheel activity, starvation-induced hypothermia and activation of the hypothalamus-pituitary-adrenal axis (Hillebrand et al., 2005c). In another study by Klenotich et al. it was demonstrated that olanzapine significantly increased survival and reduced food anticipatory activity in ABA mice (Klenotich et al., 2012). However, olanzapine did not alter food intake or overall running wheel activity (Klenotich et al., 2012).

Additionally, Klenotich et al. showed that D2/3 receptor antagonists eticlopride and amisulpride reduced weight loss and hypophagia and increased survival during ABA in mice (Klenotich et al., 2015). Furthermore, they reported that amisulpride produced larger reductions in weight loss and hypophagia than olanzapine (Klenotich et al., 2015). Treatment with either D3 receptor antagonist SB277011A or the D2 receptor antagonist L-741,626 also increased survival in ABA mice (Klenotich et al., 2015). Verhagen et al. examined the effects of different dosages of treatment with the non-selective dopaminergic antagonist *cis*-flupenthixol in ABA rats (Verhagen et al., 2009a). *cis*-flupenthixol treated ABA rats reduced body weight loss and running wheel activity and increased food intake compared to control ABA rats. Food-anticipatory activity still persists in *cis*-flupenthixol treated ABA rats (Verhagen et al., 2009a).

Tetrahydrocannabinol (THC)

Lewis et al. studied the effects of Δ9-THC treatment on ABA. Δ9-THC decreased survival in ABA mice but increased feeding in the survivors (Lewis and Brett, 2010). Contrary findings were reported by Scherma et al.: they showed that subchronic administration of the natural CB1/CB2 receptor agonist Δ9-THC and as well the synthetic CB1/CB2 receptor agonist CP-55,940 decreased body weight loss and running wheel activity in ABA rats (Scherma et al., 2017). Moreover, leptin signaling was increased, while plasma levels of corticosterone were decreased (Scherma et al., 2017). Lastly, the research group by Verty et al. found, too, that Δ9-THC treatment led to an attenuation of ABA in rats (Verty et al., 2011).

Clonidine

Rats were implanted subcutaneously with osmotic minipumps infusing 0, 30, or 300 zg/kg/day of clonidine and exposed to ABA (Rieg and Aravich, 1994). Results showed that clonidine did not affect the rate of weight loss during ABA, but increased food intake at the lower dose and wheel activity at the higher dose (Rieg and Aravich, 1994).

Recovery From ABA

Refeeding After ABA With Continuous Access to Running Wheel

Achamrah et al. examined the effects of voluntary access to a running wheel during refeeding of ABA mice and found that exercising in a running wheel during refeeding had positive effects (Achamrah et al., 2016b). Only the mice with access to running wheels completely restored their fat-free mass from before having undergone ABA and had less colonic hyperpermeability than their sedentary refeeding controls (Achamrah et al., 2016b). The general locomotor behavior and specifically the behavior in dark-light boxes of the mice that ran in running wheels improved compared to the sedentary controls (Achamrah et al., 2016b).

Taste Aversion Learning

Liang et al. compared the acquisition and extinction of a conditioned taste aversion in a naïve, ABA, and pair-fed rat group (Liang et al., 2011). The conditioned taste aversion conditioning was done after the ABA and pair-fed rats had regained all their weight from before the food restriction (Liang et al., 2011). For the CTA learning, 0.3 M sucrose consumption was followed by low doses lithium chloride (0.009 M or 0.018 M at 1.33 ml/100 g of body weight, ip) injection (Liang et al., 2011). The results showed that the ABA rats developed an aversion to sucrose significantly sooner than the naïve controls (Liang et al., 2011). Furthermore, their response was more persistent, as they completely avoided sucrose, while the naïve and pair-fed controls still tried it by the end of 10 conditioning trials (Liang et al., 2011). When extinction was assessed by 1-bottle and 2-bottle tests, it took the ABA rats longer to extinguish the aversion than the controls (Liang et al., 2011).

Neuroendocrine Changes

Mequinion et al. investigated what effects long-term energy deficits in mice exert after recovery of body weight (Mequinion et al., 2017). They showed that after a long-term energy deficit (10 weeks), mice exhibited persistent hypoleptinemia following the refeeding period (10 weeks) despite restoration of fat mass, ovarian activity, and feeding behavior (Mequinion et al., 2017). The refeeding period induced an overexpression of leptin receptor mRNA in the hypothalamus (Mequinion et al., 2017).

DISCUSSION

We performed a systematic literature review of studies on animal models for anorexia nervosa. The research on animal models for anorexia nervosa has already started decades ago and many findings contributed to the understanding of mechanisms of hunger and satiety, physical activity and cognition in an underweight state and other mechanisms relevant for anorexia nervosa in humans.

Different animal models of anorexia nervosa have been developed with advantages and disadvantages. In our review, we found and described 18 different animal models. One model of particular interest from among the genetic animal models is the anx/anx model. Interesting findings about the effects of hunger/satiety regulatory peptides like neuropeptide Y and agouti-related peptide have been made in this model. An advantage of the model is that despite the animals having *ad libitum* access to food, they still lose body weight, which mimics one feature of anorexia nervosa. A disadvantage of the model is that animals have many other neurological changes apart from hypophagia and overall have a very short survival time, therefore many researchers have concluded that their genetic expression profile along with the phenotype resembles more cachexia syndromes observed in cancer or chronic diseases rather than anorexia nervosa (Mercader et al., 2008).

The most commonly used animal model to study anorexia nervosa is the activity-based anorexia (ABA) model. It does mimic some aspects of anorexia nervosa, namely, body weight loss, increased physical activity, cessation of the estrous cycle in females and alterations in the hypothalamus-hypophysis-adrenal axis. The most frequent points of critique were the lack of psychosocial factors that play a decisive role in patients with anorexia nervosa and the acuity of the model that does not reflect the human condition that often starts in adolescence but might go on for many years. The chronic ABA models developed by Frintrop et al. for rats (Frintrop et al., 2018b) and by Mequinion et al. for mice (Mequinion et al., 2015b) do provide a more chronic time course than the acute ABA model and therefore reflect better the human condition. Two factors that are still not reflected in this model are that genetic predisposition makes some humans more susceptible to anorexia nervosa and that psychosocial factors play a role in the first manifestation and during the course of the disease.

Specific neurocognitive and behavioral changes were observed in the ABA model, including changes in anxiety-like behavior in which decreased estrogen might lead to increased anxiety (Kinzig and Hargrave, 2010; Campos et al., 2019). Apart from that an individual rat's level of anxiety behavior might correlate with its physical activity in the running wheel (Campos et al., 2019). Rats' baseline physical activity in a cage with and without a running wheel during the *ad libitum* fed period, is the best predictor for a rat's individual chance of susceptibility to ABA (Perez-Leighton et al., 2014). One study examined effects of stool transplantation of anorexia nervosa patients in germ free mice in their female offspring and the results are very interesting and warranting further research (Hata et al., 2019). Intestinal barrier alterations are observed in ABA including increased colonic permeability (Jesus et al., 2014). Neuroendocrine changes that were described in the ABA model include an increase in α4 GABA receptors in the CA1 hippocampus and amygdala (Aoki et al., 2012; Wable et al., 2014), alterations and decreased cell proliferation in the hippocampus (Chowdhury et al., 2013a) and a reduction in the density of astrocytes and a reduction in the volume of the cerebral cortex and corpus callosum (Frintrop et al., 2018a), which might be completely reversible by refeeding (Frintrop et al., 2019). Other findings were altered endocannabinoid (Casteels et al., 2014), histaminergic (Endou et al., 2001), BDNF (Gelegen et al., 2008; Ho et al., 2016), and dopaminergic (Gelegen et al., 2008; Gilman et al., 2019) transmission. Several studies investigated the effects of medication on ABA where specifically chlorpromazine (Adams et al., 2009), fluoxetine (Altemus et al., 1996), olanzapine (Klenotich et al., 2012), amisulpride (Klenotich et al., 2015), and cis-flupenthixol (Verhagen et al., 2009a) were shown to reduce ABA symptoms and point therefore in future directions of medication trials in anorexia nervosa.

There are some limiting factors to consider for this systematic review. First, by searching only from among the three most commonly used scientific databases we likely exclude some studies (e.g., so-called gray literature). These databases sometimes do not have the best fitting mesh/keywords for articles, so that many articles were found in our search that we were not looking for, that were for example human studies or animal models on other diseases than anorexia nervosa and these had to be excluded. Additionally, papers were not included that did not show up in the search. Second, we had strong exclusion criteria that reduced the total number of included studies to 108. We may have therefore excluded additional information that might have been found in the excluded reviews, including articles written in another language.

Despite the shortcomings of animal models in general and models for anorexia nervosa in particular, we do encourage the further investigation of animal models for anorexia nervosa. As we have explained above, we especially recommend future research in the chronic ABA model that is a further development of the ABA model. Although many aspects of anorexia nervosa remain poorly understood, many finding of studies discussed in this review present interesting directions toward further research. We encourage especially further research on the gut-brain-axis including intestinal microbiome changes and further research in neuronal brain circuit alterations including neurotransmitter changes.

DATA AVAILABILITY STATEMENT

The original contributions presented in the study are included in the article/supplementary material, further inquiries can be directed to the corresponding author/s.

AUTHOR CONTRIBUTIONS

SS performed the literature search and wrote the first draft of the paper. AS planned and supervised the project as well as thoroughly revised the paper. All authors contributed to the article and approved the submitted version.

FUNDING

This work was supported by funding of the German Research Foundation STE 1765/3-2 and Charité University Funding UFF 89/441-176 (AS).

ACKNOWLEDGMENTS

We acknowledge support from the German Research Foundation (DFG) and the Open Access Publication Fund of the Charité Universitätsmedizin Berlin.

REFERENCES

Achamrah, N., Nobis, S., Belmonte, L., Goichon, A., Breton, J., Legrand, R., et al. (2016a). Gender differences in mice during activity-based anorexia. *Clin. Nutr.* 35(Suppl. 1):S207. doi: 10.1016/S0261-5614(16)30780-4

Achamrah, N., Nobis, S., Breton, J., Jesus, P., Belmonte, L., Maurer, B., et al. (2016b). Maintaining physical activity during refeeding improves body composition, intestinal hyperpermeability and behavior in anorectic mice. *Sci. Rep.* 6:21887. doi: 10.1038/srep21887

Adams, K. L., Parfeniuk, G. G., and Eikelboom, R. (2009). Chlorpromazine specifically prevents the wheel-induced feeding suppression in rats. *Pharmacol. Biochem. Behav.* 93, 470–473. doi: 10.1016/j.pbb.2009.06.010

Adan, R. A., Hillebrand, J. J., Danner, U. N., Cardona Cano, S., Kas, M. J., and Verhagen, L. A. (2011). Neurobiology driving hyperactivity in activity-based anorexia. *Curr. Top. Behav. Neurosci.* 6, 229–250. doi: 10.1007/7854_2010_77

Altemus, M., Glowa, J. R., Galliven, E., Leong, Y. M., and Murphy, D. L. (1996). Effects of serotonergic agents on food-restriction-induced hyperactivity. *Pharmacol. Biochem. Behav.* 53, 123–131. doi: 10.1016/0091-3057(95)02003-9

American-Psychiatric-Association (2013) *Diagnostic and Statistical Manual of Mental Disorders,* 5th Edn. Washington, DC.

Aoki, C., Sabaliauskas, N., Chowdhury, T., Min, J. Y., Colacino, A. R., Laurino, K., et al. (2012). Adolescent female rats exhibiting activity-based anorexia express elevated levels of GABA(A) receptor alpha4 and delta subunits at the plasma membrane of hippocampal CA1 spines. *Synapse* 66, 391–407. doi: 10.1002/syn.21528

Aoki, C., Wable, G., Chowdhury, T. G., Sabaliauskas, N. A., Laurino, K., and Barbarich-Marsteller, N. C. (2014). alpha4betadelta-GABAARs in the hippocampal CA1 as a biomarker for resilience to activity-based anorexia. *Neuroscience* 265, 108–123. doi: 10.1016/j.neuroscience.2014.01.011

Aravich, P. F., Stanley, E. Z., and Doerries, L. E. (1995). Exercise in food-restricted rats produces 2DG feeding and metabolic abnormalities similar to anorexia nervosa. *Physiol. Behav.* 57, 147–153. doi: 10.1016/0031-9384(94)00277-C

Arcelus, J., Mitchell, A. J., Wales, J., and Nielsen, S. (2011). Mortality rates in patients with anorexia nervosa and other eating disorders. a meta-analysis of 36 studies. *Arch. Gen. Psychiatry* 68, 724–731. doi: 10.1001/archgenpsychiatry.2011.74

Atchley, D. P., and Eckel, L. A. (2005). Fenfluramine treatment in female rats accelerates the weight loss associated with activity-based anorexia. *Pharmacol. Biochem. Behav.* 80, 273–279. doi: 10.1016/j.pbb.2004.11.006

Atchley, D. P., and Eckel, L. A. (2006). Treatment with 8-OH-DPAT attenuates the weight loss associated with activity-based anorexia in female rats. *Pharmacol. Biochem. Behav.* 83, 547–553. doi: 10.1016/j.pbb.2006.03.016

Avraham, Y., Bonne, O., and Berry, E. M. (1996). Behavioral and neurochemical alterations caused by diet restriction - the effect of tyrosine administration in mice. *Brain Res.* 732, 133–144. doi: 10.1016/0006-8993(96)00514-8

Avraham, Y., Paturski, I., Magen, I., Vorobiev, L., and Berry, E. M. (2017). 2-Arachidonoylglycerol as a possible treatment for anorexia nervosa in animal model in mice. *Brain Res.* 1670, 185–190. doi: 10.1016/j.brainres.2017.06.003

Barbarich-Marsteller, N. C., Fornal, C. A., Takase, L. F., Bocarsly, M. E., Arner, C., Walsh, B. T., et al. (2013a). Activity-based anorexia is associated with reduced hippocampal cell proliferation in adolescent female rats. *Behav. Brain Res.* 236, 251–257. doi: 10.1016/j.bbr.2012.08.047

Barbarich-Marsteller, N. C., Marsteller, D. A., Alexoff, D. L., Fowler, J. S., and Dewey, S. L. (2005). MicroPET imaging in an animal model of anorexia nervosa. *Synapse* 57, 85–90. doi: 10.1002/syn.20160

Barbarich-Marsteller, N. C., Underwood, M. D., Foltin, R. W., Myers, M. M., Walsh, B. T., Barrett, J. S., et al. (2013b). Identifying novel phenotypes of vulnerability and resistance to activity-based anorexia in adolescent female rats. *Int. J. Eat. Disord.* 46, 737–746. doi: 10.1002/eat.22149

Belmonte, L., Achamrah, N., Nobis, S., Guerin, C., Riou, G., Bole-Feysot, C., et al. (2016). A role for intestinal TLR4-driven inflammatory response during activity-based anorexia. *Sci. Rep.* 6:35813. doi: 10.1038/srep35813

Breton, J., Giallourou, N., Nobis, S., Morin, A., Achamrah, N., Goichon, A., et al. (2020). Characterizing the metabolic perturbations induced by activity-based anorexia in the C57Bl/6 mouse using (1)H NMR spectroscopy. *Clin. Nutr.* 39, 2428–2434. doi: 10.1016/j.clnu.2019.10.026

Brown, A. J., Avena, N. M., and Hoebel, B. G. (2008). A high-fat diet prevents and reverses the development of activity-based anorexia in rats. *Int. J. Eat. Disord.* 41, 383–389. doi: 10.1002/eat.20510

Campos, G. V., de Noronha, S. R., de Souza, A. A., Lima, P. M., Abreu, A. R., Chianca, D. Jr., et al. (2019). Estrogen receptor beta activation within dorsal raphe nucleus reverses anxiety-like behavior induced by food restriction in female rats. *Behav. Brain Res.* 357–358, 57–64. doi: 10.1016/j.bbr.2018.03.029

Carrera, O., Cerrato, M., Sanchez, A., and Gutierrez, E. (2009). Long maternal separation has protective effects in rats exposed to activity-based anorexia. *Dev. Psychobiol.* 51, 616–624. doi: 10.1002/dev.20396

Casteels, C., Gerard, N., Van Kuyck, K., Pottel, L., Nuttin, B., Bormans, G., et al. (2014). Small animal PET imaging of the type 1 cannabinoid receptor in a rodent model for anorexia nervosa. *Eur. J. Nucl. Med. Mol. Imaging* 41, 308–321. doi: 10.1007/s00259-013-2522-8

Cerrato, M., Carrera, O., Vazquez, R., Echevarria, E., and Gutierrez, E. (2012). Heat makes a difference in activity-based anorexia: a translational approach to treatment development in anorexia nervosa. *Int. J. Eat. Disord.* 45, 26–35. doi: 10.1002/eat.20884

Chen, Y. W., Actor-Engel, H., and Aoki, C. (2018). alpha4-GABAA receptors of hippocampal pyramidal neurons are associated with resilience against activity-based anorexia for adolescent female mice but not for males. *Mol. Cell. Neurosci.* 90, 33–48. doi: 10.1016/j.mcn.2018.04.008

Chen, Y. W., Actor-Engel, H., Sherpa, A. D., Klingensmith, L., Chowdhury, T. G., and Aoki, C. (2017). NR2A- and NR2B-NMDA receptors and drebrin within postsynaptic spines of the hippocampus correlate with hunger-evoked exercise. *Brain Struct. Funct.* 222, 2271–2294. doi: 10.1007/s00429-016-1341-7

Chowdhury, T. G., Barbarich-Marsteller, N. C., Chan, T. E., and Aoki, C. (2013a). Activity-based anorexia has differential effects on apical dendritic branching in dorsal and ventral hippocampal CA1. *Brain Struct. Funct.* 219, 1935–1945. doi: 10.1007/s00429-013-0612-9

Chowdhury, T. G., Rios, M. B., Chan, T. E., Cassataro, D. S., Barbarich-Marsteller, N. C., Aoki, C., et al. (2014). Activity-based anorexia during adolescence disrupts normal development of the CA1 pyramidal cells in the ventral hippocampus of female rats. *Hippocampus* 24, 1421–1429. doi: 10.1002/hipo.22320

Chowdhury, T. G., Wable, G. S., Sabaliauskas, N. A., and Aoki, C. (2013b). Adolescent female C57BL/6 mice with vulnerability to activity-based anorexia exhibit weak inhibitory input onto hippocampal CA1 pyramidal cells. *Neuroscience* 241, 250–267. doi: 10.1016/j.neuroscience.2013.03.020

Collu, R., Post, J. M., Scherma, M., Giunti, E., Fratta, W., Lutz, B., et al. (2020). Altered brain levels of arachidonic acid-derived inflammatory eicosanoids in a rodent model of anorexia nervosa. *Biochim. Biophys. Acta Mol. Cell. Biol. Lipids* 1865:158578. doi: 10.1016/j.bbalip.2019.158578

Collu, R., Scherma, M., Piscitelli, F., Giunti, E., Satta, V., Castelli, M. P., et al. (2019). Impaired brain endocannabinoid tone in the activity-based model of anorexia nervosa. *Int. J. Eat. Disord.* 52, 1251–1262. doi: 10.1002/eat.23157

Duclos, M., Bouchet, M., Vettier, A., and Richard, D. (2005). Genetic differences in hypothalamic-pituitary-adrenal axis activity and food restriction-induced hyperactivity in three inbred strains of rats. *J. Neuroendocrinol.* 17, 740–752. doi: 10.1111/j.1365-2826.2005.01367.x

Endou, M., Yanai, K., Sakurai, E., Fukudo, S., Hongo, M., and Watanabe, T. (2001). Food-deprived activity stress decreased the activity of the histaminergic

neuron system in rats. *Brain Res*. 891, 32–41. doi: 10.1016/S0006-8993(00)03226-1

Farinetti, A., Aspesi, D., Marraudino, M., Marzola, E., Amianto, F., Abbate-Daga, G., et al. (2020). Sexually dimorphic behavioral effects of maternal separation in anorexic rats. *Dev. Psychobiol*. 62, 297–309. doi: 10.1002/dev.21909

Filaire, E., Rouveix, M., Massart, A., Gladine, C., Davicco, M. J., and Durand, D. (2009). Lipid peroxidation and antioxidant status in rat: effect of food restriction and wheel running. *Eur. J. Appl. Physiol*. 107, 243–250. doi: 10.1007/s00421-009-1121-7

Fraga, A., Carreira, M. C., Gonzalez-Izquierdo, A., Diéguez, C., López, M., and Gutiérrez, E. (2020). Temperature but not leptin prevents semi-starvation induced hyperactivity in rats: implications for anorexia nervosa treatment. *Sci. Rep*. 10:5300. doi: 10.1038/s41598-020-62147-z

Francois, M., Barde, S., Achamrah, N., Breton, J., do Rego, J. C., Coeffier, M., et al. (2015). The number of preproghrelin mRNA expressing cells is increased in mice with activity-based anorexia. *Neuropeptides* 51, 17–23. doi: 10.1016/j.npep.2015.04.003

Frintrop, L., Liesbrock, J., Paulukat, L., Johann, S., Kas, M. J., Tolba, R., et al. (2018a). Reduced astrocyte density underlying brain volume reduction inactivity-based anorexia rats. *World J. Biol. Psychiatry* 19, 225–235. doi: 10.1080/15622975.2016.1273552

Frintrop, L., Trinh, S., Liesbrock, J., Leunissen, C., Kempermann, J., Etdöger, S., et al. (2019). The reduction of astrocytes and brain volume loss in anorexia nervosa-the impact of starvation and refeeding in a rodent model. *Transl. Psychiatry* 9:159. doi: 10.1038/s41398-019-0493-7

Frintrop, L., Trinh, S., Liesbrock, J., Paulukat, L., Kas, M. J., Tolba, R., et al. (2018b). Establishment of a chronic activity-based anorexia rat model. *J. Neurosci. Methods* 293, 191–198. doi: 10.1016/j.jneumeth.2017.09.018

Gelegen, C., Collier, D. A., Campbell, I. C., Oppelaar, H., van den Heuvel, J., Adan, R. A. H., et al. (2007). Difference in susceptibility to activity-based anorexia in two inbred strains of mice. *Eur. Neuropsychopharmacol*. 17, 199–205. doi: 10.1016/j.euroneuro.2006.04.007

Gelegen, C., Pjetri, E., Campbell, I. C., Collier, D. A., Oppelaar, H., and Kas, M. J. H. (2010). Chromosomal mapping of excessive physical activity in mice in response to a restricted feeding schedule. *Eur. Neuropsychopharmacol*. 20, 317–326. doi: 10.1016/j.euroneuro.2009.10.001

Gelegen, C., van den Heuvel, J., Collier, D. A., Campbell, I. C., Oppelaar, H., Hessel, E., et al. (2008). Dopaminergic and brain-derived neurotrophic factor signalling in inbred mice exposed to a restricted feeding schedule. *Genes Brain Behav*. 7, 552–559. doi: 10.1111/j.1601-183X.2008.00394.x

Ghadirian, A. M., Engelsmann, F., Leichner, P., and Marshall, M. (1993). Prevalence of psychosomatic and other medical illnesses in anorexic and bulimic patients. *Behav. Neurol*. 6, 123–127. doi: 10.1155/1993/356914

Giles, E. D., Hagman, J., Pan, Z., MacLean, P. S., and Higgins, J. A. (2016). Weight restoration on a high carbohydrate refeeding diet promotes rapid weight regain and hepatic lipid accumulation in female anorexic rats. *Nutr. Metab*. 13:77. doi: 10.1186/s12986-016-0077-y

Gilman, T. L., Owens, W. A., George, C. M., Metzel, L., Vitela, M., Ferreira, L., et al. (2019). Age- and sex-specific plasticity in dopamine transporter function revealed by food restriction and exercise in a rat activity-based anorexia paradigm. *J. Pharmacol. Exp. Ther*. 371, 268–277. doi: 10.1124/jpet.119.260794

Gutiérrez, E., Baysari, M. T., Carrera, O., Whitford, T. J., and Boakes, R. A. (2006). High ambient temperature reduces rate of body-weight loss produced by wheel running. *Q. J. Exp. Psychol.* 59, 1196–1211. doi: 10.1080/17470210500417688

Gutierrez, E., Cerrato, M., Carrera, O., and Vazquez, R. (2008). Heat reversal of activity-based anorexia: implications for the treatment of anorexia nervosa. *Int. J. Eat. Disord*. 41, 594–601. doi: 10.1002/eat.20535

Gutierrez, E., Churruca, I., Zarate, J., Carrera, O., Portillo, M. P., Cerrato, M., et al. (2009). High ambient temperature reverses hypothalamic MC4 receptor overexpression in an animal model of anorexia nervosa. *Psychoneuroendocrinology* 34, 420–429. doi: 10.1016/j.psyneuen.2008.10.003

Hancock, S. D., and Grant, V. L. (2009). Sexually dimorphic effects of postnatal treatment on the development of activity-based anorexia in adolescent and adult rats. *Dev. Psychobiol*. 51, 679–695. doi: 10.1002/dev.20403

Hao, S., Avraham, Y., Bonne, O., and Berry, E. M. (2001). Separation-induced body weight loss, impairment in alternation behavior, and autonomic tone: effects of tyrosine. *Pharmacol. Biochem. Behav*. 68, 273–281. doi: 10.1016/S0091-3057(00)00448-2

Hata, T., Miyata, N., Takakura, S., Yoshihara, K., Asano, Y., Kimura-Todani, T., et al. (2019). The gut microbiome derived from anorexia nervosa patients impairs weight gain and behavioral performance in female mice. *Endocrinology* 160, 2441–2452. doi: 10.1210/en.2019-00408

Hillebrand, J. J., Heinsbroek, A. C., Kas, M. J., and Adan, R. A. (2006a). The appetite suppressant d-fenfluramine reduces water intake, but not food intake, in activity-based anorexia. *J. Mol. Endocrinol*. 36, 153–162. doi: 10.1677/jme.1.01887

Hillebrand, J. J. G., de Rijke, C. E., Brakkee, J. H., Kas, M. J., and Adan, R. A. (2005a). Voluntary access to a warm plate reduces hyperactivity in activity-based anorexia. *Physiol. Behav*. 85, 151–157. doi: 10.1016/j.physbeh.2005.03.017

Hillebrand, J. J. G., Kas, M. J. H., Scheurink, A. J. W., van Dijk, G., and Adan, R. A. H. (2006b). AgRP(83-132) and SHU9119 differently affect activity-based anorexia. *Eur. Neuropsychopharmacol*. 16, 403–412. doi: 10.1016/j.euroneuro.2005.11.004

Hillebrand, J. J. G., Koeners, M. P., de Rijke, C. E., Kas, M. J., and Adan, R. A. (2005b). Leptin treatment in activity-based anorexia. *Biol. Psychiatry* 58, 165–171. doi: 10.1016/j.biopsych.2005.03.011

Hillebrand, J. J. G., van Elburg, A. A., Kas, M. J., van Engeland, H., and Adan, R. A. (2005c). Olanzapine reduces physical activity in rats exposed to activity-based anorexia: possible implications for treatment of anorexia nervosa? *Biol. Psychiatry* 58, 651–657. doi: 10.1016/j.biopsych.2005.04.008

Ho, E. V., Klenotich, S. J., McMurray, M. S., and Dulawa, S. C. (2016). Activity-based anorexia alters the expression of BDNF transcripts in the mesocorticolimbic reward circuit. *PLoS ONE* 11:e0166756. doi: 10.1371/journal.pone.0166756

Hurel, I., Redon, B., Scocard, A., Malezieux, M., Marsicano, G., and Chaouloff, F. (2019). Beyond the activity-based anorexia model: reinforcing values of exercise and feeding examined in stressed adolescent male and female mice. *Front. Pharmacol*. 10:587. doi: 10.3389/fphar.2019.00587

Jean, A., Laurent, L., Bockaert, J., Charnay, Y., Dusticier, N., Nieoullon, A., et al. (2012). The nucleus accumbens 5-HTR(4)-CART pathway ties anorexia to hyperactivity. *Transl. Psychiatry* 2:e203. doi: 10.1038/tp.2012.131

Jean, A., Laurent, L., Delaunay, S., Doly, S., Dusticier, N., Linden, D., et al. (2017). Adaptive control of dorsal raphe by 5-HT4 in the prefrontal cortex prevents persistent hypophagia following stress. *Cell Rep*. 21, 901–999. doi: 10.1016/j.celrep.2017.10.003

Jesus, P., Ouelaa, W., Francois, M., Riachy, L., Guerin, C., Aziz, M., et al. (2014). Alteration of intestinal barrier function during activity-based anorexia in mice. *Clin. Nutr*. 33, 1046–1053. doi: 10.1016/j.clnu.2013.11.006

Johansen, J. E., Broberger, C., Lavebratt, C., Johansson, C., Kuhar, M. J., Hokfelt, T., et al. (2000). Hypothalamic CART and serum leptin levels are reduced in the anorectic (anx/anx) mouse. *Mol. Brain Res*. 84, 97–105. doi: 10.1016/S0169-328X(00)00228-X

Johnson, E. O., Kamilaris, T. C., Carter, C. S., Calogero, A. E., Gold, P. W., and Chrousos, G. P. (1996). The biobehavioral consequences of psychogenic stress in a small, social primate (*Callithrix jacchus* jacchus). *Biol. Psychiatry* 40, 317–337. doi: 10.1016/0006-3223(95)00397-5

Kim, D. Y., Yu, J., Mui, R. K., Niibori, R., Taufique, H. B., Aslam, R., et al. (2017). The tyrosine kinase receptor Tyro3 enhances lifespan and neuropeptide y (Npy) neuron survival in the mouse anorexia (anx) mutation. *DMM Dis. Model Mech*. 10, 581–595. doi: 10.1242/dmm.027433

Kinzig, K. P., and Hargrave, S. L. (2010). Adolescent activity-based anorexia increases anxiety-like behavior in adulthood. *Physiol. Behav*. 101, 269–276. doi: 10.1016/j.physbeh.2010.05.010

Klenotich, S. J., Ho, E. V., McMurray, M. S., Server, C. H., and Dulawa, S. C. (2015). Dopamine D2/3 receptor antagonism reduces activity-based anorexia. *Transl. Psychiatry*. 5:e613. doi: 10.1038/tp.2015.109

Klenotich, S. J., Seiglie, M. P., McMurray, M. S., Roitman, J. D., Le Grange, D., Dugad, P., et al. (2012). Olanzapine, but not fluoxetine, treatment increases survival in activity-based anorexia in mice. *Neuropsychopharmacology* 37, 1620–1631. doi: 10.1038/npp.2012.7

Koh, M. T., Lett, B. T., and Grant, V. L. (2000). Activity in the circular alley does not produce the activity anorexia syndrome in rats. *Appetite* 34, 153–159. doi: 10.1006/appe.1999.0307

Kumar, S., and Kaur, G. (2013). Intermittent fasting dietary restriction regimen negatively influences reproduction in young rats: a study

of hypothalamo-hypophysial-gonadal axis. *PLoS ONE* 8:e52416. doi: 10.1371/journal.pone.0052416

Legrand, R., Lucas, N., Breton, J., Azhar, S., do Rego, J. C., Dechelotte, P., et al. (2016). Ghrelin treatment prevents development of activity based anorexia in mice. *Eur. Neuropsychopharmacol.* 26, 948–958. doi: 10.1016/j.euroneuro.2016.03.010

Lewis, D. Y., and Brett, R. R. (2010). Activity-based anorexia in C57/BL6 mice: effects of the phytocannabinoid, delta9-tetrahydrocannabinol (THC) and the anandamide analogue, OMDM-2. *Eur. Neuropsychopharmacol.* 20, 622–631. doi: 10.1016/j.euroneuro.2010.04.002

L'Huillier, C., Jarbeau, M., Achamrah, N., Belmonte, L., Amamou, A., Nobis, S., et al. (2019). Glutamine, but not branched-chain amino acids, restores intestinal barrier function during activity-based anorexia. *Nutrients* 11:1348. doi: 10.3390/nu11061348

Liang, N. C., Bello, N. T., and Moran, T. H. (2011). Experience with activity based anorexia enhances conditioned taste aversion learning in rats. *Physiol. Behav.* 102, 51–57. doi: 10.1016/j.physbeh.2010.10.004

Lindfors, C., Katz, A., Selander, L., Johansen, J. E., Marconi, G., Schalling, M., et al. (2015). Glucose intolerance and pancreatic beta-cell dysfunction in the anorectic anx/anx mouse. *Am. J. Physiol. Endocrinol. Metab.* 309, E418–E427. doi: 10.1152/ajpendo.00081.2015

Lujan, M. E., Krzemien, A. A., Reid, R. L., and Van Vugt, D. A. (2006). Developing a model of nutritional amenorrhea in rhesus monkeys. *Endocrinology* 147, 483–492. doi: 10.1210/en.2005-0821

Lutter, M., Bahl, E., Hannah, C., Hofammann, D., Acevedo, S., Cui, H., et al. (2017a). Novel and ultra-rare damaging variants in neuropeptide signaling are associated with disordered eating behaviors. *PLoS ONE* 12:e0181556. doi: 10.1371/journal.pone.0181556

Lutter, M., Khan, M. Z., Satio, K., Davis, K. C., Kidder, I. J., McDaniel, L., et al. (2017b). The eating-disorder associated HDAC4^{A778T} mutation alters feeding behaviors in female mice. *Biol. Psychiatry* 81, 770–777. doi: 10.1016/j.biopsych.2016.09.024

Madra, M., and Zeltser, L. M. (2016). BDNF-Val66Met variant and adolescent stress interact to promote susceptibility to anorexic behavior in mice. *Transl. Psychiatry* 6:e776. doi: 10.1038/tp.2016.35

Maltais, L. J., Lane, P. W., and Beamer, W. G. (1984). Anorexia, a recessive mutation causing starvation in preweanling mice. *J. Hered.* 75, 468–472. doi: 10.1093/oxfordjournals.jhered.a109987

Mequinion, M., Caron, E., Zgheib, S., Stievenard, A., Zizzari, P., Tolle, V., et al. (2015b). Physical activity: benefit or weakness in metabolic adaptations in a mouse model of chronic food restriction? *Am. J. Physiol. Endocrinol. Metab.* 308, E241–E255. doi: 10.1152/ajpendo.00340.2014

Mequinion, M., Chauveau, C., and Viltart, O. (2015a). The use of animal models to decipher physiological and neurobiological alterations of anorexia nervosa patients. *Front. Endocrinol.* 6:68. doi: 10.3389/fendo.2015.00068

Mequinion, M., Le Thuc, O., Zgheib, S., Alexandre, D., Chartrel, N., Rovere, C., et al. (2017). Long-term energy deficit in mice causes long-lasting hypothalamic alterations after recovery. *Neuroendocrinology* 105, 372–383. doi: 10.1159/000455048

Mercader, J. M., Lozano, J. J., Sumoy, L., Dierssen, M., Visa, J., Gratacos, M., et al. (2008). Hypothalamus transcriptome profile suggests an anorexia-cachexia syndrome in the anx/anx mouse model. *Physiol. Genomics* 35, 341–350. doi: 10.1152/physiolgenomics.90255.2008

Nagl, M., Jacobi, C., Paul, M., Beesdo-Baum, K., Hofler, M., Lieb, R., et al. (2016). Prevalence, incidence, and natural course of anorexia and bulimia nervosa among adolescents and young adults. *Eur. Child Adolesc. Psychiatry* 25, 903–918. doi: 10.1007/s00787-015-0808-z

Nakahara, K., Takata, S., Ishii, A., Nagao, K., Bannai, M., Takahashi, M., et al. (2012). Somatostatin is involved in anorexia in mice fed a valine-deficient diet. *Amino Acids* 42, 1397–1404. doi: 10.1007/s00726-011-0836-z

Nobis, S., Achamrah, N., Goichon, A., L'Huillier, C., Morin, A., Guerin, C., et al. (2018a). Colonic mucosal proteome signature reveals reduced energy metabolism and protein synthesis but activated autophagy during anorexia-induced malnutrition in mice. *Proteomics Pract. Proteomics* 18:1700395. doi: 10.1002/pmic.201700395

Nobis, S., Goichon, A., Achamrah, N., Guérin, C., Azhar, S., Chan, P., et al. (2018b). Alterations of proteome, mitochondrial dynamic and autophagy in the hypothalamus during activity-based anorexia. *Sci. Rep.* 8:7233. doi: 10.1038/s41598-018-25548-9

Nobis, S., Morin, A., Achamrah, N., Belmonte, L., Legrand, R., Chan, P., et al. (2018c). Delayed gastric emptying and altered antrum protein metabolism during activity-based anorexia. *Neurogastroenterol. Motil.* 30:e13305. doi: 10.1111/nmo.13305

Paulukat, L., Frintrop, L., Liesbrock, J., Heussen, N., Johann, S., Exner, C., et al. (2016). Memory impairment is associated with the loss of regular oestrous cycle and plasma oestradiol levels in an activity-based anorexia animal model. *World J. Biol. Psychiatry* 17, 274–284. doi: 10.3109/15622975.2016.1173725

Perez-Leighton, C. E., Grace, M., Billington, C. J., and Kotz, C. M. (2014). Role of spontaneous physical activity in prediction of susceptibility to activity based anorexia in male and female rats. *Physiol. Behav.* 135, 104–111. doi: 10.1016/j.physbeh.2014.06.001

Petrovich, G. D., and Lougee, M. A. (2011). Sex differences in fear-induced feeding cessation: prolonged effect in female rats. *Physiol. Behav.* 104, 996–1001. doi: 10.1016/j.physbeh.2011.06.020

Pjetri, E., de Haas, R., de Jong, S., Gelegen, C., Oppelaar, H., Verhagen, L. A., et al. (2012). Identifying predictors of activity based anorexia susceptibility in diverse genetic rodent populations. *PLoS ONE* 7:e50453. doi: 10.1371/journal.pone.0050453

Reyes-Haro, D., Labrada-Moncada, F. E., Miledi, R., and Martinez-Torres, A. (2015). Dehydration-induced anorexia reduces astrocyte density in the rat corpus callosum. *Neural Plast.* 2015:474917. doi: 10.1155/2015/474917

Reyes-Haro, D., Labrada-Moncada, F. E., Varman, D. R., Kruger, J., Morales, T., Miledi, R., et al. (2016). Anorexia reduces GFAP+ cell density in the rat hippocampus. *Neural Plast.* 2016:2426413. doi: 10.1155/2016/2426413

Rieg, T. S., and Aravich, P. F. (1994). Systemic clonidine increases feeding and wheel running but does not affect rate of weight loss in rats subjected to activity-based anorexia. *Pharmacol. Biochem. Behav.* 47, 215–218. doi: 10.1016/0091-3057(94)90002-7

Scharner, S., Friedrich, T., Goebel-Stengel, M., Kobelt, P., Rose, M., and Stengel, A. (2018). Activity-based anorexia activates CRF immunoreactive neurons in female rats. *Neurosci. Lett.* 674, 142–147. doi: 10.1016/j.neulet.2018.03.049

Scharner, S., Prinz, P., Goebel-Stengel, M., Kobelt, P., Hofmann, T., Rose, M., et al. (2016). Activity-based anorexia reduces body weight without inducing a separate food intake microstructure or activity phenotype in female rats-mediation via an activation of distinct brain nuclei. *Front. Neurosci.* 10:475. doi: 10.3389/fnins.2016.00475

Scharner, S., Prinz, P., Goebel-Stengel, M., Lommel, R., Kobelt, P., Hofmann, T., et al. (2017). Activity-based anorexia activates nesfatin-1 immunoreactive neurons in distinct brain nuclei of female rats. *Brain Res.* 1677, 33–46. doi: 10.1016/j.brainres.2017.09.024

Scherma, M., Satta, V., Collu, R., Boi, M. F., Usai, P., Fratta, W., et al. (2017). Cannabinoid CB1 /CB2 receptor agonists attenuate hyperactivity and body weight loss in a rat model of activity-based anorexia. *Br. J. Pharmacol.* 174, 2682–2695. doi: 10.1111/bph.13892

Schroeder, M., Jakovcevski, M., Polacheck, T., Drori, Y., Luoni, A., Roh, S., et al. (2018). Placental miR-340 mediates vulnerability to activity based anorexia in mice. *Nat. Commun.* 9:1596. doi: 10.1038/s41467-018-03836-2

Skowron, K., Aleksandrovych, V., Kurnik-Lucka, M., Stach, P., Baranowska, A., Skowron, B., et al. (2018). Aberrations in the female reproductive organs and a role of telocytes in a rat model of anorexia nervosa. *Folia Med. Cracov.* 58, 115–125. doi: 10.24425/fmc.2018.125077

Treasure, J., Zipfel, S., Micali, N., Wade, T., Stice, E., Claudino, A., et al. (2015). Anorexia nervosa. *Nat. Rev. Dis. Primers* 1:15074. doi: 10.1038/nrdp.2015.74

van Kuyck, K., Casteels, C., Vermaelen, P., Bormans, G., Nuttin, B., and Van Laere, K. (2007). Motor- and food-related metabolic cerebral changes in the activity-based rat model for anorexia nervosa: a voxel-based microPET study. *Neuroimage* 35, 214–221. doi: 10.1016/j.neuroimage.2006.12.009

Verhagen, L. A., Luijendijk, M. C., and Adan, R. A. (2011b). Leptin reduces hyperactivity in an animal model for anorexia nervosa via the ventral tegmental area. *Eur. Neuropsychopharmacol.* 21, 274–281. doi: 10.1016/j.euroneuro.2010.11.006

Verhagen, L. A., Luijendijk, M. C., Hillebrand, J. J., and Adan, R. A. (2009a). Dopamine antagonism inhibits anorectic behavior in an animal model for anorexia nervosa. *Eur. Neuropsychopharmacol.* 19, 153–160. doi: 10.1016/j.euroneuro.2008.09.005

Verhagen, L. A., Luijendijk, M. C., Korte-Bouws, G. A., Korte, S. M., and Adan, R. A. (2009b). Dopamine and serotonin release in the nucleus accumbens during starvation-induced hyperactivity. *Eur. Neuropsychopharmacol.* 19, 309–316. doi: 10.1016/j.euroneuro.2008.12.008

Verhagen, L. A. W., Egecioglu, E., Luijendijk, M. C. M., Hillebrand, J. J. G., Adan, R. A. H., and Dickson, S. L. (2011a). Acute and chronic suppression of the central ghrelin signaling system reveals a role in food anticipatory activity. *Eur. Neuropsychopharmacol.* 21, 384–392. doi: 10.1016/j.euroneuro.2010.06.005

Verty, A. N., Evetts, M. J., Crouch, G. J., McGregor, I. S., Stefanidis, A., and Oldfield, B. J. (2011). The cannabinoid receptor agonist THC attenuates weight loss in a rodent model of activity-based anorexia. *Neuropsychopharmacology* 36, 1349–1358. doi: 10.1038/npp.2011.19

Wable, G. S., Barbarich-Marsteller, N. C., Chowdhury, T. G., Sabaliauskas, N. A., Farb, C. R., and Aoki, C. (2014). Excitatory synapses on dendritic shafts of the caudal basal amygdala exhibit elevated levels of GABAA receptor alpha4 subunits following the induction of activity-based anorexia. *Synapse* 68, 1–15. doi: 10.1002/syn.21690

Wable, G. S., Chen, Y. W., Rashid, S., and Aoki, C. (2015a). Exogenous progesterone exacerbates running response of adolescent female mice to repeated food restriction stress by changing alpha4-GABAA receptor activity of hippocampal pyramidal cells. *Neuroscience* 310, 322–341. doi: 10.1016/j.neuroscience.2015.09.006

Wable, G. S., Min, J. Y., Chen, Y. W., and Aoki, C. (2015b). Anxiety is correlated with running in adolescent female mice undergoing activity-based anorexia. *Behav. Neurosci.* 129, 170–182. doi: 10.1037/bne0000040

Welch, A. C., Zhang, J., Lyu, J., McMurray, M. S., Javitch, J. A., Kellendonk, C., et al. (2019). Dopamine D2 receptor overexpression in the nucleus accumbens core induces robust weight loss during scheduled fasting selectively in female mice. *Mol. Psychiatry.* doi: 10.1038/s41380-019-0633-8. [Epub ahead of print].

Welkenhuysen, M., Van Kuyck, K., Das, J., Sciot, R., and Nuttin, B. (2008). Electrical stimulation in the lateral hypothalamus in rats in the activity-based anorexia model. *Neurosurg. Focus* 25:E7. doi: 10.3171/FOC/2008/25/7/E7

Wojciak, R. W. (2014). Alterations of selected iron management parameters and activity in food-restricted female Wistar rats (animal anorexia models). *Eat. Weight Disord. Stud. Anorexia Bulimia Obes.* 19, 61–68. doi: 10.1007/s40519-013-0078-z

Wu, H., van Kuyck, K., Tambuyzer, T., Luyten, L., Aerts, J. M., and Nuttin, B. (2014). Rethinking food anticipatory activity in the activity-based anorexia rat model. *Sci. Rep.* 4:3929. doi: 10.1038/srep03929

Zgheib, S., Mequinion, M., Lucas, S., Leterme, D., Ghali, O., Tolle, V., et al. (2014). Long-Term physiological alterations and recovery in a mouse model of separation associated with time-restricted feeding: a tool to study anorexia nervosa related consequences. *PLoS ONE* 9:e103775. doi: 10.1371/journal.pone.0103775

Zipfel, S., Giel, K. E., Bulik, C. M., Hay, P., and Schmidt, U. (2015). Anorexia nervosa: aetiology, assessment, and treatment. *Lancet Psychiatry* 2, 1099–1111. doi: 10.1016/S2215-0366(15)00356-9

Conflict of Interest: The authors declare that the research was conducted in the absence of any commercial or financial relationships that could be construed as a potential conflict of interest.

frontiers in Neural Circuits

MINI REVIEW
published: 02 February 2021
doi: 10.3389/fncir.2021.609824

Recent Advances in Neural Circuits for Taste Perception in Hunger

Ou Fu[1], *Yasuhiko Minokoshi*[1,2] *and Ken-ichiro Nakajima*[1,2*]

[1] Division of Endocrinology and Metabolism, National Institute for Physiological Sciences, Aichi, Japan, [2] Department of Physiological Sciences, School of Life Science, SOKENDAI (The Graduate University for Advanced Studies), Okazaki, Japan

Feeding is essential for survival and taste greatly influences our feeding behaviors. Palatable tastes such as sweet trigger feeding as a symbol of a calorie-rich diet containing sugar or proteins, while unpalatable tastes such as bitter terminate further consumption as a warning against ingestion of harmful substances. Therefore, taste is considered a criterion to distinguish whether food is edible. However, perception of taste is also modulated by physiological changes associated with internal states such as hunger or satiety. Empirically, during hunger state, humans find ordinary food more attractive and feel less aversion to food they usually dislike. Although functional magnetic resonance imaging studies performed in primates and in humans have indicated that some brain areas show state-dependent response to tastes, the mechanisms of how the brain senses tastes during different internal states are poorly understood. Recently, using newly developed molecular and genetic tools as well as *in vivo* imaging, researchers have identified many specific neuronal populations or neural circuits regulating feeding behaviors and taste perception process in the central nervous system. These studies could help us understand the interplay between homeostatic regulation of energy and taste perception to guide proper feeding behaviors.

Keywords: taste, hunger, satiety, neural circuit, appetitive and consummatory behaviors

OPEN ACCESS

Edited by:
Masahiro Yamaguchi, Kōchi University, Japan

Reviewed by:
Graham William Knott, École Polytechnique Fédérale de Lausanne, Switzerland
Stefany Primeaux, Pennington Biomedical Research Center, United States

***Correspondence:**
Ken-ichiro Nakajima
knakaj@nips.ac.jp

Received: *24 September 2020*
Accepted: *08 January 2021*
Published: *02 February 2021*

Citation:
Fu O, Minokoshi Y and Nakajima K (2021) Recent Advances in Neural Circuits for Taste Perception in Hunger. Front. Neural Circuits 15:609824. doi: 10.3389/fncir.2021.609824

INTRODUCTION

Food intake is essential for survival and the neural processes mediating hunger information guide animals to initiate appetitive food seeking and subsequent consummatory feeding. Taste is important for animals to evaluate the value of food (Lindemann, 2001). It plays multiple roles in appetitive as well as in consummatory behaviors. Many brain areas show different taste responses in hunger and in satiety, indicating that taste perception is modulated by internal state. In this review, we will briefly introduce studies on taste perception in the peripheral and central nervous system, and then focus on the recent findings about the neural circuits related to the modulation of sweet or bitter taste in hunger and how they are involved in feeding.

TASTE SENSATION FROM THE TONGUE TO THE BRAIN

Humans and many mammals are able to recognize five basic tastes: sweet, umami, bitter, sour and salty. Taste substances are detected by the taste buds on the tongue. They are onion-shaped structures composed of cells that express distinct types of taste receptors. For example, sweet substances are detected by a combination of T1R2 and T1R3 G-protein-coupled receptors, while

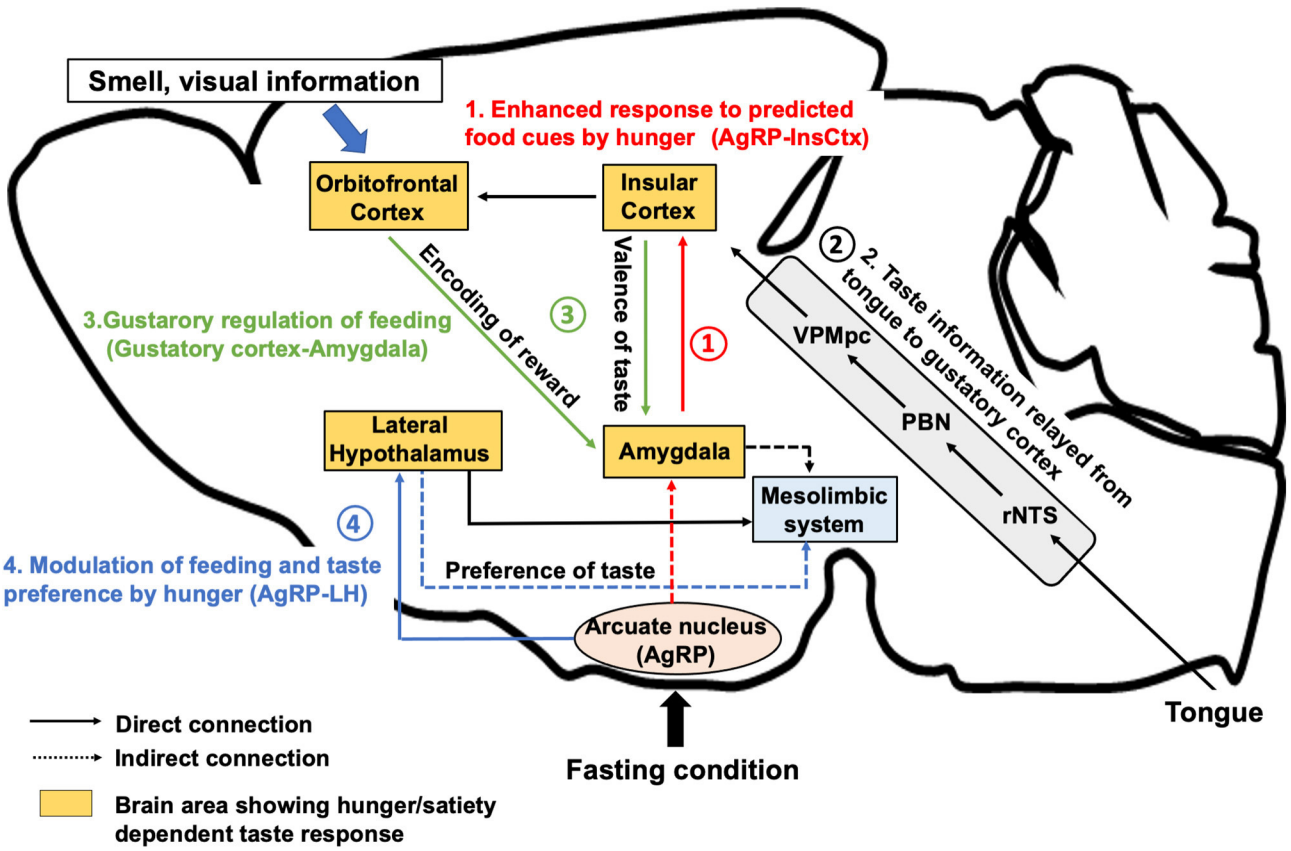

FIGURE 1 | Neural regulation of taste perception in hunger state. AgRP neurons, which are firstly activated under hunger conditions, induce food seeking and consequent consummatory behaviors. **(1)** AgRP neurons inhibit the InsCtx via AgRP-PVT-BLA-InsCtx circuits to enhance the anticipatory response toward food cue in the appetitive feeding process. **(2)** After the start of eating, taste is detected by the tongue and perceived by the gustatory cortex (the InsCtx and the OFC) through rNTS, PBN, and VPMpc. **(3)** The InsCtx encodes the positive or negative valence of taste by interacting with the BLA or the central amygdala to continue or stop feeding. The OFC integrates taste and other sensory information as well as the reward value by projecting to the BLA. **(4)** Excitatory Vglut2-expressing neurons in the lateral hypothalamus also receives inhibitory inputs from AgRP neurons to induce feeding in hunger state. Vglut2 neurons in the LH project to the LS or to the LHb to modulate palatable or aversive taste preference, respectively. The aforementioned regions largely interact with the midbrain mesolimbic system to construct reward learning for the regulation of feeding behavior. BLA, the basolateral amygdala, CeA: the central nucleus of the amygdala, InsCtx: the insular cortex; LHb, the lateral habenula; LS, the lateral septum; VPMpc, the ventral posteromedial of the thalamus; OFC, the orbitofrontal cortex; PBN, the parabrachial nucleus; rNTS, the rostral part of the nucleus tractus solitarius.

bitter substances are detected by T2R receptors (Zhao et al., 2003; Meyerhof et al., 2005; Mueller et al., 2005). As shown in **Figure 1**, taste information is then sent to the brainstem via the taste ganglion to an area called the rostral part of the nucleus tractus solitarius (rNTS) (Beckstead and Norgren, 1979). In rodents, there is a relay from the rNTS to the parabrachial nuclei (PBN), which in turn project the information to the ventral posteromedial thalamic nucleus (VPMpc) (Beckstead et al., 1980; Pritchard et al., 1989). Eventually, the taste information is received at the primary gustatory cortex, which is also called the insular cortex (InsCtx) and at the secondary gustatory cortex, which is also called the orbitofrontal cortex (OFC) (Rolls et al., 1990). Although researchers have been aware of the gustatory neuronal pathways since many years, the molecular identity of individual gustatory neurons in the brain has rarely been discovered. Some recent studies have uncovered gustatory neurons that transmit specific taste information in mice. Pdyn-expressing neurons in the rNTS respond solely to sour taste and optogenetic activation of these neurons evokes aversion (Zhang et al., 2019). In a three-port apparatus, mice were provided access to the middle port to lick various solutions (water, bitter solution, or sour solution). They were trained to go to the left (bitter solution or water) or to the right port (sour solution) to report the taste identity. While mice reported correctly by going to the left port after licking water or bitter solution, Pdyn-neuron-activated mice went to the right port after licking water to report sour taste, suggesting that these neurons are required for sour taste recognition. Another study that focused on the PBN area indicated that Satb2-expressing neurons selectively respond to sweet taste and transmit the information to the VPMpc to evoke appetitive licking behaviors (Fu et al., 2019a). As fat besides sweeteners strongly induce appetitive feeding, it has raised the

possibility of the taste of fat as the sixth taste modality. Although the oral perception of fatty acids has been previously thought to mainly rely on texture and olfaction (Rolls et al., 1999), the recent studies implied that several molecules such as CD36 and GPR120 play roles in fatty acid detection in peripheral taste systems. In CD36-positive taste cells in taste buds, Ca^{2+} concentration increased after application of long chain fatty acids (Gaillard et al., 2008). An increase in Ca^{2+} response to linoleic acid was observed in GPR120-expressing taste cells in mice (Ozdener et al., 2014). Moreover, electrophysiology recording of the mouse chorda tympani gustatory nerve indicate that GPR120 may play a role in distinguishing fatty acid taste from the other primary tastes (Yasumatsu et al., 2019).

Further studies should be conducted to clarify the molecular identity of other neurons associated with the gustatory response pathways to depict the complete taste-sensing network in the brain.

THE ROLE OF TASTE PERCEPTION IN FEEDING BEHAVIOR

Taste sensation has evolved to serve as a dominant controller of feeding behavior (Yarmolinsky et al., 2009). Feeding behaviors can be classified into homeostatic feeding to maintain body weight and metabolic function or hedonic feeding driven by sensory perception or pleasure (Berthoud, 2004; Rossi and Stuber, 2018). Notably, homeostatic and hedonic feeding systems are activated separately or simultaneously depending on various situations related to feeding (Castro et al., 2015). The activation pattern of these two systems may shift according to the taste of the food (palatable or aversive) and also according to the physiological state of the animal (hunger or satiety). Animals initiate feeding behavior in hunger state and terminate feeding when fed to satiety. This process is regulated by the homeostatic system to prevent excess caloric intake (Campos et al., 2016). However, palatable food could activate the mesolimbic reward system to induce food intake even under satiated condition. Hedonic feeding triggers appetitive behavior such as sugar craving, leading to overeating (Hajnal et al., 2004).

TASTE PERCEPTION AND INTERNAL STATE

Hungry and satiated animals exhibit different responses to attractive or potentially noxious taste substances. Neuroimaging studies in human subjects have shown that in hunger state, brain areas related to the reward system were more active after presentation of highly palatable food when compared with the same areas during satiety. This suggests that food becomes more palatable in hunger, which is described by an old saying "Hunger is the best spice" (Siep et al., 2009).

A previous study involving human taste evaluation task indicated that recognition thresholds for sucrose and salt were significantly lower during fasting state than during satiety (Zverev, 2004). Another study demonstrated that participants exhibited a significantly higher sensitivity to sweet, sour, and salty tastes during hunger state and a higher sensitivity to bitter taste during satiety (Hanci and Altun, 2016). These results indicate that internal state may directly influence the sensory perception of taste.

Some studies have also suggested that the palatability or the incentive value of taste is modulated by hunger. Hungry individuals show increased self-reporting of subjective feeling toward palatable taste (Rolls et al., 1983). Another study indicated that rats developed increased liking for sweet taste after starvation (Berridge, 1991). The authors evaluated the pleasantness of taste by using taste-reactivity facial expressions. Rats deprived of food for 48 h showed higher taste reactivity scores for sucrose–quinine mixture.

Several studies have reported that hormones and neuropeptides related to feeding may modulate peripheral taste sensitivity. Among various anorexic hormones, leptin is reported to selectively inhibit responses related to sweet taste in the taste receptor cells by biding to the functional leptin receptor Ob-Rb in the fungiform and circumvallate taste buds (Kawai et al., 2000; Shigemura et al., 2004; Yoshida et al., 2015). Glucagon-like peptide 1 (GLP-1) increases sensitivity to sweet taste via GLP-1 receptors located on the afferent nerve fibers adjacent to the taste buds (Shin et al., 2008), while cholecystokinin (CCK) on bitter taste via CCK-A receptors expressed in the taste receptor cells (Herness et al., 2002; Lu et al., 2003). Moreover, insulin seems to potentiate the response to salty taste via the epithelial sodium channels (ENaC) (Baquero and Gilbertson, 2011). Intranasal administration of insulin increased the sensitivity to sweet, bitter, salty, sour taste in human taste sensory tests (Rodriguez-Raecke et al., 2017). Neuropeptide Y, which is known as a orexigenic peptide, may influence the bitter taste sensitivity through NPY1R in the taste receptor cells (Zhao et al., 2005). Oxytocin is reported to decrease sweet sensitivity in mice via oxytocin receptors located in the taste buds (Sinclair et al., 2015). However, the central mechanism of taste modulation in hunger is still unclear.

BRAIN REGIONS SHOWING HUNGER-DEPENDENT TASTE RESPONSE

In the past, functional magnetic resonance imaging (fMRI) or electrophysiology studies have discovered brain areas including the OFC, the amygdala, the InsCtx, and the lateral hypothalamus (LH) that respond to taste cues in a hunger/satiety-dependent manner. Neuroimaging research in humans has shown that sated participants reported attenuated subjective pleasantness of a specific taste, suggesting that satiety has a negative effect on the taste perception (Rolls et al., 1983; Kringelbach et al., 2003). This decrease in pleasantness of taste showed a high correlation with a reduction in the activity of the OFC.

Electrophysiological investigations performed in primates revealed a large population of neurons in the OFC (Nakano et al., 1984; Yamamoto et al., 1984; Rolls et al., 1989), the amygdala (Nakano et al., 1986), and the LH (Burton et al., 1976) that responded to sucrose solution when the animal was hungry, but not when the animal was satiated. Importantly,

simultaneous electrophysiological recording of single neurons from the OFC, the LH, and the amygdala was conducted in food-deprived rats with free access to sucrose solution (de Araujo et al., 2006). Similar to the results in primates, rats exhibited hunger-dependent response to tastes in these brain areas. However, due to the limitation of imaging resolution in the fMRI or electrophysiology studies, the precise role of these brain areas that showed state-dependent taste response remains largely elusive.

NEURAL CIRCUITS FOR TASTE PERCEPTION AND CORRELATED FEEDING BEHAVIOR DURING HUNGER

Under fasting condition, animals need to seek food, to decide eating or rejecting the food by savoring the taste, and to consume the food for survival. It is suggested that distinct neural circuits related to appetite, taste perception, and reward work together to evoke appetitive behavior and regulate the subsequent consummatory behavior (Rolls, 2005; Ferrario et al., 2016).

To understand the role of the gustatory system during hunger state, the feeding behavior can be classified into three phases: (1) motivational and anticipatory process before the start of feeding (appetitive behavior), (2) taste perception and execution of feeding (consummatory behavior), and (3) termination of feeding (**Figure 2**). In recent years, newly developed neural manipulation methods and *in vivo* calcium imaging have allowed the study of neuronal functions related to the gustatory system and feeding regulation using high time resolution.

MOTIVATIONAL AND ANTICIPATORY PROCESS BEFORE THE START OF FEEDING

Hunger promotes motivation for appetitive behaviors to seek food and evokes feeding behaviors (Sternson et al., 2013). The hypothalamus has been considered the feeding center. It contains a variety of neuronal cell types associated with maintaining energy homeostasis. Among them, neurons that specifically express the Agouti-related protein (AgRP) within the arcuate nucleus of the hypothalamus have been identified as hunger neurons. Ablation of AgRP neurons in adult mice leads to aphagia (Wu et al., 2009). Conversely, utilization of optogenetic and chemogenetic techniques for rapid activation of cell-type-specific neurons showed that AgRP neurons are sufficient to evoke feeding behavior in fed mice within minutes and the amount of food intake is similar to that observed in overnight fasted mice (Krashes et al., 2011; Betley et al., 2013). Interestingly, GCaMP-based calcium imaging of AgRP neurons using fiber photometry has indicated that the activity of these neurons starts to decease even before a bite of the food (Chen et al., 2015), suggesting that AgRP neurons are involved in the anticipatory process to predict the caloric consumption. This anticipatory response for food sensory cues may help the transition process from seeking food to subsequent feeding behaviors.

Human fMRI studies have shown that the response of the InsCtx or the OFC to sweet solutions changes in a hunger-dependent manner (Haase et al., 2009). Taste solutions were orally delivered to hungry or satiated participants. Blood oxygenation level-dependent signal change measured by fMRI showed significant differences in the activation for sucrose, caffeine, saccharin, and citric acid in the OFC and in the InsCtx between hunger and satiety. Recent studies (Livneh et al., 2017, 2020) have demonstrated that a specific pathway from the hunger-promoting AgRP neurons to the InsCtx via the paraventricular thalamus (PVT) and the basolateral amygdala (BLA) is involved in hunger-dependent enhancement of food cue responses in mice (**Figure 1-1**). The authors applied a visual discrimination task wherein mice were trained to lick after different learned visual cues related to the delivery of a sweet solution (Ensure), a bitter solution (quinine), or water. GCaMP-based single-cell calcium imaging of the InsCtx neurons in behaving mice showed that a large population of InsCtx neurons responded to the visual food cue, licking, or sweet taste. The authors used quinine for the training of visual discrimination task to allow the mice to learn the negative food cue. However, during actual imaging, only Ensure was delivered to the mice. Interestingly, a large proportion of neurons related to food cue response were strongly activated when the mice licked the sweet solution. Imaging the same InsCtx neurons during hunger and satiety revealed that the neurons that were responsive to visual cues during hunger were abolished during satiety. Another human fMRI study suggested that seeing pictures of palatable food could activate the InsCtx (Simmons et al., 2005). These evidences suggest that the InsCtx represents food prediction and interoceptive consequences of upcoming consumption. Thus, this hypothalamus-cortical connection shows the possibility to enhance the palatability of food during hunger state.

A human fMRI study has shown that the OFC and the amygdala encode predictive reward value (Gottfried et al., 2003). *In vivo* calcium imaging study of the OFC neurons (Jennings et al., 2019), which are the direct projection targets of the InsCtx, demonstrated significant excitatory responses during caloric-reward licking in starved mice. Pairing each caloric-reward delivery with optogenetic stimulation of feeding-responsive cells significantly increased licking. Interestingly, stimulation of feeding-responsive cells does not increase licking of non-caloric sweetener saccharin, suggesting that OFC neurons are responsive to caloric reward content rather than to taste reward. It is also reported (Malvaez et al., 2019) that BLA-projecting OFC neurons encode the state-dependent incentive value of palatable food reward. Glutamate receptor activity in the BLA is necessary for reward value encoding and retrieval. Projections from the lateral OFC to the BLA are necessary and sufficient for encoding the positive value of a reward. On the other hand, projections from the medial OFC to the BLA are necessary and sufficient for retrieving this value from memory. A reinforcer devaluation paradigm study has suggested that the OFC and the BLA play different roles in mediating normal goal-directed performance (Pickens et al., 2003). The BLA seems critical to forming representations that link cues to the incentive properties of outcomes, but the OFC possibly contributes to

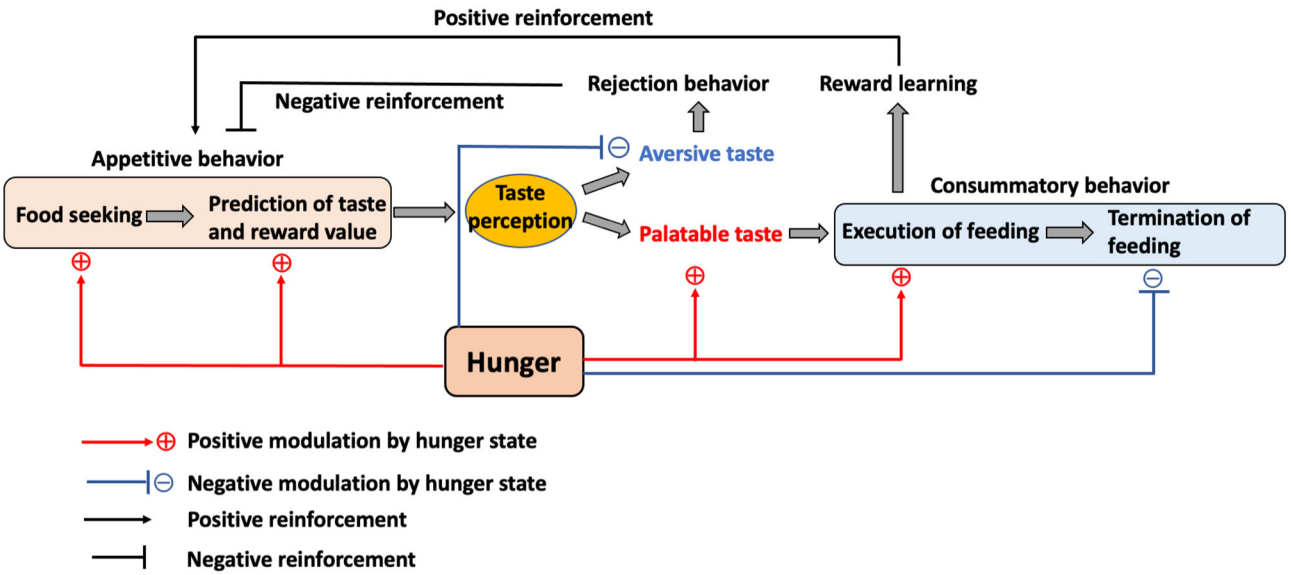

FIGURE 2 | The role of the internal state and taste in feeding. Hunger motivates animals to initiate food seeking and to promote the taste and reward value prediction in the appetitive feeding process. While palatable taste leads to food consumption, aversive taste mediates rejection. This process also contributes to the positive or negative reinforcement toward food. Hunger enhances the preference toward palatable taste while reducing the aversion toward aversive taste to promote consummatory feeding and also inhibits the termination of feeding until satiety.

maintaining these representations in memory and updating them with new information.

These results imply that the InsCtx and the OFC are not only responsive to taste identities but also play a role in the state-dependent reward prediction before feeding. While the InsCtx and the OFC are possibly involved in the prediction of taste as well as food reward, the OFC contains specific neuronal population that contributes to the prediction of the caloric content.

TASTE PERCEPTION DURING FEEDING

Food cues such as visual information and smell allow animals to predict the gustatory identity as well as the reward value of the food (Rolls, 2015). The decision to execute the actual oral feeding action depends on the identity of taste. Gustatory pathways from the brainstem to the cortical areas are important to generate the perception of taste (**Figure 1-2**). Oral exposure to food with normal taste maintains the feeding action, while palatable tastes trigger positive feeling and increase the frequency of mastication. However, aversive tastes transmit negative feeling and lead to acute termination of feeding.

A recent study (Wang et al., 2018) demonstrated that the innervation between the InsCtx and the amygdala helps transmit taste valences (**Figure 1-3**). Gustatory cortices for sweet taste and bitter taste are located in the anterior and the posterior part of the InsCtx. They innervate distinct subnuclei in the amygdala (the BLA for sweet and the central nucleus of the amygdala [CeA] for bitter). Optogenetic activation of BLA-projecting InsCtx neurons increases water-licking behavior by evoking "virtual" sweet taste sensing, while activation of CeA-projecting InsCtx neurons decreases licking toward water by mimicking the bitter taste. Another study using a tastant (sucrose/quinine)-reinforced "go/no-go" task showed that specific inhibition of neurotransmitter release from the lateral CeA (CeL)-projecting InsCtx neurons prevented mice from acquiring the "no-go" responses for quinine and impaired the "go" responses for sucrose in the "go/no-go task," indicating that the InsCtx-CeL circuit is important for the establishment of behavioral response to cues predicting appetitive or aversive tastants (Schiff et al., 2018). These results suggest that the InsCtx contains neurons that encode the innate taste valence as well as the learned taste cue prediction to evoke appetitive or rejection behaviors. However, it is unclear whether neurons related to gustatory response in the InsCtx are distinct from or overlap with the cue-predicting neurons in the InsCtx.

Considering the evidence of the connection between the amygdala and the mesolimbic reward system, the amygdala may function as a relay point to transmit the taste valence and the reward property (InsCtx-amygdala and OFC-amygdala) to trigger feeding behaviors.

TASTE AND INTERNAL STATE MODULATION FOR THE TERMINATION OF FEEDING

During energy deficiency, animals require calories to maintain the body weight and the metabolic functions. They continue consummatory feeding from hunger state until satiety to meet the caloric need. The LH is an essential neuroanatomical region for appetitive as well as for consummatory behaviors (Nieh et al.,

2015). The LH contains many distinct types of neurons and activation of GABAergic (Vgat-expressing) neurons in the LH enhances both appetitive and consummatory behaviors. Calcium imaging in freely behaving mice has indicated that individual $Vgat^{LH}$ neurons preferentially encode aspects of appetitive or consummatory behaviors (Jennings et al., 2015). In contrast, glutamatergic Vglut2 neurons, which are also abundant in the LH, play an opposite role in regulating the feeding behaviors. Optogenetic stimulation of $Vglut2^{LH}$ neurons not only decreases appetite in hungry mice but also produces an aversion to locations linked with the stimulation of these cells (Stamatakis et al., 2016). *In vivo* calcium imaging study on $Vglut2^{LH}$ neurons demonstrated a greater response during sucrose delivery in satiety when compared with the response in hunger state (Rossi et al., 2019). Although these results are opposite to the results of fMRI or electrophysiology studies of LH showing greater response in hunger than in satiety, it could be suggested that distinct neuronal populations exist in the LH and Vglut2 neurons specifically encode satiety and serve as a brake to terminate the feeding action.

An electrophysiological study (Li et al., 2013) indicated that the LH contains two distinct populations of neurons responding to appetitive and aversive tastes. A recent study revealed that physiological hunger affects preferences to appetitive as well as aversive tastes in a mouse model. These effects are induced by LH-projecting AgRP neurons (Fu et al., 2019b). In a brief-access taste test, chemogenetic and optogenetic activation of AgRP neurons in fed animals increased the number of licks for a solution containing a relatively low concentration of sucrose. In contrast, elevation in the number of licks for a bitter (denatonium) solution was also observed after optogenetic activation of AgRP neurons. Furthermore, chemogenetic inhibition of $Vglut2^{LH}$ neurons, but not of $Vgat^{LH}$ neurons recapitulated the hunger-induced taste modification. Two distinct neuronal pathways from $Vglut2^{LH}$ neurons to the lateral septum or to the lateral habenula (LHb) contribute to the modulation of appetitive and aversive taste, respectively. The LS and the LHb are parts of mesolimbic reward system, indicating that the LH may modulate the reward value of the taste (**Figure 1-4**). While $Vglut2^{LH}$ neurons that encode satiety serve as a brake to terminate consummatory behavior during hunger state (Stamatakis et al., 2016; Rossi et al., 2019), these neurons receive inhibitory inputs from the AgRP neurons. Enhancement of preference to sweet tastants and tolerance to bitter tastants through AgRP-dependent inhibition of $Vglut2^{LH}$ neurons could promote consummatory behavior to meet the emergent caloric need.

Notably, the OFC is connected both directly and indirectly with the LH (Öngür and Price, 2000; Reppucci and Petrovich, 2016), suggesting that the OFC may pass integrated sensory information into the LH, evoking motivation for palatable taste. Furthermore, the LH interacts with the mesolimbic system to induce reward learning for positive or negative reinforcement and to modulate the taste preference to trigger or to prevent future food consumption.

CONCLUSION

Feeding behaviors are regulated by homeostatic and hedonic feeding systems. Taste perception from the brainstem to the gustatory cortex serves as a regulator and driving factor for feeding by interacting with the hypothalamus and with the mesolimbic reward system. The brain integrates sensory information and interoception to guide proper feeding behaviors for survival. Understanding the mechanism by which the brain senses taste and reward modalities in different physiological states may be beneficial in therapeutic treatment of overeating in the future.

AUTHOR CONTRIBUTIONS

All authors listed have made a substantial, direct and intellectual contribution to the work, and approved it for publication.

FUNDING

KN was supported in part by Grants-in-Aid for Scientific Research (18H02160) from the Ministry of Education, Culture, Sports, Science, and by Takeda Science Foundation.

REFERENCES

Baquero, A. F., and Gilbertson, T. A. (2011). Insulin activates epithelial sodium channel (ENaC) via phosphoinositide 3-kinase in mammalian taste receptor cells. *Am. J. Physiol. Cell Physiol.* 300, C860–C871. doi: 10.1152/ajpcell.00318.2010

Beckstead, R. M., Morse, J. R., and Norgren, R. (1980). The nucleus of the solitary tract in the monkey: projections to the thalamus and brain stem nuclei. *J. Comp. Neurol.* 190, 259–282. doi: 10.1002/cne.901900205

Beckstead, R. M., and Norgren, R. (1979). An autoradiographic examination of the central distribution of the trigeminal, facial, glossopharyngeal, and vagal nerves in the monkey. *J. Comp. Neurol.* 184, 455–472. doi: 10.1002/cne.901840303

Berridge, K. C. (1991). Modulation of taste affect by hunger, caloric satiety, and sensory-specific satiety in the rat. *Appetite* 16, 103–120. doi: 10.1016/0195-6663(91)90036-R

Berthoud, H. R. (2004). Mind versus metabolism in the control of food intake and energy balance. *Physiol. Behav.* 81, 781–793. doi: 10.1016/j.physbeh.2004.04.034

Betley, J. N., Cao, Z. F. H., Ritola, K. D., and Sternson, S. M. (2013). Parallel, redundant circuit organization for homeostatic control of feeding behavior. *Cell* 155, 1337–1350. doi: 10.1016/j.cell.2013.11.002

Burton, M. J., Rolls, E. T., and Mora, F. (1976). Effects of hunger on the responses of neurons in the lateral hypothalamus to the sight and taste of food. *Exp. Neurol.* 51, 668–677. doi: 10.1016/0014-4886(76)90189-8

Campos, C. A., Bowen, A. J., Schwartz, M. W., and Palmiter, R. D. (2016). Parabrachial CGRP neurons control meal termination. *Cell Metab.* 23, 811–820. doi: 10.1016/j.cmet.2016.04.006

Castro, D. C., Cole, S. L., and Berridge, K. C. (2015). Lateral hypothalamus, nucleus accumbens, and ventral pallidum roles in eating and hunger: interactions between homeostatic and reward circuitry. *Front. Syst. Neurosci.* 9:90. doi: 10.3389/fnsys.2015.00090

Chen, Y., Lin, Y. C., Kuo, T. W., and Knight, Z. A. (2015). Sensory detection of food rapidly modulates arcuate feeding circuits. *Cell* 160, 829–841. doi: 10.1016/j.cell.2015.01.033

de Araujo, I. E., Gutierrez, R., Oliveira-Maia, A. J., Pereira, A., Nicolelis, M. A. L., and Simon, S. A. (2006). Neural ensemble coding of satiety states. *Neuron* 51, 483–494. doi: 10.1016/j.neuron.2006.07.009

Ferrario, C. R., Labouèbe, G., Liu, S., Nieh, E. H., Routh, V. H., Xu, S., et al. (2016). Homeostasis meets motivation in the battle to control food intake. *J. Neurosci.* 36, 11469–11481. doi: 10.1523/JNEUROSCI.2338-16.2016

Fu, O., Iwai, Y., Kondoh, K., Misaka, T., Minokoshi, Y., and Nakajima, K., ichiro (2019a). SatB2-expressing neurons in the parabrachial nucleus encode sweet taste. *Cell Rep.* 27, 1650–1656.e4. doi: 10.1016/j.celrep.2019.04.040

Fu, O., Iwai, Y., Narukawa, M., Ishikawa, A. W., Ishii, K. K., Murata, K., et a;. (2019b). Hypothalamic neuronal circuits regulating hunger-induced taste modification. *Nat. Commun.* 10:4560. doi: 10.1038/s41467-019-12478-x

Gaillard, D., Laugerette, F., Darcel, N., El-Yassimi, A., Passilly-Degrace, P., Hichami, A., et al. (2008). The gustatory pathway is involved in CD36-mediated orosensory perception of long-chain fatty acids in the mouse. *FASEB J.* 22, 1458–1468. doi: 10.1096/fj.07-8415com

Gottfried, J. A., O'Doherty, J., and Dolan, R. J. (2003). Encoding predictive reward value in human amygdala and orbitofrontal cortex. *Science* 301, 1104–1107. doi: 10.1126/science.1087919

Haase, L., Cerf-Ducastel, B., and Murphy, C. (2009). Cortical activation in response to pure taste stimuli during the physiological states of hunger and satiety. *Neuroimage* 44, 1008–1021. doi: 10.1016/j.neuroimage.2008.09.044

Hajnal, A., Smith, G. P., and Norgren, R. (2004). Oral sucrose stimulation increases accumbens dopamine in the rat. *Am. J. Physiol. - Regul. Integr. Comp. Physiol.* 281, R31–R37. doi: 10.1152/ajpregu.00282.2003

Hanci, D., and Altun, H. (2016). Hunger state affects both olfactory abilities and gustatory sensitivity. *Eur. Arch. Oto-Rhino-Laryngol.* 273, 1637–1641. doi: 10.1007/s00405-015-3589-6

Herness, S., Zhao, F. L., Lu, S. G., Kaya, N., and Shen, T. (2002). Expression and physiological actions of cholecystokinin in rat taste receptor cells. *J. Neurosci.* 22, 10018–10029. doi: 10.1523/JNEUROSCI.22-22-10018.2002

Jennings, J. H., Kim, C. K., Marshel, J. H., Raffiee, M., Ye, L., Quirin, S., et al. (2019). Interacting neural ensembles in orbitofrontal cortex for social and feeding behaviour. *Nature* 565, 645–649. doi: 10.1038/s41586-018-0866-8

Jennings, J. H., Ung, R. L., Resendez, S. L., Stamatakis, A. M., Taylor, J. G., Huang, J., et al. (2015). Visualizing hypothalamic network dynamics for appetitive and consummatory behaviors. *Cell* 160, 516–527. doi: 10.1016/j.cell.2014.12.026

Kawai, K., Sugimoto, K., Nakashima, K., Miura, H., and Ninomiya, Y. (2000). Leptin as a modulator of sweet taste sensitivities in mice. *Proc. Natl. Acad. Sci. U.S.A.* 97, 11044–11049. doi: 10.1073/pnas.190066697

Krashes, M. J., Koda, S., Ye, C. P., Rogan, S. C., Adams, A. C., Cusher, D. S., et al. (2011). Rapid, reversible activation of AgRP neurons drives feeding behavior in mice. *J. Clin. Invest.* 121, 1424–1428. doi: 10.1172/JCI46229

Kringelbach, M. L., O'Doherty, J., Rolls, E. T., and Andrews, C. (2003). Activation of the human orbitofrontal cortex to a liquid food stimulus is correlated with its subjective pleasantness. *Cereb. Cortex* 13, 1064–1071. doi: 10.1093/cercor/13.10.1064

Li, J. X., Yoshida, T., Monk, K. J., and Katz, D. B. (2013). Lateral hypothalamus contains two types of palatability- related taste responses with distinct dynamics. *J. Neurosci.* 33, 9462–9473. doi: 10.1523/JNEUROSCI.3935-12.2013

Lindemann, B. (2001). Receptors and transduction in taste. *Nature* 413, 219–225. doi: 10.1038/35093032

Livneh, Y., Ramesh, R. N., Burgess, C. R., Levandowski, K. M., Madara, J. C., Fenselau, H., et al. (2017). Homeostatic circuits selectively gate food cue responses in insular cortex. *Nature* 546, 611–616. doi: 10.1038/nature22375

Livneh, Y., Sugden, A. U., Madara, J. C., Essner, R. A., Flores, V. I., Sugden, L. A., et al. (2020). Estimation of current and future physiological states in insular cortex. *Neuron* 105, 1094–1111.e10. doi: 10.1016/j.neuron.2019.12.027

Lu, S. G., Zhao, F. L., and Herness, S. (2003). Physiological phenotyping of cholecystokinin-responsive rat taste receptor cells. *Neurosci. Lett.* 351, 157–160. doi: 10.1016/j.neulet.2003.07.016

Malvaez, M., Shieh, C., Murphy, M. D., Greenfield, V. Y., and Wassum, K. M. (2019). Distinct cortical–amygdala projections drive reward value encoding and retrieval. *Nat. Neurosci.* 22, 762–769. doi: 10.1038/s41593-019-0374-7

Meyerhof, W., Behrens, M., Brockhoff, A., Bufe, B., and Kuhn, C. (2005). Human bitter taste perception. *Chem. Senses* 30(Suppl. 1):i14–i15. doi: 10.1093/chemse/bjh089

Mueller, K. L., Hoon, M. A., Erlenbach, I., Chandrashekar, J., Zuker, C. S., and Ryba, N. J. P. (2005). The receptors and coding logic for bitter taste. *Nature* 434, 225–229. doi: 10.1038/nature03352

Nakano, Y., Oomura, Y., Lénárd, L., Nishino, H., Aou, S., Yamamoto, T., et al. (1986). Feeding-related activity of glucose-and morphine-sensitive neurons in the monkey amygdala. *Brain Res.* 399, 167–172. doi: 10.1016/0006-8993(86)90613-X

Nakano, Y., Oomura, Y., Nishino, H., Aou, S., Yamamoto, T., and Nemoto, S. (1984). Neuronal activity in the medial orbitofrontal cortex of the behaving monkey: modulation by glucose and satiety. *Brain Res. Bull.* 12, 381–385. doi: 10.1016/0361-9230(84)90109-6

Nieh, E. H., Matthews, G. A., Allsop, S. A., Presbrey, K. N., Leppla, C. A., Wichmann, R., et al. (2015). Decoding neural circuits that control compulsive sucrose seeking. *Cell* 160, 528–541. doi: 10.1016/j.cell.2015.01.003

Öngür, D., and Price, J. L. (2000). The organization of networks within the orbital and medial prefrontal cortex of rats, monkeys and humans. *Cereb. Cortex* 10, 206–219. doi: 10.1093/cercor/10.3.206

Ozdener, M. H., Subramaniam, S., Sundaresan, S., Sery, O., Hashimoto, T., Asakawa, Y., et al. (2014). CD36- and GPR120-mediated Ca2+ signaling in human taste bud cells mediates differential responses to fatty acids and is altered in obese mice. *Gastroenterology* 146, 995–1005. doi: 10.1053/j.gastro.2014.01.006

Pickens, C. L., Saddoris, M. P., Setlow, B., Gallagher, M., Holland, P. C., and Schoenbaum, G. (2003). Different roles for orbitofrontal cortex and basolateral amygdala in a reinforcer devaluation task. *J. Neurosci.* 23, 11078–11084. doi: 10.1523/JNEUROSCI.23-35-11078.2003

Pritchard, T. C., Hamilton, R. B., and Norgren, R. (1989). Neural coding of gustatory information in the thalamus of Macaca mulatta. *J. Neurophysiol.* 61, 1–14. doi: 10.1152/jn.1989.61.1.1

Reppucci, C. J., and Petrovich, G. D. (2016). Organization of connections between the amygdala, medial prefrontal cortex, and lateral hypothalamus: a single and double retrograde tracing study in rats. *Brain Struct. Funct.* 221, 2937–2962. doi: 10.1007/s00429-015-1081-0

Rodriguez-Raecke, R., Yang, H., Bruenner, Y. F., and Freiherr, J. (2017). Intranasal insulin boosts gustatory sensitivity. *J. Neuroendocrinol.* 29. doi: 10.1111/jne.12449

Rolls, E. T. (2005). Taste, olfactory, and food texture processing in the brain, and the control of food intake. *Physiol. Behav.* 85, 45–56. doi: 10.1016/j.physbeh.2005.04.012

Rolls, E. T. (2015). Taste, olfactory, and food reward value processing in the brain. *Prog. Neurobiol.* 127–128, 64–90. doi: 10.1016/j.pneurobio.2015.03.002

Rolls, E. T., Critchley, H. D., Browning, A. S., Hernadi, I., and Lenard, L. (1999). Responses to the sensory properties of fat of neurons in the primate orbitofrontal cortex. *J. Neurosci.* 19, 1532–1540. doi: 10.1523/JNEUROSCI.19-04-01532.1999

Rolls, E. T., Rolls, B. J., and Rowe, E. A. (1983). Sensory-specific and motivation-specific satiety for the sight and taste of food and water in man. *Physiol. Behav.* 30, 185–192. doi: 10.1016/0031-9384(83)90003-3

Rolls, E. T., Sienkiewicz, Z. J., and Yaxley, S. (1989). Hunger modulates the responses to gustatory stimuli of single neurons in the caudolateral orbitofrontal cortex of the macaque monkey. *Eur. J. Neurosci.* 1, 53–60. doi: 10.1111/j.1460-9568.1989.tb00774.x

Rolls, E. T., Yaxley, S., and Sienkiewicz, Z. J. (1990). Gustatory responses of single neurons in the caudolateral orbitofrontal cortex of the macaque monkey. *J. Neurophysiol.* 64, 1055–1066. doi: 10.1152/jn.1990.64.4.1055

Rossi, M. A., Basiri, M. L., McHenry, J. A., Kosyk, O., Otis, J. M., Van Den Munkhof, H. E., et al. (2019). Obesity remodels activity and transcriptional state of a lateral hypothalamic brake on feeding. *Science* 364, 1271–1274. doi: 10.1126/science.aax1184

Rossi, M. A., and Stuber, G. D. (2018). Overlapping brain circuits for homeostatic and hedonic feeding. *Cell Metab.* 27, 42–56. doi: 10.1016/j.cmet.2017.09.021

Schiff, H. C., Bouhuis, A. L., Yu, K., Penzo, M. A., Li, H., He, M., et al. (2018). An insula-central amygdala circuit for guiding tastant-reinforced choice behavior. *J. Neurosci.* 38, 1418–1429. doi: 10.1523/JNEUROSCI.1773-17.2017

Shigemura, N., Ohta, R., Kusakabe, Y., Miura, H., Hino, A., Koyano, K., et al. (2004). Leptin modulates behavioral responses to sweet substances by influencing peripheral taste structures. *Endocrinology* 145, 839–847. doi: 10.1210/en.2003-0602

Shin, Y. K., Martin, B., Golden, E., Dotson, C. D., Maudsley, S., Kim, W., et al. (2008). Modulation of taste sensitivity by GLP-1 signaling. *J. Neurochem.* 106, 455–463. doi: 10.1111/j.1471-4159.2008.05397.x

Siep, N., Roefs, A., Roebroeck, A., Havermans, R., Bonte, M. L., and Jansen, A. (2009). Hunger is the best spice: An fMRI study of the effects of attention, hunger and calorie content on food reward processing in the amygdala and orbitofrontal cortex. *Behav. Brain Res.* 198, 149–158. doi: 10.1016/j.bbr.2008.10.035

Simmons, W. K., Martin, A., and Barsalou, L. W. (2005). Pictures of appetizing foods activate gustatory cortices for taste and reward. *Cereb. Cortex.* 15, 1602–1608. doi: 10.1093/cercor/bhi038

Sinclair, M. S., Perea-Martinez, I., Abouyared, M., St. John, S. J., and Chaudhari, N. (2015). Oxytocin decreases sweet taste sensitivity in mice. *Physiol. Behav.* 141, 103–110. doi: 10.1016/j.physbeh.2014.12.048

Stamatakis, A. M., Van Swieten, M., Basiri, M. L., Blair, G. A., Kantak, P., and Stuber, G. D. (2016). Lateral hypothalamic area glutamatergic neurons and their projections to the lateral habenula regulate feeding and reward. *J. Neurosci.* 36, 302–311. doi: 10.1523/JNEUROSCI.1202-15.2016

Sternson, S. M., Nicholas Betley, J., and Cao, Z. F. H. (2013). Neural circuits and motivational processes for hunger. *Curr. Opin. Neurobiol.* 23, 353–360. doi: 10.1016/j.conb.2013.04.006

Wang, L., Gillis-Smith, S., Peng, Y., Zhang, J., Chen, X., Salzman, C. D., et al. (2018). The coding of valence and identity in the mammalian taste system. *Nature* 558, 127–131. doi: 10.1038/s41586-018-0165-4

Wu, Q., Boyle, M. P., and Palmiter, R. D. (2009). Loss of GABAergic signaling by AgRP neurons to the parabrachial nucleus leads to starvation. *Cell* 137, 1225–1234. doi: 10.1016/j.cell.2009.04.022

Yamamoto, T., Oomura, Y., Nishino, H., Aou, S., Nakano, Y., and Nemoto, S. (1984). Monkey orbitofrontal neuron activity during emotional and feeding behaviors. *Brain Res. Bull.* 12, 441–443. doi: 10.1016/0361-9230(84)90117-5

Yarmolinsky, D. A., Zuker, C. S., and Ryba, N. J. P. (2009). Common sense about taste: from mammals to insects. *Cell* 139, 234–244. doi: 10.1016/j.cell.2009.10.001

Yasumatsu, K., Iwata, S., Inoue, M., and Ninomiya, Y. (2019). Fatty acid taste quality information via GPR120 in the anterior tongue of mice. *Acta Physiol.* 226:e13215. doi: 10.1111/apha.13215

Yoshida, R., Noguchi, K., Shigemura, N., Jyotaki, M., Takahashi, I., Margolskee, R. F., et al. (2015). Leptin suppresses mouse taste cell responses to sweet compounds. *Diabetes* 64, 3751–3762. doi: 10.2337/db14-1462

Zhang, J., Jin, H., Zhang, W., Ding, C., O'Keeffe, S., Ye, M., et al. (2019). Sour sensing from the tongue to the brain. *Cell* 179, 392–402.e15. doi: 10.1016/j.cell.2019.08.031

Zhao, F. L., Shen, T., Kaya, N., Lu, S. G., Cao, Y., and Herness, S. (2005). Expression, physiological action, and coexpression patterns of neuropeptide Y in rat taste-bud cells. *Proc. Natl. Acad. Sci. U.S.A.* 102, 11100–11105. doi: 10.1073/pnas.0501988102

Zhao, G. Q., Zhang, Y., Hoon, M. A., Chandrashekar, J., Erlenbach, I., Ryba, N. J. P., et al. (2003). The receptors for mammalian sweet and umami taste. *Cell* 115, 255–266. doi: 10.1016/S0092-8674(03)00844-4

Zverev, Y. P. (2004). Effects of caloric deprivation and satiety on sensitivity of the gustatory system. *BMC Neurosci.* 5:5. doi: 10.1186/1471-2202-5-5

Conflict of Interest: The authors declare that the research was conducted in the absence of any commercial or financial relationships that could be construed as a potential conflict of interest.

frontiers in Human Neuroscience

ORIGINAL RESEARCH
published: 16 April 2021
doi: 10.3389/fnhum.2021.589578

Distributed Functional Connectome of White Matter in Patients With Functional Dyspepsia

Qiang Xu[1,2†], Yifei Weng[2†], Chang Liu[3], Lianli Qiu[2], Yulin Yang[3], Yifei Zhou[3], Fangyu Wang[3], Guangming Lu[1,2,4], Long Jiang Zhang[2] and Rongfeng Qi[2*]*

[1] College of Automation Engineering, Nanjing University of Aeronautics and Astronautics, Nanjing, China, [2] Department of Medical Imaging, Jinling Hospital, Medical School of Nanjing University, Nanjing, China, [3] Department of Gastroenterology, Jinling Hospital, Medical School of Nanjing University, Nanjing, China, [4] State Key Laboratory of Analytical Chemistry for Life Science, Nanjing University, Nanjing, China

OPEN ACCESS

Edited by:
Masahiro Yamaguchi,
Kôchi University, Japan

Reviewed by:
Xi Jiang,
University of Electronic Science and Technology of China, China
Wei Liao,
University of Electronic Science and Technology of China, China

***Correspondence:**
Long Jiang Zhang
kevinzhlj@163.com
Rongfeng Qi
qirongfeng@163.com

† These authors have contributed equally to this work

Specialty section:
This article was submitted to Health, a section of the journal Frontiers in Human Neuroscience

Received: 31 July 2020
Accepted: 25 February 2021
Published: 16 April 2021

Citation:
Xu Q, Weng Y, Liu C, Qiu L, Yang Y, Zhou Y, Wang F, Lu G, Zhang LJ and Qi R (2021) Distributed Functional Connectome of White Matter in Patients With Functional Dyspepsia. Front. Hum. Neurosci. 15:589578. doi: 10.3389/fnhum.2021.589578

Purpose: We aimed to find out the distributed functional connectome of white matter in patients with functional dyspepsia (FD).

Methods: 20 patients with FD and 24 age- and gender-matched healthy controls were included into the study. The functional connectome of white matter and graph theory were used to these participants. Two-sample *t*-test was used for the detection the abnormal graph properties in FD. Pearson correlation was used for the relationship between properties and the clinical and neuropsychological information.

Results: Patients with FD and healthy controls showed small-world properties in functional connectome of white matter. Compared with healthy controls, the FD group showed decreased global properties (Cp, S, Eglobal, and Elocal). Four pairs of fiber bundles that are connected to the frontal lobe, insula, and thalamus were affected in the FD group. Duration and Pittsburgh Sleep Quality Index positively correlated with the betweenness centrality of white matter regions of interest.

Conclusion: FD patients turned to a non-optimized functional organization of WM brain network. Frontal lobe, insula, and thalamus were key regions in brain information exchange of FD. It provided some novel imaging evidences for the mechanism of FD.

Keywords: functional dyspepsia, functional connectome, white matter, resting-state fMRI, graph theory

INTRODUCTION

Functional dyspepsia (FD) is one of the most prevalent functional gastrointestinal disorders, with high prevalence (5–11% of the population) (Ford et al., 2015). FD is characterized by four main symptoms: bothersome postprandial fullness, early satiety, epigastric burning, and epigastralgia (Enck et al., 2017). FD negatively affects the quality of life in patients and is a healthcare burden for society for its recurrent nature of the symptoms (El-Serag and Talley, 2003; Lacy et al., 2011). In the absence of detectable organic causes, FD was referred to be a functional disorder, which was thought to result from the dysregulation in brain–gut interaction (Koloski et al., 2012). However, the neural basis of FD remains poorly understood.

Functional neuroimaging is a meaningful tool for identifying the human brain circuitry which correlates with the clinical phenotypic and behavioral manifestations in functional gastrointestinal disorder, including FD (Van Oudenhove et al., 2007; Lee et al., 2016; Kano et al., 2018). Based on the resting-state activity or task-based responses (e.g., visceral distention), the functional neuroimaging could assist in quantifying viscerosensory inputs that reach the brain. Several brain regions were reported in the research of neurological abnormalities in patients with FD, including somatosensory cortex, frontal cortex, insula, anterior cingulate cortex, thalamus, hippocampus, and amygdala (Al Omran and Aziz, 2014; Lee et al., 2016; Kano et al., 2018). Furthermore, a previous study suggested that people with gastric fundic distension showed altered frontal-limbic network (Ladabaum et al., 2007). Another study identified that the FD patients showed abnormal pain and salience network (Lee et al., 2016). These studies suggest that the brain network analysis could be a helpful tool for understanding the mechanism of brain alteration in patients with FD.

In general, the brain network could be derived from structural connectivity, functional connectivity, and effective connectivity among the distributed brain regions (Bullmore and Sporns, 2009). Functional connectivity mainly could be built by temporal correlation or coherences between signals from brain regions (Achard and Bullmore, 2007; Biswal et al., 2010). Functional brain network analysis has been applied to the research of cognition and brain diseases/disorders (He and Evans, 2010; Ding et al., 2011; Zhang et al., 2011; Gao et al., 2013). However, most of the previous studies evaluated the functional connectivity of gray matter in blood oxygen level–dependent (BOLD) fMRI. The information of white matter (WM) in BOLD-fMRI has been ignored because the signals in white matter were thought to be noisy, unreliable, and undetectable in historical period. The role of WM in neuroimaging is still controversial.

Recently, several studies have detected the brain activity in WM in BOLD-fMRI. Evidences from amplitude and connectivity studies demonstrated that the signal of WM in BOLD-fMRI exhibited a specific distribution rather than a random distribution of noise: the WM functional connectomes exhibited a reliable and stable small-world topology, and the abnormal amplitude of low-frequency fluctuation (ALFF) in WM could provide the evidence for understanding the functional role of fiber tracts in the pathology of Parkinson's disease (Ji et al., 2017; Li et al., 2019). Moreover, WM activity was shown to be modulated under different cognitive tasks (Ji et al., 2017; Wu et al., 2017; Huang et al., 2018). In Alzheimer's disease, the WM function was associated with the regional glucose metabolism and correlated with memory function (Makedonov et al., 2016). Another study found that patients with Parkinson's disease showed increased small-worldness in the functional network of WM (Ji et al., 2019). It suggested that the functional connectivity of WM could be a useful and novel tool for investigating the alteration in brain disorders. In this study, we aimed to reveal the functional connectome of WM in FD patients. It might be helpful for the mechanism investigation with a novel insight.

MATERIALS AND METHODS

Participants

Twenty patients with functional dyspepsia (FD) (14 female, age range: 20–62 years, 40.80 ± 12.22 years) and 24 healthy controls (16 female, age range: 21–68 years, 42.29 ± 15.66 years) were included in this study. All participants were right-handed and provided written informed consent before the whole study began. The study was approved by the Medical Research Ethics Committee of Jinling Hospital in accordance with the Helsinki Declaration (Approval no. 2016NZGKJ-070).

The FD patients were diagnosed by the gastroenterologist from the Digestive Disease Clinic of Jinling Hospital by following the Rome III criteria (Drossman, 2006). The gastroenterologist has extensive experience in functional gastrointestinal disorders. The exclusion criteria were as follows: a history of gastrointestinal surgery; major medical or neurological conditions; psychiatric disorders or substance abuse; any previous treatment with centrally acting medications such as aspirin and selective serotonin reuptake inhibitors. All patients were assessed with the Pittsburgh Sleep Quality Index (PSQI). The healthy controls were recruited from the local community through printed advertisements.

MRI Data Acquisition

MRI data were collected by using a 3T MR scanner (Tim Trio, Siemens, Germany). The participants were instructed to stay still during scanning and keep their eyes closed but not fall asleep. Resting-state BOLD fMRI and high-resolution T1-weighted structural image were scanned during the study. The parameters of fMRI were as follows: TR/TE = 2,000/30 ms; FOV = 240 mm × 240 mm; matrix = 64 × 64; thickness = 4 mm with a gap of 0.4 mm between slices, 30 axial slices, with 250 brain volumes (500 s). The parameters of structural images were as follows: TR/TE = 2,300/2.98 ms; field of view = 256 mm × 256 mm; matrix size = 256 × 256, 176 sagittal slices with thickness of 1 mm, no gap between slices.

Data Preprocess

Functional images were preprocessed by using DPARSF (v4.3[1]) (Chao-Gan and Yu-Feng, 2010) and SPM12 toolkit[2]. After excluding 10 volumes, slice-timing correction and realignment were applied to the 240 left functional volumes. Subjects were excluded if his or her head motion exceeded 2.0 mm translation or 2.0° rotation. The mean frame-wise displacement (FD) was also calculated for each subject. Individuals with head motion of > 1.0 mm in translation and 1.0° in rotation were excluded. None of the participants was excluded for the head motion.

Structural images were then co-registered with the preprocessed functional images (mean functional image for each subject) and segmented into gray matter (GM), WM, and cerebrospinal fluid (CSF) using a diffeomorphic non-linear registration algorithm (DARTEL) (Ashburner, 2007) in SPM12. The mean CSF signals from 95% threshold cut-off mask, 24

[1]https://www.restfmri.net/

[2]https://www.fil.ion.ucl.ac.uk/spm/

head motion parameters (6 head motion parameters, 1 time point before, and the 12 corresponding squared items), and scrubbing parameters (FD > 0.5 mm along with one-forward and two-back neighbors) were regressed out from functional data. To avoid elimination of important neural signals, we did not remove or regress out WM or global signals (Ji et al., 2017; Li et al., 2019). To minimize mixing signal (and noise) components from the WM regions due to partial volume effect, subsequent processing of the functional images was performed for WM in accordance with previous study parameters (Li et al., 2019). First, the individual masks were generated using a rigorous 90% threshold on the probability map of WM. Functional images were spatially separated into WM images using the dot product between functional images and individual WM mask. Then the functional images in WM were spatially normalized onto Montreal Neurological Institute (MNI) space using DARTEL normalization operation and resampled to 3 mm × 3 mm × 3 mm. To minimize spurious local spatial correlations between voxels, spatial smoothing was not applied. Subsequently, linear trending and band-pass filtering (0.01–0.10 Hz) were performed to minimize any drifts as well as minimize high-frequency physiological noise sources such as the respiration rate.

Next, the individual WM masks were spatially normalized onto MNI space using DARTEL normalization operation and resampled to 3 mm × 3 mm × 3 mm. Then, only voxels identified as WM across 80% of subjects were included as part of the group-level WM mask (Li et al., 2019). To exclude the impact of deep brain structures, the probability (25% threshold) Harvard–Oxford Atlas was used to remove subcortical nuclei (i.e., bilateral thalamus, putamen, caudate, pallidum, and nucleus accumbens) from the group-level WM mask.

Parcellation of WM

The group-level WM mask was subdivided into 128 random regions of interest (ROIs) (Ji et al., 2019; Li et al., 2019) and was generated and approximately identical in size (mean ± SD = 99.24 ± 0.43 voxels across ROIs), as previously described by Zalesky et al. (2010). The WM group parcellation used here was attached as **Supplementary Information Table 1** and marked using JHU-Atlas.

Functional Connectome of WM

Pearson's correlation coefficient was used between each ROI's averaged time series. Fisher's r to Z transformation was applied to each of the correlation matrices. A schematic of the analyses is shown in **Figure 1**. Finally, we estimated the topological properties of the WM functional connectome.

Network Properties of Functional Connectome of WM

Threshold Selection

To explore the influence of thresholds on topological properties (Bullmore and Bassett, 2011), we used sparsity-based (proportional) thresholds to the weighted correlation matrix corresponding to each subject (Garrison et al., 2015). The sparsity was defined as the ratio of the real edge numbers divided by the maximum possible edge numbers in a given network at r_{thr}. We decreased the r_{thr} from 1 to 0 (from maximum to minimum) until the existing number of edges satisfied a sparsity threshold. Specifically,

$$0 \leq \text{sparsity} \leq 1 = \frac{\varepsilon_{\text{thr}}}{\text{N}(\text{N}-1)/2}$$

Where ε_{thr}expressed the existing number of edges generated by threshold at r_{thr}, and N(N − 1)/2 represents the maximum possible number of edges existing in a given network of N nodes (Bullmore and Bassett, 2011; Liao et al., 2018). In this case, when r_{thr} = 0, sparsity = 1; when r_{thr} = 1, sparsity = 0.

Topological Properties of WM Functional Network

The global and nodal topological properties of WM functional connectome were computed using Gretna software (v2.0[3]). The following global parameters were included: strength of network (S), global efficiency (Eglobal), local efficiency (Elocal), clustering coefficient (Cp), the shortest path length (Lp), normalized clustering coefficient γ()normalized shortest path length λ()and small-worldness σ()Here, S measured the connectivity capacity of the network, Eglobal quantified the capacity of information exchange across the whole network, and Elocal was the measurement of the fault tolerance of the subgraph, showing the efficiency of information exchange at the local level. The small-worldness supported both segregated and intergrated information processing.

Meanwhile, the following nodal parameters were included in the study: betweenness centrality (BC), strength (Snodal), and efficiency (Enodal). BC represents the node ability of bridging the disparate parts of the network. Snodal measures the connectivity capacity of the node, and Enodal measures the capacity of information exchange of the node. A review outlined the uses and interpretations of these topological properties (Rubinov and Sporns, 2010). The definitions of these properties are described in the **Supplementary File**.

Statistical Analysis

The statistical analysis of the demographic and neuropsychological data was carried on by using GraphPad Prism[4]. The differences of age between two groups were tested by two-sample *t*-test. Also, the sex difference was tested by χ^2 test.

The statistical analysis of the global properties was carried by using SurfStat toolbox[5]. The differences of each sparsity and those of the AUC (area under curve) were test by two-sample *t*-test under the model of general linear model. The differences of the nodal properties were tested only on the AUC condition by using the same method of the global properties.

The Pearson correlation analysis was used to find the relationship between the clinical information, neuropsychological table, and network properties.

[3]https://www.nitrc.org/projects/Gretna

[4]http://www.graphpad.com

[5]http://www.math.mcgill.ca/keith/surfstat/#ICBMagain

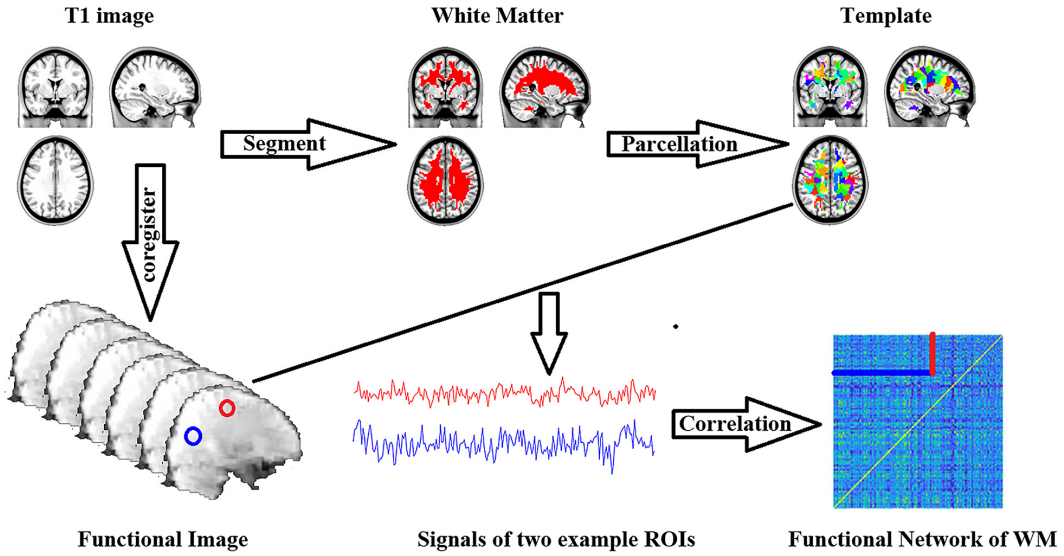

FIGURE 1 | Workflow of functional connectome of white matter construction.

TABLE 1 | Demographic and neuropsychological data.

	FD	HC	Statistical results
Sex	14F/6M	16F/8M	$\chi^2 = 0.056$, $p = 0.813$
Age (years)	40.80 ± 12.22	42.29 ± 15.66	$t = -0.347$, $p = 0.731$
Duration (months)	42.03 ± 75.92	–	–
PSQI	8.15 ± 4.32	–	–

RESULTS

Demographic and Neuropsychological Data

There was no significant difference in age and sex between the FD patients and healthy controls (**Table 1**).

Group Differences of Global Properties

Compared with the healthy controls, the FD patients showed significant decreases in Cp ($t = -3.303$, $p = 0.001$ in AUC model), S ($t = -2.184$, $p = 0.017$ in AUC model), Eglobal ($t = -1.969$, $p = 0.028$ in AUC model), and Elocal ($t = -2.116$, $p = 0.020$ in AUC model), and showed a significant increase in Lp ($t = 2.595$, $p = 0.007$ in AUC model). The differences could be detected on both AUC mode and sparsity mode. No significant difference was found in γ, λ, and σ either on AUC or on sparsity (**Table 2** and **Figure 2**).

Group Differences of Nodal Properties

For the comparison of nodal BC, the FD patients showed increases on nodes 2 (located on the right anterior corona radiata), 13 (located on the body of corpus callosum), and 42 (located on the left superior longitudinal fasciculus), and showed decreases on nodes 57 (located on the right anterior corona radiata) and 110 (located on genu of corpus callosum) (**Table 3** and **Figure 3**).

For the comparison of nodal strength, the FD patients showed decreases on nodes 12 (located on the right superior longitudinal fasciculus), 15 (located on the right anterior corona radiata), 18 (located on the left superior longitudinal fasciculus), 27 (located on the right superior longitudinal fasciculus), 64 (located on the left anterior corona radiata), 84 (located on the left posterior thalamic radiation), and 99 (located on left superior corona radiata) (**Table 3** and **Figure 3**).

For the comparison of nodal efficiency, the FD patients showed decreases on nodes 8 (located on the left posterior corona radiata), 9 (located on genu of corpus callosum), 12 (located on the right superior longitudinal fasciculus), 18 (located on the left superior longitudinal fasciculus), (located on the left anterior corona radiata), 84 (located on the left posterior thalamic radiation), 99 (located on left superior corona radiata), and 106 (unclassified on the JHU-Atlas, but located near left posterior corona radiata) (**Table 3** and **Figure 3**). All results of node comparison were corrected by false-positive adjustment (Fornito et al., 2011; Jao et al., 2013; Jin et al., 2014).

Correlation Between Clinical Information, Neuropsychological Table, and Network Properties

A positive correlation was found between duration of disorder and BC value of node 13 (located on the body of corpus callosum, $r = 0.601$, $p = 0.005$) (**Figure 4**).

Positive correlations were found between PSQI and BC values of node 2 (located on the right anterior corona radiata, $r = 0.593$, $p = 0.006$) and node 42 (located on the left superior longitudinal fasciculus, $r = 0.563$, $p = 0.010$) (**Figure 4**).

TABLE 2 | Group differences of small-world property.

	γ	λ	σ	Cp	Lp	Strength	Eglobal	Elocal
T values	−1.013	0.773	1.078	−3.303	2.595	−2.184	−1.969	−2.116
P values	0.159	0.222	0.144	0.001*	0.007*	0.017*	0.028*	0.020*

**Significant alterations.*

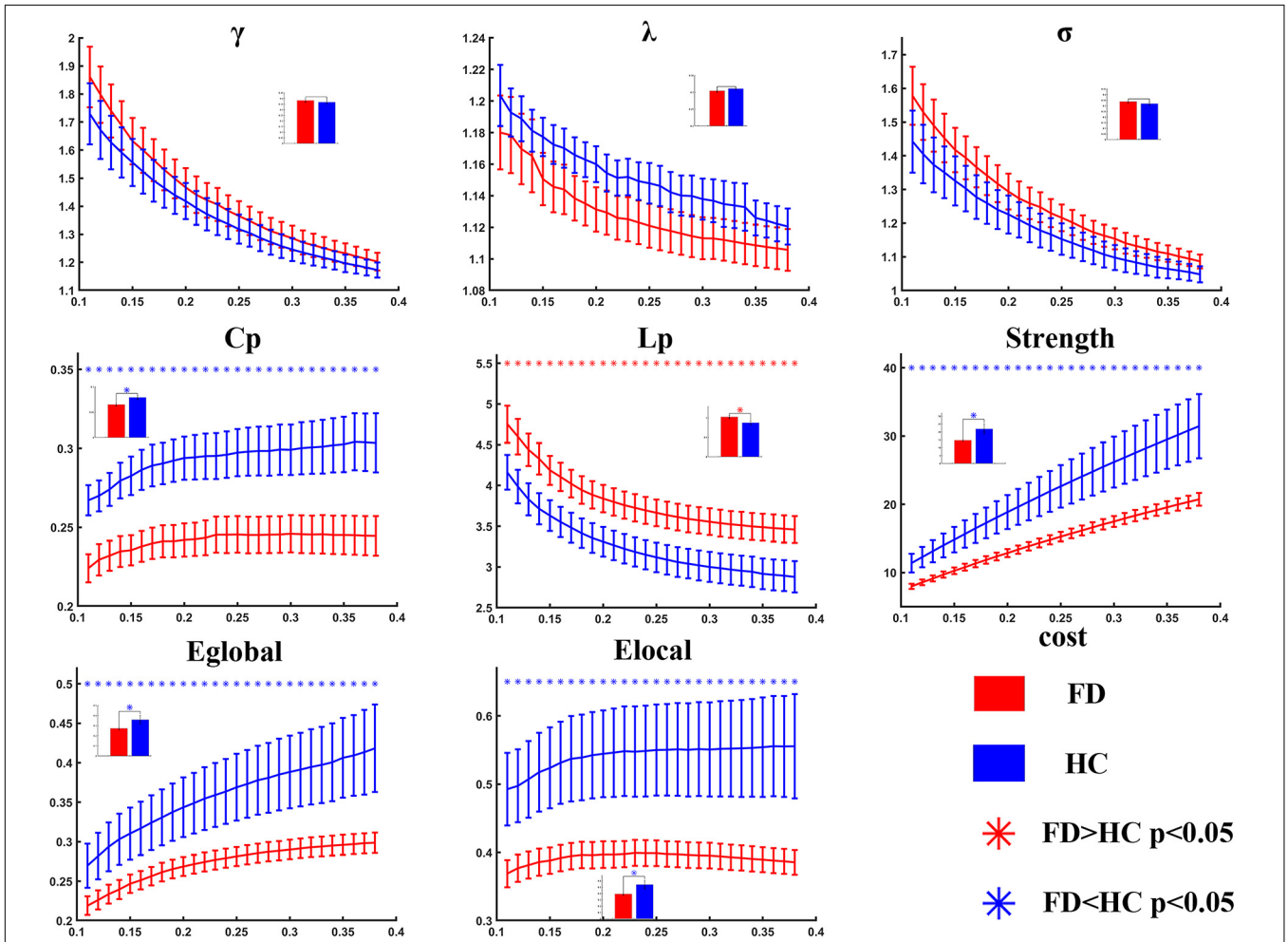

FIGURE 2 | Statistical analysis for the global properties between functional dyspepsia (FD) and healthy controls (HC). Compared with HC, the FD patients showed decreased Cp, strength, Eglobal, and Elocal, and increased Lp.

DISCUSSION

In this study, we applied the functional connectome of WM to discover the alteration of patients with FD. Both FD and HC groups showed small-world properties in the functional connectome of WM. Compared with the HC group, the FD patients showed significant decreases in global properties (Cp, S, Eglobal, and Elocal). Moreover, four pairs of fibers were affected in FD patients in the nodal properties comparison. The duration and PSQI also correlated with the alteration of nodal properties.

Graph theory provided a network prospective to investigate how the brain works interactively. The human brain is organized in a "small-world" pattern with high value and low energetic cost (Bullmore and Sporns, 2009). Small-world properties have been used to detect the alteration in brain disease, such as Alzheimer's disease (Phillips et al., 2015; Vecchio et al., 2018), epilepsy (Zhang et al., 2011; Ji et al., 2015), and stroke (Case et al., 2019). In this study, we investigated the functional architecture of WM using resting-state fMRI in FD patients. It fitted the former studies that the functional connectome of WM had a small-world structure (Ji et al., 2019; Li et al., 2019). In both patients and healthy controls, there was a small-world property in the WM functional network. As we know, this was the first time that the graph theory was applied to analyze the WM functional network in FD researches. In our result, the FD patients showed decreased strength, efficiency, and clustering coefficient, which implied

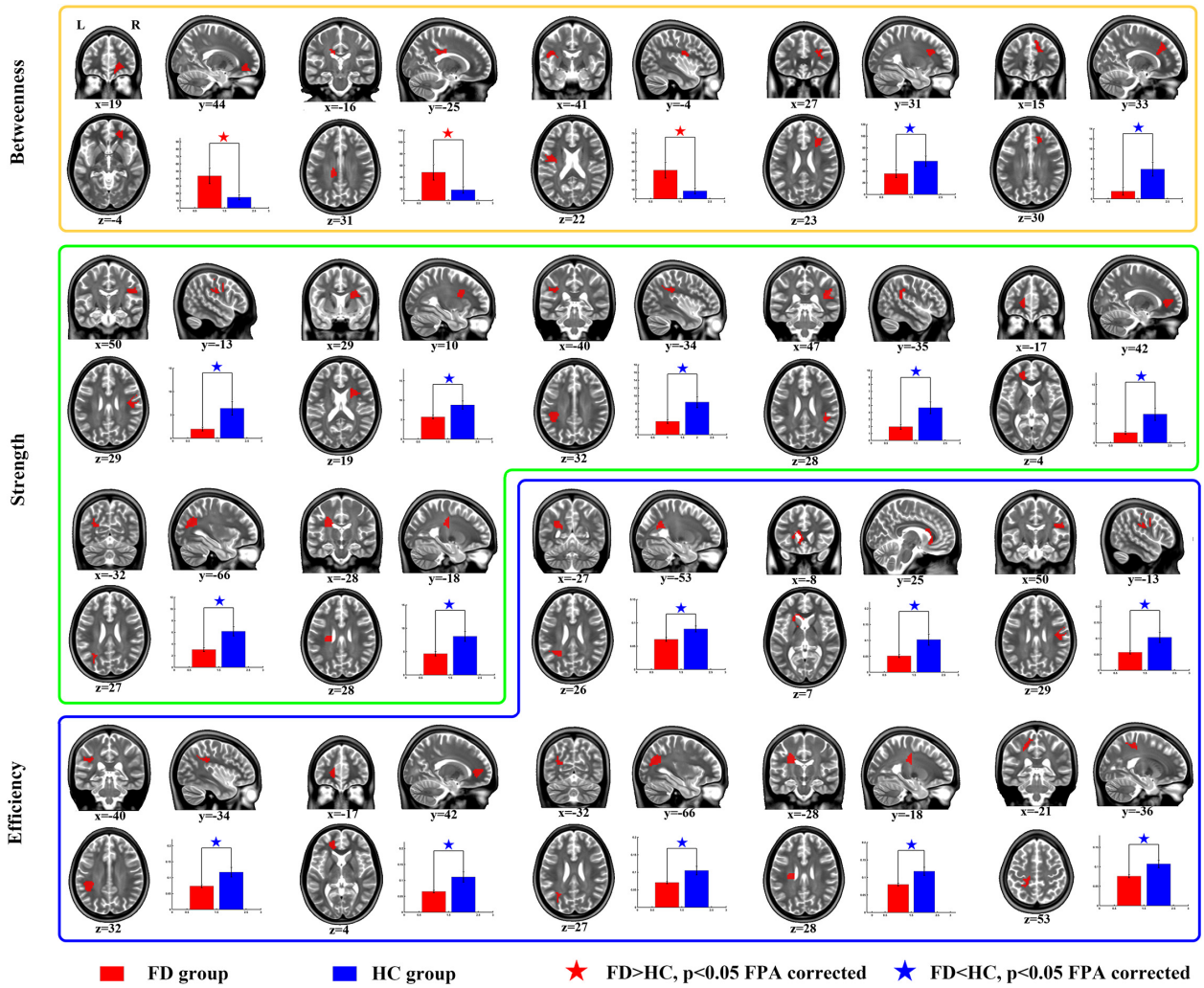

FIGURE 3 | Group differences of nodal properties between FD and HC. Compared with HC, the FD patients showed alteration in anterior corona radiata, corpus callosum, superior longitudinal fasciculus, and posterior thalamic radiation.

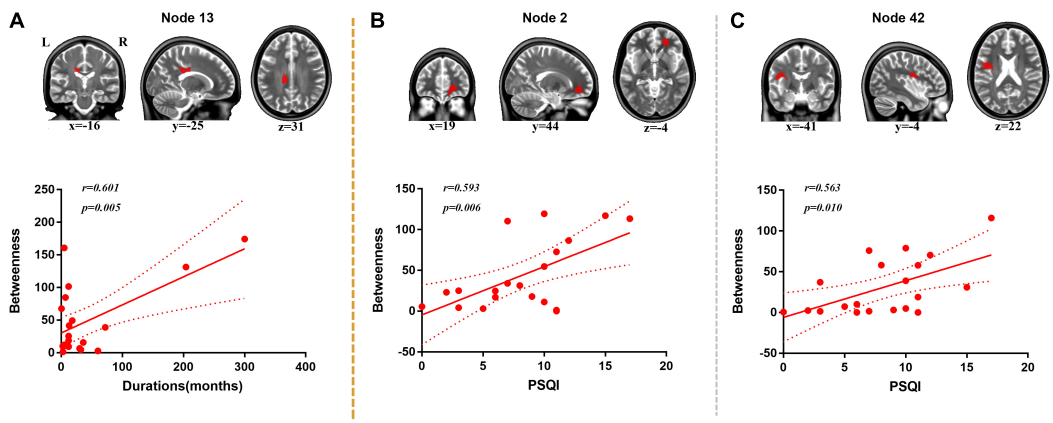

FIGURE 4 | Correlation analysis between duration, PSQI, and nodal BC. **(A)** Positive correlation was found between duration and BC of node 13 (body of corpus callosum). **(B)** Positive correlation was found between PSQI and BC of node 2 (right anterior corona radiata). **(C)** Positive correlation was found between PSQI and BC of node 42 (left superior longitudinal fasciculus).

TABLE 3 | Group differences of nodal property.

Nodal order	MNI coordinates			Localization in JHU-Atlas	T	P
	x	y	z			
Betweenness						
2	21	45	−6	Anterior_corona_radiata_R	2.847	0.003
13	−15	−30	30	Body_of_corpus_callosum	2.837	0.004
42	−42	−6	21	Superior_longitudinal_fasciculus_L	2.730	0.005
57	30	27	21	Anterior_corona_radiata_R	−2.818	0.004
110	15	33	33	Genu_of_corpus_callosum	−2.722	0.005
Strength						
12	48	−12	30	Superior_longitudinal_fasciculus_R	−2.653	0.006
15	27	9	21	Anterior_corona_radiata_R	−2.534	0.008
18	−42	−39	33	Superior_longitudinal_fasciculus_L	−2.915	0.003
27	45	−39	27	Superior_longitudinal_fasciculus_R	−2.699	0.005
64	−18	45	3	Anterior_corona_radiata_L	−2.871	0.003
84	−33	−63	27	Posterior_thalamic_radiation_(include_optic_radiation)_L	−3.432	0.001
99	−27	−18	30	Superior_corona_radiata_L	−2.944	0.003
Efficiency						
8	−27	−51	24	Posterior_corona_radiata_L	−3.003	0.002
9	−12	24	9	Genu_of_corpus_callosum	−2.554	0.007
12	48	−12	30	Superior_longitudinal_fasciculus_R	−2.536	0.008
18	−42	−39	33	Superior_longitudinal_fasciculus_L	−2.604	0.006
64	−18	45	3	Anterior_corona_radiata_L	−2.729	0.005
84	−33	−63	27	Posterior_thalamic_radiation_(include_optic_radiation)_L	−2.544	0.007
99	−27	−18	30	Superior_corona_radiata_L	−2.952	0.003
106	−21	−36	54	Unclassified	−2.831	0.004

that the FD patients showed a non-optimized structure of WM network in both global and local level properties. These findings were partially consistent with our former study in irritable bowel syndrome (IBS) patients where they showed decreased global efficiency compared with healthy controls (Qi et al., 2016a). Also, the decreased efficiency was found in other chronic pain, such as postherpetic neuralgia (Zhang et al., 2014). It suggested that the functional gastrointestinal disorders may show the information process efficiency loss.

In nodal-level statistical analysis, there were alterations in four pairs of fiber bundles in patients with FD: the anterior corona radiata, corpus callosum, superior longitudinal fasciculus, and posterior thalamic radiation. It was consistent with the findings of WM in FD patients in a former DTI study, which showed alteration in corona radiata, internal capsule, posterior thalamic radiation, corpus callosum, external capsule, sagittal stratum, and superior longitudinal fasciculus (Zhou et al., 2013). A similar alteration in WM microstructure could be found in other kinds of chronic pain, such as IBS (Chen et al., 2011), migraine (Szabó et al., 2012), and temporomandibular disorder (Moayedi et al., 2012). Besides, the anterior corona radiata was the connecting fiber bundle within the frontal lobe, the superior longitudinal fasciculus was the connecting fiber bundle from frontal lobe to insula and ends in the posterior part of the brain, the posterior thalamic radiation was the ascending fiber bundle from thalamus to cerebral cortex, and the corpus callosum was the connecting fiber bundle to bridge two hemispheres. These results also fitted the functional alteration in GM-related studies, such as decreased functional connectivity of insula (Sun et al., 2020); decreased GM density in the middle frontal gyrus, right precentral gyrus, and insula (Zeng et al., 2013); and decreased connectivity between insula and thalamus (Liu et al., 2018). Our former study also found altered amplitude of low-frequency fluctuation in insula and thalamus (Qi et al., 2020). Our results supported that the frontal lobe, insula, and thalamus were the key regions in FD patients.

In addition, correlation analysis found that the nodal BC was correlated with the duration and PSQI. No significant correlation was found between nodal properties S and efficiency. BC represents the ability of bridging different parts of the brain network (Rubinov and Sporns, 2010). The increased betweenness centrality of corpus callosum represents that the information exchange between two hemispheres was enhanced, and the positive correlation with the duration demonstrates that the duration affected this process. It was consistent with our former study of interhemispheric functional connectivity in IBS (Qi et al., 2016b). The two enhanced betweenness centrality nodes were located in the anterior corona radiata and superior longitudinal fasciculus, which were near the frontal lobe and insula (Zeng et al., 2013; Liu et al., 2018; Sun et al., 2020). The positive correlation with PSQI represents that the frontal lobe and insula might be important in the modulation of sleep quality in FD patients.

Different with the GM connectome and WM structural network, the alterations of connectome of WM might provide novel and more information for description of the mechanism

of FD. Compared with the GM connectome, the WM functional network showed a tendency toward randomization (Li et al., 2019). Previous studies showed that the effect of deoxygenated blood drainage from GM, through WM to the deep venous system, was less than 3% (Ruíz et al., 2009; Huang et al., 2018). The WM functional connectome showed more relationship to the WM structural network. According to the previous studies, the ALFF of WM showed significant correlation with FA in healthy subjects (Ji et al., 2017), but the alterations of ALFF of WM and FA were different in Parkinson's disease (Ji et al., 2019). However, the WM connectome was the promising neuromarker for the brain–behavior prediction (Li et al., 2020a). Also, it was the potential neuromarker for the classification of psychological disorder (Li et al., 2020b). It suggested that the WM connectome could extend the width of neuroimaging insight for understanding the pathophysiological mechanism for the disease.

LIMITATION

This study has several limitations. First, our results were based on a relatively small sample size and therefore should be considered preliminary. Further studies should contain more participants and even could be separated into different subtypes. Second, in this preliminary study, we did not have the diffusion MRI for further support. Third, additional results of graph theory analysis were not listed here. Further studies would consider the combined connectivity of GM and WM.

CONCLUSION

In this study, we found that the functional connectome of WM in FD patients turned to a non-optimized regularity in both global and local level. Also, the abnormal nodes were mainly located near the frontal lobe, insula, and thalamus. These findings provided a new prospective for the mechanism of FD.

DATA AVAILABILITY STATEMENT

The raw data supporting the conclusions of this article will be made available by the authors, without undue reservation.

ETHICS STATEMENT

The studies involving human participants were reviewed and approved by the Medical Research Ethics Committee of Jinling hospital. The patients/participants provided their written informed consent to participate in this study.

AUTHOR CONTRIBUTIONS

QX and YW were involved in literature review, experimental design, data analysis, and writing of the manuscript. CL contributed to the data collection and the analysis of neuropsychological data. YW, LQ, and CL contributed to the data collection. FW contributed in the experimental design. LZ and RQ contributed in the experimental design and revision of the manuscript. GL was involved in the experimental design and revision of the manuscript. All authors contributed to the article and approved the submitted version.

FUNDING

This work was supported by the National Nature Science Foundation of China (grant nos. 81671672, 81301209, and 81401402), the Jiangsu Provincial Medical Youth Talent (grant no. QNRC2016888), the China Postdoctoral Science Foundation (grant nos. 2018T111166 and 2017M623436), the Jiangsu Province Postdoctoral Science Foundation (grant no. 1701199B), and the National Key Technology (R&D) Program of the Ministry of Science and Technology (grant no. 2017YFC0108805).

SUPPLEMENTARY MATERIAL

The Supplementary Material for this article can be found online at: https://www.frontiersin.org/articles/10.3389/fnhum.2021.589578/full#supplementary-material

Supplementary Table 1 | Node position and localization in JHU-Atlas.

REFERENCES

Achard, S., and Bullmore, E. (2007). Efficiency and cost of economical brain functional networks. *PLoS Comput. Biol.* 3:e17. doi: 10.1371/journal.pcbi.0030017

Al Omran, Y., and Aziz, Q. (2014). Functional brain imaging in gastroenterology: to new beginnings. *Nat. Rev. Gastroenterol. Hepatol.* 11, 565–576. doi: 10.1038/nrgastro.2014.89

Ashburner, J. (2007). A fast diffeomorphic image registration algorithm. *Neuroimage* 38, 95–113. doi: 10.1016/j.neuroimage.2007.07.007

Biswal, B. B., Mennes, M., Zuo, X. N., Gohel, S., Kelly, C., Smith, S. M., et al. (2010). Toward discovery science of human brain function. *Proc. Natl. Acad. Sci. U S A.* 107, 4734–4739.

Bullmore, E. T., and Bassett, D. S. (2011). Brain graphs: graphical models of the human brain connectome. *Annu. Rev. Clin. Psychol.* 7, 113–140. doi: 10.1146/annurev-clinpsy-040510-143934

Bullmore, E., and Sporns, O. (2009). Complex brain networks: graph theoretical analysis of structural and functional systems. *Nat. Rev. Neurosci.* 10, 186–198. doi: 10.1038/nrn2575

Case, M., Shirinpour, S., Vijayakumar, V., Zhang, H., Datta, Y., Nelson, S., et al. (2019). Graph theory analysis reveals how sickle cell disease impacts neural networks of patients with more severe disease. *Neuroimage Clin.* 21:101599. doi: 10.1016/j.nicl.2018.11.009

Chao-Gan, Y., and Yu-Feng, Z. (2010). DPARSF: A MATLAB Toolbox for "Pipeline" Data Analysis of Resting-State fMRI. *Front. Syst. Neurosci.* 4:13. doi: 10.3389/fnsys.2010.00013

Chen, J. Y., Blankstein, U., Diamant, N. E., and Davis, K. D. (2011). White matter abnormalities in irritable bowel syndrome and relation to individual factors. *Brain Res.* 1392, 121–131. doi: 10.1016/j.brainres.2011.03.069

Ding, J. R., Liao, W., Zhang, Z., Mantini, D., Xu, Q., Wu, G. R., et al. (2011). Topological fractionation of resting-state networks. *PLoS One* 6:e26596. doi: 10.1371/journal.pone.0026596

Drossman, D. A. (2006). The functional gastrointestinal disorders and the Rome III process. *Gastroenterology* 130, 1377–1390. doi: 10.1053/j.gastro.2006.03.008

El-Serag, H. B., and Talley, N. J. (2003). Health-related quality of life in functional dyspepsia. *Aliment Pharmacol. Ther.* 18, 387–393. doi: 10.1046/j.1365-2036.2003.01706.x

Enck, P., Azpiroz, F., Boeckxstaens, G., Elsenbruch, S., Feinle-Bisset, C., Holtmann, G., et al. (2017). Functional dyspepsia. *Nat. Rev. Dis. Primers* 3:17081.

Ford, A. C., Marwaha, A., Sood, R., and Moayyedi, P. (2015). Global prevalence of, and risk factors for, uninvestigated dyspepsia: a meta-analysis. *Gut* 64, 1049–1057. doi: 10.1136/gutjnl-2014-307843

Fornito, A., Yoon, J., Zalesky, A., Bullmore, E. T., and Carter, C. S. (2011). General and specific functional connectivity disturbances in first-episode schizophrenia during cognitive control performance. *Biol. Psychiatry* 70, 64–72. doi: 10.1016/j.biopsych.2011.02.019

Gao, Q., Xu, Q., Duan, X., Liao, W., Ding, J., Zhang, Z., et al. (2013). Extraversion and neuroticism relate to topological properties of resting-state brain networks. *Front. Hum. Neurosci.* 7:257. doi: 10.3389/fnhum.2013.00257

Garrison, K. A., Scheinost, D., Finn, E. S., Shen, X., and Constable, R. T. (2015). The (in)stability of functional brain network measures across thresholds. *Neuroimage* 118, 651–661. doi: 10.1016/j.neuroimage.2015.05.046

He, Y., and Evans, A. (2010). Graph theoretical modeling of brain connectivity. *Curr. Opin. Neurol.* 23, 341–350. doi: 10.1097/wco.0b013e32833aa567

Huang, Y., Bailey, S. K., Wang, P., Cutting, L. E., Gore, J. C., and Ding, Z. (2018). Voxel-wise detection of functional networks in white matter. *Neuroimage* 183, 544–552. doi: 10.1016/j.neuroimage.2018.08.049

Jao, T., Vértes, P. E., Alexander-Bloch, A. F., Tang, I. N., Yu, Y. C., Chen, J. H., et al. (2013). Volitional eyes opening perturbs brain dynamics and functional connectivity regardless of light input. *Neuroimage.* 69, 21–34. doi: 10.1016/j.neuroimage.2012.12.007

Ji, G. J., Ren, C., Li, Y., Sun, J., Liu, T., Gao, Y., et al. (2019). Regional and network properties of white matter function in Parkinson's disease. *Hum. Brain Mapp.* 40, 1253–1263. doi: 10.1002/hbm.24444

Ji, G. J., Zhang, Z., Xu, Q., Wei, W., Wang, J., Wang, Z., et al. (2015). Connectome Reorganization Associated With Surgical Outcome in Temporal Lobe Epilepsy. *Medicine* 94:e1737. doi: 10.1097/md.0000000000001737

Ji, G.-J., Liao, W., Chen, F.-F., Zhang, L., and Wang, K. (2017). Low-frequency blood oxygen level-dependent fluctuations in the brain white matter: more than just noise. *Sci. Bull.* 62:656. doi: 10.1016/j.scib.2017.03.021

Jin, C., Qi, R., Yin, Y., Hu, X., Duan, L., Xu, Q., et al. (2014). Abnormalities in whole-brain functional connectivity observed in treatment-naive post-traumatic stress disorder patients following an earthquake. *Psychol. Med.* 44, 1927–1936. doi: 10.1017/s003329171300250x

Kano, M., Dupont, P., Aziz, Q., and Fukudo, S. (2018). Understanding Neurogastroenterology From Neuroimaging Perspective: A Comprehensive Review of Functional and Structural Brain Imaging in Functional Gastrointestinal Disorders. *J. Neurogastroenterol. Motil.* 24, 512–527. doi: 10.5056/jnm18072

Koloski, N. A., Jones, M., Kalantar, J., Weltman, M., Zaguirre, J., and Talley, N. J. (2012). The brain–gut pathway in functional gastrointestinal disorders is bidirectional: a 12-year prospective population-based study. *Gut* 61, 1284–1290. doi: 10.1136/gutjnl-2011-300474

Lacy, B. E., Everhart, K., and Crowell, M. D. (2011). Functional dyspepsia is associated with sleep disorders. *Clin. Gastroenterol. Hepatol.* 9, 410–414. doi: 10.1016/j.cgh.2011.02.010

Ladabaum, U., Roberts, T. P., and McGonigle, D. J. (2007). Gastric fundic distension activates fronto-limbic structures but not primary somatosensory cortex: a functional magnetic resonance imaging study. *Neuroimage* 34, 724–732. doi: 10.1016/j.neuroimage.2006.07.033

Lee, I. S., Wang, H., Chae, Y., Preissl, H., and Enck, P. (2016). Functional neuroimaging studies in functional dyspepsia patients: a systematic review. *Neurogastroenterol. Motil.* 28, 793–805. doi: 10.1111/nmo.12793

Li, J., Biswal, B. B., Meng, Y., Yang, S., Duan, X., Cui, Q., et al. (2020a). A neuromarker of individual general fluid intelligence from the white-matter functional connectome. *Transl. Psychiatry.* 10:147.

Li, J., Biswal, B. B., Wang, P., Duan, X., Cui, Q., Chen, H., et al. (2019). Exploring the functional connectome in white matter. *Hum. Brain Mapp.* 40, 4331–4344. doi: 10.1002/hbm.24705

Li, J., Chen, H., Fan, F., Qiu, J., Du, L., Xiao, J., et al. (2020b). White-matter functional topology: a neuromarker for classification and prediction in unmedicated depression. *Transl. Psychiatry* 10:365.

Liao, W., Li, J., Duan, X., Cui, Q., Chen, H., and Chen, H. (2018). Static and dynamic connectomics differentiate between depressed patients with and without suicidal ideation. *Hum. Brain Mapp.* 39, 4105–4118. doi: 10.1002/hbm.24235

Liu, P., Fan, Y., Wei, Y., Zeng, F., Li, R., Fei, N., et al. (2018). Altered structural and functional connectivity of the insula in functional dyspepsia. *Neurogastroenterol. Motil.* 30:e13345. doi: 10.1111/nmo.13345

Makedonov, I., Chen, J. J., Masellis, M., and MacIntosh, B. J. (2016). Physiological fluctuations in white matter are increased in Alzheimer's disease and correlate with neuroimaging and cognitive biomarkers. *Neurobiol. Aging* 37, 12–18. doi: 10.1016/j.neurobiolaging.2015.09.010

Moayedi, M., Weissman-Fogel, I., Salomons, T. V., Crawley, A. P., Goldberg, M. B., Freeman, B. V., et al. (2012). White matter brain and trigeminal nerve abnormalities in temporomandibular disorder. *Pain* 153, 1467–1477. doi: 10.1016/j.pain.2012.04.003

Phillips, D. J., McGlaughlin, A., Ruth, D., Jager, L. R., and Soldan, A. (2015). Graph theoretic analysis of structural connectivity across the spectrum of Alzheimer's disease: The importance of graph creation methods. *Neuroimage Clin.* 7, 377–390. doi: 10.1016/j.nicl.2015.01.007

Qi, R., Ke, J., Schoepf, U. J., Varga-Szemes, A., Milliken, C. M., Liu, C., et al. (2016a). Topological Reorganization of the Default Mode Network in Irritable Bowel Syndrome. *Mol. Neurobiol.* 53, 6585–6593. doi: 10.1007/s12035-015-9558-7

Qi, R., Liu, C., Weng, Y., Xu, Q., Chen, L., Wang, F., et al. (2016b). Disturbed Interhemispheric Functional Connectivity Rather than Structural Connectivity in Irritable Bowel Syndrome. *Front. Mol. Neurosci.* 9:141. doi: 10.3389/fnmol.2016.00141

Qi, R., Shi, Z., Weng, Y., Yang, Y., Zhou, Y., Surento, W., et al. (2020). Similarity and diversity of spontaneous brain activity in functional dyspepsia subtypes. *Acta Radiol.* 61, 927–935. doi: 10.1177/0284185119883391

Rubinov, M., and Sporns, O. (2010). Complex network measures of brain connectivity: uses and interpretations. *Neuroimage* 52, 1059–1069. doi: 10.1016/j.neuroimage.2009.10.003

Ruíz, D. S., Yilmaz, H., and Gailloud, P. (2009). Cerebral developmental venous anomalies: current concepts. *Ann. Neurol.* 66, 271–283. doi: 10.1002/ana.21754

Sun, R., He, Z., Ma, P., Yin, S., Yin, T., Liu, X., et al. (2020). The participation of basolateral amygdala in the efficacy of acupuncture with deqi treating for functional dyspepsia. *Brain Imaging Behav.* 15, 216–230. doi: 10.1007/s11682-019-00249-7

Szabó, N., Kincses, Z. T., Párdutz, A., Tajti, J., Szok, D., Tuka, B., et al. (2012). White matter microstructural alterations in migraine: A diffusion-weighted MRI study. *Pain* 153, 651–656. doi: 10.1016/j.pain.2011.11.029

Van Oudenhove, L., Coen, S. J., and Aziz, Q. (2007). Functional brain imaging of gastrointestinal sensation in health and disease. *World J. Gastroenterol.* 13, 3438–3445. doi: 10.3748/wjg.v13.i25.3438

Vecchio, F., Miraglia, F., Iberite, F., Lacidogna, G., Guglielmi, V., Marra, C., et al. (2018). Sustainable method for Alzheimer dementia prediction in mild cognitive impairment: Electroencephalographic connectivity and graph theory combined with apolipoprotein E. *Ann. Neurol.* 84, 302–314. doi: 10.1002/ana.25289

Wu, X., Yang, Z., Bailey, S. K., Zhou, J., Cutting, L. E., Gore, J. C., et al. (2017). Functional connectivity and activity of white matter in somatosensory pathways under tactile stimulations. *Neuroimage* 152, 371–380. doi: 10.1016/j.neuroimage.2017.02.074

Zalesky, A., Fornito, A., Harding, I. H., Cocchi, L., Yücel, M., Pantelis, C., et al. (2010). Whole-brain anatomical networks: does the choice of nodes matter?". *Neuroimage* 50, 970–983. doi: 10.1016/j.neuroimage.2009.12.027

Zeng, F., Qin, W., Yang, Y., Zhang, D., Liu, J., Zhou, G., et al. (2013). Regional brain structural abnormality in meal-related functional dyspepsia patients: a voxel-based morphometry study. *PLoS One* 8:e68383. doi: 10.1371/journal.pone.0068383

Zhang, Y., Liu, J., Li, L., Du, M., Fang, W., Wang, D., et al. (2014). A study on small-world brain functional networks altered by postherpetic neuralgia. *Magn Reson Imaging* 32, 359–365. doi: 10.1016/j.mri.2013.12.016

Zhang, Z., Liao, W., Chen, H., Mantini, D., Ding, J. R., Xu, Q., et al. (2011). Altered functional-structural coupling of large-scale brain networks in idiopathic generalized epilepsy. *Brain* 134(Pt 10), 2912–2928. doi: 10.1093/brain/awr223

Zhou, G., Qin, W., Zeng, F., Liu, P., Yang, X., von Deneen, K. M., et al. (2013). White-matter microstructural changes in functional dyspepsia: a diffusion tensor imaging study. *Am. J. Gastroenterol.* 108, 260–269. doi: 10.1038/ajg.2012.405

Conflict of Interest: The authors declare that the research was conducted in the absence of any commercial or financial relationships that could be construed as a potential conflict of interest.

frontiers in Human Neuroscience

REVIEW
published: 22 June 2021
doi: 10.3389/fnhum.2021.667709

Sweet Taste Is Complex: Signaling Cascades and Circuits Involved in Sweet Sensation

Elena von Molitor[1], Katja Riedel[2], Michael Krohn[2], Mathias Hafner[1], Rüdiger Rudolf[1,3]* and Tiziana Cesetti[1]*

[1] Institute of Molecular and Cell Biology, Hochschule Mannheim, Mannheim, Germany, [2] BRAIN AG, Zwingenberg, Germany, [3] Interdisciplinary Center for Neurosciences, Heidelberg University, Heidelberg, Germany

Sweetness is the preferred taste of humans and many animals, likely because sugars are a primary source of energy. In many mammals, sweet compounds are sensed in the tongue by the gustatory organ, the taste buds. Here, a group of taste bud cells expresses a canonical sweet taste receptor, whose activation induces Ca^{2+} rise, cell depolarization and ATP release to communicate with afferent gustatory nerves. The discovery of the sweet taste receptor, 20 years ago, was a milestone in the understanding of sweet signal transduction and is described here from a historical perspective. Our review briefly summarizes the major findings of the canonical sweet taste pathway, and then focuses on molecular details, about the related downstream signaling, that are still elusive or have been neglected. In this context, we discuss evidence supporting the existence of an alternative pathway, independent of the sweet taste receptor, to sense sugars and its proposed role in glucose homeostasis. Further, given that sweet taste receptor expression has been reported in many other organs, the physiological role of these extraoral receptors is addressed. Finally, and along these lines, we expand on the multiple direct and indirect effects of sugars on the brain. In summary, the review tries to stimulate a comprehensive understanding of how sweet compounds signal to the brain upon taste bud cells activation, and how this gustatory process is integrated with gastro-intestinal sugar sensing to create a hedonic and metabolic representation of sugars, which finally drives our behavior. Understanding of this is indeed a crucial step in developing new strategies to prevent obesity and associated diseases.

Keywords: sweet taste receptor, signaling, gustducin, calcium, GLP-1, gastro-intestinal tract, brain

OPEN ACCESS

Edited by:
Junichi Chikazoe, National Institute for Physiological Sciences (NIPS), Japan

Reviewed by:
Robert J. Lee, University of Pennsylvania, United States
Linda Barlow, University of Colorado Anschutz Medical Campus, United States

****Correspondence:***
Mathias Hafner
m.hafner@hs-mannheim.de
Rüdiger Rudolf
r.rudolf@hs-mannheim.de

Specialty section:
This article was submitted to Sensory Neuroscience, a section of the journal Frontiers in Human Neuroscience

Received: *14 February 2021*
Accepted: *20 May 2021*
Published: *22 June 2021*

Citation:
von Molitor E, Riedel K, Krohn M, Hafner M, Rudolf R and Cesetti T (2021) Sweet Taste Is Complex: Signaling Cascades and Circuits Involved in Sweet Sensation. Front. Hum. Neurosci. 15:667709. doi: 10.3389/fnhum.2021.667709

INTRODUCTION

Increased Sugar Consumption Causes Severe Health Problems

Sugars, as a prime source of calories, are used for metabolic energy production. Perhaps as a consequence of this, sweet taste is one of the most passionate sensations humans experience (DiNicolantonio et al., 2018). Already the human fetus has a preference for sweet compounds present in the amniotic fluid, and neonates show responses to sweet solutions (Tatzer et al., 1985;

Steiner et al., 2001) (for review Beauchamp and Mennella, 2011; Ventura and Mennella, 2011). Sugar attraction is generally driven by the activation of brain reward pathways (Araujo et al., 2012; Kendig, 2014; for review Han et al., 2019; Gutierrez et al., 2020) and may lead to addictive behavior (Kendig, 2014). The strong attraction to sugars is partly learned (Veldhuizen et al., 2007) and influenced by many factors, such as other sensory inputs (Ohla et al., 2012) (for review Small, 2012), emotions (Noel and Dando, 2015) and the internal metabolic state (Zhang et al., 2018). Furthermore, also genetics may influence individual variability in sweet taste preference (Keskitalo et al., 2007; Bachmanov et al., 2014).

Only 200 years ago, industrialization and colonial trading increased the global sugar availability by distributing the yield of large sugar cane fields to the world (Tappy, 2012; Chow, 2017). Since then, the consumption of the once luxury product increased steadily. Initially used to sweeten beverages such as tea, coffee and coco, the fabrication of chocolate bars, ice-creams and sodas started in the 20th century (Tappy, 2012). Nowadays, sugar has conquered virtually all food suppliers over the world (DiNicolantonio et al., 2018), and sugar consumption increased from 5 kg/person/year in 1800, to 70 kg/person/year in 2006 (Tappy, 2012). This has contributed to obesity and has become a main risk factor for many chronic disorders including type-2 diabetes, cardiovascular diseases and metabolic syndrome (Bray and Popkin, 2014; Borges et al., 2017; Chow, 2017; Kochem, 2017). However, in contrast to amino acids or fats, which are essential for the body, there is no strict physiological requirement for sugar consumption (Westman, 2002; DiNicolantonio et al., 2018).

To fight the present sugar overload, much effort has been put into finding sugar substitutes, such as non-caloric sweeteners, which are sweet, but contain no calories (Pepino, 2015). Today, there are seven principal non-caloric sweeteners on the market: advantame, saccharin, aspartame, sucralose, cyclamate, neotame and acesulfame K^+, whose daily acceptable intake dosage is approved by the FDA (Pepino, 2015). However, some of the sweeteners are known for their unpleasant bitter off-taste (Moskowitz and Klarmann, 1975; Kuhn et al., 2004; Galindo-Cuspinera et al., 2006). Although their safety has been clinically assessed (FDA/EFSA) (summarized in BfR Background Information from Bundesinstitut für Riskobewertung, 2014), recent studies suggest that they may increase the risk of cancer, obesity and diabetes. A probable reason for these unexpected side effects might be the activation sweet taste receptors in many extraoral tissues (for review Yamamoto and Ishimaru, 2013; Laffitte et al., 2014). Thus, understanding sweet taste signaling, including its effect in the gastro-intestinal tract and the brain, might help to mitigate the sugar dominance and improve global health.

Structure of the Taste Buds

According to the current knowledge, sweet taste is first sensed by the taste buds, i.e., gustatory organs, which are formed by roughly 100 specialized taste bud cells each (Lindemann, 1996; Montmayeur, 2002; Roper and Chaudhari, 2017). Humans possess about 5,000 taste buds (Suzuki, 2007; Witt, 2019). Taste bud cells can be grouped into four types (I-IV), defined by their morphology, function and expression profile (for review Roper, 2013): type I cells, with glia-like function; type II (receptor) cells, which stimulate the gustatory nerve terminals via unconventional ATP release upon detection of umami, bitter or sweet stimuli (Finger et al., 2005; Huang et al., 2007); type III cells, which transduce sour taste and make functional synapses with the afferent gustatory nerve fibers (Finger, 2005; DeFazio et al., 2006; Roper, 2013) and finally, type IV basal cells, which serve as progenitor cells (Ren et al., 2014) to replenish mature taste bud cells, as these possess a limited life span (in rodents, half-live varies form 8 to 22 days according to the cell type) (Chaudhari and Roper, 2010; Perea-Martinez et al., 2013; Liman et al., 2014; Barlow, 2015). More recently, a group of broadly responding taste bud cells has been characterized which have a type III phenotype, but respond to multiple gustatory stimuli (Dutta Banik et al., 2020). In mammals, taste buds are located in specialized papillae all over the tongue, epiglottis and palate (Lindemann, 1999; Montmayeur, 2002; Witt, 2019). Fungiform papillae, in the anterior tongue, are innervated by the chorda tympani nerve, a branch of the cranial nerve VII. Circumvallate papillae are located on the dorsal tongue and are in contact with the glossopharyngeal nerve (cranial nerve IX) (Scott, 2005; Kikut-Ligaj and Trzcielińska-Lorych, 2015). Foliate papillae, on the lateral sides of the tongue, are innervated by both nerves (Montmayeur, 2002; Witt, 2019). In the larynx there are taste buds and also single taste cells, which are in contact with the superior laryngeal branch of the vagus nerve (X) (Jowett and Shrestha, 1998; Sbarbati et al., 2004). In addition, sweet compounds stimulate the gastro-intestinal system, the brain, and other organs, either directly or indirectly via gustatory mechanisms (for review von Molitor et al., 2020c). Reciprocal cross talk occurs between oral sweet-sensation and visceral homeostatic signals. Indeed, intestinal hormones and neuropeptides have been identified in taste buds and shown to modulate taste bud cells activity (for review Dotson et al., 2013). In particular, glucagon-like-peptide 1 (GLP-1), leptin and endocannabinoids modulate sweet taste responses (Ninomiya et al., 2002; Shin et al., 2008; Martin et al., 2009; Niki et al., 2010; Martin et al., 2012).

Studying Taste in Human

Studies on taste transduction in human have progressed slowly for many reasons: (1) taste bud cells make up less than 1% of the tongue, (2) human samples are rare, and (3) primary taste bud cells have a short life span (Liman et al., 2014; Barlow, 2015). Therefore, assessment of human taste physiology has been mostly carried out by *in vivo* "taste sensitivity measurements" which probe the ability of subjects to taste a certain stimulus and determine its quality (Reed and McDaniel, 2006; Aleman et al., 2016). Such tests fall into different categories. In "quality tests" only the taste modality is defined (Galindo-Cuspinera et al., 2006; Zhang et al., 2009). In "detection threshold tests" the lowest concentration of a tastant that a subject can recognize is determined (Reed and McDaniel, 2006; Zhang et al., 2009). In "intensity tests," participants evaluate the sweetness of molecules by ranking them in a hierarchical order, often relative to a

standard (Reed and McDaniel, 2006). Alternatively, sweet taste can be analyzed using "hedonic assessment" (Reed and McDaniel, 2006), where people rate how pleasant a compound is (Kampov-Polevoy et al., 1997) and if it is preferred over another one (Liem and Mennella, 2002; Reed and McDaniel, 2006). Until now, assays to understand the underlying intracellular signaling and/or neuronal pathways are very difficult to pursue in humans. However, the sweet taste receptor inhibitor lactisol has been used in humans to investigate the perception of polysaccharides (Lapis et al., 2016; Schweiger et al., 2020). Further, a blue food-dye (Robert's Brilliant Blue FCF133) can be used for live staining of tongue papillae in humans (Shahbake et al., 2005; Zhang et al., 2009; Gardner and Carpenter, 2019). In addition, with brain imaging techniques, such as MRI (magnetic resonance imaging) and PET (positron emission tomography), the brain regions activated by sweet stimuli have been mapped in humans (Prinster et al., 2017; Canna et al., 2019; Avery et al., 2020) (for review Han et al., 2019).

Due to these limitations, taste-related signaling mechanisms have been studied mainly in rodents, although there are major species-related differences. For example, rodents have a much stronger preference for polysaccharides compared to humans (Feigin et al., 1987). Further, certain sweet taste receptor inhibitors are species specific, such as gurmarin for rodents and lactisol for humans (Hellekant, 1976; Hellekant et al., 1988; Jiang et al., 2005). An alternative experimental system consists in mammalian cell lines heterologously expressing the human sweet taste receptor and its downstream signaling molecules. In this case however, the native cellular background and the niche are missing (von Molitor et al., 2020b). Thus, a new approach, based on organoids derived from mouse taste progenitor cells, may resemble more closely the native environment (Ren et al., 2009, 2010, 2014, 2017) and organoids could be theoretically also generated from human papillae. Another recent approach consists in the generation of a stably proliferating cell line from human lingual cells, that can be used to produce 3D-cell cultures, such as spheroids (Hochheimer et al., 2014; von Molitor et al., 2020a). Thus, an optimal model to study sweet taste transduction, especially in human, has still to be established.

A LONG WAY TO THE DISCOVERY OF THE SWEET TASTE RECEPTOR

Long before the major components of taste transduction pathways were unraveled, Hänig showed that different tongue areas were more sensitive to certain taste modalities (Hanig, 1901). Unfortunately, many years later his experimental line-graph was redrawn in a simplified and mispresenting manner (Boring, 1942), leading to the common and long-lasting erroneous belief that the five taste modalities (sweet, bitter, umami, sour, salt) map to distinct tongue areas (Schiffman et al., 1986; Hoon et al., 1999). Finally, in 1974, evidence was provided that each taste modality can be sensed on every tongue part, but with different detection thresholds (Collings, 1974). Regarding sweetness, the nerve with the highest sensitivity is the glossopharyngeal in rats (Krimm et al., 1987), and chorda tympani in mice and rhesus monkeys (Hellekant et al., 1997; Danilova and Hellekant, 2003). In humans, since nerve recordings are not possible, contrasting results were obtained: the sweet detection threshold was reported to be lower either at the posterior tongue (Dastur, 1961; Okuda and Tomita, 1976) or at the tongue tip (Collings, 1974), while others reported no spatial difference (Nilsson, 1979; Sato et al., 2002). Nonetheless, subregional differences were detected even within the anterior tongue, with the edge and the lateral regions being the most sweet-sensitive areas (Stein et al., 1994). A reason for the divergence could be the heterogeneity of subjects, since taste is influenced by age (Stein et al., 1994; Ng et al., 2004), genetic variance (Bachmanov et al., 2014; Eriksson et al., 2019; Hwang et al., 2019), sex (Than et al., 1994; Fushan et al., 2010), diseases (Ng et al., 2004), and temperature (Talavera et al., 2005; Lemon, 2015).

Before the sweet taste receptor was discovered, sweet transduction in taste bud cells was proposed to involve cyclic adenosine monophosphate (cAMP) and protein-kinase A (PKA). In general, cAMP levels are regulated by its synthesis via adenyl cyclases (ACs) and hydrolysis via phosphodiesterases (PDEs) (Trubey et al., 2006). Already in 1972, a high AC activity was found in bovine tongue epithelium, enriched in taste buds (Kurihara and Koyama, 1972). Consistently, rat taste bud cells express AC 4,5 and 8 (Abaffy et al., 2003; Trubey et al., 2006). Sugars and saccharin were shown to stimulate AC in the presence of guanine nucleotides in frog, rat and pig tongue epithelium (Avenet and Lindemann, 1987; Striem et al., 1989; Naim et al., 1991; Striem et al., 1991). Electrophysiology studies revealed that application of cAMP analogs caused taste bud cell depolarization due to reduced K^+ outward currents via PKA-dependent phosphorylation (Avenet and Lindemann, 1987; Tonosaki and Funakoshi, 1988; Striem et al., 1991). Consistently, in rat and hamster taste bud cells, saccharin and sucrose elicited depolarization and generated action potentials, an effect that was mimicked by the application of a permeable analog of cAMP and cGMP and did not require extracellular Ca^{2+} (Béhé et al., 1990; Cummings et al., 1993). A different mechanism was unraveled in frog taste bud cells where saccharin and NC01 stimulation resulted in PDE-mediated cAMP hydrolysis, which in turn activated a cyclic-nucleotide-suppressible channel (CNG), mediating Ca^{2+} influx and cell depolarization (Kolesnikov and Margolskee, 1995). A direct proof of sweet-mediated cAMP/PKA pathway activation in taste bud cells is therefore still missing, hampered at that time by technical limitations, and later on possibly neglected.

In 2001, a big breakthrough was finally achieved, when multiple groups identified the "sweet taste receptor": a heterodimer formed by two G-protein coupled receptor (GPCR) subunits, T1R2 and T1R3, located at the taste pore of type II taste bud cells (Hoon et al., 1999; Bachmanov et al., 2001; Kitagawa et al., 2001; Max et al., 2001; Montmayeur et al., 2001; Nelson et al., 2001; Li et al., 2002) (for review Temussi, 2006; DuBois, 2016). This discovery was based on the observation that two mouse strains, called tasters (C57BL/6 and DBA/2), were strongly attracted by saccharin and D-phenylalanine (Bachmanov et al., 1997). *Sac* and *dpa*, which are both located

on chromosome 4, were identified as the main loci determining sweet preference in mice (Fuller, 1974; Capeless and Whitney, 1995; Lush et al., 1995; Max et al., 2001; Margolskee, 2002; Shigemura et al., 2005). Consistently, both genes were found to influence peripheral nerve response to sucrose (Bachmanov et al., 1997). The first sweet-related subunit cloned was T1R2, however, its function was not clear at that time (Hoon et al., 1999). Soon afterward, *Tas1r3,* the gene encoding the T1R3 subunit, was mapped on the human chromosome 1p36, and based on this sequence the murine ortholog was found in the *Sac* locus (Fuller, 1974; Lush, 1989; Lush et al., 1995; Kitagawa et al., 2001; Montmayeur et al., 2001; Nelson et al., 2001; Sainz et al., 2001). Commonly, heterodimers of T1R2 and T1R3 form functional sweet taste receptors, as demonstrated with recombinant systems (Nelson et al., 2001; Li et al., 2002; Zhao et al., 2003) and transgenic mouse models (Zhao et al., 2003). The T1R family contains one additional subunit: T1R1, that forms with T1R3 the umami receptor (Nelson et al., 2001; Zhao et al., 2003). All three T1R subunits belong to the class C GPCRs. Immunostainings and *in situ* hybridization in mouse tongue revealed the expression of T1R3 in about one third of taste bud cells in almost all papillae (**Table 1**; Nelson et al., 2001). Even if bitter- (T2R) and sweet taste receptors (T1R2/T1R3) were both present in type II cells, their expression did not overlap (Nelson et al., 2001). Furthermore, also sweet (T1R2) and umami (T1R1) specific subunits were mainly present in distinct type II cell populations (Hoon et al., 1999; Stone et al., 2007). Interestingly, fitting the old observations of Hänig, regional differences in the expression were recognized (**Table 1**). In rodents, T1R3 was present in all papillae, but the strongest expression was observed in circumvallate and foliate papillae, where also T1R2 showed the highest and almost exclusive expression (Montmayeur et al., 2001; Nelson et al., 2001) (for review Montmayeur, 2002). In human, T1R3 was detected in circumvallate and fungiform papillae (Max et al., 2001). Thus, the heterodimeric T1R2/T1R3 GPCR was recognized as the main molecular sensor for sugars and other sweet compounds.

SWEET TASTE RECEPTOR MEDIATED TRANSDUCTION

Not only natural sugars, such as monosaccarides or disaccharides, activate the sweet taste receptor, but also ligands with very different chemical structures, such as amino acids, proteins and non-caloric sweeteners (McCaughey, 2008), may bind to different domains of T1R2/T1R3 (Sainz et al., 2007; DuBois, 2016). In particular, in transgenic cells and animals it was shown that the human T1R2 (hT1R2) confers sensitivity to aspartame, glycyrrhizic acid, monellin and thaumatin (Zhao et al., 2003), while hT1R3 contains a binding site for neohesperidin dihydrochalcone (Li et al., 2002). It is not yet clear if also oligosaccharides, such as starch, are able to activate the sweet taste receptor (Lapis et al., 2016; Schweiger et al., 2020). In general, the change in the sweet taste receptor conformation upon ligand binding activates an intracellular downstream signaling.

The Canonical Signaling Pathway for Sweet and Bitter Taste

Sweet and bitter transduction pathways have been discovered in parallel and they share many components. In human, bitter compounds bind to a variety of ∼25 different receptors of the T2R family, that can form both homomeric and heteromeric complexes (Kuhn et al., 2004; Kuhn and Meyerhof, 2013). T2R activation leads to the release of the $\beta_3\gamma_{13}$ subunit (Huang et al., 1999; Rössler et al., 2000) from the associated G-protein, which then activates phospholipase Cβ2 (PLCβ2) (Rössler et al., 1998; Miyoshi et al., 2001; Yan et al., 2001; Zhang et al., 2003) to generate inositol-3-phosphate (IP3) (Rössler et al., 1998; Miyoshi et al., 2001; Yan et al., 2001; Zhang et al., 2003). Subsequently,

TABLE 1 | Expression of the sweet taste receptor subunits (T1R2/T1R3) in mammal taste papillae.

Subunit	*CV*	*Fungiform*	*Foliate*	*Palatal*	*Species*	*Source*
T1R3	strong	strong	strong		Mouse	Kitagawa et al., 2001
	∼30% cells	∼30% cells	∼30% cells	∼30% cells	Mouse	Nelson et al., 2001
	24% cells	15% cells	14% cells		Mouse	Montmayeur et al., 2001
	strong	strong	strong		Mouse	Max et al., 2001
	20% cells	20% cells			Human	Max et al., 2001
	100% TB, 23% cells	<4% TB, <1% cells	100% TB, 26% cells		Mouse	Sainz et al., 2001
	strong	no	Less strong	No	Mouse	Matsunami et al., 2000
	6288×10^{-7}	150600×10^{-7}	30×10^{-7}		Mouse	Choi et al., 2016
T1R2	all TBs 20–30% cells	0.5% cells	abundant	few	Rat	Hoon et al., 1999
	yes	yes	yes		Mouse	Nelson et al., 2001
	yes	no	yes		Mouse	Kitagawa et al., 2001
	strong	low	strong		Mouse	Montmayeur et al., 2001
	strong	less strong	few	few	Mouse	Matsunami et al., 2000
	7180×10^{-7}	21×10^{-7}	1170×10^{-7}		Mouse	Choi et al., 2016

Percentage refers to the cells or to the taste bud (TB), as reported. CV, circumvallate papillae. The expression was detected by in situ hybridization (Hoon et al., 1999; Kitagawa et al., 2001; Max et al., 2001; Montmayeur et al., 2001; Nelson et al., 2001; Sainz et al., 2001), immunostaining (Max et al., 2001), PCR (Matsunami et al., 2000), and qPCR (Choi et al., 2016).

IP3 binds to its receptor (IP3R) on the endoplasmic reticulum (Clapp et al., 2001; Miyoshi et al., 2001) and induces Ca^{2+} release from the stores (Akabas et al., 1988). Increased cytoplasmic Ca^{2+} levels in turn open the membrane-associated transient receptor potential channel (TRPM5) (Pérez et al., 2002; Zhang et al., 2003) permitting Na^{+} influx, followed by cell depolarization and ATP release via CALHM1/3 channel (Taruno et al., 2013; **Table 2** and **Figure 1**). The signaling network downstream the sweet taste receptor involves the same key players (**Table 2**) and it is known as the "canonical pathway." The functional role of these signaling molecules has been tested in several knockout mouse models, which displayed abolished or reduced nerve and behavioral responses to sweet compounds (**Table 2**) (for review von Molitor et al., 2020c).

Sweet Transduction May Involve Multiple G-proteins

The first described G-protein coupled to the sweet taste receptor was gustducin: a G-protein related to the G_i family, which consists of Gα-gustducin ($G\alpha_{gust}$) and $G\beta_3\gamma_{13}$ (McLaughlin et al., 1992; Huang et al., 1999). Gustducin is specifically expressed in the taste papillae and is closely related to the retinal transducin (McLaughlin et al., 1992; Margolskee, 1993). Gustducin and transducin share 80% sequence identity and many features, such as interaction with βγ subunits, GTPase activity and PDE activation (McLaughlin et al., 1993; Hoon et al., 1995; Ruiz-Avila et al., 1995). A taste specific PDE was found in bovine and rat taste tissue, and gustducin was shown to be interchangeable with transducin in a recombinant baculovirus system (Law and Henkin, 1982; McLaughlin et al., 1994; Ruiz-Avila et al., 1995). In taste buds, the expression ratio transducine/gustducin is 1/25 (McLaughlin et al., 1993; Hoon et al., 1995; Ruiz-Avila et al., 1995). The strongest evidence that the sweet taste receptor can functionally couple to $G\alpha_{gust}$ comes from experiments in recombinant systems, where T1R2/T1R3 was coexpressed with $G\alpha_{15}$ or the artificial chimeric $G\alpha_{16}$ subunit derived from murine hematopoietic cells (Nelson et al., 2001, 2002). Still, the functional coupling of $G\alpha_{gust}$ and the sweet taste receptor in native taste tissue is an open issue, as sucrose and non-caloric sweeteners were unable to activate gustducin in bovine taste membrane extract (Ruiz-Avila et al., 1995; Ming et al., 1998).

Further observations suggested that gustducin may be one, but not the only player in sweet taste transduction, since: (1) only a subset of sweet taste receptor expressing cells are positive for gustducin, with publications reporting from 1/10 to 2/3 of double positive cells (Hoon et al., 1999; Montmayeur et al., 2001; Max et al., 2001), and (2) in gustducin-knockout mice the responses to sweet compounds were reduced but not abolished (Wong et al., 1996; Ruiz-Avila et al., 2001; He et al., 2002; Danilova et al., 2006). Regarding $G\alpha_{gust}$ expression, regional differences occur and they are species-specific. In rats, taste buds of the fungiform papillae contain three time less gustducin-positive cells than those of the circumvallate papillae and the palate (Boughter et al., 1997). By contrast, in mice, $G\alpha_{gust}$ is coexpressed with T1R2/T1R3 in fungiform papillae and palatal taste bud cells, but not in the circumvallate papillae (Kim et al., 2003; Stone et al., 2007). This is consistent with the observation that in gustducin-knockout mice electrophysiological recordings from the chorda tympani nerve, showed an almost abolished response to sweet compounds (Wong et al., 1996), while the response of the glossopharyngeal nerve was less affected (Danilova et al., 2006). This suggests that sweet taste transduction may use different pathways according to the location of the taste bud cells, with species-specific differences. Little can be said about gustducin's functional role in humans as there is only one immunostaining study showing its expression in circumvallate and foliate papillae (Takami et al., 1994).

Gustducin is activated when an agonist binds to a bitter-, sweet- or umami-taste receptor. The conformational change of the GPCR induces GDP/GTP exchange on the Gα subunit, which then dissociates to transduce the signal into the cell (Hoon et al., 1995). For bitter stimuli, the Gα and βγ subunits were proposed to activate distinct downstream effector molecules (Sainz et al., 2007): Gα may induce PDE-mediated cAMP hydrolysis, while βγ may activate PLCβ2/IP3 signaling (Yan et al., 2001). Further, gustducin-knockout mice had elevated basal cAMP levels and bitter responses were unmasked only upon inhibition of PKA (Clapp et al., 2008), proposing that $G\alpha_{gust}$ activates PDEs and is important to maintain low levels of cAMP in resting states (Lindemann, 1996; Spielman, 1998; Clapp et al., 2008). Unfortunately, this scenario was not investigated for sweet taste responses therefore, we can only speculate whether the sweet-mediated pathway similarly requires gustducin to expand the functional range of cAMP changes. Nevertheless, this hypothesis provides a framework for understanding the reduced sweet preference in gustducin-knockout mice (Wong et al., 1996).

The picture is further complicated by the fact that additional G-proteins have been found in taste bud cells (**Table 3**).

TABLE 2 | Overview of signaling molecules involved in bitter and sweet signaling.

Signaling molecule	*Bitter*	*Sweet*
$G\beta_3$	Rössler et al., 2000	Max et al., 2001
$G\gamma_{13}$	Huang et al., 1999	Max et al., 2001
PLCβ2	Rössler et al., 1998; Miyoshi et al., 2001; Yan et al., 2001; Zhang et al., 2003	Asano-Miyoshi et al., 2000; Max et al., 2001; Miyoshi et al., 2001; Zhang et al., 2003
IP3	Hwang et al., 1990; Ogura et al., 1997; Spielman, 1998; Huang et al., 1999	Bernhardt et al., 1996; Uchida and Sato, 1997; Usui-Aoki et al., 2005
IP3R	Clapp et al., 2001; Miyoshi et al., 2001	Miyoshi et al., 2001
Ca^{2+} release from stores	Akabas et al., 1988	Bernhardt et al., 1996; Uchida and Sato, 1997
TRPM5	Pérez et al., 2002; Zhang et al., 2003	Pérez et al., 2002; Zhang et al., 2003; Talavera et al., 2005

Involvement of the signaling molecules was demonstrated with knockout mouse models, where Ca^{2+} signals in taste bud cells, nerve responses and/or behavioral attraction were measured upon stimulation. Immunostainings were used for localization of the signaling molecules.

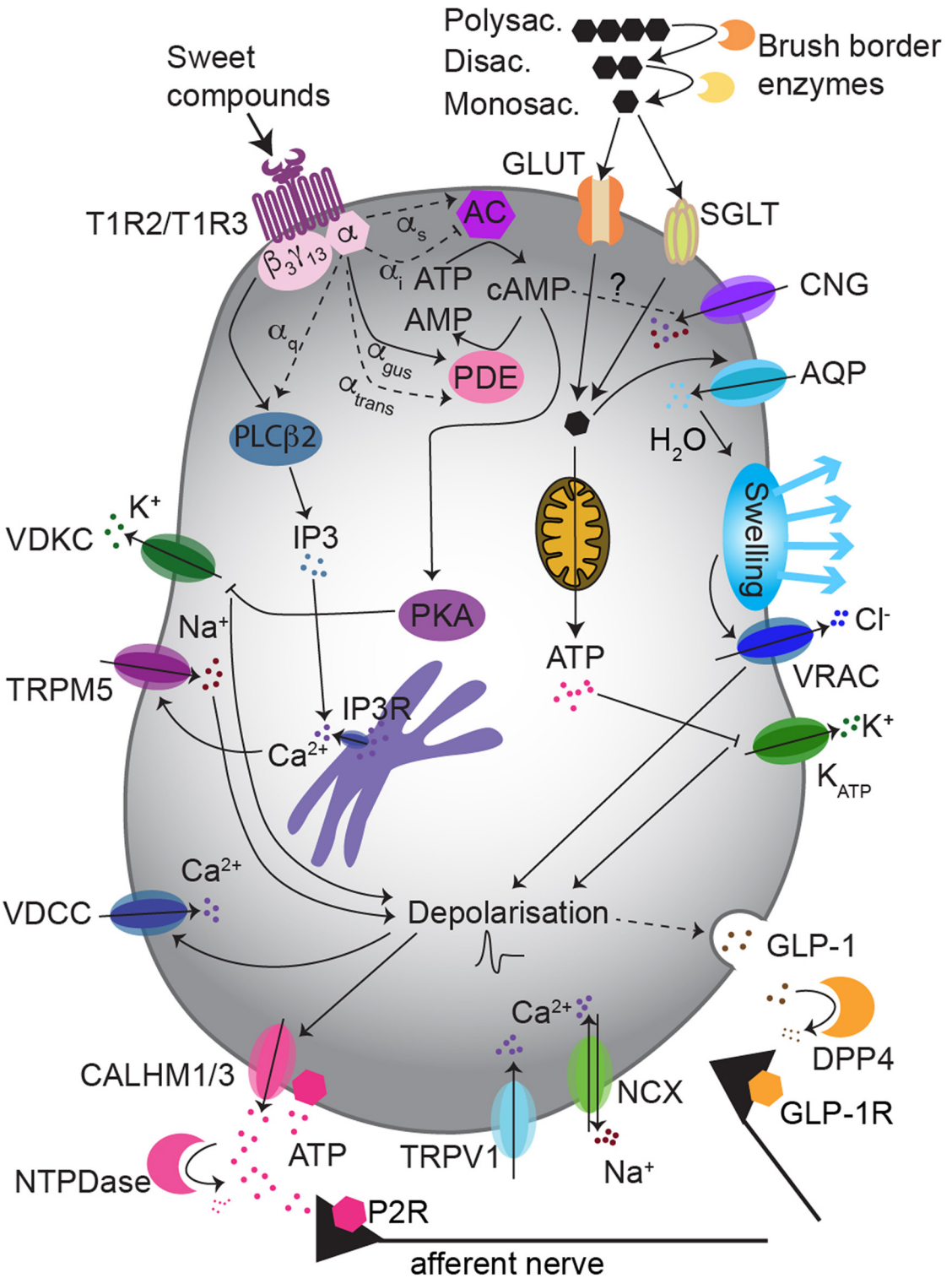

FIGURE 1 | Sweet taste transduction uses multiple pathways in type II taste bud cells. The "canonical pathway" implies the activation of gustducin by T1R3/T1R2 receptor, which then promotes: intracellular Ca^{2+} rise via PLCβ2/IP3 signaling, cell depolarization via TRPM5 and ATP release. Non-caloric sweeteners may preferentially use the PLCβ2/IP3 pathway, while sugars may rather activate a cAMP/PKA pathway, depolarizing the cell via K^+ channels inhibition. The "alternative pathway" possibly involves glucose influx via GLUTs and/or SGLT1, increase of ATP and inhibition of K_{ATP}-mediated K^+ outflow. This may induce GLP-1 release. Abbreviations: AQP, aquaporins; DPP4, dipeptidyl peptidase 4; CALHM1/3, Ca^{2+} homeostasis modulator 1/3; VDKC, voltage-dependent K^+ channel; P2R, purinergic receptor class 2; GLP-1R, GLP-1 receptor.

TABLE 3 | Overview of G-protein subunits expression in the taste buds.

Trimeric G proteins	*Species*	*Source*
$G\alpha_{gust}$	Recombinant in baculovirus	Hoon et al., 1995
	Mouse	Wong et al., 1996; Huang et al., 1999; Ruiz-Avila et al., 2001; He et al., 2002; Kim et al., 2003; Danilova et al., 2006; Miura et al., 2007; Stone et al., 2007
	Rat	McLaughlin et al., 1992, 1994; Yang et al., 1999; Kusakabe et al., 2000
	Human	Max et al., 2001
$G\alpha_{trans}$	Mouse	He et al., 2002
	Rat	Ruiz-Avila et al., 1995; Yang et al., 1999
	Bovine	Ruiz-Avila et al., 1995
$G\alpha_{s}$	Rat	McLaughlin et al., 1992, 1994; Kusakabe et al., 2000
$G\alpha_{i-2}$	Rat	McLaughlin et al., 1992, 1994; Asano-Miyoshi et al., 2000; Kusakabe et al., 2000
$G\alpha_{i-3}$	Rat	McLaughlin et al., 1992, 1994; Kusakabe et al., 2000
$G\alpha_{i-4}$	Rat	McLaughlin et al., 1992, 1994
$G\alpha_{12}$	Rat	McLaughlin et al., 1992, 1994
$G\alpha_{15}$	Mouse	Shindo et al., 2008; Tizzano et al., 2008
$G\alpha_{q}$	Rat	Kusakabe et al., 1998
$\beta_3\gamma_{13}$	Mouse, human	Huang et al., 1999
$\beta_3\gamma_{13}$	Rat	Rössler et al., 2000

The expression was detected by immunofluorescence (Ruiz-Avila et al., 1995; Kusakabe et al., 2000; Max et al., 2001; Shindo et al., 2008), in situ hybridization (Yang et al., 1999; Kusakabe et al., 2000; Kim et al., 2003; Shindo et al., 2008), PCR (Kusakabe et al., 1998; Tizzano et al., 2008), Southern (Kusakabe et al., 2000), and Northern blot (Kusakabe et al., 1998), as well as gene expression profiling (Huang et al., 1999).

Besides $G\alpha_{gust}$, also the mRNA for $G\alpha_{i-2}$, $G\alpha_{i-3}$, $G\alpha_{s}$ and $G\alpha_{14}$ was found in rat taste tissue (McLaughlin et al., 1992). Immunostaining analysis showed that also $G\alpha_{15}$ and $G\alpha_{q}$ were localized in rat taste buds (Kusakabe et al., 1998). The expression of $G\alpha_{i-2}$, $G\alpha_{i-3}$, $G\alpha_{s}$, and $G\alpha_{gust}$ was confirmed in rat circumvallate papillae with different techniques, proving that one taste bud cell can coexpress multiple Gα subunits, and $G\alpha_{gust}$ may not be the dominant species (Kusakabe et al., 1998; Kusakabe et al., 2000). This finding suggests that different, mutually interacting pathways might coexist in individual taste bud cells. Conversely, other evidence supports the idea that multiple pathways may be segregated in different cell subpopulations: for example in mouse taste bud cells, $G\alpha_{14}$ was found to be coexpressed with T1R3, but not with gustducin (Shindo et al., 2008; Tizzano et al., 2008). The $G\alpha_{14}$ subunit may be involved in PLC activation and IP3 generation (Kusakabe et al., 1998; Shindo et al., 2008; Tizzano et al., 2008). Based on a differential hybridization screen, $G\beta_3\gamma_{13}$ expression was detected in all $G\alpha_{gust}$ positive receptor cells (Rebecchi and Pentyala, 2000). Additionally, also the $G\beta_1\gamma_{13}$ subunit was found in receptor cells, and stimulation with a bitter compound revealed its functionality (Huang et al., 1999). $G\gamma_{13}$ colocalizes with $G\alpha_{gust}$ and mediates production of IP3 via PLCβ2 upon bitter stimulation (Yan et al., 2001). Finally, also $G\gamma_3$ was found in taste bud cells, coexpressed with PLCβ2, $G\alpha_{gust}$ and $G\beta_3$ (Rössler et al., 2000). Hence, this plethora of observations suggests a heterogenous picture, with several G-proteins and multiple downstream signaling options involved in the sweet taste pathway.

In summary, it has been generally accepted that sweet taste transduction in taste bud cells is mediated by $G\alpha_{gust}$. However, there are still many open questions, and several factors have to be considered in the interpretation of this transduction model: (1) functional studies are still very limited and mainly conducted in recombinant systems, (2) gustducin-knockout mice showed residual sweet taste responses, (3) besides $G\alpha_{gust}$, also other $G\alpha_{q}$ and $G\alpha_{i}$ subunits have been found in taste bud cells (**Table 3**), (4) several second messengers are mobilized by sweet taste receptor activation. One could speculate that the relative importance of a certain signaling pathway varies among species. Indeed, in mice the Gβγ pathway may dominate, while in rats and hamsters the Gα pathway seems to be more prominent (Trubey et al., 2006). Therefore, it is likely that several G-proteins and different pathways are involved in sweet taste transduction, which may be similar for human sweet taste sensation as well.

THE SWEET TASTE RECEPTOR-INDEPENDENT PATHWAY

Residual Sugar Attraction in Sweet Taste Receptor Deficient Mice

After the discovery of the sweet taste receptor, it has been assumed that the taste of sugars and of non-caloric sweeteners is almost exclusively transduced via the heterodimer T1R2/T1R3. However, additional mechanisms mediating sugar perception in taste bud cells have been reported. Indeed, a small residual response to highly concentrated sugars, but not to non-caloric sweeteners, was observed in T1R2 and T1R3 single-knockout mice (Zhao et al., 2003). In another T1R3-knockout strain, no response to non-caloric sweeteners was observed, but chorda tympani responses to disaccharides were only moderately diminished and those to glucose were even preserved (Damak et al., 2003). Further evidence in favor of a sweet-sensing pathway independent of the classical sweet taste receptor, comes from knockout mice models for crucial downstream signaling molecules, such as PLCβ2 (Zhang et al., 2003; Dotson et al., 2005), TRPM5 (Zhang et al., 2003; Talavera et al., 2005; Damak et al., 2006; Sclafani et al., 2007; Ren et al., 2010; Eddy et al., 2012) or gustducin (Wong et al., 1996; He et al., 2002; Ruiz et al., 2003; Glendinning et al., 2005; Danilova et al., 2006; Sclafani et al., 2007), in which behavioral and nerve

responses to sugars were not completely abolished (for review von Molitor et al., 2020c). Thus, it was proposed that, although the canonical T1R2/T1R3-mediated pathway is of principal importance for sweet sensation, additional sweet taste receptor independent pathways might sense caloric sugars (von Molitor et al., 2020c). These might employ T1R3 homodimers and/or completely different downstream signalings.

The Sweet Taste Receptor Independent Pathway May Use Glucose Transporters

In search of potential candidates for such alternative pathways, tissues involved in glucose homeostasis can be taken as models. Metabolic homeostasis in the body is achieved upon glucose absorption in the gastro-intestinal tract and glycemia regulation via pancreatic insulin release. Accordingly, gastro-intestinal and pancreatic cells use specialized mechanisms to sense and take up glucose. These include glucose transporters (GLUTs) and sodium-driven glucose symporters (SGLTs). The GLUT family contains 13 members with tissue-specific expression and functional diversity (**Table 4**). The SGLTs comprise only three family members (Scheepers et al., 2004; Zhao and Keating, 2007; Deng and Yan, 2016). In β-cells, GLUT2-mediated glucose entry elevates, via oxidative metabolism, the intracellular ATP level, which in turn leads to K_{ATP} channel inhibition (Ashcroft et al., 1984; Miki et al., 1998). This drives cell depolarization and triggers insulin release (Ashcroft, 2005; Yamamoto and Ishimaru, 2013; Laffitte et al., 2014). Alternatively, at hyperglycemic conditions, β-cell depolarization occurs via osmotic swelling and consequent activation of volume-regulated anion channels (VRACs), that mediates depolarizing outward Cl^- currents (Matsumura et al., 2007; Best et al., 2010; Louchami et al., 2012). Conversely, SGLT1 activation directly depolarizes the cells since glucose entry is coupled to the influx of Na^+. Furthermore, in contrast to GLUT, SGLT1 is activated also by non-metabolizable glucose analogs (Sclafani et al., 2020; Yasumatsu et al., 2020). In general, GLUTs and SGLT1 shuttle caloric sugars with different affinities (**Table 3**), but not non-caloric sweeteners. Considering the similarities between the taste papillae and the epithelia of the gastro-intestinal system (see chapter 7), the possibility that glucose transporters may be responsible for the residual response to sugars, as observed in sweet taste receptor deficient mice, was explored.

Notably, in human taste bud cells, glucose absorption has been long known (Kurosaki et al., 1998; Oyama et al., 1999; Toyono et al., 2011; Yee et al., 2011) and expression of both SGLT1 and GLUTs, was observed in taste papillae of different species (**Table 4**). Fittingly, also potential downstream players of GLUTs were found in taste bud cells (for review von Molitor et al., 2020c), supporting the hypothesis that GLUT and SGLT1 may be responsible for the residual glucose preference in T1R3-knockout mice (Damak et al., 2003). Specifically, the involvement of SGLT1 in T1R3-independent sugar responses in mice was recently reported. Yasumatzu et al. showed that NaCl selectively increased sweet responses to glucose and sucrose, but not to non-caloric sweeteners, nor to other taste modalities, both in wild type and T1R3-knockout mice (Yasumatsu et al., 2020). This increase was ablated by phlorizin, a SGLT1 blocker. Additionally, afferent sweet-responsive fibers showed three different response patterns to sweet stimuli: (1) fibers with a maximal response to sugars were sensitive to NaCl and phlorizin, (2) fibers with a maximal response to non-caloric sweeteners were unaffected by NaCl and phlorizin, and (3) fibers with a mixed behavior also responded to NaCl and phlorizin (Yasumatsu et al., 2020). This suggests that there are some sweet-responding taste bud cells expressing only SGLT1, some that express only T1R2/T1R3 and a third group expressing both (Yasumatsu et al., 2020). Whether SGLT1-expressing cells represent type II or another cell population, such as the recently discovered "broadly responsive" cells, needs further investigation (Dutta Banik et al., 2020; Yasumatsu et al., 2020). It is still unknown if the SGLT1-mediated pathway induces Ca^{2+} signals,

TABLE 4 | GLUTs and SGLT expression in taste bud cells.

Transporter	*Substrate*	*Species*	*Papillae*	*Source*
GLUT2 (Slc2A2)	glucose, mannose, galactose, fructose, glucosamine (Thorens, 2015)	Mouse	CV, foliate, fungiforme	Yee et al., 2011
		Rat	CV	Merigo et al., 2011
GLUT4 (Slc2A4)	glucose, dehydroacetic acid (Huang and Czech, 2007; Vargas et al., 2019)	Mouse	CV, foliate, fungiform	Yee et al., 2011
Glut5 (Slc2A5)	fructose (Douard and Ferraris, 2008)	Rat	CV	Merigo et al., 2011
Glut8 (Slc2A8)	glucose, fructose, galactose (Schmidt et al., 2009)	Mouse	CV, foliate, fungiform	Yee et al., 2011
		Macaque	CV, fungiform	Hevezi et al., 2009
Glut9 (Slc2A9)	glucose, fructose, urate (Doblado and Moley, 2009)	Mouse	CV, foliate, fungiform papillae	Yee et al., 2011
Glut10 (Slc2A10)	glucose, galactose (Dawson et al., 2001)	Macaque	CV, fungiform	Hevezi et al., 2009
Glut13 (Slc2A13)	glucose, IP3 (Zhao and Keating, 2007)	Macaque	CV, fungiform	Hevezi et al., 2009
SGLT1 (Slc5)	glucose, galactose (Sabino-Silva et al., 2010; Wright et al., 2011)	Mouse	CV, foliate, fungiform	Yee et al., 2011
		Rat	CV papillae	Merigo et al., 2011

Expression was detected by PCR (Merigo et al., 2011; Yee et al., 2011), immunohistochemistry (Merigo et al., 2011; Yee et al., 2011), or an affymetrix genome wide array (Hevezi et al., 2009). CV, circumvallate papillae.

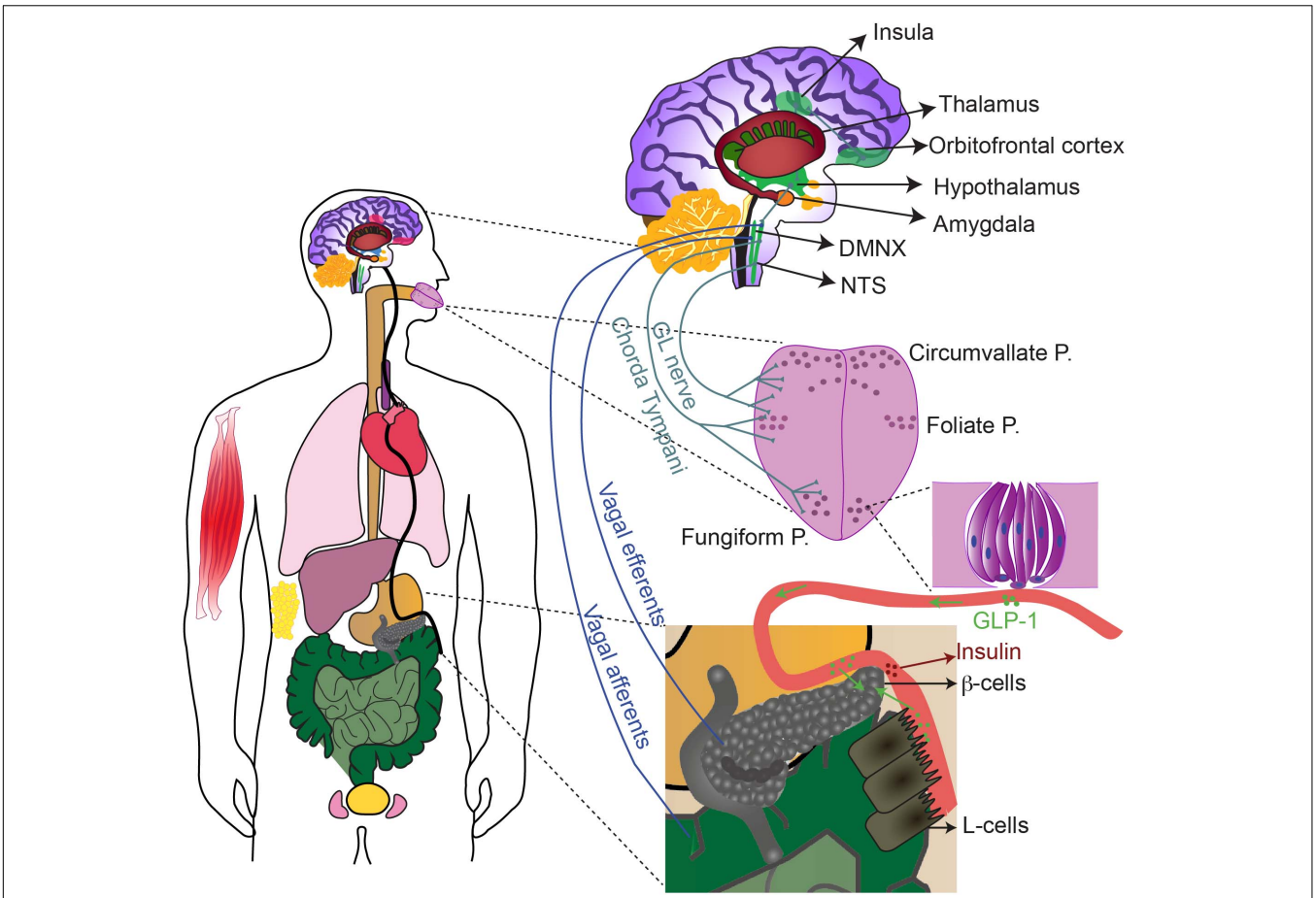

FIGURE 2 | The sweet taste receptor contributes to gustation and extraoral sugar-sensing. T1R2/T1R3, and possibly T1R3 homomers, are expressed with their downstream signaling molecules in multiple extraoral tissues (in color), including: oesophagus, stomach, liver, pancreas, intestine, bladder, testis, skeletal muscle, respiratory tract and adipose tissue. Activation of sweet-sensitive taste bud cells leads to purinergic stimulation of the chorda tympani and the glossopharyngeal (GL) nerves that send information, upon relay in the NTS and the thalamus, up to the insula. The insula communicates with several other brain regions (some are depicted) to regulate reward, motivation and energy homeostasis. Taste bud cells release also GLP-1 that can activate the afferent fibers as well. Sweet stimulation of taste bud cells thereby generates CPIR, possibly via NTS-DMNX communication and consequent activation of efferent vagal fibers. GLP-1 released by taste bud cells in the circulation, may also reach the pancreas, the intestine and the brain, exerting there paracrine effects.

TRMP5 activation and ATP release, or uses a completely different intracellular mechanism and neurotransmitter. In further support of the SGLT1 hypothesis, all sweet-responsive afferent fibers in T1R3-knockout mice were phlorizin sensitive and could be activated by the non-metabolizable sugar αMDG. In addition, NaCl increased licking of glucose solution in T1R3-knockout animals, an effect blocked by phlorizin (Yasumatsu et al., 2020), providing evidence that the SGLT1-based pathway mediates sugar attraction. Theoretically, also disaccharides could be detected via the alternative pathway. Indeed, mouse taste cells express a group of disaccharidases, called "brush border" enzymes, that hydrolyze the disaccharides to monosaccharides, which in turn can enter the taste cells via the transporters (Merigo et al., 2009; Sukumaran et al., 2016). Additionally, live-cell imaging in taste bud cells using a FRET-based glucose sensor (Deuschle et al., 2005) or (NAD(P)H,FAD) fluorescent imaging, may help to understand the contribution of SGLT1 and GLUTs to sweet responses. To unravel whether the alternative pathway also generates Ca^{2+} events to transduce gustatory responses, live Ca^{2+} imaging should be performed in taste bud cells of T1R3-knockout mice.

Neurotransmitter and Physiological Role of the Alternative Pathway

The alternative pathway may use not only a distinct intracellular signaling, but also a different neurotransmitter. A likely candidate for signal transmission from taste bud cells to gustatory nerves is glucagon-like peptide-1 (GLP-1) (**Figures 1**, **2**). Indeed, GLP-1 and its synthetizing enzyme convertase, were detected in a subset of type II and type III cells in mouse circumvallate papillae (Feng et al., 2008; Shin et al., 2010; Kokrashvili et al., 2014) (for review von Molitor et al., 2020c), while the related receptor (GLP-1R) was found in intragemmal nerve fibers (Shin et al., 2008; Takai et al., 2015). GLP-1 released by taste bud cells is selectively sweet- and lipid-dependent and it potentiates sweet

taste mediated attraction (Martin et al., 2009; Martin et al., 2012). Besides this, taste bud cells may contribute to systemic GLP-1, releasing it in the blood stream (**Figure 2**). In the body, GLP-1 is mainly released from enteroendocrine L-cells upon glucose uptake, via a mechanism involving SGLT1-mediated depolarization and activation of voltage-dependent calcium channels (VDCCs) (Best et al., 2010; Brubaker, 2017). Generally, GLP-1 controls fasting plasma glucagon, influences motoric mechanisms of gastric emptying, inhibits short-term food intake and potentiates pancreatic insulin release (Meier and Nauck, 2005; Schirra and Göke, 2005). In particular, GLP-1 induces the "cephalic phase insulin release" (CPIR). This is an innate response to sweet food ingestion that occurs prior its absorption, through which pancreatic insulin release occurs before blood glucose level rises (Louis-Sylvestre, 1976; Just et al., 2008). CPIR is important to prepare the body for ingestion, digestion, and storage of carbohydrate (Ahrén and Holst, 2001; Smeets et al., 2010). In healthy humans and rodents, CPIR is induced by oral exposure to sweet substances, but not to umami, salty or bitter compounds (Tonosaki et al., 2007; Just et al., 2008; Dušková et al., 2013). However, further studies are required to reveal the mechanism of GLP-1 release from sweet-sensitive taste bud cells and how this may induce CPIR (for review von Molitor et al., 2020c). Nonetheless, the alternative sweet-sensitive pathway could be a new interesting drug target (Laffitte et al., 2014; ZhuGe et al., 2020). If the idea holds true that taste bud cells mediate CPIR via oral secretion of GLP-1 (Chambers et al., 2017; Svendsen et al., 2018), controlling GLP-1 signaling in the tongue may help to control glycemia or even to treat diabetes (von Molitor et al., 2020c).

CALORIC SUGARS AND NON-CALORIC SWEETENERS MAY UTILIZE DISTINCT PATHWAYS

Before the discovery of the sweet taste receptor, taste bud cells responses to caloric and non-caloric sweeteners were proposed to be mediated by two different pathways. In rat taste buds, caloric sugars were shown to augment cAMP concentrations, while non-caloric sweeteners mainly raised intracellular IP3 concentration (Striem et al., 1991; Bernhardt et al., 1996). Moreover, with Ca^{2+} imaging experiments, it was shown that extracellular Ca^{2+} is required only for nutritive sugar-mediated responses (Bernhardt et al., 1996). Thus, the response to sugars seems to involve the cAMP/PKA pathway and to depend on Ca^{2+} influx, while non-caloric sweeteners probably induce IP3-mediated Ca^{2+} release from the stores (Bernhardt et al., 1996). However, it remains elusive, whether such a strict separation holds true, since saccharin was reported to activate both pathways: at low concentrations the cAMP/PKA-signaling, and at higher concentrations the IP3-pathway (Nakashima and Ninomiya, 1999). Presumably, saccharin can switch its activity from sweet to bitter agonist in a concentration-dependent manner (Kuhn, 2004; Galindo-Cuspinera, 2006; Behrens, 2017). Since mice deficient for PLCβ2 (Zhang et al., 2003; Dotson et al., 2005) and TRPM5 (Zhang et al., 2003; Talavera et al., 2005; Damak et al., 2006) were shown to be insensitive to non-caloric sweeteners and to have largely reduced responses to natural sugars, PLCβ2 and TRPM5 may be crucial signaling molecules for perception of both caloric and non-caloric sweet tastants (for review von Molitor et al., 2020c). Furthermore, in rat taste buds the very same cells responded to sucrose and artifical sweeteners (Bernhardt et al., 1996; Lindemann, 1996). This can be interpreted as either both types of sweet stimuli activate the same pathway, or that two different pathways coexist in the same cell and interact. For example, GPCRs can mediate different signaling pathways via either, the α or βγ subunit (Zhu et al., 1994; Zhu and Birnbaumer, 1996). In support of the two-pathways hypothesis, non-caloric sweeteners mediated responses differ from those elicited by natural sugars as they have a higher potency, a delayed on- and off-set, and a lower sweetness intensity (DuBois et al., 1991; DuBois, 2016; Wee et al., 2018). Therefore, they are ranked less sweet than sugars by humans (Antenucci and Hayes, 2015) and mice (Smith and Sclafani, 2002). Stimulation of taste buds with sugars and non-caloric sweeteners also evokes different physiological responses. Natural sugars were able to induce CPIR in humans, as described in most studies (Goldfine et al., 1969; Berthoud et al., 1980; Yamazaki and Sakaguchi, 1986; Tonosaki et al., 2007; Just et al., 2008; Shinozaki et al., 2008; Dušková et al., 2013; Dhillon et al., 2017), but for non-caloric sweeteners this is still controversial (reviewed Han et al., 2019; von Molitor et al., 2020c). Along the same line, there is clear evidence that GLP-1 is released by taste bud cells upon nutritive sugar consumption, but a corresponding efficacy of non-caloric sweeteners is debated (for review Renwick and Molinary, 2010; von Molitor et al., 2020c). Furthermore, upon oral perception, both caloric sugars and non-caloric sweeteners activated the gustatory cortex, but their responses differed in terms of intensity and activated regions (Frank et al., 2008; Chambers et al., 2009). Finally, while natural sugars activated brain reward areas, such as the dopaminergic midbrain area (Frank et al., 2008) and the striatum (Chambers et al., 2009), non-caloric sweeteners failed to do so (for review Han et al., 2019). Considering the broad consumption of non-caloric sweeteners, it is crucial to find an answer to these many open questions to better interpretate and predict their physiological effect.

Ca^{2+} PATHWAYS IN TASTE RECEPTOR CELLS

Sweet taste responses rely on intracellular Ca^{2+} signals, that are translated into afferent-fiber activity in order to send the information to upper brain centers. In this context, type II cells released Ca^{2+} from the stores via PLC/IP3-mediated signaling upon saccharin stimulation (Bernhardt et al., 1996; Rebello et al., 2013). Consistent with this observation, neither VDCCs gene expression nor depolarization-induced Ca^{2+} signals were observed in type II cells (Clapp et al., 2006; DeFazio et al., 2006). However, others reported voltage-dependent Ca^{2+} influx in a subpopulation of bitter-responding cells, that may feature both type II and type III cells (Hacker and Medler, 2008) (for review Medler, 2015). Consistenly, the presence of "broadly responsive"

taste bud cells has been recently reported, that are positive for the type III cell marker SNAP25, and respond to KCl-mediated depolarization with Ca^{2+} influx. Further, they responded to bitter, umami and/or sweet stimuli with Ca^{2+} signals mediated, in this case, by a different PLC: the PLCβ3. Thus, these "broadly responsive" cells feature both voltage-dependent Ca^{2+} influx and intracellular Ca^{2+} release, even if it remained elusive, wether they express VDCCs, T2R and T1R. In all papillae types, such cells represented about 20–30% of all taste bud cells and about 50% of type III cells. Furthermore, since PLCβ3-knockout mice have a reduced licking behavior to bitter, sweet and umami stimuli, this cell population crucially contributes to taste perception (Banik et al., 2018; Dutta Banik et al., 2020).

Further potential Ca^{2+} mobilization routes include: cyclic nucleotide gated (CNG) channels, store-operated Ca^{2+} channels (SOCs), vanilloid-receptor-1 (TRPV1), and Calcium Sensing Receptor (CaSR) (**Figure 1** and **Table 5**).

First, CNG channels are pivotal in decoding visual and olfactory sensations (Bradley et al., 2005). In frog taste bud cells, electrophysiological experiments have shown the presence of a CNG conductance that was inhibited by cAMP/cGMP. This argued for a sequence of events, whereby tastant-induced transducin activation would trigger PDE, leading to cyclic nucleotide degradation, CNG channel activation, depolarization and Ca^{2+} influx (Kolesnikov and Margolskee, 1995). In 1997, Misaka et al. cloned another CNG from rat tongue epithelial tissue that was present specifically in taste buds of circumvallate papillae at the pore side, whose expression disappeared upon glossopharyngeal nerve denervation. In contrast to the channel described by Kolesnikov and Margolskee, this channel was shown, in a recombinant system, to be activated by cGMP and cAMP (Misaka et al., 1997). However, it remained elusive whether it is able to conduct Ca^{2+}, if it is functional in the native tissue and if it is linked to the sweet taste transduction pathway.

Second, SOCs may provide another way for Ca^{2+} entry into taste bud cells. In general, they are responsible for capacitive Ca^{2+} entry upon depletion of the store. In mouse taste bud cells, SOCs are composed of the proteins orai-1 and orai-3, which are under the control of an endoplasmatic-Ca^{2+} depletion sensor, i.e., stromal interaction molecule-1 (STIM-1). STIM-1 was shown to mediate the perception of fatty acids by the induction of Ca^{2+} signals (Dramane et al., 2012; Abdoul-Azize et al., 2014). Orai-1 and orai-3 are expressed in CD36 positive cells (Dramane et al., 2012), with CD36 and GPR120 being considered as receptors for fatty acids. In mouse, both receptors are expressed in some type II and type III cells (Matsumura et al., 2009; Gilbertson and Khan, 2014). They mediate Ca^{2+} signals and the release of serotonin and GLP-1 (Ozdener et al., 2014). Since long-chain fatty acids reinforce attraction to sugars (Martin et al., 2012), there might be a cross talk between signaling pathways triggered by fatty acids and sweet tastants. Indeed, TRPM5 may be a key signaling component in both pathways, since TRPM5-knockout mice had not only a reduced sweet taste sensitivity, but also an abolished fat preference (Sclafani et al., 2007). Interestingly, store-operated Ca^{2+} entry is involved in responses to prolonged bitter stimulation, meaning that not only Ca^{2+} release but also Ca^{2+} influx may be important for transduction (Ogura et al., 2002). Probably, this mechanism has been often underestimated, since the majority of electrophysiological and functional imaging experiments used only brief taste stimuli applications. Still, it is not known if prolonged sweet stimuli also require store-operated Ca^{2+} influx.

Third, the vanilloid-receptor-1 (TRPV1) is a non-selective cation channel permeable to Na^+, Ca^{2+}, K^+ and NH_4^+ which

TABLE 5 | Possible Ca^{2+} signaling pathways in type II taste bud cells.

Molecule	*Activation*	*Effect*	*Source*
VDCC	depolarization	Ca^{2+} influx	Béhé et al., 1990; Medler et al., 2003; Hacker and Medler, 2008
ORAI/STIM	Ca^{2+} release from the store	Ca^{2+} influx	Ogura et al., 2002; Matsumura et al., 2009; Gilbertson and Khan, 2014; Ozdener et al., 2014
TRMP5/TRPM4	depolarization and Ca^{2+}	Na^+ influx and depolarization	Pérez et al., 2002; Prawitt et al., 2003; Talavera et al., 2005; Kaske et al., 2007
CNG	cAMP/cGMP	Na^+ influx and depolarization	Kolesnikov and Margolskee, 1995; Misaka et al., 1997
Ryanodine Receptor	Ca^{2+}, L-type VDCC	Ca^{2+} release from the store	Rebello and Medler, 2010; Rebello et al., 2013
IP3R	IP3	Ca^{2+} release from the store	Clapp et al., 2001; Hacker and Medler, 2008
TRPV1	capsaicine, temperature, H^+	Ca^{2+}, Na^+, K^+, Mg^{2+} influx	Lyall et al., 2004; Hacker and Medler, 2008; Laskowski and Medler, 2009
CaSR	glutation, Ca^{2+}	Ca^{2+} release from the store	Maruyama et al., 2012; Medina et al., 2016

Expression and functionality were assessed with RT-PCR (Prawitt et al., 2003; Hacker and Medler, 2008; Laskowski and Medler, 2009; Matsumura et al., 2009; Rebello and Medler, 2010; Maruyama et al., 2012) immunohistochemistry (Misaka et al., 1997; Clapp et al., 2001; Medler et al., 2003; Kaske et al., 2007; Hacker and Medler, 2008; Matsumura et al., 2009; Rebello and Medler, 2010; Maruyama et al., 2012; Rebello et al., 2013; Medina et al., 2016), in situ hybridization (Pérez et al., 2002), live-microscopy imaging (Ogura et al., 2002; Hacker and Medler, 2008; Laskowski and Medler, 2009; Rebello and Medler, 2010; Maruyama et al., 2012; Rebello et al., 2013; Ozdener et al., 2014; Medina et al., 2016), and electrophysiology (Béhé et al., 1990; Kolesnikov and Margolskee, 1995; Misaka et al., 1997; Medler et al., 2003; Prawitt et al., 2003; Lyall et al., 2004; Talavera et al., 2005).

TABLE 6 | Gastro-intestinal expression of sweet taste signaling molecules.

Organ	*T1R2*	*T1R3*	*T2R*	*$G\alpha_{gust}$*	*PLCβ2*	*TRPM5*	*GLUT/SGLT*	*K_{ATP}*	*Species*	*Source*
Oeso-phagus		✓		✓ low		✓ low			Human	Young et al., 2009
Stomach	✓	✓	✓	✓	✓	✓	✓	✓	Mouse	Hass et al., 2007; Kaske et al., 2007; Bezençon et al., 2008; Hass et al., 2010; Janssen et al., 2011; Widmayer et al., 2011; Sakata et al., 2012
Intestine	✓	✓	✓		✓ low	✓			Human	Bezençon et al., 2007; Jang et al., 2007; Young et al., 2009
	✓	✓	✓	✓			✓		Mouse	Dyer et al., 2005; Margolskee et al., 2007; Janssen et al., 2011
							✓	✓	Rat	Kuhre et al., 2015
Colon		✓	✓	✓					Human	Taniguchi, 2004; Rozengurt et al., 2006
	✓	✓		✓ low					Mouse	Bezençon et al., 2008; Reimann et al., 2008
							✓ low		Rat	Jie et al., 2015
Pancreas		✓				✓	✓	✓	Human	Prawitt et al., 2003; Taniguchi, 2004
	✓	✓		✓		✓	✓	✓	Mouse	Prawitt et al., 2003; Nakagawa et al., 2009; Colsoul et al., 2010; Nakagawa et al., 2014
							✓	✓	Rat	Cook and Hales, 1984; Inagaki et al., 1995; Vos et al., 1995

Methods included: PCR (Prawitt et al., 2003; Dyer et al., 2005; Rozengurt et al., 2006; Margolskee et al., 2007; Bezençon et al., 2008; Nakagawa et al., 2009; Young et al., 2009; Widmayer et al., 2011; Sakata et al., 2012), in situ hybridization (Hass et al., 2007; Margolskee et al., 2007), immunohistochemistry (Taniguchi, 2004; Rozengurt et al., 2006; Hass et al., 2007; Jang et al., 2007; Kaske et al., 2007; Margolskee et al., 2007; Bezençon et al., 2008; Colsoul et al., 2010; Janssen et al., 2011; Widmayer et al., 2011), biochemical measurement (Kuhre et al., 2015), or transcriptome analysis (Jie et al., 2015).

is modulated by diverse stimuli such as vanilline, temperature, voltage and capsaicine. It was proposed to be responsible for salt detection, since it mediates amiloride-insensitive responses of the chorda tympani nerve not only to Na^+, but also to Ca^{2+}, K^+ and NH_4^+ (Lyall et al., 2004). It is responsible for constitutive Ca^{2+} entry, which is then regulated by mitochondrial Ca^{2+} buffering and membrane Ca^{2+} extrusion via the Na^+-Ca^{2+} exchanger (NCX) (Hacker and Medler, 2008; Laskowski and Medler, 2009). The concerted action of these players may contribute to the regulation of intracellular Ca^{2+} homeostasis in taste bud cells. In fact, both pharmacological alteration of the mitochondrial potential (Hacker and Medler, 2008) and blocking of NCX, induced Ca^{2+} signals in taste bud cells (Laskowski and Medler, 2009). Also, mitochondria were shown to differentially contribute to Ca^{2+} buffering in type II and type III cells (Hacker and Medler, 2008; Medler, 2015), and metabolic stimuli may affect intracellular Ca^{2+} homeostasis by interfering with mitochondrial activity: in type II cells, changes in mitochondrial potential induced by glucose metabolism may decrease mitochondrial Ca^{2+} buffering and affect intracellular Ca^{2+} transients (Hacker and Medler, 2008; Medler, 2015).

Fourth, an additional taste, called *kokumi*, makes use of the CaSR to induce specialized Ca^{2+} signals (Maruyama et al., 2012; Medina et al., 2016). CaSR is a typical GPCR which plays a central role in mammalian Ca^{2+} homeostasis (Chattopadhyay et al., 1997). It is present in both type II and type III cells, but it is not coexpressed with T1R3 (Bystrova et al., 2010; Maruyama et al., 2012). In rodents, most CaSR-positive cells were found in circumvallate and foliate papillae (San Gabriel et al., 2009). CaSR is activated by glutathione and cations such as Ca^{2+}, Mg^{2+} and Gd^{3+}. Although these CaSR agonists alone have no flavor, they enhanced the intensity of sweet or umami sensation. When recombinant CaSR was expressed in HEK cells, glucose and sucrose were able to elicit Ca^{2+} transients in the presence of extracellular Ca^{2+}, suggesting that CaSR can be allosterically modulated by sugars to mobilize Ca^{2+} via a downstream pathway (Medina et al., 2016). Indeed, in mouse taste cells, *kokumi* substances induced intracellular Ca^{2+} release via PLC (Maruyama et al., 2012). CaSR can also be activated by bitter compounds (Rogachevskaja et al., 2011) and may, therefore, exert an ubiquitous and still largely unknown modulatory effect on several taste modalities.

PRESENCE AND ROLE OF SWEET TASTE RECEPTOR IN EXTRAORAL TISSUES

Apparently, T1R2/T1R3 is not only responsible for sweet taste detection in the oral cavity, since it is also expressed in several extra oral tissues (**Figure 2**), together with its downstream signaling molecules (**Table 6** and **Figure 2**) (for review Yamamoto and Ishimaru, 2013; Laffitte et al., 2014). Most of these tissues are involved in carbohydrate metabolism and there, the sweet taste receptor is involved in nutrient sensing, monitoring changes in energy storage and triggering metabolic and behavioral responses to maintain the energy balance (Lee and Owyang, 2017). Thus, the wide expression of the sweet taste receptor highlights potential health risks that sweeteners pose, due to their multiple targets in the body (Laffitte et al., 2014). The following paragraphs briefly introduce the main findings on extraoral expression of sweet taste receptors and the knowledge on their function there.

Sweet Taste Receptors in the Gastrointestinal Tract

In the esophagus, mainly T1R3-homodimers are present (Young et al., 2009), while in the mouse stomach, T1R3 is expressed at higher levels than T1R2, supporting the hypothesis that homomeric and dimeric receptors may be both present (Hass et al., 2010). Gustducin expression in rat stomach, duodenum, and the pancreatic duct was already known in 1996 (Höfer et al., 1996). Later, Hass et al. identified a cluster of gustducin, PLCβ2 and TRPM5 expressing cells in the mouse stomach. Even if colocalization studies were not possible, they noticed that gustducin and TRPM5 positive cells were scattered, whereas PLCβ2 positive cells were restricted to a basolateral sub-compartment (Hass et al., 2007). PLCβ2 positive cells further expressed cytokeratin 18, a marker for brush cells (Hass et al., 2007). In a follow up study, they showed also T1R3 expression in this region (Hass et al., 2010). Thus, these brush cell clusters may have chemosensory function and support the gastric compartment to sense nutrients. This may not only initiate the appropriate gastric processes for digestion and regulate gastric emptying (Rozengurt, 2006; Kendig et al., 2014), but may also be relevant to transmit information to the hypothalamic nuclei governing food intake (Hass et al., 2010). Accordingly, gustducin and T1R3 are coexpressed with the hunger hormone ghrelin (Hass et al., 2010; Janssen et al., 2011). Concerning the sweet taste receptor independent pathway, mRNAs encoding GLUT1,4,5 and components of the K_{ATP} channel (Kir6.2 and SUR1), were also detected in the pool of gastric mucosal cells secreting ghrelin. However, activators or inhibitors of the K_{ATP} channel did not change ghrelin release, as shown with mouse ghrelinoma cells kept at low density (Sakata et al., 2012). Hence, both the canonical and the alternative pathway may play a role in a ghrelin releasing cells of the stomach.

RT-PCR results have shown that humans and mice similarly express T1R2, T1R3, gustducin, PLCB2 and TRMP5 in gastro-intestinal tissues, with the exception of T1R2 that was not detected in the stomach (Bezençon et al., 2007). In rodent intestinal cell lines, T1R2/T1R3 is coexpressed with α-gustducin (Dyer et al., 2005; Margolskee et al., 2007). Additionally, in humans, the sweet taste receptor is highly expressed in the jejunum and duodenum and to a lesser content in the ileum (Dyer et al., 2005; Young et al., 2009). Moreover, gustducin was detected in more than 90% of human L-cells, in less than 50% of K-cells, and in other cell types in the duodenum (Jang et al., 2007). Gustducin expression was most prominent in the mid-jejunum (Young et al., 2009), the place where carbohydrate-induced reflexes are likely to be initiated (Lin et al., 1989). Besides this, the expression of PLCβ2 (Young et al., 2009) and TRPM5 (Prawitt et al., 2003; Young et al., 2009) has been demonstrated in gastro-intestinal cells, where they might be involved in sugar

sensing via canonical sweet signaling (**Table 6**; Dyer et al., 2005; Bezençon et al., 2007). While the release of ghrelin by T1R3-expressing brush and endocrine cells (Hass et al., 2010) seemed to be sweet taste receptor and gustducin independent in mice (Steensels et al., 2016), the canonical pathway may mediate the release of GLP-1. Indeed, intestinal cells, expressing T1R2 and T1R3, released GLP-1 (Dyer et al., 2005; Jang et al., 2007), which was reduced in T1R3-knockout mice and upon sweet taste receptor inhibition (Jang et al., 2007). Furthermore, T1R3 and gustducin were shown to regulate the expression of SGLT1 in enterocytes, since sugars and non-caloric sweeteners stimulated SGLT1 expression and glucose absorptive capacity in wild-type mice, but not in T1R3- or gustducin-knockout mice (Margolskee et al., 2007). More recently, glucose intake via GLUT2 was found to induce the release of GLP-1 in rat intestine via glucose metabolism and ATP-mediated closure of K_{ATP} (Kuhre et al., 2015). Thus, as in the taste buds, both sweet taste receptor dependent and independent pathways may coexist.

The expression of T1R3 and gustducin has been shown also in human enteroendocrine L-cells of the colon (Rozengurt et al., 2006). Curiously, in mouse colon cells, gustducin is coexpressed with TRPM5, but not with PLCβ2 nor T1R3 (Bezençon et al., 2008). Further, SGLT1 and K_{ATP} expression in rat colon cells is low (Reimann et al., 2008). As gustducin expression was found in L-cells, which secrete GLP-1 and peptide tyrosine tyrosine (PYY), sweet taste receptors there may be involved in energy homeostasis (Rozengurt et al., 2006; Rozengurt, 2006). Additionally, it was proposed that T1R3/T1R2, along with T2R, may play a role in the peristaltic reflex (Rozengurt, 2006; Kendig et al., 2014).

Sweet Taste Receptors in the Pancreas

Another key player in glucose homeostasis is the pancreas, where increased blood glucose levels are sensed via GLUT2. Upon glucose transport into β-cells, oxidative phosphorylation occurs which increases intracellular ATP that in turn inactivates K^+ channels to mediate cell depolarization. This mechanism links glycolysis to hormonal release, since subsequent VDCCs-mediated Ca^{2+} influx triggers insulin secretion (Yamamoto and Ishimaru, 2013; Laffitte et al., 2014). Additionally, the pancreas senses sweet compounds via T1R3 and T1R2, which are both coexpressed with gustducin, as shown in MIN6 cells and mouse β-cells (Nakagawa et al., 2009; Medina et al., 2014). However, low mRNA levels of T1R2 were detected, suggesting that here T1R3-homodimers may be present and contribute to sweet taste receptor function (Young et al., 2009; Medina et al., 2014). T1R3 activation was shown to increase ATP production by promoting mitochondrial metabolism (Nakagawa et al., 2014; Kojima et al., 2015). Stimulation of β-cells with fructose, sucralose or non-caloric sweeteners led to increased insulin blood levels (Nakagawa et al., 2009), an effect blocked by knocking out T1R3 or inhibiting it with gurmarin, suggesting T1R3 functionality in β-cells (Geraedts et al., 2012; Nakagawa et al., 2013; Medina et al., 2014). In addition, TRMP5-knockout mice showed diminished glucose-mediated insulin secretion (Colsoul et al., 2010). Thus, in the pancreas, the canonical sweet taste pathway may function in synergy with the GLUT-mediated pathway.

Sweet Taste Receptors in Other Tissues

Sweet taste receptor expression has been additionally documented in multiple other tissues not directly involved in glucose homeostasis, such as respiratory tract (Lee and Cohen, 2014; Workman et al., 2015), liver (Taniguchi, 2004), testes (Gong et al., 2016), heart (Wauson et al., 2012), bladder (Elliott et al., 2011), skeletal muscle (Kokabu et al., 2017), and adipose tissue (Masubuchi et al., 2013; **Figure 2**). The role of sweet taste receptors in these tissues is reviewed elsewhere (Lee and Cohen, 2015).

Besides metabolic functions, taste receptors may play a role also in the innate immune response. In support of this, human solitary chemosensory cells (SCCs) expressed T2R and T1R receptors (Lee et al., 2014). SCCs are discrete, non-ciliated cells of the nasal respiratory epithelium (Yamamoto and Ishimaru, 2013; Maina et al., 2018). As shown in rodents, they express gustducin (Finger et al., 2003) and TRPM5 (Lin et al., 2008). During infection of the upper airways, gram-negative bacteria release bitter noxious substances, called acyl-homoserine lactones (AHLs), which are agonists of T2R38 (Lee et al., 2012). Accordingly, human neutrophils can identify AHLs via T2R38 (Maurer et al., 2015) and additional T2R members (Yan et al., 2017). T2R stimulation then leads to PLCβ2 activation and increased intracellular Ca^{2+} which spreads to neighboring ciliated cells via gap junctions to induce secretion of anti-microbial peptides for killing pathogenic microbes (Finger et al., 2003; Lee et al., 2014) (for review see Maina et al., 2018; Triantafillou et al., 2018). Stimulation of the sweet taste receptor, expressed in the same cells, led to inhibition of this defense pathway (Lee et al., 2014). However, when bacteria metabolize glucose, its concentration in the airway mucus decreases and this interrupts the tonic activation of T1R2/T1R3, boosting the immune response (Maina et al., 2018). Thus, the combination of sweet taste receptor antagonists with bitter receptor agonists could be a new potential pharmacological approach to treatment chronic rhinosinusitis or airway infections (reviewed in Workman et al., 2015; Maina et al., 2018).

The ubiquitous expression of sweet taste receptors indicates that sweet compounds and other allosteric binding partners of T1R2/T1R3 (Kojima and Nakagawa, 2011) and T1R3-homomeric receptors (Young et al., 2009; Medina et al., 2014) may induce potential health risks via inappropriate metabolic effects, such as: stimulating the release of gut or pancreatic hormones, altering glucose absorption, or modulating immune responses (Geraedts et al., 2012; Laffitte et al., 2014). The other way around, this may open new theraputical prospectives for the treatment of obesity related metabolic disfunctions (Laffitte et al., 2014; Workman et al., 2015; Maina et al., 2018).

HOW SUGARS AFFECT THE BRAIN

The ability to detect sugars is crucial in human nutrition as it orients food choice and energy intake. Sugars not only provide the energy necessary for metabolism, but also guide the behavior. Our preference for sugars is innate (Steiner et al., 2001), but affective responses to flavors are acquired based on experience

(Araujo et al., 2020), allowing the organism to learn which food is rich in energy. Further, sugar preference mediates attraction and reward mechanisms (for review Gutierrez et al., 2020). Thus, both nutritional and sensory properties regulate food intake.

Sugar preference and intake are controlled at least on three levels: gustation, gut-brain axis and brain-glucose sensing. The brain can sense glucose either directly or indirectly via oro- and visceral-sensation. Sensory, hedonic and metabolic values are encoded by separate brain circuitries working in parallel (Araujo et al., 2012) (for review Han et al., 2019; Gutierrez et al., 2020). Notably, preference for sugars does not seem to depend on its caloric content (Wright et al., 2011; Zukerman et al., 2013) nor on sweet taste receptors (Araujo et al., 2008; Ren et al., 2010; Oliveira-Maia et al., 2012; Tan et al., 2020), and even if food palatability affects what we eat, it does not influence how much we eat (Araujo, 2016). Rather, post-oral mechanisms are critical in controlling sugar intake and establishing long-term preference (Araujo, 2011). Therefore, different factors and pathways appear to regulate our preference for sugars on the one hand, and the amount of sugar consumption on the other hand.

Gustatory Representation

Consciously, sweetness can be perceived only upon activation of the sweet taste receptor in the oral cavity. Therefore, type II cells communicate with afferent gustatory fibers; these send the information, via several relay stations, up to the cortex (**Figure 2**; Ohla et al., 2019). How the taste quality is conveyed to the brain, is still a matter of debate. Yet, it is widely accepted that taste bud cells are hardwired to a defined behavior, i.e., not the identity of the taste receptor but of the perceiving cells determine the behavioral response. For example, when an opiate (Zhao et al., 2003) or a bitter-taste receptor (Mueller et al., 2005) was expressed in type II sweet-sensitive cells of mice, these transgenic animals were attracted by tasteless synthetic opiates or by bitter tastants, respectively. Thus, it was thought that sweet-responding taste bud cells respond only to this taste modality, however this view has been recently challenged by the discovery of broadly responding taste cells (Banik et al., 2018; Dutta Banik et al., 2020).

Afferent neurons may respond either to only one (best stimulus) or to multiple qualities (broadly tuned), and their tuning may vary according the stimulus concentration (Barretto et al., 2015; Wu et al., 2015). The cell bodies of the afferent neurons are located either in the geniculate, petrosal or nodose ganglia, projecting to the rostral portion of the solitary tract nucleus (rNTS) (Corson and Erisir, 2013). In human, the rNTS secondary neurons send their axons directly to the parvocellular portion of the Vetroposteromedial nucleus of the thalamus (VPMpc), while in rodents they make a first relay in the parabrachial nucleus (Samuelsen et al., 2013). From the thalamus, the information is conveyed to the primary gustatory cortex, called insula (IC), that further projects to the orbitofrontal cortex (for review Small, 2012; Ohla et al., 2019; **Figure 2**).

Electrophysiological and live-imaging experiments in rodents have shown that along the neural axis, both specialized and generalized neurons encode the sweet taste (Spector and Travers, 2005; Ohla et al., 2019). Moving toward higher brain centers, a growing percentage of neurons responds to multiple stimuli (broadly tuned). Here, combinatorial and temporal coding are crucial for taste decoding, thus the neuronal ensembles and their firing frequency pattern decode important gustatory information (Spector and Travers, 2005; Stapleton et al., 2007; Ohla et al., 2019). Accordingly, sweet taste intensity is decoded by neuronal firing frequency in the insular cortex and in the orbitofrontal cortex (Fonseca et al., 2018). In human, a gustatopic map has been recognized in the insula, where discrete regions were activated by oral exposure to a defined taste modality, and even the concentration intensity was represented by a spatial gradient (Prinster et al., 2017; Canna et al., 2019; Chikazoe et al., 2019; Porcu et al., 2020). On the contrary, other data support rather a distributed pattern of activity (Ohla et al., 2019; Porcu et al., 2020). Accordingly, no insular region revealed a consistent preference for a specific taste quality (Avery et al., 2020) and taste representation was not only highly variable across subjects (Schoenfeld et al., 2004; Avery et al., 2020), but also within subjects on different days (Avery et al., 2020). It is controversially discussed also for rodents whether the different taste modalities are encoded by topographically distinct cortical fields (Chen et al., 2011; Fletcher et al., 2017; for review Ohla et al., 2019). Optogenetic stimulation of the sweet responsive insular region induced increased licking of water in mice, suggesting that they perceived it as a sweet solution (Peng et al., 2015). Thus, the internal representation in the insula may underlie innate sweet preference. The insula not only encodes the chemical identity, but also the palatability of tastants (Araujo et al., 2006) and communicates with higher and lower-order neural relays, such as the striatum (Small et al., 2003; Oliveira-Maia et al., 2012) and the orbitofrontal cortex (Haase et al., 2008). Thus, as shown by electrophysiolgical recordings in mice, palatability is encoded by a widespread network including multiple brain regions (Parabrachial Nucleus, VPMpc, Basolateral Amygdala, Nucleus Accumbens Shell and lateral hypothalamic area) (for review Gutierrez et al., 2020). The coordinated action of these neural pathways motivates sugar intake. Furthermore, the insula preferentially interacts with the hypothalamus when the stimulus is nutritive (Rudenga et al., 2010). While it is still discussed whether the sweet taste itself can stimulate hunger (for review Low et al., 2014), sugars can induce attraction even in the absence of sweet taste receptor-mediated oral sensation, as shown with different ageusic transgenic mice (Nelson et al., 2001; Araujo et al., 2008; Sclafani et al., 2014). Oral sweet-sensing influences the initial food acceptance, but it does not determine the daily caloric intake (Glendinning et al., 2010; Ren et al., 2010). Other senses also influence sweet perception and hedonic value, via multisensory integration in the NST (Travers and Norgren, 1995), in the insula and in the orbitofrontal cortex (Rolls and Baylis, 1994) (for review Small, 2012). Sweet perception is additionally influenced by expectation (Veldhuizen et al., 2007), emotions (Noel and Dando, 2015), and metabolic state (Zhang et al., 2018).

Gut-Brain Axis

To feel pleasure and develop attraction to sugars, taste recognition needs to be integrated with energy-value sensing. Preference for a certain flavor develops only when its taste is

paired to post-ingestive reward signals (for review Kim et al., 2018; Gutierrez et al., 2020). Accordingly, mice develop a preference for sugars over non-caloric sweeteners within 48 h, when solutions, perceived equivalenty sweet, were provided (Tan et al., 2020). The mechanism involved is also responsible for sugar craving (Volkow et al., 2011). Sensing of the metabolic value occurs in the gastro-intestinal tract and/or the portal vein, both sending signals via vagal afferent fibers to the NTS and from here to upper brain centers. Specifically, in mice, proenkephaline-positive neurons of the caudal nucleus of the solitary tract (cNTS) were strongly activated by ingestion or intragastric application of sugars, but not of non-caloric sweeteners. This was mediated by vagal sensory neurons of the nodose ganglia receiving input from the duodenum and synapsing to cNTS excitatory neurons (Tan et al., 2020). Silencing these vagal afferents or the proenkephaline-positive neurons prevented the development of sugar preference, but left innate sweet attraction intact. Thus, innate sweet attraction and learned sugar preferences use different neural circuitries. Substrates of SGLT1, such as non-metabolizable 3-OMG and galactose, were also able to activate vagal sensory neurons in the intestine. The lack of responses to non-caloric sweeteners, fructose and mannose further supported the involvement of SGLT1, since they are no substrates of SGLT1 (Tan et al., 2020). Consistently, in SGLT1-deficient mice, flavor conditioning to glucose was impaired, while natural preference was not affected (Sclafani et al., 2016). Tan et al. further provided evidence that this neural circuitry in mice is involved in the development of novel preference: when a stimulus was paired with chemo-genetic activation of cNTS proenkephaline-neurons, it became the preferred stimulus, thus less sweet solutions were preferred over sweeter ones, while silencing their synaptic activity prevented the development of preference (Tan et al., 2020). However, non-caloric sweeteners failed to activate the post-oral reward circuitry and to induce incretin hormone release, that mediates CPIR and satiety signals (for review Pepino and Bourne, 2011; Low et al., 2014). The uncoupling of gustatory signal and metabolic value, that occurs with non-caloric sweeteners, seems to alter reward and satiation responses also in human (for review Han et al., 2019). This may explain some adverse effects of non-caloric sweeteners and why they are not so effective in reducing weight (Swithers and Davidson, 2008; Lohner et al., 2017). In summary, visceral signals regulate feeding independently of the sweet taste receptor and its downstream signaling (Araujo et al., 2008; Ren et al., 2010; Oliveira-Maia et al., 2012; Tan et al., 2020). Thus, although post-oral sugar sensing does not convey taste perception, it is important to develop preference and it activates also neurons in the cortical region responsible for gustation. Indeed, activation of the dorsal insula is required to develop sugar preference in ageusic mice (TRPM5-knockout) with a conditioning protocol (Oliveira-Maia et al., 2012). Recent evidence suggests that sweetness and nutritional signals engage distinct brain networks, to motivate ingestion, both in mice and in humans (Tellez et al., 2016; Thanarajah et al., 2019).

Indeed, a recent study in healthy subjects combined fMRI and PET imaging to show that orosensory and post-ingestive mechanisms underly two distinct peaks in dopamine and recruit segregated brain circutries. The first dopaminergic response involved the dorsal striatum, the mesolimbic system, the orosensory pathways and areas participating in reward value signaling, while the second, delayed response was visible in distinct regions, such as the amygdala and the caudate nucleus (Thanarajah et al., 2019). In mice, sweet tasting stimulated dopamine release in the ventral striatum, via projection of the ventral tegmental area, while nutritional visceral sensing induced dopamine release in the dorsal striatum from the Substantia Nigra pars compacta neurons (SNpc). Thus, mesolimbic and nigrostriatal pathways detected taste and food energy, respectively (Tellez et al., 2016). However, the level of dopamine released in both regions was dependent on glucose oxidation rates, and glucose induced higher dopamine release compared to isocaloric serine. Thus, carbohydrate-specific preference can develop independently of taste quality or caloric load. Rather, it is associated with the ability of the body to use carbohydrates as a fuel (Ren et al., 2010). Similar results were obtained in humans with fMRI imaging, showing that glucose metabolism was a critical signal for regulating NAc and hypothalamic responses to food cues, independently of flavor liking (Araujo et al., 2013). However, the exact pathway linking sweet visceral sensing to dopamine release in the brain still needs to be elucidated in humans.

Recently, a pathway connecting gut-chemosensation to brain reward-circuitries was proposed in mice. It involves vagal afferent fibers originating from the stomach and the duodenum, which project, via the right nodose ganglia, to the ventromedial area of the NTS. At the end, via further projections, the dopaminergic neurons of the SNpc are activated to release dopamine in the dorsal striatum (Han et al., 2018). However, it is unlikely that this pathway is activated by sugars, since subdiaphragmatic vagotomy did not alter the preference to glucose (Qu et al., 2019). Rather, the mesenteric portal system, which transports glucose from the proximal intestine to the liver, may be crucially involved in food preference acquisition. Mechanistically, this might involve glucose sensing via SGLT1 and GLUT2 followed by information transmission to upper neural stations (Berthoud, 2004; Zukerman et al., 2013; Sclafani et al., 2016; Zhang et al., 2019). Further, bypass surgery of obese people has brought evidence that the gut-brain axis regulates food reward and motivation to eat also in humans (for review Orellana et al., 2019). In Roux-en-Y gastric bypass (RYGB), a small pouch of the stomach is connected with a distal part of the small intestine. This surgery shows the higher efficacy in inducing large and permanent reductions in body weight. Notably, this is not only due to reduced volume and absorbtion of the ingested food, but also to neural and hormonal changes (Ochner et al., 2011; Goldstone et al., 2016; Kim et al., 2018; Tsouristakis et al., 2019). Presumably, both neural and hormonal mechanisms are responsible for the enhanced intake of healthy food as well as for the selective reduction of high-caloric food preference and of hunger, which are observed in RYGB patients (Nance et al., 2020). It appears, that such behavioral changes have a neural correlate. Indeed, RYGB seems to restore the balance in the dopaminergic reward systems, which is altered by overeating. In obese people, the availability of striatal dopaminergic D2R is reduced (Wang et al., 2001), while several prefrontal cortex

regions are overactivated upon meal consumption or exposure to food cues (Tomasi and Volkow, 2013) (for review Volkow et al., 2011). Conversely, RYGB reduces prefrontal cortex activation and may restore striatal D2R availability (Hamilton et al., 2018). In summary, postingestive sugar sensing is important for body homeostasis as well as sweet gustation, but the exact mechanisms underlying post-oral learned sugar preference still need to be elucidated.

Brain Glucose Sensing

Glucose is the preferred brain fuel. Substituting it with lactate, the major metabolic alternative for neurons, specifically impaired neuronal network activities that require high energy expenditure, such as gamma- and theta-oscillations (Hollnagel et al., 2020). Thus, only glucose supports optimal information processing in awake animals. In addition to this, some brain areas have specialized neurons working as "glucose sensors": their firing activity is indeed regulated by extracellular glucose levels. Possibly, these neurons are not activated by intracellular glucose metabolism, but rather by sensing extracellular glucose via the sweet taste receptor (Ren et al., 2009; Kohno, 2017). The genes of the sweet taste receptor subunits, *Tas1r2* and *Tas1r3*, and of the associated G-protein gustducin are active in several mammalian brain regions: most abundantly in the hypothalamus, but also in the hippocampus, the habenula, the cortex and the epithelial intraventricular cells of the choroid plexus (Ren et al., 2009).

The hypothalamus is a major regulator of energy balance, as it regulates food intake and metabolism (Kohno, 2017). Here, the first step in energy regulation, i.e., energy sensing, is executed by direct neuronal glucose sensing: some neurons respond to high glucose with excitation and some with inhibition (Fioramonti et al., 2007). It is still open, if this is directly linked to hunger induction, however, two hypothalamic neuronal populations might be particularly relevant in that context: AgRP (orexigenic neuropeptide Y/agouti-related peptide) and POMC (proopiomelanocortin) neurons located in the arcuate nuclei (ARC). Transition of AgRP neurons from active to inactive states was proportional to calories ingested, driving hunger and promoting food intake (Chen et al., 2016; Beutler et al., 2017). Via multiple downstream relay stations, AgRP neurons control also the neuronal activity in the insula, influencing food salience (Livneh et al., 2017). Conversely, POMC neuron activation led to suppression of appetite and food intake (Aponte et al., 2011). Several mechanisms have been described underlying these effects, some related to glucose metabolism and ATP production, and some independent of it, possibly mediated by the sweet taste receptor (for review see Kohno, 2017). Specifically, in the hypothalamus, T1R2 and T1R3 expression was regulated by the nutritional state: it was increased under food deprivation and decreased upon obesity (Ren et al., 2009). Mimicking this situation *in vitro*, exposure to a low glucose medium selectively promoted higher T1R2 expression in a mouse hypothalamic neuronal cell line, while hyperglycemic media reduced its expression, independently of glucose metabolism (Ren et al., 2009). The non-caloric sweetener sucralose regulated T1R2 expression as well, confirming a metabolism-independent pathway (Ren et al., 2009). Overall, this suggests that sweet taste receptor expression in hypothalamic neurons is under the control of ligand concentration and energy status. However, the regulation is bidirectional as activation of the sweet taste receptor in the ARC hypothalamic nuclei controls neuronal activity and, thus, food intake. In particular, mainly non-POMC leptine-responsive neurons in mice responded to high glucose and/or sucralose with Ca^{2+} increase that was mediated by the sweet taste receptor and L-type Ca^{2+} channels (Kohno et al., 2016). However, in 33% of these neurons the response was not blocked by gurmarine, which specifically interacts with gustducin to block sweet signal transduction, therefore additional mechanisms may be involved (Kohno et al., 2016). Further studies are required to unravel the neuronal types in the ARC that respond to glucose and their physiological role in controlling hunger and satiety.

In summary, sugars can motivate their consumption independently of their sweet taste. Paring signals arising from the tongue and from the gastrointestinal systems is a way to develop and reinforce preference for sugars. Reinforcement occurs when taste is coupled to nutritional value sensing, assuring that absorption, metabolism and energy production follow gustation.

THE JOURNEY OF UNRAVELING SWEET TASTE

The field of sweet gustation research can be divided in two eras: before and after the discovery of the sweet taste receptor (**Figure 3**). The cloning of the sweet taste receptor, which occurred at the beginning of this millenium, was the result of a longstanding research and opened new perspectives, new methods and new approaches (Temussi, 2006; von Molitor et al., 2020c).

However, investigation of sweet taste signal transduction has started already in the 70s (**Table 6**), long before the sweet taste receptor was identified. These studies revealed the involvement of the cAMP/PKA pathway in sweet transduction in different species (Kurihara and Koyama, 1972; Avenet and Lindemann, 1987; Tonosaki and Funakoshi, 1988). In the 90s, gustducin was discovered (McLaughlin et al., 1992; Takami et al., 1994) and it took further ∼10 years of intensive research to finally unravel the identity of the sweet taste receptor (Bachmanov et al., 2001; Kitagawa et al., 2001; Max et al., 2001; Montmayeur et al., 2001; Nelson et al., 2001; Li et al., 2002). This was followed by a boost of research which progressively uncovered the components of the PLCβ2/IP3 downstream-pathway. This was made possible by the parallel discoveries on bitter-mediated signaling (**Table 2**). Thus, many assumptions true for bitter transduction were transferred to sweet signaling, even if there were only weak or even contradictory evidences. At some point, it became a kind of common sense that sweet, bitter and umami receptors share a similar intracellular signaling mechanism, called "canonical pathway." Since bitter, sweet and umami receptors were found to be mainly expressed in different subgroups of type II cells, it was proposed that the specificity of the response is assured by the type of taste bud cell activated (Finger, 2005). Furthermore, sweet-responsive taste bud cells were shown to be hard-wired via a

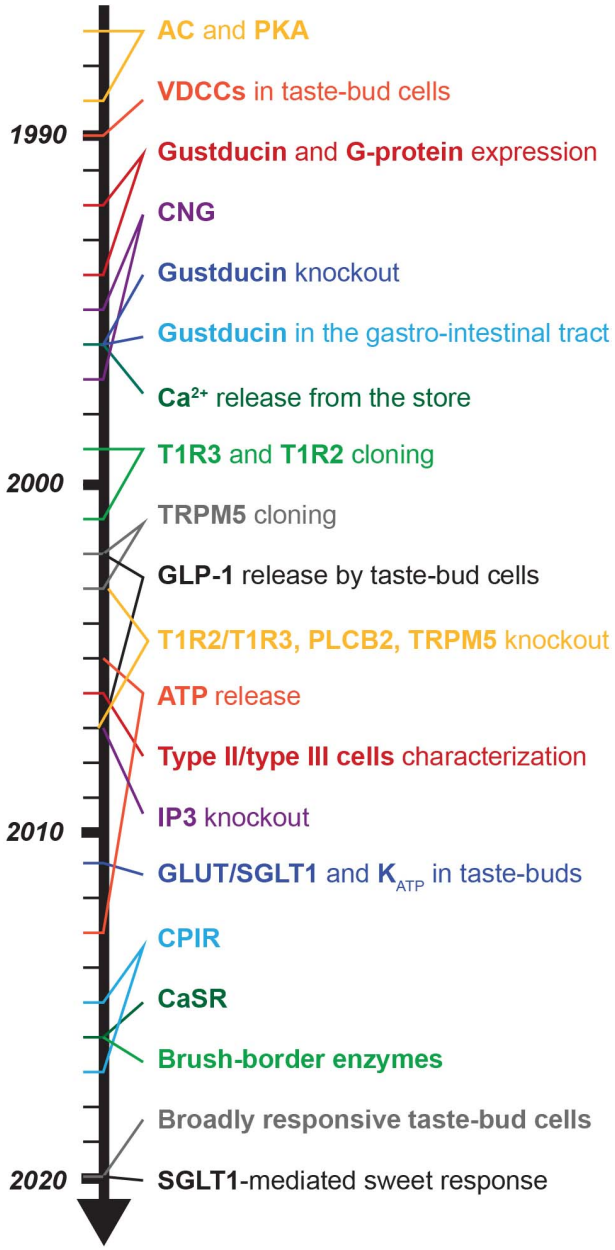

FIGURE 3 | Time-line of the most important findings in sweet taste signaling. The years of the most important publications are marked by lines. The scheme refers to findings related to sweet signaling transduction and focus mainly on the taste bud cells.

specific neural connection to a defined behavioral response (Zhao et al., 2003; Mueller et al., 2005). Thus, the first 10 years from the discovery of the sweet taste receptor were mainly dedicated to the characterization of the cell types (Finger, 2005; Clapp et al., 2006; DeFazio et al., 2006), the downstream molecules (**Table 2**) and the mechanism of taste bud cells communication (Finger et al., 2005; Huang et al., 2007; Taruno et al., 2013) with afferent fibers and neighboring cells. This reinforced the concept and the importance of the "canonical pathway," but it also marginalized the involvement of the cAMP/PKA-signaling and alternative viewpoints in sugar-mediated responses. A simplified interpretation of sweet taste coding in the taste buds was put forward: one-signaling mechanism and one-cell type (Zhao et al., 2003; Mueller et al., 2005).

However, it became increasingly clear that the picture was much more complicated. Knockout mice models for T1R2/T1R3 (Zhao et al., 2003) and its downstream molecules such as gustducin, PLCβ2 (Zhang et al., 2003), IP3R (Hisatsune et al., 2007), and TRMP5 (Zhang et al., 2003), verified their functional roles in sweet taste transduction, but residual responses to caloric sugars and not to non-caloric sweeteners (Damak et al., 2003) called for alternative mechanisms responsible for oral-mediated sweet gustation (Glendinning et al., 2015, 2017; Yasumatsu et al., 2020) (for review von Molitor et al., 2020c). In analogy to the mechanisms of glucose-sensing in extraoral tissue, some possible players, such as SGLT1, GLUT2, and K_{ATP} channels, have raised interest starting from the 2011 (Merigo et al., 2011; Yee et al., 2011), since they are expressed in taste bud cells, however their function is still debated (for review von Molitor et al., 2020c). Nonetheless, a physiological role was proposed for this alternative pathway, as it could be important to recognize the caloric value of food already in the mouth, and to drive CPIR (Glendinning et al., 2015, 2017). At the same time, sweet taste receptor expression was detected in many other organs (for review Yamamoto and Ishimaru, 2013; Laffitte et al., 2014). Since then, most publications have focused on studying taste transduction in extraoral tissues as they may offer new therapeutic possibilities. Accordingly, less projects still focus on fundamental sweet-signaling in taste bud cells, though there are still many open questions, even about the canonical signaling pathway. From the broad extraoral expression of sweet taste receptor, it became evident that the effects of sugars and non-caloric sweeteners are mediated not only by gustation, but also by sweet visceral-sensing (Araujo et al., 2008; Ren et al., 2010; Oliveira-Maia et al., 2012). Thus, for optimal energy homeostasis, glucose sensing in the tongue, intestine, pancreas and the brain need to be coordinated in order to drive the appropriate behavior. Recently, it was proposed that attraction to sugars is not only linked to conscious perception of sweetness, but also to visceral sugar-sensing, being especially relevant for the activation of reward circuitries and for learned sweet-preference (Kim et al., 2018; Han et al., 2019; Gutierrez et al., 2020). If this novel concept can be applied to human, it will challenge the whole interpretation of food-associated diseases, such as obesity and diabetes type II, and it will open new perspectives for their treatment (Neiers et al., 2016). We have also started to understand that non-caloric sweeteners, causing metabolic disregulation, increase the risk of these diseases (Renwick and Molinary, 2010; Pepino, 2015; Lohner et al., 2017). Consistently, extraoral sweet taste receptors are now in the focus of pharmaceutical industry (Sprous and Palmer, 2010). However, we should not stop investigating the sweet-signaling pathways in taste bud cells, since many questions are still open. Furthermore, discovering alternative sweet-sensitive taste mechanisms, their functional role and their ligands, may open the possibility to control energy homeostasis and our eating behavior already at the level of the

mouth. In this context, it will be important to develop new and more physiological *in vitro* models to study sweet taste transduction in human.

AUTHOR CONTRIBUTIONS

EM and TC contributed to conceptualization, writing, and visualization. KR, MH, and RR contributed to writing – review and editing and contributed to supervision. RR contributed to project administration. MH and RR contributed to funding acquisition. All authors have read and agreed to the published version of the manuscript.

FUNDING

This work was funded by the German Federal Ministry of Education and Research (BMBF) as part of the Innovation Partnership M^2Aind, project M^2OGA (03FH8I02IA) within the framework Starke Fachhochschulen–Impuls für die Region (FH-Impuls).

REFERENCES

Abaffy, T., Trubey, K. R., and Chaudhari, N. (2003). Adenylyl cyclase expression and modulation of cAMP in rat taste cells. *Am. J. Physiol. Cell Physiol.* 284:2002. doi: 10.1152/ajpcell.00556.2002

Abdoul-Azize, S., Selvakumar, S., Sadou, H., Besnard, P., and Khan, N. A. (2014). Ca2+ signaling in taste bud cells and spontaneous preference for fat: Unresolved roles of CD36 and GPR120. *Biochimie* 96, 8–13. doi: 10.1016/j.biochi.2013.06.005

Ahrén, B., and Holst, J. J. (2001). The cephalic insulin response to meal ingestion in humans is dependent on both cholinergic and noncholinergic mechanisms and is important for postprandial glycemia. *Diabetes* 50, 1030–1038. doi: 10.2337/diabetes.50.5.1030

Akabas, M. H., Dodd, J., and Al-Awqati, Q. (1988). A bitter substance induces a rise in intracellular calcium in a subpopulation of rat taste cells. *Science* 242, 1047–1050. doi: 10.1126/science.3194756

Aleman, M. G., Marconi, L. J., Nguyen, N. H., Park, J. M., Patino, M. M., Wang, Y., et al. (2016). The Influence of Assay Design, Blinding, and Gymnema sylvestre on Sucrose Detection by Humans. *J. Undergrad. Neurosci. Educ.* 15, A18–A23.

Antenucci, R. G., and Hayes, J. E. (2015). Nonnutritive sweeteners are not supernormal stimuli. *Int. J. Obes.* 39, 254–259. doi: 10.1038/ijo.2014.109

Aponte, Y., Atasoy, D., and Sternson, S. M. (2011). AGRP neurons are sufficient to orchestrate feeding behavior rapidly and without training. *Nat. Neurosci.* 14, 351–355. doi: 10.1038/nn.2739

Araujo, I. E. (2011). "Multiple reward layers in food reinforcement," in *Neurobiology of Sensation and Reward*, ed. J. A. Gottfried (Boca Raton, FL: CRC Press), 263–286.

Araujo, I. E. (2016). Circuit organization of sugar reinforcement. *Physiol. Behav.* 164, 473–477. doi: 10.1016/j.physbeh.2016.04.041

Araujo, I. E., Ferreira, J. G., Tellez, L. A., Ren, X., and Yeckel, C. W. (2012). The gut-brain dopamine axis: a regulatory system for caloric intake. *Physiol. Behav.* 106, 394–399. doi: 10.1016/j.physbeh.2012.02.026

Araujo, I. E., Gutierrez, R., Oliveira-Maia, A. J., Pereira, A., Nicolelis, M. A. L., and Simon, S. A. (2006). Neural ensemble coding of satiety states. *Neuron* 51, 483–494. doi: 10.1016/j.neuron.2006.07.009

Araujo, I. E., Lin, T., Veldhuizen, M. G., and Small, D. M. (2013). Metabolic regulation of brain response to food cues. *Curr. Biol.* 23, 878–883. doi: 10.1016/j.cub.2013.04.001

Araujo, I. E., Oliveira-Maia, A. J., Sotnikova, T. D., Gainetdinov, R. R., Caron, M. G., Nicolelis, M. A. L., et al. (2008). Food reward in the absence of taste receptor signaling. *Neuron* 57, 930–941. doi: 10.1016/j.neuron.2008.01.032

Araujo, I. E., Schatzker, M., and Small, D. M. (2020). Rethinking Food Reward. *Annu. Rev. Psychol.* 71, 139–164. doi: 10.1146/annurev-psych-122216-011643

Asano-Miyoshi, M., Abe, K., and Emori, Y. (2000). Co-expression of calcium signaling components in vertebrate taste bud cells. *Neurosci. Lett.* 283, 61–64. doi: 10.1016/S0304-3940(00)00911-3

Ashcroft, F. M. (2005). ATP-sensitive potassium channelopathies: focus on insulin secretion. *J. Clin. Invest.* 115, 2047–2058. doi: 10.1172/JCI25495

Ashcroft, F. M., Harrison, D. E., and Ashcroft, S. J. H. (1984). Glucose induces closure of single potassium channels in isolated rat pancreatic β -cells. *Nature* 312, 446–448.

Avenet, P., and Lindemann, B. (1987). Patch-clamp study of isolated taste receptor cells of the frog. *J. Membr. Biol.* 97, 223–240.

Avery, J. A., Liu, A. G., Ingeholm, J. E., Riddell, C. D., Gotts, S. J., and Martin, A. (2020). Taste Quality Representation in the Human Brain. *J. Neurosci.* 40, 1042–1052. doi: 10.1523/JNEUROSCI.1751-19.2019

Bachmanov, A. A., Bosak, N. P., Lin, C., Matsumoto, I., Ohmoto, M., Reed, D. R., et al. (2014). Genetics of taste receptors. *Curr. Pharm. Des.* 20, 2669–2683. doi: 10.2174/13816128113199990566

Bachmanov, A. A., Li, X., Reed, D. R., Ohmen, J. D., Li, S., Chen, Z., et al. (2001). Positional cloning of the mouse saccharin preference (Sac) locus. *Chem. Senses* 26, 925–933. doi: 10.1093/chemse/26.7.925

Bachmanov, A. A., Reed, D. R., Ninomiya, Y., Inoue, M., Tordoff, M. G., Price, R. A., et al. (1997). Sucrose consumption in mice: major influence of two genetic loci affecting peripheral sensory responses. *Mamm. Genome* 8, 545–548. doi: 10.1007/s003359900500

Banik, D. D., Martin, L. E., Freichel, M., Torregrossa, A.-M., et al. (2018). TRPM4 and TRPM5 are both required for normal signaling in taste receptor cells. *Proc. Natl. Acad. Sci. U S A.* 115, E772–E781. doi: 10.1073/pnas.1718802115

Barlow, L. A. (2015). Progress and renewal in gustation: New insights into taste bud development. *Development* 142, 3620–3629. doi: 10.1242/dev.120394

Barretto, R. P. J., Gillis-Smith, S., Chandrashekar, J., Yarmolinsky, D. A., Schnitzer, M. J., Ryba, N. J. P., et al. (2015). The neural representation of taste quality at the periphery. *Nature* 517, 373–376. doi: 10.1038/nature13873

Beauchamp, G. K., and Mennella, J. A. (2011). Flavor perception in human infants: development and functional significance. *Digestion* 83(Suppl. 1), 1–6. doi: 10.1159/000323397

Béhé, P., DeSimone, J. A., Avenet, P., and Lindemann, B. (1990). Membrane currents in taste cells of the rat fungiform papilla. Evidence for two types of Ca currents and inhibition of K currents by saccharin. *J. Gen. Physiol.* 96, 1061–1084. doi: 10.1085/jgp.96.5.1061

Bernhardt, S. J., Naim, M., Zehavi, U., and Lindemann, B. (1996). Changes in IP3 and cytosolic Ca2+ in response to sugars and non-sugar sweeteners in transduction of sweet taste in the rat. *J. Physiol.* 490(Pt 2), 325–336. doi: 10.1113/jphysiol.1996.sp021147

Berthoud, H. R., Trimble, E. R., Siegel, E. G., Bereiter, D. A., and Jeanrenaud, B. (1980). Cephalic-phase insulin secretion in normal and pancreatic islet-transplanted rats. *Am. J. Physiol.* 238, E336–E340. doi: 10.1152/ajpendo.1980.238.4.E336

Berthoud, H.-R. (2004). Anatomy and function of sensory hepatic nerves. *Anat. Rec. A Discov. Mol. Cell Evol. Biol.* 280, 827–835. doi: 10.1002/ar.a.20088

Best, L., Brown, P. D., Sener, A., and Malaisse, W. J. (2010). Electrical activity in pancreatic islet cells: The VRAC hypothesis. *Islets* 2, 59–64. doi: 10.4161/isl.2.2.11171

Beutler, L. R., Chen, Y., Ahn, J. S., Lin, Y.-C., Essner, R. A., and Knight, Z. A. (2017). Dynamics of Gut-Brain Communication Underlying Hunger. *Neuron* 96, 461.e–475.e. doi: 10.1016/j.neuron.2017.09.043

Bezençon, C., Fürholz, A., Raymond, F., Mansourian, R., Métairon, S., Le Coutre, J., et al. (2008). Murine intestinal cells expressing Trpm5 are mostly brush cells and express markers of neuronal and inflammatory cells. *J. Comp. Neurol.* 509, 514–525. doi: 10.1002/cne.21768

Bezençon, C., Le Coutre, J., and Damak, S. (2007). Taste-signaling proteins are coexpressed in solitary intestinal epithelial cells. *Chem. Senses* 32, 41–49. doi: 10.1093/chemse/bjl034

Borges, M. C., Louzada, M. L., Sá, T. H., Laverty, A. A., Parra, D. C., Garzillo, J. M. F., et al. (2017). Artificially Sweetened Beverages and the Response to the Global Obesity Crisis. *PLoS Med.* 14:e1002195. doi: 10.1371/journal.pmed.1002195

Boring, E. G. (1942). *Sensation and perception in the history of experimental psychology*. New York,NY: Irvington Pub.

Boughter, J. D. Jr., Pumplin, D. W., Yu, C., Christy, R. C., and Smith, D. V. (1997). Differential Expression of α -Gustducin in Taste Bud Populations of the Rat and Hamster. *J. Neurosci.* 17, 2852–2858. doi: 10.1523/JNEUROSCI.17-08-02852.1997

Bradley, J., Reisert, J., and Frings, S. (2005). Regulation of cyclic nucleotide-gated channels. *Curr. Opin. Neurobiol.* 15, 343–349. doi: 10.1016/j.conb.2005.05.014

Bray, G. A., and Popkin, B. M. (2014). Dietary sugar and body weight: Have we reached a crisis in the epidemic of obesity and diabetes? health be damned! Pour on the sugar. *Diabetes Care* 37, 950–956. doi: 10.2337/dc13-2085

Brubaker, P. L. (2017). Species-Dependent Mechanisms Regulating Glucose-Dependent GLP-1 Secretion? *Diabetes* 66, 2063–2065. doi: 10.2337/dbi17-0020

Bundesinstitut für Riskobewertung (2014). *Bewertung von Süßstoffen und Zuckeraustauschstoffen*. Berlin: Bundesinstitut für Riskobewertung.

Bystrova, M. F., Romanov, R. A., Rogachevskaja, O. A., Churbanov, G. D., and Kolesnikov, S. S. (2010). Functional expression of the extracellular-Ca2+-sensing receptor in mouse taste cells. *J. Cell Sci.* 123, 972–982. doi: 10.1242/jcs.061879

Canna, A., Prinster, A., Cantone, E., Ponticorvo, S., Russo, A. G., Di Salle, F., et al. (2019). Intensity-related distribution of sweet and bitter taste fMRI responses in the insular cortex. *Hum. Brain Mapp.* 40, 3631–3646. doi: 10.1002/hbm.24621

Capeless, C. G., and Whitney, G. (1995). The genetic basis of preference for sweet substances among inbred strains of mice: preference ratio phenotypes and the alleles of the Sac and dpa loci. *Chem. Senses* 20, 291–298. doi: 10.1093/chemse/20.3.291

Chambers, A. P., Sorrell, J. E., Haller, A., Roelofs, K., Hutch, C. R., Kim, K.-S., et al. (2017). The Role of Pancreatic Preproglucagon in Glucose Homeostasis in Mice. *Cell Metab.* 25, 927.e–934.e. doi: 10.1016/j.cmet.2017.02.008

Chambers, E. S., Bridge, M. W., and Jones, D. A. (2009). Carbohydrate sensing in the human mouth: effects on exercise performance and brain activity. *J. Physiol.* 587, 1779–1794. doi: 10.1113/jphysiol.2008.164285

Chattopadhyay, N., Vassilev, P. M., and Brown, E. M. (eds) (1997). Calcium-sensing receptor: roles in and beyond systemic calcium homeostasis. *Biol. Chem.* 378, 759–768.

Chaudhari, N., and Roper, S. D. (2010). The cell biology of taste. *J. Cell Biol.* 190, 285–296. doi: 10.1083/jcb.201003144

Chen, X., Gabitto, M., Peng, Y., Ryba, N. J. P., and Zuker, C. S. (2011). A gustotopic map of taste qualities in the mammalian brain. *Science* 333, 1262–1266. doi: 10.1126/science.1204076

Chen, Y., Lin, Y.-C., Zimmerman, C. A., Essner, R. A., and Knight, Z. A. (2016). Hunger neurons drive feeding through a sustained, positive reinforcement signal. *Elife* 5:18640. doi: 10.7554/eLife.18640

Chikazoe, J., Lee, D. H., Kriegeskorte, N., and Anderson, A. K. (2019). Distinct representations of basic taste qualities in human gustatory cortex. *Nat. Commun.* 10:1048. doi: 10.1038/s41467-019-08857-z

Choi, H.-J., Cho, Y.-K., Chung, K.-M., and Kim, K.-N. (2016). Differential expression of taste receptors in tongue papillae of DBA mouse. *Int. J. Oral Biol.* 41, 25–32.

Chow, K. F. (2017). A review of excessive sugar metabolism on oral and general health. *Chin. J. Dent. Res.* 20, 193–198.

Clapp, T. R., Medler, K. F., Damak, S., Margolskee, R. F., and Kinnamon, S. C. (2006). Mouse taste cells with G protein-coupled taste receptors lack voltage-gated calcium channels and SNAP-25. *BMC Biol.* 4:7. doi: 10.1186/1741-7007-4-7

Clapp, T. R., Stone, L. M., Margolskee, R. F., and Kinnamon, S. C. (2001). Immunocytochemical evidence for co-expression of Type III IP3receptor with signaling components of bitter taste transduction. *BMC Neurosci.* 2:6. doi: 10.1186/1471-2202-2-6

Clapp, T. R., Trubey, K. R., Vandenbeuch, A., Stone, L. M., Margolskee, R. F., Chaudhari, N., et al. (2008). Tonic activity of Galpha-gustducin regulates taste cell responsivity. *FEBS Lett.* 582, 3783–3787. doi: 10.1016/j.febslet.2008.10.007

Collings, V. B. (1974). Human taste response as a function of locus of stimulation on the tongue and soft palate. *Percept. Psychophys.* 16, 169–174. doi: 10.3758/BF03203270

Colsoul, B., Schraenen, A., Lemaire, K., Quintens, R., van Lommel, L., Segal, A., et al. (2010). Loss of high-frequency glucose-induced Ca2+ oscillations in pancreatic islets correlates with impaired glucose tolerance in Trpm5-/- mice. *Proc. Natl. Acad. Sci. U S A.* 107, 5208–5213. doi: 10.1073/pnas.0913107107

Cook, D. L., and Hales, C. N. (1984). Intracellular ATP directly blocks K+ channels in pancreatic B-cells. *Nature* 311, 271–273. doi: 10.1038/311271a0

Corson, J. A., and Erisir, A. (2013). Monosynaptic convergence of chorda tympani and glossopharyngeal afferents onto ascending relay neurons in the nucleus of the solitary tract: a high-resolution confocal and correlative electron microscopy approach. *J. Comp. Neurol.* 521, 2907–2926. doi: 10.1002/cne.23357

Cummings, T. A., Powell, J., and Kinnamon, S. C. (1993). Sweet taste transduction in hamster taste cells: Evidence for the role of cyclic nucleotides. *J. Neurophysiol.* 70, 2326–2336. doi: 10.1152/jn.1993.70.6.2326

Damak, S., Rong, M., Yasumatsu, K., Kokrashvili, Z., Pérez, C. A., Shigemura, N., et al. (2006). Trpm5 null mice respond to bitter, sweet, and umami compounds. *Chem. Senses* 31, 253–264. doi: 10.1093/chemse/bjj027

Damak, S., Rong, M., Yasumatsu, K., Kokrashvili, Z., Varadarajan, V., Zou, S., et al. (2003). Detection of sweet and umami taste in the absence of taste receptor T1r3. *Science* 301, 850–853. doi: 10.1126/science.1087155

Danilova, V., and Hellekant, G. (2003). Comparison of the responses of the chorda tympani and glossopharyngeal nerves to taste stimuli in C57BL/6J mice. *BMC Neurosci.* 4:5. doi: 10.1186/1471-2202-4-5

Danilova, V., Damak, S., Margolskee, R. F., and Hellekant, G. (2006). Taste responses to sweet stimuli in alpha-gustducin knockout and wild-type mice. *Chem. Senses* 31, 573–580. doi: 10.1093/chemse/bjj062

Dastur, D. K. (1961). The relationship between terminal lingual innervation and gustation. A clinical and histological study. *Brain* 84, 499–513. doi: 10.1093/brain/84.3.499

Douard, V., and Ferraris, R. P. (2008). Regulation of the fructose transporter GLUT5 in health and disease. *Am. J. Physiol. Endocrinol. Metab.* 295, E227–E237. doi: 10.1152/ajpendo.90245.2008

Dawson, P. A., Mychaleckyj, J. C., Fossey, S. C., Mihic, S. J., Craddock, A. L., and Bowden, D. W. (2001). Sequence and functional analysis of GLUT10: a glucose transporter in the Type 2 diabetes-linked region of chromosome 20q12-13.1. *Mol. Genet. Metab.* 74, 186–199. doi: 10.1006/mgme.2001.3212

DeFazio, R. A., Dvoryanchikov, G., Maruyama, Y., Kim, J. W., Pereira, E., Roper, S. D., et al. (2006). Separate populations of receptor cells and presynaptic cells in mouse taste buds. *J. Neurosci.* 26, 3971–3980. doi: 10.1523/JNEUROSCI.0515-06.2006

Deng, D., and Yan, N. (2016). GLUT, SGLT, and SWEET: Structural and mechanistic investigations of the glucose transporters. *Protein Sci.* 25, 546–558. doi: 10.1002/pro.2858

Deuschle, K., Okumoto, S., Fehr, M., Looger, L. L., Kozhukh, L., and Frommer, W. B. (2005). Construction and optimization of a family of genetically encoded metabolite sensors by semirational protein engineering. *Protein Sci.* 14, 2304–2314. doi: 10.1110/ps.051508105

Dhillon, J., Lee, J. Y., and Mattes, R. D. (2017). The cephalic phase insulin response to nutritive and low-calorie sweeteners in solid and beverage form. *Physiol. Behav.* 181, 100–109. doi: 10.1016/j.physbeh.2017.09.009

DiNicolantonio, J. J., O'Keefe, J. H., and Wilson, W. L. (2018). Sugar addiction: is it real? A narrative review. *Br. J. Sports Med.* 52, 910–913. doi: 10.1136/bjsports-2017-097971

Doblado, M., and Moley, K. H. (2009). Facilitative glucose transporter 9, a unique hexose and urate transporter. *Am. J. Physiol. Endocrinol. Metab.* 297, E831–E835. doi: 10.1152/ajpendo.00296.2009

Dotson, C. D., Geraedts, M. C. P., and Munger, S. D. (2013). Peptide regulators of peripheral taste function. *Semin. Cell Dev. Biol.* 24, 232–239. doi: 10.1016/j.semcdb.2013.01.004

Dotson, C. D., Roper, S. D., and Spector, A. C. (2005). PLCbeta2-independent behavioral avoidance of prototypical bitter-tasting ligands. *Chem. Senses* 30, 593–600. doi: 10.1093/chemse/bji053

Dramane, G., Abdoul-Azize, S., Hichami, A., Vögtle, T., Akpona, S., Chouabe, C., et al. (2012). STIM1 regulates calcium signaling in taste bud cells and preference for fat in mice. *J. Clin. Invest.* 122, 2267–2282. doi: 10.1172/JCI59953

DuBois, G. E. (2016). Molecular mechanism of sweetness sensation. *Physiol. Behav.* 164, 453–463. doi: 10.1016/j.physbeh.2016.03.015

DuBois, G. E., Orthoefer, F. T., and Walters, D. E. (1991). *Sweeteners: Discovery, Molecular Design, and Chemoreception: Developed from a Symposium Sponsored by the Division of Agricultural and Food Chemistry at the 199th National Meeting of the American Chemical Society, Boston, Massachusetts, April 22-27, 1990*. Boston: American Chemical Society.

Dušková, M., Macourek, M., Šrámková, M., Hill, M., and Stárka, L. (2013). The role of taste in cephalic phase of insulin secretion. *Prague Med. Rep.* 114, 222–230. doi: 10.14712/23362936.2014.11

Dutta Banik, D., Benfey, E. D., Martin, L. E., Kay, K. E., Loney, G. C., Nelson, A. R., et al. (2020). A subset of broadly responsive Type III taste cells contribute to the detection of bitter, sweet and umami stimuli. *PLoS Genet.* 16:e1008925. doi: 10.1371/journal.pgen.1008925

Dyer, J., Salmon, K. S. H., Zibrik, L., and Shirazi-Beechey, S. P. (2005). Expression of sweet taste receptors of the T1R family in the intestinal tract and enteroendocrine cells. *Biochem. Soc. Trans.* 33, 302–305. doi: 10.1042/BST0330302

Eddy, M. C., Eschle, B. K., Peterson, D., Lauras, N., Margolskee, R. F., and Delay, E. R. (2012). A conditioned aversion study of sucrose and SC45647 taste in TRPM5 knockout mice. *Chem. Senses* 37, 391–401. doi: 10.1093/chemse/bjr093

Elliott, R. A., Kapoor, S., and Tincello, D. G. (2011). Expression and distribution of the sweet taste receptor isoforms T1R2 and T1R3 in human and rat bladders. *J. Urol.* 186, 2455–2462. doi: 10.1016/j.juro.2011.07.083

Eriksson, L., Esberg, A., Haworth, S., Holgerson, P. L., and Johansson, I. (2019). Allelic Variation in Taste Genes Is Associated with Taste and Diet Preferences and Dental Caries. *Nutrients* 11:nu1107149. doi: 10.3390/nu11071491

Feigin, M. B., Sclafani, A., and Sunday, S. R. (1987). Species differences in polysaccharide and sugar taste preferences. *Neurosci. Biobehav. Rev.* 11, 231–240. doi: 10.1016/S0149-7634(87)80031-3

Feng, X.-H., Liu, X.-M., Zhou, L.-H., Wang, J., and Liu, G.-D. (2008). Expression of glucagon-like peptide-1 in the taste buds of rat circumvallate papillae. *Acta Histochem.* 110, 151–154. doi: 10.1016/j.acthis.2007.10.005

Finger, T. E. (2005). Cell types and lineages in taste buds. *Chem. Senses* 30(Suppl. 1), i54–i55. doi: 10.1093/chemse/bjh110

Finger, T. E., Böttger, B., Hansen, A., Anderson, K. T., Alimohammadi, H., and Silver, W. L. (2003). Solitary chemoreceptor cells in the nasal cavity serve as sentinels of respiration. *Proc. Natl. Acad. Sci. U S A.* 100, 8981–8986. doi: 10.1073/pnas.1531172100

Finger, T. E., Danilova, V., Barrows, J., Bartel, D. L., Vigers, A. J., Stone, L., et al. (2005). ATP signaling is crucial for communication from taste buds to gustatory nerves. *Science* 310, 1495–1499. doi: 10.1126/science.1118435

Fioramonti, X., Contié, S., Song, Z., Routh, V. H., Lorsignol, A., and Pénicaud, L. (2007). Characterization of glucosensing neuron subpopulations in the arcuate nucleus: integration in neuropeptide Y and pro-opio melanocortin networks? *Diabetes* 56, 1219–1227. doi: 10.2337/db06-0567

Fletcher, M. L., Ogg, M. C., Lu, L., Ogg, R. J., and Boughter, J. D. (2017). Overlapping Representation of Primary Tastes in a Defined Region of the Gustatory Cortex. *J. Neurosci.* 37, 7595–7605. doi: 10.1523/JNEUROSCI.0649-17.2017

Fonseca, E., Lafuente, V., Simon, S. A., and Gutierrez, R. (2018). Sucrose intensity coding and decision-making in rat gustatory cortices. *Elife* 7:41152. doi: 10.7554/eLife.41152

Frank, G. K. W., Oberndorfer, T. A., Simmons, A. N., Paulus, M. P., Fudge, J. L., Yang, T. T., et al. (2008). Sucrose activates human taste pathways differently from artificial sweetener. *Neuroimage* 39, 1559–1569. doi: 10.1016/j.neuroimage.2007.10.061

Fuller, J. L. (1974). Single-locus control of saccharin preference in mice. *J. Hered.* 65, 33–36. doi: 10.1093/oxfordjournals.jhered.a108452

Fushan, A. A., Simons, C. T., Slack, J. P., and Drayna, D. (2010). Association between common variation in genes encoding sweet taste signaling components and human sucrose perception. *Chem. Senses* 35, 579–592. doi: 10.1093/chemse/bjq063

Galindo-Cuspinera, V., Winnig, M., Bufe, B., Meyerhof, W., and Breslin, P. A. S. (2006). A TAS1R receptor-based explanation of sweet 'water-taste'. *Nature* 441, 354–357.

Gardner, A., and Carpenter, G. H. (2019). Anatomical stability of human fungiform papillae and relationship with oral perception measured by salivary response and intensity rating. *Sci. Rep.* 9:9759. doi: 10.1038/s41598-019-46093-z

Geraedts, M. C. P., Takahashi, T., Vigues, S., Markwardt, M. L., Nkobena, A., Cockerham, R. E., et al. (2012). Transformation of postingestive glucose responses after deletion of sweet taste receptor subunits or gastric bypass surgery. *Am. J. Physiol. Endocrinol. Metab.* 303, E464–E474. doi: 10.1152/ajpendo.00163.2012

Gilbertson, T. A., and Khan, N. A. (2014). Cell signaling mechanisms of oro-gustatory detection of dietary fat: Advances and challenges. *Progress Lipid Res.* 53, 82–92. doi: 10.1016/j.plipres.2013.11.001

Glendinning, J. I., Beltran, F., Benton, L., Cheng, S., Gieseke, J., Gillman, J., et al. (2010). Taste does not determine daily intake of dilute sugar solutions in mice. *Am. J. Physiol. Regul. Integr. Comp. Physiol.* 299:2010. doi: 10.1152/ajpregu.00331.2010

Glendinning, J. I., Bloom, L. D., Onishi, M., Zheng, K. H., Damak, S., Margolskee, R. F., et al. (2005). Contribution of alpha-gustducin to taste-guided licking responses of mice. *Chem. Senses* 30, 299–316. doi: 10.1093/chemse/bji025

Glendinning, J. I., Frim, Y. G., Hochman, A., Lubitz, G. S., Basile, A. J., and Sclafani, A. (2017). Glucose elicits cephalic-phase insulin release in mice by activating KATP channels in taste cells. *Am. J. Physiol. Regul. Integr. Comp. Physiol.* 312, R597–R610. doi: 10.1152/ajpregu.00433.2016

Glendinning, J. I., Stano, S., Holter, M., Azenkot, T., Goldman, O., Margolskee, R. F., et al. (2015). Sugar-induced cephalic-phase insulin release is mediated by a T1r2+T1r3-independent taste transduction pathway in mice. *Am. J. Physiol. Regul. Integr. Comp. Physiol.* 309, R552–R560. doi: 10.1152/ajpregu.00056.2015

Goldfine, I. D., Ryan, W. G., and Schwartz, T. B. (1969). The effect of glucola, diet cola and water ingestion on blood glucose and plasma insulin. *Proc. Soc. Exp. Biol. Med.* 131, 329–330. doi: 10.3181/00379727-131-33870

Goldstone, A. P., Miras, A. D., Scholtz, S., Jackson, S., Neff, K. J., Pénicaud, L., et al. (2016). Link Between Increased Satiety Gut Hormones and Reduced Food Reward After Gastric Bypass Surgery for Obesity. *J. Clin. Endocrinol. Metab.* 101, 599–609. doi: 10.1210/jc.2015-2665

Gong, T., Wei, Q., Mao, D., and Shi, F. (2016). Expression patterns of taste receptor type 1 subunit 3 and α -gustducin in the mouse testis during development. *Acta Histochem.* 118, 20–30. doi: 10.1016/j.acthis.2015.11.001

Gutierrez, R., Fonseca, E., and Simon, S. A. (2020). The neuroscience of sugars in taste, gut-reward, feeding circuits, and obesity. *Cell Mol. Life Sci.* 77, 3469–3502. doi: 10.1007/s00018-020-03458-2

Haase, L., Cerf-Ducastel, B., and Murphy, C. (2008). Cortical Activation in Response to Pure Taste Stimuli During the Physiological States of Hunger and Satiety. *Neuroimage* 44, 1008–1021. doi: 10.1016/j.neuroimage.2008.09.044

Hacker, K., and Medler, K. F. (2008). Mitochondrial calcium buffering contributes to the maintenance of Basal calcium levels in mouse taste cells. *J. Neurophysiol.* 100, 2177–2191. doi: 10.1152/jn.90534.2008

Hamilton, J., Swenson, S., Hajnal, A., and Thanos, P. K. (2018). Roux-en-Y gastric bypass surgery normalizes dopamine D1, D2, and DAT levels. *Synapse* 2018:22058. doi: 10.1002/syn.22058

Han, P., Bagenna, B., and Fu, M. (2019). The sweet taste signalling pathways in the oral cavity and the gastrointestinal tract affect human appetite and food intake: a review. *Int. J. Food Sci. Nutr.* 70, 125–135. doi: 10.1080/09637486.2018.1492522

Han, W., Tellez, L. A., Perkins, M. H., Perez, I. O., Qu, T., Ferreira, J., et al. (2018). A Neural Circuit for Gut-Induced Reward. *Cell* 175, 665.e–678.e. doi: 10.1016/j.cell.2018.08.049

Hanig, D. P. (1901). *Zur Psychophysik des Geschmackssinnes.* Wiesloch: Engelmann.

Hass, N., Schwarzenbacher, K., and Breer, H. (2007). A cluster of gustducin-expressing cells in the mouse stomach associated with two distinct populations of enteroendocrine cells. *Histochem. Cell Biol.* 128, 457–471.

Hass, N., Schwarzenbacher, K., and Breer, H. (2010). T1R3 is expressed in brush cells and ghrelin-producing cells of murine stomach. *Cell Tissue Res.* 339, 493–504. doi: 10.1007/s00441-009-0907-6

He, W., Danilova, V., Zou, S., Hellekant, G., Max, M., Margolskee, R. F., et al. (2002). Partial rescue of taste responses of alpha-gustducin null mice by transgenic expression of alpha-transducin. *Chem. Senses* 27, 719–727. doi: 10.1093/chemse/27.8.719

Hellekant, G. (1976). On the gustatory effects of gymnemic acid and miraculin in dog, pig and rabbit. *Chem. Senses* 2, 85–95. doi: 10.1093/chemse/2.1.85

Hellekant, G., Danilova, V., and Ninomiya, Y. (1997). Primate sense of taste: behavioral and single chorda tympani and glossopharyngeal nerve fiber recordings in the rhesus monkey. *Macaca Mulatta*. *J. Neurophysiol.* 77, 978–993. doi: 10.1152/jn.1997.77.2.978

Hellekant, G., DuBois, G. E., Roberts, T. W., and van der Wel, H. (1988). On the gustatory effect of amiloride in the monkey (Macaca mulatto). *Chem. Senses* 13, 89–93. doi: 10.1093/chemse/13.1.89

Hevezi, P., Moyer, B. D., Lu, M., Gao, N., White, E., Echeverri, F., et al. (2009). Genome-wide analysis of gene expression in primate taste buds reveals links to diverse processes. *PLoS One* 4:e6395. doi: 10.1371/journal.pone.0006395

Hisatsune, C., Yasumatsu, K., Takahashi-Iwanaga, H., Ogawa, N., Kuroda, Y., Yoshida, R., et al. (2007). Abnormal taste perception in mice lacking the type 3 inositol 1,4,5-trisphosphate receptor. *J. Biol. Chem.* 282, 37225–37231. doi: 10.1074/jbc.M705641200

Hochheimer, A., Krohn, M., Rudert, K., Riedel, K., Becker, S., Thirion, C., et al. (2014). Endogenous gustatory responses and gene expression profile of stably proliferating human taste cells isolated from fungiform papillae. *Chem. Senses* 39, 359–377. doi: 10.1093/chemse/bju009

Höfer, D., Püschel, B., and Drenckhahn, D. (1996). Taste receptor-like cells in the rat gut identified by expression of alpha-gustducin. *Proc. Natl. Acad. Sci. U S A.* 93, 6631–6634. doi: 10.1073/pnas.93.13.6631

Hollnagel, J.-O., Cesetti, T., Schneider, J., Vazetdinova, A., Valiullina-Rakhmatullina, F., Lewen, A., et al. (2020). Lactate Attenuates Synaptic Transmission and Affects Brain Rhythms Featuring High Energy Expenditure. *iScience* 23:101316. doi: 10.1016/j.isci.2020.101316

Hoon, M. A., Adler, E., Lindemeier, J., Battey, J. F., Ryba, N. J., and Zuker, C. S. (1999). Putative Mammalian Taste Receptors: A Class of Taste-Specific GPCRs with Distinct Topographic Selectivity. *Cell* 96, 541–551. doi: 10.1016/S0092-8674(00)80658-3

Hoon, M. A., Northup, J. K., Margolskee, R. F., and Ryba, N. J. (1995). Functional expression of the taste specific G-protein, alpha-gustducin. *Biochem. J.* 309(Pt 2), 629–636. doi: 10.1042/bj3090629

Huang, L., Shanker, Y. G., Dubauskaite, J., Zheng, J. Z., Yan, W., Rosenzweig, S., et al. (1999). Ggamma13 colocalizes with gustducin in taste receptor cells and mediates IP3 responses to bitter denatonium. *Nat. Neurosci.* 2, 1055–1062. doi: 10.1038/15981

Huang, S., and Czech, M. P. (2007). The GLUT4 glucose transporter. *Cell Metab.* 5, 237–252. doi: 10.1016/j.cmet.2007.03.006

Huang, Y.-J., Maruyama, Y., Dvoryanchikov, G., Pereira, E., Chaudhari, N., and Roper, S. D. (2007). The role of pannexin 1 hemichannels in ATP release and cell-cell communication in mouse taste buds. *Proc. Natl. Acad. Sci. U S A.* 104, 6436–6441. doi: 10.1073/pnas.0611280104

Hwang, L.-D., Lin, C., Gharahkhani, P., Cuellar-Partida, G., Ong, J.-S., An, J., et al. (2019). New insight into human sweet taste: a genome-wide association study of the perception and intake of sweet substances. *Am. J. Clin. Nutr.* 109, 1724–1737. doi: 10.1093/ajcn/nqz043

Hwang, P. M., Verma, A., Bredt, D. S., and Snyder, S. H. (1990). Localization of phosphatidylinositol signaling components in rat taste cells: Role in bitter taste transduction. *Proc. Natl. Acad. Sci. U S A.* 87, 7395–7399. doi: 10.1073/pnas.87.19.7395

Inagaki, N., Gonoi, T., Clement, J. P., Namba, N., Inazawa, J., Gonzalez, G., et al. (1995). Reconstitution of IKATP: an inward rectifier subunit plus the sulfonylurea receptor. *Science* 270, 1166–1170. doi: 10.1126/science.270.5239.1166

Jang, H.-J., Kokrashvili, Z., Theodorakis, M. J., Carlson, O. D., Kim, B.-J., Zhou, J., et al. (2007). Gut-expressed gustducin and taste receptors regulate secretion of glucagon-like peptide-1. *Proc. Natl. Acad. Sci. U S A.* 104, 15069–15074. doi: 10.1073/pnas.0706890104

Janssen, S., Laermans, J., Verhulst, P.-J., Thijs, T., Tack, J., and Depoortere, I. (2011). Bitter taste receptors and α -gustducin regulate the secretion of ghrelin with functional effects on food intake and gastric emptying. *Proc. Natl. Acad. Sci. U S A.* 108, 2094–2099. doi: 10.1073/pnas.1011508108

Jiang, P., Cui, M., Zhao, B., Liu, Z., Snyder, L. A., Benard, L. M. J., et al. (2005). Lactisole interacts with the transmembrane domains of human T1R3 to inhibit sweet taste. *J. Biol. Chem.* 280, 15238–15246. doi: 10.1074/jbc.M414287200

Jie, P. B., Qi, Z. H., Li, Z. Y., Hao, X. S., and Zheng, W. (2015). Chlorogenic acid maintains glucose homeostasis through modulating the expression of SGLT-1, GLUT-2, and PLG in different intestinal segments of Sprague-Dawley rats fed a high-fat diet. *Biomed. Environ. Sci.* 28, 894–903.

Jowett, A., and Shrestha, R. (1998). Mucosa and taste buds of the human epiglottis. *J. Anat.* 193(Pt 4), 617–618. doi: 10.1046/j.1469-7580.1998.19340617.x

Just, T., Pau, H. W., Engel, U., and Hummel, T. (2008). Cephalic phase insulin release in healthy humans after taste stimulation? *Appetite* 51, 622–627. doi: 10.1016/j.appet.2008.04.271

Kampov-Polevoy, A., Garbutt, J. C., and Janowsky, D. (1997). Evidence of preference for a high-concentration sucrose solution in alcoholic men. *Am. J. Psychiatry* 154, 269–270. doi: 10.1176/ajp.154.2.269

Kaske, S., Krasteva, G., König, P., Kummer, W., Hofmann, T., Gudermann, T., et al. (2007). TRPM5, a taste-signaling transient receptor potential ion-channel, is a ubiquitous signaling component in chemosensory cells. *BMC Neurosci.* 8:49. doi: 10.1186/1471-2202-8-49

Kendig, D. M., Hurst, N. R., Bradley, Z. L., Mahavadi, S., Kuemmerle, J. F., Lyall, V., et al. (2014). Activation of the umami taste receptor (T1R1/T1R3) initiates the peristaltic reflex and pellet propulsion in the distal colon. *Am. J. Physiol. Gastrointest Liver Physiol.* 307, G1100–G1107. doi: 10.1152/ajpgi.00251.2014

Kendig, M. D. (2014). Cognitive and behavioural effects of sugar consumption in rodents. *Rev. Appet.* 80, 41–54. doi: 10.1016/j.appet.2014.04.028

Keskitalo, K., Knaapila, A., Kallela, M., Palotie, A., Wessman, M., Sammalisto, S., et al. (2007). Sweet taste preferences are partly genetically determined: identification of a trait locus on chromosome 16. *Am. J. Clin. Nutr.* 86, 55–63. doi: 10.1093/ajcn/86.1.55

Kikut-Ligaj, D., and Trzcielińska-Lorych, J. (2015). How taste works: cells, receptors and gustatory perception. *Cell Mol. Biol. Lett.* 20, 699–716. doi: 10.1515/cmble-2015-0042

Kim, K.-S., Seeley, R. J., and Sandoval, D. A. (2018). Signalling from the periphery to the brain that regulates energy homeostasis. *Nat. Rev. Neurosci.* 19, 185–196. doi: 10.1038/nrn.2018.8

Kim, M.-R., Kusakabe, Y., Miura, H., Shindo, Y., Ninomiya, Y., and Hino, A. (2003). Regional expression patterns of taste receptors and gustducin in the mouse tongue. *Biochem. Biophys. Res. Communicat.* 312, 500–506. doi: 10.1016/j.bbrc.2003.10.137

Kitagawa, M., Kusakabe, Y., Miura, H., Ninomiya, Y., and Hino, A. (2001). Molecular genetic identification of a candidate receptor gene for sweet taste. *Biochem. Biophys. Res. Commun.* 283, 236–242. doi: 10.1006/bbrc.2001.4760

Kochem, M. (2017). Type 1 Taste Receptors in Taste and Metabolism. *Ann. Nutr. Metab.* 70(Suppl. 3), 27–36. doi: 10.1159/000478760

Kohno, D. (2017). Sweet taste receptor in the hypothalamus: a potential new player in glucose sensing in the hypothalamus. *J. Physiol. Sci.* 67, 459–465. doi: 10.1007/s12576-017-0535-y

Kohno, D., Koike, M., Ninomiya, Y., Kojima, I., Kitamura, T., and Yada, T. (2016). Sweet Taste Receptor Serves to Activate Glucose- and Leptin-Responsive Neurons in the Hypothalamic Arcuate Nucleus and Participates in Glucose Responsiveness. *Front. Neurosci.* 10:502. doi: 10.3389/fnins.2016.00502

Kojima, I., and Nakagawa, Y. (2011). The Role of the Sweet Taste Receptor in Enteroendocrine Cells and Pancreatic β -Cells. *Diabetes Metab. J.* 35, 451–457. doi: 10.4093/dmj.2011.35.5.451

Kojima, I., Nakagawa, Y., Ohtsu, Y., Hamano, K., Medina, J., and Nagasawa, M. (2015). Return of the glucoreceptor: Glucose activates the glucose-sensing receptor T1R3 and facilitates metabolism in pancreatic β -cells. *J. Diabetes Investig.* 6, 256–263. doi: 10.1111/jdi.12304

Kokabu, S., Lowery, J. W., Toyono, T., Sato, T., and Yoda, T. (2017). On the Emerging Role of the Taste Receptor Type 1 (T1R) Family of Nutrient-Sensors in the Musculoskeletal System. *Molecules* 22:molecules22030469. doi: 10.3390/molecules22030469

Kokrashvili, Z., Yee, K. K., Ilegems, E., Iwatsuki, K., Li, Y., Mosinger, B., et al. (2014). Endocrine taste cells. *Br. J. Nutr.* 111(Suppl. 1), S23–S29. doi: 10.1017/S0007114513002262

Kolesnikov, S. S., and Margolskee, R. F. (1995). A cyclic-nucleotide-suppressible conductance activated by transducin in taste cells. *Nature* 376, 85–88. doi: 10.1038/376085a0

Krimm, R. F., Nejad, M. S., Smith, J. C., Miller, I. J., and Beidler, L. M. (1987). The effect of bilateral sectioning of the chorda tympani and the greater superficial

petrosal nerves on the sweet taste in the rat. *Physiol. Behav.* 41, 495–501. doi: 10.1016/0031-9384(87)90086-2

Kuhn, C., and Meyerhof, W. (2013). Oligomerization of sweet and bitter taste receptors. *Methods Cell Biol.* 117, 229–242. doi: 10.1016/B978-0-12-408143-7.00013-X

Kuhn, C., Bufe, B., Winnig, M., Hofmann, T., Frank, O., Behrens, M., et al. (2004). Bitter taste receptors for saccharin and acesulfame K. *J. Neurosci.* 24, 10260–10265. doi: 10.1523/JNEUROSCI.1225-04.2004

Kuhre, R. E., Frost, C. R., Svendsen, B., and Holst, J. J. (2015). Molecular mechanisms of glucose-stimulated GLP-1 secretion from perfused rat small intestine. *Diabetes* 64, 370–382. doi: 10.2337/db14-0807

Kurihara, K., and Koyama, N. (1972). High activity of adenyl cyclase in olfactory and gustatory organs. *Biochem. Biophys. Res. Commun.* 48, 30–34. doi: 10.1016/0006-291X(72)90339-7

Kurosaki, Y., Yano, K., and Kimura, T. (1998). Perfusion cells for studying regional variation in oral mucosal permeability in humans. 2. A specialized transport mechanism in D-glucose absorption exists in dorsum of tongue. *J. Pharm. Sci.* 87, 613–615. doi: 10.1021/js9703028

Kusakabe, Y., Yamaguchi, E., Tanemura, K., Kameyama, K., Chiba, N., Arai, S., et al. (1998). Identification of two α -subunit species of GTP-binding proteins, Gα 15 and Gα q, expressed in rat taste buds. *Biochim. Biophys. Acta Mol. Cell Res.* 1403, 265–272. doi: 10.1016/S0167-4889(98)00062-7

Kusakabe, Y., Yasuoka, A., Asano-Miyoshi, M., Iwabuchi, K., Matsumoto, I., Arai, S., et al. (2000). Comprehensive study on G protein alpha-subunits in taste bud cells, with special reference to the occurrence of Galphai2 as a major Galpha species. *Chem. Senses* 25, 525–531. doi: 10.1093/chemse/25.5.525

Laffitte, A., Neiers, F., and Briand, L. (2014). Functional roles of the sweet taste receptor in oral and extraoral tissues. *Curr. Opin. Clin. Nutr. Metab. Care* 17, 379–385. doi: 10.1097/MCO.0000000000000058

Lapis, T. J., Penner, M. H., and Lim, J. (2016). Humans Can Taste Glucose Oligomers Independent of the hT1R2/hT1R3 Sweet Taste Receptor. *Chem. Senses* 2016:bjw088. doi: 10.1093/chemse/bjw088

Laskowski, A. I., and Medler, K. F. (2009). Sodium-calcium exchangers contribute to the regulation of cytosolic calcium levels in mouse taste cells. *J. Physiol.* 587, 4077–4089. doi: 10.1113/jphysiol.2009.173567

Law, J. S., and Henkin, R. I. (1982). Taste bud adenosine -3'5'-monophosphate phosphodiesterase: Activity, subcellular distribution and kinetic parameters. *Res. Commun. Chem. Pathol. Pharmacol.* 38, 439–452.

Lee, A. A., and Owyang, C. (2017). Sugars, Sweet Taste Receptors, and Brain Responses. *Nutrients* 9:nu9070653. doi: 10.3390/nu9070653

Lee, R. J., and Cohen, N. A. (2014). Bitter and sweet taste receptors in the respiratory epithelium in health and disease. *J. Mol. Med.* 92, 1235–1244. doi: 10.1007/s00109-014-1222-6

Lee, R. J., and Cohen, N. A. (2015). Taste receptors in innate immunity. *Cell Mol. Life Sci.* 72, 217–236. doi: 10.1007/s00018-014-1736-7

Lee, R. J., Kofonow, J. M., Rosen, P. L., Siebert, A. P., Chen, B., Doghramji, L., et al. (2014). Bitter and sweet taste receptors regulate human upper respiratory innate immunity. *J. Clin. Invest.* 124, 1393–1405. doi: 10.1172/JCI72094

Lee, R. J., Xiong, G., Kofonow, J. M., Chen, B., Lysenko, A., Jiang, P., et al. (2012). T2R38 taste receptor polymorphisms underlie susceptibility to upper respiratory infection. *J. Clin. Invest.* 122, 4145–4159. doi: 10.1172/JCI64240

Lemon, C. H. (2015). Perceptual and neural responses to sweet taste in humans and rodents. *Chemosens. Percept.* 8, 46–52. doi: 10.1007/s12078-015-9177-8

Li, X., Staszewski, L., Xu, H., Durick, K., Zoller, M., and Adler, E. (2002). Human receptors for sweet and umami taste. *Proc. Natl. Acad. Sci. U S A.* 99, 4692–4696. doi: 10.1073/pnas.072090199

Liem, D. G., and Mennella, J. A. (2002). Sweet and sour preferences during childhood: role of early experiences. *Dev. Psychobiol.* 41, 388–395. doi: 10.1002/dev.10067

Liman, E. R., Zhang, Y. V., and Montell, C. (2014). Peripheral coding of taste. *Neuron* 81, 984–1000. doi: 10.1016/j.neuron.2014.02.022

Lin, H. C., Doty, J. E., Reedy, T. J., and Meyer, J. H. (1989). Inhibition of gastric emptying by glucose depends on length of intestine exposed to nutrient. *Am. J. Physiol.* 256, G404–G411. doi: 10.1152/ajpgi.1989.256.2.G404

Lin, W., Ogura, T., Margolskee, R. F., Finger, T. E., and Restrepo, D. (2008). TRPM5-expressing solitary chemosensory cells respond to odorous irritants. *J. Neurophysiol.* 99, 1451–1460. doi: 10.1152/jn.01195.2007

Lindemann, B. (1996). Taste reception. *Physiol. Rev.* 76, 719–766. doi: 10.1152/physrev.1996.76.3.719

Lindemann, B. (1999). Receptor seeks ligand: On the way to cloning the molecular receptors for sweet and bitter taste. *Nat. Med.* 5, 381–382. doi: 10.1038/7377

Livneh, Y., Ramesh, R. N., Burgess, C. R., Levandowski, K. M., Madara, J. C., Fenselau, H., et al. (2017). Homeostatic circuits selectively gate food cue responses in insular cortex. *Nature* 546, 611–616. doi: 10.1038/nature22375

Lohner, S., Toews, I., and Meerpohl, J. J. (2017). Health outcomes of non-nutritive sweeteners: analysis of the research landscape. *Nutr. J.* 16:55. doi: 10.1186/s12937-017-0278-x

Louchami, K., Best, L., Brown, P., Virreira, M., Hupkens, E., Perret, J., et al. (2012). A new role for aquaporin 7 in insulin secretion. *Cell Physiol. Biochem.* 29, 65–74. doi: 10.1159/000337588

Louis-Sylvestre, J. (1976). Preabsorptive insulin release and hypoglycemia in rats. *Am. J. Physiol.* 230, 56–60. doi: 10.1152/ajplegacy.1976.230.1.56

Low, Y. Q., Lacy, K., and Keast, R. (2014). The role of sweet taste in satiation and satiety. *Nutrients* 6, 3431–3450. doi: 10.3390/nu6093431

Lush, I. E. (1989). The genetics of tasting in mice: VI. Saccharin, acesulfame, dulcin and sucrose. *Genet. Res.* 53, 95–99. doi: 10.1017/S0016672300027968

Lush, I. E., Hornigold, N., King, P., and Stoye, J. P. (1995). The genetics of tasting in mice VII. Glycine revisited, and the chromosomal location of Sac and Soa. *Genet. Res.* 66, 167–174. doi: 10.1017/S0016672300034510

Lyall, V., Heck, G. L., Vinnikova, A. K., Ghosh, S., Phan, T.-H. T., Alam, R. I., et al. (2004). The mammalian amiloride-insensitive non-specific salt taste receptor is a vanilloid receptor-1 variant. *J. Physiol.* 558, 147–159. doi: 10.1113/jphysiol.2004.065656

Maina, I. W., Workman, A. D., and Cohen, N. A. (2018). The role of bitter and sweet taste receptors in upper airway innate immunity: Recent advances and future directions. *World J. Otorhinolaryngol. Head Neck Surg.* 4, 200–208. doi: 10.1016/j.wjorl.2018.07.003

Margolskee, R. F. (1993). The molecular biology of taste transduction. *Bioessays* 15, 645–650. doi: 10.1002/bies.950151003

Margolskee, R. F. (2002). Molecular mechanisms of bitter and sweet taste transduction. *J. Biol. Chem.* 277, 1–4. doi: 10.1074/jbc.R100054200

Margolskee, R. F., Dyer, J., Kokrashvili, Z., Salmon, K. S. H., Ilegems, E., Daly, K., et al. (2007). T1R3 and gustducin in gut sense sugars to regulate expression of Na+-glucose cotransporter 1. *Proc. Natl. Acad. Sci. U S A.* 104, 15075–15080. doi: 10.1073/pnas.0706678104

Martin, B., Dotson, C. D., Shin, Y.-K., Ji, S., Drucker, D. J., Maudsley, S., et al. (2009). Modulation of taste sensitivity by GLP-1 signaling in taste buds. *Ann. N Y. Acad. Sci.* 1170, 98–101. doi: 10.1111/j.1749-6632.2009.03920.x

Martin, C., Passilly-Degrace, P., Chevrot, M., Ancel, D., Sparks, S. M., Drucker, D. J., et al. (2012). Lipid-mediated release of GLP-1 by mouse taste buds from circumvallate papillae: putative involvement of GPR120 and impact on taste sensitivity. *J. Lipid Res.* 53, 2256–2265. doi: 10.1194/jlr.M025874

Maruyama, Y., Yasuda, R., Kuroda, M., and Eto, Y. (2012). Kokumi substances, enhancers of basic tastes, induce responses in calcium-sensing receptor expressing taste cells. *PLoS One* 7:e34489. doi: 10.1371/journal.pone.0034489

Masubuchi, Y., Nakagawa, Y., Ma, J., Sasaki, T., Kitamura, T., Yamamoto, Y., et al. (2013). A novel regulatory function of sweet taste-sensing receptor in adipogenic differentiation of 3T3-L1 cells. *PLoS One* 8:e54500. doi: 10.1371/journal.pone.0054500

Matsumura, K., Chang, B. H.-J., Fujimiya, M., Chen, W., Kulkarni, R. N., Eguchi, Y., et al. (2007). Aquaporin 7 Is a β -Cell Protein and Regulator of Intraislet Glycerol Content and Glycerol Kinase Activity, β -Cell Mass, and Insulin Production and Secretion?†. *Mol. Cell Biol.* 27, 6026–6037. doi: 10.1128/MCB.00384-07

Matsumura, S., Eguchi, A., Mizushige, T., Kitabayashi, N., Tsuzuki, S., Inoue, K., et al. (2009). Colocalization of GPR120 with phospholipase-Cβ 2 and α -gustducin in the taste bud cells in mice. *Neurosci. Lett.* 450, 186–190. doi: 10.1016/j.neulet.2008.11.056

Matsunami, H., Montmayeur, J. P., and Buck, L. B. (2000). A family of candidate taste receptors in human and mouse. *Nature* 404, 601–604. doi: 10.1038/35007072

Maurer, S., Wabnitz, G. H., Kahle, N. A., Stegmaier, S., Prior, B., Giese, T., et al. (2015). Tasting *Pseudomonas aeruginosa* Biofilms: Human Neutrophils Express

the Bitter Receptor T2R38 as Sensor for the Quorum Sensing Molecule N-(3-Oxododecanoyl)-l-Homoserine Lactone. *Front. Immunol.* 6:369. doi: 10.3389/fimmu.2015.00369

Max, M., Shanker, Y. G., Huang, L., Rong, M., Liu, Z., Campagne, F., et al. (2001). Tas1r3, encoding a new candidate taste receptor, is allelic to the sweet responsiveness locus Sac. *Nat. Genet.* 28, 58–63. doi: 10.1038/88270

McCaughey, S. A. (2008). The taste of sugars. *Neurosci. Biobehav. Rev.* 32, 1024–1043. doi: 10.1016/j.neubiorev.2008.04.002

McLaughlin, S. K., McKinnon, P. J., and Margolskee, R. F. (1992). Gustducin is a taste-cell-specific G protein closely related to the transducins. *Nature* 357, 563–569. doi: 10.1038/357563a0

McLaughlin, S. K., McKinnon, P. J., Robichon, A., Spickofsky, N., and Margolskee, R. F. (1993). Gustducin and transducin: a tale of two G proteins. *Ciba Found Symp.* 179, 186–196. doi: 10.1002/9780470514511.ch12

McLaughlin, S. K., McKinnon, P. J., Spickofsky, N., Danho, W., and Margolskee, R. F. (1994). Molecular cloning of G proteins and phosphodiesterases from rat taste cells. *Physiol. Behav.* 56, 1157–1164. doi: 10.1016/0031-9384(94)90360-3

Medina, A., Nakagawa, Y., Ma, J., Li, L., Hamano, K., Akimoto, T., et al. (2014). Expression of the glucose-sensing receptor T1R3 in pancreatic islet: changes in the expression levels in various nutritional and metabolic states. *Endocr. J.* 61, 797–805. doi: 10.1507/endocrj.ej14-0221

Medina, J., Nakagawa, Y., Nagasawa, M., Fernandez, A., Sakaguchi, K., Kitaguchi, T., et al. (2016). Positive Allosteric Modulation of the Calcium-sensing Receptor by Physiological Concentrations of Glucose. *J. Biol. Chem.* 291, 23126–23135. doi: 10.1074/jbc.M116.729863

Medler, K. F. (2015). Calcium signaling in taste cells. *Biochim. Biophys. Acta* 1853, 2025–2032. doi: 10.1016/j.bbamcr.2014.11.013

Medler, K. F., Margolskee, R. F., and Kinnamon, S. C. (2003). Electrophysiological Characterization of Voltage-Gated Currents in Defined Taste Cell Types of Mice. *J. Neurosci.* 23, 2608–2617. doi: 10.1523/jneurosci.23-07-02608.2003

Meier, J. J., and Nauck, M. A. (2005). Glucagon-like peptide 1(GLP-1) in biology and pathology. *Diabetes Metab. Res. Rev.* 21, 91–117. doi: 10.1002/dmrr.538

Merigo, F., Benati, D., Cecchini, M. P., Cristofoletti, M., Osculati, F., and Sbarbati, A. (2009). Amylase expression in taste receptor cells of rat circumvallate papillae. *Cell Tissue Res.* 336, 411–421. doi: 10.1007/s00441-009-0789-7

Merigo, F., Benati, D., Cristofoletti, M., Osculati, F., and Sbarbati, A. (2011). Glucose transporters are expressed in taste receptor cells. *J. Anat.* 219, 243–252. doi: 10.1111/j.1469-7580.2011.01385.x

Miki, T., Nagashima, K., Tashiro, F., Kotake, K., Yoshitomi, H., Tamamoto, A., et al. (1998). Defective insulin secretion and enhanced insulin action in KATP channel-deficient mice. *Proc. Natl. Acad. Sci. U S A.* 95, 10402–10406.

Ming, D., Ruiz-Avila, L., and Margolskee, R. F. (1998). Characterization and solubilization of bitter-responsive receptors that couple to gustducin. *Proc. Natl. Acad. Sci. U S A.* 95, 8933–8938. doi: 10.1073/pnas.95.15.8933

Misaka, T., Kusakabe, Y., Emori, Y., Gonoi, T., Arai, S., and Abe, K. (1997). Taste buds have a cyclic nucleotide-activated channel, CNGgust. *J. Biol. Chem.* 272, 22623–22629. doi: 10.1074/jbc.272.36.22623

Miura, H., Nakayama, A., Shindo, Y., Kusakabe, Y., Tomonari, H., and Harada, S. (2007). Expression of gustducin overlaps with that of type III IP3 receptor in taste buds of the rat soft palate. *Chem. Senses* 32, 689–696. doi: 10.1093/chemse/bjm036

Miyoshi, M. A., Abe, K., and Emori, Y. (2001). IP(3) receptor type 3 and PLCbeta2 are co-expressed with taste receptors T1R and T2R in rat taste bud cells. *Chem. Senses* 26, 259–265. doi: 10.1093/chemse/26.3.259

Montmayeur, J. (2002). Receptors for bitter and sweet taste. *Curr. Opin. Neurobiol.* 12, 366–371. doi: 10.1016/S0959-4388(02)00345-8

Montmayeur, J. P., Liberles, S. D., Matsunami, H., and Buck, L. B. (2001). A candidate taste receptor gene near a sweet taste locus. *Nat. Neurosci.* 4, 492–498. doi: 10.1038/87440

Moskowitz, H. R., and Klarmann, L. (1975). The tastes of artificial sweetners and their mixtures. *Chem. Senses* 1, 411–421. doi: 10.1093/chemse/1.4.411

Mueller, K. L., Hoon, M. A., Erlenbach, I., Chandrashekar, J., Zuker, C. S., and Ryba, N. J. P. (2005). The receptors and coding logic for bitter taste. *Nature* 434, 225–229. doi: 10.1038/nature03352

Naim, M., Ronen, T., Striem, B. J., Levinson, M., and Zehavi, U. (1991). Adenylate cyclase responses to sucrose stimulation in membranes of pig circumvallate taste papillae. *Comparat. Biochem. Physiol. Part B Comparat. Biochem.* 100, 455–458. doi: 10.1016/0305-0491(91)90203-P

Nakagawa, Y., Nagasawa, M., Mogami, H., Lohse, M., Ninomiya, Y., and Kojima, I. (2013). Multimodal function of the sweet taste receptor expressed in pancreatic β -cells: generation of diverse patterns of intracellular signals by sweet agonists. *Endocr. J.* 60, 1191–1206. doi: 10.1507/endocrj.ej13-0282

Nakagawa, Y., Nagasawa, M., Yamada, S., Hara, A., Mogami, H., Nikolaev, V. O., et al. (2009). Sweet taste receptor expressed in pancreatic beta-cells activates the calcium and cyclic AMP signaling systems and stimulates insulin secretion. *PLoS One* 4:e5106. doi: 10.1371/journal.pone.0005106

Nakagawa, Y., Ohtsu, Y., Nagasawa, M., Shibata, H., and Kojima, I. (2014). Glucose promotes its own metabolism by acting on the cell-surface glucose-sensing receptor T1R3. *Endocr. J.* 61, 119–131. doi: 10.1507/endocrj.ej13-0431

Nakashima, K., and Ninomiya, Y. (1999). Transduction for sweet taste of saccharin may involve both inositol 1,4,5-trisphosphate and cAMP pathways in the fungiform taste buds in C57BL mice. *Cell Physiol. Biochem.* 9, 90–98. doi: 10.1159/000016305

Nance, K., Acevedo, M. B., and Pepino, M. Y. (2020). Changes in taste function and ingestive behavior following bariatric surgery. *Appetite* 146: 104423.

Neiers, F., Canivenc-Lavier, M.-C., and Briand, L. (2016). What Does Diabetes "Taste" Like? *Curr. Diab. Rep.* 16:49. doi: 10.1007/s11892-016-0746-2

Nelson, G., Chandrashekar, J., Hoon, M. A., Feng, L., Zhao, G., Ryba, N. J. P., et al. (2002). An amino-acid taste receptor. *Nature* 416, 199–202. doi: 10.1038/nature726

Nelson, G., Hoon, M. A., Chandrashekar, J., Zhang, Y., Ryba, N. J., and Zuker, C. S. (2001). Mammalian Sweet Taste Receptors. *Cell* 106, 381–390. doi: 10.1016/S0092-8674(01)00451-2

Ng, K., Woo, J., Kwan, M., Sea, M., Wang, A., Lo, R., et al. (2004). Effect of age and disease on taste perception. *J. Pain Symptom Manage.* 28, 28–34. doi: 10.1016/j.jpainsymman.2003.11.007

Niki, M., Jyotaki, M., Yoshida, R., and Ninomiya, Y. (2010). Reciprocal modulation of sweet taste by leptin and endocannabinoids. *Results Probl. Cell Differ.* 52, 101–114. doi: 10.1007/978-3-642-14426-4_9

Nilsson, B. (1979). Taste acuity of the human palate. III. Studies with taste solutions on subjects in different age groups. *Acta Odontol. Scand.* 37, 235–252. doi: 10.3109/00016357909027585

Ninomiya, Y., Shigemura, N., Yasumatsu, K., Ohta, R., Sugimoto, K., Nakashima, K., et al. (2002). "Leptin and sweet taste," in *Vitamins and Hormones*, ed. G. Litwack (Amsterdam: Elsevier), 221–248.

Noel, C., and Dando, R. (2015). The effect of emotional state on taste perception. *Appetite* 95, 89–95. doi: 10.1016/j.appet.2015.06.003

Ochner, C. N., Kwok, Y., Conceição, E., Pantazatos, S. P., Puma, L. M., Carnell, S., et al. (2011). Selective reduction in neural responses to high calorie foods following gastric bypass surgery. *Ann. Surg.* 253, 502–507. doi: 10.1097/SLA.0b013e318203a289

Ogura, T., Mackay-Sim, A., and Kinnamon, S. C. (1997). Bitter Taste Transduction of Denatonium in the Mudpuppy Necturus maculosus. *J. Neurosci.* 17, 3580–3587. doi: 10.1523/JNEUROSCI.17-10-03580.1997

Ogura, T., Margolskee, R. F., and Kinnamon, S. C. (2002). Taste receptor cell responses to the bitter stimulus denatonium involve Ca2+ influx via store-operated channels. *J. Neurophysiol.* 87, 3152–3155. doi: 10.1152/jn.2002.87.6.3152

Ohla, K., Toepel, U., Le Coutre, J., and Hudry, J. (2012). Visual-gustatory interaction: orbitofrontal and insular cortices mediate the effect of high-calorie visual food cues on taste pleasantness. *PLoS One* 7:e32434. doi: 10.1371/journal.pone.0032434

Ohla, K., Yoshida, R., Roper, S. D., Di Lorenzo, P. M., Victor, J. D., Boughter, J. D., et al. (2019). Recognizing Taste: Coding Patterns Along the Neural Axis in Mammals. *Chem. Senses* 44, 237–247. doi: 10.1093/chemse/bjz013

Okuda, Y., and Tomita, H. (eds) (1976). *Differences in sensitivity to taste on the tongue and in the soft palate*. Tokyo: University of Tokyo.

Oliveira-Maia, A. J., Araujo, I. E., Monteiro, C., Workman, V., Galhardo, V., and Nicolelis, M. A. L. (2012). The insular cortex controls food preferences independently of taste receptor signaling. *Front. Syst. Neurosci.* 6:5. doi: 10.3389/fnsys.2012.00005

Orellana, E. R., Covasa, M., and Hajnal, A. (2019). Neuro-hormonal mechanisms underlying changes in reward related behaviors following weight loss surgery:

Potential pharmacological targets. *Biochem. Pharmacol.* 164, 106–114. doi: 10.1016/j.bcp.2019.04.004

Oyama, Y., Yamano, H., Ohkuma, A., Ogawara, K., Higaki, K., and Kimura, T. (1999). Carrier-mediated transport systems for glucose in mucosal cells of the human oral cavity. *J. Pharm. Sci.* 88, 830–834. doi: 10.1021/js980298f

Ozdener, M. H., Subramaniam, S., Sundaresan, S., Sery, O., Hashimoto, T., Asakawa, Y., et al. (2014). CD36- and GPR120-mediated Ca^{2+} signaling in human taste bud cells mediates differential responses to fatty acids and is altered in obese mice. *Gastroenterology* 146, 995–1005. doi: 10.1053/j.gastro.2014.01.006

Peng, Y., Gillis-Smith, S., Jin, H., Tränkner, D., Ryba, N. J. P., and Zuker, C. S. (2015). Sweet and bitter taste in the brain of awake behaving animals. *Nature* 527, 512–515. doi: 10.1038/nature15763

Pepino, M. Y. (2015). Metabolic effects of non-nutritive sweeteners. *Physiol. Behav.* 152, 450–455. doi: 10.1016/j.physbeh.2015.06.024

Pepino, M. Y., and Bourne, C. (2011). Non-nutritive sweeteners, energy balance, and glucose homeostasis. *Curr. Opin. Clin. Nutr. Metab. Care* 14, 391–395. doi: 10.1097/MCO.0b013e3283468e7e

Perea-Martinez, I., Nagai, T., and Chaudhari, N. (2013). Functional cell types in taste buds have distinct longevities. *PLoS One* 8:e53399. doi: 10.1371/journal.pone.0053399

Pérez, C. A., Huang, L., Rong, M., Kozak, J. A., Preuss, A. K., Zhang, H., et al. (2002). A transient receptor potential channel expressed in taste receptor cells. *Nat. Neurosci.* 5, 1169–1176. doi: 10.1038/nn952

Porcu, E., Benz, K. M., Ball, F., Tempelmann, C., Hanke, M., and Noesselt, T. (2020). Macroscopic information-based taste representations in insular cortex are shaped by stimulus concentration. *Proc. Natl. Acad. Sci. U S A.* 117, 7409–7417. doi: 10.1073/pnas.1916329117

Prawitt, D., Monteilh-Zoller, M. K., Brixel, L., Spangenberg, C., Zabel, B., Fleig, A., et al. (2003). TRPM5 is a transient Ca2+-activated cation channel responding to rapid changes in Ca2+i. *Proc. Natl. Acad. Sci. U S A.* 100, 15166–15171. doi: 10.1073/pnas.2334624100

Prinster, A., Cantone, E., Verlezza, V., Magliulo, M., Sarnelli, G., Iengo, M., et al. (2017). Cortical representation of different taste modalities on the gustatory cortex: A pilot study. *PLoS One* 12:e0190164. doi: 10.1371/journal.pone.0190164

Qu, T., Han, W., Niu, J., Tong, J., and Araujo, I. E. (2019). On the roles of the Duodenum and the Vagus nerve in learned nutrient preferences. *Appetite* 139, 145–151. doi: 10.1016/j.appet.2019.04.014

Rebecchi, M. J., and Pentyala, S. N. (2000). Structure, function, and control of phosphoinositide-specific phospholipase C. *Physiol. Rev.* 80, 1291–1335. doi: 10.1152/physrev.2000.80.4.1291

Rebello, M. R., and Medler, K. F. (2010). Ryanodine receptors selectively contribute to the formation of taste-evoked calcium signals in mouse taste cells. *Eur. J. Neurosci.* 32, 1825–1835. doi: 10.1111/j.1460-9568.2010.07463.x

Rebello, M. R., Maliphol, A. B., and Medler, K. F. (2013). Ryanodine Receptors Selectively Interact with L Type Calcium Channels in Mouse Taste Cells. *PLoS One* 8:e68174. doi: 10.1371/journal.pone.0068174

Reed, D. R., and McDaniel, A. H. (2006). The human sweet tooth. *BMC Oral Health* 6(Suppl. 1):S17. doi: 10.1186/1472-6831-6-S1-S17

Reimann, F., Habib, A. M., Tolhurst, G., Parker, H. E., Rogers, G. J., and Gribble, F. M. (2008). Glucose sensing in L cells: a primary cell study. *Cell Metab.* 8, 532–539. doi: 10.1016/j.cmet.2008.11.002

Ren, W., Aihara, E., Lei, W., Gheewala, N., Uchiyama, H., Margolskee, R. F., et al. (2017). Transcriptome analyses of taste organoids reveal multiple pathways involved in taste cell generation. *Sci. Rep.* 7:4004. doi: 10.1038/s41598-017-04099-5

Ren, W., Lewandowski, B. C., Watson, J., Aihara, E., Iwatsuki, K., Bachmanov, A. A., et al. (2014). Single Lgr5- or Lgr6-expressing taste stem/progenitor cells generate taste bud cells ex vivo. *Proc. Natl. Acad. Sci. U S A.* 111, 16401–16406. doi: 10.1073/pnas.1409064111

Ren, X., Ferreira, J. G., Zhou, L., Shammah-Lagnado, S. J., Yeckel, C. W., and Araujo, I. E. (2010). Nutrient selection in the absence of taste receptor signaling. *J. Neurosci.* 30, 8012–8023. doi: 10.1523/JNEUROSCI.5749-09.2010

Ren, X., Zhou, L., Terwilliger, R., Newton, S. S., and Araujo, I. E. (2009). Sweet taste signaling functions as a hypothalamic glucose sensor. *Front. Integr. Neurosci.* 3:12. doi: 10.3389/neuro.07.012.2009

Renwick, A. G., and Molinary, S. V. (2010). Sweet taste receptors, low-energy sweeteners, glucose absorption and insulin release. *Br. J. Nutr.* 104, 1415–1420. doi: 10.1017/S0007114510002540

Rogachevskaja, O. A., Churbanov, G. D., Bystrova, M. F., Romanov, R. A., and Kolesnikov, S. S. (2011). Stimulation of the extracellular Ca^{2+}-sensing receptor by denatonium. *Biochem. Biophys. Res. Commun.* 416, 433–436. doi: 10.1016/j.bbrc.2011.11.095

Rolls, E. T., and Baylis, L. L. (1994). Gustatory, olfactory, and visual convergence within the primate orbitofrontal cortex. *J. Neurosci.* 14, 5437–5452. doi: 10.1523/JNEUROSCI.14-09-05437.1994

Roper, S. D. (2013). Taste buds as peripheral chemosensory processors. *Semin. Cell Dev. Biol.* 24, 71–79. doi: 10.1016/j.semcdb.2012.12.002

Roper, S. D., and Chaudhari, N. (2017). Taste buds: Cells, signals and synapses. *Nat. Rev. Neurosci.* 18:485. doi: 10.1038/nrn.2017.68

Rössler, P., Boekhoff, I., Tareilus, E., Beck, S., Breer, H., and Freitag, J. (2000). G protein betagamma complexes in circumvallate taste cells involved in bitter transduction. *Chem. Senses* 25, 413–421. doi: 10.1093/chemse/25.4.413

Rössler, P., Kroner, C., Freitag, J., Noè, J., and Breer, H. (1998). Identification of a phospholipase C β subtype in rat taste cells. *Eur. J. Cell Biol.* 77, 253–261. doi: 10.1016/S0171-9335(98)80114-3

Rozengurt, E. (2006). Taste receptors in the gastrointestinal tract. I. Bitter taste receptors and alpha-gustducin in the mammalian gut. *Am. J. Physiol. Gastrointest. Liver Physiol.* 291, G171–G177. doi: 10.1152/ajpgi.00073.2006

Rozengurt, N., Wu, S. V., Chen, M. C., Huang, C., Sternini, C., and Rozengurt, E. (2006). Colocalization of the alpha-subunit of gustducin with PYY and GLP-1 in L cells of human colon. *Am. J. Physiol. Gastrointest. Liver Physiol.* 291, G792–G802. doi: 10.1152/ajpgi.00074.2006

Rudenga, K., Green, B., Nachtigal, D., and Small, D. M. (2010). Evidence for an Integrated Oral Sensory Module in the Human Anterior Ventral Insula. *Chem. Senses* 35, 693–703. doi: 10.1093/chemse/bjq068

Ruiz, C. J., Wray, K., Delay, E., Margolskee, R. F., and Kinnamon, S. C. (2003). Behavioral evidence for a role of alpha-gustducin in glutamate taste. *Chem. Senses* 28, 573–579. doi: 10.1093/chemse/bjg049

Ruiz-Avila, L., McLaughlin, S. K., Wildman, D., McKinnon, P. J., Robichon, A., Spickofsky, N., et al. (1995). Coupling of bitter receptor to phosphodiesterase through transducin in taste receptor cells. *Nature* 376, 80–85. doi: 10.1038/376080a0

Ruiz-Avila, L., Wong, G. T., Damak, S., and Margolskee, R. F. (2001). Dominant loss of responsiveness to sweet and bitter compounds caused by a single mutation in alpha -gustducin. *Proc. Natl. Acad. Sci. U S A.* 98, 8868–8873. doi: 10.1073/pnas.151235798

Sabino-Silva, R., Mori, R. C., David-Silva, A., Okamoto, M. M., Freitas, H. S., and Machado, U. F. (2010). The Na(+)/glucose cotransporters: from genes to therapy. *Braz. J. Med. Biol. Res.* 43, 1019–1026. doi: 10.1590/s0100-879x2010007500115

Sainz, E., Cavenagh, M. M., LopezJimenez, N. D., Gutierrez, J. C., Battey, J. F., Northup, J. K., et al. (2007). The G-protein coupling properties of the human sweet and amino acid taste receptors. *Dev. Neurobiol.* 67, 948–959. doi: 10.1002/dneu.20403

Sainz, E., Korley, J. N., Battey, J. F., and Sullivan, S. L. (2001). Identification of a novel member of the T1R family of putative taste receptors. *J. Neurochem.* 77, 896–903. doi: 10.1046/j.1471-4159.2001.00292.x

Sakata, I., Park, W.-M., Walker, A. K., Piper, P. K., Chuang, J.-C., Osborne-Lawrence, S., et al. (2012). Glucose-mediated control of ghrelin release from primary cultures of gastric mucosal cells. *Am. J. Physiol. Endocrinol. Metab.* 302, E1300–E1310. doi: 10.1152/ajpendo.00041.2012

Samuelsen, C. L., Gardner, M. P. H., and Fontanini, A. (2013). Thalamic contribution to cortical processing of taste and expectation. *J. Neurosci.* 33, 1815–1827. doi: 10.1523/JNEUROSCI.4026-12.2013

San Gabriel, A., Uneyama, H., Maekawa, T., and Torii, K. (2009). The calcium-sensing receptor in taste tissue. *Biochem. Biophys. Res. Commun.* 378, 414–418. doi: 10.1016/j.bbrc.2008.11.060

Sato, K., Endo, S., and Tomita, H. (2002). Sensitivity of three loci on the tongue and soft palate to four basic tastes in smokers and non-smokers. *Acta Otolaryngol. Suppl.* 2020, 74–82. doi: 10.1080/00016480260046445

Sbarbati, A., Merigo, F., Benati, D., Tizzano, M., Bernardi, P., and Osculati, F. (2004). Laryngeal chemosensory clusters. *Chem. Senses* 29, 683–692. doi: 10.1093/chemse/bjh071

Scheepers, A., Joost, H.-G., and Schürmann, A. (2004). The glucose transporter families SGLT and GLUT: molecular basis of normal and aberrant function. *JPEN J. Parenter Enteral. Nutr.* 28, 364–371. doi: 10.1177/0148607104028005364

Schiffman, S. S., Diaz, C., and Beeker, T. G. (1986). Caffeine intensities taste of certain sweeteners: Role of adenosine receptor. *Pharmacol. Biochem. Behav.* 24, 429–432. doi: 10.1016/0091-3057(86)90536-8

Schmidt, S., Joost, H.-G., and Schürmann, A. (2009). GLUT8, the enigmatic intracellular hexose transporter. *Am. J. Physiol. Endocrinol. Metab.* 296, E614–E618. doi: 10.1152/ajpendo.91019.2008

Schirra, J., and Göke, B. (2005). The physiological role of GLP-1 in human: incretin, ileal brake or more? *Regul. Pept.* 128, 109–115. doi: 10.1016/j.regpep.2004.06.018

Schoenfeld, M. A., Neuer, G., Tempelmann, C., Schüssler, K., Noesselt, T., Hopf, J.-M., et al. (2004). Functional magnetic resonance tomography correlates of taste perception in the human primary taste cortex. *Neuroscience* 127, 347–353. doi: 10.1016/j.neuroscience.2004.05.024

Schweiger, K., Grüneis, V., Treml, J., Galassi, C., Karl, C. M., Ley, J. P., et al. (2020). Sweet Taste Antagonist Lactisole Administered in Combination with Sucrose, But Not Glucose, Increases Energy Intake and Decreases Peripheral Serotonin in Male Subjects. *Nutrients* 12:nu12103133. doi: 10.3390/nu12103133

Sclafani, A., Koepsell, H., and Ackroff, K. (2016). SGLT1 sugar transporter/sensor is required for post-oral glucose appetition. *Am. J. Physiol. Regul. Integr. Comp. Physiol.* 310, R631–R639. doi: 10.1152/ajpregu.00432.2015

Sclafani, A., Marambaud, P., and Ackroff, K. (2014). Sucrose-conditioned flavor preferences in sweet ageusic T1r3 and Calhm1 knockout mice. *Physiol. Behav.* 126, 25–29. doi: 10.1016/j.physbeh.2013.12.003

Sclafani, A., Zukerman, S., and Ackroff, K. (2020). Residual Glucose Taste in T1R3 Knockout but not TRPM5 Knockout Mice. *Physiol. Behav.* 222:112945. doi: 10.1016/j.physbeh.2020.112945

Sclafani, A., Zukerman, S., Glendinning, J. I., and Margolskee, R. F. (2007). Fat and carbohydrate preferences in mice: the contribution of alpha-gustducin and Trpm5 taste-signaling proteins. *Am. J. Physiol. Regul. Integr. Comp. Physiol.* 293, R1504–R1513. doi: 10.1152/ajpregu.00364.2007

Scott, K. (2005). Taste Recognition: Food for Thought. *Neuron* 48, 455–464. doi: 10.1016/j.neuron.2005.10.015

Shahbake, M., Hutchinson, I., Laing, D. G., and Jinks, A. L. (2005). Rapid quantitative assessment of fungiform papillae density in the human tongue. *Brain Res.* 1052, 196–201. doi: 10.1016/j.brainres.2005.06.031

Shigemura, N., Yasumatsu, K., Yoshida, R., Sako, N., Katsukawa, H., Nakashima, K., et al. (2005). The role of the dpa locus in mice. *Chem. Senses* 30(Suppl. 1), i84–i85. doi: 10.1093/chemse/bjh125

Shin, Y.-J., Park, J.-H., Choi, J.-S., Chun, M.-H., Moon, Y. W., and Lee, M.-Y. (2010). Enhanced expression of the sweet taste receptors and alpha-gustducin in reactive astrocytes of the rat hippocampus following ischemic injury. *Neurochem. Res.* 35, 1628–1634. doi: 10.1007/s11064-010-0223-2

Shin, Y.-K., Martin, B., Golden, E., Dotson, C. D., Maudsley, S., Kim, W., et al. (2008). Modulation of taste sensitivity by GLP-1 signaling. *J. Neurochem.* 106, 455–463. doi: 10.1111/j.1471-4159.2008.05397.x

Shindo, Y., Miura, H., Carninci, P., Kawai, J., Hayashizaki, Y., Ninomiya, Y., et al. (2008). G alpha14 is a candidate mediator of sweet/umami signal transduction in the posterior region of the mouse tongue. *Biochem. Biophys. Res. Commun.* 376, 504–508. doi: 10.1016/j.bbrc.2008.09.035

Shinozaki, K., Shimizu, Y., Shiina, T., Morita, H., and Takewaki, T. (2008). Relationship between taste-induced physiological reflexes and temperature of sweet taste. *Physiol. Behav.* 93, 1000–1004. doi: 10.1016/j.physbeh.2008.01.006

Small, D. M. (2012). Flavor is in the brain. *Physiol. Behav.* 107, 540–552. doi: 10.1016/j.physbeh.2012.04.011

Small, D. M., Jones-Gotman, M., and Dagher, A. (2003). Feeding-induced dopamine release in dorsal striatum correlates with meal pleasantness ratings in healthy human volunteers. *Neuroimage* 19, 1709–1715. doi: 10.1016/s1053-8119(03)00253-2

Smeets, P. A. M., Erkner, A., and Graaf, C. (2010). Cephalic phase responses and appetite. *Nutr. Rev.* 68, 643–655. doi: 10.1111/j.1753-4887.2010.00334.x

Smith, J. C., and Sclafani, A. (2002). Saccharin as a sugar surrogate revisited. *Appetite* 38, 155–160. doi: 10.1006/appe.2001.0467

Spector, A. C., and Travers, S. P. (2005). The representation of taste quality in the mammalian nervous system. *Behav. Cogn. Neurosci. Rev.* 4, 143–191. doi: 10.1177/1534582305280031

Spielman, A. I. (1998). Gustducin and its role in taste. *J. Dent. Res.* 77, 539–544. doi: 10.1177/00220345980770040601

Sprous, D., and Palmer, R. K. (2010). "Chapter 6 - The T1R2/T1R3 Sweet Receptor and TRPM5 Ion Channel: Taste Targets with Therapeutic Potential," in *Progress in Molecular Biology and Translational Science : Membrane Proteins as Drug Targets*, ed. C. A. Lunn (Florida,FL: Academic Press), 151–208.

Stapleton, J. R., Lavine, M. L., Nicolelis, M. A. L., and Simon, S. A. (2007). Ensembles of gustatory cortical neurons anticipate and discriminate between tastants in a single lick. *Front. Neurosci.* 1:161–174. doi: 10.3389/neuro.01.1.1.012.2007

Steensels, S., Vancleef, L., and Depoortere, I. (2016). The Sweetener-Sensing Mechanisms of the Ghrelin Cell. *Nutrients* 8:nu8120795. doi: 10.3390/nu8120795

Stein, N., Laing, D. G., and Hutchinson, I. (1994). Topographical differences in sweetness sensitivity in the peripheral gustatory system of adults and children. *Dev. Brain Res.* 82, 286–292. doi: 10.1016/0165-3806(94)90170-8

Steiner, J. E., Glaser, D., Hawilo, M. E., and Berridge, K. C. (2001). Comparative expression of hedonic impact: affective reactions to taste by human infants and other primates. *Neurosci. Biobehav. Rev.* 25, 53–74. doi: 10.1016/S0149-7634(00)00051-8

Stone, L. M., Barrows, J., Finger, T. E., and Kinnamon, S. C. (2007). Expression of T1Rs and gustducin in palatal taste buds of mice. *Chem. Senses* 32, 255–262. doi: 10.1093/chemse/bjl053

Striem, B. J., Naim, M., and Lindemann, B. (1991). Generation of Cyclic AMP in Taste Buds of the Rat Circumvallate Papilla in Response to Sucrose. *Cell Physiol. Biochem.* 1, 46–54. doi: 10.1159/000154592

Striem, B. J., Pace, U., Zehavi, U., Naim, M., and Lancet, D. (1989). Sweet tastants stimulate adenylate cyclase coupled to GTP-binding protein in rat tongue membranes. *Biochem. J.* 260, 121–126. doi: 10.1042/bj2600121

Sukumaran, S. K., Yee, K. K., Iwata, S., Kotha, R., Quezada-Calvillo, R., Nichols, B. L., et al. (2016). Taste cell-expressed α -glucosidase enzymes contribute to gustatory responses to disaccharides. *Proc. Natl. Acad. Sci. U S A.* 113, 6035–6040. doi: 10.1073/pnas.1520843113

Suzuki, T. (2007). Cellular mechanisms in taste buds. *Bull. Tokyo Dent. Coll.* 48, 151–161. doi: 10.2209/tdcpublication.48.151

Svendsen, B., Larsen, O., Gabe, M. B. N., Christiansen, C. B., Rosenkilde, M. M., Drucker, D. J., et al. (2018). Insulin Secretion Depends on Intra-islet Glucagon Signaling. *Cell Rep.* 25, 1127.e–1134.e. doi: 10.1016/j.celrep.2018.10.018

Swithers, S. E., and Davidson, T. L. (2008). A role for sweet taste: calorie predictive relations in energy regulation by rats. *Behav. Neurosci.* 122, 161–173. doi: 10.1037/0735-7044.122.1.161

Takai, S., Yasumatsu, K., Inoue, M., Iwata, S., Yoshida, R., Shigemura, N., et al. (2015). Glucagon-like peptide-1 is specifically involved in sweet taste transmission. *FASEB J.* 29, 2268–2280. doi: 10.1096/fj.14-265355

Takami, S., Getchell, T. V., McLaughlin, S. K., Margolskee, R. F., and Getchell, M. L. (1994). Human taste cells express the G protein α -gustducin and neuron-specific enolase. *Mol. Brain Res.* 22, 193–203. doi: 10.1016/0169-328X(94)90047-7

Talavera, K., Yasumatsu, K., Voets, T., Droogmans, G., Shigemura, N., Ninomiya, Y., et al. (2005). Heat activation of TRPM5 underlies thermal sensitivity of sweet taste. *Nature* 438, 1022–1025. doi: 10.1038/nature04248

Tan, H.-E., Sisti, A. C., Jin, H., Vignovich, M., Villavicencio, M., Tsang, K. S., et al. (2020). The gut-brain axis mediates sugar preference. *Nature* 580, 511–516. doi: 10.1038/s41586-020-2199-7

Taniguchi, K. (2004). Expression of the sweet receptor protein, T1R3, in the human liver and pancreas. *J. Vet. Med. Sci.* 66, 1311–1314. doi: 10.1292/jvms.66.1311

Tappy, L. (2012). Q&A: 'toxic' effects of sugar: should we be afraid of fructose? *BMC Biol.* 10:42. doi: 10.1186/1741-7007-10-42

Taruno, A., Vingtdeux, V., Ohmoto, M., Ma, Z., Dvoryanchikov, G., Li, A., et al. (2013). CALHM1 ion channel mediates purinergic neurotransmission of sweet, bitter and umami tastes. *Nature* 495, 223–226. doi: 10.1038/nature11906

Tatzer, E., Schubert, M. T., Timischl, W., and Simbruner, G. (1985). Discrimination of taste and preference for sweet in premature babies. *Early Hum. Dev.* 12, 23–30. doi: 10.1016/0378-3782(85)90133-1

Tellez, L. A., Han, W., Zhang, X., Ferreira, T. L., Perez, I. O., Shammah-Lagnado, S. J., et al. (2016). Separate circuitries encode the hedonic and nutritional values of sugar. *Nat. Neurosci.* 19, 465–470. doi: 10.1038/nn.4224

Temussi, P. (2006). The history of sweet taste: Not exactly a piece of cake. *J. Mol. Recognit.* 19, 188–199. doi: 10.1002/jmr.767

Than, T. T., Delay, E. R., and Maier, M. E. (1994). Sucrose threshold variation during the menstrual cycle. *Physiol. Behav.* 56, 237–239. doi: 10.1016/0031-9384(94)90189-9

Thanarajah, S. E., Backes, H., DiFeliceantonio, A. G., Albus, K., Cremer, A. L., Hanssen, R., et al. (2019). Food Intake Recruits Orosensory and Post-ingestive Dopaminergic Circuits to Affect Eating Desire in Humans. *Cell Metab.* 29, 695.e–706.e. doi: 10.1016/j.cmet.2018.12.006

Thorens, B. (2015). GLUT2, glucose sensing and glucose homeostasis. *Diabetologia* 58, 221–232. doi: 10.1007/s00125-014-3451-1

Tizzano, M., Dvoryanchikov, G., Barrows, J. K., Kim, S., Chaudhari, N., and Finger, T. E. (2008). Expression of Galpha14 in sweet-transducing taste cells of the posterior tongue. *BMC Neurosci.* 9:110. doi: 10.1186/1471-2202-9-110

Tomasi, D., and Volkow, N. D. (2013). Striatocortical pathway dysfunction in addiction and obesity: differences and similarities. *Crit. Rev. Biochem. Mol. Biol.* 48, 1–19. doi: 10.3109/10409238.2012.735642

Tonosaki, K., and Funakoshi, M. (1988). Cyclic nucleotides may mediate taste transduction. *Nature* 331, 354–356. doi: 10.1038/331354a0

Tonosaki, K., Hori, Y., Shimizu, Y., and Tonosaki, K. (2007). Relationships between insulin release and taste. *Biomed. Res.* 28, 79–83.

Toyono, T., Seta, Y., Kataoka, S., Oda, M., and Toyoshima, K. (2011). Differential expression of the glucose transporters in mouse gustatory papillae. *Cell Tissue Res.* 345, 243–252. doi: 10.1007/s00441-011-1210-x

Travers, S. P., and Norgren, R. (1995). Organization of orosensory responses in the nucleus of the solitary tract of rat. *J. Neurophysiol.* 73, 2144–2162. doi: 10.1152/jn.1995.73.6.2144

Triantafillou, V., Workman, A. D., Kohanski, M. A., and Cohen, N. A. (2018). Taste Receptor Polymorphisms and Immune Response: A Review of Receptor Genotypic-Phenotypic Variations and Their Relevance to Chronic Rhinosinusitis. *Front. Cell Infect. Microbiol.* 8:64. doi: 10.3389/fcimb.2018.00064

Trubey, K. R., Culpepper, S., Maruyama, Y., Kinnamon, S. C., and Chaudhari, N. (2006). Tastants evoke cAMP signal in taste buds that is independent of calcium signaling. *Am. J. Physiol. Cell Physiol.* 291, C237–C244. doi: 10.1152/ajpcell.00303.2005

Tsouristakis, A. I., Febres, G., McMahon, D. J., Tchang, B., Conwell, I. M., Tsang, A. J., et al. (2019). Long-Term Modulation of Appetitive Hormones and Sweet Cravings After Adjustable Gastric Banding and Roux-en-Y Gastric Bypass. *OBES Surg.* 29, 3698–3705. doi: 10.1007/s11695-019-04111-z

Uchida, Y., and Sato, T. (1997). Changes in outward K+ currents in response to two types of sweeteners in sweet taste transduction of gerbil taste cells. *Chem. Senses* 22, 163–169. doi: 10.1093/chemse/22.2.163

Usui-Aoki, K., Matsumoto, K., Koganezawa, M., Kohatsu, S., Isono, K., Matsubayashi, H., et al. (2005). Targeted expression of Ip3 sponge and Ip3 dsRNA impaires sugar taste sensation in Drosophila. *J. Neurogenet.* 19, 123–141. doi: 10.1080/01677060600569713

Vargas, E., Podder, V., and Sepulveda, M. A. C. (2019). *Physiology, Glucose Transporter Type 4 (GLUT4).* Treasure Island, FL: StatPearls Publishing.

Veldhuizen, M. G., Bender, G., Constable, R. T., and Small, D. M. (2007). Trying to detect taste in a tasteless solution: modulation of early gustatory cortex by attention to taste. *Chem. Senses* 32, 569–581. doi: 10.1093/chemse/bjm025

Ventura, A. K., and Mennella, J. A. (2011). Innate and learned preferences for sweet taste during childhood. *Curr. Opin. Clin. Nutr. Metab. Care* 14, 379–384. doi: 10.1097/MCO.0b013e328346df65

Volkow, N. D., Wang, G.-J., and Baler, R. D. (2011). Reward, dopamine and the control of food intake: implications for obesity. *Trends Cogn. Sci.* 15, 37–46. doi: 10.1016/j.tics.2010.11.001

von Molitor, E., Nürnberg, E., Ertongur-Fauth, T., Scholz, P., Riedel, K., Hafner, M., et al. (2020a). Analysis of calcium signaling in live human Tongue cell 3D-Cultures upon tastant perfusion. *Cell Calcium* 87:102164. doi: 10.1016/j.ceca.2020.102164

von Molitor, E., Riedel, K., Hafner, M., Rudolf, R., and Cesetti, T. (2020b). Sensing Senses: Optical Biosensors to Study Gustation. *Sensors* 20:s20071811. doi: 10.3390/s20071811

von Molitor, E., Riedel, K., Krohn, M., Rudolf, R., Hafner, M., and Cesetti, T. (2020c). An alternative pathway for sweet sensation: possible mechanisms and physiological relevance. *Pflugers Arch.* 472, 1667–1691. doi: 10.1007/s00424-020-02467-1

Vos, A., Heimberg, H., Quartier, E., Huypens, P., Bouwens, L., Pipeleers, D., et al. (1995). Human and rat beta cells differ in glucose transporter but not in glucokinase gene expression. *J. Clin. Invest.* 96, 2489–2495. doi: 10.1172/JCI118308

Wang, G.-J., Volkow, N. D., Logan, J., Pappas, N. R., Wong, C. T., Zhu, W., et al. (2001). Brain dopamine and obesity. *Lancet* 357, 354–357.

Wauson, E. M., Zaganjor, E., Lee, A.-Y., Guerra, M. L., Ghosh, A. B., Bookout, A. L., et al. (2012). The G protein-coupled taste receptor T1R1/T1R3 regulates mTORC1 and autophagy. *Mol. Cell* 47, 851–862. doi: 10.1016/j.molcel.2012.08.001

Wee, M., Tan, V., and Forde, C. (2018). A Comparison of Psychophysical Dose-Response Behaviour across 16 Sweeteners. *Nutrients* 10:nu10111632. doi: 10.3390/nu10111632

Westman, E. C. (2002). Is dietary carbohydrate essential for human nutrition? *Am. J. Clin. Nutr.* 75, 951–953. doi: 10.1093/ajcn/75.5.951

Widmayer, P., Breer, H., and Hass, N. (2011). Candidate chemosensory cells in the porcine stomach. *Histochem. Cell Biol.* 136, 37–45.

Witt, M. (2019). Anatomy and development of the human taste system. *Handb. Clin. Neurol.* 164, 147–171. doi: 10.1016/B978-0-444-63855-7.00010-1

Wong, G. T., Gannon, K. S., and Margolskee, R. F. (1996). Transduction of bitter and sweet taste by gustducin. *Nature* 381, 796–800. doi: 10.1038/381796a0

Workman, A. D., Palmer, J. N., Adappa, N. D., and Cohen, N. A. (2015). The Role of Bitter and Sweet Taste Receptors in Upper Airway Immunity. *Curr. Allergy Asthma Rep.* 15:72. doi: 10.1007/s11882-015-0571-8

Wright, E. M., Loo, D. D. F., and Hirayama, B. A. (2011). Biology of human sodium glucose transporters. *Physiol. Rev.* 91, 733–794. doi: 10.1152/physrev.00055.2009

Wu, A., Dvoryanchikov, G., Pereira, E., Chaudhari, N., and Roper, S. D. (2015). Breadth of tuning in taste afferent neurons varies with stimulus strength. *Nat. Commun.* 6:8171. doi: 10.1038/ncomms9171

Yamamoto, K., and Ishimaru, Y. (2013). Oral and extra-oral taste perception. *Semin. Cell Dev. Biol.* 24, 240–246. doi: 10.1016/j.semcdb.2012.08.005

Yamazaki, M., and Sakaguchi, T. (1986). Effects of D-glucose anomers on sweetness taste and insulin release in man. *Brain Res. Bull.* 17, 271–274. doi: 10.1016/0361-9230(86)90126-7

Yan, C. H., Hahn, S., McMahon, D., Bonislawski, D., Kennedy, D. W., Adappa, N. D., et al. (2017). Nitric oxide production is stimulated by bitter taste receptors ubiquitously expressed in the sinonasal cavity. *Am. J. Rhinol. Allergy* 31, 85–92. doi: 10.2500/ajra.2017.31.4424

Yan, W., Sunavala, G., Rosenzweig, S., Dasso, M., Brand, J. G., and Spielman, A. I. (2001). Bitter taste transduced by PLC-beta(2)-dependent rise in IP(3) and alpha-gustducin-dependent fall in cyclic nucleotides. *Am. J. Physiol. Cell Physiol.* 280, C742–C751. doi: 10.1152/ajpcell.2001.280.4.C742

Yang, H., Wanner, I. B., Roper, S. D., and Chaudhari, N. (1999). An optimized method for in situ hybridization with signal amplification that allows the detection of rare mRNAs. *J. Histochem. Cytochem.* 47, 431–446. doi: 10.1177/002215549904700402

Yasumatsu, K., Ohkuri, T., Yoshida, R., Iwata, S., Margolskee, R. F., and Ninomiya, Y. (2020). Sodium-glucose cotransporter 1 as a sugar taste sensor in mouse tongue. *Acta Physiol.* 2020:e13529. doi: 10.1111/apha.13529

Yee, K. K., Sukumaran, S. K., Kotha, R., Gilbertson, T. A., and Margolskee, R. F. (2011). Glucose transporters and ATP-gated K+ (KATP) metabolic sensors are present in type 1 taste receptor 3 (T1r3)-expressing taste cells. *Proc. Natl. Acad. Sci. U S A.* 108, 5431–5436. doi: 10.1073/pnas.1100495108

Young, R. L., Sutherland, K., Pezos, N., Brierley, S. M., Horowitz, M., Rayner, C. K., et al. (2009). Expression of taste molecules in the upper gastrointestinal tract in humans with and without type 2 diabetes. *Gut* 58, 337–346. doi: 10.1136/gut.2008.148932

Zhang, G.-H., Zhang, H.-Y., Wang, X.-F., Zhan, Y.-H., Deng, S.-P., and Qin, Y.-M. (2009). The relationship between fungiform papillae density and detection

threshold for sucrose in the young males. *Chem. Senses* 34, 93–99. doi: 10.1093/chemse/bjn059

Zhang, J., Jin, H., Zhang, W., Ding, C., O'Keeffe, S., Ye, M., et al. (2019). Sour Sensing from the Tongue to the Brain. *Cell* 179, 392.e–402.e. doi: 10.1016/j.cell.2019.08.031

Zhang, L., Han, W., Lin, C., Li, F., and Araujo, I. E. (2018). Sugar Metabolism Regulates Flavor Preferences and Portal Glucose Sensing. *Front. Integr. Neurosci.* 12:57. doi: 10.3389/fnint.2018.00057

Zhang, Y., Hoon, M. A., Chandrashekar, J., Mueller, K. L., Cook, B., Wu, D., et al. (2003). Coding of Sweet, Bitter, and Umami Tastes. *Cell* 112, 293–301. doi: 10.1016/S0092-8674(03)00071-0

Zhao, F.-Q., and Keating, A. (2007). Functional Properties and Genomics of Glucose Transporters. *CG* 8, 113–128. doi: 10.2174/138920207780368187

Zhao, G. Q., Zhang, Y., Hoon, M. A., Chandrashekar, J., Erlenbach, I., Ryba, N. J. P., et al. (2003). The receptors for mammalian sweet and umami taste. *Cell* 115, 255–266. doi: 10.1016/s0092-8674(03)00844-4

Zhu, X., and Birnbaumer, L. (1996). G protein subunits and the stimulation of phospholipase C by Gs-and Gi-coupled receptors: Lack of receptor selectivity of Galpha(16) and evidence for a synergic interaction between Gbeta gamma and the alpha subunit of a receptor activated G protein. *Proc. Natl. Acad. Sci. U S A.* 93, 2827–2831. doi: 10.1073/pnas.93.7.2827

Zhu, X., Gilbert, S., Birnbaumer, M., and Birnbaumer, L. (1994). Dual signaling potential is common among Gs-coupled receptors and dependent on receptor density. *Mol. Pharmacol.* 46, 460–469.

ZhuGe, R., Roura, E., and Behrens, M. (2020). Editorial: Extra-Oral Taste Receptors: Function, Disease and Evolution. *Front. Physiol.* 11:607134. doi: 10.3389/fphys.2020.607134

Zukerman, S., Ackroff, K., and Sclafani, A. (2013). Post-oral appetite stimulation by sugars and nonmetabolizable sugar analogs. *Am. J. Physiol. Regul. Integr. Comp. Physiol.* 305, R840–R853. doi: 10.1152/ajpregu.00297.2013

Conflict of Interest: KR and MK were employed by the company BRAIN-Biotech.

The remaining authors declare that the research was conducted in the absence of any commercial or financial relationships that could be construed as a potential conflict of interest.

Advantages of publishing in Frontiers

OPEN ACCESS
Articles are free to read for greatest visibility and readership

FAST PUBLICATION
Around 90 days from submission to decision

HIGH QUALITY PEER-REVIEW
Rigorous, collaborative, and constructive peer-review

TRANSPARENT PEER-REVIEW
Editors and reviewers acknowledged by name on published articles

Frontiers
Avenue du Tribunal-Fédéral 34
1005 Lausanne | Switzerland

Visit us: www.frontiersin.org
Contact us: frontiersin.org/about/contact

REPRODUCIBILITY OF RESEARCH
Support open data and methods to enhance research reproducibility

DIGITAL PUBLISHING
Articles designed for optimal readership across devices

FOLLOW US
@frontiersin

IMPACT METRICS
Advanced article metrics track visibility across digital media

EXTENSIVE PROMOTION
Marketing and promotion of impactful research

LOOP RESEARCH NETWORK
Our network increases your article's readership